New Methods for the Asymmetric Synthesis of α-Alkylated Ketones and 1,3-Amino Alcohols

Christina M. McSweeney, B.Sc.

University College Cork
Coláiste na hOllscoile Corcaigh

Thesis presented for the degree of Doctor of Philosophy to National University of Ireland, Cork.

Analytical and Biological Chemistry Research Facility (ABCRF)

Department of Chemistry

April 2015

Supervisor: Dr. Gerard P. McGlacken

Head of Department: Prof. Martyn Pemble

To my parents,

Mary and Terence

Accept what is, let go of what was,

and have faith in what will be.

Acknowledgments

I would first like to thank my supervisor for giving me the opportunity to be the first PhD student to join his research group. You have been an excellent mentor in guiding me from an undergraduate student to a research chemist. I have gained invaluable research and scientific writing skills thanks to your enthusiasm and knowledge of the subject, which have opened up great opportunities for me in my future career.

I would like to thank SFI for funding for my PhD research.

I would sincerely like to thank all of the technical and research staff in the department. Dr. Dan McCarthy, Dr. Lorraine Bateman and Dr. Denis Lynch for NMR work, Barry O'Mahony for microanalysis, Dr. Florence McCarthy and Mick O'Shea for mass spectrometry, Dr. Simon Lawrence and his research group for single crystal analysis and Derry Kearney for glass blowing repairs (and glass sculptures to cheer me up in unhappier times!). A special thanks to Dr. Matthias Jauch for IT services and all you help with my Dell laptop, without you it would not have made it over the line.

To all the members of the GMG research group, it was a lonely year until everyone began to filter in and now we are like one big family. You have all been a pleasure to work with and I wish you all the best in your futures. A special thanks to Vera, my 'sparteine buddy' you were a shoulder to lean on when the research didn't go exactly the way we wanted. To Leti, thank you for all your help along the way, I can't thank you enough (and yes now we can party!).

To all the researchers on the 4th floor of the Kane and 2nd floor of the Cavanagh building, I have made many great friends, all of whom have made my time more enjoyable and unforgettable. In particular, Dawn, Lorna and Danielle, the lunch bunch, ye truly will be lifelong friends no matter where life takes us. To Kevin, for his extremely humorous conversations and Starbucks coffee rants. To Denis Lynch, thanks for all your help over the years, you truly are a wealth of knowledge, a genius and an absolute gent.

Finally, I would like to thank my parents, without whom this would not be possible. You have always encouraged me to be the best person I can be and supported me with every decision I have made to date. I would not be the person I am today if it were not for both of you and for that I am eternally grateful.

Declaration

I hereby confirm that the body of work described within this thesis, for the degree of Doctor of Philosophy, is the result of my own research work, carried out under the supervision of Dr. Gerard McGlacken, and has not been previously submitted.

Signed: _____

Abstract

A large number of optically active drugs and natural products contain α-functionalised ketones or simple derivatives thereof. Furthermore, chiral α-alkylated ketones are useful synthons and have found widespread use in total synthesis. The asymmetric alkylation of ketones represents one of the most powerful and longstanding procedures in organic chemistry. Surprisingly, however, only one effective methodology is available, and this involves the use of chiral auxiliaries. This is discussed in Chapter 1, which also provides a background of other key topics discussed throughout the thesis.

Expanding on the existing methodology of chiral auxiliaries, Chapter 2 details the synthesis of a novel chiral auxiliary containing a pyrrolidine ring and its use in the asymmetric preparation of α-alkylated ketones with good enantioselectivity. The synthesis of racemic α-alkylated ketones as reference standards for GC chromatography is also reported in this chapter.

Chapter 3 details a new approach to chiral α-alkylated ketones using an intermolecular chirality transfer methodology. This approach employs the use of simple non-chiral dimethylhydrazones and their asymmetric alkylation using the chiral diamine ligands, (+)- and (-)-sparteine. The methodology described represents the first example of an asymmetric alkylation of non-chiral azaenolates. Enantiomeric ratios up to 83 : 17 are observed.

Chapter 4 introduces the first aldol-Tishchenko reaction of an imine derivative for the preparation of 1,3-aminoalcohol precursors. 1,3-Aminoalcohols can be synthesised via indirect routes involving various permutations of stepwise construction with asymmetric induction. Our approach offers an alternative highly diastereomeric route to the synthesis of this important moiety utilising N-*tert*-butanesulfinyl imines in an aldol-Tishchenko-type reaction.

Chapter 5 details the experimental procedures for all of the above work.

Chapter 6 discusses the results of a separate research project undertaken during this PhD. 2-alkyl-quinolin-4-ones and their *N*-substituted derivatives have several important biological functions such as the role of *Pseudomonas* quinolone signal (PQS) in quorum sensing. Herein, we report the synthesis of its biological precursor, 2-heptyl-4-hydroxy-quinoline (HHQ) and possible isosteres of PQS; the C-3 Cl, Br and I analogues. *N*-Methylation of the iodide was also feasible and the usefulness of this compound showcased in Pd-catalysed cross-coupling reactions, thus allowing access to a diverse set of biologically important molecules.

Abbreviations

α	stereochemical descriptor
$[\alpha]_D^T$	specific rotation
Å	amstrong
@	at
Ac	acetyl
ACC	amino cyclic carbamate
AcOH	acetic acid
AHL	acyl homoserine lactone
alkyl.	alkylation
anal.	analysis
aq	aqueous
β	stereochemical descriptor
BINOL	1,1'-bi-2-naphthol
Bn	benzyl
Boc	*tert*-butyloxycarbonyl
BOX	bisoxazoline
br s	broad singlet
Bu	butyl
C	centi (10^{-2})
	concentration, for rotation
ºC	Celsius degrees
^{13}C NMR	carbon nuclear magnetic resonance
ca.	circa, about
calcd	calculated
cat.	catalyst
cf.	compare
COSY	correlation spectroscopy
δ	NMR chemical shift
d	Doublet
D	Deuterium
DABCO	1,4-diazabicyclo[2.2.2]octane

dba	dibenzylideneacetone
DCC	N,N'-dicyclohexylcarbodiimide
dd	doublet of doublets
ddd	doublet of doublets of doublets
deg	degree
deprot.	deprotonation
DEPT	distortionless enhancement by polarization transfer
DFT	density functional theory
DIBAL-H	diisobutylaluminium hydride
DiPAMP	Ethane-1,2-diylbis[(2-methoxyphenyl)phenylphosphane]
DKR	dynamic kinetic resolution
DMAP	4-dimethylaminopyridine
DME	1,2-dimethoxyethane
DMF	dimethylformamide
DMPU	1,3-Dimethyl-3,4,5,6-tetrahydro-2(1H)-pyrimidinone
DNA	deoxyribonucleic acid
DNase	deoxyribonuclease
DOPA	3-(3,4-dihydroxyphenyl)alanine
DPPBA	diphenylphosphino benzoic acid
dq	doublet of quartets
dr	diastereomeric ratio
dt	doublet of triplets
DTR	dynamic thermodynamic resolution
DuPhos	phospholane ligands
E	electrophile
E	entgegen configuration
e.g.	for example
EDG	electron donating group
EDS	enantiodeterming step
ee	enantiomeric excess
EQ	external quenching
equiv.	equivalent

er	enantiomeric ratio
ESI	electrospray ionization
Et	ethyl
et al.	and others
Expt	experiment
EWG	electron withdrawing group
g	gram
GC	gas chromatography
h	hour
^{1}H NMR	proton nuclear magnetic resonance
HCLA	homo chiral lithium amide
HHQ	2-heptyl-4-hydroxy-quinolone
HIV	human immunodeficiency virus
HMBC	heteronuclear multiple-bond correlation spectroscopy
HMPA	hexamethylphosphoramide
HRMS	high-resolution mass spectrometry
HSL	homoserine lactone
HSQC	heteronuclear single-quantum correlation spectroscopy
Hz	Hertz
i	Iso
i.e.	that is
Inc.	incorporated
IQ	internal quenching
IR	infrared
J	coupling constant
k	rate constant
KDA	potassium diisopropylamide
KHMDS	potassium bis(trimethylsilyl)amide
L	liter
LC-MS	liquid chromatography-mass spectrometry
LDA	lithium diisopropylamide
LHMDS, LiHMDS	lithium bis(trimethylsilyl)amide

LRMS	low resolution mass spectra
LTMP, LiTMP	lithium tetramethylpiperidide
μ	micro (10^{-6})
m	meter
	mili (10^{-3})
	multiplet
	medium
M	metal
	molar
m/z	mass-to-charge ratio
max	maximum
m-CPBA	*m*-chloroperoxybenzoic acid
Me	methyl
MHz	megahertz
min	minute
mol	mole
	molecular
mol%	mol percent
Mp	melting point
MS	mass spectrometry
MTBE	methyl *tert*-butyl ether
ν_{max}	frequency of maximum absorption
n	nano (10^{-9})
n	normal
NDA	sodium diisopropylamide
NMR	nuclear magnetic resonance
NOE	nuclear Overhauser effect
NOESY	nuclear Overhauser enhancement spectroscopy
o	ortho
OD	optical density
o/n	overnight
π	type of orbital, electron

p	para
P	primitive
P.	*Pseudomonas*
Pe	pentyl
Ph	phenyl
PhD	Doctorate of Philosophy
PMDTA	*N*,*N*,*N*′,*N*′,*N*″-pentamethyldiethylenetriamine
ppm	parts per million
PQS	*Pseudomonas* quinoline signal
Pr	propyl
p-TsOH	*p*-toluenesulfonic acid
q	quartet
quin	quintet
QSI	quorum sensing inhibitor
R	rectus configuration
RAMBO	(2*R*,3a*R*,6a*R*)-2-(methoxymethyl)hexahydrocyclopenta[*b*]pyrrol-1(2*H*)-amine
RAMP	(*R*)-1-amino-2-methoxymethylpyrrolidine
R_f	retention factor
R factor	reliability factor
RNA	ribonucleic acid
RT	room temperature
s	second
	singlet
	strong
S	sinister configuration
SADP	(*S*)-2-(2-methoxypropan-2-yl)pyrrolidin-1-amine
SAEP	(*S*)-2-(3-methoxypentan-3-yl)pyrrolidin-1-amine
SAMP	(*S*)-1-amino-2-methoxymethylpyrrolidine
SAPP	(*S*)-2-(methoxydiphenylmethyl)pyrrolidin-1-amine
sec	secondary
sept	septet

sext	sextet
SOMO	singly occupied molecular orbital
sp	sparteine
t	triplet
t, tert	tertiary
TADDOL	α,α,α,α-tetraaryl-1,3-dioxolane-4,5-dimethanol
TBDPS	*tert*-butyldiphenylsilyl ether
TBS	*tert*-butyldimethylsilyl ether
temp	temperature
TFA	trifluoroacetic acid
TfO, triflate	trifluoromethanesulfonate
THF	tetrahydrofuran
TLC	thin-layer chromatography
TMEDA	tetramethylethylenediamine
TMS	tetramethylsilane
	tetramethylsilyl
t_R	retention time
Ts	4-toluenesulfonyl, tosyl
w	weak
wt	weight
Z	zusammen configuration

*Note: Descriptors of stereoisomer composition and stereoselectivity used throughout, are in accordance with the original papers.

Table of Contents

Chapter 1 – Introduction

1.1 Asymmetric Synthesis and Stereochemistry 3

1.2 α-Substitution of Ketones 7

1.3 Chiral Auxiliaries 9

1.4 Homo Chiral Lithium Amide Bases 19

1.5 Other Methods for the α-Alkylation of Ketones 28

1.6 Dialkylhydrazone Methodology and Recovery of Carbonyl Compounds 32

1.7 Chiral Ligands 36

1.8 (-)-Sparteine and its Use in Asymmetric Synthesis 38

1.9 Sulfinimines and 1,3-Amino Alcohols 43

1.10 The Aldol-Tishchenko Reaction 47

Chapter 2 - Synthesis of Racemic α-Alkylated Ketones and the Development of a Novel Chiral Auxiliary for their Enantioselective Preparation

2.1 Introduction 59

2.2 Results and Discussion 60

2.2.1 Preparation of Racemic α-Alkylated Ketones 60

2.2.2 Synthesis of a Novel Diamine-based Chiral Auxiliary 63

2.2.3 Investigation of a Novel Chiral Auxiliary in the Asymmetric α-Alkylation of Ketones 69

2.3 Conclusions and Future Work 75

Chapter 3 - Intermolecular Chirality Transfer using Sparteine as a Chiral Ligand

3.1 Introduction 79

3.2 Results and Discussion 82

3.2.1 Synthesis of *N*,*N*-Dimethylhydrazones for Asymmetric α-Alkylation via Intermolecular Chirality Transfer 82

3.2.2 Determination of Optimum Reaction Conditions for Asymmetric α-Alkylation via Intermolecular Chirality Transfer 87

3.2.3 Substrate Scope in Asymmetric α-Alkylation via Intermolecular Chirality Transfer 93
3.2.4 Yield Optimisation for Asymmetric α-Alkylation via Intermolecular Chirality Transfer 98
3.2.5 Further Studies of Hydrazone Cleavage Methods 100
3.2.6 Addition of Lithium Salts 102
3.2.7 Mechanistic Investigations 103
3.2.8 Preparation of Chiral Ligands and their Use in the Asymmetric Synthesis of α-Alkylated Ketones 112
3.2.9 NMR Investigations of Asymmetric Alkylation with (+)-Sparteine 125
3.2.10 Aldol & Michael Reactions using (-)- and (+)-Sparteine 131
3.3 Conclusions and Future Work 136

Chapter 4 - Asymmetric α-Alkylation and Synthesis of 1,3-Amino Alcohol Precursors using Chiral Sulfinimines
4.1 Introduction 141
4.2 Results and Discussion 142
4.2.1 Synthesis of *N*-*tert*-Butanesufinyl Imines and their Use in Asymmetric α-Alkylation reactions 142
4.2.2 Synthesis of 1,3-Amino Alcohol Precursors 145
4.3 Conclusions and Future Work 161

Chapter 5 - Experimental
5.1 General Procedures 165
5.2 Synthesis of Racemic α-Alkylated Ketones 167
5.3 Synthesis of a Novel Diamine Chiral Auxiliary 173
5.3.1 Synthesis of (2*R*,5*S*)-trichloromethyl-1-aza-3-oxabicyclo-[3.3.0]-octan-4-one 173
5.3.2 Preparation of (*S*)-2-(pyrrolidin-1-ylmethyl)pyrrolidin-1-amine 174
5.4 Asymmetric α-Alkylation using Novel Diamine Chiral Auxiliary 177
5.4.1 Solvent Screen for Asymmetric Alkylation using Chiral Auxiliary 177

5.5 Synthesis *N*,*N*-Dimethylhydrazones for Asymmetric α-Alkylation via Intermolecular Chirality Transfer 179

5.6 Asymmetric α-Alkylation via Intermolecular Chirality Transfer 183

5.6.1 Temperature, Solvent and Base Variations 183

5.6.2 Substrate Investigations 185

5.6.3 Procedures for Work-up Investigations 195

5.6.4 Hydrazone Cleavage Methods 197

5.6.5 Addition of Lithium Salts 199

5.6.6 Procedures for Mechanistic Investigations 200

5.7 Preparation of Chiral Ligands and their Use in the Asymmetric Synthesis of α-Alkylated Ketones 201

5.7.1 Preparation of 2,2'-isopropylidenebis[(4*S*)-4-phenyl-4,5-dihydro-1,3-oxazole] 201

5.7.2 Preparation of (1*S*,2*S*)-N^1,N^1,N^2,N^2-tetramethyl-1,2-diphenylethane-1,2-diamine 204

5.7.3 Preparation of (1*R*,2*R*)-1,2-dimethoxy-1,2-diphenylethane 205

5.7.4 Preparation of (*S*)-1-methyl-2-pyrrolidin-1-ylmethyl)pyrrolidine 206

5.7.5 Preparation of (1*S*,2*S*)-N^1,N^2-bis (3,3-dimethylbutyl)- N^1,N^2-dimethylcyclohexane-1,2-diamine 208

5.7.6 Preparation of N^1,N^1,N^2,N^2-tetramethylcyclohexane-1,2-diamine 212

5.7.7 Chiral Ligand Screen in the Asymmetric Synthesis of α-Alkylated Ketones 213

5.8 Aldol & Michael Reactions using (-)- and (+)-Sparteine 215

5.9 Procedures for NMR Investigations of Asymmetric Alkylation with (+)-Sparteine 218

5.10 Asymmetric α-Alkylation and Synthesis of a 1,3-Amino Alcohol Precursors using Chiral Sulfinimines 220

5.10.1 Synthesis of *N*-*tert*-Butanesulfinyl Imines 220

5.10.2 Asymmetric α-Alkylation using Chiral Sulfinimines 222

5.10.3 Synthesis of 1,3-Amino Alcohol Precursors 223

Chapter 6 - Reference List 230

Appendix 1 - Structure-function Analysis of the C-3 position in Analogues of Microbial Behavioral Modulator, HHQ

1.1 Introduction 3

1.1.1 Background 3

1.1.2 The Biosynthesis of PQS 5

1.1.3 Cell-Cell Communication 8

1.1.4 Biological Functions and Applications 9

1.2 Results and Discussion 11

1.2.1 Introduction 11

1.2.2 Synthesis of 2-heptylquinolin-4(1*H*)-one 14

1.2.3 Synthesis of 3-halo-analogues of 2-heptylquinolin-4(1*H*)-one 17

1.2.4 Biological Results and Discussion 22

1.3 Conclusions and Future Work 26

1.4 Experimental 27

1.4.1 Synthesis of 2-heptylquinolin-4(1*H*)-one 27

1.4.2 Synthesis of 3-halo-analogues of 2-heptylquinolin-4(1*H*)-one 30

1.4.3 *N*-Methylation and the Suzuki-Miyaura Reaction 32

Appendix 2

Chapter 1

Introduction

1.1 Asymmetric Synthesis and Stereochemistry

Asymmetric synthesis, also called chiral synthesis, enantioselective or stereoselective synthesis is a type of organic synthesis that introduces one or more, new and desired elements of chirality. The word *chiral* comes from the Greek word *cheir*, which means hand. Our hands are chiral – our right hand is a mirror image of our left hand – as are most of life's molecules.

Nature yields an enormous variety of chiral compounds, and often only one of the two possible enantiomers. Consequently, only one of the mirror image forms of amino acids, and therefore peptides, enzymes and other proteins, are found in nature. Carbohydrates and nucleic acids like DNA and RNA are other examples.[1]

A publication in 2006 states that in the pharmaceutical industry, 56% of the drugs in use are chiral products, with 88% of these marketed as racemates, consisting of an equimolar mixture of two enantiomers.[2]

Although they have the same chemical structure, most enantiomers of racemic drugs exhibit marked differences in biological activities such as pharmacology, toxicology, pharmacokinetics, metabolism etc. The importance of stereochemical purity in pharmaceutical products has been one driving force in the quest for improved control over the stereochemical outcome of organic reactions. Biological systems, in most cases, recognise a pair of enantiomers as different substances and the two enantiomers will often elicit different responses. Thus one enantiomer may act as a very effective therapeutic drug whereas the other enantiomer may be highly toxic.[3]

The striking example of the drug Thalidomide is well known. A West German Pharmaceutical Company, Chemie Grünenthal, first introduced Thalidomide, in 1957, as a sedative or sleep aid. It was proclaimed a 'wonder drug' for insomnia, coughs, colds and headaches. It was also found to be effective in reducing morning sickness and so thousands of pregnant women took the drug to relieve their symptoms. During its use, reports began to emerge of instances of neuritis. It became evident Thalidomide was having a toxic effect on the nervous system of the user. At the time of the drug's development it was not thought likely that any drug could pass from the mother across the placental barrier and harm the developing foetus. However while Thalidomide was in use from 1957 to 1961 between 10,000 and 20,000 babies were affected. Many were born with deformities and there were also cases where the infants were stillborn or

died shortly after birth.[4] The same birth defects are now being found in second- and third-generation Thalidomide users.

It was discovered that the desired physiological activity was found to reside solely with the *R*-(+)-enantiomer **(*R*)-1** and the corresponding *S*-(-)-enantiomer **(*S*)-1** was teratogenic (Figure 1.1.1). Although, it is now known that the 'safe' isomer can be converted to the teratogenic isomer once in the human body.

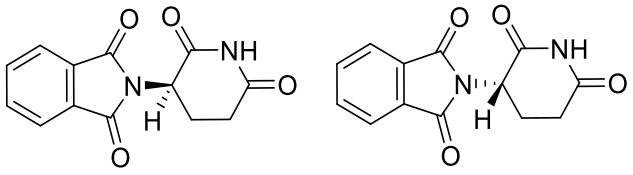

R-Enantiomer **(*R*)-1**

S-Enantiomer **(*S*)-1**

Figure 1.1.1

There are other, less dramatic examples of how two enantiomers can affect our cells differently. Limonene (Figure 1.1.2), for example, is chiral and the receptors in our nose can differentiate between both enantiomers. One form smells of lemons but the other of oranges.

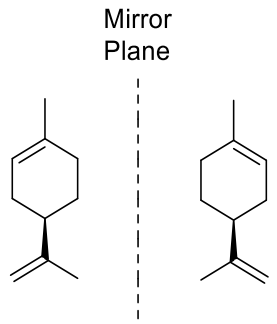

Figure 1.1.2

The importance of asymmetric synthesis as a tool to obtain enantiomerically pure or enriched compounds has been fully acknowledged to date by chemists in synthetic organic chemistry, medicinal chemistry, and the pharmaceutical industries and agricultural industries.

In order to achieve asymmetric synthesis, at least one component of the reaction must be chiral and non-racemic. If there is no asymmetric component in the reaction, then transition states which lead to enantiomers will be equal in energy, and a racemate must be formed. In general terms, any feature of the reacting system which would cause the transition states to be diastereomeric, could lead to the preferential formation of one diastereoisomer or enantiomer.

Transition states which are diastereomeric need not be of the same energy and consequently one of the possible products could be formed preferentially.[5]

The range and scope of the reactions used in asymmetric synthesis are very large and consequently they are difficult to classify. However, the following are common types of asymmetric synthesis.

1. *Chiral Auxiliaries* –This method is based on a three step process. The achiral substrate is combined with a chiral reagent known as a chiral auxiliary to form a chiral intermediate. Treatment of this intermediate with a suitable reagent produces a compound with a new asymmetric centre. The chiral auxiliary causes, by steric or other means, the reaction to favour the production of one of the possible stereoisomers in preference to the other. Completion of the reaction is followed by removal of the chiral auxiliary, which may be recovered and recycled.[6]

2. *Chiral Reagents* – A chiral control element is incorporated into the structure of the reagent in order to direct the stereochemistry at newly formed stereocentres in a reaction. The reagent is used in stoichiometric quantities in the reaction and is usually not recovered for re-use. Examples include chiral reducing agents and chiral bases.

3. *Chiral Catalysts* – Similar to chiral reagents, chirality is introduced through the structure of the reagent, however one molecule of catalyst can lead to many molecules of chiral product by virtue of regeneration of the chiral catalyst during the reaction.

    - *Biocatalysis* – This method involves the use of natural catalysts, such as enzymes, to perform chemical transformations on organic compounds. Biocatalysis is economical in its use of chiral material but suffers from the disadvantage that it requires large quantities of the enzyme to produce significant quantities of the target compound.[6]

    - *Transition Metal Catalysis* – This is an enantiopure organic compound which combines with a metal centre by chelation to form an asymmetric catalyst. This catalyst engages in a chemical reaction and transfers its chirality to the reaction product, which as a result also becomes chiral and potentially enantiomerically enhanced.

- *Organocatalysis* – This is the acceleration of chemical transformations with a substoichiometric amount of an organic compound which does not contain a metal atom.[7]

1.2 α-Substitution of Ketones

The carbonyl moiety remains among the most utilized and well-studied functional groups in organic chemistry. In particular, functionalization of a carbonyl group at the α-position via carbon–carbon or carbon–heteroatom bond formation is a powerful transformation in chemical synthesis with broad application in the construction of complex organic architecture.

A large number of optically active drugs and natural products contain α-functionalized ketones, or simple derivatives thereof. Furthermore, chiral α-alkylated ketones are very useful synthons and have found widespread use in total synthesis.[8-10]

The Paterson ketone **2** is a simple chiral ethyl ketone used in the synthesis of polyketide and propionate based natural products. It was used in the synthesis of oleandolide **3**, the aglycon of the macrolide antibiotic oleandomycin **4** (Figure 1.2.1), a 14-membered macrolide antibiotic produced by the actinomycete *Streptomyces antibioticus*.[11]

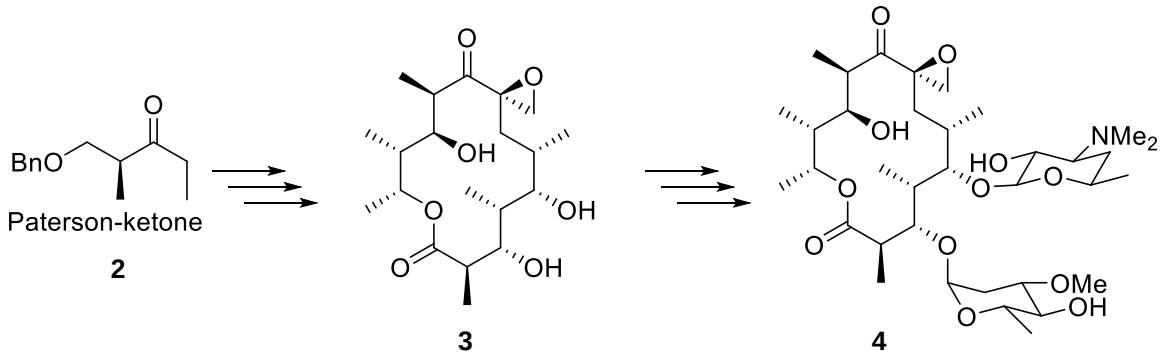

Figure 1.2.1

Stigmatellin A, (+)-pectinatone, (+)-maritimol and ulapualide A are all further examples of natural products, which use asymmetric alkylation reactions as one of their key synthetic steps (Figure 1.2.2).[9,10]

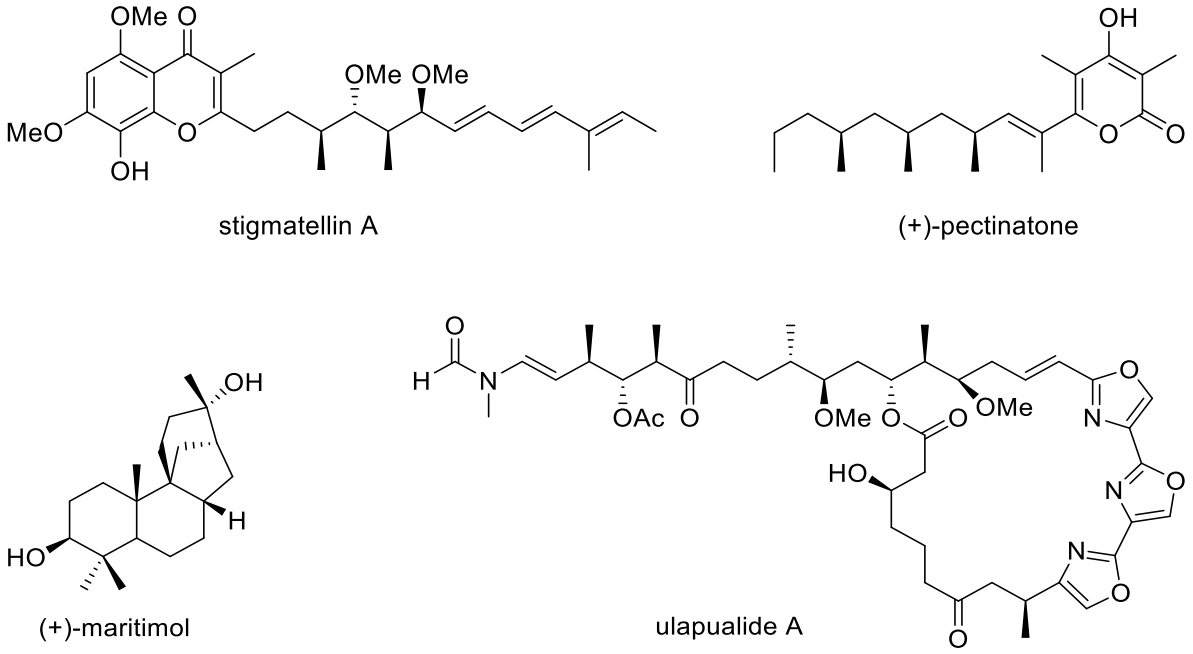

Figure 1.2.2

Traditionally, carbonyl functionalization typically involves the pre-generation or in situ formation of nucleophilic enols, enolates, alkyl/silyl enol ethers, enamines and azaenolates, which readily combine with aryl, alkyl, heteroatom, or halogen-centred electrophiles.

Enolate chemistry is inherently complex because multiple reaction pathways, in addition to the desired one may be operative for a given transformation.[12,13] As a result, numerous challenges have had to be overcome in developing effective asymmetric α-alkylation methods.

In the case of symmetrical ketone derivatives, a general and widely applicable asymmetric method has to control geometry about the double bond of the enolate, as well as the facial approach of the electrophile to the enolate. In some non-symmetrical ketones the situation is even more complex as the regioselectivity of the deprotonation must also be controlled.[8]

In light of these challenges, early attempts suffered from low enantioselectivity and were limited in terms of the nature of the alkylating agent. However the field has undergone significant development and highly selective asymmetric methods are now available.

1.3 Chiral Auxiliaries

The use of chiral auxiliaries in chemical reactions, in many regards, parallels that of a protecting group. The moiety must be attached to the substrate molecule, it must be stable to the reaction conditions, and it must be removed at the end of the reaction. However, unlike a protecting group that is a passive partner in the reaction, a chiral auxiliary acts as a vehicle for asymmetric induction. This induction can also be accomplished by interactive means, such as by sterically blocking reaction at one face of the substrate. Unlike chiral catalysts, auxiliaries are used stoichiometrically since they add to the substrate molecule via a covalent bond to facilitate asymmetric induction in the subsequent reaction.[14] An arsenal of chiral auxiliaries have been developed over the years for α-alkylation with varying degrees of success.[15-19]

Yamada et al. published the first asymmetric synthesis of α-alkyl-cyclohexanone via enamine chemistry based on an (*S*)-proline-derived auxiliary in 1969.[16] The enantiomeric excesses for the reaction of enamine **5** with Michael acceptors to afford the 1,4-adducts **6** were moderate (Scheme 1.3.1).

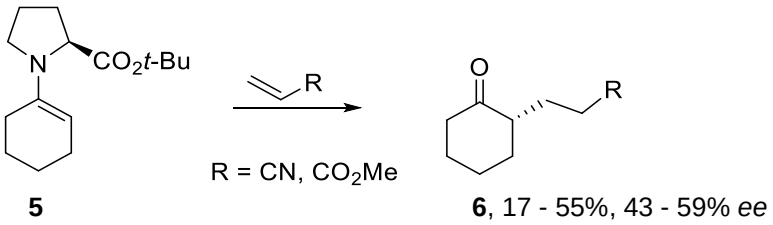

5 **6**, 17 - 55%, 43 - 59% *ee*

Scheme 1.3.1

Meyers reported in 1976 that the alkylation of metallated azaenolates with an acyclic amino acid-based auxiliary **7** gave good yields and very good enantioselectivity of the corresponding ketones **8** (82 - 95% *ee*) (Scheme 1.3.2).[18]

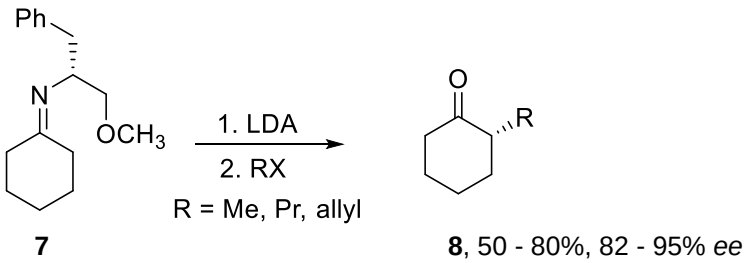

7 **8**, 50 - 80%, 82 - 95% *ee*

Scheme 1.3.2

These pioneering studies laid the ground work for the introduction of the now widely used auxiliaries, (*S*)-1-amino-2-methoxymethylpyrrolidine (SAMP) **(*S*)-9** and its enantiomer (*R*)-1-amino-2-methoxymethylpyrrolidine (RAMP) **(*R*)-9** by Enders in 1976.[10,20,21]

SAMP **(*S*)-9** RAMP **(*R*)-9**

Figure 1.3.1

SAMP **(*S*)-9** can be obtained on a 1 mol scale in 57% yield in six steps from the cheap commercially available amino acid, (*S*)-proline **10** (Scheme 1.3.3).[22] Reduction of **10** with lithium aluminium hydride followed by treatment of resulting alcohol **(*S*)-11** with methyl formate leads to formamide **12**. Methylation followed by removal of the amine protecting group with potassium hydroxide yields the pyrrolidine **13**. Reaction with potassium cyanate affords amide **14** followed by *N*-amination via Hofmann degradation to give SAMP **(*S*)-9**.

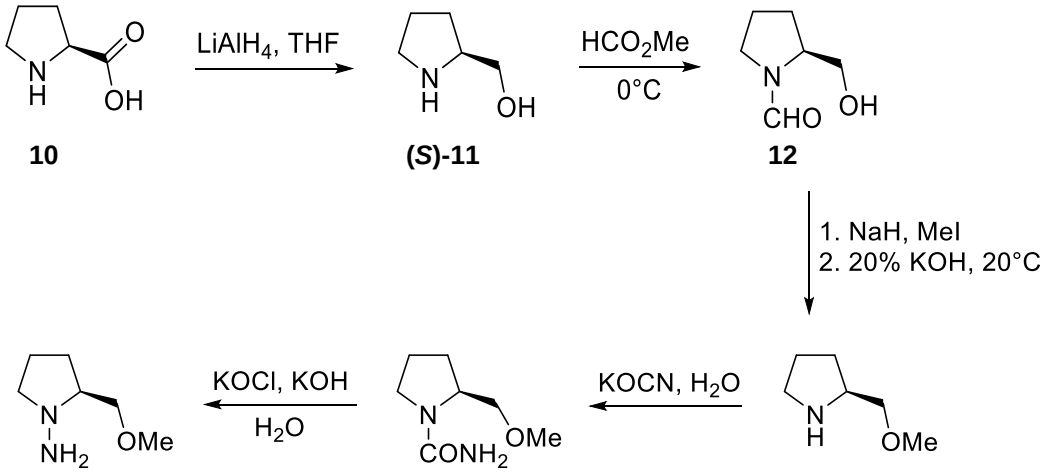

Scheme 1.3.3

An alternative four-step procedure is available (Scheme1.3.4), however it is less desirable as it proceeds through the highly toxic nitrosamine intermediate **15**.

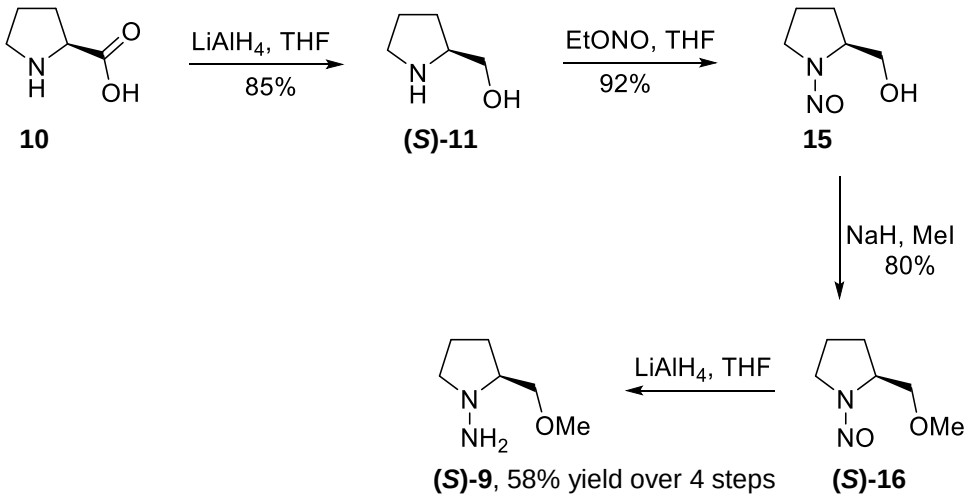

Scheme 1.3.4

Due to the difficulty in obtaining (*R*)-proline, its enantiomer, RAMP **(*R*)-9** is best formed from (*R*)-glutamic acid in six steps with 35% overall yield (Scheme 1.3.5).[23] The relatively inexpensive (*R*)-glutamic acid **(*R*)-17** is transformed into (*R*)-pyroglutamic acid **18** by refluxing in water and then purification over an ion-exchange column. Although it was possible to reduce **18** to **(*R*)-11** in 57% yield, this was lowered to *ca.* 15% in large scale preparations. If however **18** was first transformed with diazomethane into the methyl ester, the $LiAlH_4$ reduction of the lactam and ester moiety in one step works well in 76% yield. Following the procedure used for SAMP **(*S*)-9**, nitrosation followed by treatment with sodium hydride/methyl iodide in THF gives nitrosamine **(*R*)-16**. Reduction with $LiAlH_4$ affords RAMP **(*R*)-9** in a 35% yield over six steps.

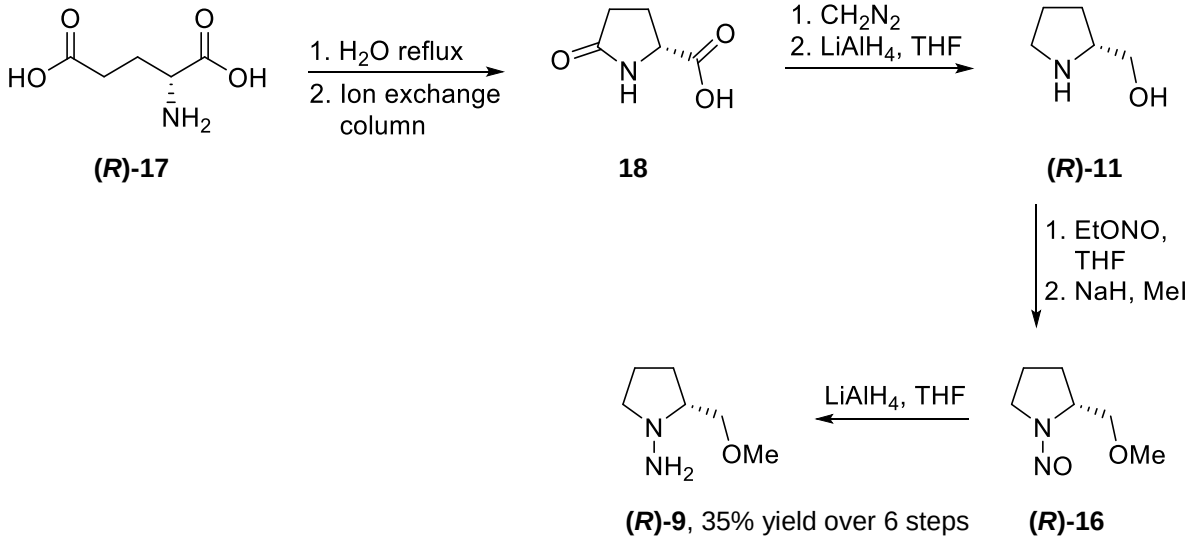

Scheme 1.3.5

If more steric demand is required the auxiliaries SADP **19**, SAEP **20** and SAPP **21** can be prepared in a seven step sequence,[24] while the even-more sterically demanding RAMBO **22** can be prepared from the corresponding amino acid derivative in the usual methods (Figure 1.3.2).[25,26]

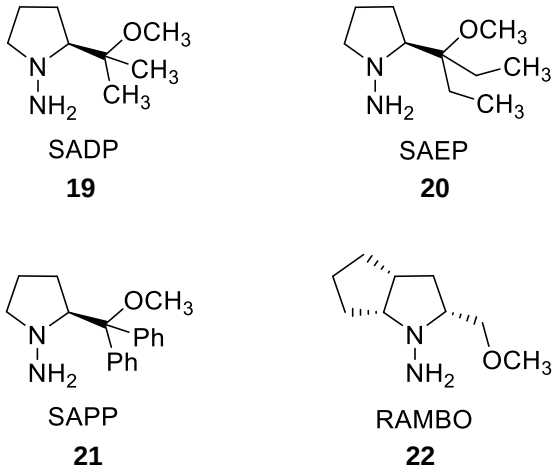

Figure 1.3.2

The chiral hydrazones are easily obtained by mixing SAMP **(*S*)-9** or its analogues and the carbonyl compound.[27] The condensation reaction with aldehydes runs quickly at 0°C without solvent, while ketones require reflux with a catalytic amount of acid and a solvent such as cyclohexane or benzene. Often purification of the hydrazones is unnecessary and they can be stored at -20°C under an inert atmosphere without decomposition (Scheme 1.3.6).

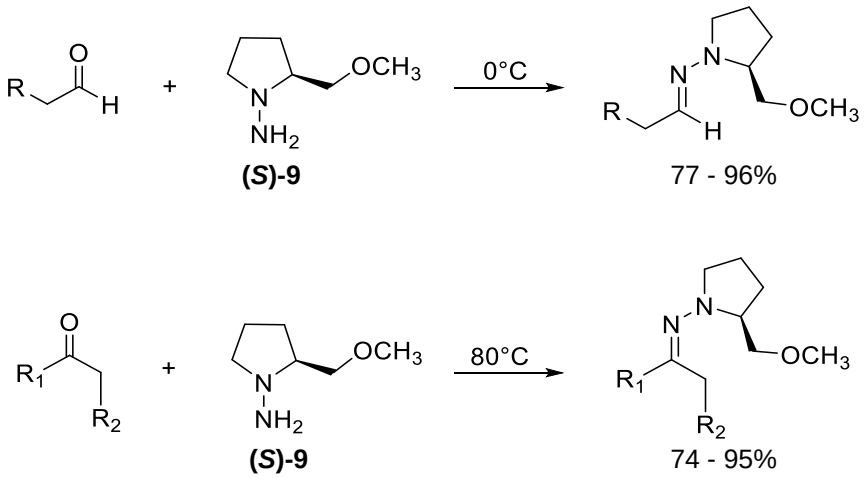

Scheme 1.3.6

SAMP-hydrazones can be deprotonated with lithium diisopropylamide or other lithium bases and the resulting azaenolates can be trapped by electrophiles to obtain diastereomerically

enriched compounds. A single reaction pathway makes it possible to predict the orientation of the resulting diastereomer. By use of either SAMP **(*S*)-9** or RAMP **(*R*)-9** as the chiral inductor, the synthesis of the desired enantiomer can therefore be controlled.

A compelling feature of the Enders' asymmetric α-alkylation methodology is the diversity of the alkylation agents that can be employed while maintaining high yields and stereoselectivities. In the case of ketones complex alkyl halides, Michael acceptors, carbonyl compounds, halide-substituted esters, epoxides, disulfides, oxiranes, aziridines and cyclopropene acetals can be employed. After workup, distillation or column chromatography can be used to purify the crude α-substituted hydrazones. Subsequent cleavage of the hydrazones (**23**), for example, using ozone or MeI and HCl/pentane, restores the original carbonyl function to provide substituted ketones or aldehydes (**24**) (Scheme 1.3.7).[28]

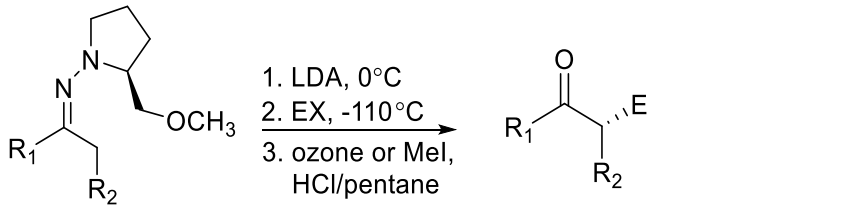

23 **24**, 51 - 99%, 31 - 99% ee

Scheme 1.3.7

SAMP-hydrazones have also been successfully used in a wide range of other synthetic transformations including aldol reactions, Michael additions, [2,3]-Wittig rearrangements, Carroll rearrangements, nucleophilic additions to C=N, Diels-Alder reactions and organometallic-mediated chemistry.[10]

Investigations into the azaenolate geometry formed when SAMP-hydrazones are deprotonated with LDA under standard conditions in diethyl ether, showed that only the $E_{CC}Z_{CN}$-species is formed. This has been confirmed by trapping experiments,[20,28] spectroscopic investigations[29] and X-ray analysis.[30] In the transition state shown in Figure 1.3.3, the lithium atom of the enehydrazide is located about 20° below the plane and is intramolecularly chelated by the oxygen of the methoxy group. Electrophilic attack is sterically disfavoured from 'above' due to the rigid 5-membered ring. This diastereofacial differentiation results in diastereomerically enriched hydrazones. The configuration of the new stereogenic centre is predictable. The SAMP-/RAMP-hydrazone method was therefore also used as a reliable standard procedure for the determination of the absolute configuration of chiral compounds.[31]

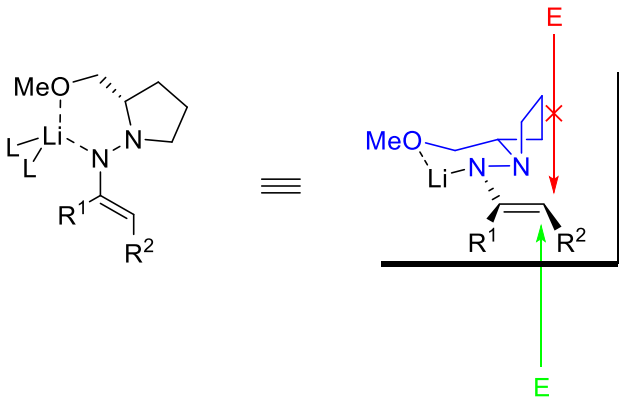

Figure 1.3.3

Monosubstituted hydrazones **25**, obtained by α-alkylation of **26**, can undergo a second regioselective α-alkylation reaction, giving rise to pseudo-C_2-symmetric hydrazones **27** with complete diastereoselectivity.[32] A single diastereomer of the C_2-symmetric ketones **28** was provided by subsequent treatment with ozone (Scheme 1.3.8).

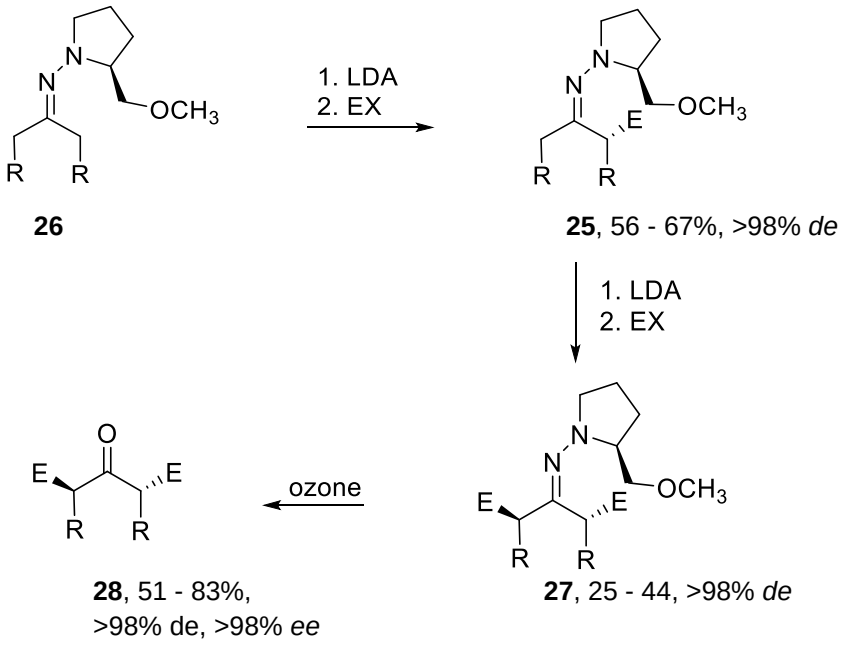

26

25, 56 - 67%, >98% *de*

28, 51 - 83%, >98% de, >98% *ee*

27, 25 - 44, >98% *de*

Scheme 1.3.8

Extension of the use of SAMP/RAMP auxiliaries to natural product synthesis includes a number of elegant transformations. For example, Nicolaou et al. applied the SAMP/RAMP aldehyde alkylation in the asymmetric total synthesis of epothilone A **29** (Scheme 1.3.9).[33,34] Like Taxol, these compounds exhibit potent microtubule destabilizing activity. Propanal-derived hydrazone **30** is treated with LDA, and the resulting azaenolate undergoes alkylation with **31** to provide **32**, a synthetic precursor to epothilone A **29**.

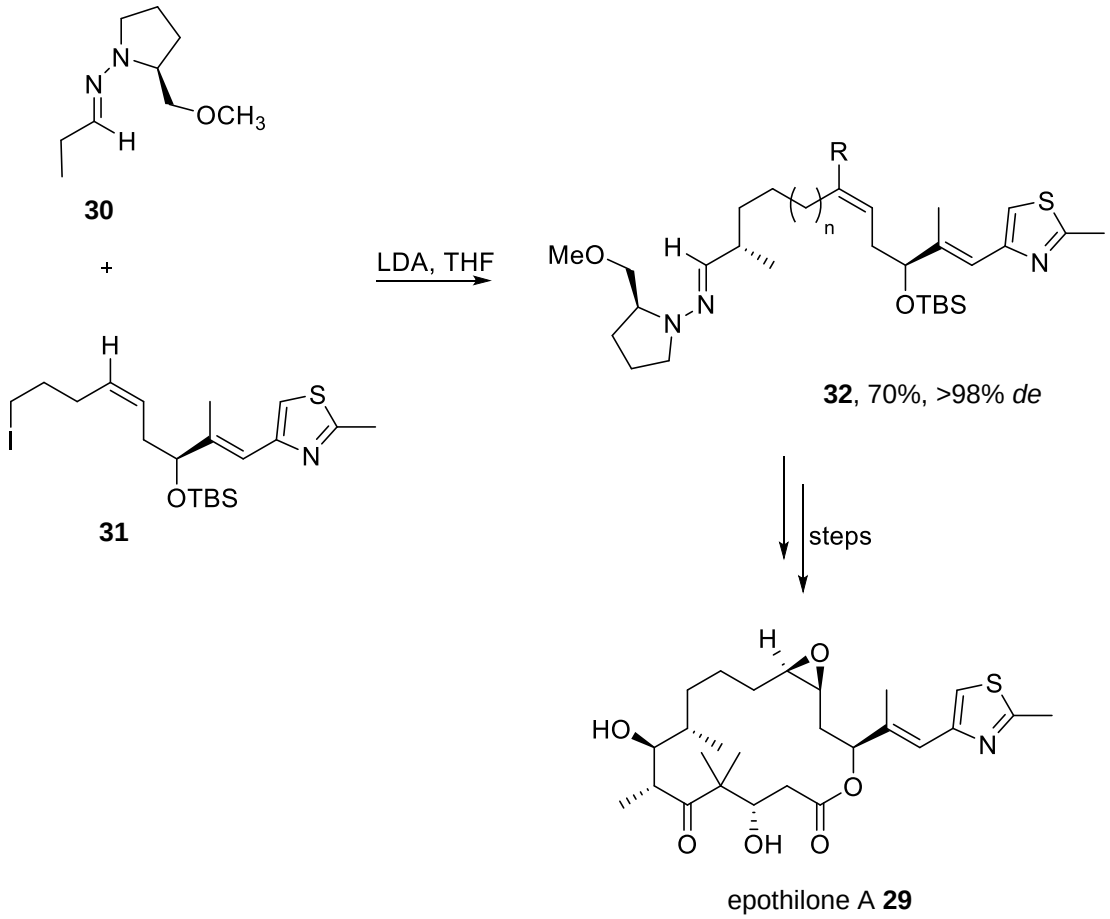

Scheme 1.3.9

In 2008, Coltart and co-workers introduced the *N*-amino cyclic carbamate (ACC) chiral auxiliaries **33** and **34** (Figure 1.3.4).[35] The advantage of these auxiliaries over the SAMP/RAMP chiral auxiliaries is twofold: Firstly deprotonation of the hydrazone is rapid, and alkylation does not require the extremely low temperatures required by SAMP **(*S*)-9**, yet it proceeds with consistently high yields and excellent stereoselectivity. Secondly, regioselective α,α-bisalkylation is possible.

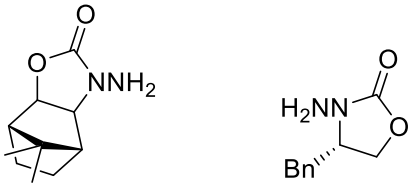

Figure 1.3.4

Of the ACCs investigated, the camphor-derived auxiliary **33** proved to be the most versatile and successful. A key design feature of these auxiliaries was the placement of a carbonyl group

adjacent to the hydrazone moiety for enhanced α-proton acidity and tight chelation at the level of the azaenolate.[36]

The selectivity in the alkylation of the ACC azaenolate follows a mechanism where the formation of the azaenolate from the hydrazone **35** is controlled by the orientation of the carbonyl group. The ACC hydrazone prefers to exist in the conformation depicted in Scheme 1.3.10, where steric interactions between the methyl group and the bulky bicyclo group on the auxiliary are minimized. Coordination of LDA to the carbonyl group in a five-membered chelate, leads to a '*syn*-directed' deprotonation and formation of the $E_{CC}Z_{CN}$ azaenolate. The bottom face of the azaenolate is sterically blocked, and alkylation takes place selectively from the top (β) face.[37]

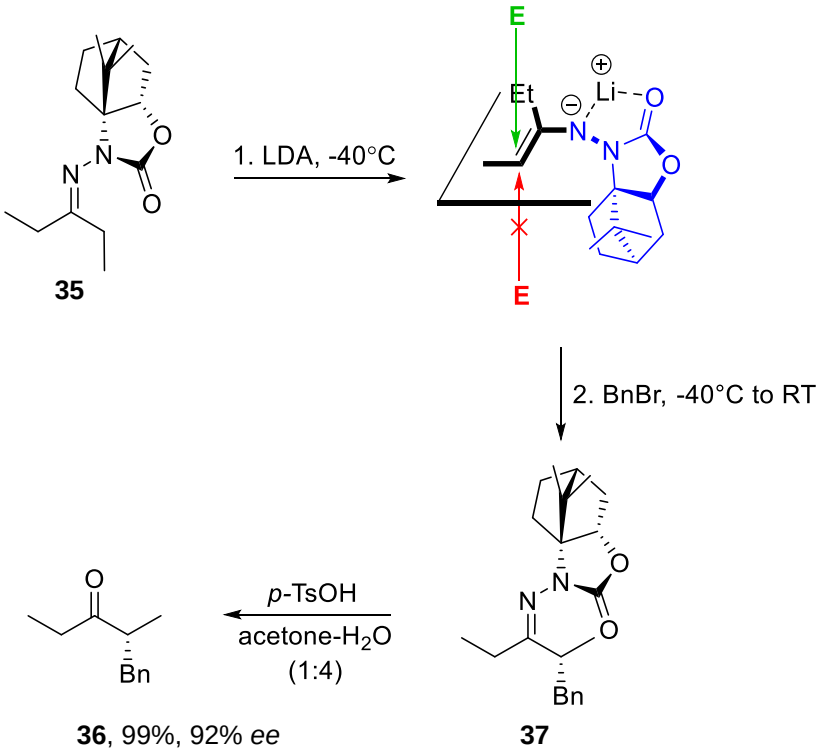

Scheme 1.3.10

With *p*-toluenesulfonic acid, hydrazone **37** can be transformed to the corresponding ketone **36** in almost quantitative yields.

The ACC methodology has also been utilized in the synthesis of several biologically important compounds,[38] for example in the first asymmetric total synthesis of the antiviral agent (+)-clusianone **38**. ACC alkylation of **39** affords **40** in excellent enantiomeric ratios, which is converted to the target product **38** (Scheme 1.3.11).

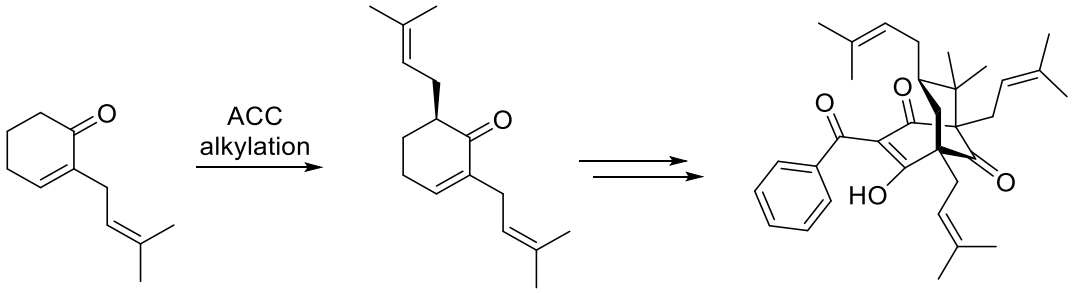

39 **40**, 99 : 1 *er* (+)-clusianone **38**

Scheme 1.3.11

Regiocontrol in LDA-mediated deprotonation of ketones, dialkylhydrazones (e.g. SAMP/RAMP) and imines is usually derived from the removal of the most sterically accessible proton (kinetic deprotonation). As a result, the controlled asymmetric α,α-bisalkylation of ketones having indistinguishable α-, α'-protons is not possible. However with ACC hydrazones this has been accomplished. In the case of acetone derived hydrazone **41** (Scheme 1.3.12), treatment with LDA, followed by the addition of the alkylating agent resulted in **42** with regioselective monoalkylation with >99 : 1 α- : -α' ratio. A second alkylation proceeded with both regio- and stereochemical control, to afford the α,α-bisalkylated product **43** and cleavage of the auxiliary affords **44** in excellent yield and a >99 : 1 *dr*. Conveniently, in some cases, both diastereomers of the bisalkylated hydrazone can be obtained in an equally high *dr* using the same auxiliary, simply by altering the order of addition of the alkylating agents.

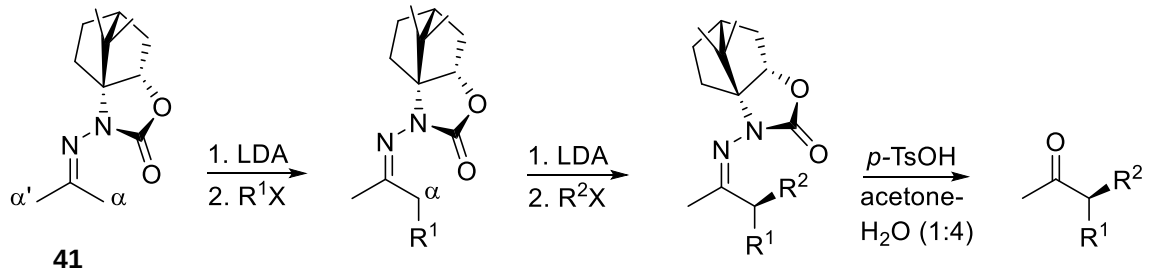

41 **42** **43** **44**, 95-98%, >99 : 1 *er*

Scheme 1.3.12

The reliability, broad substrate tolerance and high levels of efficiency and selectivity, contribute to the popularity of the chiral auxiliary strategy. Unfortunately, the multiple steps for the preparation, incorporation and removal of the auxiliary in the synthesis render this process inefficient, which is undesirable for large-scale processes. The need for stoichiometric amounts of the chiral auxiliary means catalysis is never possible.

1.4 Homo Chiral Lithium Amide Bases

Given the growing importance of asymmetric synthesis, it is not surprising that the race for simple methods of asymmetric induction is extremely competitive. Optically pure lithium amide bases have proven to be a versatile tool in modern asymmetric synthesis. Homo chiral lithium amide bases (HCLAs) are a class of compounds usually formed in situ when, for example, *n*-BuLi is added to the corresponding chiral amine. HCLAs have to date enjoyed success in mainly three areas: Enantioselective rearrangement of epoxides to allylic alcohols, enantioselective deprotonation of prochiral ketones and aromatic and benzyl functionalization of tricarbonyl (η^6-arene) chromium complexes.[39]

It was Koga[40] and Simpkins[41] who independently recognised that a carefully chosen HCLA should be able to distinguish between the conformationally locked, axial α-protons in the cyclohexanone ring. In the first report by Koga, a large number of HCLAs were generated and used in the asymmetric deprotonation of substituted cyclohexanones **45**. The products were isolated as their corresponding trimethylsilyl enol ethers **46** (Scheme 1.4.1).

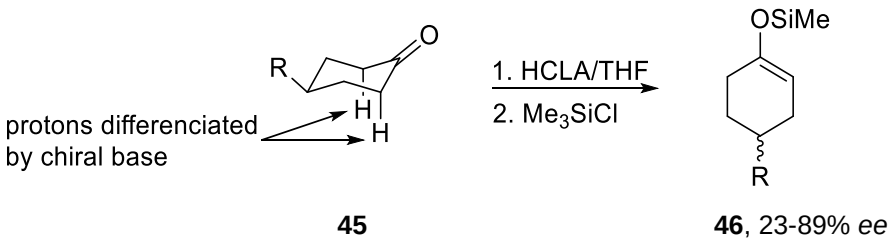

45 **46**, 23-89% *ee*

Scheme 1.4.1

Initial experiments by Simpkins in this area involved deprotonation of cis-2,6-dimethylcyclohexanone **47** using lithium amide **48** and trapping of the resulting enolate with allyl bromide. Enantiomeric excesses for the corresponding products **49**, were moderate but promising (Scheme 1.4.2).[41,42]

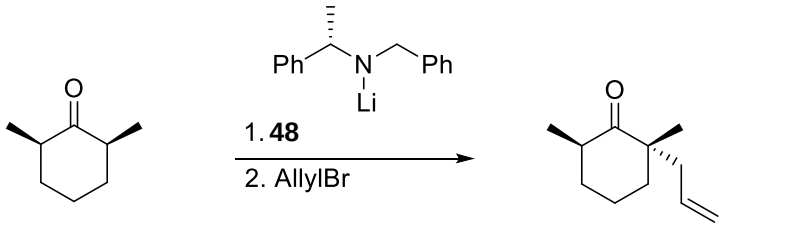

47 **49**, 65%, 25% *ee*

Scheme 1.4.2

The opposite enantiomer **48** and two other HCLA bases **50** and **51** (Figure 1.4.1) were used in the deprotonation of dimethylated cyclohexanone.[41]

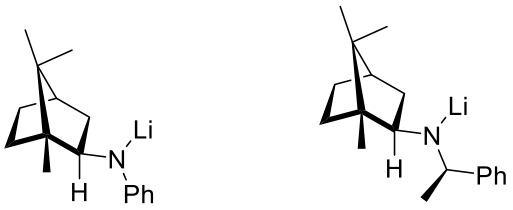

50 **51**

Figure 1.4.1

Using HCLA **50** and quenching with acetic anhydride, resulted in the best selectivity and formation of **52** with an *ee* of 74% (Scheme 1.4.3 and Table 1.4.1).[41]

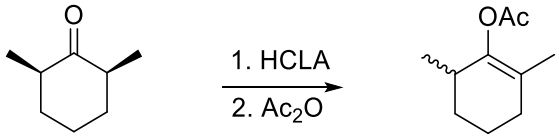

47 **52**

Scheme 1.4.3

HCLA	% *ee*	Configuration of 52
48	29	*R*
50	74	*R*
51	65	*S*

Table 1.4.1

Having achieved good enantioselectivity with HCLA **50**, quenching with different electrophiles such as chlorotrimethyl silane opened up new synthetic pathways such as the synthesis of α-hydroxy ketones **53** via the epoxide intermediate generated by the addition of mCPBA to the silyl enol ether **54** (Scheme 1.4.4).[43]

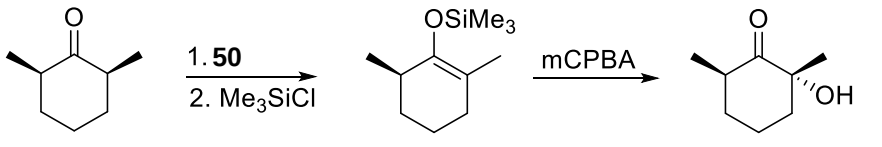

47 **54** **53,** 70% *ee*

Scheme 1.4.4

New bases and reaction methods were quickly being employed in the race to increase enantioselectivity. When the internal quenching technique devised by Corey[44] was used with the new HCLA **55** the enantiomeric excesses improved to an excellent 96% (Scheme 1.4.5).[45] The internal quenching protocol involved having the trimethylsilyl chloride present during the deprotonation. Thus, as soon as the enolate is selectively formed it is trapped as the silyl enol ether to afford **54**.

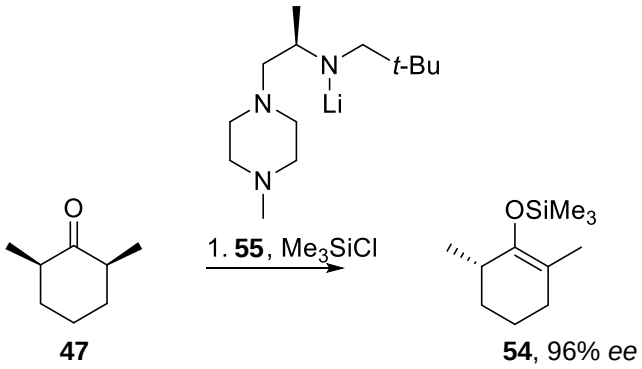

47 **54**, 96% *ee*

Scheme 1.4.5

The improvement in this reaction was explained by the fact that HCLA **55** contains an internal ligation site in the form of a nitrogen atom in the piperazine ring.

When Koga published the full details of his work on 4-substituted cyclohexanone the enantiomeric excesses were, in general very good.[46] For example, in the reaction of 4-*tert*-butyl-cyclohexanone **56** with the corresponding silyl enol ether using HCLA **57,** product **58** was isolated in 87% yield with an *ee* of 77% (Scheme 1.4.6). The reactions were carried out at -78°C using Corey's internal quenching method.[44]

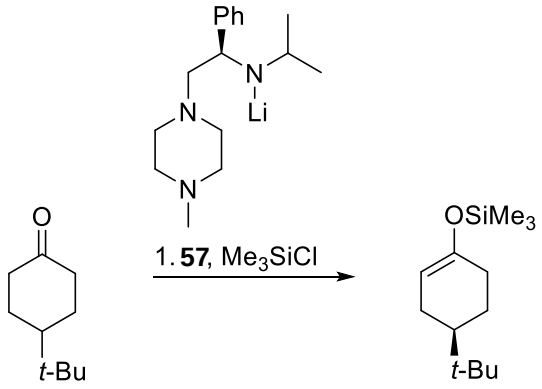

56 **58**, 77% *ee*

Scheme 1.4.6

When the reaction (Scheme 1.4.6) was carried out at -105°C the enantiomeric excess was increased to 89%. Simpkins noted a similar temperature dependence when using the HCLA **59** in the same reaction (Scheme 1.4.7).[42] The enantiomeric excess was raised from 69 to 88% upon lowering the reaction temperature from -78 to -90°C.

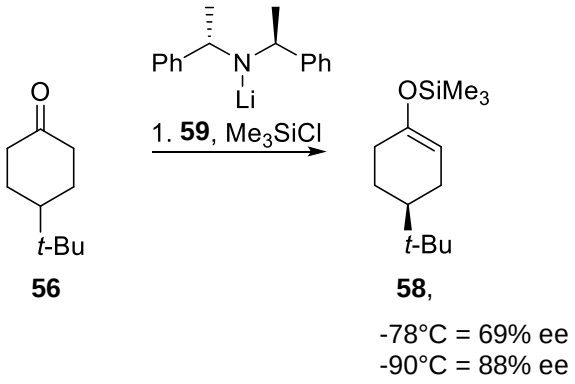

Scheme 1.4.7

Both Simpkins and Koga have shown that in order to obtain high levels of enantioselectivity in chiral base-mediated ketone deprotonations, it is necessary to trap the lithium enolates as silyl enol ethers using the Corey internal quench protocol. In the above reaction (Scheme 1.4.7) at -78°C using external quenching conditions the enantiomeric excess was lowered considerably to 23% (*cf*. 69% for internal quench). Similar results were obtained in the conversion of bi-cyclic ketone **60** to silyl enol ether **61** where the *ee* was reduced from 82 to 33% when the internal quenching technique was replaced by external quenching (Scheme 1.4.8).[47]

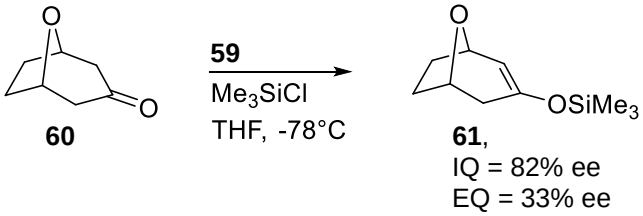

Scheme 1.4.8

When lithium chloride was employed in this reaction (Scheme 1.4.8) under external quenching conditions the enantioselectivity was raised from 33 to 84% (Table 1.4.2).

LiCl equiv.	% *ee*
0	33
0.1	84
0.7	83
1.5	84

Table 1.4.2

It is therefore shown that similar enantiomeric excesses can be obtained with internal quenching without LiCl, and external quenching with LiCl. It was postulated that lithium chloride is generated in the case of internal quenching by reaction of the chiral base with trimethylsilyl chloride directly or by silylation of the lithium enolate during the course of the reaction.[48]

When base **59** was used in the aldol reaction of tropinone **62** and benzaldehyde to give **63** (Scheme 1.4.9) by Majewski, enantioselectivities increased steadily as up to 1 equiv. of lithium chloride was added (Table 1.4.3).[49,50]

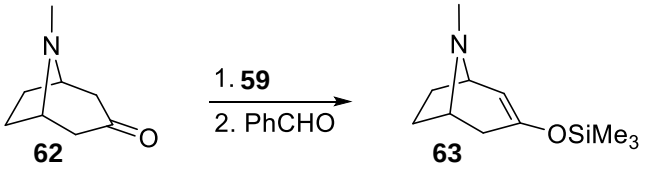

62 **63**

Scheme 1.4.9

LiCl equiv.	% *ee*
0	35
0.25	78
0.5	85
1.0	88
1.0[a]	95

[a]Lithium chloride generated by premixing *n*-butyllithium and the hydrochloride of the chiral amine prior to addition of the ketone.

Table 1.4.3

With a view to understanding these interesting results Koga carried out two sets of experiments. Firstly, he revisited the reaction of the 4-substituted cyclohexanone using chiral base **59** (Scheme 1.4.10) and various equivalents of LiCl, under external quenching conditions (Table 1.4.4).[47,51]

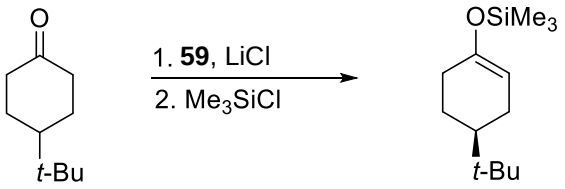

56 **58**

Scheme 1.4.10

LiCl equiv.	% *ee*
0	44
0.5	87
1.0	88
3.0	88

Table 1.4.4

He found that even the addition of sub-stoichiometric amounts of LiCl greatly improved the enantioselectivity.

Secondly Koga carried out the same reaction with different lithium halide salts introduced as the appropriate trimethysilyl halide (Me_3SiX) in an internal quench. He found that going down group 8 of the periodic table decreases enantioselectivity (Table 1.4.5).[51]

LiX	% *ee*
Cl	90
Br	65
I	31

Table 1.4.5

Koga has provided an elegant rationalisation of such results.[51] He proposed that in the absence of any lithium chloride (external quenching conditions) the lithium amide base **59** exists as the homo-dimer **64** (Figure 1.4.2).

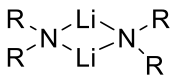

64

Figure 1.4.2

^{6}Li and ^{15}N NMR spectroscopic studies on **59** have revealed that dimer **64** was, in fact, the major component in a solution of the lithium amide base in THF. This claim was verified by crystallographic analysis of crystals of **59** formed from THF and hexane by Simpkins and Mair.[37]

When ^{6}Li and ^{15}N NMR spectroscopic studies were carried out on **59** containing more than 0.5 equiv. LiCl it was found that the major component in a solution of THF was mixed-dimer **65** (Figure 1.4.3).

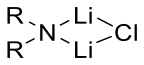

65

Figure 1.4.3

It was therefore concluded that the mixed-dimer **65** is responsible for the high level of enantioenrichment. In the case of lithium bromide and lithium iodide, the equivalent mixed-dimer may not be as thermodynamically stable, consequently its contribution is small.[51]

Koga has also reported the catalytic use of HCLA bases in the asymmetric deprotonation of 4-substituted cyclohexanones **45**. The catalytic cycle that Koga proposed is shown in Scheme 1.4.11. In this system, the chiral base is regenerated by using a stoichiometric amount of achiral lithium amide **66**. He suggested that catalysis would be possible since lithium amides with two coordinating nitrogen groups (as in **66**) are less reactive in ketone deprotonations than those such as **67** derived from diamines.

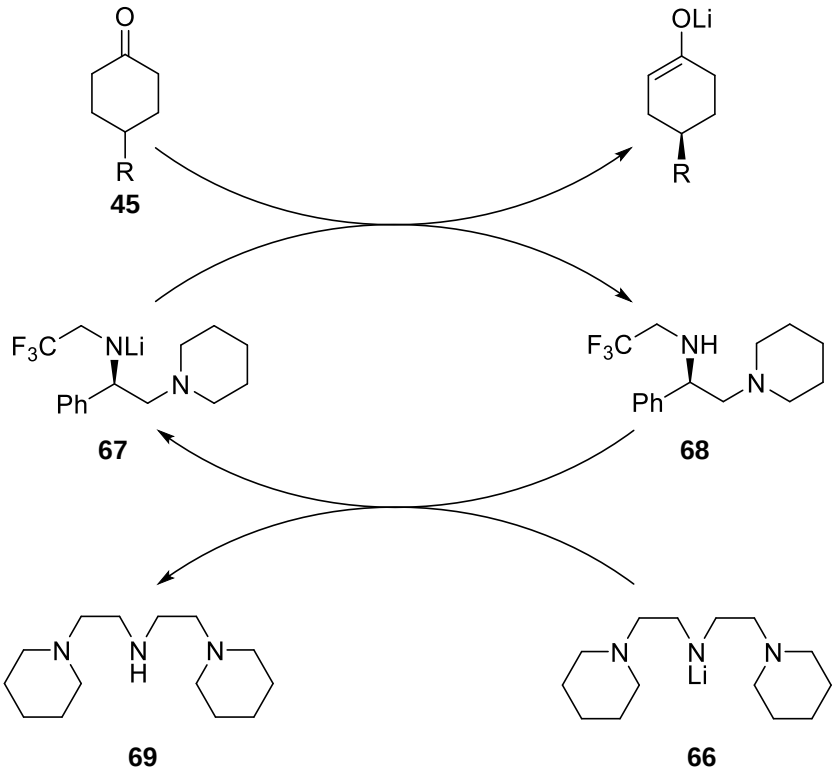

Scheme 1.4.11

The optimum conditions required the use of excess DABCO and HMPA as additives and the enolate was trapped with Me_3SiCl under external quench conditions since *N*-silylation of **68** occurred with an internal quench. These conditions were applied using cyclohexanone **56**, 0.3 equiv. of **68** and 2.4 equiv. of **66** resulting in the formation of silyl enol ether **58** in 79% *ee* and 83% yield (Scheme 1.4.12).[52] The enantioselectivities achieved were slightly lower than that obtained using a stoichiometric amount of chiral base, however this result clearly demonstrates the success of the catalytic cycle.

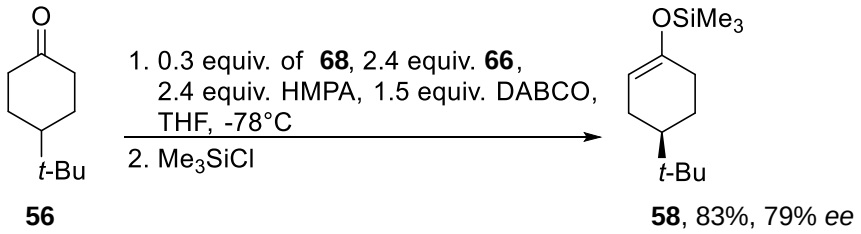

Scheme 1.4.12

Koga has also reported the catalytic use of HCLA bases in the alkylation of silyl enol ether **70**. The lithium enolate is generated in the presence of lithium bromide, and subsequent reaction with benzyl bromide using 0.05 equivalents of HCLA **71** and 2.0 equivalents of diamine **72** gave alkylated product **73** in 96% *ee* (Scheme 1.4.13).[53]

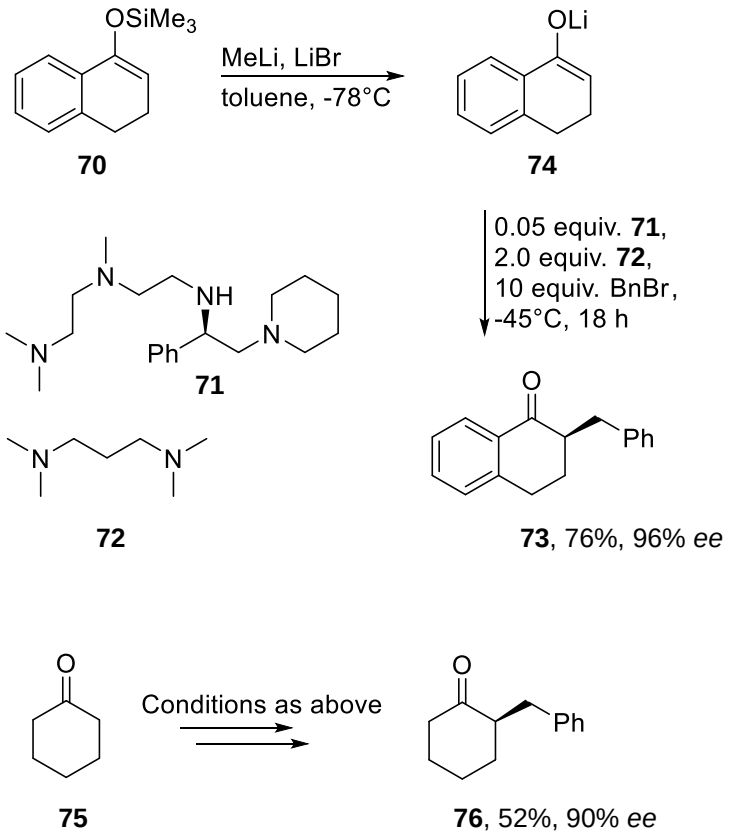

Scheme 1.4.13

Catalysis was possible in this reaction because the lithium enolate **74** is activated to alkylation by complexation of diamine **72.** In the absence of diamine **72**, less than 1% of alkylation product was obtained. Cyclohexanone **75** was also successfully alkylated under these catalytic conditions (Scheme 1.4.13).

Even though HCLA bases have been studied extensively they have only been reported in the asymmetric α-alkylation of cyclic and conformationally locked ketones.

1.5 Other Methods for the α-Alkylation of Ketones

The Tsuji–Trost reaction employs a chiral palladium catalyst to generate an enantiodefined electrophilic palladium π-allyl intermediate. A nucleophile attacks the catalytic intermediate to arrive at carbonyl α-quaternary centres with high levels of enantioselectivity.[54] This work was first pioneered by Tsuji in 1965.[55] Trost and co-workers further developed this process with the introduction of phosphine ligands.[56] An enantioselective variant was introduced in 1977.[57]

In 1999, Trost reported the first enantioselective Pd-catalysed allylic alkylation of tin enolates **77** of 2-methyl-tetralone **78** (Scheme 1.5.1).[58] These were subjected to allylations with a wide range of allylic substrates in the presence of the bidentate ligand (*S*,*S*)-DPPBA **79** to afford **80**.

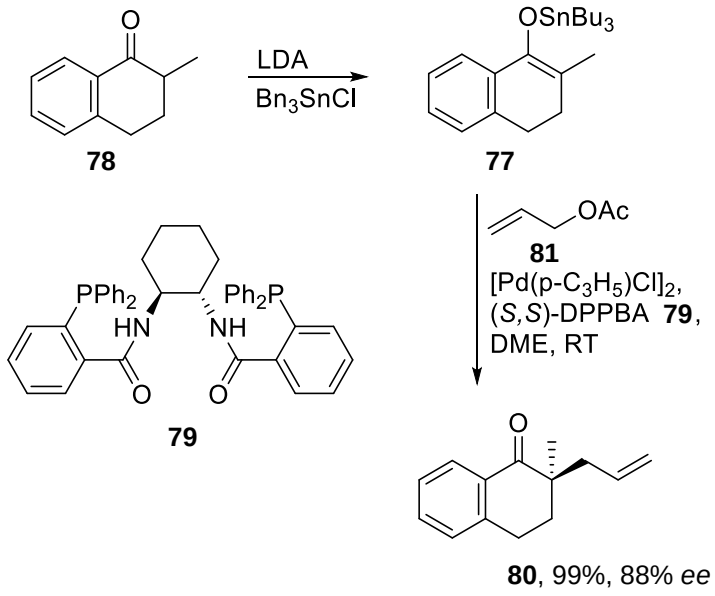

Scheme 1.5.1

The Stoltz group later reported an enantioselective decarboxylative asymmetric allylic alkylation using ligand **82**, where substrates of the form **83** or **84** undergo decarboxylation resulting in the formation of a palladium π-allyl intermediate.[59] The transformation works well for the formation of quaternary allylic stereocenters such as **85** (Scheme 1.5.2).

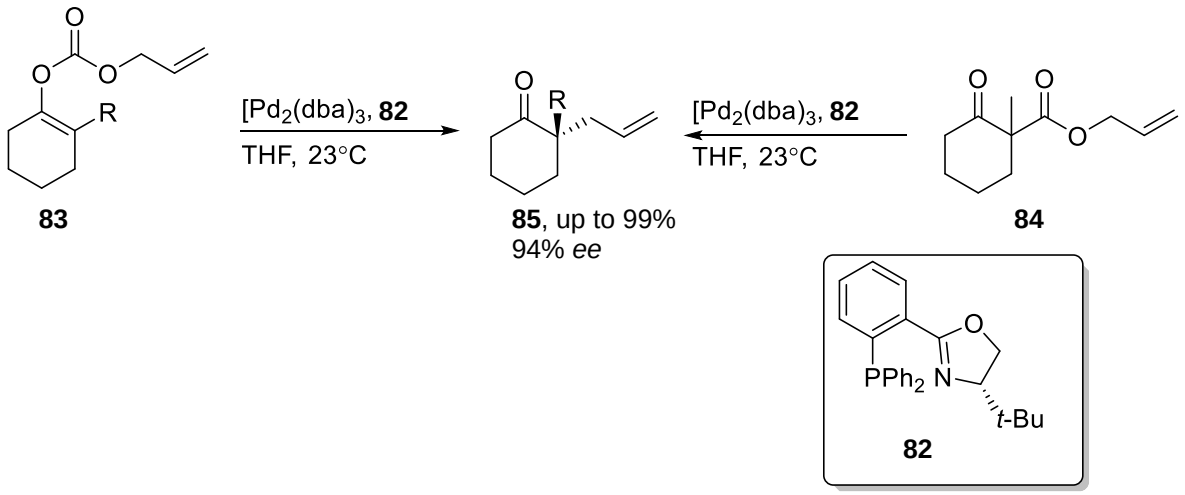

Scheme 1.5.2

A significant limitation of the Stoltz and the earlier mentioned Trost work was its restriction to cyclic ketones. In 2005, Trost and Xu provided the first examples of acyclic ketones in these allylic alkylations, using the allyl enol carbonate **86** and the bidentate ligand **87**, ketones **88** were obtained in good enantioselectivities (Scheme 1.5.3).[60]

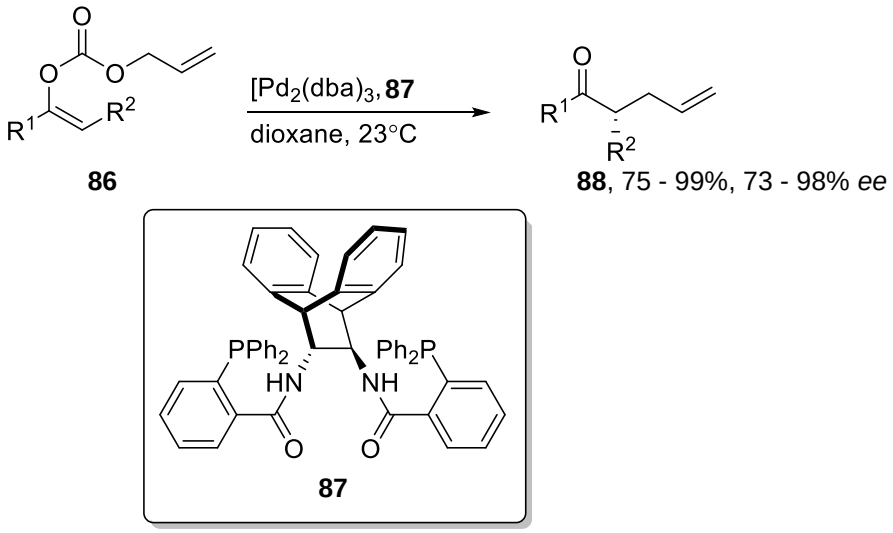

Scheme 1.5.3

Also in 2005, Jacobsen and co-workers introduced a general ketone α-alkylation strategy employing catalytic chromium-salen complexes **89** (Scheme 1.5.4).[61] α-Alkylation to form quaternary centres (**90**) proceeds under mild conditions with very good to excellent selectivities and efficiencies using cyclic tin enolates **91**. A variety of common alkyl halides, including methyl iodide and benzyl bromide, can participate in this reaction.

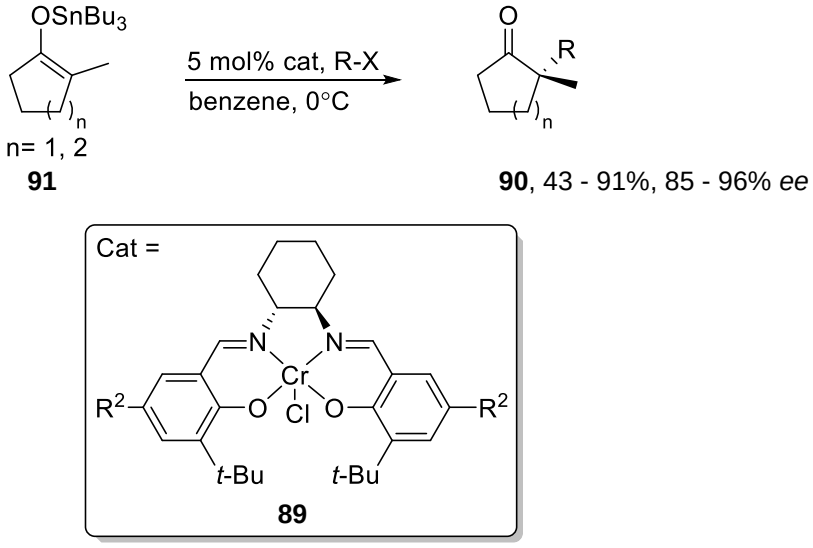

Scheme 1.5.4

A pioneering study by a Merck research group in 1984, triggered the development of asymmetric phase-transfer catalysis, for the preparation of enantioenriched α-alkylated cyclic ketones.[62] Dolling and co-workers utilized the cinchonine-derived quaternary ammonium salt **92** as the catalyst for the methylation of phenylindanone derivatives **93** under liquid–liquid phase-transfer conditions (toluene : 50% aq. NaOH solution) and succeeded in obtaining the alkylated product **94** in excellent yield and high enantiomeric excess (Scheme 1.5.5).

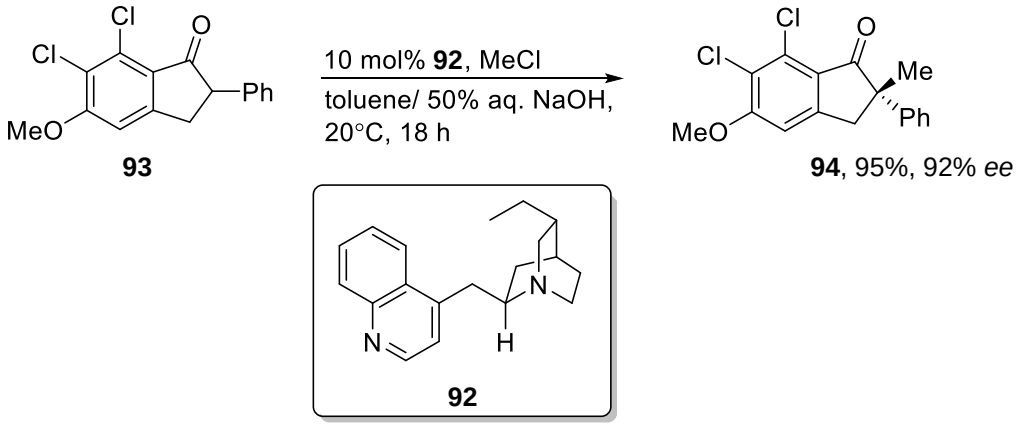

Scheme 1.5.5

In 2010, MacMillan and co-workers introduced the first enantioselective organocatalytic α-allylation of cyclic ketones to give allylated compounds **95**, via singly occupied molecular orbital (SOMO) catalysis (Scheme 1.5.6).[63]

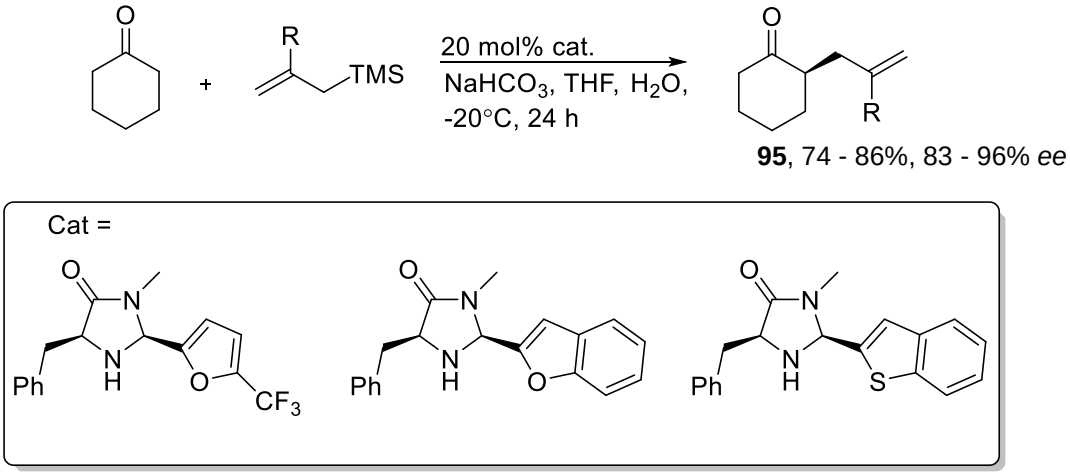
O
R
TMS
20 mol% cat.
NaHCO3, THF, H2O,
-20°C, 24 h
O
R
95, 74 - 86%, 83 - 96% ee
Cat =
O
N
N
H
Ph
O
CF3
O
N
N
H
Ph
O
O
N
N
H
Ph
S

Scheme 1.5.6

1.6 Dialkylhydrazone Methodology and Recovery of Carbonyl Compounds

The usefulness of *N*,*N*-dialkylhydrazones of the form **96** in synthetic organic chemistry arises mostly from the broad reactivity of their organolithium derivatives.[64] The hydrazone moiety has two bonds which are readily cleaved, yet it is usually stable enough to allow problem-free transformations at other parts of the hydrazone molecule. The C=N bond is susceptible to hydrolytic, oxidative, and reductive cleavage, to restore the carbonyl group, and the N–N bond is predisposed to reductive cleavage to produce primary amines (Figure 1.6.1).

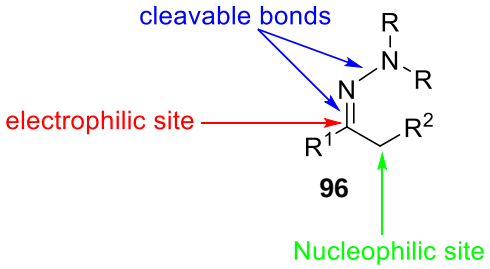

Figure 1.6.1

The protons at the α-carbon of the hydrazone are deemed to be less acidic, compared to the α-carbon of the parent carbonyl, by 10 orders of magnitude.[64] Hydrazone conjugate bases are generally more reactive towards electrophiles. This is an advantage over synthetically equivalent ketone compounds. The acidity of the α-proton and the stability of metallated hydrazones (due to coordination of the metal to the nitrogen atoms) usually allows α-metallation of the hydrazones with alkali metal amides such as lithium diisopropylamide (LDA) or even alkyl lithium bases such as *n*-BuLi and *sec*-BuLi.[65,66] Furthermore, the acidity of the hydrazone α-proton is usually low enough to prevent racemisation of stereogenic centres at the α-carbon of chiral hydrazones by typical bases, which is in contrast to the higher racemisation rate in equivalent ketones.

Typically, the regioselectivity for the deprotonation of hydrazones is high and predictable.[67,68] It is known to take place at the less substituted carbon atom unless there is an anion-stabilising group present at the competing site.[67,68] As a result, subsequent electrophilic attack at the formed azaenolates gives regioselectively functionalised or branched hydrazones. Alkylation of hydrazones occurs selectively at the α-carbon, unlike ketones where *O*-alkylation often competes with C-alkylation. Dialkylhydrazones offer other advantages such as selective

monoalkylation (no problem with polyalkylation), and dialkylhydrazones do not undergo self-condensation (often a problem with the parent carbonyl compounds).[12,13,64] There is also the possibility of using the hydrazone moiety as a chiral auxiliary (such as in the SAMP/RAMP methodology discussed previously in Section 1.3).

Simple lithio-*N*,*N*-dimethylhydrazones have been shown to form aggregates in solution. For example, tetramers have been reported for lithiated cyclohexanone dimethylhydrazone.[69] In general, complex homonuclear and heteronuclear (with a lithium amide such as LDA) aggregation and metal coordination may be expected for metalo-*N*,*N*-dimethylhydrazones and related simple hydrazones.[70] On the basis of the investigation of configurations of lithiated SAMP-hydrazone species in solution (NMR of dimethyl- and SAMP-hydrazone)[29,71] and by crystallography,[30] it was confirmed that they form four possible rotational isomers.[67,71] The most stable configuration is $E_{CC}Z_{CN}$ (Figure 1.6.2).

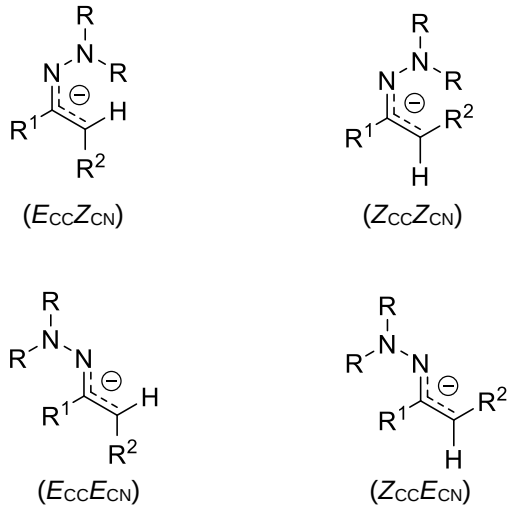

Figure 1.6.2

N,*N*-dialkylhydrazones **96** can be easily formed from simple aldehydes and ketones **97** by condensation with dialkyl hydrazines, mixed neat or in benzene, dichloromethane, or hexane solutions. Hindered, or less reactive aldehydes and especially ketones may require acidic catalysts (AcOH, TFA, *p*-TsOH) and heating with concomitant removal of water (azeotropic or by molecular sieves or other water scavengers) to achieve high conversions or reasonable reaction times (Scheme 1.6.1).[10,72]

N,*N*-dialkylhydrazones **96** can be cleaved to the parent carbonyl compound **97** by a multitude of methods.[9] Recovery of carbonyl compounds **97** from *N*,*N*-dimethyl- and SAMP/RAMP-

hydrazones have been thoroughly reviewed and include oxidative, hydrolytic and reductive protocols (Scheme 1.6.1).

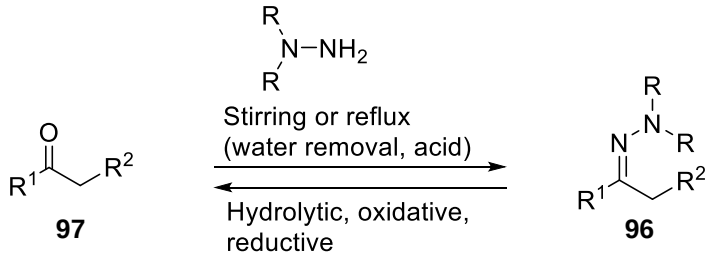

Scheme 1.6.1

N,*N*-dialkylhydrazones did not gain widespread application in synthesis until the pioneering work on alkylation of metalated *N*,*N*-dimethylhydrazones was published by Corey and Enders in the years 1976-1978.[65,66,73-77]

Lithium and potassium azaenolates are the most commonly used metalated hydrazones.[72,78] These are prepared by deprotonation of hydrazones with LDA (sometimes with additives such as HMPA, LiBr, and TMEDA), *n*-BuLi (sometimes with additives such as HMPA, TMEDA, and DMPU), *t*-BuLi, LTMP, *t*-BuOK, NDA,[21] KDA (potassium diisopropylamide made from diisopropylamine, *t*-BuOK, and *n*-BuLi),[79] and the Lochmann-Schlosser superbase, i.e., *t*-BuOK/*n*-BuLi.[80]

Once formed, azaenolates can react with a number of electrophiles. The known synthetically useful C-C bond forming reactions of simple α-metalated hydrazones include Michael-type additions, aldol-type reactions, Claisen-type acylations and α-alkylation protocols (Scheme 1.6.2).[72]

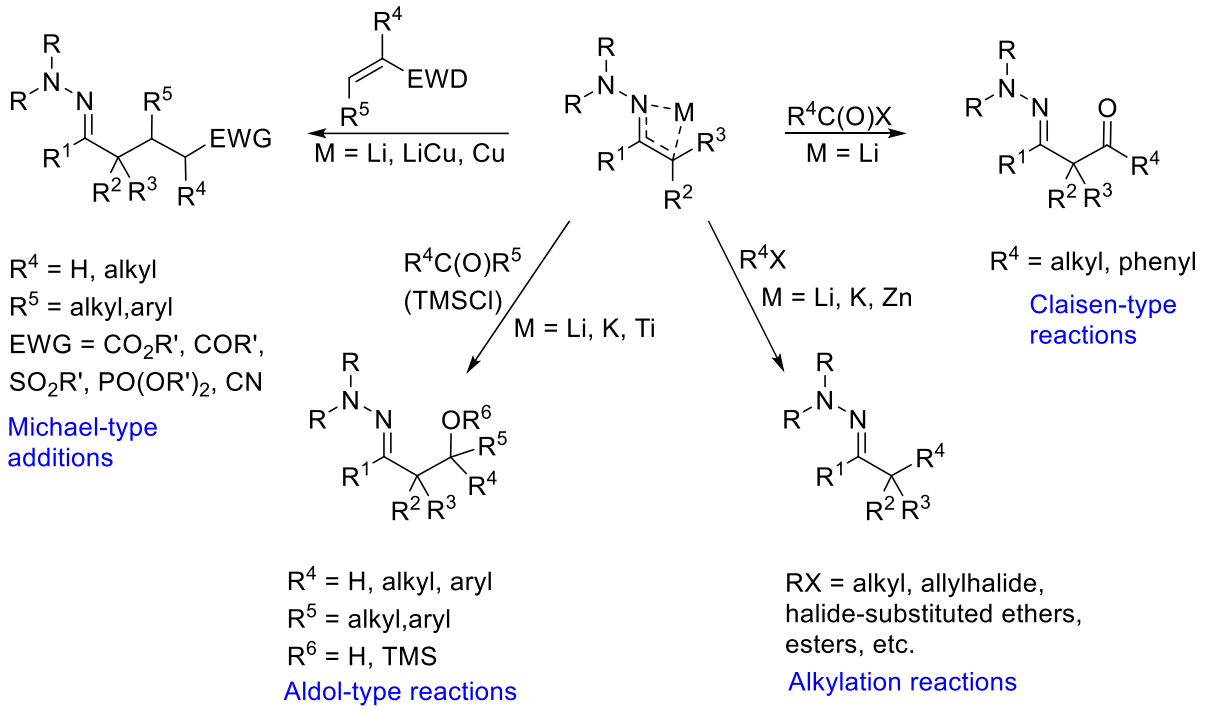

Scheme 1.6.2

Electrophilic alkylations were among the first synthetically useful transformations of hydrazones and still remain the most frequently used reactions of hydrazones.

1.7 Chiral Ligands

A chiral ligand is an enantiopure organic compound which combines with a metal centre via chelation to form an asymmetric reagent. When this catalyst engages in a chemical reaction, it can transfer its chirality to the reaction product. In an ideal reaction, only a substoichiometric amount of the catalyst would be necessary, enabling the synthesis of a large amount of a chiral compound from achiral precursors with the use of a very small (often expensive) amount of chiral ligand.

The first successful, chiral ligand, the diphosphine DiPAMP **98** was developed in 1968 by Knowles.[81] This ligand was utilised in the industrial production of *L*-DOPA **99** (Scheme 1.7.1).[82]

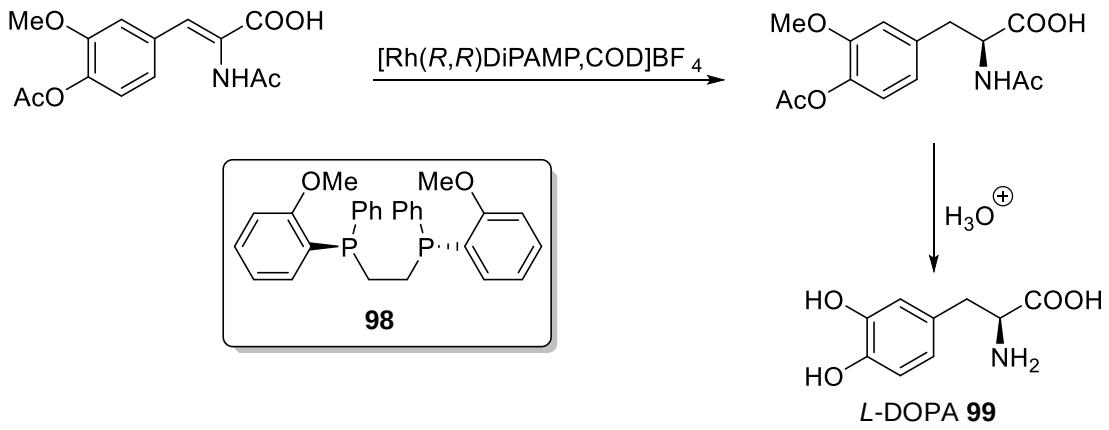

Scheme 1.7.1

Of the hundreds of chiral ligands prepared so far, a relatively small number of structural classes stand out because of their broad applicability. These 'privileged ligands' (Figure 1.7.1), as they are called, allow high levels of enantiocontrol in many different metal-catalysed reactions. A survey of their structures reveals that a surprisingly large number of them possess C_2-symmetry.[83]

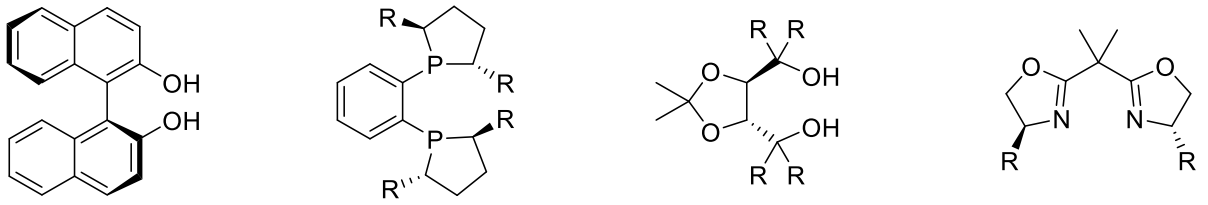

Figure 1.7.1

C_2-symmetry can have a beneficial effect on enantioselectivity as it reduces the number of competing diastereomeric reaction pathways, enables a straightforward analysis of substrate catalyst interaction and the simplification of mechanistic and structural studies.[84] The key design features of successful C_2-symmetric ligands are:

1. They are easy to modify.
2. They have a rigid chiral pocket.
3. The stereogenic centres are positioned in close proximity to the coordination site.
4. They bind to metals strongly.

Although the concept of C_2-symmetry has been well-exploited, there is no fundamental reason why C_2-symmetric ligands should necessarily be superior to their nonsymmetrical counterparts.[84]

Diamines have become widely studied by many groups as chiral auxiliaries, chiral reagents and chiral external ligands.[85] In the chiral diamines, the element of chirality can be located in three places: Between the nitrogen atoms (internal chirality), on the nitrogen substituents (external chirality), or on the nitrogen atom itself.[85]

1.8 (-)-Sparteine and its Use in Asymmetric Synthesis

(-)-Sparteine **(-)-sp 100** or lupinidine (Figure 1.8.1) is a bitter tasting, lupine alkaloid, obtained from the broom *Cytisus scoparius* or the lupin *Lupinus luteus*. It is a transparent, oily liquid, colourless when fresh, turning brown on exposure to air. It was discovered by Stenhouse in 1851.[86] (+)-Sparteine **(+)-sp 100** or pachycarpine is also naturally occurring, but much less abundant. It is found in the shrub *Sophora pachycarpa*.[87]

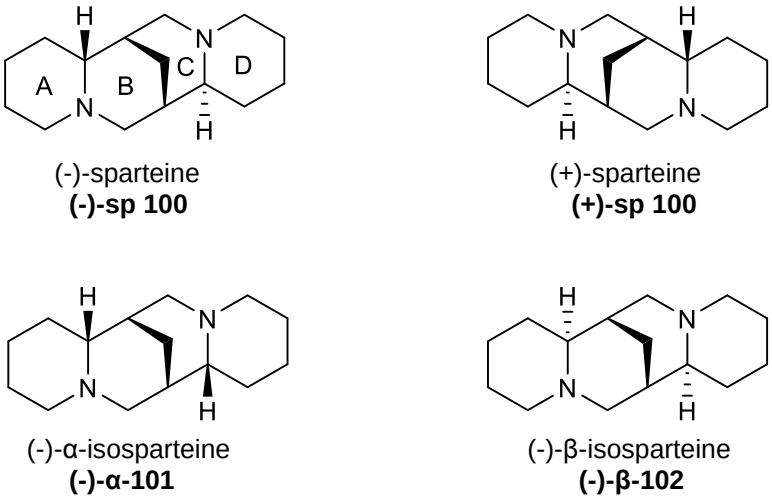

Figure 1.8.1

In contrast to its diastereomers, (-)-α-isosparteine **101** and (-)-β-isosparteine **102** (Figure 1.8.1), **(-)-sp 100** and **(+)-sp 100** deviate from C_2-symmetry. Diamines **(-)-α-101** and **(-)-β-102** also occur naturally, but they are best obtained by isomerization of **(-)-sp 100** via the dehydro derivatives **103** and **104** (Figure 1.8.2).[88]

Figure 1.8.2

Diamine **(-)-sp 100** consists of four rings. The A/B rings form a double chair system and are relatively resistant to conformational-configurational changes. The other ring systems (C/D) are more susceptible to conformational changes especially at nitrogen atom N-16 and can occur in two distinct forms, the *trans* boat chair or the cis double chair configuration (Figure 1.8.3). The position of the two nitrogen atoms N-1 and N-16 makes sparteine an excellent ligand for coordination to metal complexes. This alkaloid in a free form shows a transoid conformation

and the C-ring adopts the boat conformation and a *trans* C/D ring juncture.[89,90] On protonation or formation of metal complexes inversion of configuration on N-16 takes place resulting in adoption of cisoid conformation with *cis* C/D ring juncture,[88,91] and a cavity between two nitrogen atoms allowing **(-)-sp 100** to function as a bidendate ligand (Figure 1.8.3).

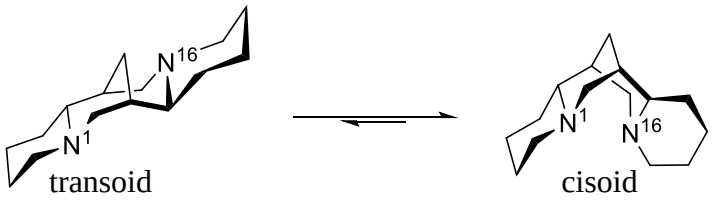

Figure 1.8.3

(-)-Sp 100 has shown itself to be admirably suited as a chiral bidentate ligand.[88] The application of **(-)-sp 100** in organic chemistry ranges from asymmetric synthesis[92] and polymerisation reactions[93] to kinetic resolution of secondary alcohols.[94] In almost all of its applications in asymmetric synthesis, a stoichiometric amount of the chiral ligand was required for the reaction. However, in some reported cases, the use of substoichiometric or a catalytic amount of the ligand has been successful.

Beak et al. has used **(-)-sp 100** in the asymmetric deprotonation of *N*-Boc pyrrolidines **105**. Deprotonation of **105** leads, through enantiotopic differentiation and removal of the pro-*S* H atom, to the configurationally stable intermediate **106**, which can be substituted with retention of configuration, by various electrophiles to give **107** (Scheme 1.8.1).

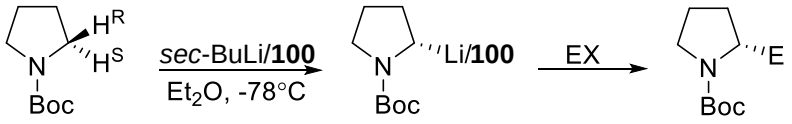

105 **106** **107a-d**

107a EX = $MeOSO_2OMe$, 88%, 94% *ee*
107b EX = CO_2, 55%, 88% *ee*
107c EX = Ph_2CO, 75%, 90% *ee*
107d EX = Bu_3SnCl, 83%, 96% *ee*

Scheme 1.8.1

Diamine **(-)-sp 100** was also used in the asymmetric addition of organolithium reagents to imines by Denmark and co-workers in 1994.[92] The group also compared the efficiency of bis-oxazoline ligands, e.g. **108**, to that of **(-)-sp 100** as chiral ligands for lithium. A clear solvent effect was observed for the reaction of organolithium reagents in the presence of chiral chelating

ligands. It was observed that ethers such as Et_2O and *i*-Pr_2O gave the best results. For the reaction with a selected imine **109** and *n*-BuLi, **(-)-sp 100** gave the highest enantioselectivity for **110**, when both catalytic and stoichiometric amounts of the ligand was used, as shown in Scheme 1.8.2 and Table 1.8.1.

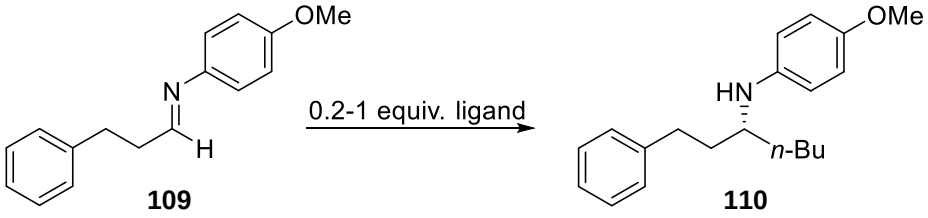

109 **110**

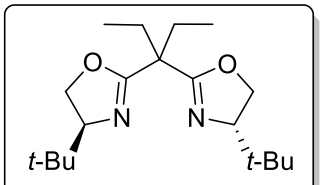

108

Scheme 1.8.2

Ligand	Equivalents	Solvent	Yield	%*ee* (*R*)
(-)-sp 100	1	Et_2O	90	91
108	1	*i*-Pr_2O	86	69
(-)-sp 100	0.2	Et_2O	91	79
108	0.2	*i*-Pr_2O	92	51

Table 1.8.1

One distinct disadvantage of **(-)-sp 100** as a chiral ligand is the difficulty in accessing the other enantiomer. As previously noted, **(+)-sp 100** also occurs in nature but is scarce. In an attempt to alleviate this problem, O'Brien and co-workers have pioneered the work to find a suitable alternative.[95,96] They developed a simple and short synthetic sequence that furnished multigram quantities of a (+)-sparteine equivalent without recourse to resolution. They reasoned that diamine **(+)-111** (Figure 1.8.4), which lacks one of the rings and chiral centres of **(+)-sp 100**, would be a good (+)-sparteine mimic.

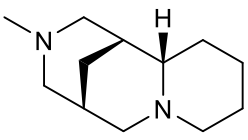

(+)-111

Figure 1.8.4

Diamine **(+)-111** was tested in Beak's lithiation/electrophilic trapping of *N*-Boc pyrrolidine **105** to give **112**. Similar yields and identical enantiomeric ratios were observed for both **(-)-sp 100** and **(+)-111** (Scheme 1.8.3).

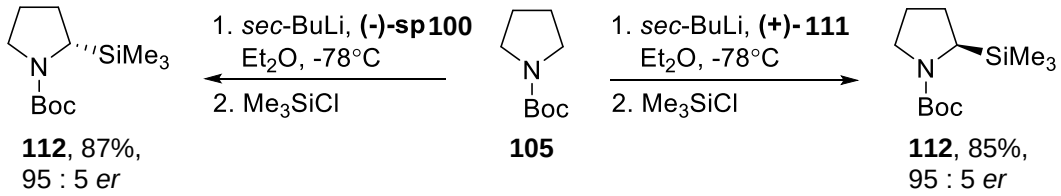

Scheme 1.8.3

In 2008,[97] it was also shown that diamine **113** (Figure 1.8.5) (previously developed by the Alexakis group)[98,99] could serve as another alternative to **(-)-sp 100**. This time both enantiomeric forms were easily accessible.

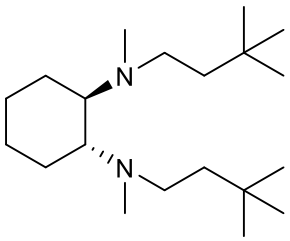

113

Figure 1.8.5

O'Brien has also successfully employed **(-)-sp 100** in a catalytic asymmetric deprotonation reaction via a ligand exchange protocol.[100] Bispidine **114** was discovered to be a slow lithiator. Thus, it was used with both **(-)-sp 100** and **(+)-111** in the lithiation/Me_3SiCl trapping of *N*-Boc pyrrolidine **105** (Scheme 1.8.4).

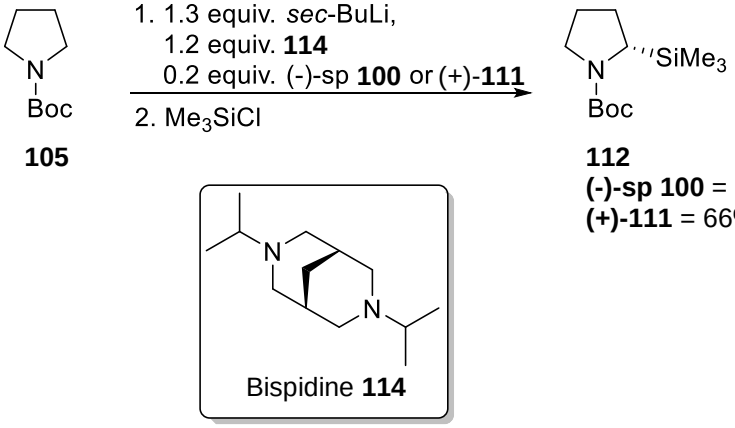

Scheme 1.8.4

O'Brien and co-workers hypothesised that a stoichiometric achiral diamine **115** would complex with *sec*-BuLi to give **116**. This would displace (-)-sparteine from complex **117** thus producing a new organolithium/diamine complex **118**. The active *sec*-BuLi/(-)-sp complex **119** would be regenerated and could re-enter the catalytic cycle. Electrophilic trapping of **117** or **118** (or both) would then produce **112** (Scheme 1.8.5). For such an approach to work, several criteria must be met: (i) Ligand exchange must occur, (ii) Organolithium **117** and **118** must be configurationally stable during the ligand exchange and (iii) Deprotonation of **105** using *sec*-BuLi/(-)-sparteine complex **119** must be faster than that using the achiral *sec*-BuLi/diamine complex **116**.

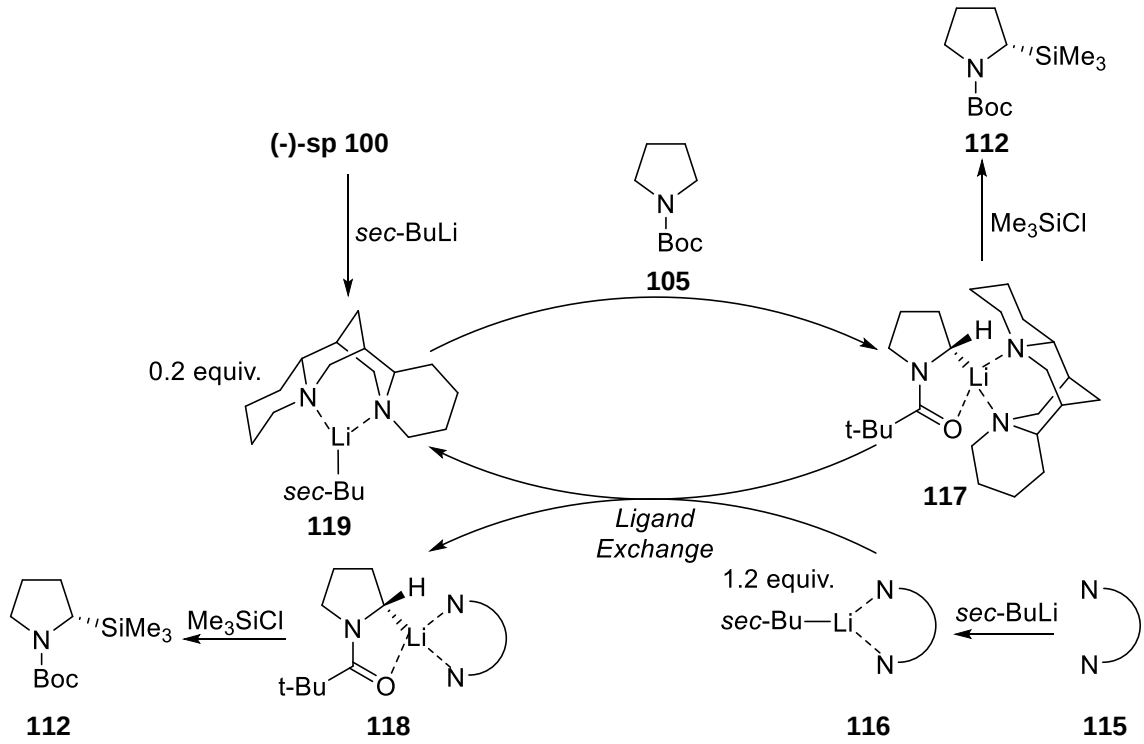

Scheme 1.8.5

1.9 Sulfinimines and 1,3-Amino Alcohols

N-Sulfinyl imines or sulfinimines **120-125** are a special class of imines bearing a sulfinyl group attached to nitrogen. They display unique reactivity and stereoselectivity due to the presence of the chiral and electron withdrawing *N*-sulfinyl group.[101] Their widespread application over the last four decades, has led to the development of an array of chiral sulfinyl motifs, offering the opportunity to fine-tune the reactivity of the sulfinimines towards specific requirements (Figure 1.9.1).[102]

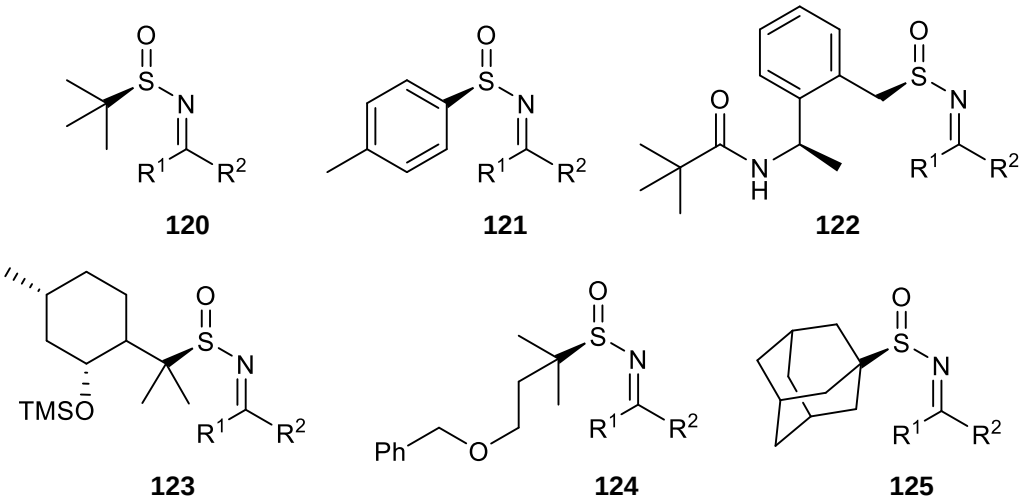

Figure 1.9.1

Sulfinimines have played an important role in the asymmetric synthesis of a variety of structurally diverse nitrogen-containing molecules because they provide a general protocol for the asymmetric addition of organometallic reagents to chiral imines. [103]

The C=N is activated for nucleophilic addition by the electron-withdrawing sulfinyl group, which facilitates reaction at low temperatures. The chiral *N*-sulfinyl group exerts a strong stereodirecting effect, resulting in the addition of enolates and organometallic reagents to both enolisable and nonenolisable sulfinimines with high and predictable asymmetric induction. Epimerization of the newly created carbon stereocenter in the sulfinamide product is inhibited because the sulfinyl group stabilises anions at nitrogen.[101]

The preparation and reaction of sulfinimines, including their applications in asymmetric synthesis, have been the subject of several reviews that cover the literature from their first preparation.[101,102,104,105]

For any motif to be truly valuable as a synthetic tool, it is vital for it to be readily available. The most common and versatile method for the preparation of generic sulfinimines is through the condensation of an aldehyde or ketone **126** with an amine **127** in the presence of a mild Lewis acid dehydrating reagent such as $Ti(OEt)_4$. This provides access to a diverse range of substituted imines **128** (Scheme 1.9.1).[105,106]

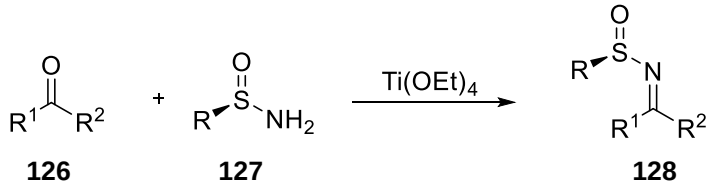

Scheme 1.9.1

Of these sulfinimines, Ellman's 2-methyl-2-propanesulfinamide (*N*-*tert*-butanesulfinamide) **120** has proved to be a versatile chiral auxiliary and has found applications in both academia and industry. *N*-*tert*-butanesulfinyl imines **129** have been used as intermediates in the asymmetric synthesis of many versatile building blocks including *syn*- and *anti*-1,3[107-109] or 1,2-amino alcohols[110,111] **130**, **131**, β-amino acids and esters[112-114] **132** and α,α-quaternary amines **133**,[106,115] α-branched amines **134** and α-amino acids[116,117] **135** (Scheme 1.9.2).

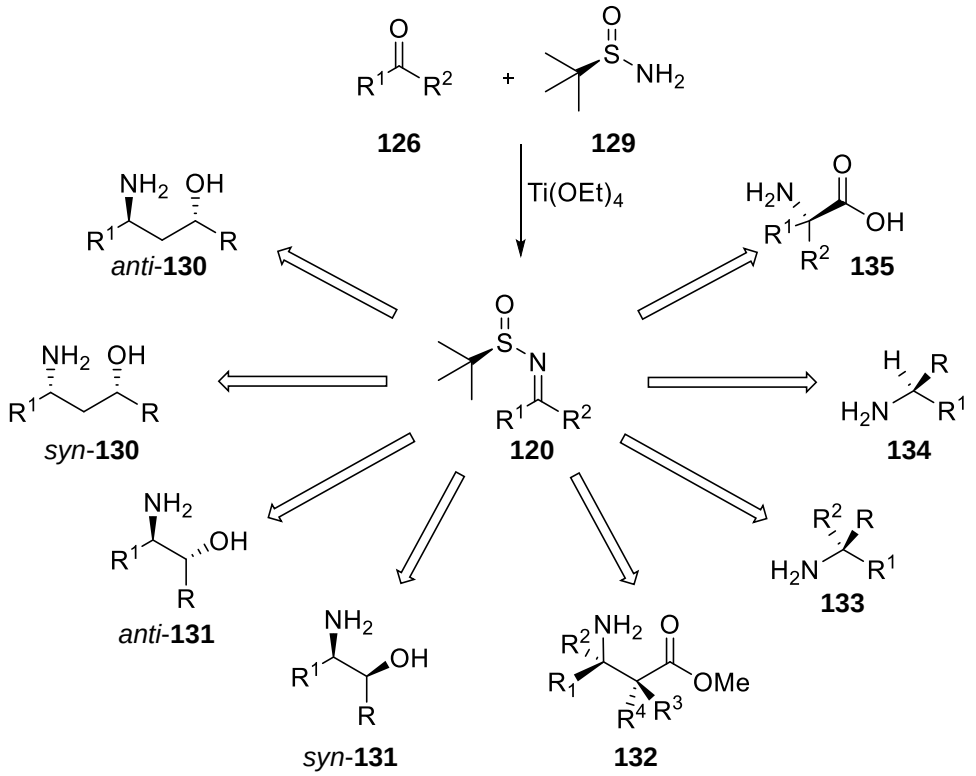

Scheme 1.9.2

Amino alcohols are of great interest because of their biological and structural importance. For example, acyclic 1,3-amino alcohols are key structural components of numerous natural products,[118-123] potent drugs,[124,125] and components of numerous medicinal compounds such as HIV-protease inhibitors,[126] μ-opioid receptor antagonists,[127] potent antibiotic negamycin,[128-130] serotonin reuptake inhibitor and antidepressants.[131] 1,3-amino alcohols have also been used as ligands for asymmetric catalysts and as chiral auxiliaries.[132-139] Despite their prevalence and the importance of acyclic 1,3-amino alcohols, there are only a few efficient synthetic methods reported in the literature to access this important class of compounds.[140-143]

Ellman's preparation of 1,3-amino alcohols is straightforward and can furnish both *syn*- and *anti*-1,3-amino alcohols.[110,111] The metalloenamines derived from the *N*-*tert*-butanesulfinyl imines **136** of structurally diverse methyl ketones (by the deprotonation and metalation with LDA and $ZnBr_2$ or $MgBr_2$) were added to a range of aldehydes with high diastereoselectivities. Stereoselective methods were identified for the reduction of the β-hydroxy *N*-sulfinyl imine products **137** to provide both the *syn*- and *anti*-1,3-amino alcohol precursors **138** with high diastereoselectivities and yields (Scheme 1.9.3). A number of reducing agents were screened. Reduction of **137** with lithium triethylborohydride gives the *anti*-1,3-amino alcohol while reduction with catecholborane yields the *syn* product in the best selectivities.

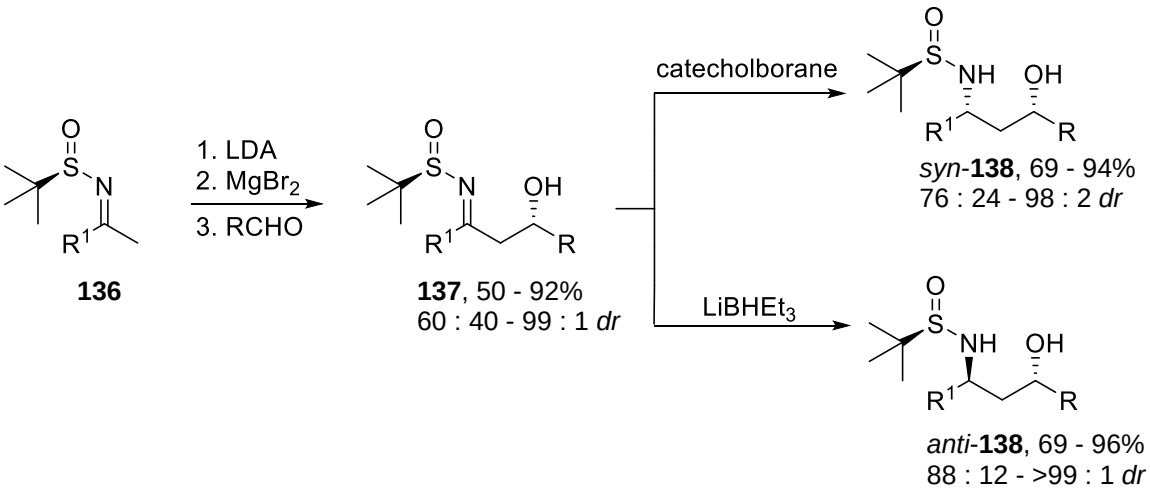

Scheme 1.9.3

The outcomes of the reduction products are controlled by the stereochemistry of the *tert*-butanesulfinyl group. According to X-ray data, the ketimine intermediate has an *E*-geometry. The $LiBHEt_3$ will not change this geometry while catecholborane is capable of giving a six-

membered ring intermediate (Scheme 1.9.4). In result, the *E*-imine will isomerize to the *Z*-imine to ultimately give the *syn* product.[111]

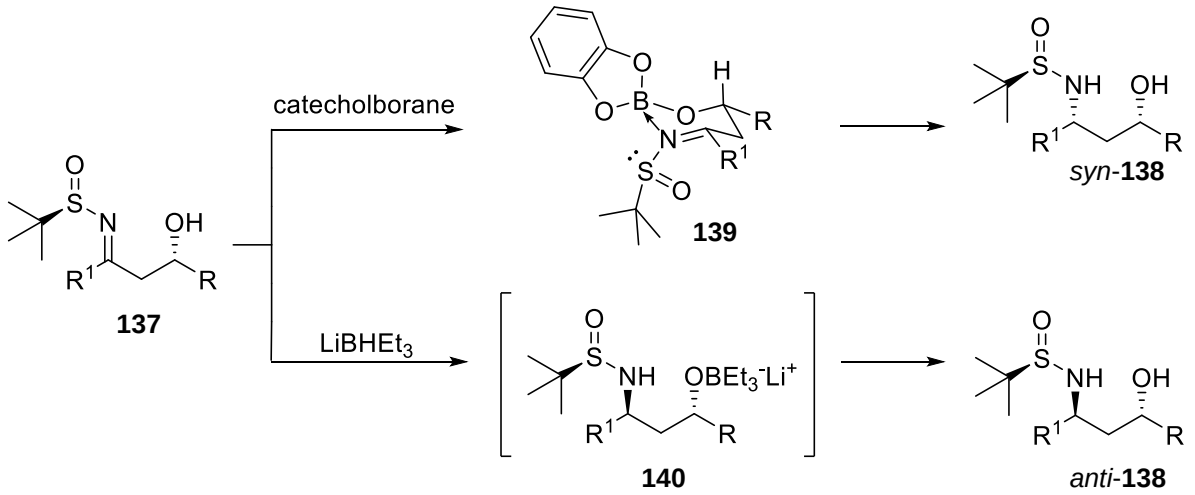

Scheme 1.9.4

The *N*-*tert*-butanesulfinyl group of the 1,3-amino alcohol precursors *syn*- and *anti*-**138** is easily removed to afford the free amino alcohol using HCl in methanol.[144] While this methodology provides a simple, general synthesis of a diverse range of 1,3-amino alcohols, there are clear limitations. These include the requirement of additives, such as magnesium bromide and the necessity for expensive reducing agents, such as superhydride (lithium triethylborohydride).

1.10 The Aldol-Tishchenko Reaction

Nucleophilic substitution of a ketone or an aldehyde is usually very difficult, due to the fact that the alkyl and hydrogen substituents involved are poor leaving groups (unlike the leaving groups normally employed in carboxylic acid derivatives). The Cannizzaro reaction is one exception and was one of the first synthetic hydride transfer reactions.[145] The Cannizzaro reaction involves nucleophilic attack by the hydroxide on an aldehyde such as **141**, followed by intermolecular hydride transfer affording the oxidation product, benzoic acid **142** and the reduction product, benzyl alcohol **143** (Scheme 1.10.1).

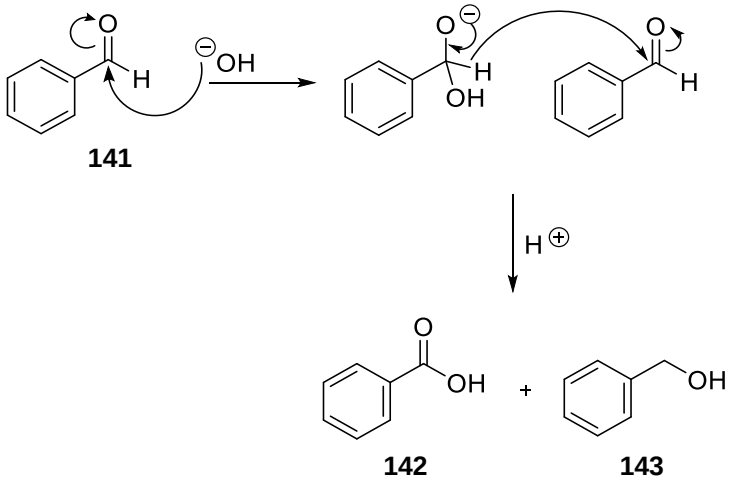

Scheme 1.10.1

When sodium alkoxide is used as base with benzaldehyde, Claisen found that a similar reaction takes place, but benzyl benzoate **144** is formed.[146] The likely route involves a hydride transfer giving ethyl benzoate **145**, followed by transesterification affording **144** (Scheme 1.10.2).

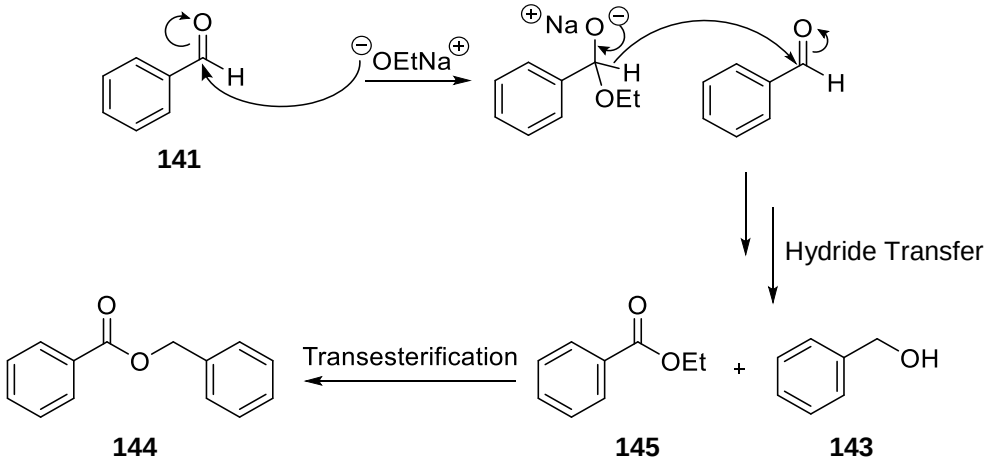

Scheme 1.10.2

Tishchenko showed that both aliphatic and aromatic aldehydes can also be condensed in this way in the presence of a metal catalyst (Scheme 1.10.3).[147]

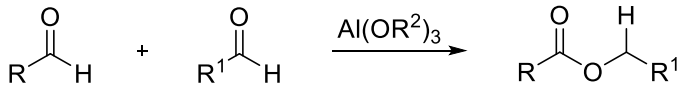

Scheme 1.10.3

In 1990 Evans and Hoveyda reported the samarium-catalysed intramolecular Tishchenko reduction of β-hydroxy ketones **146** affords **147** in excellent yields and stereoselectivity (Scheme 1.10.4 and Table 1.10.1).[148]

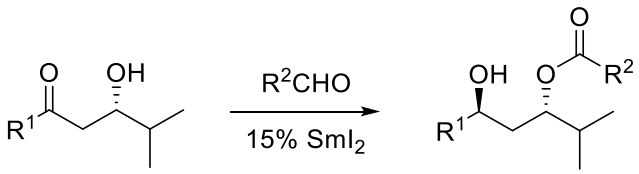

146 *anti*-**147**

Scheme 1.10.4

R^1	R^2	Yield	*anti* : *syn*
n-hexyl	Me	96%	>99 : 1
n-hexyl	$MeCH_2$	95%	>99 : 1
n-hexyl	Ph	94%	>99 : 1
i-Pr	Me	85%	>99 : 1
i-Pr	Ph	99%	>99 : 1

Table 1.10.1

Treatment of the β-hydroxy ketones with between 4 and 8 equiv. of aldehyde in THF at -10°C in the presence of SmI_2, resulted in the rapid formation of *anti*-1,3-diol monoesters. A variety of aldehydes can be used and the reaction is complete within an hour. The use of excess aldehyde is not mandatory but does serve to increase the rate of the reaction. The authors suggest a mechanism involving coordination of the hydroxy ketone **146** and the aldehyde to the catalyst, hemiacetal **148** formation followed by intramolecular hydride transfer to give **147** (Scheme 1.10.5).

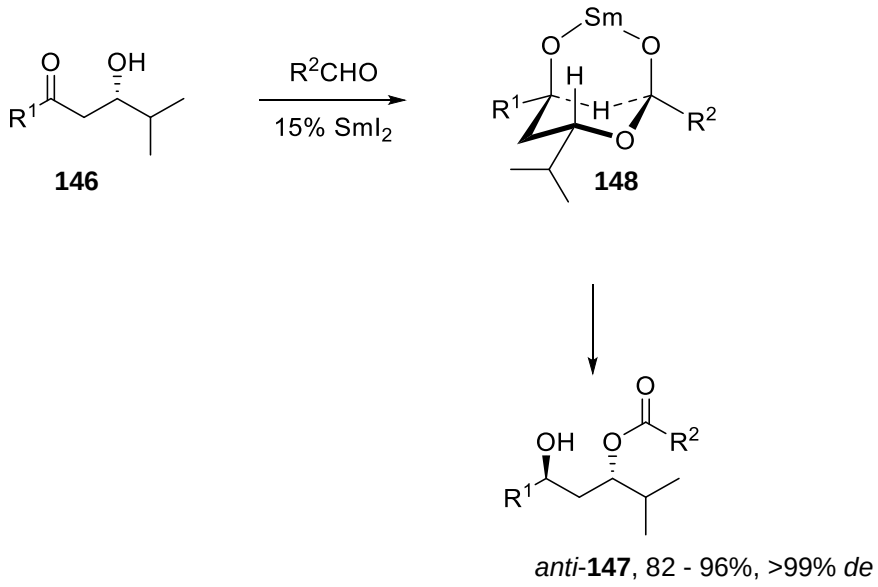

Scheme 1.10.5

Reduction of the hydroxy ketone **149** with CD_3CDO (Scheme 1.10.6) resulted in complete incorporation of deuterium at the newly generated carbinol centre (**150**) demonstrating that the aldehyde is the exclusive source of the hydride.[148]

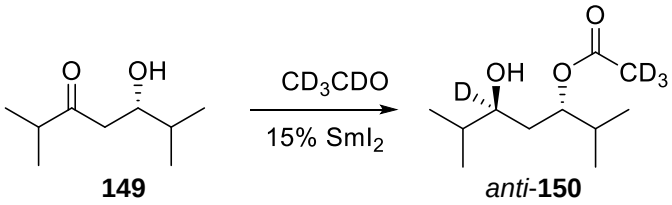

Scheme 1.10.6

This report by Evans and Hoveyda prompted an interesting communication wherein a similar reduction was noticed. Treatment of a racemic sample of epoxide **151** with LDA followed by the usual work-up, resulted in a single isomer of alcohol **152** being formed (23%, stereochemistry not determined) (Scheme 1.10.7). [149]

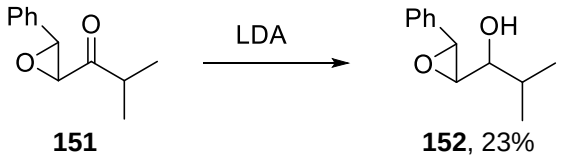

Scheme 1.10.7

Replacement of LDA with LiTMP allowed nucleophilic attack of the enolate on benzaldehyde at -78°C resulting in formation of racemic alcohol **153** (Scheme 1.10.8).[149]

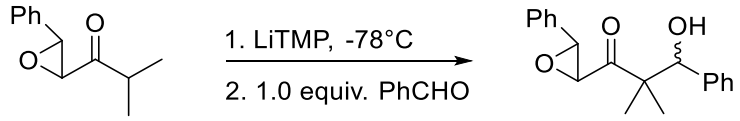

151 **153**, 58%

Scheme 1.10.8

However, allowing longer reaction times and higher temperatures (room temperature, over-night) a single stereoisomer of ester **154** was isolated (26%) and upon using 3 equiv. of benzaldehyde, a single isomer was formed in 63% yield (Scheme 1.10.9).

151 **154**, 63%

Scheme 1.10.9

The structure of **154** was confirmed by X-ray analysis. An interesting experiment shed some light on the mechanistic details. When an isomeric mixture of 1,3-hydroxy ketone **153** was deprotonated with a base (LDA) and treated with benzaldehyde, a single isomer of **154** was again isolated (Scheme 1.10.10) in 47% yield.

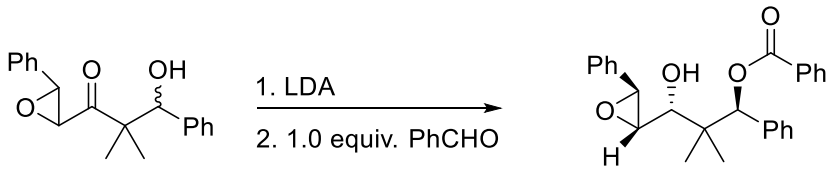

153
Isomeric mixture

154, 47%
Single Isomer

Scheme 1.10.10

It having been already noted that addition of the first molecule of benzaldehyde is non-stereoselective giving **153** as a mixture of stereoisomers, it was proposed that addition of **151** to the two molecules of aldehyde, as well as hydride transfer all occur in a concerted fashion. This would account for the stereoselectivity of the reaction. Because the reaction could not be forced to completion, it was suggested that these stages may occur in equilibrium.

Heathcock noted when excess paraformaldehyde was used to achieve higher conversion of the ketone **155** to 1,3-hydroxyketone **156**, diol monoformate ester **157** was formed instead (Scheme 1.10.11).[150]

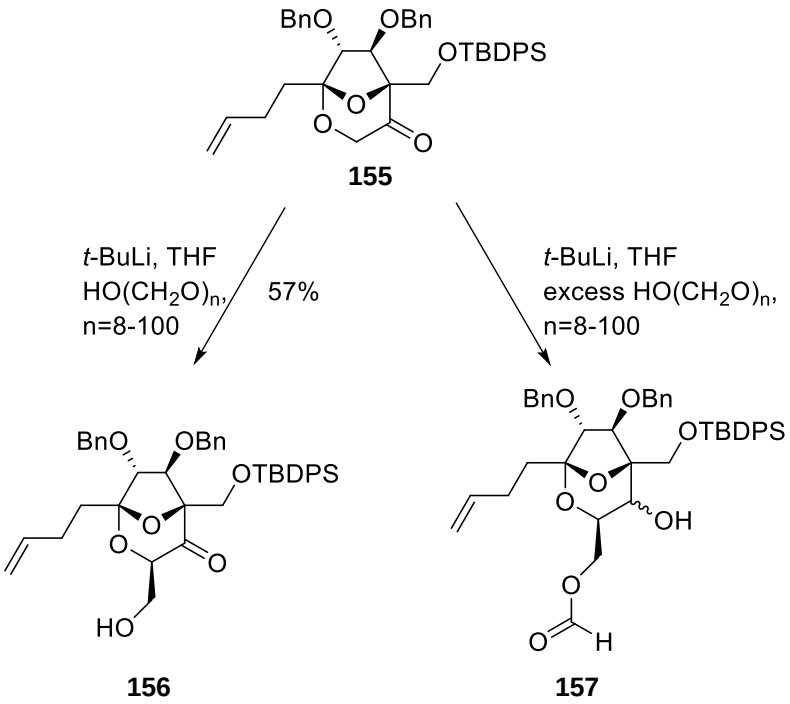

Scheme 1.10.11

The substrate scope for the synthesis of *anti*-1,3 diols was still limited at this time prompting further work on the aldol-Tishchenko reaction. In 1996, Mahrwald et al. reported, a one-pot aldol-Tishchenko reaction of 3-pentanone **158** with aldehydes using substoichiometric amounts of titanium ate complexes, to furnish *anti*-1,3-diol monoesters **159** in a high level of stereoselectivity (Scheme 1.10.12).[151]

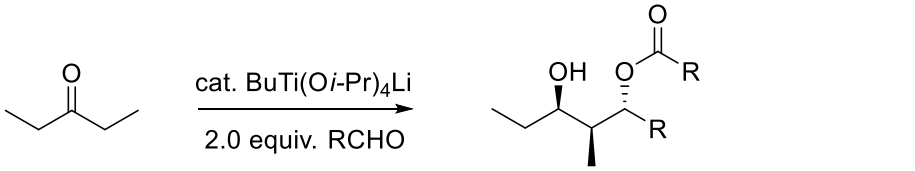

158 *anti*-**159**, 63 - 86%, 94 - 98% *de*

Scheme 1.10.12

Hydrolysis of monoesters **159** occurs easily affording the corresponding diastereomerically pure 1,3-*anti*-diols.

In 1997 Woerpel reported several tandem aldol-Tishchenko reactions of lithium enolates including a simple method for the synthesis of polyoxgenated compounds with up to five stereocenters, which were generated with excellent diastereoselectivity.[152]

The lithium enolates of a number of ketones **160** were treated with 2.2 equiv. of aldehyde at -78°C followed by warming to 22°C for 12 h affording, almost exclusively, one diastereoisomer of **161** in good yield (Scheme 1.10.13). The stereochemistry of the product was determined by comparison to reference compounds and analysis of the derived 1,3-diol **162**.[153,154] No β-hydroxy ketones (simple aldol addition products) were isolated in these reactions.

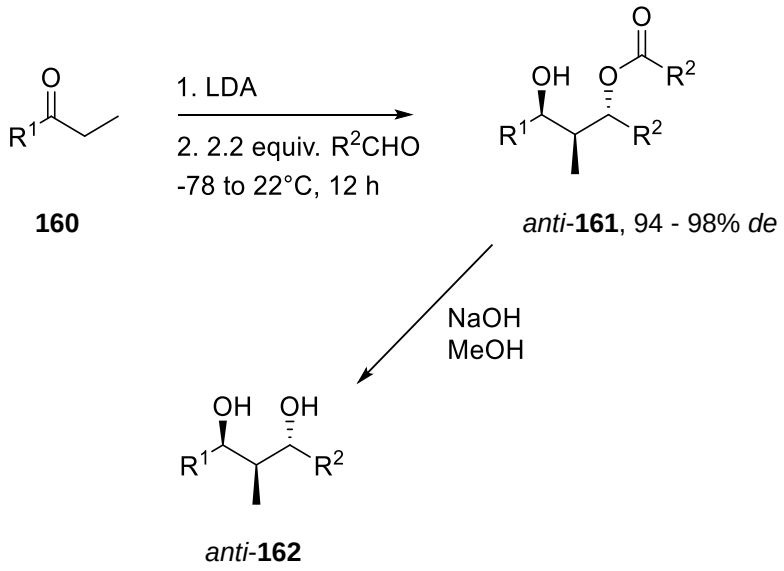

Scheme 1.10.13

In contrast to aldol addition reactions of **160** to **163** which are known to proceed in extremely short reaction times (less than 10 s) at -78°C (Scheme 1.10.14),[155] these aldol-Tishchenko reactions take place at room temperature over several hours.

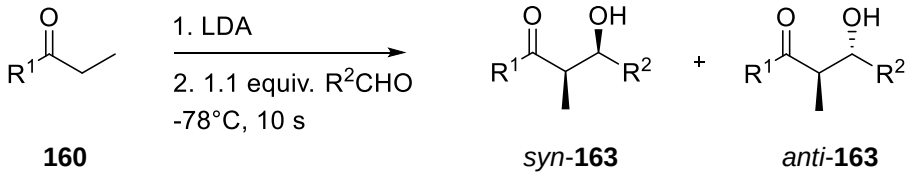

Scheme 1.10.14

Treatment of *syn*-aldol adduct *syn*-**164** with LDA followed by 1.1 equivalent of propionaldehyde resulted in a 1 : 1 ratio of diol **165** (R=*i*-Pr) and crossover product **166** (R = Et) after hydrolysis (Scheme 1.10.15).

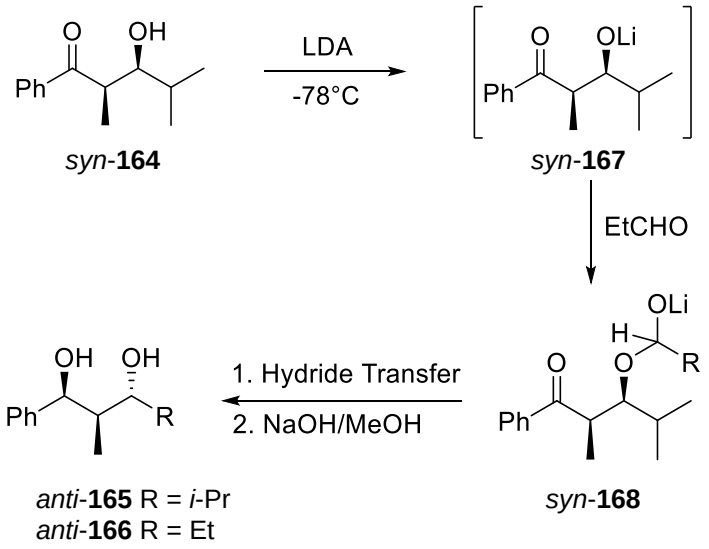

Scheme 1.10.15

The same ratio was obtained when the *anti*-isomer of **164** was used. Since the stereochemical relationship of the products is not dependent upon the structure of the aldolate, it can be concluded that the aldol step is reversible and non-stereodetermining.

To determine the relative rates of the aldol and Tishchenko reactions a solution of aldolate **167** was quenched at different temperatures (Scheme 1.10.16).

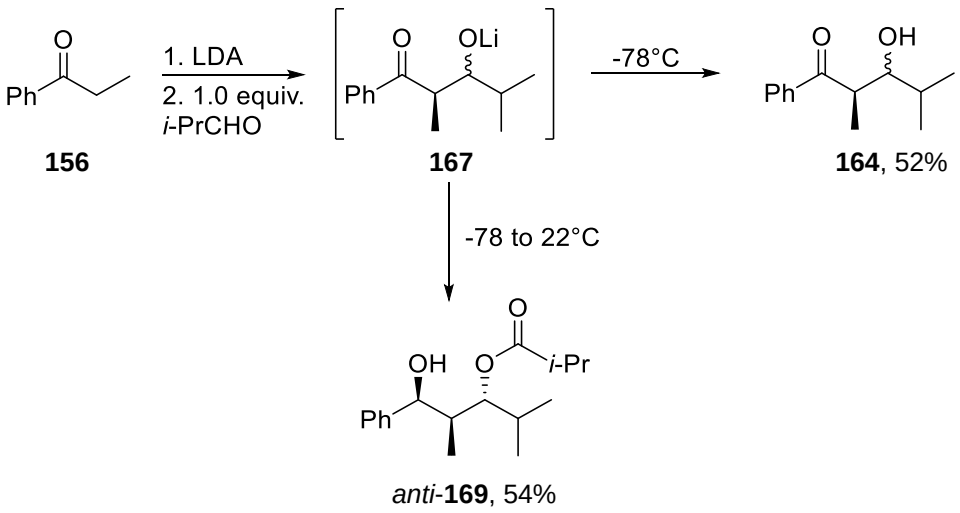

Scheme 1.10.16

When the reaction was quenched after 10 s at -78°C expected aldol products **164** were formed as a *ca.* 1 : 1 mixture of diastereoisomers in a yield of 52%. However, when the reaction mixture was allowed warm to room temperature for 12 h, mono-ester **169** was formed along with some

aldol products **164** (11%). This shows that the rate of the aldol reaction (10 s at -78°C) is greater than the Tishchenko reduction (several hours at room-temperature).

The high stereoselectivity of the reaction can be rationalised by a mechanism involving a reversible aldol reaction followed by intramolecular hydrogen transfer via a six-membered transition state (Scheme 1.10.17).

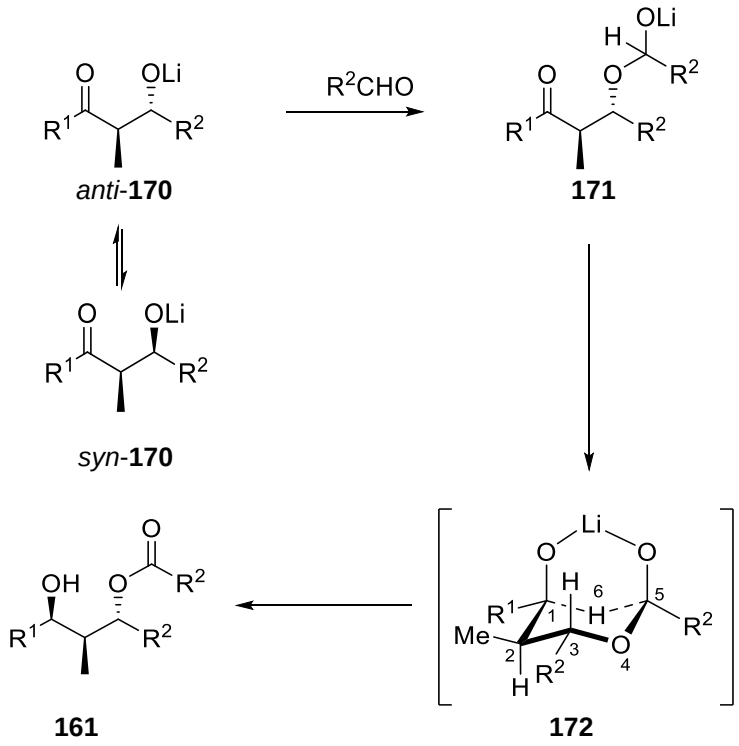

Scheme 1.10.17

Attack by lithium enolate **170** on the aldehyde will result in hemi-acetal **171** which can adopt a highly structured 6-membered transition state **172** with both the methyl group at C-2 and the R^2 group at C-3 in the preferred equatorial position. The 1- and 5- positions are fixed via coordination to the lithium ion. This model is also in agreement with that proposed by Evans and Hoveyda in the samarium catalysed Tishchenko reduction of β-hydroxy ketones.[148]

In 2001, Morken and co-workers described the first catalytic asymmetric aldol-Tishchenko reaction of two different aldehydes, **173** and **174**, catalysed by an yttrium-salen complex (Scheme 1.10.18).[157]

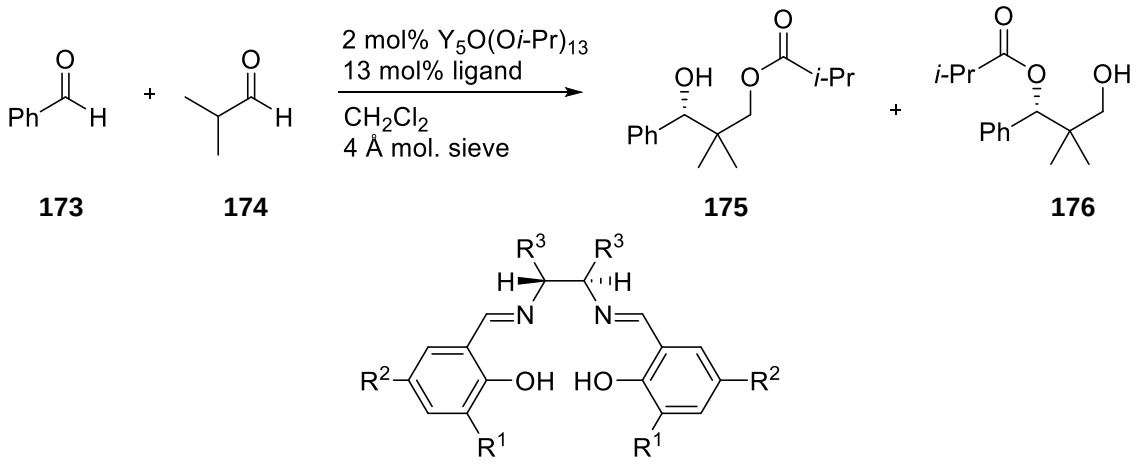

Scheme 1.10.18

The reaction provides two regioisomeric esters **175** and **176** in similar enantiopurity suggesting a nonselective intramolecular acyl migration after formation of the aldol-Tishchenko adduct.

Bulky substituents *ortho* to the salen oxygen atom (R^1) were necessary for reactivity and selectivity, whereas the presence of *para* substituents (R^2) were not essential for asymmetric induction (Table 1.10.2). The highest enantioselectivities were obtained when ligand **177f** was employed.

Ligand	R^1	R^2	R^3	Yield	*er* of 175
177a	*t*-Bu	*t*-Bu	$(CH_2)_4$	44% (3.4 : 1)	78 : 22
177b	*t*-Bu	H	$(CH_2)_4$	36% (3.0 : 1)	78 : 22
177c	Me	H	$(CH_2)_4$	54% (1.6 : 1)	57 : 43
177d	adamantyl	Me	$(CH_2)_4$	42% (3.2 : 1)	83 : 17
177e	*t*-Bu	*t*-Bu	Ph	48% (3.3 : 1)	82 : 18
177f	adamantyl	Me	Ph	70% (>15 : 1)	87 : 13

Table 1.10.2

Mlynarski and Mitura presented the first catalytic asymmetric aldol-Tishchenko reaction of aldehydes and simple aliphatic ketones in 2004.[158] They employed chiral ytterbium complexes to catalyse the condensation of aromatic aldehydes with 3-pentanone **158** (and other ketones) giving rise to the *anti*-1,3-diol monoesters **178** and **179**, however yields and enantioselectivity were moderate (Scheme 1.10.19).

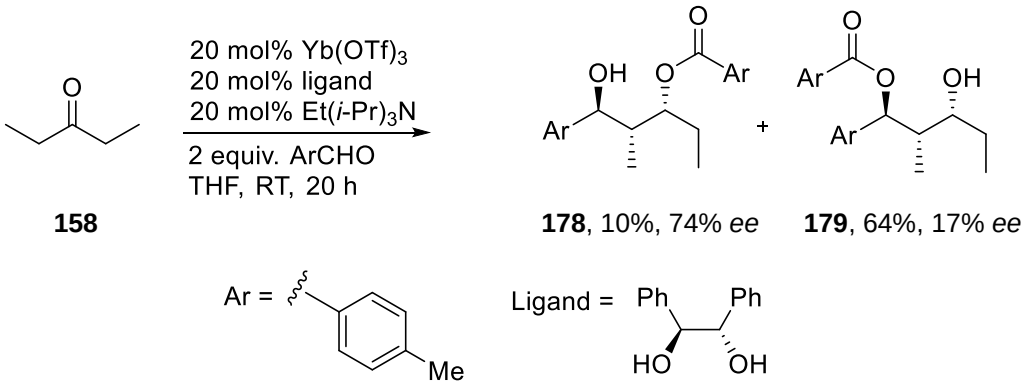

Scheme 1.10.19

Shibasaki disclosed the first catalytic direct aldol–Tishchenko reactions of aryl aldehydes (e.g. **180**) and aryl ketones (e.g. **181**) that resulted, after hydrolysis of the intermediate 1,3-diol monoesters, in *anti*-1,3-diols **182** in moderate to good yield and high enantioselectivity (Scheme 1.10.20).[159]

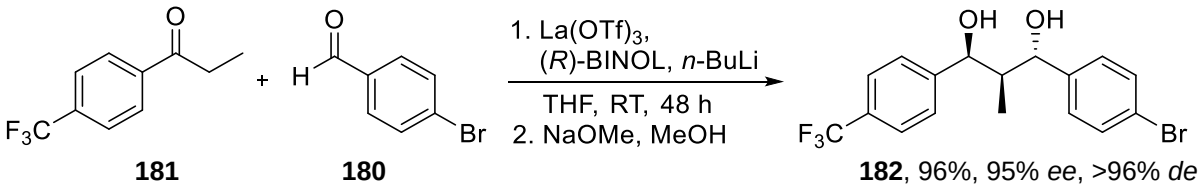

Scheme 1.10.20

Chapter 2

Synthesis of Racemic α-Alkylated Ketones and the Development of a Novel Chiral Auxiliary for their Enantioselective Preparation

2.1 Introduction

In this chapter the synthesis of a compilation of racemic ketones is described. It was necessary to prepare the target compounds of this project to become familiar with the stability and volatility of the α-alkylated products and establish suitable methods for isolation, purification and storage before attempting their asymmetric synthesis.

Moreover, these racemic ketones would serve as reference standards. Optimum separation conditions via GC analysis were determined for each compound using these racemic samples, which would provide accurate determination of enantiomeric ratios of the enantioenriched products.

The synthesis of a novel chiral diamine-based chiral auxiliary is also detailed in this chapter. Its use, in the asymmetric α-alkylation of ketones, was also investigated and the results are presented.

2.2 Results and Discussion

2.2.1 Preparation of Racemic α-Alkylated Ketones

The simple aliphatic ketone 3-pentanone was chosen as the substrate for initial investigations in establishing a new route to asymmetric α-alkylated ketones. 3-pentanone was chosen to be a suitable substrate as it would be a very useful synthon in the synthesis of polyketide and propionate-based natural products.[160] 2-methyl-3-pentanone and propiophenone would also be employed in substrate scope investigations. Therefore α-alkylated products of these ketones were prepared as part of a racemic reference library.

Preparation of the racemic substrates **36** and **183-188** was accomplished by addition of the ketone to freshly prepared LDA in THF at -78°C. The reaction was stirred for 1 h at -78°C and the electrophile was added slowly. The reaction was then warmed to room temperature overnight. The reaction was quenched with saturated NH_4Cl, extracted with diethyl ether and the organic layers combined, dried and concentrated under reduced pressure. The crude product was then purified using column chromatography on silica gel to afford the pure alkylated ketones (Scheme 2.2.1).

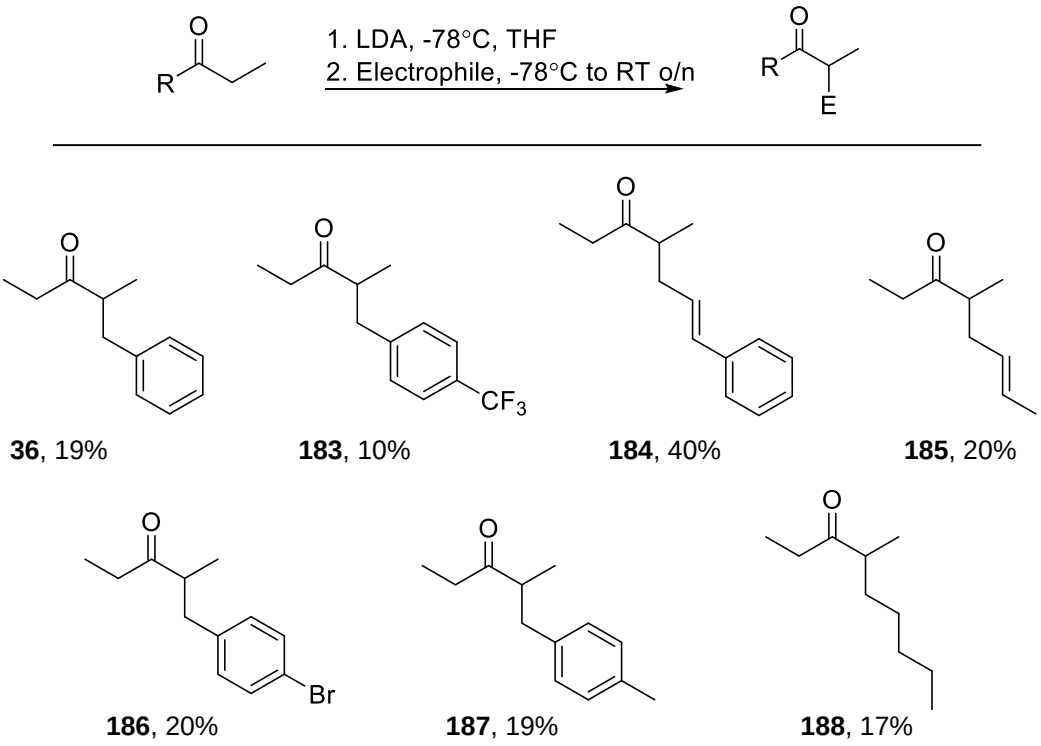

Scheme 2.2.1

Initially ethyl acetate was employed as solvent for extractions and for purification of the ketone using column chromatography. However, due to volatility of the ketones, diethyl ether was later utilised.

The yields obtained for α-alkylated ketones using 3-pentanone were poor to modest. It is well known that aldehyde and ketone alkylation is challenging due to competing side reactions, such as aldol condensations, Cannizzaro and Tishchenko reactions, and *O*-alkylation.[12,13] Furthermore, Molander and co-workers have demonstrated the allylation of 3-pentanone occurs in a poor yield (30%).[161] Additionally, these products were very volatile and a notable decrease in mass was observed upon rotary evaporation.

Improved yields were observed for the alkylation of 2-methyl-3-pentanone and propiophenone. Benzylation of 2-methyl-3-pentanone resulted in **189** in 40% yield. In the case of propiophenone, the products obtained, **190** and **191**, were not volatile, however the reactions did not go to completion in the timescale of the reaction (Scheme 2.2.2).

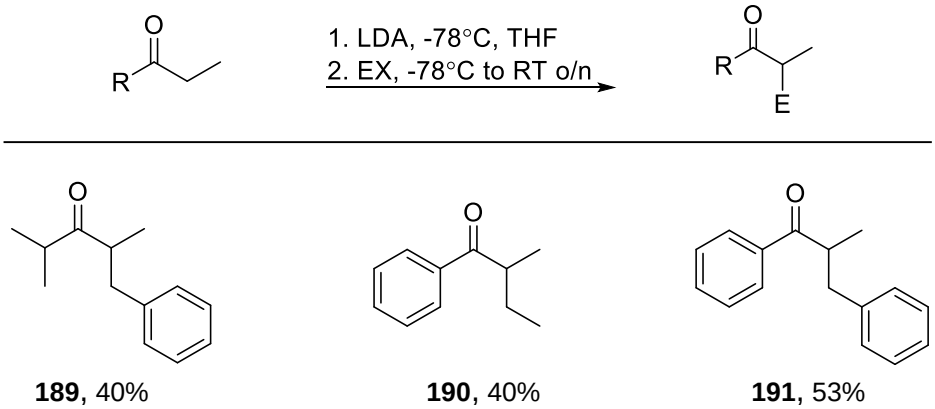

189, 40% **190**, 40% **191**, 53%

Scheme 2.2.2

Having successfully synthesised this range of racemic ketones, each was subjected to chiral GC analysis and conditions were determined to achieve baseline resolution of enantiomers. As an example, Scheme 2.2.2 shows the chromatograph obtained for the separation of 2-methyl-1-phenylpentan-3-one **36** using chiral GC chromatography (Figure 2.2.1).

Sample Info : 120C hold 10min ramp 10C/min to 140C hold 5min, flow 1ml/min, Inj vol. 0.2ul, split ratio 10:1, front inlet 150C, detector 155C

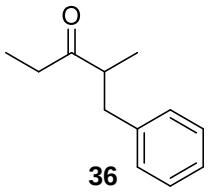

36

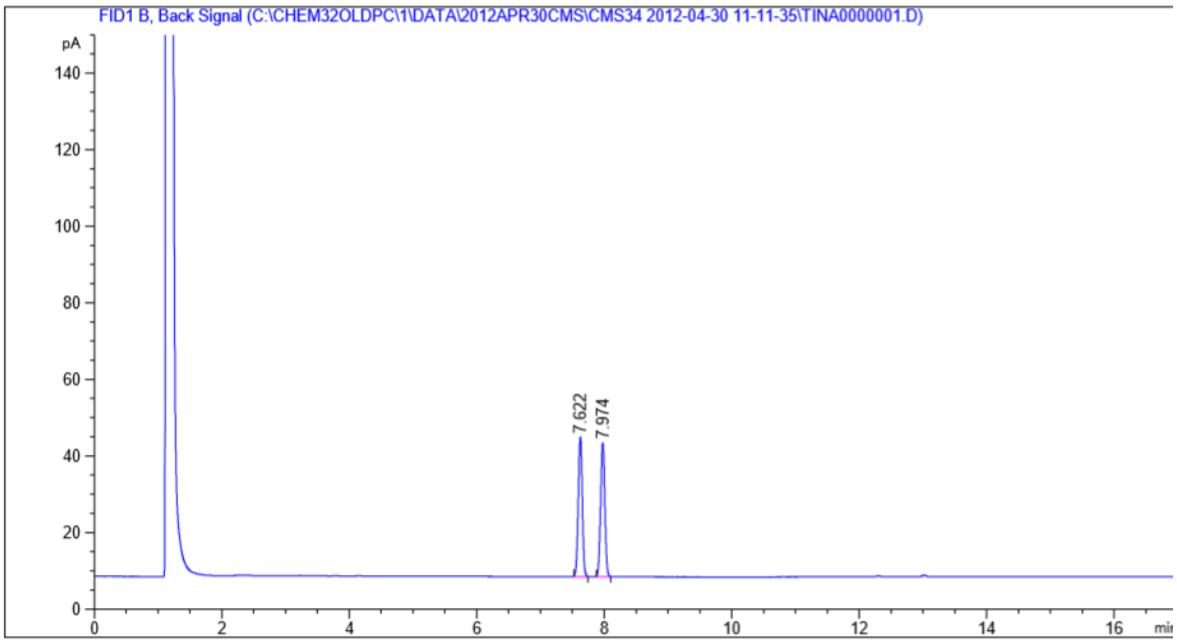

Figure 2.2.1

2.2.2 Synthesis of a Novel Diamine-based Chiral Auxiliary

Expanding on the existing chiral ligand methodology, a novel diamine-based chiral auxiliary, **(*S*)-192** was synthesised and it use in the asymmetric α-alkylation of ketones was investigated. Given that SAMP **(*S*)-9** and its bulkier analogues contain an oxygen at the additional chelation site, we were interested in investigating the effect of changing this to a nitrogen (as part of a pyrrolidine system) and determine the enantioselectivity of the resulting alkylated products. Our auxiliary offers a distinct advantage in that it can be accessed in two steps from the commercially available amine **(*S*)-193** (Scheme 2.2.3).

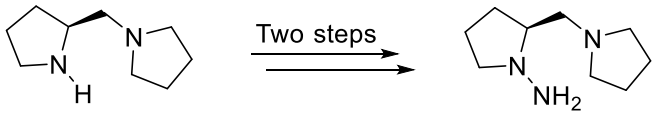

(*S*)-193 **(*S*)-192**

Scheme 2.2.3

To obtain larger quantities of chiral diamine **(*S*)-193** we began with (*S*)-proline **(*S*)-194**. The literature procedure described by Amedjkouh et al. was used for the preparation of **(*S*)-193**.[162] The first step involved preparation of the bicyclo, oxazolidinone **(*R,S*)-195** (Scheme 2.2.4). This was achieved by addition of anhydrous chloral **196** to a stirred solution of the amino acid (*S*)-proline **(*S*)-194**, dissolved in chloroform. The resulting solution was then heated for 10 h under reflux using a reverse Dean-Stark apparatus to remove water. The mixture was then cooled to room temperature and washed with water. The resulting water layers were washed with dichloromethane and the combined organic layers were dried and concentrated under reduced pressure. The crude product, a brown crystalline solid was purified by recrystallisation from ethanol. The bicyclo product **(*R,S*)-195** was produced in a 42% yield as white crystalline needles.

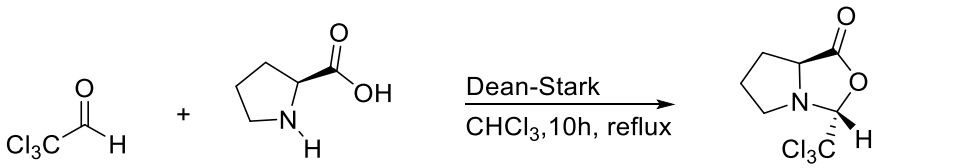

196 **(*S*)-194** **(*R,S*)-195**, 42%

Scheme 2.2.4

The mechanism probably proceeds as outlined in Scheme 2.2.5.

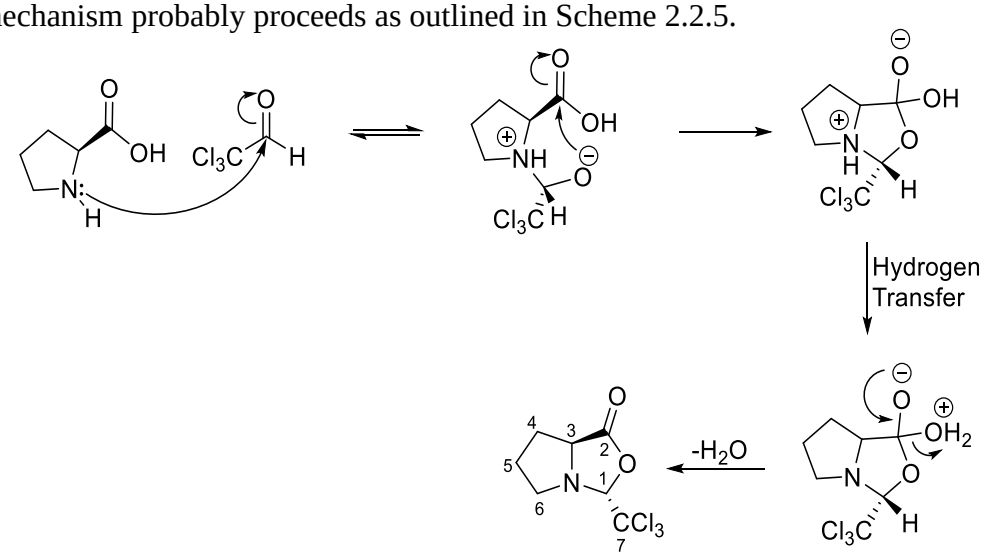

Scheme 2.2.5

From the analytical data obtained it was possible to conclude that the bicyclo intermediate **(*R*,*S*)-195** was successfully formed.[162] In the ^{1}H NMR, a 1H doublet of doublets was observed at 4.11 ppm which is indicative of the hydrogen at C-3. A 1H singlet at 5.16 ppm represented the proton at C-1, next to the trichloromethyl-carbon. The three adjacent CH_2 groups (C-4, C-5 and C-6) all showed multiplets between 1.80 and 3.50 ppm. In the ^{13}C NMR spectra, the CH_2 carbons appeared at 25.4 (C-5), 29.9 (C-4) and 57.9 (C-6) ppm respectively and the CH of C-3 was observed at 62.4 ppm. The carbonyl-carbon appeared at 175.5 ppm. A positive mass spectrum confirmed the presence of the protonated molecular ion at m/z = 244. An optical rotation, $[\alpha]_D^{20}$ of + 29.8 was obtained at 20°C, which was consistent with that found in the literature and confirmed that the product **(*R*,*S*)-195** was obtained.

In the second step of the synthesis, the bicyclo oxazolidinone **(*R*,*S*)-195** was suspended in ethanol. Pyrrolidine **197** was added dropwise at 0˚C and the solution was allowed to stir at room temperature. After 4.5 hours, TLC analysis (1 : 1, hexane : ethyl acetate) showed all starting material had reacted. Once the solvent had been removed under reduced pressure, the product **(*S*)-198** was obtained as a yellow oil and used in the next step without further purification (Scheme 2.2.6).

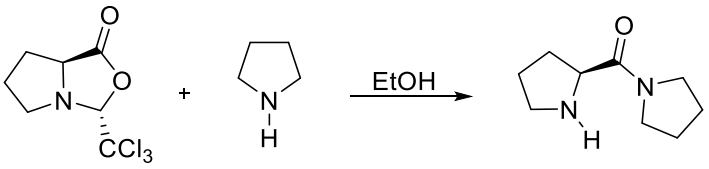

(*R,S*)-195 **197** **(*S*)-198**

Scheme 2.2.6

The mechanism for this reaction probably proceeds as outlined in Scheme 2.2.7.

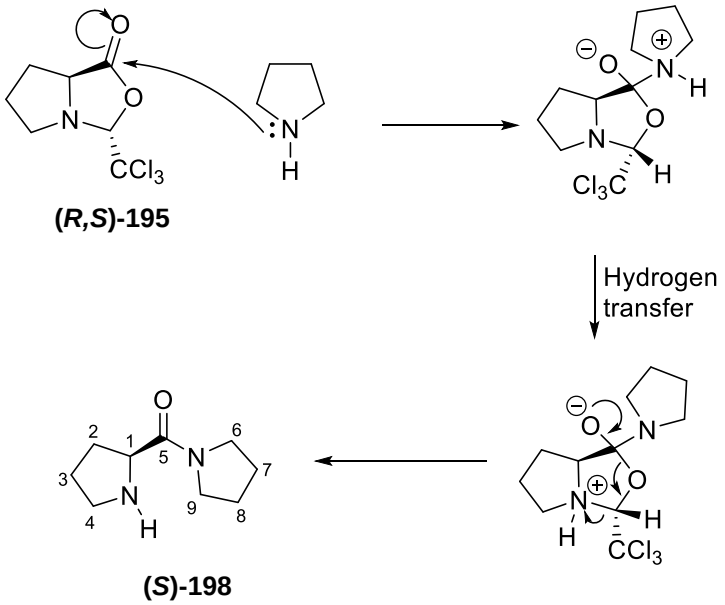

(*R,S*)-195

(*S*)-198

Scheme 2.2.7

The ^{1}H NMR spectrum was consistent with that in the literature.[162] A characteristic doublet of doublets was observed at 3.79 ppm for the proton at C-1, due to splitting by the diastereomeric protons at C-2. A 4H multiplet between 3.35-3.57 ppm corresponded to the protons at C-6 and C-9. In the ^{13}C NMR spectrum, the CH at C-1 was observed at 59.44 ppm. The CH_2 groups at C-4, C-6, C-9 are more downfield, than the remaining CH_2 groups, at 45.8, 45.9, 47.6 ppm respectively. The positive mass spectrum confirmed the presence of the protonated molecular ion at m/z = 169.

The next step en route to the chiral auxiliary **(*S*)-192** involved reduction of amide **(*S*)-198** to tertiary amine **(*S*)-193** using lithium aluminium hydride. The reducing agent was first dissolved in dry THF under a nitrogen atmosphere, the amide was then added dropwise at 0˚C over a 30 minute period in THF. The reaction mixture was returned to room temperature and allowed to stir overnight. It was then heated at reflux for 2.5 h. The mixture was allowed to cool to room temperature and quenched by slow addition of water, 15% sodium hydroxide and water. The

mixture was stirred until a white precipitate had formed. The reaction mixture was then filtered through Celite® and the filtrate concentrated under reduced pressure to give the crude product as an orange oil. Kugelrohr distillation was employed, affording the product **(*S*)-193** as a clear oil in 40% yield over two steps (Scheme 2.2.8).

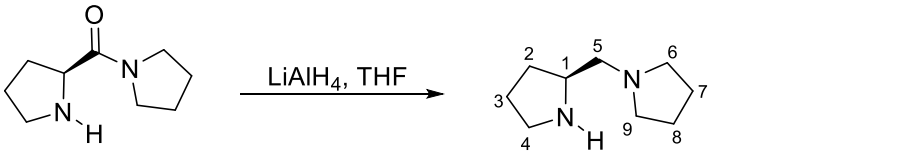

(*S*)-198 **(*S*)-193**, 40% over two steps

Scheme 2.2.8

The ^{1}H NMR spectrum confirmed that amide **(*S*)-198** was successfully reduced to amine **(*S*)-193**. All methylene groups of the proline rings appeared as multiplets. The proton at C-1, which appeared as a doublet of doublets in **(*S*)-198** was now observed as a multiplet at 3.15-3.29 ppm due to additional coupling to protons at C-5, as well as C-2. The carbon spectra confirmed the absence of the carbonyl of amide **(*S*)-198**, instead a peak was observed at 62.1 ppm, which corresponded to the CH_2 of C-5. The infrared spectra showed characteristic peaks for **(*S*)-193**, a strong stretch at 3320 cm^{-1} for the N-H stretch, peaks between 2961-2793 cm^{-1} for C-H stretches and medium stretches between 1146-1108 cm^{-1} for the C-N. A positive ESI mass spectrum showed the protonated molecular ion at m/z = 155. An optical rotation, $[\alpha]_D^{20}$ of + 5.2 was obtained in ethanol at a concentration of 2.4 g/100 ml and was in reasonable agreement with the literature value of + 8.9.[162]

The fourth step of the synthesis was the preparation of nitroso intermediate **(*S*)-199**. Great care was taken in handling nitroso product **(*S*)-199**, as it is a possible carcinogen. Three pairs of gloves were used at all time, and reactions were carried out with extra caution. Following the reaction all glassware was washed in a base bath, then an acid bath followed by water and acetone.

A procedure by Lazny *et al.* was chosen for the nitrosation reaction of **(*S*)-193** to **(*S*)-199**.[163] This involved addition of *tert*-butyl nitrite to a solution of amine **(*S*)-193** in THF. The mixture was stirred for 18 h at room temperature in the absence of light. However TLC analysis showed only starting materials remained. The following day the mixture was refluxed for 5 h. The solvent and the excess *tert*-butyl nitrite were removed under reduced pressure to afford a brown oil. ^{1}H NMR spectra showed the reaction was unsuccessful and that only the starting material remained.

As this procedure was unsuccessful, **(*S*)-199** was subsequently prepared using a procedure described by Curtin et al.[164] The amine starting material **(*S*)-193** was dissolved in water and 37% hydrochloric acid was added. Acetic acid was then added, followed by sodium nitrite at 0˚C and the solution left to stir at this temperature for 30 minutes. The reaction mixture was then returned to room temperature for 90 minutes. A TLC using 9 : 1, dichloromethane : methanol showed all starting material had reacted. The solution was cooled to 0˚C for addition of the 10% sodium carbonate until it just turned basic. Ethyl acetate was added, the aqueous layer was then removed and washed twice with ethyl acetate. The combined organic layers were dried and the solvent removed under reduced pressure to give the product **(*S*)-199** as a yellow oil. It was used in the next step without further purification (Scheme 2.2.9).

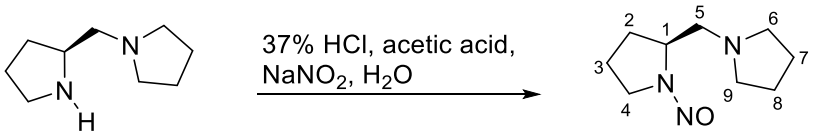

(*S*)-193 **(*S*)-199**

Scheme 2.2.9

Due to the toxic nature of the compound **(*S*)-199**, only ^{1}H NMR analysis was obtained. The equivalent hydrogens of C-7 and C-8 of the proline ring were observed at 1.73-1.82 ppm. A signal was detected for the proton at C-1, which appeared at 3.15-3.29 ppm for the diamine **(*S*)-193**, but was now seen as a multiplet at 4.56-4.68 ppm for nitroso **(*S*)-199**. This is due to the electron withdrawing nitroso group causing a deshielding effect. Two 1H doublet of doublets were observed for C-5 between 2.80 and 2.99 ppm.

For the final step of the chiral auxiliary synthesis, lithium aluminium hydride was used to reduce nitroso intermediate **(*S*)-199** to hydrazine **(*S*)-192**. To a suspension of lithium aluminium hydride in dry THF under a nitrogen atmosphere, cooled to 0°C, was added **(*S*)-199** in dry THF, slowly over a 30 minute period. The mixture was allowed warm to room temperature and left to stir for a period of 6 hours. The reaction was quenched by slow addition of water, 15% sodium hydroxide and water. A white precipitate formed, which was filtered through Celite® and washed with ethyl acetate and THF. The filtrate was then concentrated under reduced pressure to give the crude product as a yellow oil. Purification of **(*S*)-192** was achieved via kugelrohr distillation. Pure chiral auxiliary **(*S*)-192** was isolated in 40% yield over two steps (nitrosation and reduction) (Scheme 2.2.10).

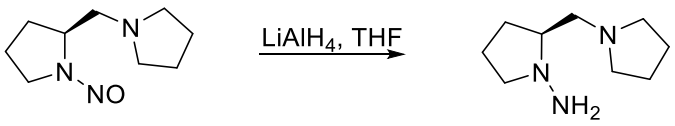

(*S*)-199 **(*S*)-192**

Scheme 2.2.10

The mechanism for this reaction is outlined below in Scheme 2.2.11.

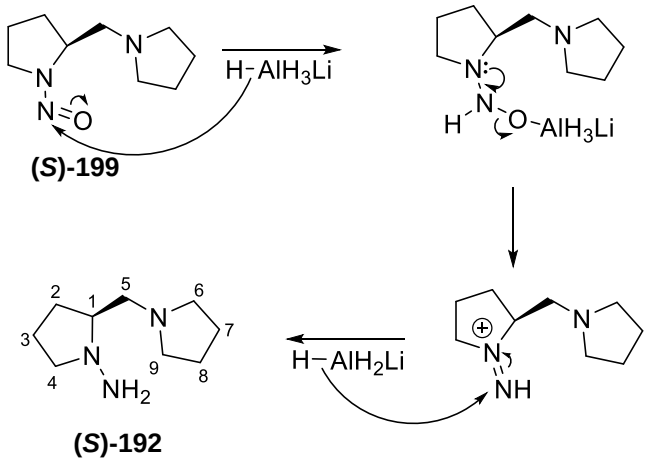

Scheme 2.2.11

The ^{1}H NMR spectra of **(*S*)-192** showed a characteristic doublet of doublets for the hydrogen at C-5 at 2.88 ppm. The ^{13}C NMR spectrum displayed peaks at 20.6 (C-2), 23.7 (C-7 and C-8) and 28.7 ppm (C-3) being the most upfield. The only CH in the molecule at C-1 was observed at 67.8 ppm, which was confirmed using a DEPT-90 spectrum. The infrared spectra showed a medium stretch at 3306 cm^{-1} for the N-H stretch. The C-H stretches were observed between 2961-2789 cm^{-1}. A positive high resolution mass spectrum was also obtained for this product and showed the protonated molecular ion at m/z = 170.1674 compared to a calculated m/z = 170.1657. An optical rotation, $[\alpha]_D^{20}$ of -11.4 in ethanol, at a concentration of 1 g/100 ml was observed.

2.2.3 Investigation of a Novel Chiral Auxiliary in the Asymmetric α-Alkylation of Ketones

Chiral auxiliary **(*S*)-192** was investigated in the asymmetric alkylation of 3-pentanone **158**. Hydrazone **(*S*)-200** was formed by reaction of hydrazine **(*S*)-192** in cyclohexane, followed by addition of 3-pentanone **158** and 2 grains of *p*-toluenesulfonic acid. This mixture was stirred for 5 h at room temperature, under a nitrogen atmosphere. NMR analysis showed the reaction had gone to completion (Scheme 2.2.12). Diethyl ether was added to the solution and this was washed with water. The organic layers were combined, dried and concentrated under reduced pressure to give the crude product **(*S*)-200** as a yellow oil. This was used in the next step without further purification. We did investigate purification of this hydrazone but found it was problematic. Using column chromatography on alumina gel, only 3% of the pure hydrazone **(*S*)-200** was isolated. We concluded the hydrazone was being retained on the column. The crude product was later deemed to be of sufficient purity for use in the next step.

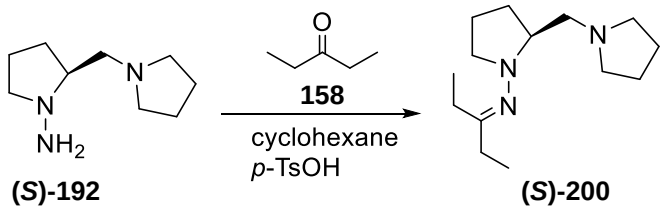

Scheme 2.2.12

The mechanism of this reaction is depicted on Scheme 2.2.13.

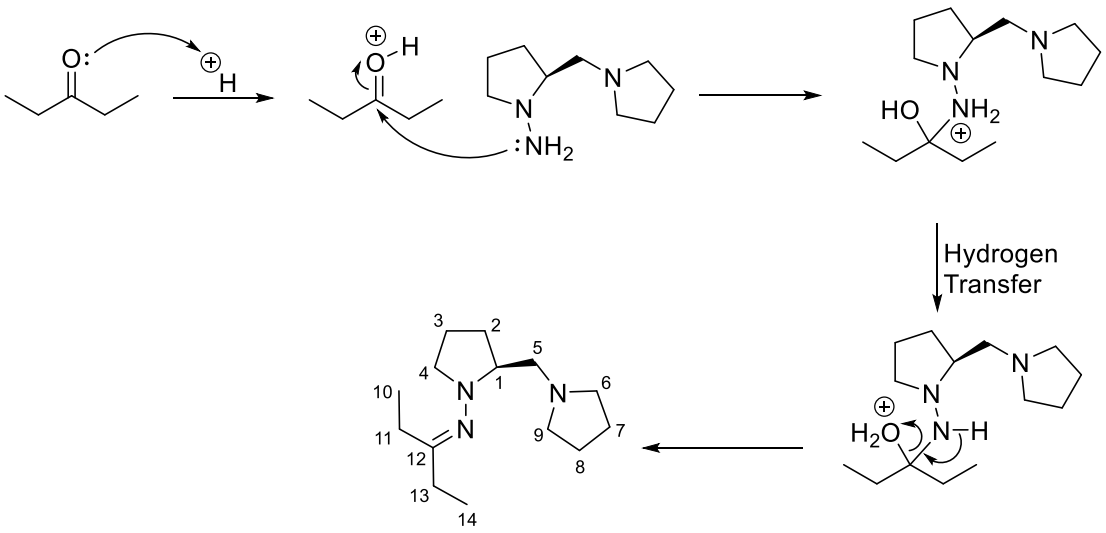

Scheme 2.2.13

The ^{1}H NMR spectra showed two overlapping 3H triplets, at 1.06 and 1.08 ppm for the methyl groups at C-10 and C-14. The methyl group at C-14 is tentatively assigned as the signal at 1.08, being the more downfield of the two methyl groups due to the proximity the nitrogen of the auxiliary through space causing a deshielding effect. In the ^{13}C NMR the distinctive C=N carbon was observed at 173.3 ppm confirming successful formation of the hydrazone **(*S*)-200**. The IR spectrum also confirmed the presence of a C=N group with a strong stretch at 1637 cm^{-1}. The high resolution mass spectrum for the product showed the protonated molecular ion at m/z = 238.2283 compared to the calculated value 238.2277. An optical rotation, $[\alpha]_D^{20}$ of +114.0 in ethanol at a concentration of 1 g/100 ml was recorded for hydrazone **(*S*)-200**.

Chiral hydrazone **(*S*)-200** was than alkylated as follows. Lithium diisopropylamide was freshly prepared. To dry THF, dry diisopropylamine was added at room temperature. This was cooled to 0°C and *n*-BuLi was added dropwise. The reaction mixture was left to stir for 30 min at 0°C, then cooled to -78°C. The hydrazone **(*S*)-200** was added dropwise and stirred for 15 min. The reaction was then returned to room temperature and stirred for 4 h. The reaction was cooled to -110°C (cryocooler temperature) and benzyl bromide was added and allowed to stir for 30 min. The reaction mixture was allowed warm to room temperature overnight. The following day saturated NH_4Cl was added and left to stir for a few min to quench the reaction. The reaction mixture was then extracted with diethyl ether, dried and the solvent removed.

The resulting oil was hydrolysed, using a biphasic 4M HCl/diethyl ether system and vigorous stirring. Once TLC (5 : 1, hexane : diethyl ether) showed the reaction had gone to completion, water was added and the mixture extracted with diethyl ether. The combined organic fractions were combined and dried over anhydrous magnesium sulphate, filtered, and concentrated under reduced pressure. This crude product was then purified using column chromatography on silica gel to give the pure product **(*S*)-36** as a clear oil in a poor yield of 15% (Scheme 2.2.14).

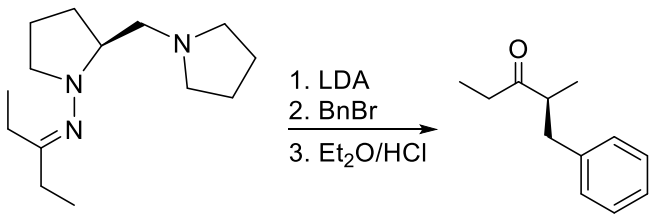

(*S*)-200 **(*S*)-36**

Scheme 2.2.14

All spectroscopic data recorded were consistent with that of **(*S*)-36** obtained previously. GC analysis was carried out using the conditions previously established with racemic **36**, and confirmed that no enantioinduction had occurred and a racemic mixture was obtained (Figure 2.2.2 (a)). This reaction was later repeated by another member of the group and 61% ee was achieved,[165] therefore this result was put down to experimental error.

This reaction was repeated using diethyl ether as the solvent and again the spectroscopic data obtained was consistent with that previously obtained.

We were extremely pleased to obtain an excellent enantiomeric ratio of 6 : 94 when the solvent was changed to diethyl ether. Diethyl ether is evidently the best solvent for this reaction resulting in improved yields and considerably better enantiomeric ratios (Figure 2.2.2 (b)). The results are summarised in the Table 2.2.1.

(a). 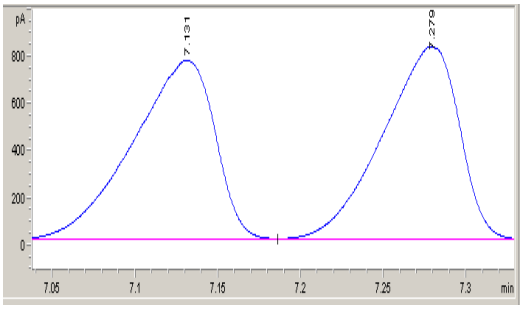

(b). 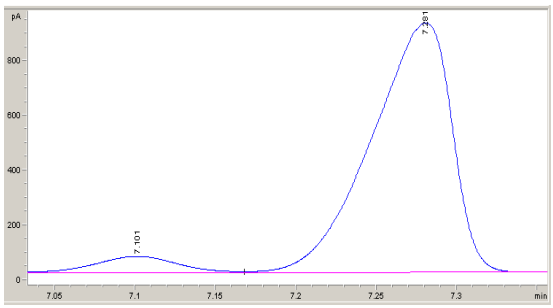

Figure 2.2.2 (a). GC chromatograph for reaction carried out in THF. (b). GC chromatograph for reaction carried out in diethyl ether.

Entry	Solvent	Ketone	Yield[a]	*er R* : *S*	% *ee*
1	THF	**36**	14%	50 : 50	Racemic
1	Et_2O	**(*S*)-36**	33%	6 : 94	88%

[a]Isolated yield is over two steps.

Table 2.2.1 Solvent investigations for asymmetric alkylation using novel chiral auxiliary.

The chiral shift reagent, Europium tris[3-(trifluoromethylhydroxymethylene)-(+)-camphorate] **(+)-201** (Figure 2.2.3) was also used to confirm the enantioselectivity of **(*S*)-36**.

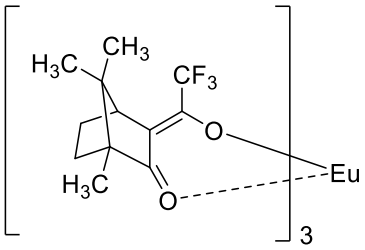

(+)-201

Figure 2.2.3

Chiral shift reagent **(+)-201** was added to a 10 mg sample of racemic **36** in 2 mg increments and the NMR spectrum recorded (Figure 2.2.4). We can see the doublet at 1.08 ppm begins to split into two doublets corresponding to the (*S*)- and (*R*)-enantiomer. The best resolution was obtained with an NMR sample containing 8 mg of europium complex **(+)-201** and 10 mg of ketone in deuterated chloroform.

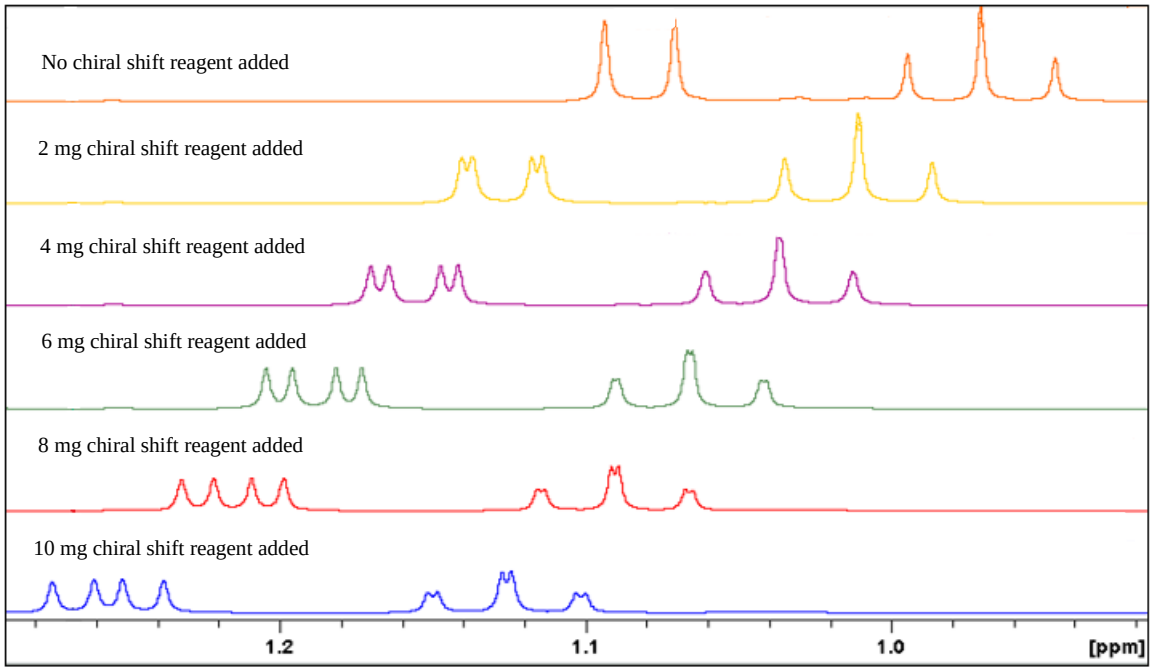

Figure 2.2.4

When these conditions were applied to **(*S*)-36**, full baseline resolution was not achieved. However the good enantioselectivity previously determined by GC was confirmed (**Figure** 2.2.5).

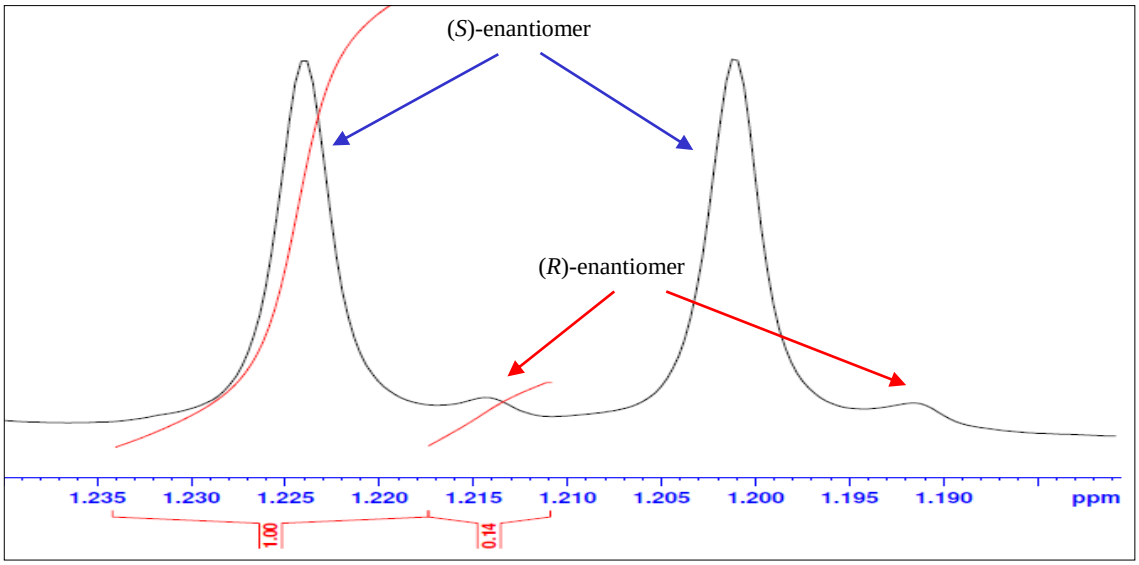

Figure 2.2.5

The mechanism for the hydrolysis step is depicted in Scheme 2.2.15.

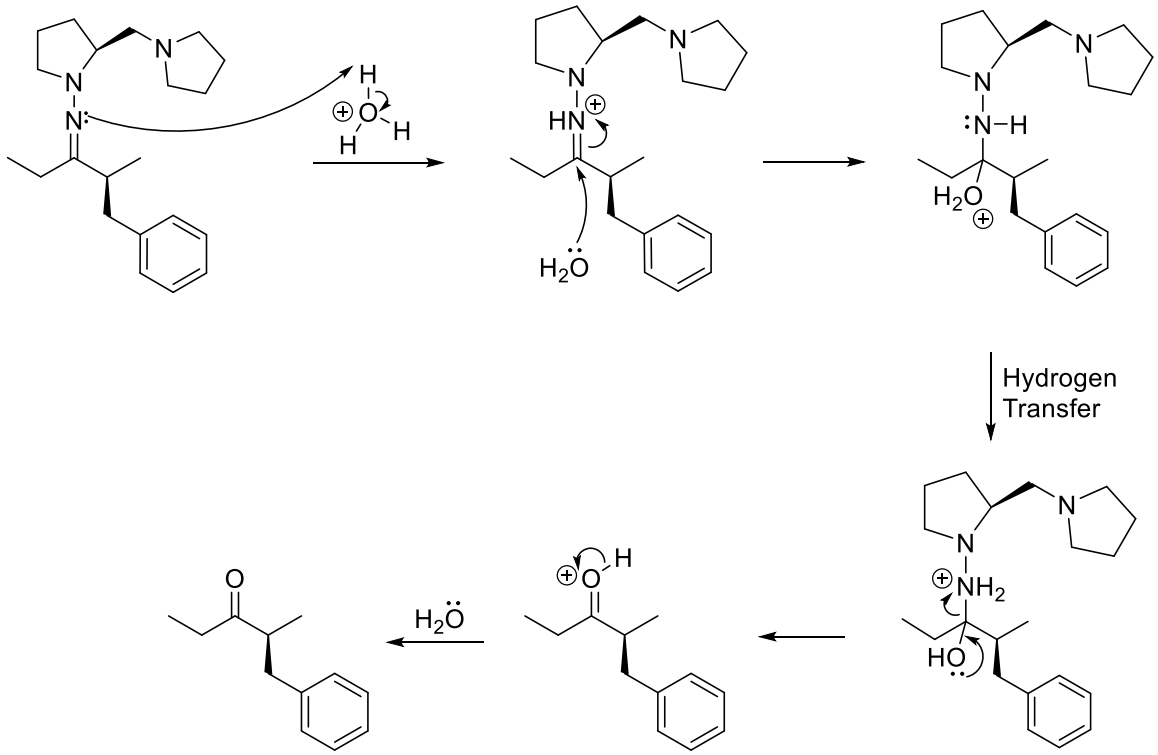

Scheme 2.2.15

We surmise a similar transition state to the SAMP system, involving the selective formation of an $E_{CC}Z_{CN}$ intermediate (Figure 2.2.6). Electrophilic attack is sterically disfavoured from 'above' due to the rigid 5-membered ring. This diastereofacial differentiation results in

diastereomerically enriched hydrazones and ultimately enantiomerically enriched α-substituted ketones upon cleavage of the chiral auxiliary.

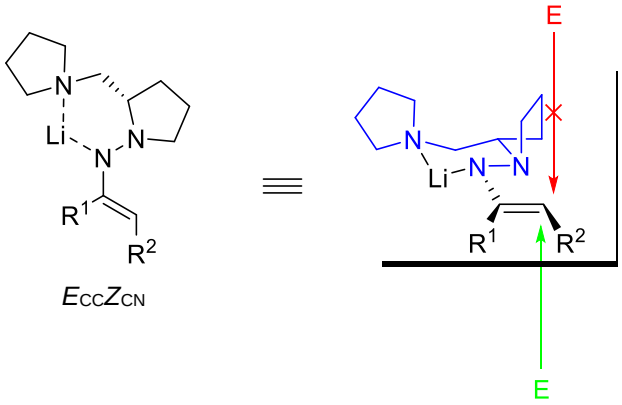

Figure 2.2.6

2.3 Conclusions and Future Work

A novel chiral auxiliary **(*S*)-192** with a pyrrolidine arm was successfully prepared in five synthetic steps from commercially available (*S*)-proline **(*S*)-194**, without the need for column chromatography. This auxiliary **(*S*)-192** successfully effected the asymmetric α-alkylation of the simple aliphatic ketone 3-pentanone **158** in an excellent enantiomeric ratio of 94 : 6 using diethyl ether as solvent. Given the positive results obtained with **(*S*)-192** and its potential to rival the SAMP **(*S*)-9** auxiliary, it was worthy of further optimisation and full substrate scope investigations. The work was subsequently carried on by another member of the group. Optimisation and a full substrate scope was completed and the results were published.[165]

Chapter 3

Intermolecular Chirality Transfer using Sparteine as a Chiral ligand

3.1 Introduction

While we were delighted with the success of the previously discussed chiral auxiliary **(*S*)-192** (as discussed in Chapter 2) we felt this work would only have a moderate impact given the numerous successful auxiliaries available. This prompted us to explore a new protocol for the α-alkylation of ketones. Herein, we present a strategy for the generation of enantiomerically enriched α-alkylated acyclic ketones using an intermolecular chirality transfer protocol, and the results obtained to date are discussed.

Many optically active drugs and natural products contain the α-functionalised ketone moiety. As previously discussed, enantioenriched α-alkylated ketones are very useful synthons and have found widespread use in synthesis.[8-10] Thus, the asymmetric alkylation of ketones represents a very useful transformation in organic chemistry. Surprisingly however, only one effective methodology applicable to simple acyclic ketones exists, and this involves the use of chiral auxiliaries (Scheme 3.1.1).[35]

(i) Ender's SAMP Chiral Auxiliary

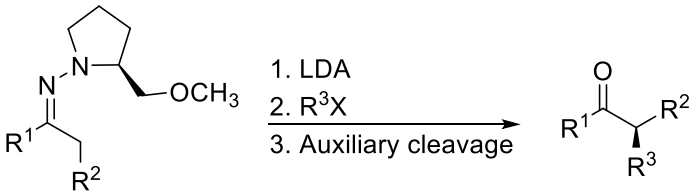

(ii) Coltart's ACC Chiral Auxiliary

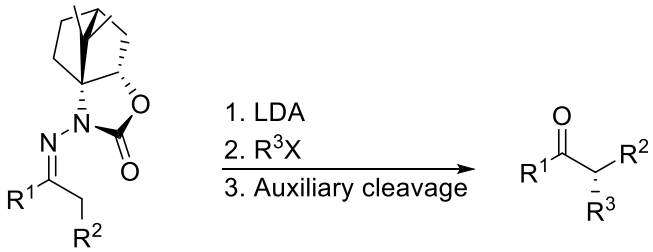

Scheme 3.1.1

The well-known, proline derived, SAMP/RAMP auxiliaries have found numerous applications in asymmetric alkylation (Scheme 3.1.1) (discussed in Chapter 1, Section 1.3).[10] For example, Nicolaou et al. employed the SAMP hydrazone of 3-pentanone in an asymmetric alkylation en route to swinholide A **202** (Scheme 3.1.2).[166,167]

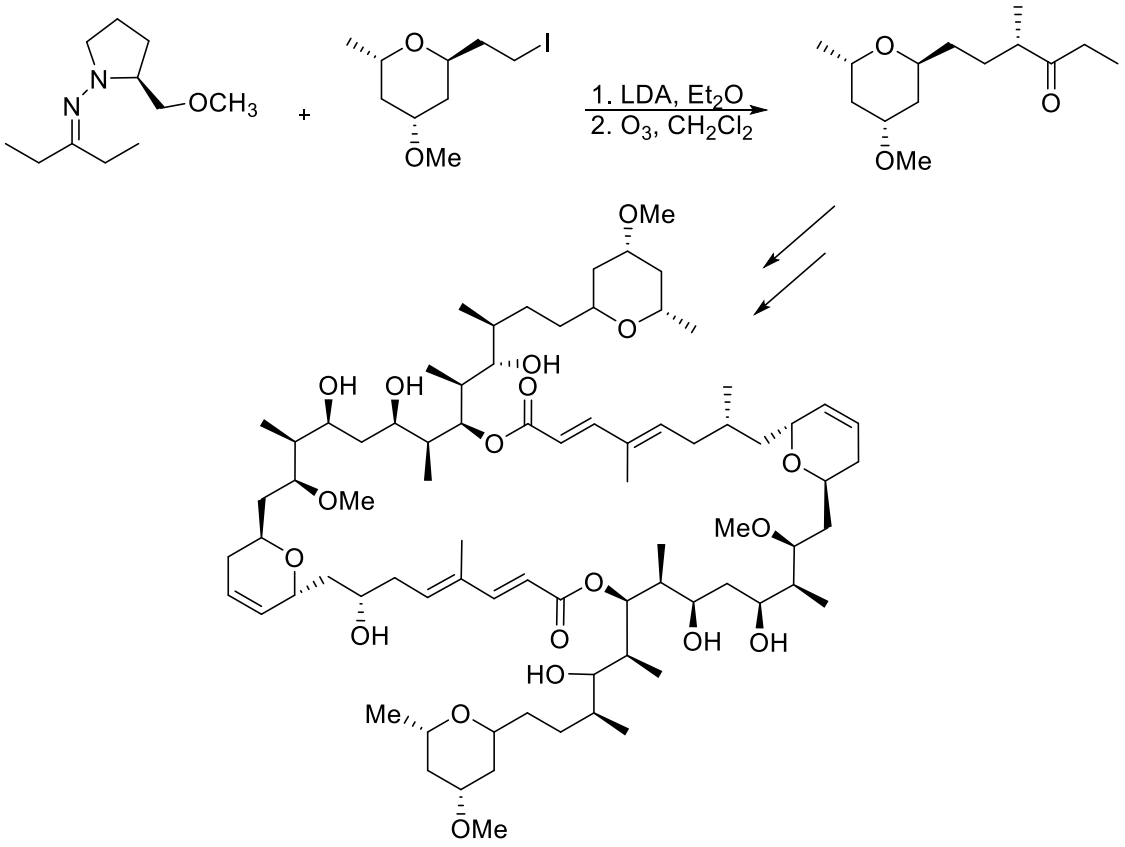

Swinholide A **202**

Scheme 3.1.2

More recently Coltart has introduced *N*-amino cyclic carbamate (ACC) chiral auxiliaries (discussed in Chapter 1, Section 1.3). These auxiliaries do not require the extremely low alkylation temperatures used with SAMP/RAMP hydrazones. The ACC methodology has already been utilised in the synthesis of several biologically important compounds.[38]

Despite advances in the use of homo chiral lithium amide bases,[53,168-170] transition metal catalysis[60,171,172] and organocatalysis, none of these areas of research have managed to achieve the asymmetric α-alkylation of acyclic ketones.[63]

Our approach to enantiomerically enriched α-alkylated ketones involves the use of simple non-chiral dimethylhydrazones and effecting their asymmetric alkylation using a chiral diamine ligand. As we have previous demonstrated (discussed in Chapter 2, Section 2.2.1), the use of lithium bases to furnish small aliphatic α-alkylated ketones, via deprotonation and alkylation of ketones, often proceeds in poor yield.[161]

In light of this, we chose to introduce the dimethylhydrazone methodology into our system, (discussed in Chapter 1, Section 1.6).[173] Hydrazone **203** would act as a ketone surrogate to

facilitate smoother alkylation. We postulated that deprotonation using an alkyl lithium/chiral diamine system would furnish a highly structured azaenolate intermediate **204**, which would benefit from added chelation with the dimethylamino group. In such a rigid system we would expect high facial selectivity to provide chiral, alkylated dimethylhydrazones **(*S*)-205**. Hydrazone cleavage using a biphasic HCl/diethyl ether system would easily return the enantioenriched ketone moiety **(*S*)-206** (Scheme 3.1.3).

Intermolecular Chirality Transfer Methodology

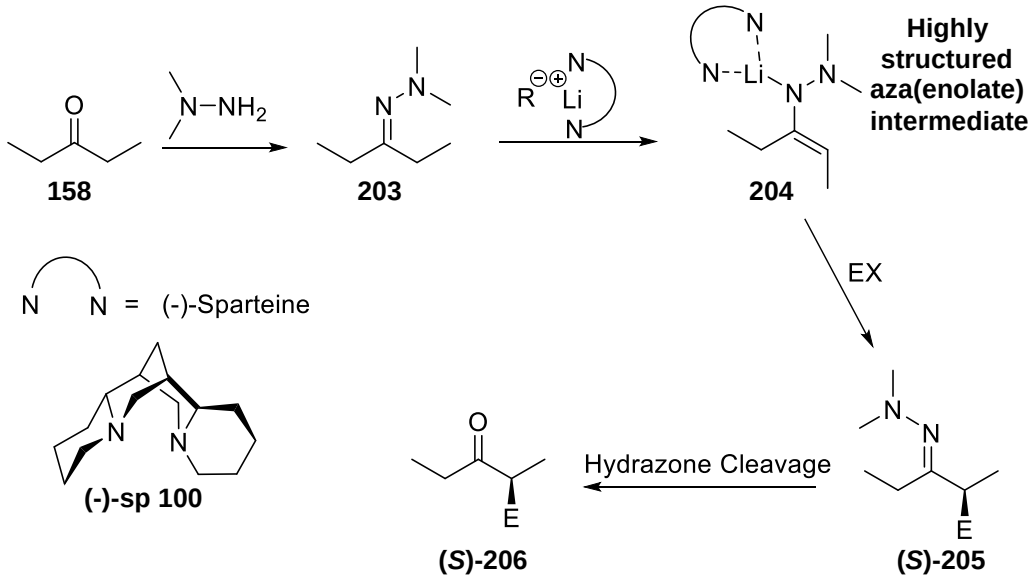

Scheme 3.1.3

Of the numerous chiral diamines available,[85] (-)-sparteine **(-)-sp 100** was chosen as the chiral ligand for this work, as its use in enantioselective synthesis has been heavily documented in the literature.[88] For example, sparteine/lithium systems have proven useful in a number of transformations involving asymmetric deprotonations and substitutions.[97,100,174-180]

3.2 Results and Discussion

3.2.1 Synthesis of *N,N*-Dimethylhydrazones for Asymmetric α-Alkylation via Intermolecular Chirality Transfer

Initial investigations into this methodology were attempted using the parent ketone, however only a trace amount of product, with no enantioenrichment, was detected by GC chromatography. In addition the methyl and methylene regions of the ^{1}H NMR showed a complex array of peaks due to compounds formed from the multiple reactions pathways viable for ketone enolates.[12,13] Therefore the intermolecular chirality transfer methodology was developed using *N,N*-dimethylhydrazones.

During the course of this project a selection of *N,N*-dimethylhydrazones were prepared in excellent yields using *N,N*-dimethylhydrazine, in the presence of a catalytic amount of AcOH, and purified via kugelrohr distillation. (Scheme 3.2.1).

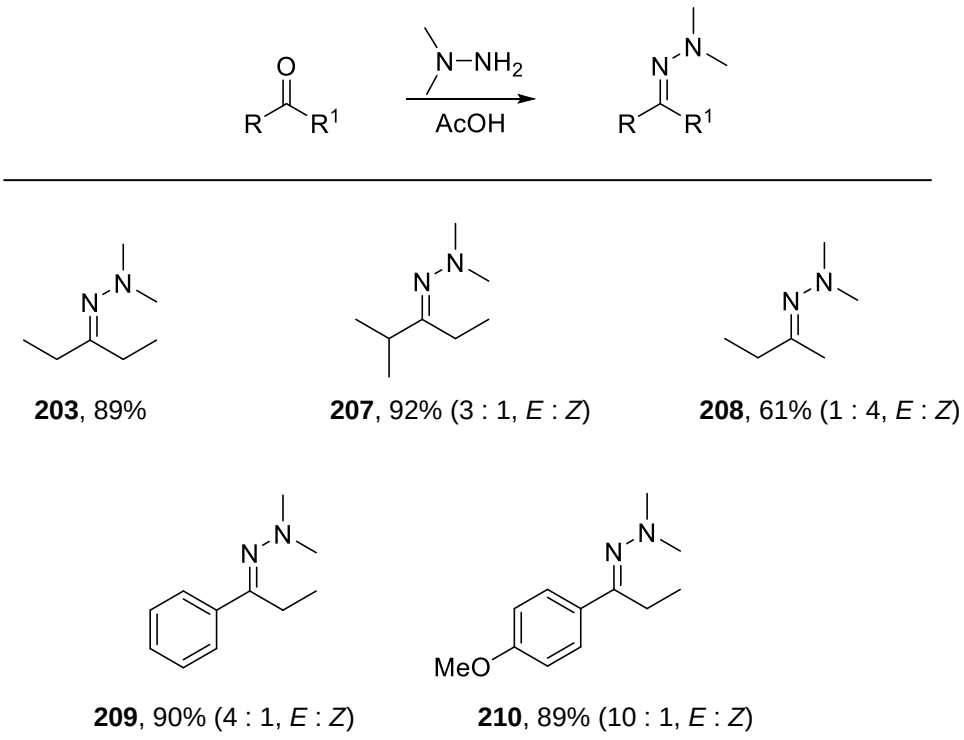

203, 89% **207**, 92% (3 : 1, *E* : *Z*) **208**, 61% (1 : 4, *E* : *Z*)

209, 90% (4 : 1, *E* : *Z*) **210**, 89% (10 : 1, *E* : *Z*)

Scheme 3.2.1

Excellent yields were observed for each of these hydrazones with the exception of hydrazone **208**. A decreased yield of 61% for this compound was due to its volatility and some product was lost upon purification with high vacuum apparatus.

Hydrazone **211** was also prepared during the project for use in the synthesis of a precursor to (*R*)-stigmolone (discussed later in Section 3.2.2).[181] To prepare hydrazone **211**, hydrazone **207** was deprotonated in the presence of freshly prepared LDA in THF at -78°C. The reaction was allowed warm to room temperature and stirred for 6 h. 2-iodopropane was added slowly at -78°C and the reaction allowed warm to room temperature overnight with continued stirring. The reaction was quenched with saturated NH_4Cl, extracted with diethyl ether and the organic layers combined, dried and concentrated under reduced pressure. The ^1H NMR spectrum of the crude reaction mixture showed the reaction had gone to completion. We believe product was lost upon work up and purification of this volatile product as only 37% of pure hydrazone **211** was isolated after column chromatography on silica gel (Scheme 3.2.2). Furthermore, TLC analysis also showed evidence for the cleavage of the hydrazone to its parent ketone upon chromatography which also contributed to the depleted yield.[182] Hydrazone **211** was observed as a mixture of two isomers in 8 : 1 ratio (as determined by NMR of the crude material). The product quickly isomerised to a 1 : 1 ratio over the timescale of purification.

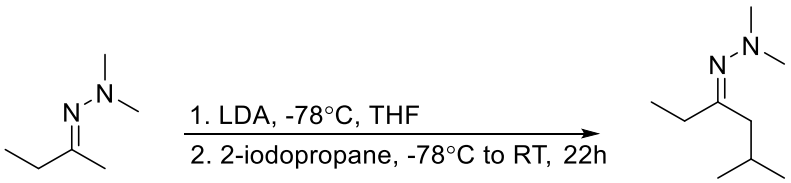

207 **211**, 37%

Scheme 3.2.2

All other unsymmetrical hydrazones **11-15** were also clearly visible as two isomers by NMR spectroscopy. For example, both isomers of hydrazone **210** were clearly distinguishable in the ^1H and ^{13}C NMR spectra. The ratio of isomers was observed as 10 : 1, *E* : *Z*. The major isomer for hydrazones is always the least sterically hindered.[183] Here also, the less sterically encumbered isomer (*E*-configuration) is shown to be the major isomer. This is the favoured configuration as steric interactions between the phenyl group and the dimethyl group are minimised (Scheme 3.2.3).

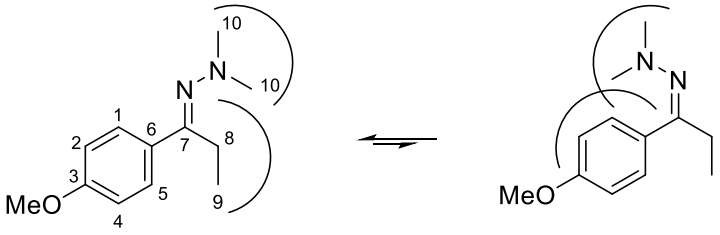

***E*-210** ***Z*-210**

Scheme 3.2.3

	^{1}H NMR				^{13}C NMR				
	H-8	H-9	H-10	OMe	C-7	C-8	C-9	C-10	OMe
***E*-210**	2.88, q, J = 7.6	1.08, t, J = 7.6	2.54, s	3.82, s	169.1	21.5	12.1	47.9	55.3
***Z*-210**	2.51, q, J = 7.6	1.01, t, J = 7.6	2.36, s	3.86, s	166.7	31.4	11.9	47.0	55.4

Table 3.2.1 ^{1}H and ^{13}C NMR spectra of ***E*-210** and ***Z*-210**.

The striking difference between both isomers, is the difference of 10 ppm in the chemical shift of C-8 in the ^{13}C NMR spectrum (Table 3.2.1). It can be seen in Scheme 3.2.3 that the two dimethyl groups may have a shielding effect on C-8 of the *E*-isomer accounting for the up-field resonance. However this effect is not observed in the ^{1}H spectra, the reality is probably more complex and may involve some form of hyper-conjugation.

When a proton is radiated, spatially-close protons may experience an intensity enhancement, which is termed the Nuclear Overhauser Effect (NOE). The NOE is unique among NMR methods because it does not depend upon through-bond couplings but depends only on the spatial proximity between protons.

The NOESY spectrum (Figure 3.2.1) for **210** showed a correlation between the protons of the dimethyl groups at 2.54 ppm and the protons of C-8 at 2.88 ppm, for the major isomer. This correlation indicates that the dimethyl amino group resides on the side of the alkyl groups, confirming ***E*-210** as the major isomer, which is in agreement with a previous report in the literature.[183]

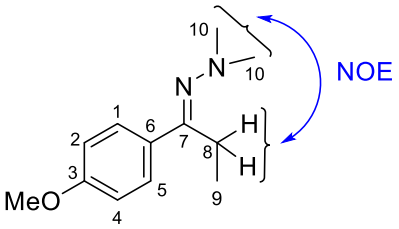

***E*-210**

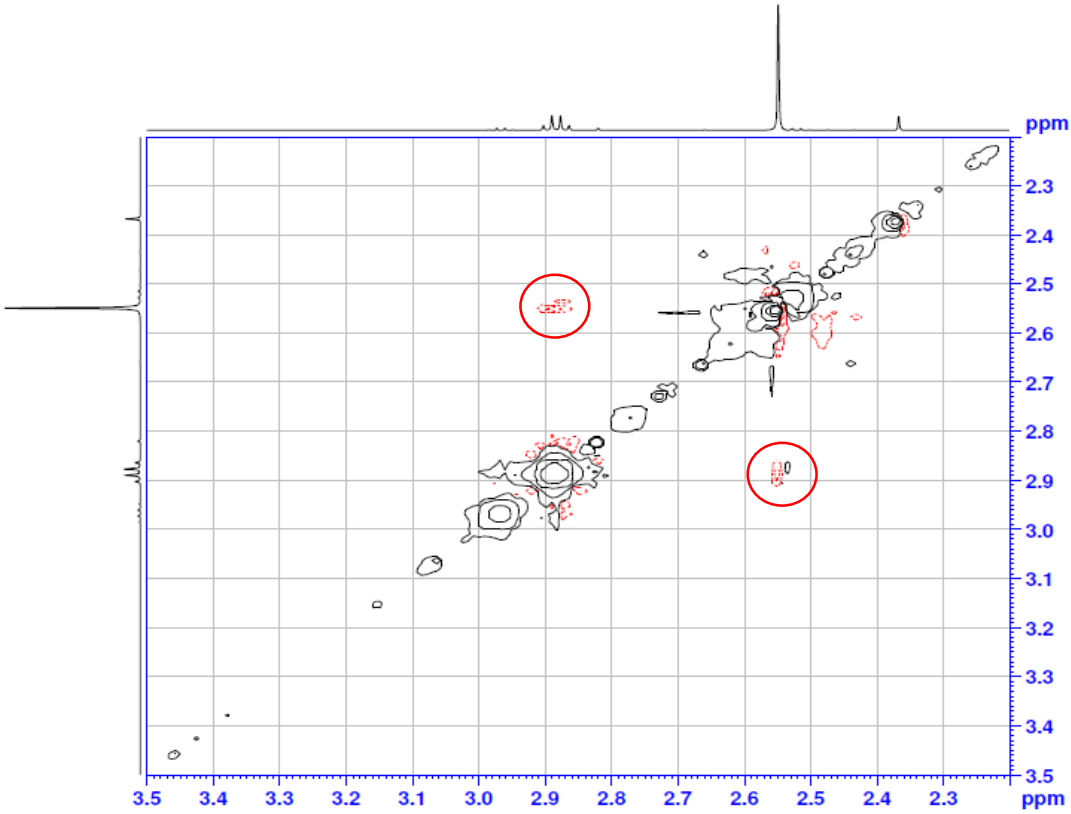

Figure 3.2.1 NOESY sprectrum for ***E*-210**

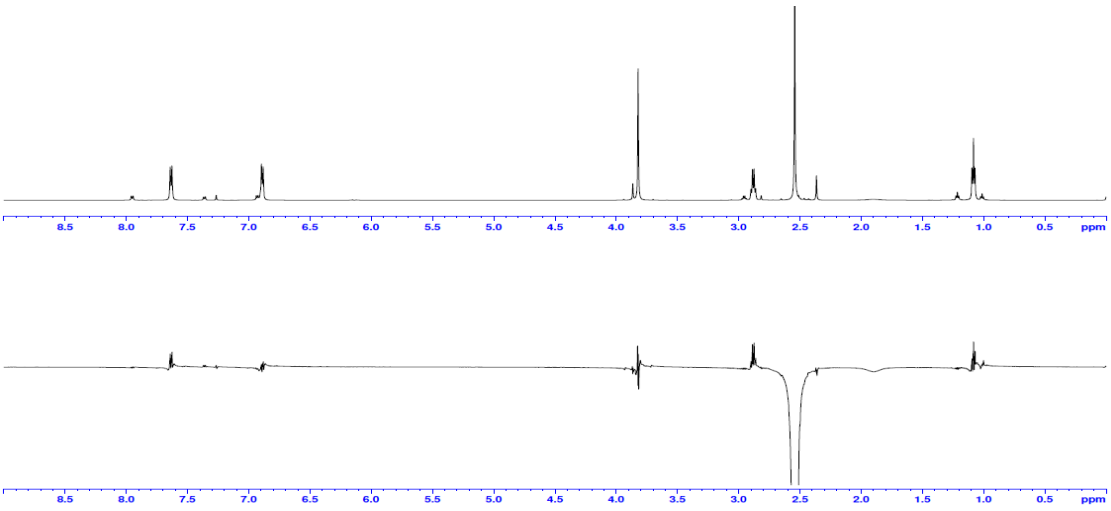

Figure 3.2.2 NOE difference sprectrum for ***E*-210**

This observation was further supported by NOE difference experiments where irradiation of the signal for the dimethyl group protons causes a notable enhancement in the signals for the protons C-8 (2.88 ppm) and C-9 (1.08 ppm), in comparison to the signals for the *ortho*-protons C-1 and C-5 (Figure 3.2.2). This also signified the spatial proximity of the dimethyl groups to the C-8 protons, and hence supported the *E*-configuration. However the NOE detected here is small for the signals at 1.08 and 2.88 ppm.

The size of the NOE enhancement for a particular pair of protons is principally a function of two variables - the primary one is the distance between the 'sending' and 'receiving' protons. The secondary is consideration of what other protons are contributing to the dipole-dipole relaxation of the 'receiving' proton. If there are other protons that are closer than the 'sending' one, then the 'receiving' proton will of inevitability show a smaller NOE enhancement. Thus when a methyl group, for example, is the receiver, the NOE enhancement is always small (<5%) even when the 'sending' proton is very close. This is because each methyl proton has two, much closer, dipole-dipole coupled partners which provide the primary relaxation pathway, resulting in only a small input from more distant protons outside the methyl group.[184] This might explain the small NOE observed here for ***E*-210** between the dimethyl group protons and the protons of C-8 and C-9.

3.2.2 Determination of Optimum Reaction Conditions for Asymmetric α-Alkylation via Intermolecular Chirality Transfer

Hydrazone **203** was chosen as our standard substrate for investigations into asymmetric α-alkylation via intermolecular chirality transfer, because as previously mentioned 3-pentanone **158** is a very useful synthon in the synthesis of natural products.[160,166,167]

These asymmetric alkylation reactions were air sensitive and required a nitrogen environment to proceed. Ligand **(-)-sp 100** and toluene were distilled prior to use and all equipment had to be thoroughly dried. Scheme 3.2.4 shows our model reaction used to establish suitable conditions. Hydrazone **203** was deprotonated in the presence of **(-)-sp 100** and *sec*-BuLi to form azaenolate intermediate **204**. Subsequent reaction with BnBr or iodopentane, yields the enantioenriched hydrazone **(*S*)-205**. The hydrazone moiety was hydrolysed using a biphasic 4M HCl/diethyl ether system to afford benzylated ketone product **(*S*)-36** or **(*S*)-188**. This cleavage method was chosen, as the ketone products could be isolated within 30 minutes.

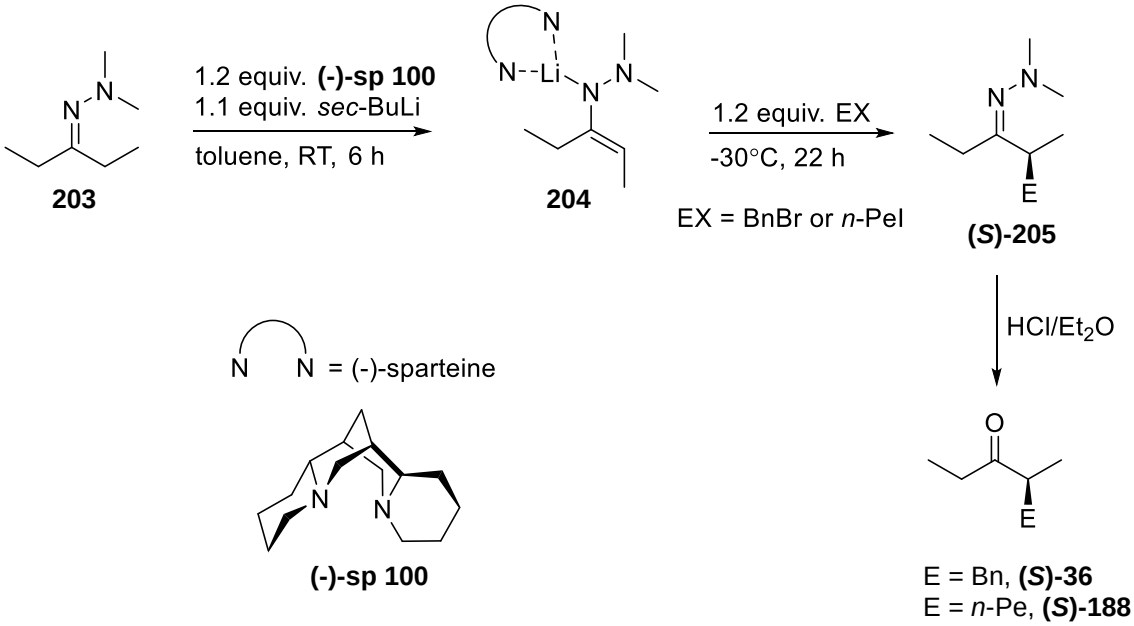

Scheme 3.2.4

Our initial studies focused on establishing the optimum reaction temperature for enantioselectivity to occur. Firstly, keeping the deprotonation constant at room temperature, a range of alkylation temperatures were investigated (Table 3.2.2). Since stereoselective reactions are usually achieved under kinetic control, lower temperatures usually result in higher stereoselectivity.

Entry	Ligand	Deprot. Temp.	Alkyl. Temp.	Solvent	Yield[a]	Ketone	*er R* : *S*	% *ee*
1	**(-)-sp 100**	RT	-78°C to RT	Toluene	53%	**(*S*)-36**	20 : 80	60%
2	**(-)-sp 100**	RT	-70°C	Toluene		no reaction occurred		
3	**(-)-sp 100**	RT	-55°C	Toluene	50%	**(*S*)-36**	28 : 72	44%
4	**(-)-sp 100**	RT	-30°C	Toluene	57%	**(*S*)-36**	24 : 76	52%
5	**(-)-sp 100**	RT	0°C	Toluene	50%	**(*S*)-36**	27 : 73	46%
6	**(-)-sp 100**	RT	RT	Toluene	55%	**(*S*)-36**	29 : 71	42%
7	**(-)-sp 100**	RT	70°C	Toluene	53%	**(*S*)-36**	30 : 70	40%

[a]Isolated yield is over two steps.

Table 3.2.2 Alkylation temperature investigations.

When the reaction was alkylated at -70°C, no reaction occurred (entry 2). Alkylation did take place at -55°C with moderate enantioselectivity (28 : 72 *er*) (entry 3). An improvement in the enantiomeric ratio was observed at -30°C when an enantiomeric ratio of 24 : 76 was achieved (entry 4). As the temperature was increased enantioselectivities began to drop off (entries 5-7). It was interesting to note that when the alkylating agent was added at -78°C and the reaction mixture allowed warm up overnight the best enantioselectivity was achieved (entry 1). However attempts to replicate this result failed, reflecting a rather uncontrolled warm-up protocol. Therefore, an alkylation temperature of -30°C was chosen as our standard going forward.

Before continuing with further studies on this methodology we were eager to ensure racemisation of the chiral centre was not occurring during the acid hydrolysis used for the hydrazone cleavage. To ensure this was not the case, we carried out the hydrolysis for 24 hours and no erosion of enantioselectivity was observed.

We next investigated higher deprotonation temperatures, in an attempt to manipulate the system and produce the thermodynamically most stable azaenolate, which could possibly give better enantioselectivity (Table 3.2.3).

Entry	Ligand	Deprot. Temp.	Alkyl. Temp.	Solvent	Yield[a]	Ketone	*er R* : *S*	% *ee*
1	**(-)-sp 100**	32°C	-30°C	Toluene	45%	**(*S*)-36**	23 : 77	54%
2	**(+)-sp 100**	40°C	-30°C	Toluene	32%	**(*R*)-36**	70 : 30	40%
3	**(-)-sp 100**	40°C	40°C	Toluene	52%	**(*S*)-36**	33 : 67	34%
4	**(-)-sp 100**	70°C	70°C	Toluene	54%	**(*S*)-36**	36 : 64	28%

[a]Isolated yield is over two steps.

Table 3.2.3 Deprotonation temperature investigations.

Unfortunately these efforts did not improve the enantiomeric ratios. While some selectivity is observed, it is quite poor compared to our standard conditions (deprotonation at room temperature and alkylation at -30°C). A marginal increase in enantioselectivity is observed when deprotonation takes place at 32°C, however it was not significant enough to have warranted a change in our standard conditions. A deprotonation time of six hours was found to be necessary in order to produce satisfactory yields. Later NMR investigations (see Section 3.2.9) showed deprotonation was complete in 30 minutes, however, although the enantioselectivities obtained were the same, we could not replicate the yields achieved with the six hour deprotonation.

Next, we examined the outcome of changing the solvent. Again, hydrazone **203** was subjected to sparteine/*sec*-BuLi deprotonation (room temperature for 6 h) and alkylation with either benzyl bromide or 1-iodopentane (-30°C for 22 h), in a range of solvents. The resulting alkylated hydrazones were hydrolysed using the HCl/diethyl ether system and the enantiomeric excess of the ketones **36** and **188** determined (Table 3.2.4).

Entry	Ligand	Electrophile	Solvent	Yield	Ketone	*er R* : *S*	% *ee*
1	**(-)-sp 100**	BnBr	Toluene	57%[a]	**(*S*)-36**	24 : 76	52%
2	**(-)-sp 100**	BnBr	Cumene	62%[b]	**(*S*)-36**	25 : 75	50%
3	**(-)-sp 100**	BnBr	Benzene	45%[a]	**(*S*)-36**	31 : 69	38%
4	**(-)-sp 100**	BnBr	Cyclohexane	23%[a]	**(*S*)-36**	31 : 69	38%
5	**(-)-sp 100**	BnBr	THF	40%[a]	**(*S*)-36**	Racemic	
6	**(-)-sp 100**	*n*-PeI	Toluene	46%[a]	**(*S*)-188**	17 : 83	66%
7	**(+)-sp 100**	*n*-PeI	Et_2O	43%[a]	**(*R*)-188**	78 : 22	56%
8	**(-)-sp 100**	*n*-PeI	MTBE	32%[a]	**(*S*)-188**	33 : 67	34%

[a]Isolated yield is over two steps. [b]Yield determined using NMR and 1,3,5-trimethoxybenzene as internal standard.

Table 3.2.4 Solvent screen.

The enantioselectivity showed a high solvent dependence. Cumene as solvent gave good conversion to alkylated ketone **(*S*)-36** (62% yield by NMR over 2 steps) (entry 2), however complete removal of this high boiling point solvent in the presence of volatile ketones proved difficult and the ketone product was lost as a result. Use of diethyl ether afforded ketone **(*R*)-188** in good enantioselectivity (78 : 22 *er*) and moderate yield (43%) over 2 steps (entry 7). In this case, to demonstrate the accessibility of both enantiomers of the chiral ketone, **(+)-sp 100** was utilised. The use of benzene, cyclohexane and MTBE gave lower enantioselectivity (entry 3, 4 and 8).

Toluene was found to be the prime solvent for these reactions giving the best enantioenrichment of both **(*S*)-36** and **(*S*)-188**, 24 : 76 *er* (entry 1) and 83 : 17 *er* (entry 6), respectively. While conversion to product in toluene was high, yields remained moderate, most likely due to the high volatility of the resulting ketones.

The use of THF as solvent, afforded ketone **(*S*)-36** with no enantioenrichment (entry 5), probably due to competing coordination of THF and **(-)-sp 100** to the lithium. O'Brien and co-workers observed a similar effect in the asymmetric deprotonation of *N*-Boc pyrrolidine in THF.[185] They discovered, via NMR experiments, there is no complexation of **(-)-sp 100** to the *sec*-BuLi in THF until ≥3 equivalents of **(-)-sp 100** is used.

Next we probed the effect of varying the alkyl lithium base. Again, using our standard conditions for deprotonation (room temperature for 6 h) and alkylation (benzyl bromide -30°C for 22 h) the following alkyl- and aryllithium reagents were tested (Table 3.2.5).

Entry	Ligand	Electrophile	Alkyl Lithium Reagent	Yield[a]	Ketone	*er R* : *S*	% *ee*
1	**(-)-sp 100**	BnBr	PhLi	16%	**(*S*)-36**	20 : 80	60%
2	**(-)-sp 100**	BnBr	*n*-BuLi	44%	**(*S*)-36**	28 : 72	44%
3	**(-)-sp 100**	BnBr	*sec*-BuLi	57%	**(*S*)-36**	24 : 76	52%
4	**(-)-sp 100**	BnBr	*t*-BuLi	35%	**(*S*)-36**	24 : 76	52%

[a]Isolated yield is over two steps.

Table 3.2.5 Evaluation of alkyl lithium reagent.

While PhLi gave the best enantioselectivity (20 : 80 *er*), the yield was very poor (16%) (entry 1). Therefore, *sec*-BuLi (entry 3) became the base of choice as it gave the best yield (57 %) of all alkyl lithium reagents screened and its enantioselectivity (24 : 76 *er*) was only marginally less than with PhLi. *t*-BuLi gave the same enantiomeric ratio (24 : 76 *er*) as *sec*-BuLi, however the yield was much lower (35%) (entry 4). Using *n*-BuLi resulted in a moderate yield (44%) and the lowest enantioselectivity (28 : 72 *er*) of all the alkyl lithium reagents investigated (entry 2).

The variance in enantioselectivities observed for the various alkyl lithium reagents could be rationalised by their different aggregate structures when coordinated to sparteine. Strohmann and co-workers have published a comprehensive discussion on the solid-state and solution structures of organolithium reagents.[186] For instance, *n*-BuLi is described as having a hexameric

parent structure (*n*-BuLi)$_6$ (Figure 3.2.3), which deaggregates to a dimeric species upon coordination of sparteine.

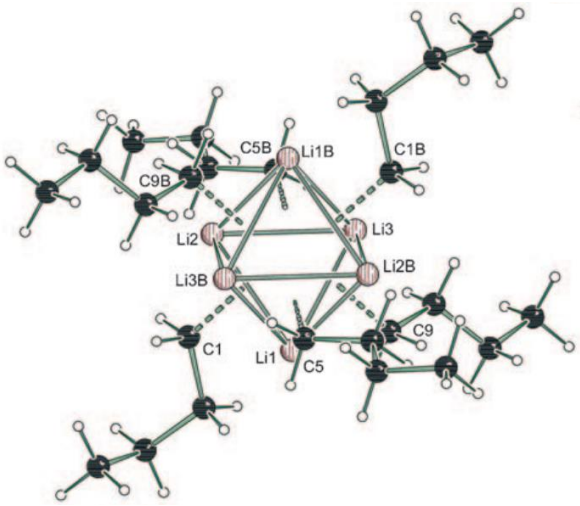

(*n*-BuLi)$_6$

Figure 3.2.3[186]

t-BuLi on the other hand has a tetrameric parent structure (*t*-BuLi)$_4$ (Figure 3.2.4), but is a monomer when coordinated to sparteine (Figure 3.2.4).

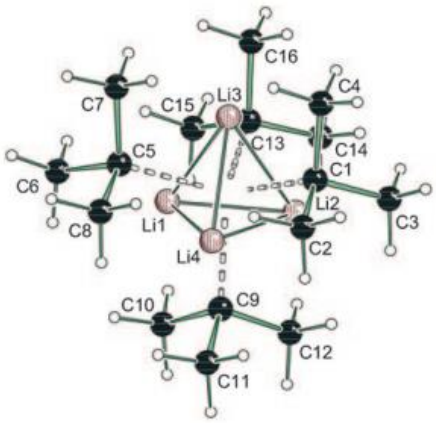

(*t*-BuLi)$_4$

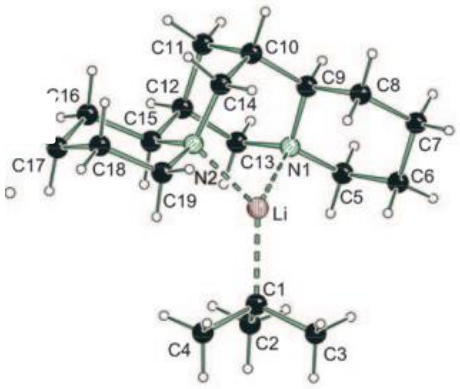

t-BuLi•(-)-sp

Figure 3.2.4[186]

These different aggregate states can often lead to different reactivity.[187] Lower aggregates appear to be more reactive in most cases, but the relative reactivity of aggregates has rarely been determined.[188]

At this stage we considered the different enantioselectivities observed for each alkyl lithium base as evidence for an asymmetric deprotonation mechanism (see Section 3.2.6 for a detailed discussion of possible reaction mechanisms). Certainly, if the reaction takes place via an asymmetric deprotonation step the structure of the alkyl lithium base (monomer or aggregate) would be crucial to the rate and selectivity of deprotonation and thus the enantioselectivity of the alkylated product. However the differences are minimal and an asymmetric alkylation was not ruled out.

3.2.3 Substrate Scope in Asymmetric α-Alkylation via Intermolecular Chirality Transfer

Having established optimal conditions for the asymmetric alkylation, we then explored the scope of the reaction with a range of simple alkyl halides (Scheme 3.2.5).

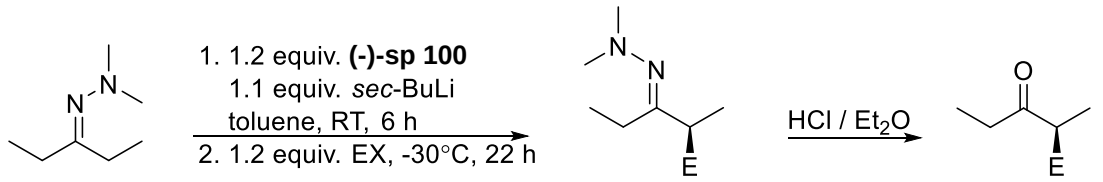

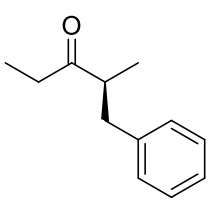

(*S*)-36, 57%
24 : 76 *er* (52% *ee*)

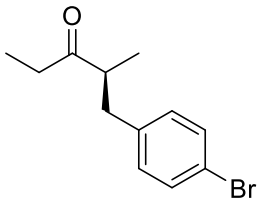

(*S*)-186, 28%
30 : 70 *er* (40% *ee*)

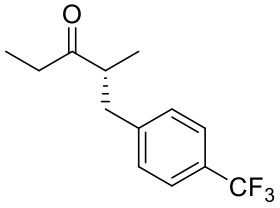

(*R*)-183*, 46%
66 : 34 *er* (32% *ee*)

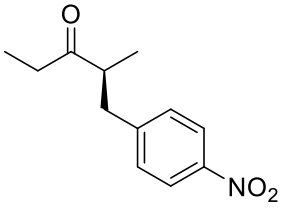

(*S*)-212, 22%
40 : 60 *er* (20% *ee*)

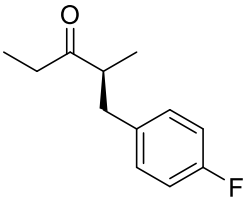

(*S*)-213, 26%
30 : 70 *er* (40% *ee*)

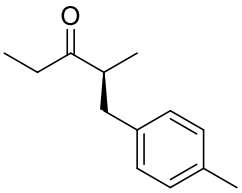

(*S*)-187, 50%
27 : 73 *er* (46% *ee*)

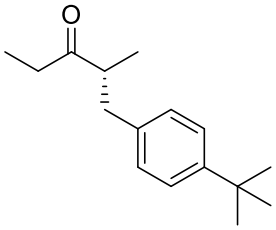

(*R*)-214*, 62%
71 : 29 *er* (42% *ee*)

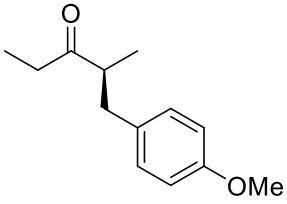

(*S*)-215, 33%
33 : 67 *er* (34% *ee*)

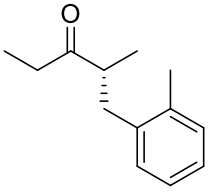

(*R*)-216*, 54%
76 : 24 *er* (52% *ee*)

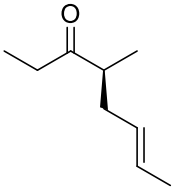

(*S*)-185, 20%
35 : 65 *er* (30% *ee*)

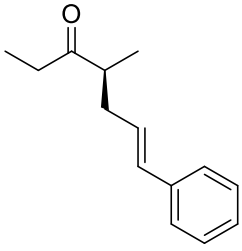

(*S*)-184, 30%
21 : 79 *er* (42% *ee*)

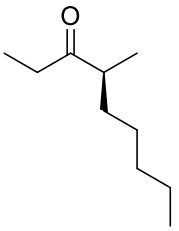

(*S*)-188, 46%
17 : 83 *er* (66% *ee*)

*Note: Change in configuration is due to the use of **(+)-sp 100** as the chiral ligand for these substrates.

Scheme 3.2.5

Carbonyl α-benzylation, leading to the formation of homobenzylic stereocenters, is a significant structural motif incorporated in important biological molecules, including neurotransmitters, hormones and complex metabolites.[189-191] Also their use in hydrazone chiral auxiliary

methodology has been very limited. In fact, no thorough investigation of benzyl based electrophiles has been reported using chiral hydrazone methodology. In light of this we chose a range of benzyl-derived alkylating agents for our initial substrate scope studies. Benzyl bromide gave a moderate yield and enantioselectivity, 57% and 24 : 76 *er*, respectively. An optical rotation of + 31.7 was obtained for this compound. On comparison with a literature value of + 70.9 for the *S*-enantiomer with an *er* of 0.5 : 99.5,[192] we concluded the configuration was also *S*- for our system. This is inferred for other substrates where literature values for optical rotations do not exist.

We also inspected benzyl electrophiles with varying electronic properties. Electron-deficient, *para*-substituted aromatics are interesting from a biological and pharmaceutical stand point as they are more stable towards metabolic oxidation and are used in several industries.[193] In particular nitro-aromatic compounds can resist microbial degradation.[194] In our system these faster reacting electrophiles resulted in a decrease in both yield and enantiomeric ratio (**(*S*)-186**, **(*R*)-183**, **(*S*)-212** and **(*S*)-213**). The *para*-halogenated benzyl bromides (bromine and fluorine) resulted in the same enantiomeric ratios (**(*S*)-186** and **(*S*)-213**, 30 : 70 *er*). The fluorine and trifluoromethyl analogues were also chosen due to the growing importance of organofluoro compounds in the pharmaceutical industry.[195]

The introduction of inductively-electron-donating alkyl groups in the *para* position of benzyl bromides such as **(*S*)-187** (Me), **(*R*)-214** (*tert*-butyl), also led to a decrease in enantiomeric ratio, 27 : 73 *er* and 71 : 29 *er* respectively. However, the effect was less dramatic than that observed with electron-withdrawing substituents. Also the strongly, resonance donating methoxy group **(*S*)-215** resulted in a greater decrease in enantioselectivity (33 : 67 *er*), as well as a decrease in yield.

2-Methylbenzyl bromide was utilised in order to install a small steric repulsion on approach of the electrophile (**(*R*)-216,** 76 : 24 *er*). A slight increase in selectivity was observed for this electrophile over its 4-methyl analogue.

It was interesting that crotyl bromide resulted in poor yield and selectivity (**(*S*)-185**, 20%, 35 : 65 *er*), but on changing the methyl group of crotyl bromide to a phenyl substituent, a substantial increase in enantiomeric ratio was observed (**(*S*)-184**, 21 : 79 *er*). Introduction of the *n*-pentyl moiety required use of an iodide leaving group and we were pleased to discover this slower

reacting electrophile resulted in the highest enantioenrichment achieved to date (**(*S*)-188**, 17 : 83 *er*).

While the yields remain moderate for most of these substrates, increased yields were observed for electrophiles resulting in less volatile ketone products (**(*R*)-214** 62%, 71 : 29 *er*).

Dimethylhydrazones derived from non-C_2 symmetric ketones and aryl ketones were then subjected to our optimised conditions. Hydrazone **207** (prepared as discussed in Section 3.2.1) was deprotonated using sparteine/*sec*-BuLi under the standard conditions (room temperature for 6 h), and alkylated (-30°C for 22 h), with benzyl bromide to afford the product **(*R*)-189** (48%, 54 : 46 *er*) after hydrolysis (Scheme 3.2.6).

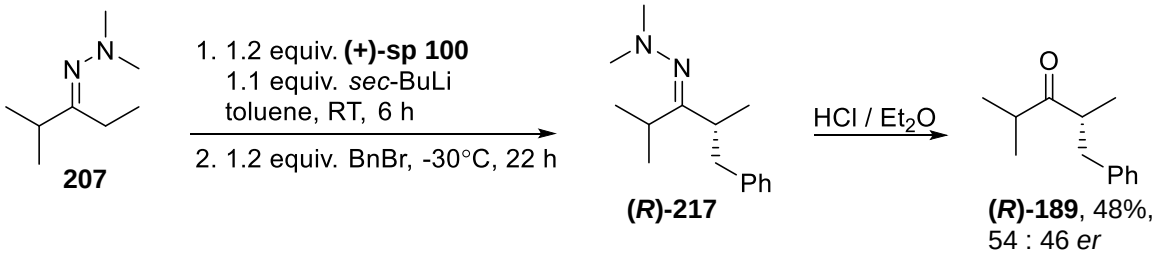

207 **(*R*)-217** **(*R*)-189**, 48%, 54 : 46 *er*

Scheme 3.2.6

A dramatic decrease in enantioselectivity is observe for this substrate in comparison to the 3-pentanone analogues. This may be due to its non-symmetrical nature, which may lead to the formation of a different aza(enolate), which does not result in the same high facial selectivity as observed with 3-pentanone substrates.

The use of hydrazones **209** and **210** also led to disappointing results (Scheme 3.2.7).

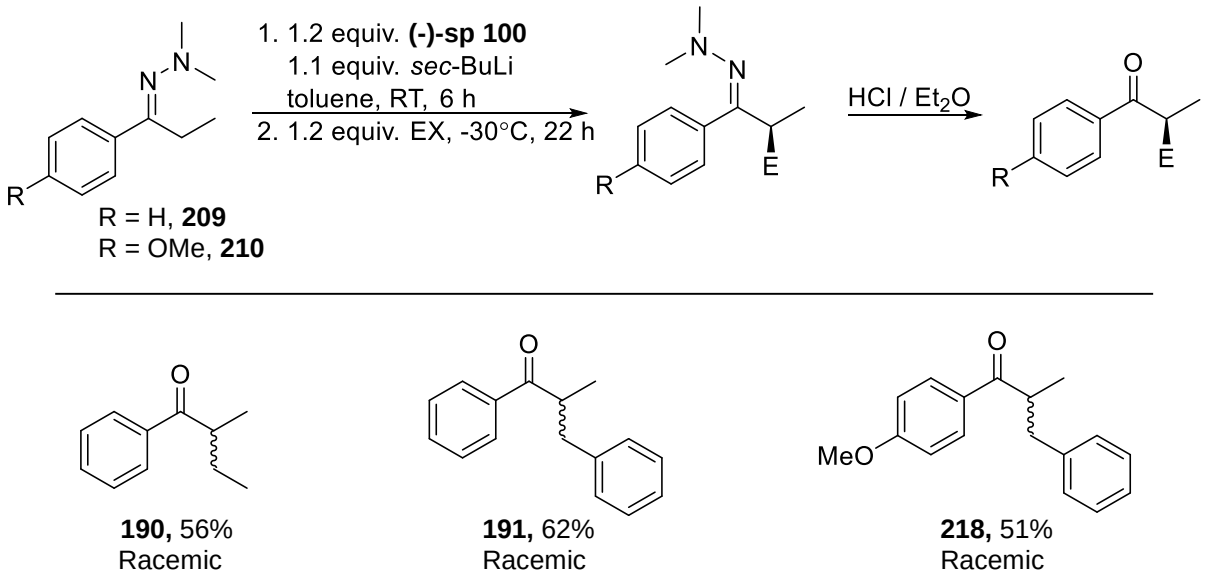

Scheme 3.2.7

Here hydrazones **209** and **210** were deprotonated using sparteine/*sec*-BuLi (room temperature for 6 h) and alkylated (-30°C for 22 h) with ethyl iodide or benzyl bromide. After cleavage of the hydrazone, the parent ketones were isolated as racemic mixtures, in all cases for **190**, **191** and **218**. We believe these disappointing results were due to the unsymmetrical nature of the hydrazone, as was observed above for **(*R*)-189**. Again a different geometry of the azaenolate may arise, resulting in a transition state where facial discrimination does not occur.

Another possible explanation for this observation could be racemisation of the chiral centre during cleavage of the hydrazone. Cleavage of the hydrazone was carried out using the biphasic diethyl ether/HCl system. It is possible that the lack of an additional enolisable site alpha to the carbonyl on the opposite side of the chiral centre results in racemisation (Scheme 3.2.8). No other cleavage protocols were investigated for these substrates.

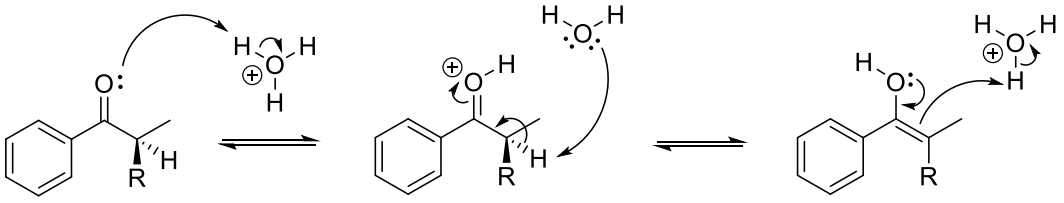

Scheme 3.2.8

A possible test to investigate this theory going forward, would be to carry out the hydrolysis in deuterium chloride (DCl) and deuterium oxide (D_2O), and monitoring deuterium incorporation at the chiral centre.

We also extended this methodology to the preparation of **(*R*)-219** from hydrazone **211** (prepared earlier in Section 3.2.1). **(*R*)-219** is a precursor in the synthesis of stigmolone **(*R*)-220**, an aggregation pheromone of the myxobacterium *Stigmatella aurantiaca* (Scheme 3.2.9).[181]

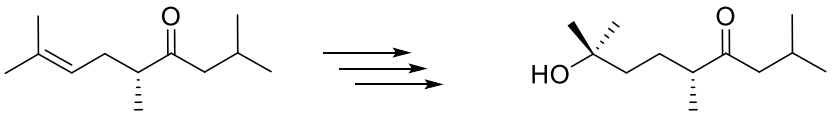

(*R*)-219 **(*R*)-220**

Scheme 3.2.9

Hydrazone **211** was alkylated using our intermolecular chirality transfer protocol with 3,3-dimethylallyl bromide under the standard conditions (deprotonation at room temperature for 6 h and alkylation at -30°C for 22 h) (Scheme 3.2.10).

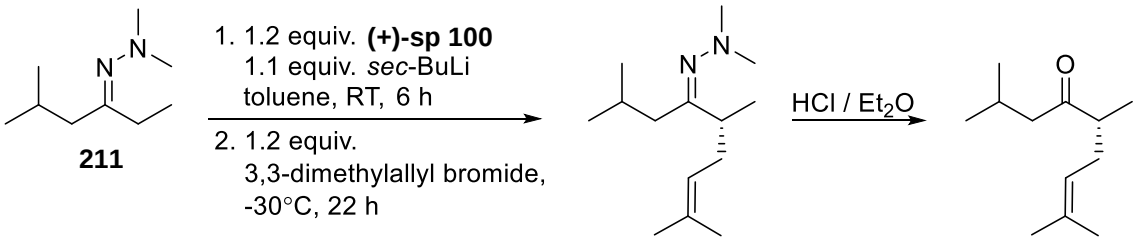

(*R*)-221 **(*R*)-219**, 28%, 65 : 35 *er*

Scheme 3.2.10

Again a decrease in enantioselectivity is observed for this substrate in comparison with the 3-pentanone analogues. In light of the poor selectivity obtained in the synthesis of **(*R*)-219** we did not continue the synthesis of stigmolone **(*R*)-220**.

3.2.4 Yield Optimisation for Asymmetric α-Alkylation via Intermolecular Chirality Transfer

Given that good yields were observed for ketone **(*R*)-214** (62%, 71 : 29 *er*), this substrate was used to investigate other work up conditions to maximise recovery and further improve yields.

The standard work-up conditions used to give 62% yield involved addition of saturated ammonium chloride to the reaction mixture at -30°C to quench the reaction. The mixture was then allowed warm to room temperature. Diethyl ether was added and the mixture was washed with ammonium chloride which removes sparteine. The organic layer was dried, and concentrated under reduced pressure. The crude hydrazone was subjected to the HCl hydrolysis method and the crude ketone purified using column chromatography to give **(*R*)-214** as a clear oil in 62% yield and 71 : 29 *er*.

Juaristi and co-workers have previously employed a methanol quench in reactions involving sparteine/lithium complexes.[196] Applying this protocol to our reaction conditions, methanol was added to the reaction mixture at -30°C. Once the reaction mixture had warmed to room temperature, it was concentrated under reduced pressure. Water was added to the residue and following extraction with diethyl ether, the organic layers were combined, dried and concentrated under reduced pressure. The crude hydrazone was purified using column chromatography to give the pure hydrazone which was immediately subjected to the HCl hydrolysis method. The crude ketone was also purified using column chromatography and the title compound **(*R*)-214** isolated in 53% yield and the same enantiomeric ratio of 71 : 29 *er*.

We also investigated the use of a pH 7 buffer solution to quench the reaction. This protocol had previously been utilised by Enders in the synthesis of (*E*)-(*S*)-4-methyloct-6-en-3-one **(*S*)-185**.[197] Thus a pH 7 buffer solution was added to the reaction mixture at -30°C and allowed warm to room temperature. The mixture was then extracted with diethyl ether. The organic layers were combined, dried and concentrated under reduced pressure. The crude hydrazone was purified using column chromatography to remove the ligand before hydrolysis. The pure hydrazone was immediately subjected to the HCl hydrolysis method. The crude ketone was also purified using column chromatography and the title compound **(*R*)-214** isolated in 53% yield and an enantiomeric ratio of 71 : 29 *er*.

Each of the three work-up conditions provided products with the same enantioselectivities for the product (**(*R*)-214**, 71 : 29 *er*), however a decreased yield was observed when the methanol

quench and pH 7 buffer solution quench methods were employed. The loss of yield for both methods can be attributed to the additional chromatography step of the hydrazone. The hydrazones from both of these methods required purification to remove the chiral ligand before hydrolysis in order to avoid sparteine disrupting the hydrolysis step. In the cases where an ammonium chloride wash was incorporated, all traces of sparteine were removed and therefore purification of the hydrazone was deemed unnecessary.

3.2.5 Further Studies of Hydrazone Cleavage Methods

Upon reading a report by Smith and co-workers,[198] we decided to revisit the issue of racemisation during the cleavage of the hydrazone.

During a synthetic program directed towards the total synthesis of (+)-nodulisporic acid A, Smith and co-workers observed epimerisation during the cleavage of the SAMP auxiliary via hydrolytic cleavage using oxalic acid. They eventually, successfully cleaved the auxiliary using an oxidative protocol using pH 7 buffered peroxyselenous acid conditions.[198] Peroxyselenous acid, generated in situ from SeO_2 and 30% H_2O_2 (1 : 4) was a superior oxidant for the removal of the chiral auxiliary from SAMP hydrazones, however some epimerization was observed.[198] The epimerization problem was alleviated by the introduction of a pH 7 buffer.

We applied Smith's optimised conditions for the cleavage of the dimethyl hydrazone of **(*R*)-216**. Hydrazone **203** was subjected to asymmetric alkylation using **(+)-sp 100** to form hydrazone **(*R*)-222**, which was cleaved using SeO_2, 30% H_2O_2 and a pH 7 phosphate buffer. **(*R*)-216** was isolated in 46% yield over two steps with the same enantiomeric ratio as that observed using the biphasic system of diethyl ether/4 M HCl (76 : 24 *er*) (Scheme 3.2.11).

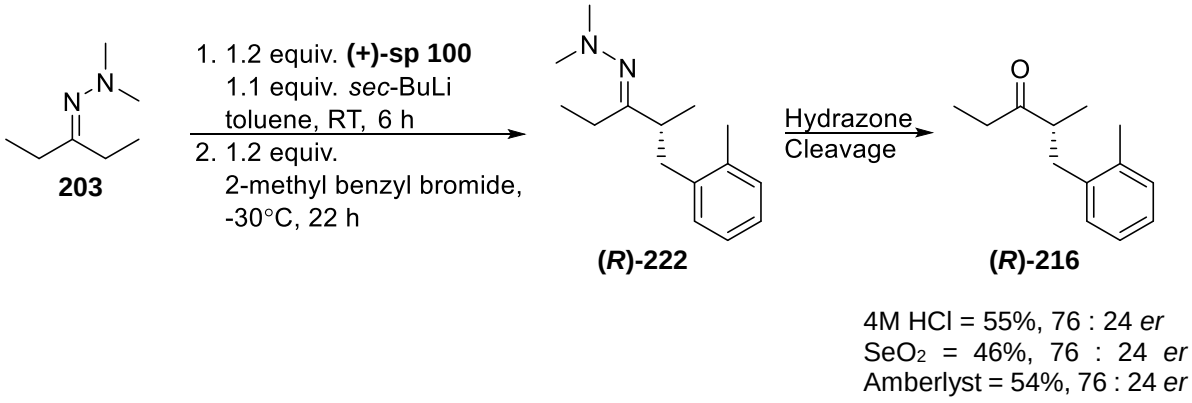

Scheme 3.2.11

The mechanism for the pH 7 buffered peroxyselenous acid cleavage is shown in (Scheme 3.2.12).

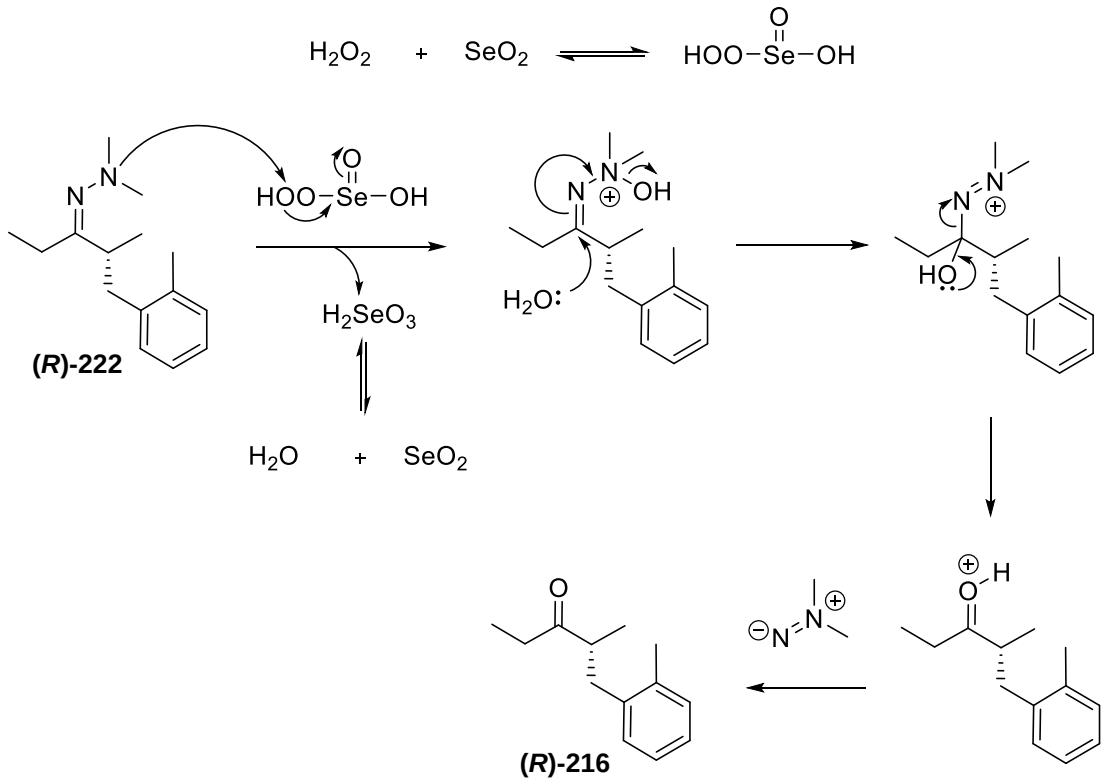

Scheme 3.2.12

Amberlyst® 15 hydrogen form beads have also been described as an excellent and far superior catalyst for regeneration of carbonyl compounds from nitrogeneous derivatives, like tosylhydrazones, oximes, 2,4-dinitrophenylhydrazones and semicarbazones.[199] In our system the use of Amberlyst® 15 refluxing in acetone/water resulted in isolation of **(*R*)-216** in 54% yield over the two steps and 76 : 24 *er* (Scheme 3.2.11).

Given that the same enantioselectivities were observed for all three cleavage procedures we were confident that racemisation was not occurring during hydrolytic cleavage using diethyl ether/4 M HCl.

3.2.6 Addition of Lithium Salts

Organolithium reagents are known to exist as aggregated species in solution.[186] The degree of aggregation strongly depends on the carbanion structure, solvent polarity, and the presence of donor ligands like TMEDA, PMDTA and HMPA. Sometimes the observed aggregates are the actual reactive species; elsewhere, lower aggregates have been shown to be active.[187,200]

If aggregation was a potential problem in our system, we felt using aggregate-breaking additives, such as lithium halide salts, in the reactions may improve results (Table 3.2.6).

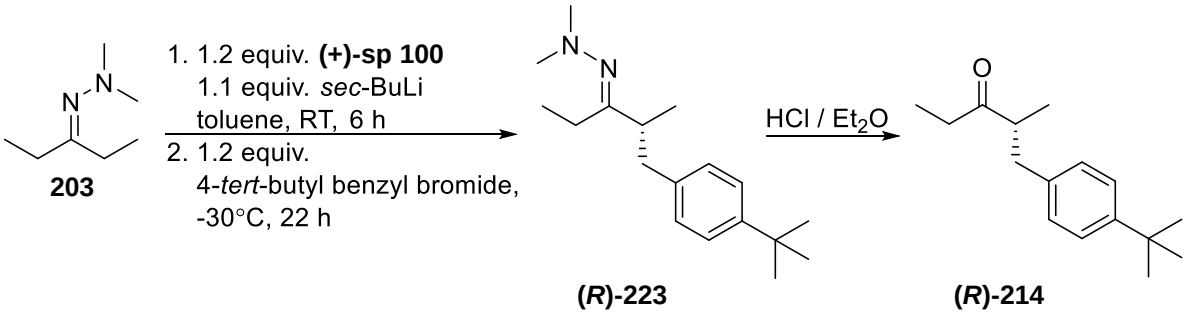

Entry	Ligand	Lithium Salt	Yield[a]	Ketone	*er R* : *S*	% *ee*
1	**(+)-sp 100**	LiCl	35%	**(*R*)-214**	69 : 31	38%
2	**(+)-sp 100**	LiBr	9%	**(*R*)-214**	59 : 41	18%
3	**(+)-sp 100**	LiI	7%	**(*R*)-214**	61 : 39	22%
4	**(+)-sp 100**	LiBr	59%	**(*R*)-214**	71 : 29	42%[b]

[a]Yield determined using NMR and 1,3,5-trimethoxybenzene as internal standard. [b]2 equiv. lithium bromide were added after the deprotonation and allowed to stir for 45 min at room temperature, before cooling to -30°C for alkylation.

Table 3.2.6 Addition of Lithium Additives.

The addition of the lithium halogen salts had a detrimental effect both on yield and enantioselectivity. In the case of entries 1-3, the additive was introduced at the beginning of the reaction. In entry 4 lithium bromide was added after deprotonation, and a far less adverse effect was observed on both enantioselectivity and yield. This led us to believe that these additives prevented deprotonation from taking place, not alkylation. Although aggregate-breaking additives have been shown to work well in other systems, lithium halogen salts were not amenable to good yields or enantioselectivities in our system.

3.2.7 Mechanistic Investigations

During the course of this project, we also undertook a mechanistic study in the hope that by gaining an insight into how the reaction progresses we would be better equipped to optimise and improve enantiomeric induction in these reactions.

Typically, the introduction of asymmetry in a chiral ligand mediated lithiation-substitution requires diastereomeric interactions in an intermediate or transition state. In these types of systems the enantiodetermining step can be either the lithiation step, i.e. asymmetric deprotonation or a post-deprotonation step, i.e. asymmetric substitution (Scheme 3.2.13).

In an asymmetric deprotonation, an organolithium reagent is complexed to a chiral ligand. This chiral base selectively abstracts an enantiotopic proton from a prochiral substrate **224**. The enantioenriched organolithium intermediate **225•L** is usually configurationally stable and reacts with an electrophile maintaining stereochemical integrity and providing the enantioenriched product **226**. In an asymmetric substitution, the enantiodetermining step occurs after deprotonation. This racemic organolithium **225** can afford enantioenriched product **226**, on reaction with an electrophile, under the influence of the chiral ligand.[201]

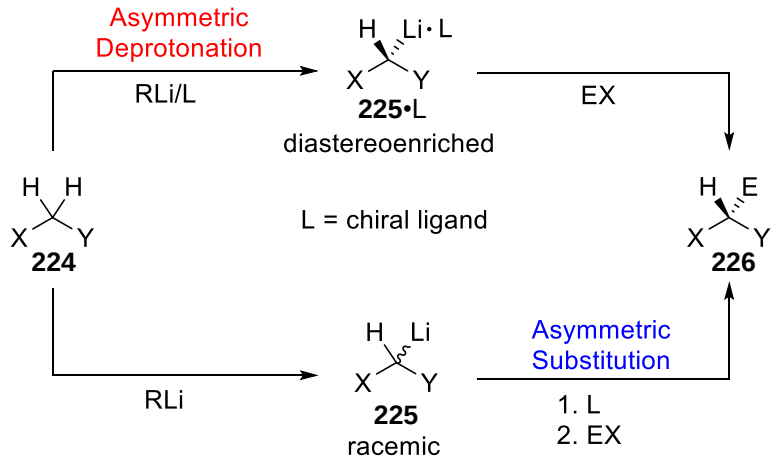

Scheme 3.2.13

In an attempt to distinguish between these pathways in our intermolecular chirality transfer alkylations, we undertook an experiment where hydrazone **203** was deprotonated for 6 hours using *sec*-butyllithium, in the absence of any chiral ligand. **(-)-Sp 100** was then added to the reaction at room temperature and allowed to complex for 45 minutes. Alkylation with benzyl bromide at -30°C and hydrazone cleavage resulted in formation of **(*S*)-36** with an enantiomeric

ratio that is comparable to that obtained when the chiral ligand is present from the start (Table 3.2.7).

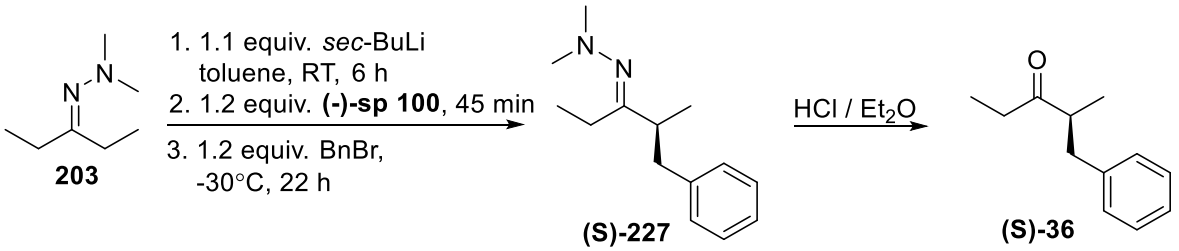

Entry	Ligand	Variation	Electrophile	Yield[a]	*er R* : *S*	% *ee*
1	**(-)-sp 100**	**(-)-sp 100** added @ RT after deprot.[b]	benzyl bromide	25%	23 : 77	54%
2	**(-)-sp 100**	**(-)-sp 100** present for deprot.	benzyl bromide	57%	24 : 76	52%

[a]Isolated yield over two steps. [b]Ligand was added after the deprotonation and allowed to stir for 45 min, before alkylation @ -30°C.

Table 3.2.7 Mechanistic Investigations.

These results show that the enantioselectivity of this reaction can be established after the deprotonation. However, it does not explicitly rule out the possibility of an initial asymmetric deprotonation followed by formation of a planar azaenolate and asymmetric alkylation, or initial asymmetric deprotonation followed by an interconverting species, then an asymmetric alkylation.

While the pathway of asymmetric deprotonation is well documented, transfer of stereoinformation in a post-deprotonation step (the pathway of asymmetric substitution) is less so. Asymmetric substitutions are applicable to organolithium intermediates regardless of their mode of formation and can involve configurationally labile carbanions.[202]

Two limiting pathways have been postulated to rationalize enantioselectivities observed in asymmetric substitutions. In one pathway deprotonation of **224** followed by complexation with the ligand results in the formation of diastereomeric complexes (**225**•L and *epi*-**225**•L) which are configurationally stable (not interconverting) with respect to their rate of reaction with the electrophile. The diastereomeric complexes (**225**•L and *epi*-**225**•L) are formed in a fixed ratio and both react with the electrophile at a similar rate to form the enantioenriched product **226**. *Epi*-**225**•L would also react with EX to give the other enantiomer of **226** (not shown). In this case the enantioselectivity of the products is determined by the ratio of the diastereomeric

complexes established before the substitution step. This is termed **Dynamic Thermodynamic Resolution** (DTR) because the ratio of complexes is dynamically controlled prior to reaction with electrophile (Scheme 3.2.14).

Dynamic Thermodynamic Resolution

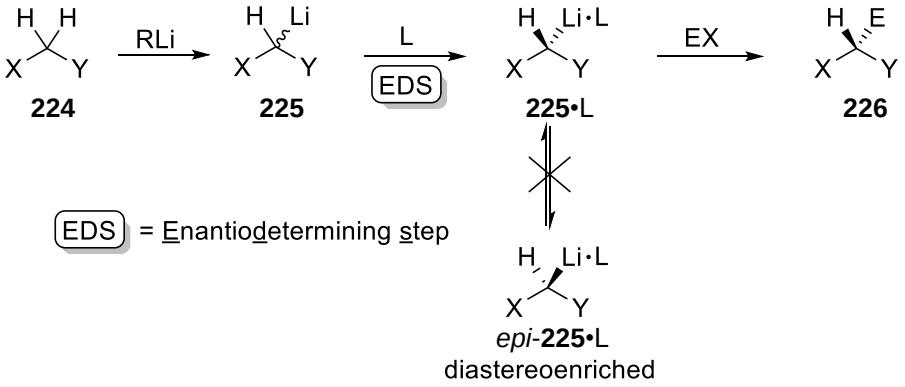

Scheme 3.2.14

In the other pathway, the diastereomeric complexes (**225**•L and *epi*-**225**•L) are configurationally labile (rapidly interconverting) with respect to their rate of reaction with the electrophile. Here, the stereogenic reactive centre undergoes rapid epimerization and one of the diastereomeric complexes reacts faster with the electrophile than the other epimer, under the reaction conditions, to form the enantioenriched **226**. In this case, the enantioselectivity is determined by the difference in the diastereomeric transition state energies for the reaction with the electrophiles, i.e. the rates of reaction will determine the enantioselectivity of **226**. This is a case of **Dynamic Kinetic Resolution** (DKR) (Scheme 3.2.15).

Dynamic Kinetic Resolution

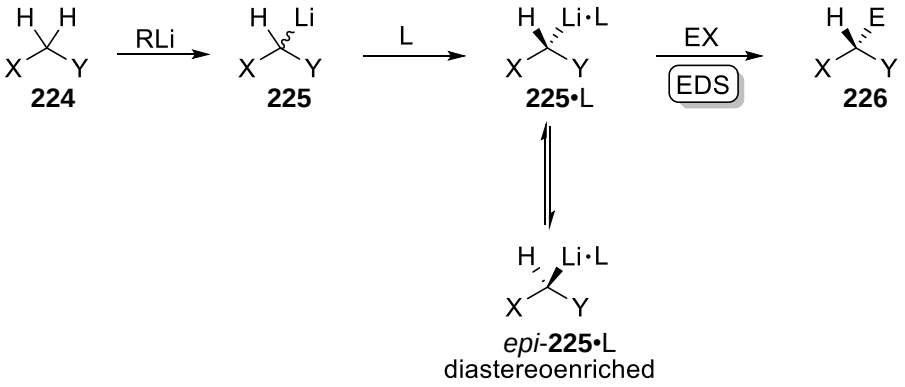

Scheme 3.2.15

To distinguish between these pathways in our system, the configurational stability must be determined with respect to the rate of reaction with an electrophile. Hoffmann has provided an elegant method for determining configurational stabilities in certain conditions. The Hoffmann Test takes advantage of the kinetic resolution of diastereomers in a reaction of a racemic organolithium reagent with a chiral electrophile in racemic and enantioenriched forms (Scheme 3.2.16).[203-206]

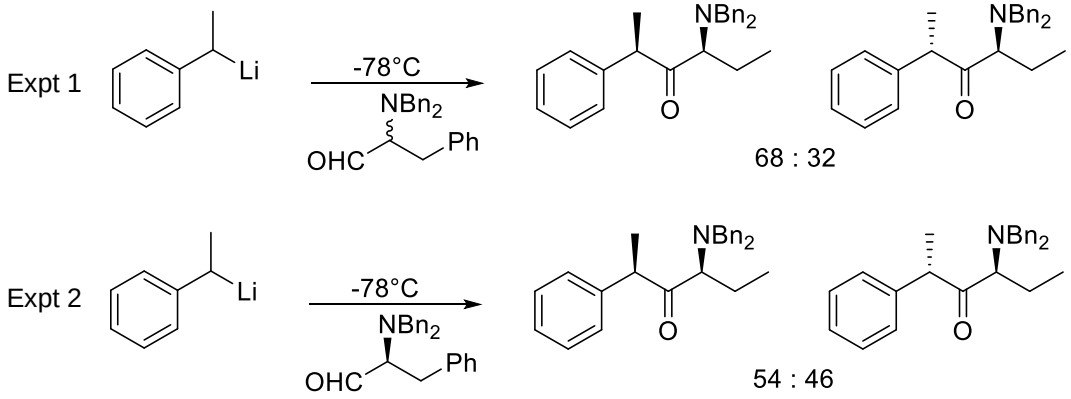

Scheme 3.2.16

If the ratios for Expt 1 and Expt 2 are not equal to each other, it can be concluded that the reaction is configurationally stable. Equal ratios of product enantiomers suggest fast epimerisation about the benzylic centre relative to the rate of reaction.

Beak and co-workers described a variant of this test in which organolithium species which are diastereomeric by virtue of complexation with a chiral ligand undergo reaction with an achiral electrophile via diastereomeric transition states.[202] They referred to this as the 'poor man's Hoffmann Test', as it does not require a chiral enantioenriched electrophile.[201] The tests can be carried out either by determining the stereoselectivity with a deficiency and excess of the electrophile or by monitoring the stereoselectivity of the substitution product as a function of the alkylation progress (Scheme 3.2.17).

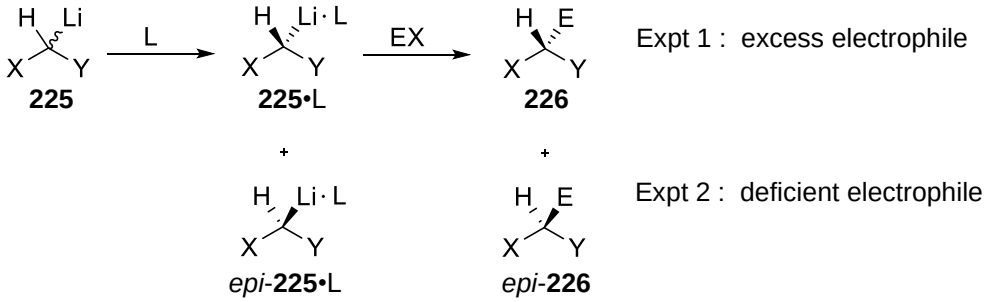

Scheme 3.2.17

We applied both of Beak's tests to our intermolecular chirality transfer reactions. Firstly deficient and excess electrophile was investigated. The alkylation of hydrazone **203** with 0.2 equiv. of 2-methylbenzyl bromide provided **(*R*)-216** with an *er* of 76 : 24, the same level of enantioinduction was observed when excess electrophile was used (Table 3.2.8). This result disfavours a DTR system where nonequilibrating diastereomeric complexes react with the electrophile but does not rule out the possibility of configurationally stable complexes with indistinguishable rates of reaction of each diastereomer.

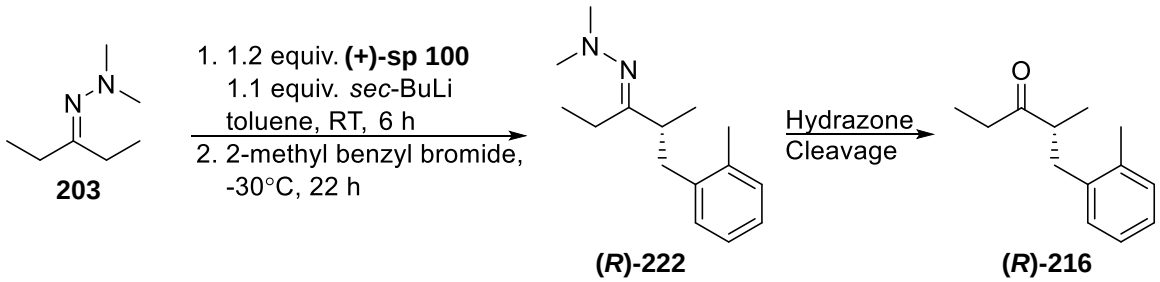

Entry	Ligand	Variation	Electrophile	Yield[a]	*er R* : *S*	% *ee*
1	**(+)-sp 100**	Excess electrophile	2-methylbenzyl bromide	54%	76 : 24	52%
2	**(+)-sp 100**	0.2 equiv. electrophile	2-methylbenzyl bromide	18%	76 : 24	52%

[a]Yield determined using NMR and 1,3,5-trimethoxybenzene as internal standard.

Table 3.2.8 Mechanistic Investigations

The second test involved treatment of hydrazone **203** with sparteine/*sec*-BuLi at room temperature for 6 hours followed by reaction with 4-*tert*-butylbenzyl bromide. The reaction provided product **(*R*)-214** with an *er* of 71 : 29, irrespective of the extent of reaction (Table

3.2.9). This observation is consistent with a mechanism of rapidly equilibrating diastereomeric complexes.

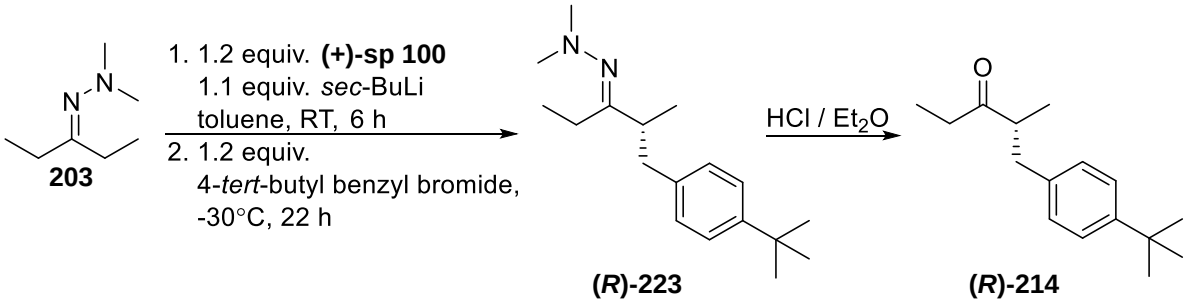

Entry	Ligand	Variation	Electrophile	Yield	*er R* : *S*	% *ee*
1	**(+)-sp 100**	22 h alkylation	4-*tert*-butylbenzyl bromide	62%[a]	71 : 29	42%
2	**(+)-sp 100**	2 h alkylation	4-*tert*-butylbenzyl bromide	43%[b]	71 : 29	42%

[a]Isolated yield over two steps. [b]Yield determined using NMR and 1,3,5-trimethoxybenzene as internal standard.

Table 3.2.9 Mechanistic Investigations

While these results somewhat suggest a mechanism involving DKR. We feel our system may be further complicated by the possible formation of four azaenolate isomer forms.

DFT calculations carried out prior to the undertaking of this project, show the $E_{CC}Z_{CN}$ geometry of the azaenolate to be the most stable isomeric form (Figure 3.2.5).[207]

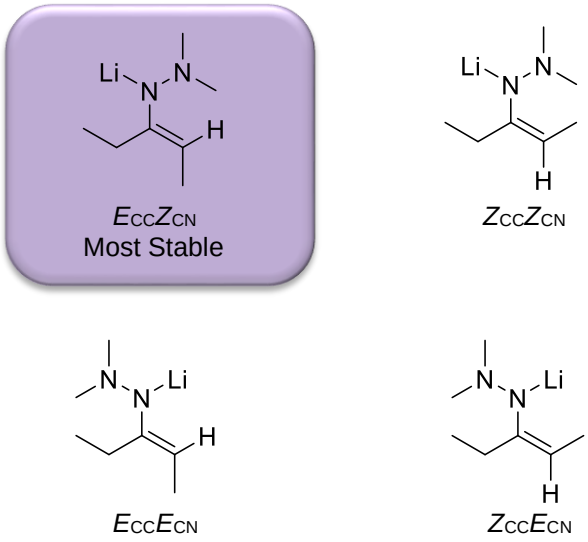

Figure 3.2.5

On this basis it is possible that a mechanism more like that observed for the SAMP/RAMP auxiliaries (discussed in Chapter 1, Section 1.3) could be operative.

During this project we also investigated the possibility of using a catalytic amount of the chiral ligand. O'Brien has successfully employed sparteine in catalytic asymmetric deprotonation reaction via a ligand exchange protocol (discussed in Section 1.8).[100]

In order for catalysis to be possible it would be necessary for the rate of alkylation to be greater in the presence of the chiral ligand than when no ligand is present (Scheme 3.2.18).

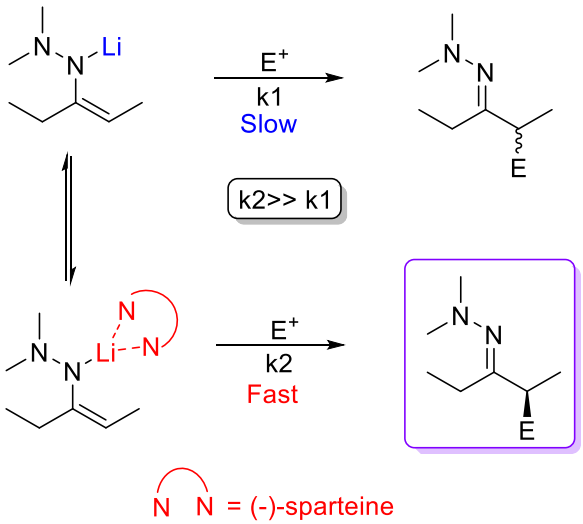

Scheme 3.2.18

A second requirement for catalysis is the ability of sparteine to reattach to an azaenolate once expelled after alkylation. This would likely involve dislodging coordinating solvent molecules or perhaps more likely, the breaking up of aggregate species.

Firstly we needed to determine the rate of reaction for the alkylation step in the presence of sparteine/*sec*-BuLi verses the rate with *sec*-BuLi alone (no sparteine present). Both reactions were stopped after a set period of time before alkylation was complete. Comparison of the extent of conversion indicates that the reaction is faster in the presence of the chiral ligand (Table 3.2.10).

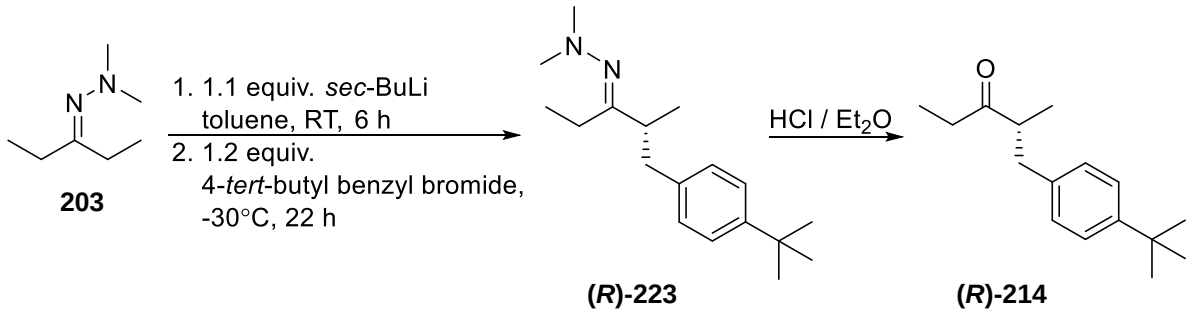

203 **(*R*)-223** **(*R*)-214**

Entry	Ligand	Variation from standard conditions	Electrophile	Yield[a]	*er R* : *S*	% *ee*
1	**(+)-sp 100**	1.5 h alkylation	4-*tert*-butylbenzyl bromide	20%	68 : 32	36%
2	No sparteine added	1.5 h alkylation	4-*tert*-butylbenzyl bromide	10%	n/a	n/a

[a]Yield determined using NMR and 1,3,5-trimethoxybenzene as internal standard.

Table 3.2.10

Since the reaction fulfilled the first criteria for a catalytic reaction, we tried the reaction using 0.4 equivalents of **(+)-sp 100**. The reaction was carried out in the usual manner with the chiral ligand present for the deprotonation step.

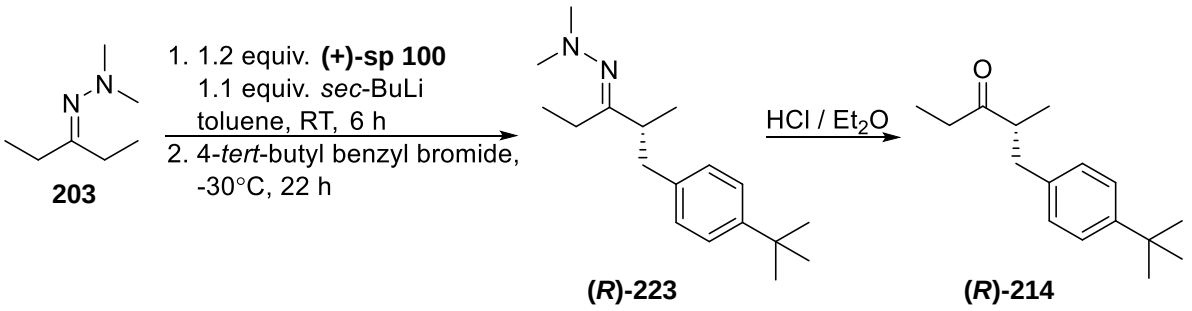

203 **(*R*)-223** **(*R*)-214**

Entry	Ligand	Variation from standard conditions	Electrophile	Yield[a]	*er R* : *S*	% *ee*
1	**(+)-sp 100**	Standard conditions	4-*tert*-butylbenzyl bromide	62%	71 : 29	42%
2	**(+)-sp 100**	0.4 equiv. **(+)-sp 100**	4-*tert*-butylbenzyl bromide	38%	68 : 32	36%
3	**(+)-sp 100**	0.4 equiv. **(+)-sp 100** in ether	4-*tert*-butylbenzyl bromide	34%	59 : 41	18%

[a]Yield determined using NMR and 1,3,5-trimethoxybenzene as internal standard.

Table 3.2.11

The target compound **(*R*)-214** was isolated in 32% yield with an enantiomeric ratio of 68 : 32 (entry 2). Only a slight decrease in enantiomeric ratio was observed, however a considerable decrease in yield was noticable. It is clear from these results that sparteine does not reattach to and promote the reaction. The slight decrease in enantiomeric ratio is probably due to a competing racemic alkylation (Table 3.2.11).

The reaction was also carried out using diethyl ether as solvent and a similar effect was observed (entry 3). Even lower enantiomeric ratios were witnessed here due to the ineffectiveness of diethyl ether in these reactions (discussed earlier in Section 3.2.2).

3.2.8 Preparation of Chiral Ligands and their Use in the Asymmetric Synthesis of α-Alkylated Ketones

Having exhausted all other avenues in our attempts to improve the enantiomeric ratios. We next examined the effect of changing the chiral diamine.

The use of sparteine as a chiral ligand has been unrivalled, in terms of its breadth of application. However, it does suffer from a number of drawbacks: 1) Limited scope for derivatisation or modification, 2) Difficulty in accessing both enantiomers and 3) Expensive and limited in supply.

In light of this, we sought to evaluate other chiral ligands with varying structures, in order to find a ligand-scaffold suited to our system. By studying the effect of the chiral ligands on our system, we hoped to learn more about the structural aspects necessary for stereochemical control.

The following ligands were chosen for our investigations (Figure 3.2.6).

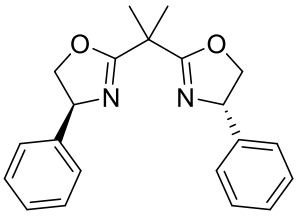

(*S*,*S*)-227

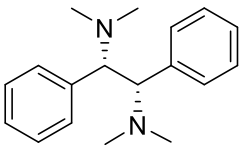

(*S*,*S*)-228

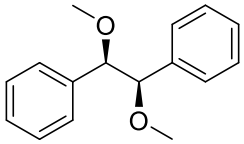

(*R*,*R*)-229

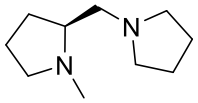

(*S*)-230

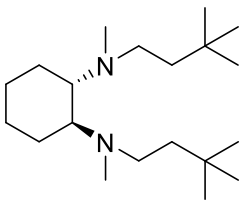

(*S*,*S*)-113

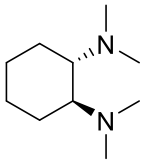

(*S*,*S*)-231

Figure 3.2.6

Bisoxazoline **(*S*,*S*)-227** was chosen as bisoxazolines (BOX) are a class of privileged chiral ligands and have been successful in a wide array of asymmetric reactions. They have been extensively reviewed and there are many structural variations commercially available.[208] BOX ligands also benefit from being C_2-symmetric. Ligands possessing C_2-symmetry often improve the enantioselectivity in asymmetric transformations, by reducing the number of transition states with a unique geometry. The benefits of C_2-symmetry in BOX ligands have been

reviewed in depth.[209,210] In general, for methylene bridged BOX ligands the stereochemical outcome is consistent with a twisted square planar intermediate, which was proposed based on crystal structures.[211,212] The R-substituent blocks one enantiotopic face of the substrate, leading to enantioselectivity (Figure 3.2.7).[210]

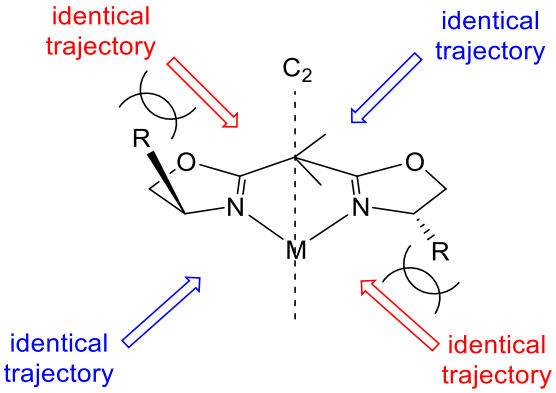

Figure 3.2.7

(*S*,*S*)-227 was synthesised according to Evans's procedure (Scheme 3.2.19).[213]

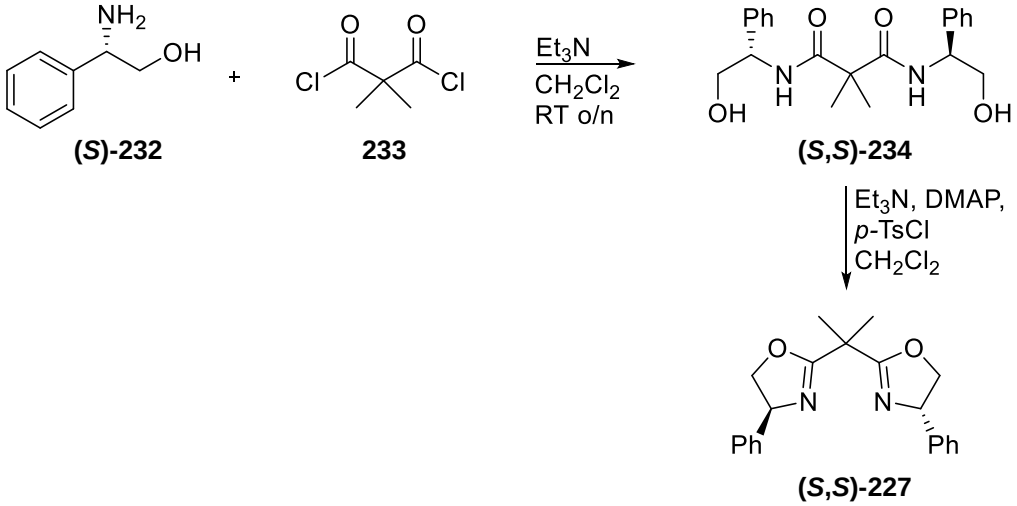

Scheme 3.2.19

Firstly, amino alcohol **(*S*)-232** was prepared in 97% yield from the corresponding amino acid, (*S*)-phenylgylcine **(*S*)-235** using a method described by Meyers, which employed sodium borohydride and boron trifluoride diethyl etherate (Scheme 3.2.20).[214]

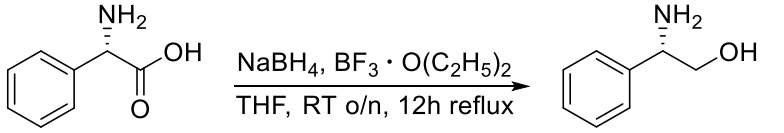

(*S*)-235 **(*S*)-232**, 97%

Scheme 3.2.20

We also attempted reduction of **(*S*)-235** using lithium aluminium hydride, however this proved unsuccessful.

The acyl chloride, **233** was prepared from **236** using thionyl chloride as the chlorinating agent in 55 % yield (Scheme 3.2.21).

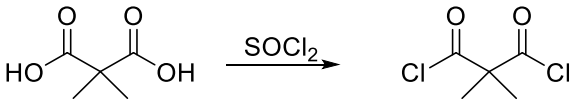

236 **233**, 55%

Scheme 3.2.21

While higher yields are reported using oxalyl chloride and DMF for the chlorination,[213] we avoided this procedure due to the formation of a minor by-product, dimethylcarbamoyl chloride **237** (Figure 3.2.8) which is a potent carcinogen.

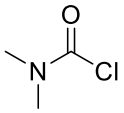

237

Figure 3.2.8

The next step involved acylation of amino alcohol **(*S*)-232** with acyl chloride **233** to form the bisamide **(*S*,*S*)-234** in 71% yield (Scheme 3.2.22).

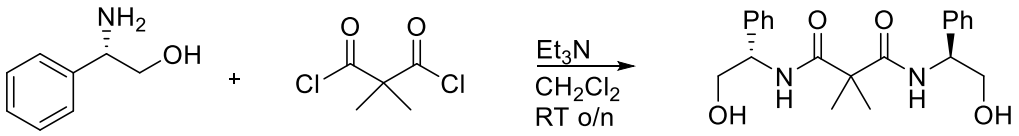

(*S*)-232 **233** **(*S*,*S*)-234**, 71%

Scheme 3.2.22

Initial isolation of this product proved problematic due to the formation of a solid precipitate. However good yields were achieved by adjustment of the work-up as follows: filtration of the solid which had formed, followed by washing of the mother liquor with 10% HCl solution. We

were surprised by the apparent insolubility of bisamide **(*S*,*S*)-234**. A crystal structure was obtained which indicated a dihydrate of the bisamide had been formed, which appeared to render the product only partially soluble in dichloromethane but fully soluble in the polar protic solvent, methanol (Figure 3.2.9).

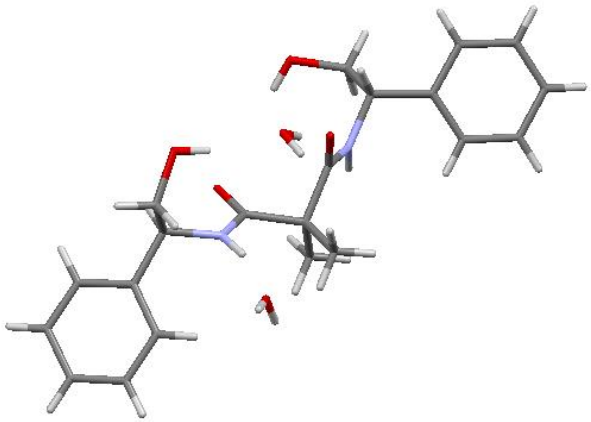

Figure 3.2.9

(*S*,*S*)-234 was found to have the space group, *P* 2_1, indicating it is primitive (it contains one lattice point), monoclinic (it has three different cell lengths), two of the angles in a unit cell are 90° and the third angle is not 90° (Table 3.2.12). Two molecules are contained in each unit cell. The R-factor, (reliability factor) for **(*S*,*S*)-234** is excellent at 0.0411.

Chemical formula	**$C_{20}H_{25}NO_6$**
Space group	*P* 2_1
Cell dimensions (Å)	*a* = 8.423 (3)
	b = 11.261 (3)
	c = 11.347 (4)
	α = 90
	β = 91.054
	γ = 90
No. of molecules (Z)	2
R (Reliability factor)	0.0411 (2599)

Table 3.2.12 Crystallograhic data for **(*S*,*S*)-234**

Clear intermolecular hydrogen bond interactions are evident between the hydrogen of a water molecule and the carbonyl oxygen of **(*S*,*S*)-234** and between the oxygen of a water molecule and the hydrogen of the hydroxyl group of **(*S*,*S*)-234** (Figure 3.2.10).

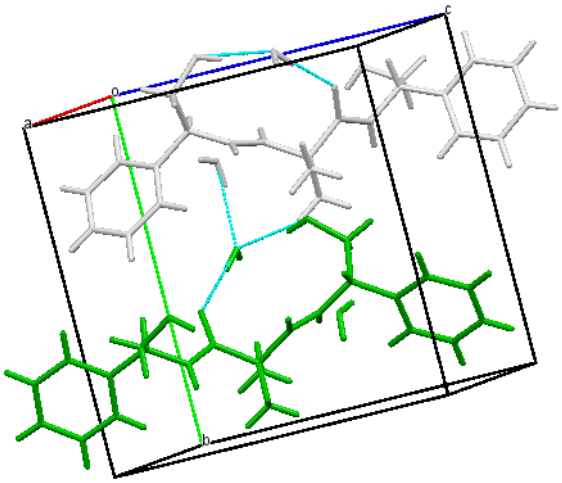

Figure 3.2.10

We were able to successfully form the oxazoline ring by treatment of bisamide **(*S*,*S*)-234** with *para*-toluenesulfonyl chloride and triethylamine in the presence of catalytic quantities of 4-(dimethylamino)pyridine. The bis(tosylate) formed in situ, undergoes cyclisation to provide the BOX ligand (Scheme 3.2.23).

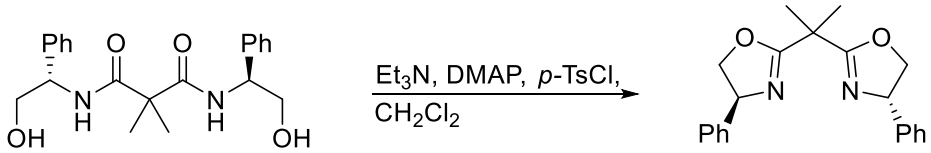

(*S*,*S*)-234 **(*S*,*S*)-227**, 10%

Scheme 3.2.23

While analysis of the ^{1}H NMR spectrum of the crude material showed complete consumption of **(*S*,*S*)-234** and high mass recovery was achieved, purification using column chromatography proved problematic and only a 10% yield of **(*S*,*S*)-227** was isolated.

Given the lack of sufficient quantities of BOX ligand **(*S*,*S*)-227** for investigation in our asymmetric alkylation reactions, we decided to employ Fraile's one pot synthesis of BOX ligands.[215,216] This approach involved condensation of chiral amino alcohol **(*S*)-232** with dimethyl malononitrile **238** using stoichiometric amounts of zinc triflate (Scheme 3.2.24).

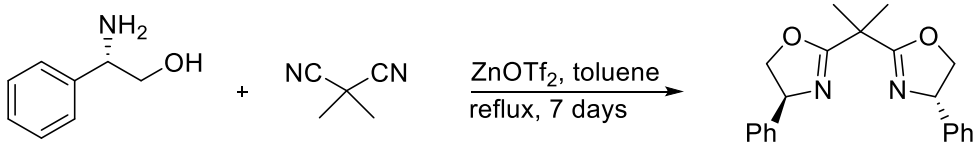

(*S*)-232 **238** **(*S*,*S*)-227**, 41%

Scheme 3.2.24

The reaction was monitored by ^{1}H NMR until all starting material had fully reacted. This reaction took seven days to complete. We believe this was due to the zinc triflate being displaced to the top of the reaction vessel during stirring, reducing the amount accessible in the reaction medium and hindering the reaction. Once the reaction was complete, the crude mixture was subjected to purification via column chromatography. Given the difficulty observed in the purification of this ligand, we made a slight modification. We found that the addition of 0.4% triethylamine to the eluent (4 : 1, hexane : EtOAc) considerably increased the amount of BOX ligand **(*S*,*S*)-227** eluted from the column and 41% yield was achieved.

As we now had sufficient quantities of BOX ligand **(*S*,*S*)-227**, we investigated its use as a chiral ligand in our intermolecular chirality transfer alkylation. BOX ligand **(*S*,*S*)-227** was subjected to our standard conditions for deprotonation (room temperature for 6 h) and alkylation (iodopentane, -30°C for 22 h) (Table 3.2.13). We were disappointed to discover that no reaction had occurred under these conditions (entry 1).

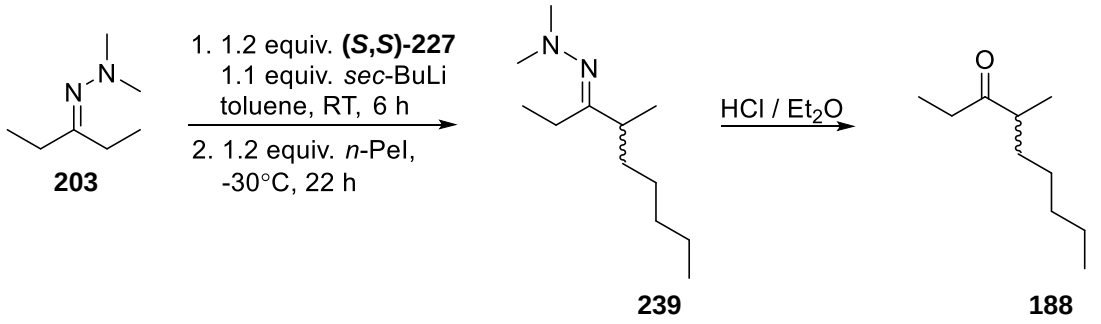

Entry	Ligand	Electrophile	Deprot. Temp.	Alkyl. Temp.	Yield[a]
1	**(*S*,*S*)-227**	*n*-PeI	RT	-30°C	No reaction occurred
2	**(*S*,*S*)-227**	*n*-PeI	RT	Warm to RT	No reaction occurred
3	**(*S*,*S*)-227**	*n*-PeI	40°C	Warm to RT	No reaction occurred
4	**(*S*,*S*)-227**	*n*-PeI	RT (ligand added after deprot.)	-30°C	No reaction occurred

Table 3.2.13 Intermolecular chirality transfer alkylation using bisoxazoline ligand.

We next increased the temperature of the alkylation step. The reaction was allowed warm room temperature overnight but again this did not result in product formation (entry 2). Next, the deprotonation temperature was increased to 40°C and the reaction was again allowed warm to room temperature during alkylation (entry 3). However these changes failed to promote any conversion to product and only starting material was isolated.

To ensure deprotonation was occurring, we carried out the deprotonation at room temperature for 5 hours using *sec*-BuLi in the absence of ligand, then the BOX ligand **(*S*,*S*)-227** was added and the reaction was stirred for 1 hour before addition of the alkylating agent at -30°C, however this also failed to yield any product (entry 4). We concluded that the BOX ligand **(*S*,*S*)-227** was interrupting the alkylation step. It is possible that the BOX ligand **(*S*,*S*)-227** formed an intermediate with the hydrazone azaenolate where the site of alkylation was blocked and rendered unreactive.

We then chose to test the diphenylethane derivatives, diamine **(*S*,*S*)-228** and diether **(*R*,*R*)-229** (Figure 3.2.11).

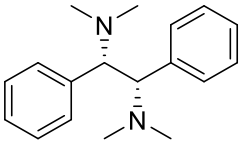

(*S*,*S*)-228

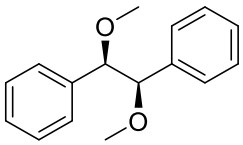

(*R*,*R*)-229

Figure 3.2.11

These ligands have previously been utilised by Tomioka, in the enantioselective addition of organolithium reagent to imines.[156,217] The imines used, derived from 1-naphthaldehyde and cyclohexylamine, selectively underwent conjugate addition (Scheme 3.2.25). The product was directly hydrolysed leading to an aldehyde which is quite sensitive to rearomatisation, and therefore was reduced quickly to the stable corresponding alcohol **240**. When diamine **(*S*,*S*)-228** was used, the alcohol **(1*S*,2*R*)-240** was obtained in only 11% *ee*, while diether **(*R*,*R*)-229** was much more efficient and afforded **(1*R*,2*S*)-229** in 91% *ee*.

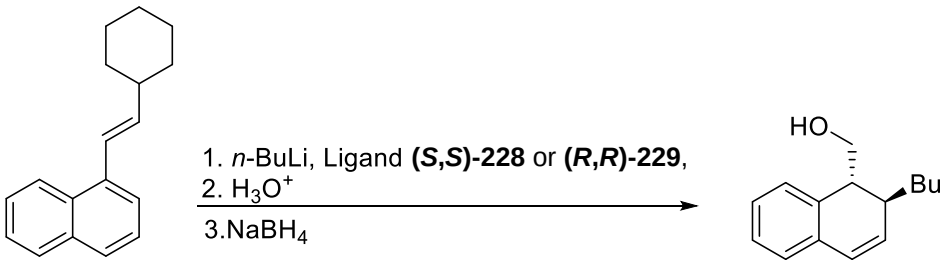

241

(1*S*, 2*R*)-240, 26%, 11% *ee*
(1*R*, 2*S*)-240, 80%, 91% *ee*

Scheme 3.2.25

Chiral diether **(*R*,*R*)-229** was prepared using a procedure described by Tomioka which involved dimethylation of optically pure (+)-hydrobenzoin **(*R*,*R*)-242** using sodium hydride and dimethyl sulfate. It was isolated as a stable, non-hygroscopic, colourless crystalline solid in 68% (Scheme 3.2.26).[156]

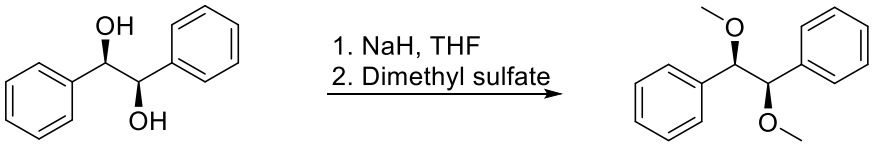

(*R*,*R*)-242 **(*R*,*R*)-229**, 68%

Scheme 3.2.26

Diamine **(*S*,*S*)-228** was prepared from **(*S*,*S*)-243** using an Eschweiler-Clarke methylation using excess formic acid and formaldehyde in 45% yield (Scheme 3.2.27).[156]

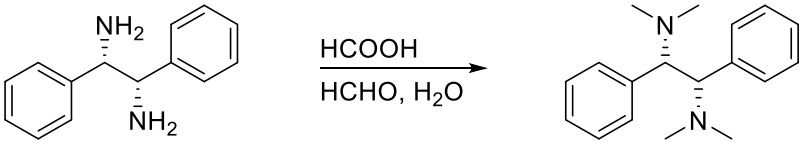

(*S*,*S*)-243 **(*S*,*S*)-228**, 45%

Scheme 3.2.27

This processes does not produce quaternary ammonium salts and chiral amines typically do not racemise under the conditions reported.

Both ligands were then investigated in our asymmetric alkylation under standard conditions (deprotonation at room temperature for 6 h and alkylation using benzyl bromide at -30°C for 22 h) (Table 3.2.14).

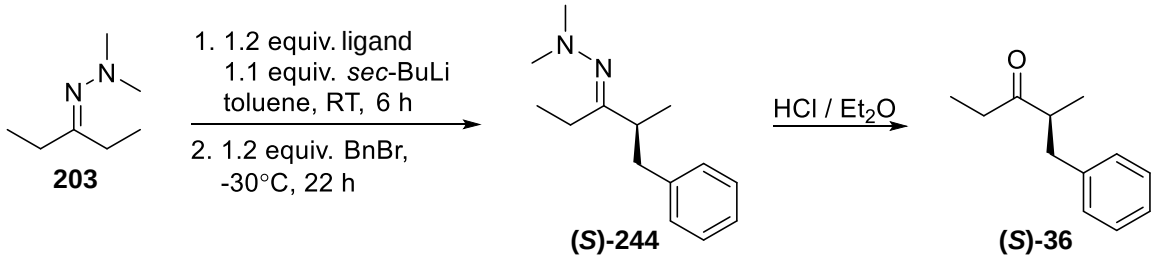

203 **(*S*)-244** **(*S*)-36**

Entry	Ligand	Electrophile	Deprot. Temp.	Alkyl. Temp.	Yield[a]	*er R* : *S*	% *ee*
1	**(*S*,*S*)-228**	BnBr	RT	-30°C	31%	45 : 55	10%
2	**(*R*,*R*)-229**	BnBr	RT	-30°C	27%	57 : 43	14%

[a]Isolated yield over two steps

Table 3.2.14

We were disappointed to observe poor conversion to product under our standard conditions for both ligands, as well as very low enantioselectivities.

We then examined **(*S*)-230**, which is derived from (*S*)-proline. These types of ligands have previously been employed in the enantioselective reduction of ketones **245** to alcohols using stannous chloride and DIBAL-H as shown in Scheme 3.2.28.[218] The best reported selectivity was obtained with diamine **(*S*)-246**, which afforded **(*S*)-247** in 78% *ee*, while diamines **(*S*)-248** and **(*S*)-230** led to the product in 46% *ee* and 64% *ee*, respectively.

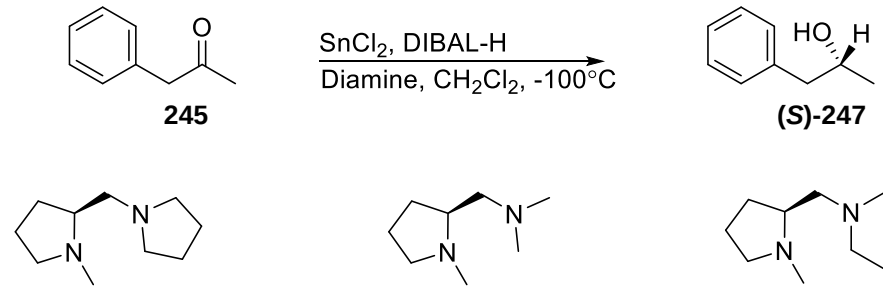

245 **(*S*)-247**

(*S*)-230, 59%, 64% *ee* **(*S*)-248**, 47%, 46% *ee* **(*S*)-246**, 71%, 78% *ee*

Scheme 3.2.28

Diamine **(*S*)-230** was chosen for our studies, as it was easily accessible in one step from chiral amine **(*S*)-193**, used previously in the synthesis of novel chiral auxiliary **(*S*)-192** (discussed in chapter 2). If this ligand could induce even moderate enantioselectivity in our system we would have considerable scope for optimisation, given the quantity of proline derived ligands synthetically accessible.[85]

An Eschweiler-Clarke methylation was used for the preparation of **(*S*)-230** from amine **(*S*)-193**,[156] however isolation of the product during work-up proved difficult. The portion that was isolated was purified using kugelrohr distillation to afford pure ligand **(*S*)-230** in 38% overall yield (Scheme 3.2.29).

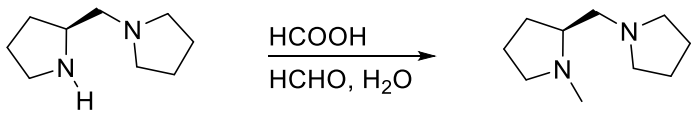

(*S*)-193 **(*S*)-230,** 38%

Scheme 3.2.29

Given the difficulty in preparing **(*S*)-230**, we investigated another synthetic route. (*S*)-Boc-proline **(*S*)-249** was reacted with pyrrolidine via a DCC coupling to form the amide **(*S*)-250** in

35% yield after a troublesome purification using column chromatography.[219] Subsequent reduction using lithium aluminium hydride afforded **(*S*)-230** in 51% yield (Scheme 3.2.30).

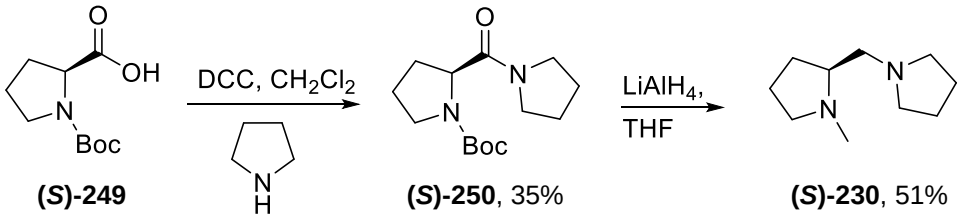

(*S*)-249 **(*S*)-250**, 35% **(*S*)-230**, 51%

Scheme 3.2.30

We then investigated the use of **(*S*)-230** as a chiral ligand in our asymmetric alkylation under our standard conditions (deprotonation at room temperature for 6 h and alkylation using iodopentane at -30°C for 22 h) (Scheme 3.2.31).

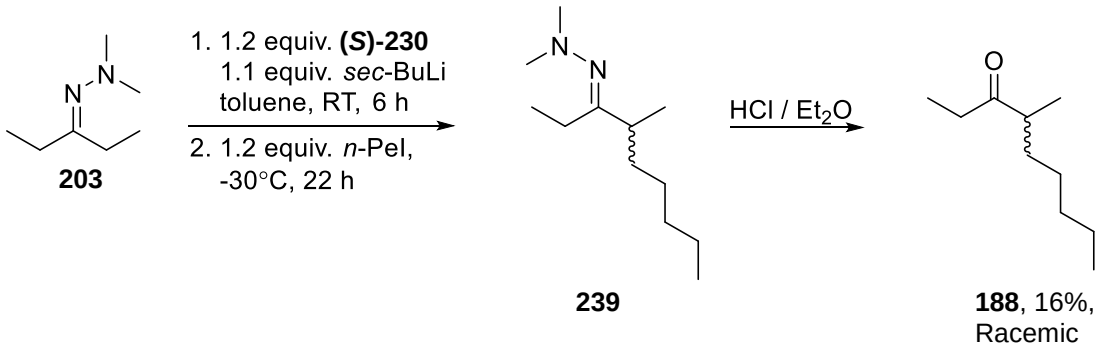

203 **239** **188**, 16%, Racemic

Scheme 3.2.31

Surprisingly this ligand did not induce any enantioselectivity in our system. We concluded that this ligand must either not have complexed with our azaenolate or alternatively did not provide any diastereo-discrimination when complexed.

Given this disappointing result no further investigation or optimisation using this ligand scaffold was carried out.

Alexakis has reported the synthesis of C_2-symmetric diamines, derived from *trans*-cyclohexane-1,2-diamine, in which both nitrogens bear two different substituents, e.g. **(*S*,*S*)-113** (Figure 3.2.12). In the cyclic complex formed with an organolithium reagent, **(*S*,*S*)-113**-Li, the nitrogen atom becomes stereogenic and brings the chirality closer to the reactive site (Figure 3.2.12).[99,220,221]

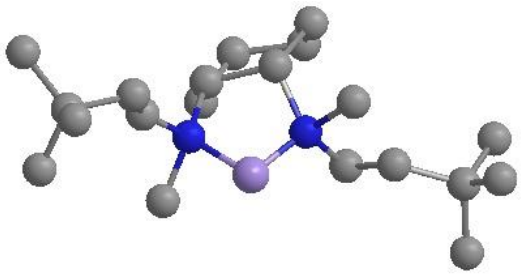

(*S*,*S*)-113-Li

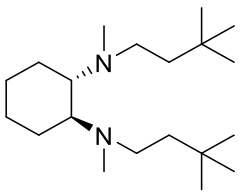

(*S*,*S*)-113

Figure 3.2.12

In 2008, it was reported that diamine **(*R*,*R*)-113** is as effective as **(-)-sp 100** for the asymmetric deprotonation of *N*-Boc pyrrolidine **105** (Scheme 3.2.32).[97] Thus, **(*S*)-112** was obtained with the same degree of enantioinduction using both ligands.

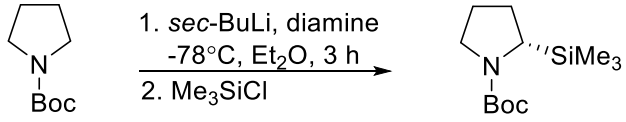

105 **(*S*)-112**

(-)-sp 100, 87%, 95 : 5 *er*
(*R*,*R*)-113, 72%, 95 : 5 *er*

Scheme 3.2.32

Compared to **(-)-sp 100**, diamine **(*R*,*R*)-113** can be prepared in a relatively straightforward manner. Also there is ample scope for modification and both enantiomers are accessible.

Diamine **(*S*,*S*)-113** was prepared on multigram scale using a reported synthesis.[97] First, (-)-*trans*-cyclohexane-1,2-diamine was resolved using L- and D-tartaric acid to give both salts **(*R*,*R*)-251** and **(*S*,*S*)-251** in 76% and 99% yield respectively. Reaction of **(*S*,*S*)-251** with NaOH and methyl chloroformate afforded a bis-methyl carbamate, which was reduced using lithium aluminium hydride to give **(*S*,*S*)-252**. Diamine **(*S*,*S*)-252** was then acylated using *tert*-butylacetyl chloride to deliver the crude bis-amide. Reduction using lithium aluminium hydride gave diamine **(*S*,*S*)-113** after purification by kugelrohr distillation in 41% yield over 4 steps (Scheme 3.2.33).

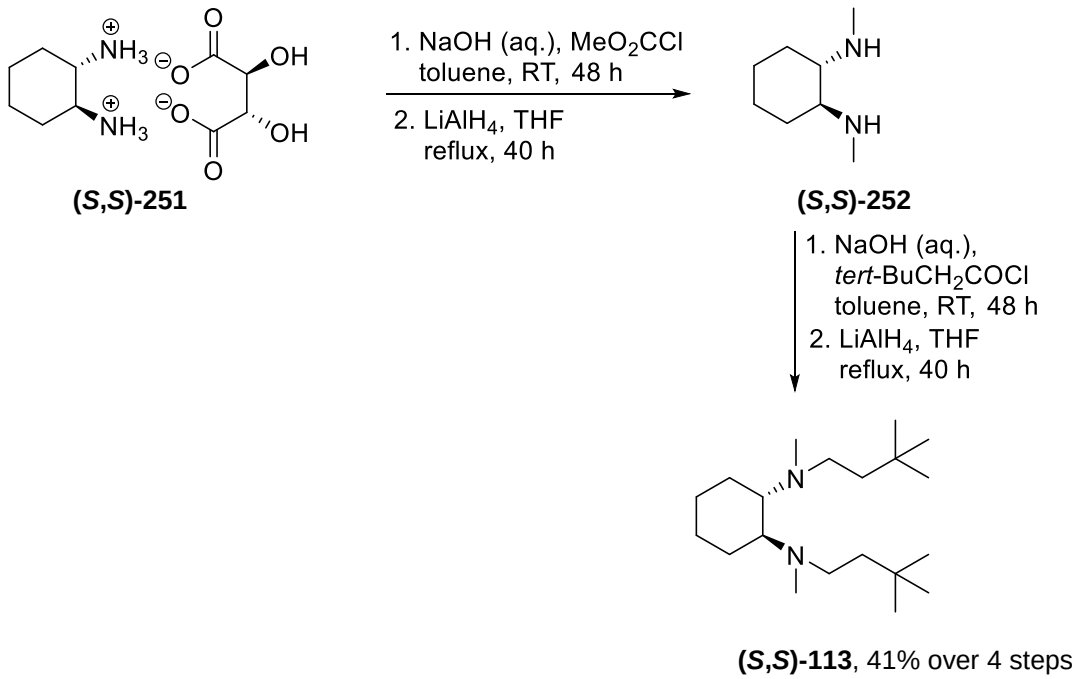

(*S*,*S*)-251 **(*S*,*S*)-252** **(*S*,*S*)-113**, 41% over 4 steps

Scheme 3.2.33

Ligand **(*S*,*S*)-231** was also prepared for comparison, as it was easily accessible via methylation of the salt **(*S*,*S*)-251** in 71% yield (Scheme 3.2.34).

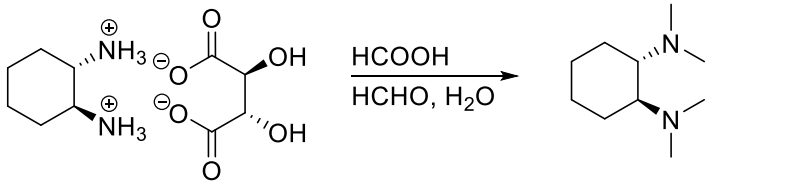

(*S*,*S*)-251 **(*S*,*S*)-231**, 71%

Scheme 3.2.34

With diamines **(*S*,*S*)-113** and **(*S*,*S*)-231** in hand, we evaluated them in our asymmetric alkylation reactions under our standard conditions (deprotonation at room temperature for 6 h and alkylation using iodopentane at -30°C for 22 h) (Table 3.2.15).

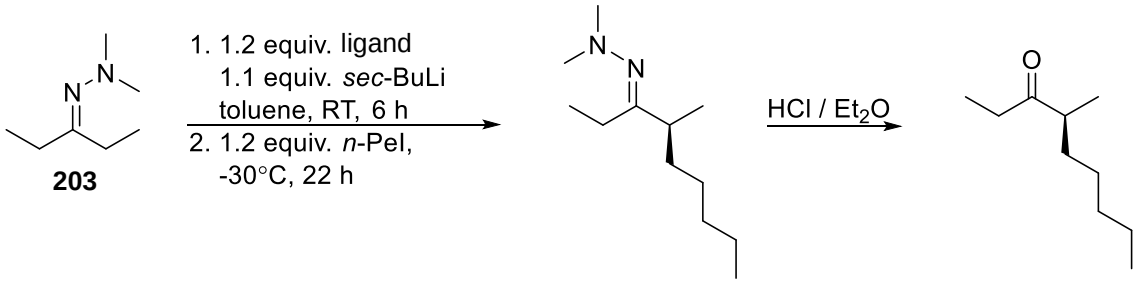

203 **239** **188**

Entry	Ligand	Electrophile	Yield[a]	Product	*er R* : *S*	% *ee*
1	**(*S*,*S*)-113**	*n*-PeI	53%	**(*S*)-188**	29 : 71	42%
2	**(*S*,*S*)-231**	*n*-PeI	23%	**(*R*)-188**	58 : 42	16%
3	**(-)-sp 100**	*n*-PeI	34%	**(*S*)-188**	17 : 83	66%

[a]Isolated yield over two steps

Table 3.2.15 Intermolecular chirality transfer alkylation using cyclohexane derived ligands.

Not surprisingly, **(*S*,*S*)-231** did not perform well and resulted in a poor enantiomeric ratio of 58 : 42. Interestingly the use of **(*S*,*S*)-231** gave the opposite sense of chirality than **(-)-sp 100** or **(*S*,*S*)-113**. It is evident that the introduction of sterically bulkier substituents results in good levels of enantioinduction in this reaction. Pleasingly, a moderate enantiomeric ratio of 29 : 71 *er* was achieved using **(*S*,*S*)-113**. While the selectivity observed using **(*S*,*S*)-113** did not rival that of **(-)-sp 100**, it did provide us with a ligand scaffold suitable for derivatisation in future projects.

3.2.9 NMR Investigations of Asymmetric Alkylation with (+)-Sparteine

The formation of monomeric azaenolate species allows for the depiction of four different geometrical isomers. This has been thoroughly discussed in the literature for lithiated SAMP-hydrazone species in solution (Figure 3.2.13).[29,71] The preferred configuration is $E_{CC}Z_{CN}$.

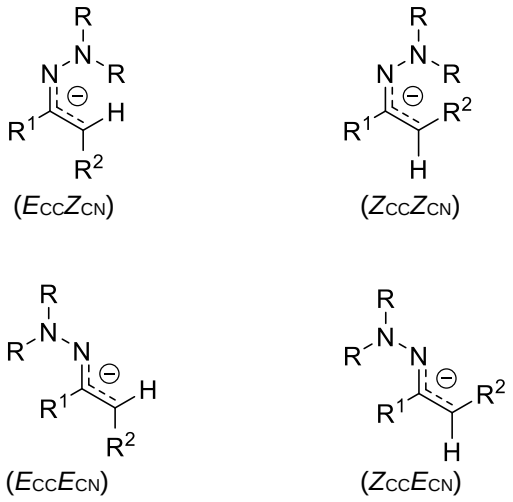

Figure 3.2.13

We hoped it would be possible to identify each of these species by NMR studies and determine the most abundant isomer after deprotonation, in our system. If more than one azaenolate was present this could explain why only moderate enantiomeric ratios have been achieved to date. We envisaged that NOESY experiments could establish the structures of the azaenolates present.

The reaction outlined in Scheme 3.2.35 was carried out in the usual manner except deuterated toluene was employed, to allow NMR experiments to be ran without solvent interference. Two reactions were carried out, one with **(+)-sp 100** present and one without.

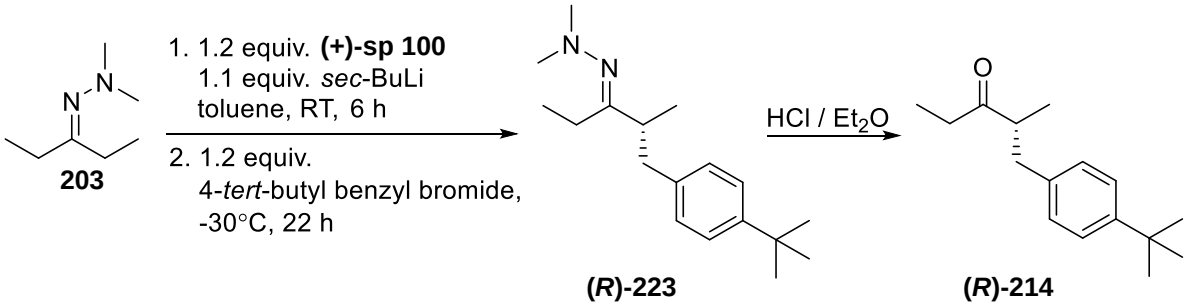

Scheme 3.2.35

An NMR tube, fitted with a rubber septum and wrapped in parafilm, was placed under vacuum via a needle connected to a schlenk line. The tube was heated gently and refilled with nitrogen and then the NMR tube was allowed to cool. Using a glass syringe, 0.6 mL of the reaction mixture was removed under inert atmosphere (Figure 3.2.14) and transferred to the NMR tube (Figure 3.2.15). The samples were analysed at 600 MHz on a Bruker AVANCE 600 instrument.

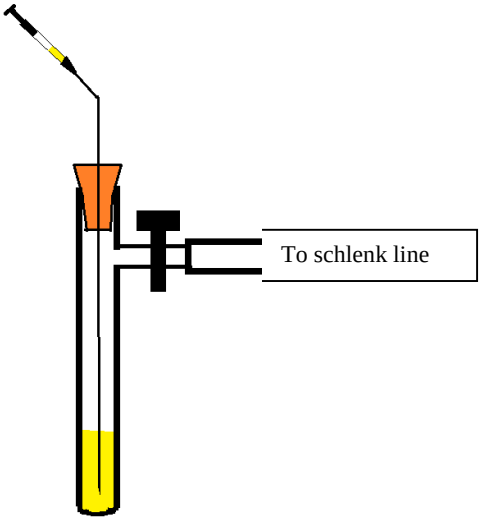

Figure 3.2.14

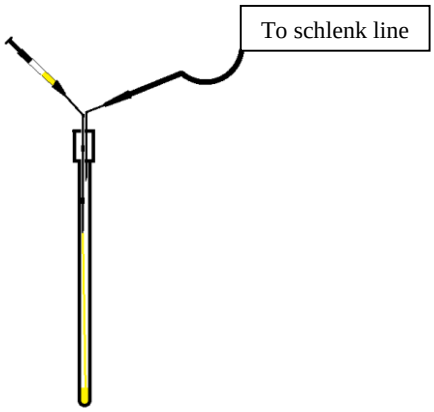

Figure 3.2.15

Initially we envisaged ^{1}H NMR would allow us to characterise the azaenolates, in a similar manner as reported by Enders with SAMP/RAMP hydrazones.[28,71] However, when **(+)-sp 100** was employed, we were unable to identify any peaks corresponding to azaenolates in the ^{1}H NMR spectra. When **(+)-sp 100** was absent from the reaction the ^{1}H NMR spectrum was complex and no clear assignments were possible. Given the complexity of the ^{1}H NMR spectra, NOESY experiments also proved inconclusive.

^{13}C NMR spectra for both reactions were more decipherable, since the interesting C=N signals appear at low field and do not overlap with the strong solvent and **(+)-sp 100** peaks. Figure 3.2.16 shows a portion of the ^{13}C NMR spectra obtained.

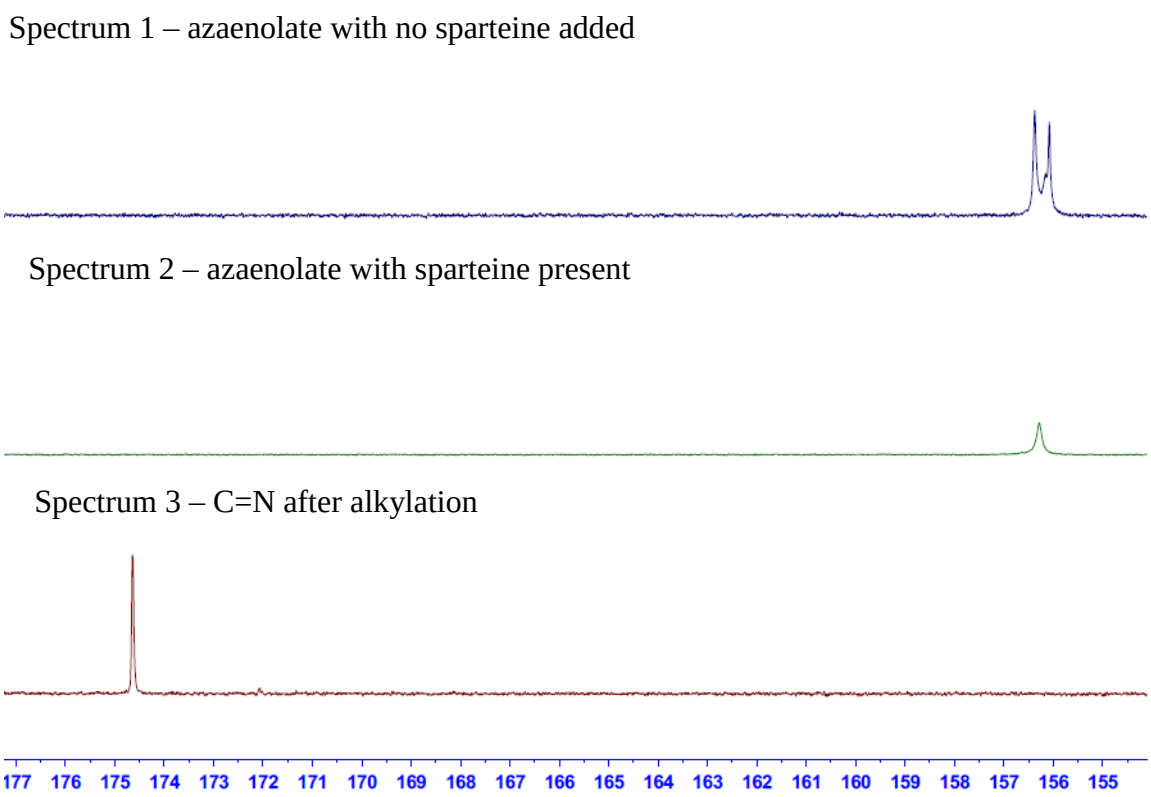

Figure 3.2.16

Spectrum 1 and 2 are samples which were taken from the reaction mixture after 30 minutes. Both clearly show the disappearance of the C=N signal of **203** which is present at 174.5 ppm. This indicated full deprotonation had occurred in this time. An interesting occurrence in both spectrum 1 and 2 is the appearance of a signal between 156 - 156.5 ppm. We assign this signal as the C=N carbon of the hydrazone in its azaenolate form, which now appears more upfield due to shielding effects. In the case of spectrum 1, where no sparteine was added to the reaction, this signal appears as 2-3 peaks, which suggests the possibility of different azaenolate intermediates. In spectrum 2, where **(+)-sp 100** was present during the deprotonation, the signal between 156 - 156.5 ppm was observed as a singlet leading us to believe that either one azaenolate or a quickly equilibrating mixture is present when chelated to the lithium and the ligand. This observation is agreement with DFT calculations which show the $E_{CC}Z_{CN}$ geometry of the azaenolate to be the most stable isomeric form when sparteine is present (Figure 3.2.17) (discussed in Section 3.2.6).

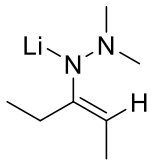

($E_{CC}Z_{CN}$)

Figure 3.2.17

Both reactions displayed identical ^{13}C NMR spectra upon alkylation, with the restoration of the C=N moiety in **223**, shown in spectrum 3 and indicated by the signal at 174.6 ppm.

The argument for the preferential formation of the $E_{CC}Z_{CN}$ azaenolate when sparteine was present, was further supported by the NOESY spectrum (Figure 3.2.18) for **(*R*)-223**, which showed a correlation between the protons of the dimethyl groups at 2.27 ppm and the protons of C-4 at 3.93 ppm, for the major isomer. This correlation indicates that the dimethyl amino group resides on the newly substituted side, confirming the *Z*-geometry for hydrazone **(*R*)-223**. Since the dimethyl group resides on the side of alkylation this is good evidence for the complexation of the dimethylamino group with sparteine during deprotonation.

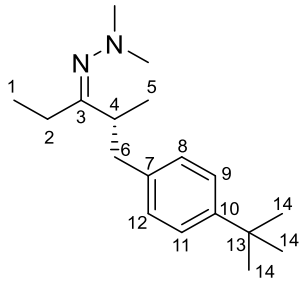

(*R*)-223 *Z*-geometry

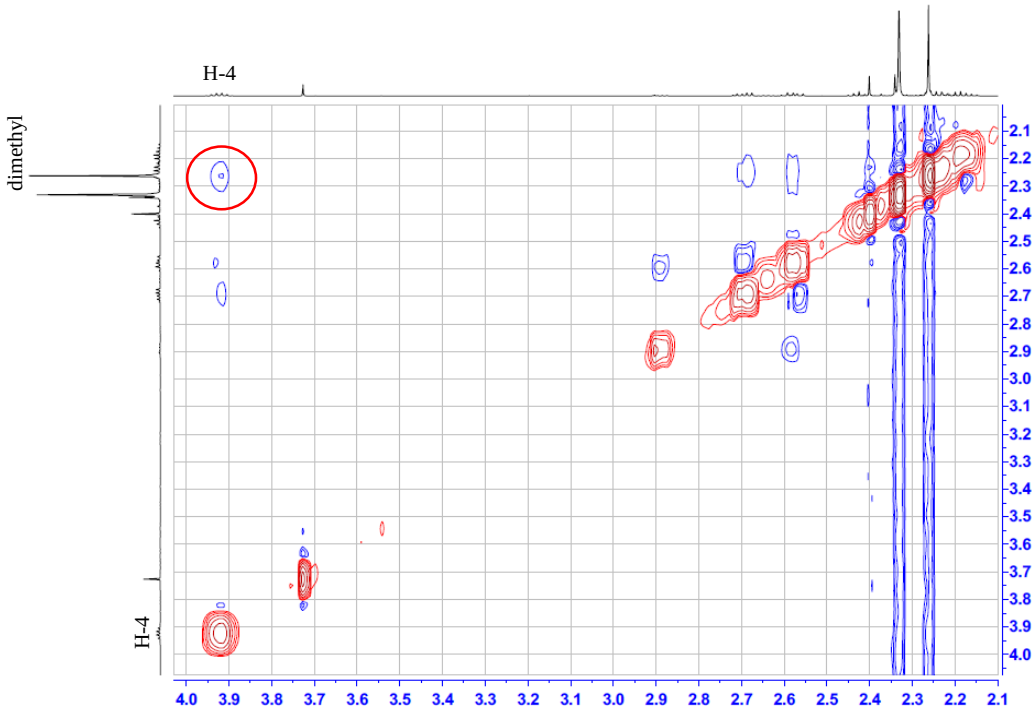

Figure 3.2.18

In Figure 3.2.19 we can see, over time the dimethylamino group 'flips' to the less sterically hindered *E*-geometry via analysis of the ^{1}H NMR spectra of the crude material. A decrease in diagnostic peaks for the *Z*-hydrazone and increase in the signals which can be assigned to the *E*-hydrazone was observed. Unfortunately, NOSEY experiments to confirm that the dimethyl now resides on the side with C-1 and C-2 were inconclusive (*E*-hydrazone). This observation is consistent with our hypothesis of formation of the $E_{CC}Z_{CN}$ azaenolate when sparteine is present. Corey reported a similar observation in the case of α-silylated cyclohexanone-dimethylhydrazone, where the *Z*-hydrazone is formed upon silylation and 'flips' to the more stable *E*-hydrazone.[76]

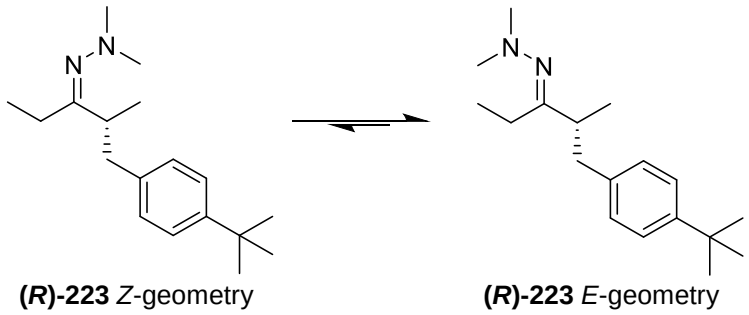

(*R*)-223 *Z*-geometry **(*R*)-223** *E*-geometry

Z-hydrazone

E-hydrazone

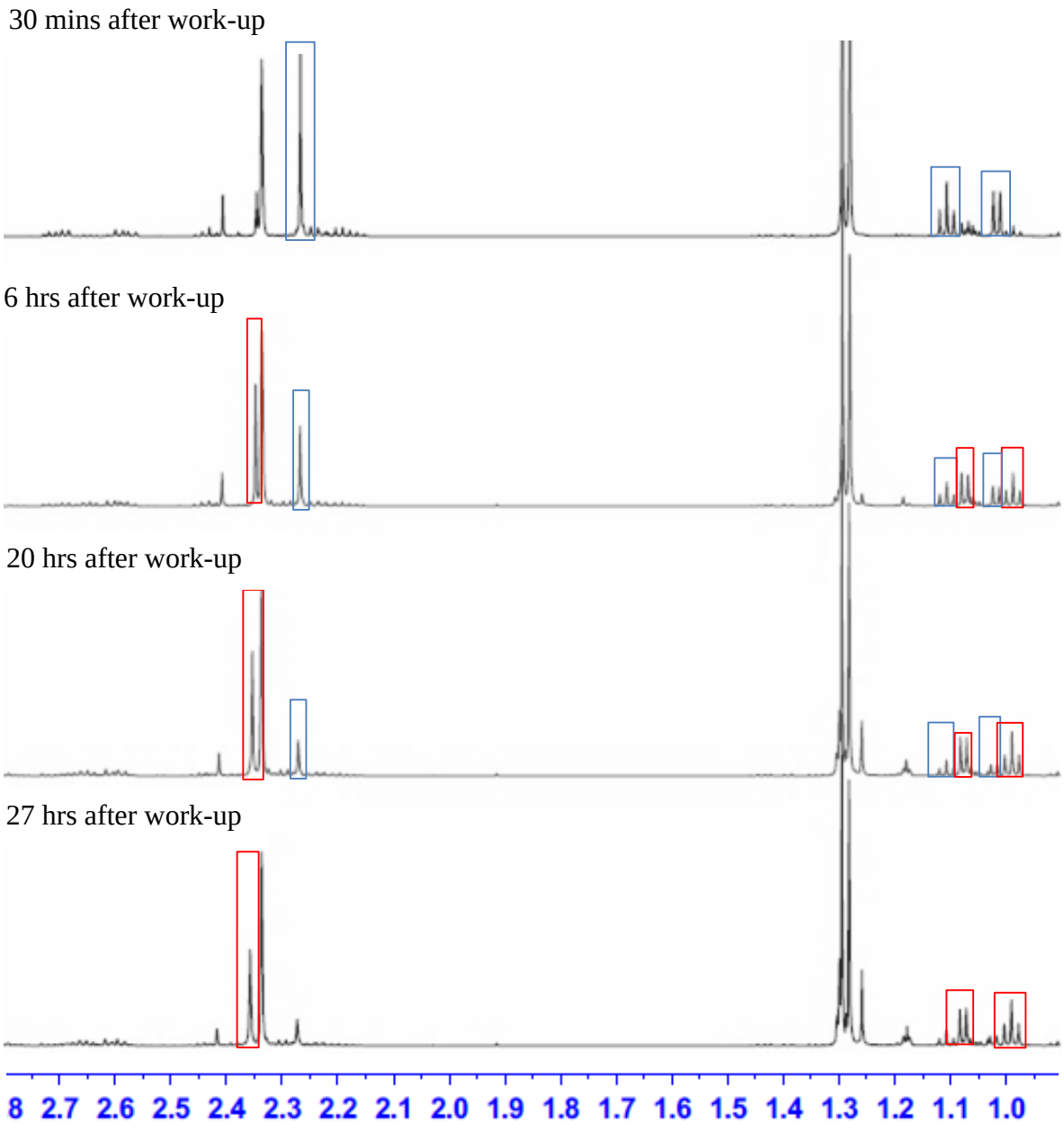

Figure 3.2.19

3.2.10 Aldol & Michael Reactions using (-)- and (+)-Sparteine

We also sought to investigate if the scope of the intermolecular chirality transfer methodology could extend to the generation of two chiral centres in one pot, such as in the aldol and Michael reactions.

The aldol reaction involves the condensation of a nucleophilic enolate species with an electrophilic carbonyl moiety. The product of the reaction is an important synthon used in the synthesis of macrolides and polyether antibiotics. Furthermore, this reaction is one of the basic biosynthetic transformations. The aldol reaction has been broadly studied with numerous metals and many combinations of substrates and reagents in order to synthesise *syn* or *anti* aldol products with a high level of selectivity.[222-225]

Hydrazone **203** was deprotonated in the presence of **(-)-sp 100** and *sec*-BuLi and subsequent reaction with benzaldehyde resulted in formation of the diastereomeric hydrazone **253**. Cleavage of the hydrazone lead to the desired aldol product **254** (Scheme 3.2.36). A test reaction was conducted on hydrazone **253** using the biphasic 4M HCl/diethyl ether hydrazone cleavage method. However, this method of cleavage afforded the ketone product **254**, as a racemic mixture. We suspected these more labile substrates may have been epimerised by the HCl. In light of this, Amberlyst® 15[199] in refluxing acetone/water was employed and aldol product **254** was formed, as an inseparable mixture of diastereomers after column chromatography in 65% yield over two steps. The diastereomeric ratio was 60 : 40 as determined by NMR of the crude product, and the enantiomeric ratio was 76 : 24 for the *syn* and 35 : 65 for the *anti*- products.

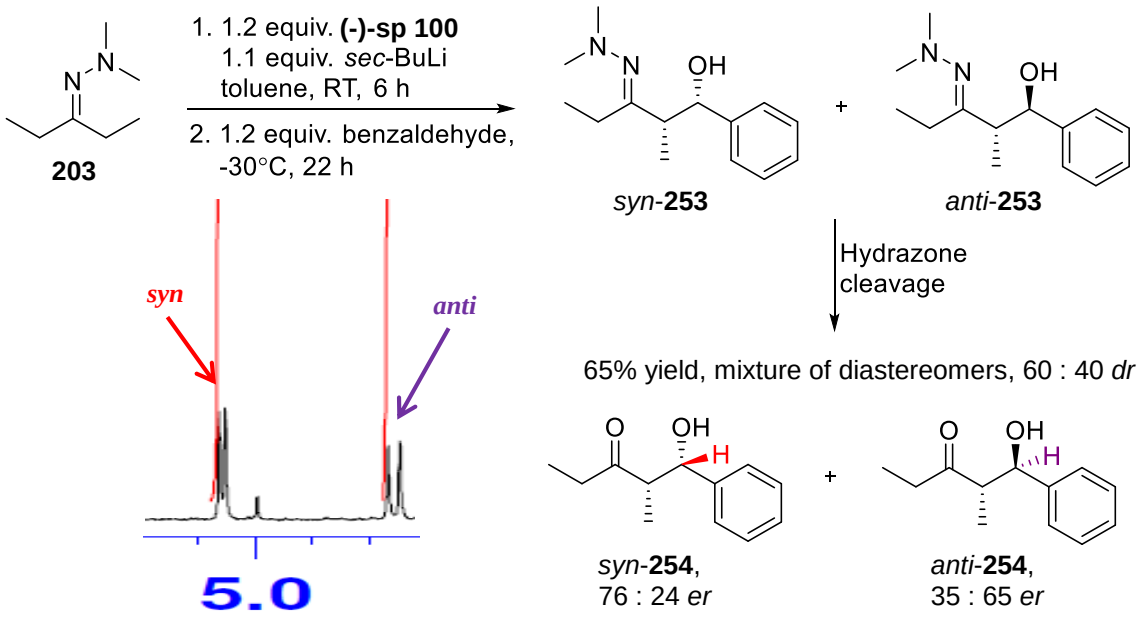

*Note: absolute configuration was not determined. Dashed/wedged notation used to differentiate *syn*- and *anti*-products and clarify results.

Scheme 3.2.36

The diastereomeric ratio and enantioselectivities were determined on the crude sample immediately after work-up (Figure 3.2.20) as the aldol products were observed to epimerise rapidly over time as determined using gas chromatography.

	syn	***anti***
dr	60	40
er R : S	76 : 24	35 : 65
% ee	52%	30%

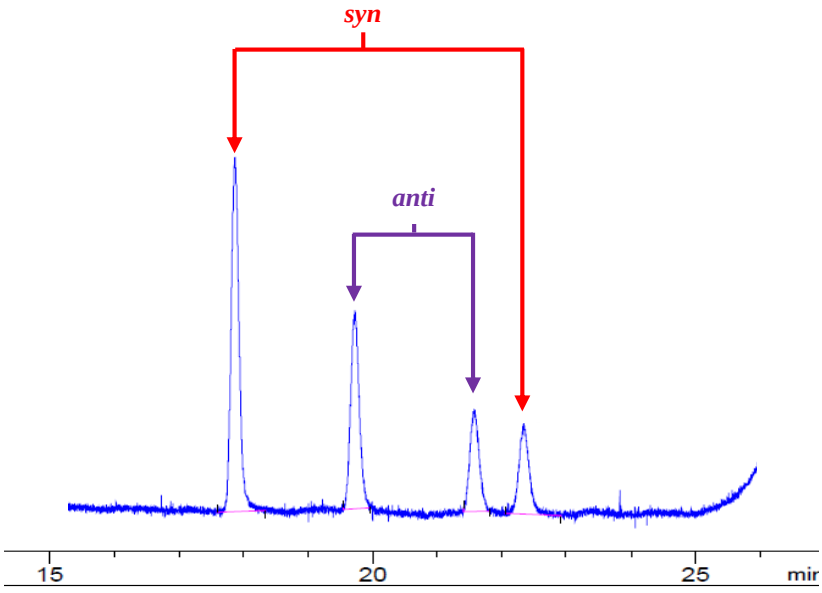

Figure 3.2.20

While the *syn* and *anti* products could not be completely separated using column chromatography, sufficient amounts of each were isolated from the racemic mixture to allow for them to be distinguished by GC. ^{1}H NMR spectroscopy was used to identify the most abundant diastereomer in each of the separated samples by comparison to the known ^{1}H NMR data in the literature. The NMR sample was then subjected to GC which determined the retention times of each diastereomer.

The Michael addition of carbonyl compounds to nitroalkenes[226] is a challenging benchmark for newly developed protocols involving enolates and similar intermediates, owing to its potential for the construction of a C-C bond with simultaneous generation of up to three adjacent stereogenic centres and because of the pivotal importance of the nitro group as a precursor to many functionalities.[72] While bifunctional thioureas[227] and chiral Brønsted bases[228,229] have been developed to control the stereochemistry of the process with malonate esters and related methylene-active substrates,[230] stereocontrol during the reaction involving aldehydes and ketones is most often effected from chiral cyclic secondary amines via enamine formation.[231] However, despite the recent efforts in the area, unmet challenges remain with regard to substrate generality and reaction selectivity, including both diastereo- and enantioselectivity. We hoped our intermolecular chirality transfer methodology could help move towards overcoming some of the challenges in this area.

Hydrazone **203** was deprotonated in the presence of **(+)-sp 100** and *sec*-BuLi and reacted with β-nitrostyrene at -70°C, which resulted in the formation of diastereomeric hydrazones, *syn*- and *anti*-**255**. Hydrazone cleavage using HCl/diethyl ether afforded the product **256** (Scheme 3.2.37). Both diastereomers were separable from each other using column chromatography, *syn*-**256** was isolated in 45% yield and *anti*-**256** in 8% yield.

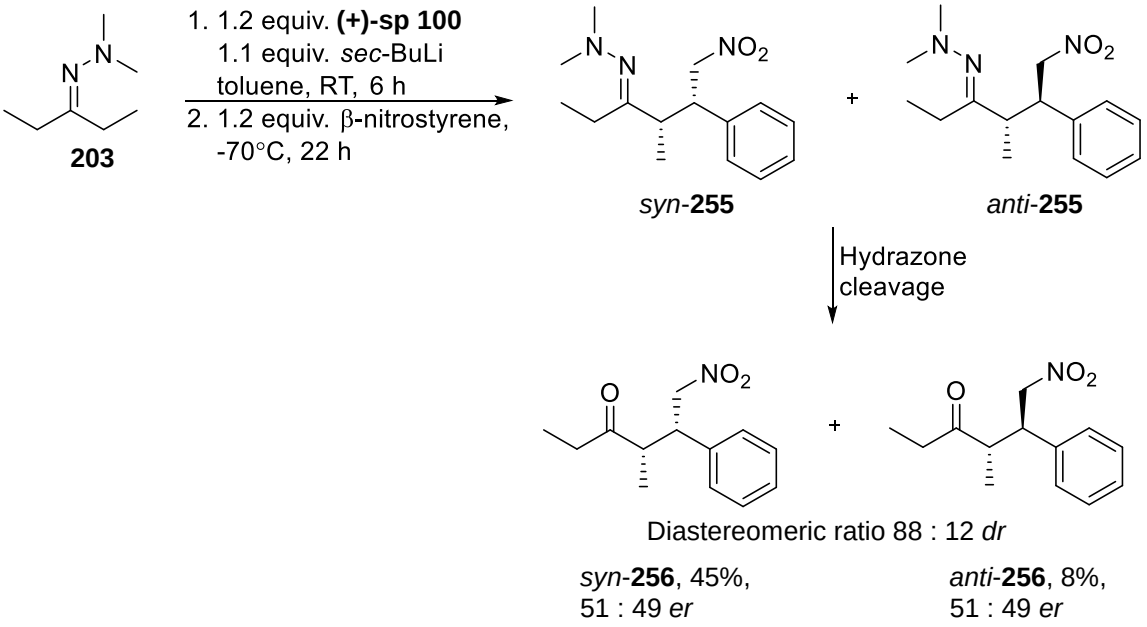

Scheme 3.2.37

The diastereomeric ratio and enantioselectivities were determined on the crude sample immediately after work-up using gas chromatography (Figure 3.2.21).

	syn	*anti*
dr	88	12
er R : S	59 : 41	59 : 41
% ee	2%	2%

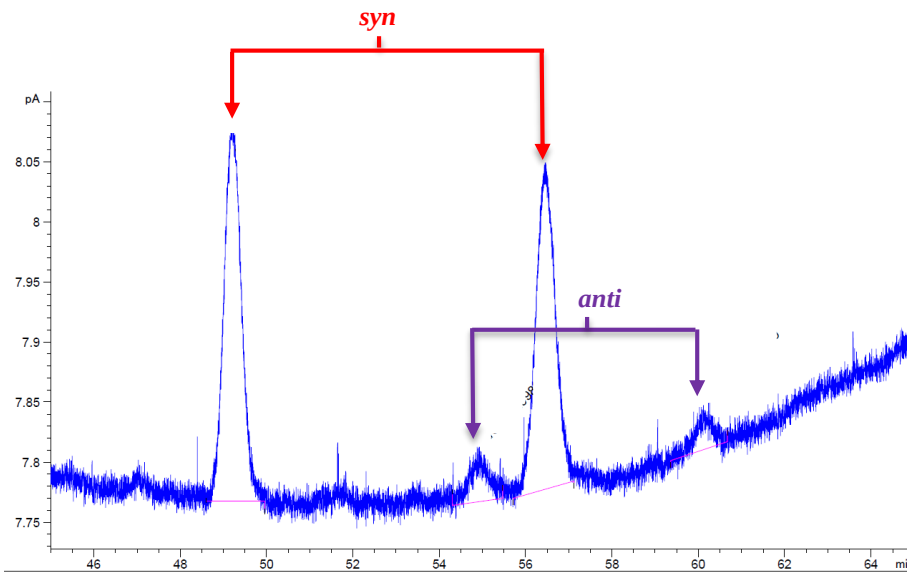

Figure 3.2.21

The *syn* and *anti* peaks were distinguished from each other by comparison of the GC traces with those of the separated diastereomers. ^{1}H NMR spectroscopy of the separated diastereomers allowed us to assign the *syn* and *anti* products in conjunction with the known ^{1}H NMR data in the literature.

3.3 Conclusions and Future Work

The α-alkylation of dimethylhydrazones via an intermolecular chirality transfer strategy for the preparation of enantioenriched α-alkylated ketones is presented. To the best of our knowledge this work details the first example of asymmetric alkylation to a non-chiral acyclic azaenolate. To date optimised conditions have been established with enantiomeric ratios up to 83 : 17.

Key reaction parameters have been investigated including the alkyllithium reagent, solvent, temperature and ligand. Both hydrolytic and oxidative cleavage of the hydrazone have been explored and substrate scope investigations including a number of benzyl based electrophiles have been conducted. Seven chiral ligands have been evaluated, leading to the discovery of a useful ligand scaffold suitable for derivatisation and modification. Preliminary mechanistic and NMR investigations have also been carried out.

Future work on this project will focus on the following:

- Study the effect of changing the metal centre (Na, K, Mg).
- Synthesis and investigation of other ligands.
- Expand catalysis investigation to the inclusion of a ligand exchange protocol.
- Application of this methodology in the α-alkylation of aldehydes and other classes of electrophiles.
- Investigate the use of this methodology in Pd-catalysed arylations.

Chapter 4

Asymmetric α-Alkylation and Synthesis of 1,3-Amino Alcohol Precursors using Chiral Sulfinimines

4.1 Introduction

This chapter describes the use of Ellman's auxiliary in the preparation of α-alkylated ketones and the synthesis of 1,3-amino alcohols using an aldol-Tishchenko protocol. Ellman's auxiliary, 2-methyl-2-propanesulfinamide (*N*-*tert*-butanesulfinamide) **(*R*)-129** (Figure 4.1.1) has proved to be a versatile chiral auxiliary and has been utilised in the preparation of *syn*- and *anti*- 1,2[107-109] or 1,3-amino alcohols,[110,111] α-branched and α,α-quaternary amines,[106,115] α-amino acids[116,117] and β-amino acids and esters.[112-114]

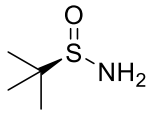

(*R*)-129

Figure 4.1.1

Ellman and co-workers have previously employed this auxiliary for the α-alkylation of *N*-*tert*-butanesulfinyl amidines **257** to afforded alkylated sulfinimines **258** in excellent selectivities (Scheme 4.1.1).[232]

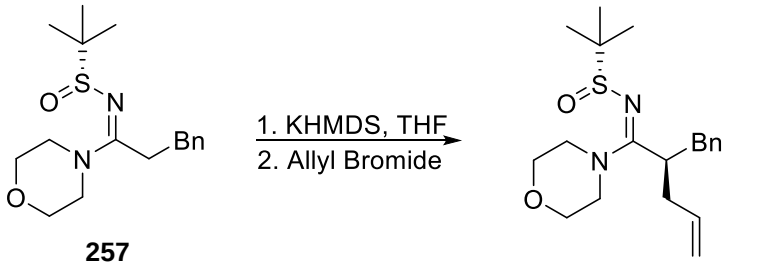

257

258, 92%, 99 : 1 *dr*

Scheme 4.1.1

Also detailed in this chapter is the highly diastereoselective synthesis of 1,3-amino alcohols via addition of *N*-*tert*-butanesulfinyl imines to an aldehyde using an tandem aldol-Tishchenko protocol, in high yields and diastereoselectivity. This is also the first known example of an aldol-Tishchenko reaction involving hydride addition to a C=N moiety.

4.2 Results and Discussion

4.2.1 Synthesis of *N*-*tert*-butanesulfinyl Imines and their Use in Asymmetric α-Alkylation Reactions

The use of *N*-*tert*-butanesulfinamide in the alkylation of simple aliphatic ketones has not been reported in the literature. We felt we could contribute to the existing chiral auxiliary methodology by utilising the *N*-*tert*-butanesulfinamide in the alkylation of 3-pentanone and propiophenone.

Firstly a selection of *N*-*tert*-butanesulfinyl imines were prepared, by condensation of the (*S*)-*N*-*tert*-butanesulfinamide with the corresponding ketone in the presence of $Ti(OEt)_4$ in THF (Scheme 4.2.1).[105,106]

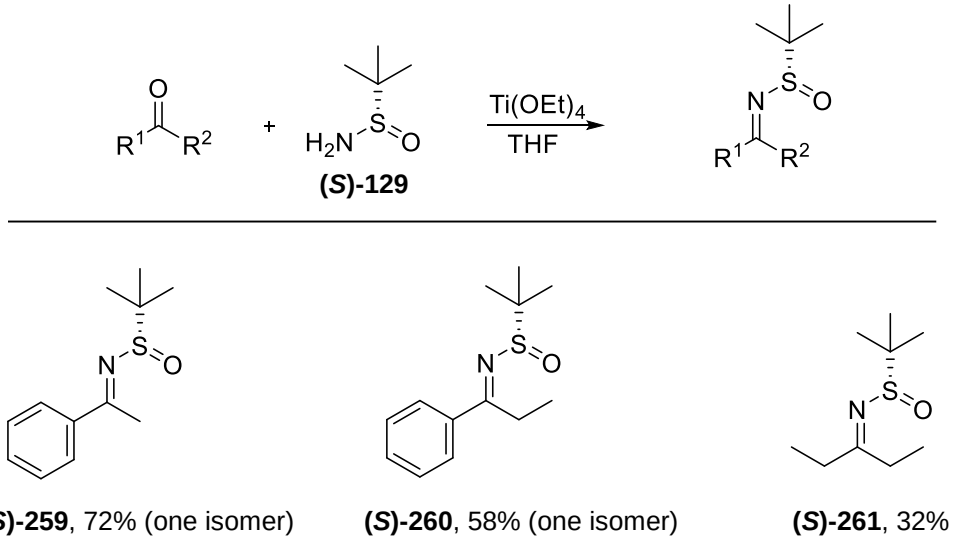

Scheme 4.2.1

A complicating feature of these ketimines is the possibility of forming two imine isomers *E* and *Z* (Figure 4.2.1), which directly impacts on the diastereoselective addition of nucleophiles.[113]

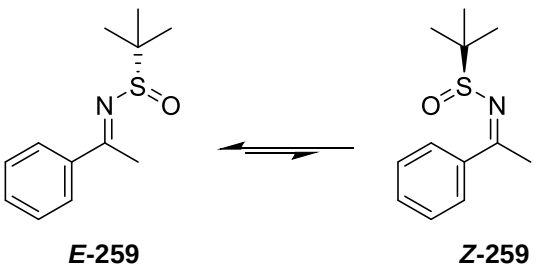

Figure 4.2.1

Fortunately, due to the steric properties of the *N*-*tert*-butanesulfinyl group, only the *E* imine isomer was observed for both **(*S*)-259** and **(*S*)-260**.

Asymmetric α-benzylation was attempted using the sulfinimines **(*S*)-260** and **(*S*)-261**. However both reactions resulted in a complex mixture of products.

In the case of **(*S*)-260** a mixture of the desired alkylation product **262** and by-products including dialkylated product **263**, enamine **264** and starting material were observed in the ^{1}H NMR and mass spectra of the crude material (Scheme 4.2.2).

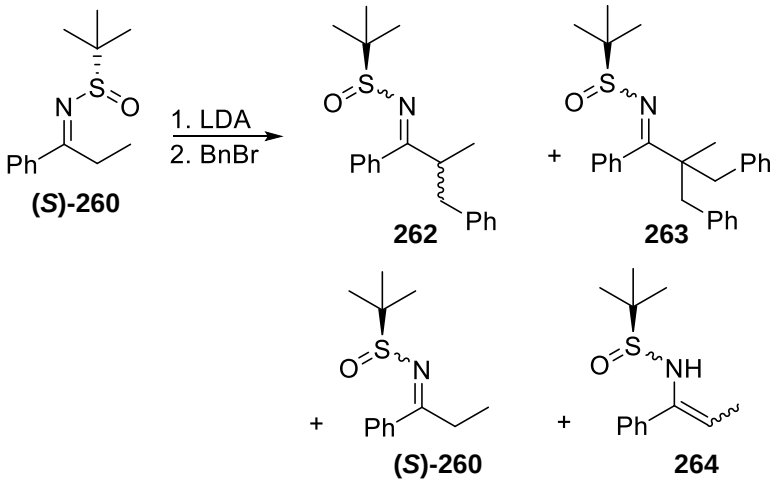

Scheme 4.2.2

This result was unexpected, given that α-alkylations of metalloenamines are often performed to install a stereocenter at the α-position of carbonyl compounds.[10]

We believe the formation of significant amounts of these by-products maybe attributed to the strong electron-withdrawing character of the *N*-sulfinyl group, which attenuates the nucleophilicity of the metalloenamine **265**.[233] This reduces the rate of reaction of the metalloenamine **265** with benzyl bromide, allowing deprotonation of **262** to occur. The more substituted metalloenamine **266**, which is less aggregated, reacts quickly with benzyl bromide resulting in formation of **263** (Scheme 4.2.3).[234]

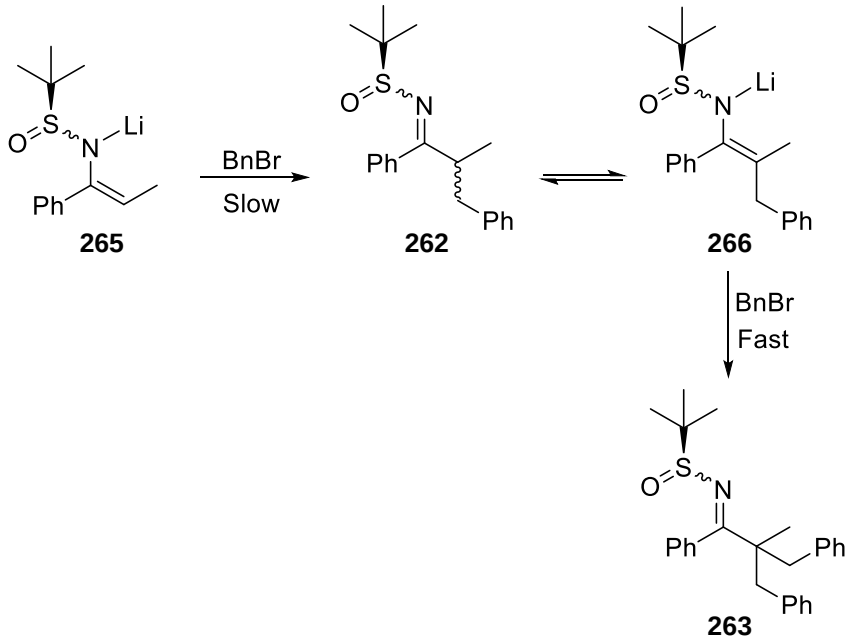

Scheme 4.2.3

4.2.2 Synthesis of 1,3-Amino Alcohol Precursors

As previously stated in section 1.9, chiral 1,3-amino alcohols and their derivatives containing two stereogenic centres are key structural motifs in many natural products and biologically active compounds.[118-131] The moiety is also found in a number of natural products, such as the HIV protease inhibitor, lopinavir **267** (Figure 4.2.2).

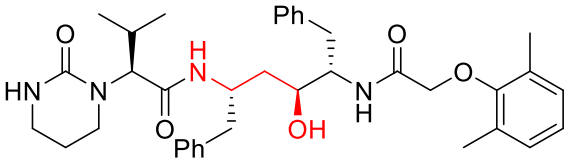

267

Figure 4.2.2

In addition, they are useful building blocks in asymmetric synthesis.[132-139] Various methods have been developed for the preparation of enantiomerically enriched 1,3-amino alcohols. Recent strategies include diastereoselective reduction of enantiopure substrates,[110,111,133,134,136,235-238] an iterative organocatalytic approach[238] and ring opening of chiral piperidines[239-243] or tetrahydropyrans.[244]

Inspired by their unique biological properties and prevalence in natural products we sought to develop a one-pot synthesis of diastereomerically pure 1,3-amino alcohol precursors.

Ellman previously described the preparation of 1,3-amino alcohols using metalloenamines derived from the *N*-*tert*-butanesulfinyl imines **(*R*)-136**. Reduction of the β-hydroxy *N*-sulfinyl imine products **137** provided both the *syn*- and *anti*-1,3-amino alcohol precursors, *syn*- and *anti*-**138** with high diastereoselectivities and yields (Scheme 4.2.4). [110,111]

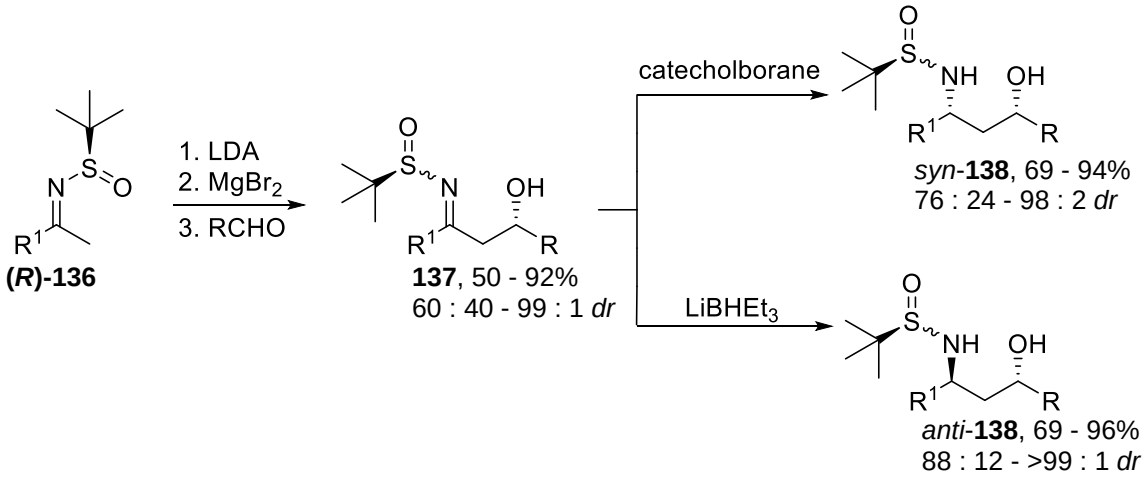

Scheme 4.2.4

We felt we could dramatically improve this methodology by employing a tandem aldol-Tishchenko reaction where an initial aldol reaction would be followed by in situ reduction via a hydride transfer from a second equivalent of aldehyde.

Bodnar and Woerpel previously described the one-pot aldol-Tishchenko reaction of lithium enolates with aldehydes. The lithium enolate reacts with one equivalent of aldehyde followed by attack of the lithium aldolate on a second equivalent. Transfer of the aldehydic hydrogen as a *hydride* occurs in high diastereoselectivity via an organised 6-membered transition state with the bulkiest groups arranged in the equatorial positions (**172**, Figure 4.2.3) as discussed in section 1.10.[152]

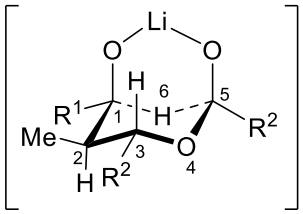

172

Figure 4.2.3

We envisaged the use of Ellman's *tert*-butanesulfinyl imines in an analogous reaction could provide useful diastereomerically and enantiomerically pure aminoalcohol precursors (Scheme 4.2.5).

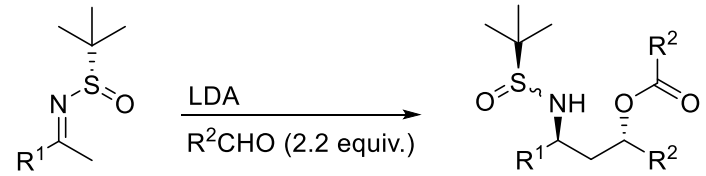

(*S*)-268 *anti*-**269**

Scheme 4.2.5

We chose the chiral sulfinamide as substrate for three reasons:

1. It should provide the required electrophilicity for a Tishchenko hydride transfer (which would not be possible with hydrazone **203** used in Chapter 3 for example).
2. Removal of the group post reaction is easily carried out.
3. The bulky *tert*-butyl group on the sulfur could further enhance the diastereoselectivity in this transformation and crucially introduce enantioselectivity.

Our route to 1,3-amino alcohols would offer distinct advantages over Ellman's synthesis (discussed in section 1.9).[110,111] The in situ reduction using an inexpensive extra equivalent of aldehyde produces precursors to 1,3-amino alcohols without the use of extra additives such as $MgBr_2$. The need for a diastereoselective reduction is also eliminated, avoiding expensive reducing agents such as super hydride and catecholborane. Another advantage of our route is that we install both chiral centres in one pot.

Sulfinimine **(*S*)-259** (prepared in section 4.2.1) was initially subjected to the conditions used by Ellman for the diastereoselective aldol reaction. Thus **(*S*)-259** was deprotonated for 1 h at -78°C using LDA, $MgBr_2$ (2 equiv.) was added in one portion and the reaction mixture was allowed to stir for a further 45 min. Our procedure then deviates from Ellman's and 2.2 equiv. of pivaldehyde were added to the azaenolate and the reaction allowed warm to room temperature (Scheme 4.2.6).

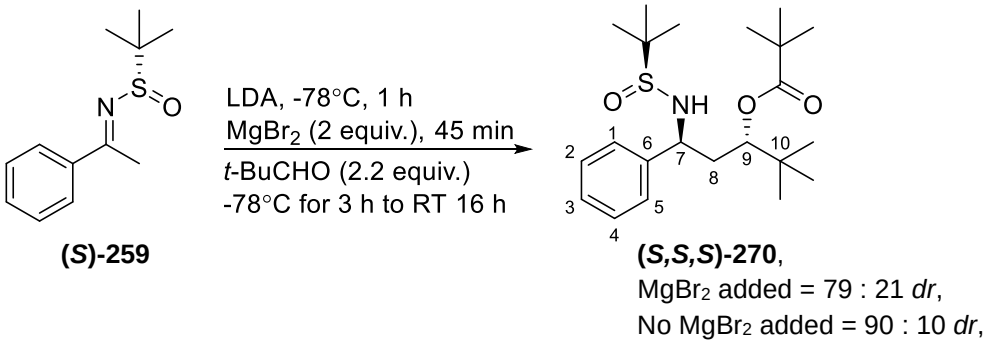

(*S*)-259

(*S,S,S*)-270,
$MgBr_2$ added = 79 : 21 *dr*,
No $MgBr_2$ added = 90 : 10 *dr*,

Scheme 4.2.6

Remarkably, the aldehyde acted as aldol acceptor and hydride donor in this reaction and the aldol-Tishchenko product **(*S,S,S*)-270** was isolated in 15% yield after column chromatography, as a mixture of diastereomers, with a *dr* of 79 : 21, *anti* : *syn*. This was confirmed by spectroscopic and crystallographic analysis.

The ^{13}C NMR showed a peak at 178.6 ppm, indicative of the carbonyl of the ester. This was further supported by the infrared spectrum where a signal at 1725 cm^{-1} was observed, also corresponding to the carbonyl of an ester. Also the ^{13}C NMR spectrum CH signals at 57.3 and 77.3 were characteristic of the carbons at C-7 and C-9 respectively. The exact structural assignment was also confirmed using COSY, HSQC and HMBC experiments. High resolution mass spectrometry found the protonated molecular ion at 396.2559 which was in good agreement with the calculated value of 396.2572.

Further optimisation of the reaction conditions revealed that $MgBr_2$ was unnecessary. In fact, when $MgBr_2$ was omitted from the reaction mixture, the yield was raised to 64% (mixture of diastereomers) and the diastereomeric ratio was increased to 90 : 10, *anti* : *syn*. Again the diastereomeric ratio was determined from the crude ^1H NMR spectrum (Figure 4.2.4).

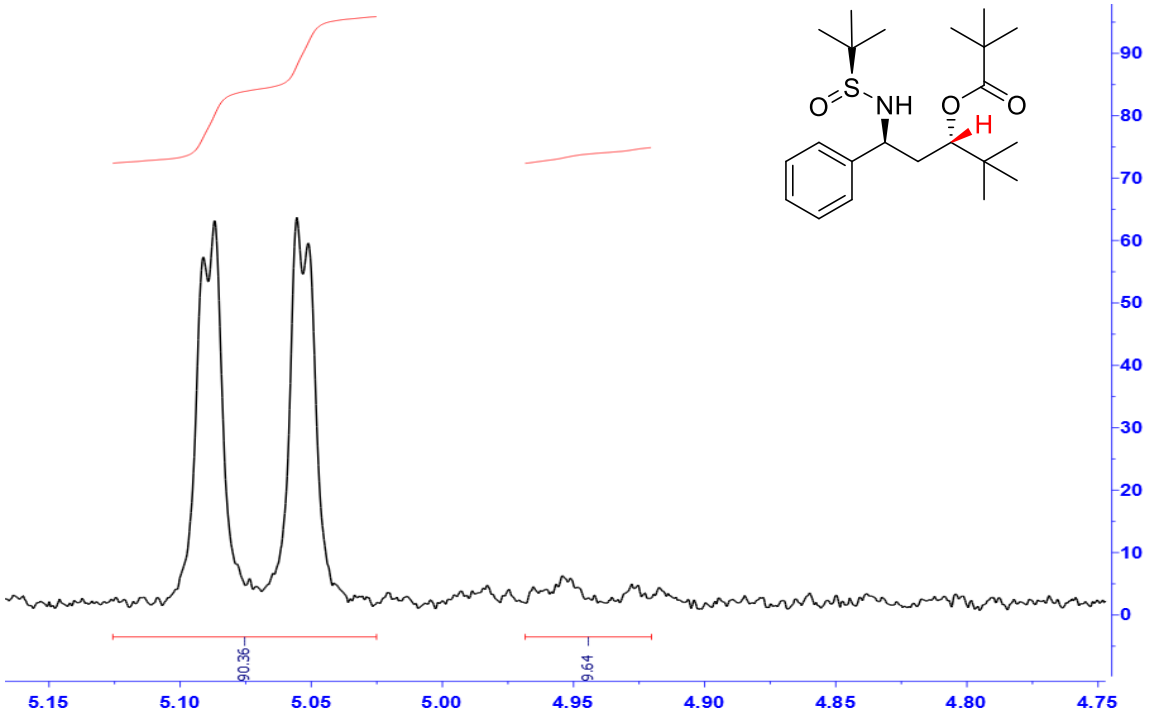

Figure 4.2.4

The major diastereomer and minor diastereomers were isolated separately in 59% and 5% yield respectively, after column chromatography. The absolute stereochemistry of the major diastereomer was determined using X-ray crystallographic analysis (Figure 4.2.5).

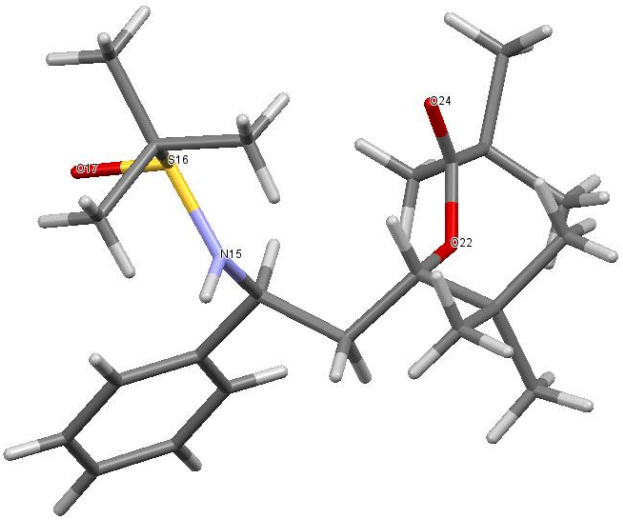

Figure 4.2.5

It can be clearly seen from the crystal structure (Figure 4.2.5), the geometry of N-15 and O-22 are *anti* to one another in the case of **(*S*,*S*,*S*)-270** and all chiral centres could be assigned as the *S*-configuration. **(*S*,*S*,*S*)-270** was found to have the space group, *P* $2_12_12_1$, indicating it is primitive (it contains one lattice point), it is orthorhombic (the has three different cell lengths) and each angle in a unit cell is 90°. The cell length in the c axis is quiet large, indicating the crystals are likely packing in an elongated fashion (Table 4.2.1).

Chemical formula	$C_{20}H_{25}NO_6$
Space group	*P* $2_12_12_1$
Cell dimensions (Å)	*a* = 9.6296 (11)
	b = 10.9154 (19)
	c = 23.692 (4)
	α = 90
	β = 90
	γ = 90
No. of molecules (Z)	4
R (Reliability factor)	0.0494 (3289)

Table 4.2.1 Crystallograhic data for **(*S*,*S*,*S*)-270**

The R-factor, (reliability factor) which is a measure of the agreement between the crystallographic model and the experimental X-ray diffraction data, is very good for **(*S*,*S*,*S*)-270** at 0.0494.

We were very interested to observe the opposite stereochemistry to that of Ellman at the C-O chiral centre (Scheme 4.2.7).

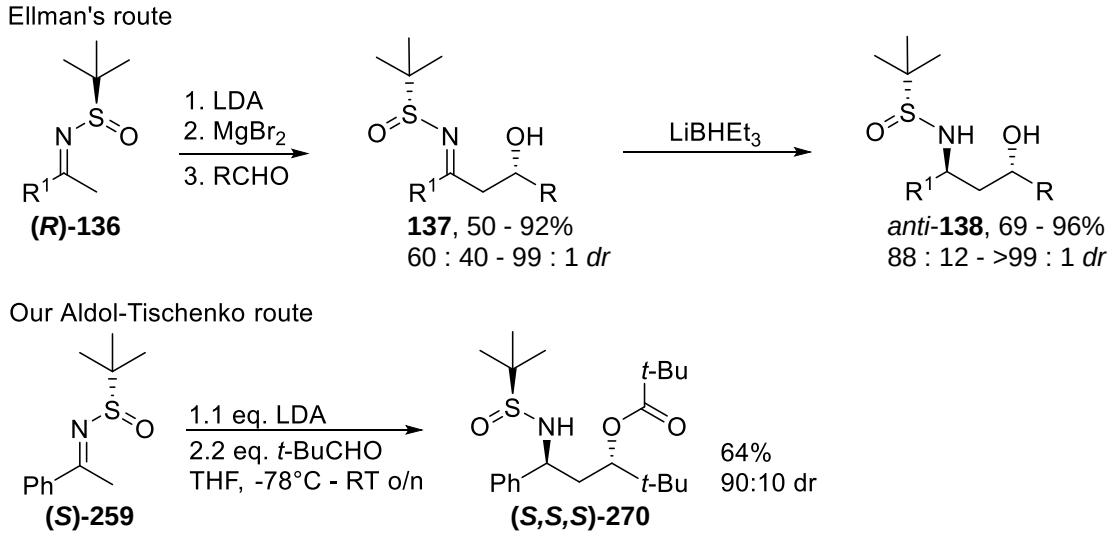

Scheme 4.2.7

Based on the results published by Ellman[110] – and the transition states proposed therein – formation of the *R*-alkoxide **(*S*,*R*)-274** is most likely favoured initially, subsequently giving the adduct **(*S*,*R*)-271** as the major alkoxide species in the reaction (Scheme 4.2.8). However we hypothesised that a six membered transition state (**272a** and **272b**) for the hydride reduction step, with the bulkiest substituents arranged in the preferred equatorial positions, similar to that proposed by Bodnar and Woerpel,[152] would be the key difference in our system. On examining these transition states **272a** and **272b** (using a molecular modelling kit), the more activated transition state **272a** which would lead to the *anti*-product **(*S*,*R*,*R*)-270**, has a very sterically unfavourable interaction. In this state, in order for the sulfoxide oxygen to coordinate to the lithium, and generate a reactive anionic reducing species, the *tert*-butyl group of the auxiliary has to be directed in towards the centre of the six-membered transition state, giving an unfavourable steric interaction with the *tert*-butyl group at C-9.

As the final hydride transfer is essentially irreversible, the transition state leading to successful transfer will ultimately dictate the final product, with equilibrium effects funnelling all intermediates towards this transition state. This means that although the major intermediate is likely to be **(*S*,*R*)-271**, it is the activated transition state **272b**, arising from intermediate **(*S*,*S*)-271**, which has the bulky *tert*-butyl group directed away from the six-membered transition state and lacks unfavourable steric interactions, that is more likely to form and successfully lead to hydride transfer. This transition state **272b** results in faster hydride transfer and leads to the stereochemistry observed in the major final product **(*S*,*S*,*S*)-270** which is opposite to that which would be expected in the major intermediates, as proposed based on Ellman's work. For our hypothesis to hold true we would require the aldol addition step to be reversible. Recent work within the group before publication of this thesis has shown that the aldol addition is in fact reversible.[245] Overall, these transition states **272a** and **272b** do allow for the influence of the chirality of the auxiliary in producing the observed stereochemistry. If the *tert* -butyl group was a purely steric effect and not directed by the initial stereochemistry of the auxiliary, then an equal mixture of the two possible anti isomers **(*S*,*S*,*S*)-270** and **(*S*,*R*,*R*)-270** should be observed as the major product.

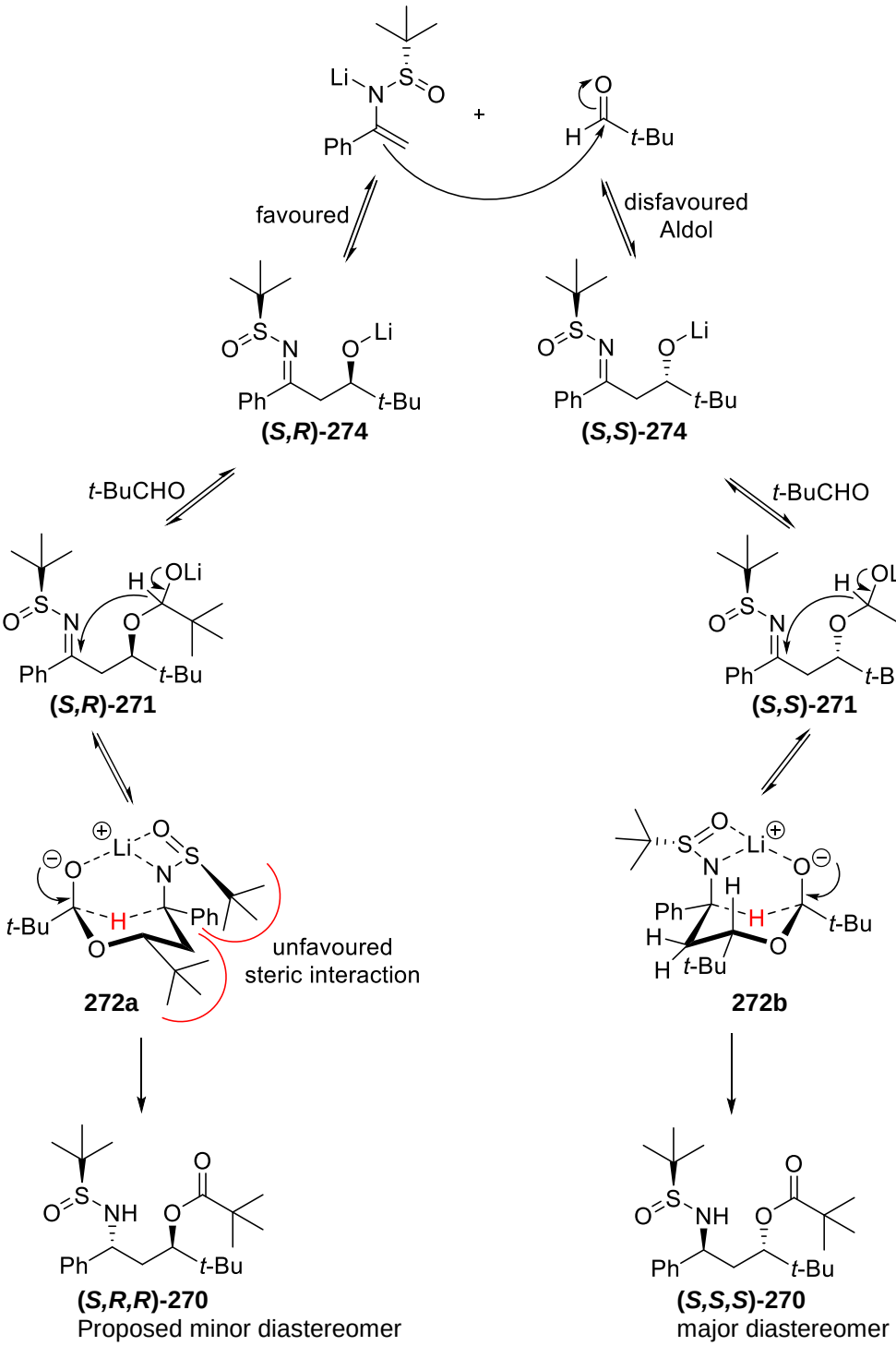

Scheme 4.2.8

Additionally if we were to look solely at the relationship between the observed vicinal coupling constant (H-C-C-H, ^{3}J) and the dihedral angle between coupled protons, i.e. the Karplus equation, we can also make an assumption about the stereochemistry of the major and minor diastereomers formed in our reaction. The Karplus relationship is based on the observation, supported by theoretical considerations, that vicinal H-H couplings will be maximal with

protons with 180° and 0° dihedral angles (anti or eclipsed relationship results in optimal orbital overlap) and that coupling will be minimal (near 0) for protons that are 90° from each other.

Looking at the coupling constants for the protons on C-7, C-8 and C-9, of the major diastereomer, and the relationship to the dihedral, we can make an assumption about the structure of the product in solution. While one might predict the structure of **(*S*,*S*,*S*)-270** to lie in the chair confirmation indicated in Figure 4.2.6.

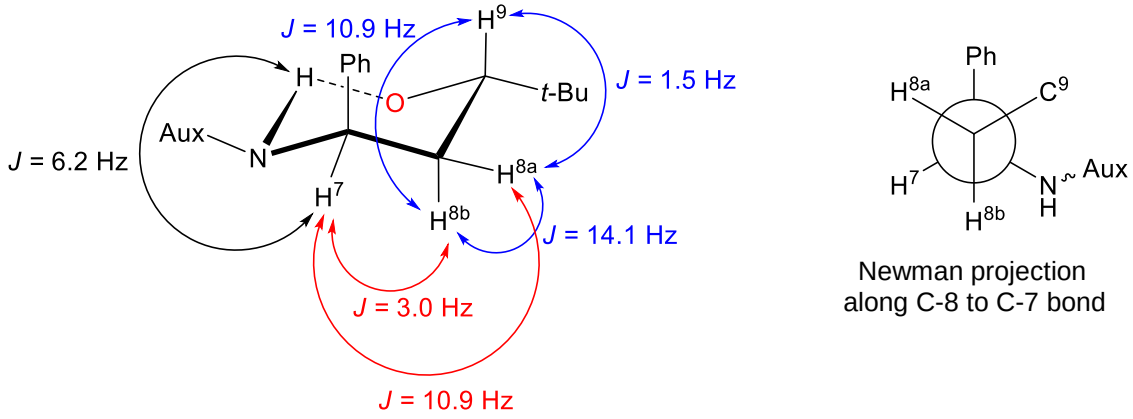

Figure 4.2.6

However, while all coupling constants indicated in blue do satisfy the Karplus equation, the coupling constants indicated in red, for the coupling between the proton of C-7, H^7 and the protons of C-8, H^{8a} and H^{8b}, do not agree with predictions from the Karplus equation in this particular confirmation. Both H^{8a} and H^{8b} have dihedral angle of 60° with H^7 (see Newman projection Figure 4.2.6) and therefore should have similar coupling constants of between 2-5 Hz.[246]

For all the observed coupling constants of **(*S*,*S*,*S*)-270** to be in agreement with the Karplus equation then **(*S*,*S*,*S*)-270** would have to adopt a boat confirmation (Figure 4.2.7), where C-7 is flipped down resulting in H^7 having a dihedral angle of 180° with H^{8a} (J = 8-15 Hz) and 60° (J = 2-5 Hz) with H^{8b}.[246]

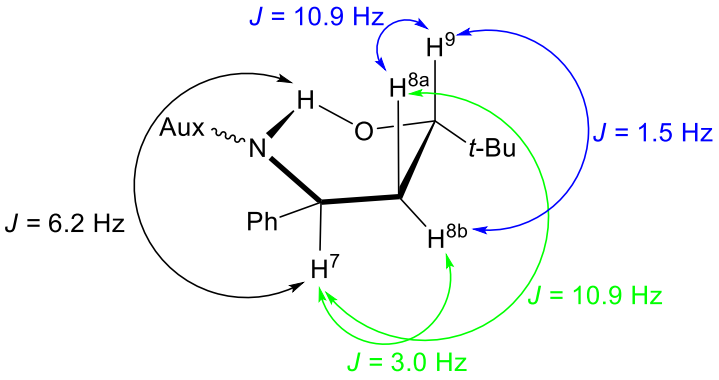

Figure 4.2.7

Given that the minor diastereomer has the same coupling constant pattern it is possible that it assumes as similar structure where C-7 and C-9 have an *anti*- relationship. This observation provides further evidence for our proposed mechanistic pathways discussed earlier.

During the purification of **(*S*,*S*,*S*)-270**, impurity **(*S*)-273** was isolated in 25% yield. Analysis of the spectroscopic data and X-ray crystallographic analysis, identified **(*S*)-273** as the compound in Figure 4.2.8.

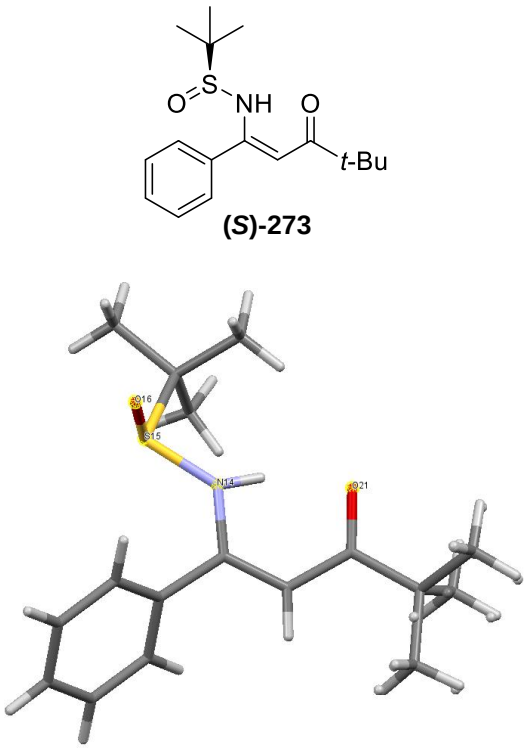

Figure 4.2.8

(*S*)-273 was found to have the space group *P* 2_1, indicating it is primitive (it contains one lattice point), it is monoclinic (has three different cell lengths two of the angles in a unit cell are 90° and the third angle is not 90°) (Table 4.2.2). Two molecules are contained in each unit cell. The R-factor, (reliability factor) for **(*S*)-273** is excellent at 0.0411.

Chemical formula	**$C_{20}H_{25}NO_6$**
Space group	*P* 2_1
Cell dimensions (Å)	*a* = 10.200 (9)
	b = 9.406 (8)
	c = 10.462 (9)
	α = 90
	β = 116.167 (13)
	γ = 90
No. of molecules (Z)	2
R (Reliability factor)	0.0632 (1776)

Table 4.2.2 Crystallograhic data for **(*S*)-273**

For **(*S*)-273**, a characteristic peak was observed in the infrared spectrum at 1558 cm^{-1} indicative of a carbonyl group. In the ^{1}H NMR spectrum a peak at 5.69 ppm suggested the presence of an alkenyl proton and in the ^{13}C NMR spectrum the peak at 207.7 ppm further confirmed the presence of a ketone carbonyl group. High resolution mass spectrometry indicated a protonated molecular ion of 308.1684, which was in good agreement with the calculated value of 308.1688.

We rationalised this impurity may have been a result of a Meerwein–Ponndorf–Verley reduction/Oppenauer oxidation (Scheme 4.2.9).[247,248] Traditionally achieved using an aluminium metal centre,[247,248] there is also precedent for the use of lithium in this transformation.[249]

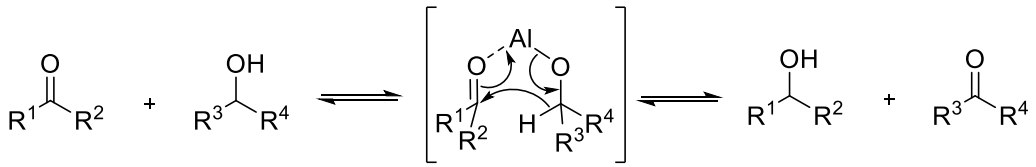

Scheme 4.2.9

We believe this transformation occurs in competition with the formation of **(*S*,*S*,*S*)-270**. We propose the following mechanism for the formation of **(*S*)-273** (Scheme 4.2.10).

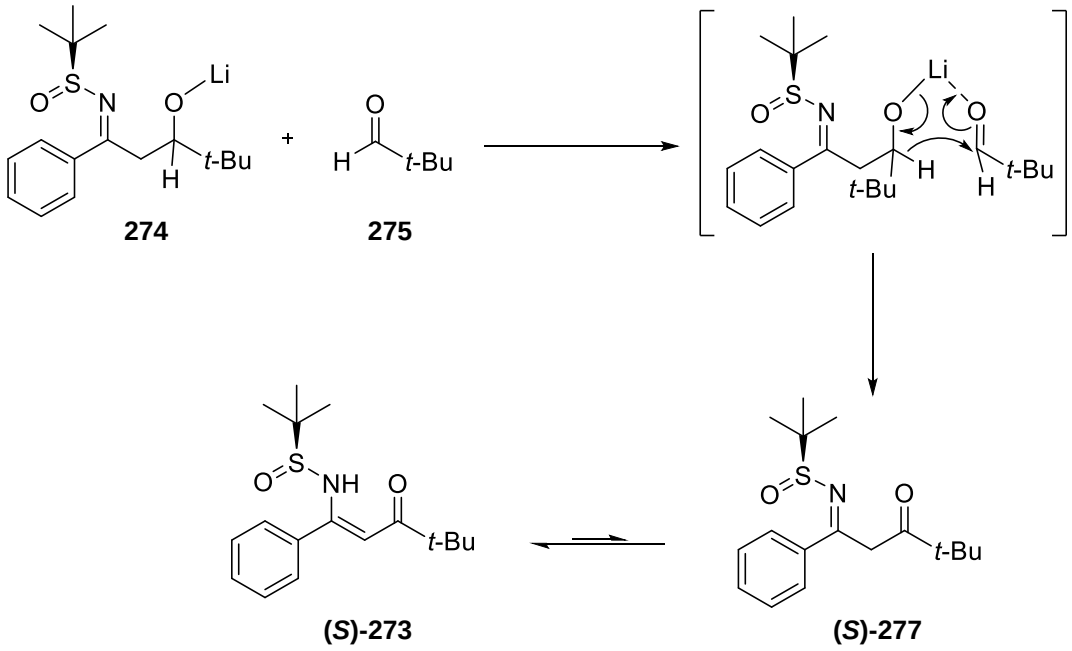

Scheme 4.2.10

Lithium aldolate **274** undergoes an Oppenauer oxidation to form the keto-imine **(*S*)-277**, via which tautomerises to the enamine **(*S*)-273**. The aldehyde **275** undergoes Meerwein–Ponndorf–

Verley reduction to the alcohol. At this stage we surmise that reducing the final temperature during the warm up stage may limit the formation of **(*S*)-273**. Certainly avoiding the formation of the by-product (25%) would significantly improve our yields and enhance the applicability of our reaction.

Cleavage of the ester group to afford the β-hydroxy amine was investigated next. Pivalate esters can be cleaved by a range of methods,[250] including bases such as potassium hydroxide or potassium *tert*-butoxide.

To further enhance the synthetic utility of this synthesis we wanted to establish a simple cleavage method which would be efficient and low cost.

For this reason the relatively inexpensive strong base, potassium hydroxide was investigated for the removal of the pivalate ester **(*S*,*S*,*S*)-270**. Potassium hydroxide was added to **(*S*,*S*,*S*)-270**, in a 1 : 1 mixture of ethanol and water. After 24 hours the desired product **(*S*,*S*,*S*)-278** was not formed and only starting material was isolated (Scheme 4.2.11).

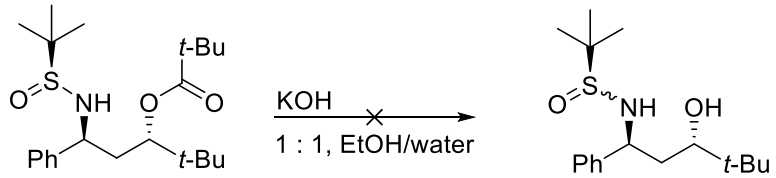

(*S*,*S*,*S*)-270 **(*S*,*S*,*S*)-278**

Scheme 4.2.11

The reaction was repeated with potassium carbonate in methanol and heated at reflux overnight.[251] Again only starting material was isolated.

We believe both of these procedures failed due to the steric bulk surrounding the carbonyl of the pivalate ester. With two *tert*-butyl groups in close proximity, attack of the nucleophile necessary in the cleavage mechanism is hindered and therefore unsuccessful.

Cleavage of the pivalate group was achieved using a DIBAL-H reduction (Scheme 4.2.12).

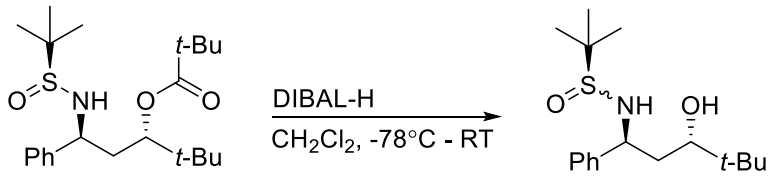

(*S*,*S*,*S*)-270 **(*S*,*S*,*S*)-278**, 51%

Scheme 4.2.12

Pivalate ester **(*S*,*S*,*S*)-270** was added to DIBAL-H in anhydrous dichloromethane, under N_2 atmosphere at -78°C. The reaction was allowed warm to room temperature overnight. The reaction was cooled to 0°C and methanol was added slowly to quench the excess DIBAL-H. The reaction was allowed warm to room temperature and aqueous 10% HCl solution was slowly added to hydrolyse the aluminium salts. After work-up, the cleaved β-hydroxy amine, **(*S*,*S*,*S*)-**

278 was successfully isolated in 51% yield. Subsequent work by others in the group has shown other esters (e.g. *i*-Pr) are easily cleavage using potassium hydroxide.[245]

Analysis of the spectroscopic data confirmed successful cleavage of the ester moiety. Most notably, the absence of the peak at 178.6 ppm for the ester carbonyl in the ^{13}C NMR spectrum and the presence of the broad singlet at 2.77 ppm for the alcohol proton suggested the formation of **(*S*,*S*,*S*)-278**. The exact structural assignment was determined using COSY, HSQC and HMBC experiments. Using the HMBC spectrum (Figure 4.2.9) it was possible to assign the signal which corresponds to the carbon of C-7. The quaternary carbon of the aromatic ring showed a correlation with the peak at 4.71 ppm, i.e. a 2-bond coupling to the protons of the adjacent carbon, C-7. A correlation was also observed with the peak at 1.89 ppm, i.e. a 3-bond coupling to the protons at C-8.

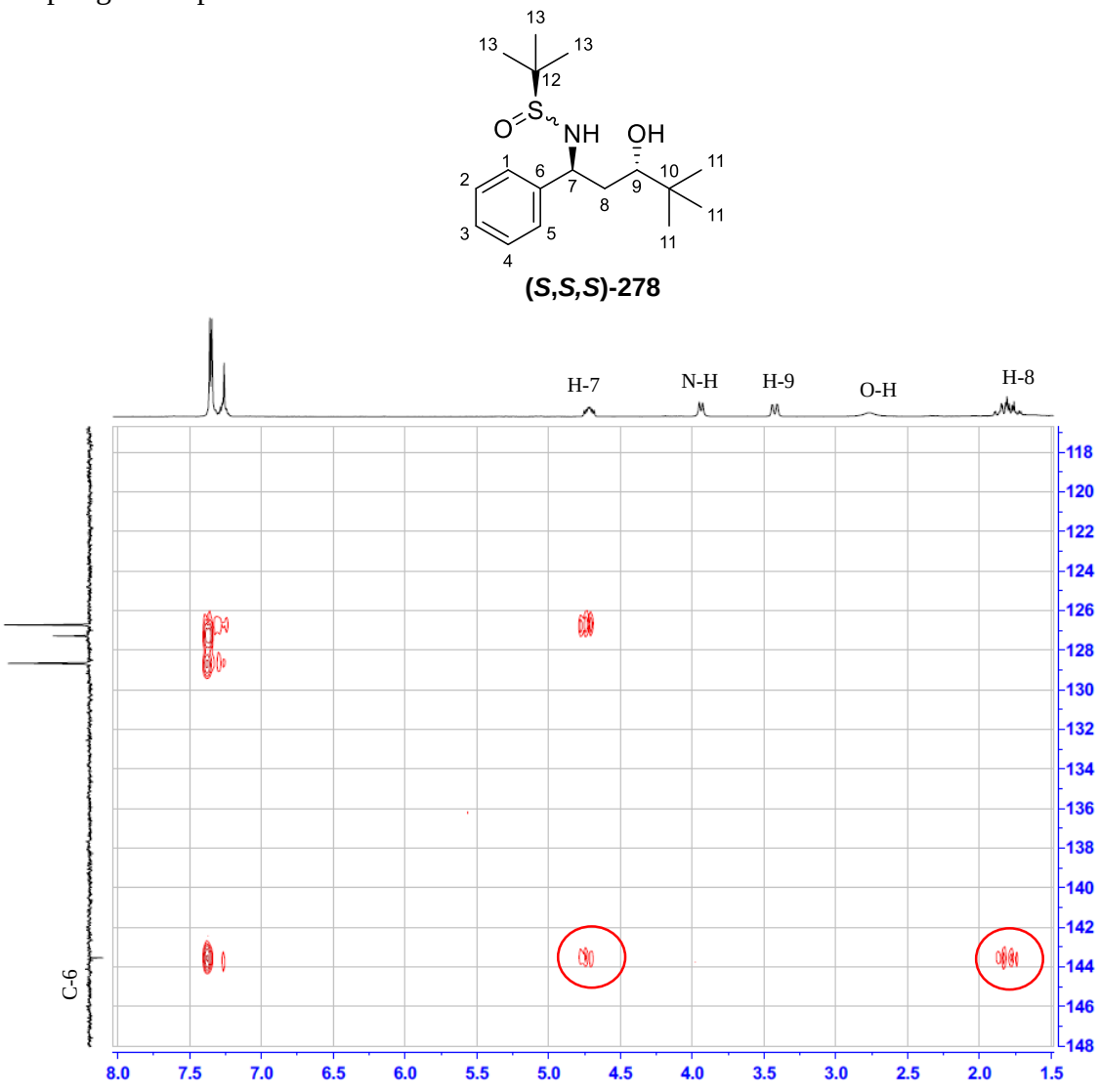

Figure 4.2.9 HMBC spectrum for **(*S*,*S*,*S*)-278**

In the COSY spectrum, the peak at 4.71 ppm also showed a correlation with the peaks at 1.89 (H-8) and 3.94 (N-H) ppm, which further confirmed the assignment of the C-7 (Figure 4.2.10).

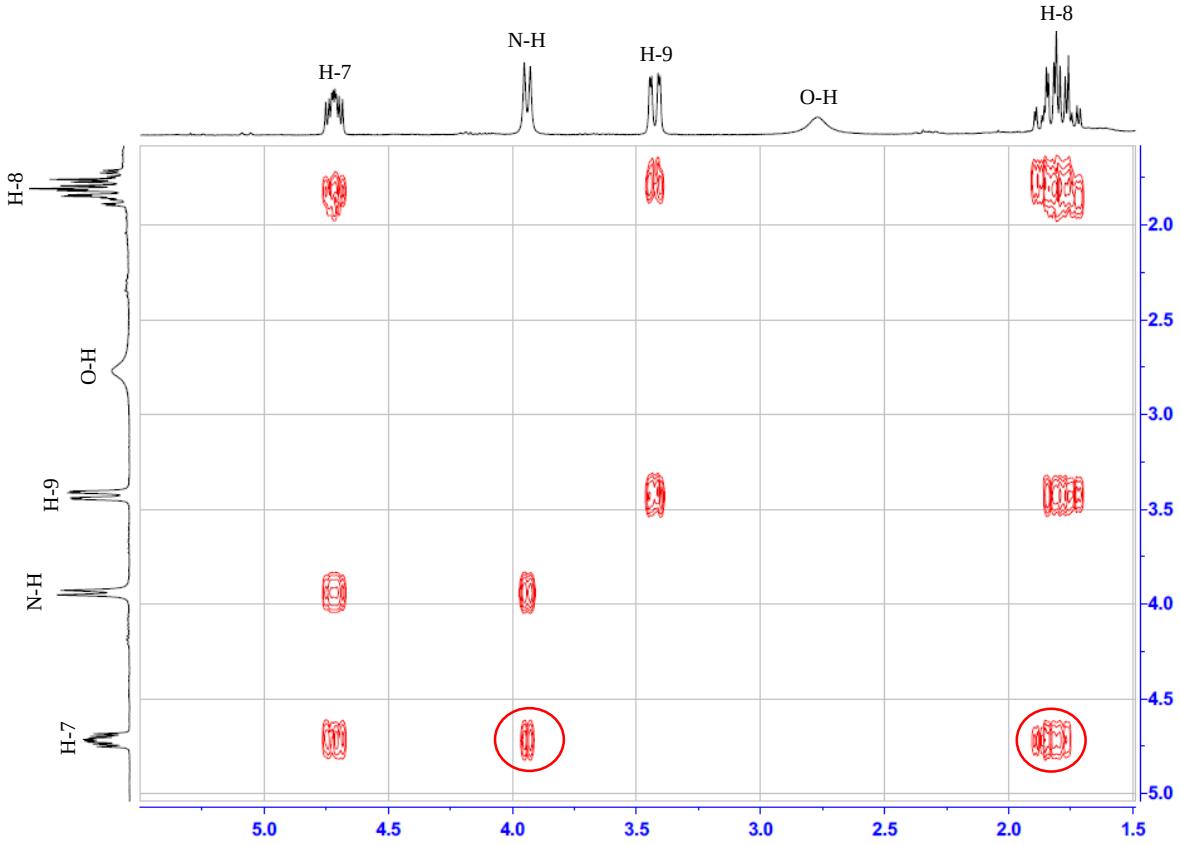

Figure 4.2.10 COSY spectrum for **(*S*,*S*,*S*)-278**

The successful cleavage of pivalate esters, using hydrochloric acid in 1,4-dioxane, has been reported.[252] Given that hydrochloric acid is also used for the cleavage of the *N-tert*-butanesulfinyl auxiliary,[144] we hoped that the removal of both the auxiliary and the ester could be achieved in one step.

To **(*S*,*S*,*S*)-270** in 1,4-dioxane was added 4 M HCl. The reaction mixture was heated at reflux overnight. The reaction mixture was then cooled to room temperature and concentrated under reduced pressure. Ethyl acetate was added, at which point the product crashed out of solution. The formed solid was filtered and dried. Analysis of the spectroscopic data confirmed the auxiliary was successfully cleaved, however the ester group remained and **(*S*,*S*)-279** was isolated as the HCl salt in 85% yield (Scheme 4.2.13).

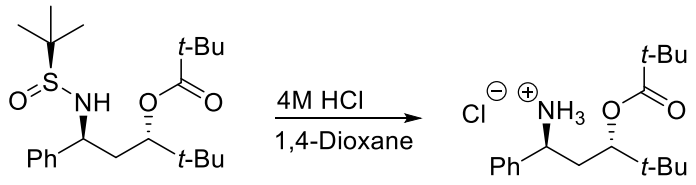

(*S*,*S*,*S*)-270 **(*S*,*S*)-279**

Scheme 4.2.13

The ^{13}C NMR spectrum showed a distinctive peak at 179.1 corresponding to the presence of an ester carbonyl group. High resolution mass spectrometry found the protonated molecular ion at 292.2276 which was in good agreement with the calculated value of 292.2277.

4.3 Conclusions and Future Work

A new method for the preparation of chiral *anti*-1,3-amino alcohols is described. The first application of a tandem aldol-Tishchenko reaction on C=N is reported resulting in *anti*-1,3-amino alcohol precursors in high levels of diastereoselectivity. Also to the best of our knowledge this is the first synthesis of 1,3-amino alcohols that installs both chiral centres (C-N and C-O) concomitantly in one pot.

Expanding on this successful work, we would hope to optimise the reaction conditions in an attempt to improve yields and minimise formation of the impurity **(*S*)-273**. We also intend to perform substrate scope investigations, which would include changing the *N*-*tert*-butanesulfinamide and varying the aldehyde. The *tert*-butyl ester is a particularly difficult functional group to cleave using simple bases and we would hope to showcase our methodology with the avoidance of DIBAL-H in future reactions. Mechanistic studies will also be carried out, as well as extension of the methodology to the formation of three and five chiral centres in one pot. Future work will also focus on the investigation of the use of catalysts such as samarium diiodide previously utilised by Evans.[148]

Chapter 5

Experimental

5.1 General Procedures

Solvents employed were distilled prior to use as follows:
Cyclohexane was distilled from calcium hydride. THF, diethyl ether (Et_2O) and toluene were distilled from sodium benzophenone ketyl. Methyl *tert*-butyl ether (MTBE), benzene and cumene were purchased as anhydrous solvents from Sigma Aldrich. Sparteine was distilled prior to use, using a Kugelrohr distillation apparatus. (-)-Sparteine **(-)-sp 100** was purchased from Santa Cruz Technologies Inc. (+)-Sparteine **(+)-sp 100** was purchased from Beta Pharma. All other reagents were purchased from Sigma Aldrich unless otherwise noted.

Wet flash column chromatography was carried out using Kieselgel silica gel 60, 0.040-0.063 mm (Merck). Thin layer chromatography (TLC) was carried out on pre-coated silica gel plates (Merck 60 PF254). Visualisation was achieved by potassium permanganate staining.

Melting points were measured on a Thomas Hoover Capillary Melting Point apparatus.

Infrared (IR) spectra were recorded on a Perkin-Elmer FT-IR Paragon 1000 spectrophotometer. Liquid samples were examined as thin films interspersed between sodium chloride plates. Solid samples were dispersed in potassium bromide and recorded as pressed discs. The intensity of peaks were expressed as strong (s), medium (m) and weak (w).

NMR spectra were run in $CDCl_3$ using tetramethylsilane (TMS) as the internal standard, unless otherwise specified. ^1H NMR spectra were recorded at 300 MHz on a Bruker AVANCE 300 spectrometer and ^{13}C NMR spectra were recorded at 75 MHz on a Bruker AVANCE 300 instrument, unless otherwise stated. All spectra were recorded at University College Cork. Chemical shifts δ_H and δ_C are expressed as parts per million (ppm), positive shift being downfield from TMS; coupling constants (*J*) are expressed in hertz (Hz). Splitting patterns in ^1H NMR spectra are designated as s (singlet), br s (broad singlet), d (doublet), dd (doublet of doublets), dt (doublet of triplets), t (triplet), q (quartet), quin (quintet), sext (sextet), sept (septet), and m (multiplet). For ^{13}C NMR spectra, the number of attached protons for each signal was determined using the DEPT pulse sequence run in the DEPT-90 and DEPT-135 modes. The terms C, CH, CH_2, and CH_3 are used to designate the signals as $C(H)_n$; n = 0, 1, 2, 3. HSQC, COSY and HMBC experiments were routinely performed to aid the NMR assignment of novel chemical structures.

Low resolution mass spectra (LRMS) were recorded on a Waters Quattro Micro triple quadrupole instrument in electrospray ionization (ESI) mode using 50% acetonitrile- water containing 0.1% formic acid as eluent. Samples were made up in acetonitrile. High resolution precise mass spectra (HRMS) were recorded on a Waters LCT Premier Tof LC-MS instrument in electrospray ionization (ESI) mode using 50% acetonitrile-water containing 0.1% formic acid as eluent. Samples were prepared in acetonitrile.

Enantiopurity of the chiral compounds was determined by chiral gas chromatography performed on an Astec CHIRALDEX^{TM} G-TA, fused silica capillary column, 20 m x 0.25 mm x 0.12 µm film thickness. GC analysis was performed on an Agilent Technologies 7820 A GC system. All chiral columns were purchased from Sigma-Aldrich Supelco. Conditions for separation were determined using the following operating conditions as standard, flow rate: 1 mL/min, injection volume: 0.2 µL, split ratio: 10 : 1, front inlet temperature: 150°C, detector temperature: 155°C.

Optical rotations were measured on a Perkin-Elmer 141 polarimeter at 589 nm in a 10 cm cell. Concentrations (c) are expressed in g/100 mL. α_D^T is the specific rotation of a compound and is expressed in units of 10^{-1} deg cm^2 g^{-1}.

The Microanalysis Laboratory, National University of Ireland, Cork, performed elemental analysis using a Perkin-Elmer 240 and Exeter Analytical CE440 elemental analysers.

Single crystal X-ray analysis was conducted by Dr. S.E. Lawrence, Department of Chemistry, National University of Ireland, Cork, or other members of his group using a Nonius Mach 3 diffractometer with graphite monochromatised Mo-Ka radiation. Calculations were performed on a PC with the maXus (C.J. Gilmore et al, University of Glasgow, 1998), SHELXL-97 (G.M. Sheldrick, University of Gottingen, 1998) and Platon (A.L. Spek, University of Utrecht, 1998) suite of programs

^{1}H NMR spectra, ^{13}C NMR spectra, LRMS and melting point (if solid) analyses were recorded for all previously prepared compounds. For novel compounds, in addition to the previously mentioned analysis, IR, HRMS and elemental analysis (if possible) were also obtained. Optical rotations were used to assign absolute stereochemistry for known compounds.

An arbitrary numbering system was employed to aid the assignment of ^{1}H NMR and ^{13}C NMR spectra.

5.2 Synthesis of Racemic α-Alkylated Ketones

General Procedure for Synthesis of Racemic α-Alkylated Ketones

To a schlenk tube under N_2 atmosphere, containing diisopropylamine (1.2 equiv.) in anhydrous THF (5 mL), was added *n*-BuLi (1.1 equiv.) at 0°C. The mixture was allowed to stir at 0°C for 30 min. The reaction mixture was cooled to -78°C, the **ketone** (1 equiv.) was added dropwise and allowed to stir for 1 h. The **electrophile** (1.2 equiv.) was added dropwise and the reaction was allowed warm to room temperature and stirred overnight. The reaction was quenched with saturated NH_4Cl (1.5 mL), Et_2O (10 mL) and NH_4Cl (10 mL) were added and the mixture was extracted with Et_2O (3 x 30 mL). The organic layers were combined and dried over anhydrous $MgSO_4$, filtered, and concentrated under reduced pressure.

2-methyl-1-phenylpentan-3-one 36

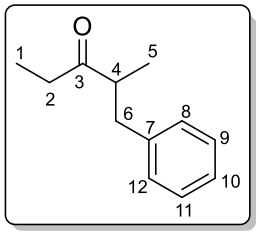

Prepared following the general procedure outlined above using 3-pentanone and benzyl bromide. The crude product was purified using column chromatography (10 : 1, hexane : Et_2O) on silica gel to give the title compound **36** as a clear oil (0.365 g, 19%).

Spectroscopic characteristics were consistent with previously reported data.[192] R_f = 0.45 (5 : 1, hexane : Et_2O). ^{1}H NMR (300 MHz, $CDCl_3$): δ 0.95 (3H, t, *J* = 7.3 Hz, H-1), 1.08 (3H, d, *J* = 6.0 Hz, H-5), 2.25 (1H, dq, *J* = 17.9, 7.3 Hz, H-2), 2.44 (1H, dq, *J* = 17.9, 7.3 Hz, H-2), 2.57 (1H, dd, *J* = 7.2, 14.2 Hz, H-6), 2.78-2.89 (1H, m, H-4), 2.97 (1H, dd, *J* = 7.2, 14.2 Hz, H-6), 7.12-7.30 (5H, m, Ar-H) ppm; ^{13}C NMR (75.5 MHz, $CDCl_3$): δ 7.6 (C-1), 16.6 (C-5), 35.2 (C-2), 39.3 (C-6), 47.9 (C-4), 120.2 (Ar-CH), 128.4 (2 x Ar-CH), 128.9 (2 x Ar-CH), 139.9 (Ar-C), 214.8 (C-3) ppm; MS (ESI) *m/z*: 177 $[M + H]^+$.

GC analysis: t_R = 7.4 and 7.8 min (120°C hold for 10 min, ramp 10°C/min to 140°C, hold for 5 min).

2-methyl-1-(4-(trifluoromethyl)phenyl)pentan-3-one 183

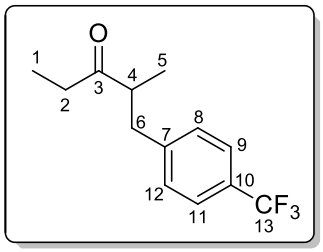

Prepared following the general procedure outlined above using 3-pentanone and 4-trifluoromethylbenzyl bromide. The crude product was purified using column chromatography (15 : 1, hexane : Et_2O) on silica gel to give the title compound **183** as a clear oil (0.237 g, 10%).

Spectroscopic characteristics were consistent with previously reported data.[253]

R_f = 0.45 (10 : 1, hexane : Et_2O). ^{1}H NMR (300 MHz, $CDCl_3$): δ 0.98 (3H, t, *J* = 7.5 Hz, H-1), 1.10 (3H, d, *J* = 6.9 Hz, H-5), 2.26 (1H, dq, *J* = 17.7, 7.5 Hz, H-2), 2.48 (1H, dq, *J* = 17.7, 7.5 Hz, H-2), 2.62 (1H, dd, *J* = 7.2, 12.9 Hz, H-6), 2.79-2.91 (1H, m, H-4), 3.05 (1H, dd, *J* = 7.2, 12.9 Hz, H-6), 7.25 (2H, d, *J* = 7.9 Hz, Ar-H), 7.53 (2H, d, *J* = 7.9, Ar-H) ppm; ^{13}C NMR (75.5 MHz, $CDCl_3$): δ 7.6 (C-1), 16.8 (C-5), 35.1 (C-2), 38.7 (C-6), 47.6 (C-4), 124.2 (q, $J_{C\text{-}F}$ = 277.5 Hz, C-13), 125.3 (q, $^3J_{C\text{-}F}$ = 3.8 Hz, C-9, C-11), 128.6 (q, $^2J_{C\text{-}F}$ = 32.5 Hz, C-10), 129.3 (C-8, C-12), 144.1 (C-7), 214.7 (C-3) ppm; MS (ESI) *m/z*: 245 $[M + H]^+$.

GC analysis: t_R = 10.4 and 12.1 min (120°C hold for 10 min, ramp 5°C/min to 140°C, hold for 5 min).

(*E*)-4-methyl-7-phenylhept-6-en-3-one 184

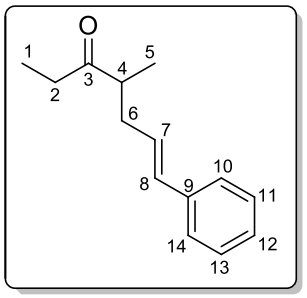

Prepared following the general procedure outlined above using 3-pentanone and 3-bromo-1-phenyl-1-propene. The crude product was purified using column chromatography (15 : 1, hexane : Et_2O) on silica gel to give the title compound **184** as a clear oil (0.8 g, 40%).

Spectroscopic characteristics were consistent with previously reported data.[254]

R_f = 0.4 (10 : 1, hexane : Et_2O). ^{1}H NMR (300 MHz, $CDCl_3$): δ 1.05 (3H, t, *J* = 7.2 Hz, H-1), 1.13 (3H, d, *J* = 6.9 Hz, H-5), 2.19-2.29 (1H, m, H-6), 2.40-2.59 (3H, m, H-2, H-6), 2.63-2.74 (1H, m, H-4), 6.06-6.17 (1H, m, H-7), 6.40 (1H, d, *J* = 15.9 Hz, H-8), 7.25-7.33 (5H, m, Ar-H) ppm; ^{13}C NMR (75.5 MHz, $CDCl_3$): δ 7.7 (C-1), 16.4 (C-5), 34.6 (C-2), 36.3 (C-6), 46.1 (C-4), 126.1 (2 x Ar-CH), 127.2 (C-7), 127.6 (C-8), 128.5 (2 x Ar-CH), 131.9 (Ar-CH), 137.4 (C-9), 214.6 (C-3) ppm; MS (ESI) *m/z*: 203 $[M + H]^+$.

GC analysis: t_R = 25.2 and 26.5 min (130°C hold for 30 min, ramp 10°C/min to 140°C, hold for 5 min).

(*E*)-4-methyloct-6-en-3-one 185

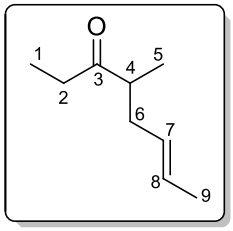

Prepared following the general procedure outlined above using 3-pentanone and crotyl bromide. The crude product was purified using column chromatography (50 : 1, hexane : Et_2O) on silica gel to give the title compound **185** as a clear oil (0.275 g, 20%).

Spectroscopic characteristics were consistent with previously reported data.[197]

R_f = 0.57 (20 : 1, hexane : Et_2O). ^{1}H NMR (300 MHz, $CDCl_3$): δ 1.03 (3H, t, *J* = 7.4 Hz, H-1), 1.05 (3H, d, *J* = 7.3 Hz, H-5), 1.59-1.68 (3H, m, H-9), 1.93-2.07 (1H, m, H-6), 2.19-2.38 (1H, m, H-6), 2.38-2.72 (3H, m, H-2, H-4), 5.26-5.38 (1H, m, H-7), 5.38-5.52 (1H, m, H-8) ppm; ^{13}C NMR (75.5 MHz, $CDCl_3$): δ 7.7 (C-1), 16.1 (C-5), 17.9 (C-9), 34.4 (C-2), 36.1 (C-6), 46.2 (C-4), 127.3 (C-7), 128.1 (C-8), 214.9 (C-3) ppm; MS (ESI) *m/z*: 141 $[M + H]^+$.

GC analysis: t_R = 4.0 and 4.4 min (90°C hold for 5 min, ramp 10°C/min to 140°C, hold for 5 min).

1-(4-bromophenyl)-2-methylpentan-3-one 186

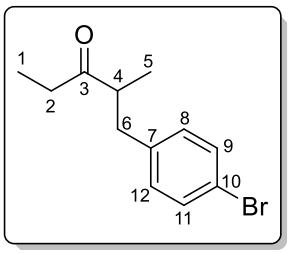

Prepared following the general procedure outlined above using 3-pentanone and 4-bromobenzyl bromide. The crude product was purified using column chromatography (10 : 1, hexane : Et_2O) on silica gel to give the title compound **186** as a clear oil (0.19 g, 20%).

Spectroscopic characteristics were consistent with previously reported data.[35]

R_f = 0.58 (5 : 1, hexane : Et_2O). ^{1}H NMR (300 MHz, $CDCl_3$): δ 0.97 (3H, t, *J* = 7.5 Hz, H-1), 1.08 (3H, d, *J* = 6.9 Hz, H-5), 2.24 (1H, dq, *J* = 17.9, 7.2 Hz, H-2), 2.45 (1H, dq, *J* = 17.9, 7.2 Hz, H-2), 2.51 (1H, dd, *J* = 7.2, 13.3 Hz, H-6), 2.72-2.86 (1H, m, H-4), 2.91 (1H, dd, *J* = 7.2, 13.3 Hz, H-6), 6.97-7.04 (2H, m, Ar-H), 7.35-7.5 (2H, m, Ar-H) ppm; ^{13}C NMR (75.5 MHz, $CDCl_3$): δ 7.6 (C-1), 16.7 (C-5), 35.2 (C-2), 38.5 (C-6), 47.7 (C-4), 120.0 (Ar-C), 130.7 (2 x Ar-CH), 131.4 (2 x Ar-CH), 138.9 (Ar-C), 214.3 (C-3) ppm; MS (ESI) *m/z*: 255 $[M + H]^+$.

GC analysis: t_R = 15.7 and 16.7 min (140°C hold for 20 min).

2-methyl-1-*p*-tolylpentan-3-one 187

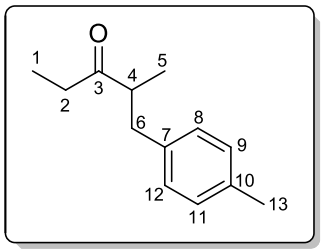

Prepared following the general procedure outlined above using 3-pentanone and 4-methylbenzyl bromide. The crude product was purified using column chromatography (20 : 1, hexane : Et_2O) on silica gel to give the title compound **187** as a clear oil (0.365 g, 19%).

R_f = 0.42 (10 : 1, hexane : Et_2O). IR (NaCl) $\bar{\nu}_{max}$: 2974-2876 (C-H stretch, s), 1713 (C=O stretch, s), 1515 (Aromatic C=C stretch, s), 1458 (C-H bending, m) cm^{-1}; ^1H NMR (300 MHz, $CDCl_3$): δ 0.97 (3H, t, *J* = 7.2 Hz, H-1), 1.06 (3H, d, *J* = 6.9 Hz, H-5), 2.26 (1H, dq, *J* = 17.8, 7.2 Hz, H-2), 2.30 (3H, s, H-13), 2.43 (1H, dq, *J* = 17.8, 7.2 Hz, H-2), 2.52 (1H, dd, *J* = 7.2, 13.2 Hz, H-6), 2.74-2.74 (1H, m, H-4), 2.92 (1H, dd, *J* = 7.2, 13.2 Hz, H-6), 7.00-7.10 (4H, m, Ar-H) ppm; ^{13}C NMR (75.5 MHz, $CDCl_3$): δ 7.6 (C-1), 16.6 (C-5), 21.0 (C-13), 35.1 (C-2), 38.9 (C-6), 47.9 (C-4), 128.8 (2 x Ar-CH), 129.1 (2 x Ar-CH), 135.7 (Ar-C), 136.7 (Ar-C), 214.9 (C-3) ppm; HRMS (ESI) *m/z* calcd for $C_{13}H_{19}O$ $[M + H]^+$: 191.1436, found 191.1428. GC analysis: t_R = 12.2 and 12.8 min (120°C hold for 5 min, ramp 10°C/min to 140°C, hold for 5 min).

4-methylnonan-3-one 188

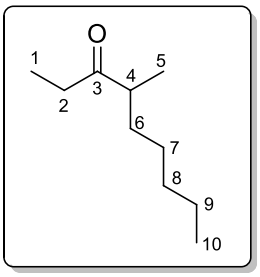

Prepared following the general procedure outlined above using 3-pentanone and 1-iodopentane. The crude product was purified using column chromatography (10 : 1, hexane : Et_2O) on silica gel to give the title compound **188** as a clear oil (0.03 g, 17%).

R_f = 0.68 (4 : 1, hexane : Et_2O). IR (NaCl) $\bar{\nu}_{max}$: 2960-2858 (C-H stretch, s), 1716 (C=O stretch, s), 1460 (C-H bending, s) cm^{-1}; ^1H NMR (300 MHz, $CDCl_3$) δ: 0.88 (3H, t, *J* = 6.9 Hz, H-10), 1.04 (3H, t, *J* = 7.3 Hz, H-1), 1.06 (3H, d, *J* = 6.8 Hz, H-5), 1.13-1.41 (7H, m, H-6, H-7, H-8, H-9), 1.52-1.73 (1H, m, H-6), 2.35-2.61 (3H, m, H-2, H-4) ppm; ^{13}C NMR (75.5 MHz, $CDCl_3$): δ 7.8 (C-1), 14.0 (C-10), 16.5 (C-5), 22.5, 27.0, 31.9, 33.1, 34.2 (C-2, C-6, C-7, C-8, C-9), 46.1 (C-4), 215.5 (C-3) ppm; HRMS (ESI) *m/z* calcd for $C_{10}H_{21}O$ $[M + H]^+$: 157.1592, found 157.1588.

GC analysis: t_R = 3.6 and 3.8 min (105°C hold for 10 min, ramp 10°C/min to 140°C, hold for 5 min).

2,4-dimethyl-1-phenylpentan-3-one 189

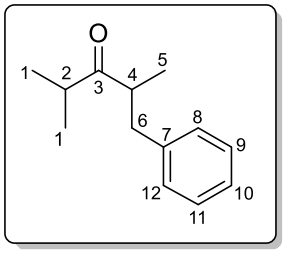

Prepared following the general procedure outlined above using 2-methyl-3-pentanone and benzyl bromide. The crude product was purified using column chromatography (10 : 1, hexane : Et_2O) on silica gel to give the title compound **189** as a clear oil (0.076 g, 40%).

Spectroscopic characteristics were consistent with previously reported data.[255]

R_f = 0.74 (5 : 1, hexane : Et_2O). ^{1}H NMR (300 MHz, $CDCl_3$): δ 0.87 (3H, d, *J* = 6.9 Hz, H-1), 1.01 (3H, d, *J* = 6.9 Hz, H-1), 1.08 (3H, d, *J* = 6.9 Hz, H-5), 2.43-2.61 (2H, m, H-2, H-6), 2.88-3.10 (2H, m, H-4, H-6), 7.09-7.32 (5H, m, Ar-H) ppm; ^{13}C NMR (75.5 MHz, $CDCl_3$): δ 17.2 (C-5), 17.7 (C-1), 18.0 (C-1), 39.5 (C-6), 40.4 (C-2), 46.5 (C-4), 126.2 (Ar-CH), 128.4 (2 x Ar-CH), 128.9 (2 x Ar-CH), 139.9 (C-7), 214.8 (C-3) ppm (Note: Exact structural assignment confirmed using COSY and HSQC); MS (ESI) *m/z*: 191 $[M + H]^+$.

GC analysis: t_R = 10.8 and 11.1 min (110°C hold for 20 min, ramp 10°C/min to 140°C, hold for 5 min).

2-methyl-1-phenylbutan-1-one 190

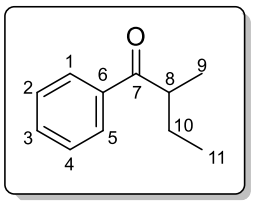

Prepared following the general procedure outlined above using propiophenone and ethyl iodide. The crude product was purified using column chromatography (10 : 1, hexane : Et_2O) on silica gel to give the title compound **190** as a clear oil (0.651 g, 40%).

Spectroscopic characteristics were consistent with previously reported data.[256]

R_f = 0.62 (4 : 1, hexane : Et_2O). ^{1}H NMR (300 MHz, $CDCl_3$): δ 0.92 (3H, t, *J* = 7.4 Hz, H-11), 1.19 (3H, d, *J* = 6.9 Hz, H-9), 1.40-1.58 (1H, m, H-10), 1.75-1.93 (1H, m, H-10), 3.33-3.48 (1H, m, H-8), 7.41-7.51 (2H, m, Ar-H), 7.51-7.59 (1H, m, Ar-H), 7.91-7.99 (2H, m, Ar-H) ppm; ^{13}C NMR (75.5 MHz, $CDCl_3$): δ 11.8 (C-11), 16.8 (C-9), 26.7 (C-10), 42.1 (C-8), 128.3 (2 x Ar-CH), 128.6 (2 x Ar-CH), 132.8 (Ar-CH), 136.8 (C-6), 204.5 (C-7) ppm; MS (ESI) *m/z*: 163 $[M + H]^+$.

GC analysis: t_R = 14.0 and 14.9 min (100°C hold for 20 min, ramp 5°C/min to 140°C, hold for 5 min).

2-methyl-1,3-diphenylpropan-1-one 191

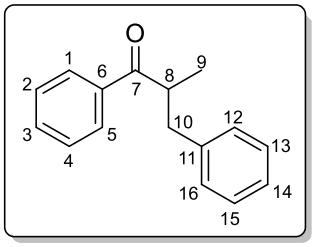

Prepared following the general procedure outlined above using propiophenone and benzyl bromide. The crude product was purified using column chromatography (10 : 1, hexane : Et_2O) on silica gel to give the title compound **191** as a clear oil (0.48 g, 53%).

Spectroscopic characteristics were consistent with previously reported data.[256]

R_f = 0.56 (4 : 1, hexane : Et_2O). ^{1}H NMR (300 MHz, $CDCl_3$): 1.18 (3H, d, *J* = 6.9 Hz, H-9), 2.68 (1H, dd, *J* = 6.9, 13.7 Hz, H-10), 3.16 (1H, dd, *J* = 6.9, 13.7 Hz, H-10), 3.66-3.80 (1H, m, H-8), 7.13-7.31 (5H, m, Ar-H), 7.35-7.57 (3H, m, Ar-H), 7.86-7.99 (2H, m, Ar-H) ppm; ^{13}C NMR (75.5 MHz, $CDCl_3$): δ 17.5 (C-9), 39.4 (C-10), 42.8 (C-8), 126.2 (Ar-CH), 128.3 (2 x Ar-CH), 128.4 (2 x Ar-CH), 128.7 (2 x Ar-CH), 129.1 (2 x Ar-CH), 132.9 (Ar-CH), 136.5 (Ar-C), 140.0 (Ar-C), 203.7 (C-7) ppm; MS (ESI) *m/z*: 245 $[M + H]^+$.

GC analysis: t_R = 53.2 and 57.2 min (90°C hold for 5 min, ramp 10°C/min to 140°C, hold for 5 min).

5.3 Synthesis of a Novel Diamine Chiral Auxiliary

5.3.1 Synthesis of (2*R*,5*S*)-trichloromethyl-1-aza-3-oxabicyclo-[3.3.0]-octan-4-one

(2*R*,5*S*)-trichloromethyl-1-aza-3-oxabicyclo-[3.3.0]-octan-4-one (*R*,*S*)-195

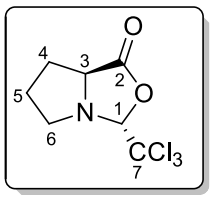

To a stirred solution of (*S*)-proline (30 g, 0.26 mol) in chloroform (350 mL) was added anhydrous chloral (57.6 g, 0.39 mol). The reaction mixture was heated at reflux for 10 h using a reverse Dean-Stark apparatus. The water collected was measured (4.5 mL) and the reaction mixture was cooled to room temperature. The cooled mixture was washed with water (2 x 100 mL) and the resulting water layers were washed with CH_2Cl_2 (2 x 50 mL). The organic layers were combined and dried over anhydrous $MgSO_4$, filtered, and concentrated under reduced pressure. The residue was crystallized from EtOH to give the product **(*R*,*S*)-195** as white needles (26.21 g, 41%). Mp 106-109°C (lit.[162] 107°C).

Spectroscopic characteristics were consistent with previously reported data.[162]

$[\alpha]_D^{20}$ + 29.8 (c 2, C_6H_6) (lit.[162] $[\alpha]_D^{20}$ + 32.7 (c 2, C_6H_6) for *R*,*S*-enantiomer). ^{1}H NMR (300 MHz, $CDCl_3$): δ 1.64-1.79 (1H, m, H-5), 1.84-1.99 (1H, m, H-5), 2.02-2.30 (2H, m, H-4), 3.02-3.20 (1H, m, H-6), 3.32-3.50 (1H, m, H-6), 4.11 (1H, dd, *J* = 4.7, 8.8 Hz, H-3), 5.14 (1H, s, H-1) ppm; ^{13}C NMR (75.5 MHz, $CDCl_3$): δ 25.4 (C-5), 29.9 (C-4), 57.9 (C-6), 62.4 (C-3), 100.6 (C-7), 103.7 (C-1), 175.5 (C-2) ppm; MS (ESI) *m/z*: 244 $[M+H]^+$ (for ^{35}Cl).

5.3.2 Preparation of (*S*)-2-(pyrrolidin-1-ylmethyl)pyrrolidin-1-amine

(*S*)-prolyl-pyrrolidine (*S*)-198

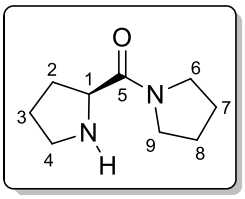

To (2*R*,5*S*)-trichloromethyl-1-aza-3-oxabicyclo-[3.3.0]-octan-4-one **(*R*,*S*)-195** (8.032 g, 0.0327 mol), dissolved in EtOH (120 mL), was added pyrrolidine (6.975 g, 0.98 mol), dropwise. The resulting mixture was allowed to stir for 4.5 h at room temperature, until all starting material had reacted (determined by TLC analysis (1 : 1, hexane : EtOAc)). The reaction mixture was concentrated under reduced pressure to give the product **(*S*)-198** as a yellow oil. The crude product was used in the next step without further purification.

Spectroscopic characteristics were consistent with previously reported data.[162]

Rotamers were observed for this compound. The minor rotamer was not observed in this case. ^{1}H NMR (300 MHz, $CDCl_3$): δ 1.60-2.22 (8H, m, H-2, H-3, H-7, H-8), 2.77-2.89 (1H, m, H-4), 3.13-3.25 (1H, m, H-4), 3.33-3.59 (4H, m, H-6, H-9), 3.79 (1H, dd, *J* = 6.3, 8.1 Hz, H-1), 8.10 (1H, bs, N-H) ppm; ^{13}C NMR (75.5 MHz, $CDCl_3$): δ 24.0, 25.9, 26.1, 30.4, 45.8, 45.9, 47.6 (C-2, C-3, C-4, C-6, C-7, C-8, C-9), 59.4 (C-1), 172.7 (C-5) ppm; MS (ESI) *m/z*: 169 $[M+H]^+$.

(*S*)-(1-pyrrolidinylmethyl)-pyrrolidine (*S*)-193

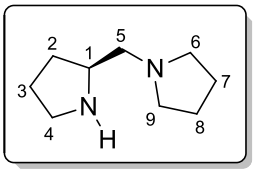

To $LiAlH_4$ (3.10 g, 0.0817 mol) in anhydrous THF (100 mL), under a N_2 atmosphere at 0°C, was added (*S*)-prolyl-pyrrolidine **(*S*)-198** (max. 0.0327 mol) in anhydrous THF (100 mL). The reaction mixture was brought to room temperature and allowed to stir overnight. The reaction mixture was heated at reflux for 2.5 h. The mixture was allowed cool to room temperature and quenched by the slow addition of water (14 mL), 15% NaOH solution (14 mL) and water (42 mL) and allowed to stir for 1 h, until a white precipitate had formed. The mixture was filtered through a pad of Celite® to remove the inorganic salts and washed with EtOAc (100 mL). The filtrate was dried over anhydrous $MgSO_4$, filtered, and concentrated under reduced pressure to give the crude product as an orange oil. The product was further purified by kugelrohr distillation to give **(*S*)-193**, as a colourless oil (2.73 g, 54% over two steps).

Spectroscopic characteristics were consistent with previously reported data.[162]

$[\alpha]_D^{20}$ + 5.188 (c 2.4, EtOH) (lit.[162] $[\alpha]_D^{20}$ + 8.9 (c 2.4, EtOH) for S-enantiomer). ^{1}H NMR (300 MHz, $CDCl_3$): δ 1.26-1.42 (1H, m, H-2), 1.62-1.84 (6H, m, H-2, H-3, H-7, H-8), 1.84-1.94 (1H, m, H-3), 2.34 (1H, dd, *J* = 5.2, 11.9 Hz, H-5), 2.41-2.63 (5H, m, H-5, H-6, H-9), 2.81 (1H, bs,

N-H), 2.85 (1H, dt, *J* = 7.1, 10.2 Hz, H-4), 2.98 (1H, dt, *J* = 6.6, 10.2 Hz, H-4), 3.15-3.29 (1H, m, H-1) ppm; ^{13}C NMR (75.5 MHz, $CDCl_3$): δ 23.4 (C-7, C-8), 25.0, 30.1, 41.3 (C-2, C-3, C-4), 54.5 (C-6, C-9), 57.4 (C-1), 62.1 (C-5) ppm; MS (ESI) *m/z*: 155 $[M + H]^+$.

(*S*)-1-nitroso-2-(pyrrolidinylmethyl)-pyrrolidine (*S*)-199

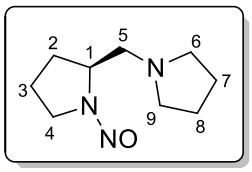

Method A

To a solution of the amine **(*S*)-193** (0.1 g, 0.65 mmol) in THF (1 mL) was added *tert*-butyl nitrite (0.206 g, 2 mmol). The mixture was allowed to stir at room temperature, for 18 h, without admission of light. After such time, the reaction mixture was heated at reflux for 5 h, cooled to room temperature and allowed to stir again overnight. The solvent and excess *tert*-butyl nitrite, were removed under reduced pressure to give a brown, oily residue.

^{1}H NMR analysis showed the reaction was unsuccessful and that only starting material remained.

Method B

To a stirred solution of the amine **(*S*)-193** (5 g, 0.033 mol) in water (100 mL) was added 37% HCl solution (8 mL). To the solution, acetic acid (50 mL) was added, followed by $NaNO_2$ (6.4 g, 0.093 mol) at 0°C. The reaction mixture was allowed to stir for 30 min at 0°C and at room temperature for 2 h, until all starting material had reacted (determined by TLC analysis (9 : 1, CH_2Cl_2 : MeOH)). The solution was cooled to 0°C and 10% Na_2CO_3 (50 mL) was added slowly. EtOAc (50 mL) was added and the aqueous layer extracted and washed with EtOAc (2 x 50 mL). Additional 10% Na_2CO_3 was added to the aqueous layer, until it was basic. The aqueous was extracted again with EtOAc (2 x 150 mL). The organic layers were combined and dried over anhydrous $MgSO_4$, filtered, and concentrated under reduced pressure to give the product **(*S*)-199**, as a yellow oil (4.51 g, 75%). The crude product was used in the next step without further purification.

^{1}H NMR (300 MHz, $CDCl_3$): δ 1.71-1.86 (4H, m, H-7, H-8), 1.86-2.28 (4H, m, H-2, H-3), 2.51-2.69 (4H, m, H-6, H-9), 2.80 (1H, dd, *J* = 7.0, 12.3 Hz, H-5), 2.99 (1H, dd, *J* = 7.7, 12.3, H-5), 3.51-3.62 (1H, m, H-4), 3.62-3.75 (1H, m, H-4), 4.56-4.68 (1H, m, H-1) ppm. To limit handling of the potential carcinogenic nitroso compound **(*S*)-199** only a ^{1}H NMR spectrum was obtained.

(*S*)-2-(pyrrolidin-1-ylmethyl)pyrrolidin-1-amine (*S*)-192

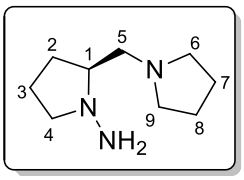

To $LiAlH_4$ (1.25 g, 0.033 mol) in anhydrous THF (60 mL) under a N_2 atmosphere at 0°C, was added (*S*)-1-nitroso-2-(pyrrolidinylmethyl)-pyrrolidine **(*S*)-199** (3.01 g, 0.0164 mol) in anhydrous THF (60 mL). The reaction was allowed warm to room temperature and allowed to stir for 6 h, until all starting material had reacted (determined by TLC analysis (9 : 1, CH_2Cl_2 : MeOH)). The reduction was quenched by slow addition of water (1.3 mL), 15% NaOH solution (1.3 mL) and water (3.9 mL) and allowed to stir for 1 h, until a white precipitate had formed. The mixture was filtered through a pad of Celite® to remove the inorganic salts and washed with EtOAc and THF. The filtrate was dried over anhydrous $MgSO_4$, filtered, and concentrated under reduced pressure. This was purified using kugelrohr distillation and the pure product **(*S*)-192** was isolated as a clear oil (1.37 g, 49% over two steps).

$[\alpha]_D^{20}$ – 11.40 (c 1, EtOH). IR (NaCl) $\bar{\nu}_{max}$: 3306 (N-H stretch, m), 2961-2789 (C-H stretch, s), 1591 (N-H bending, m), 1459-1446 (C-H bending, m), 1137 (C-N stretch, m) cm^{-1}; ^1H NMR (300 MHz, $CDCl_3$): δ 1.38-1.62 (1H, m, H-2), 1.62-1.87 (6H, m, H-2, H-3, H-7, H-8), 1.91-2.09 (1H, m, H-3), 2.22-2.42 (3H, m, H-4, H-5), 2.42-2.64 (4H, m, H-6, H-9), 2.88 (1H, dd, *J* = 6.3, 11.5 Hz, H-5), 3.06 (bs, N-H_2), 3.20-3.29 (1H, m, H-1); ^{13}C NMR (75.5 MHz, $CDCl_3$): δ 20.6 (C-2), 23.7 (C-7, C-8), 28.7 (C-3), 54.9 (C-6, C-9), 59.5, 61.5 (C-4, C-5), 67.8 (C-1) ppm; HRMS (ESI) *m/z* calcd for $C_9H_{20}N_3$ $[M + H]^+$: 170.1657, found 170.1674.

5.4 Asymmetric α-Alkylation using Novel Diamine Chiral Auxiliary

5.4.1 Solvent Screen for Asymmetric Alkylation using Chiral Auxiliary

(*S*)-*N*-(pentan-3-ylidene)-2-(pyrrolidin-1-ylmethyl)pyrrolidin-1-amine (*S*)-200

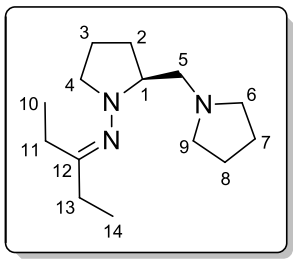

To a solution of hydrazine **(*S*)-192** (1.57 g, 9.29 mmol) in cyclohexane was added 3-pentanone (4 g, 46.45 mmol) and 2 grains of *p*-toluenesulfonic acid. The mixture was allowed to stir at room temperature for 5 h, under a N_2 atmosphere, until all starting material had reacted (determined by NMR and TLC analysis (2 : 1, hexane : EtOAc)). Et_2O (80 mL) was added to the solution and the mixture was washed with water (3 x 30 mL). The organic layer was dried over anhydrous $MgSO_4$, filtered, and concentrated under reduced pressure to give the crude product **(*S*)-200** as a yellow oil (0.86 g, 38%).

$[\alpha]_D^{20}$ + 114 (c 1, EtOH). IR (NaCl) $\bar{\nu}_{max}$: 2964-2790 (C-H stretch, s), 1637 (C=N stretch, s), 1460 (C-H bending, s), 1138 (C-N stretch, m) cm^{-1}; ^1H NMR (300 MHz, $CDCl_3$): δ 1.06 and 1,08 (2 x 3H, t, *J* = 6.3 Hz, H-10 and H-14), 1.53-1.63 (1H, m, H-2), 1.70-1.85 (6H, m, H-2, H-3, H-7, H-8), 2.02-2.13 (1H, m, H-3), 2.16-2.51 (11H, m, H-4, H-5, H-6, H-9, H-11, H-13), 2.97-3.09 (2H, m, H-1, H-5); ^{13}C NMR (75.5 MHz, $CDCl_3$): δ 10.9 (C-10), 11.9 (C-14), 21.8 (C-2), 23.4 (C-7, C-8), 23.5, 28.6, 28.7, 54.8 (C-3, C-4, C-11, C-13), 54.9 (C-6, C-9), 61.4 (C-5), 66.1 (C-1), 173.3 (C-12) ppm; HRMS (ESI) *m/z* calcd for $C_{14}H_{27}N_3$ $[M + H]^+$: 238.2277, found 238.2283.

General Procedure for the Asymmetric Alkylations with Chiral Auxiliary

To diisopropylamine (1.716 mmol, 0.24 mL) in anhydrous **solvent** (3 mL) at 0°C, was added *n*-BuLi (1.6 M, 1.87 mmol, 1.17 mL). The reaction mixture was allowed to stir for 30 min, cooled to -78°C. The chiral hydrazone **(*S*)-200** (0.37 g, 1.56 mmol) was added dropwise and allowed to stir for 15 min. The reaction was allowed warm to room temperature and allowed to stir for 4 h. The reaction was cooled to -110°C and benzyl bromide (1.87 mmol, 0.22 mL) was added dropwise and allowed to stir for 30 min. The reaction mixture was allowed warm to room temperature overnight.

After such time, saturated NH_4Cl (0.5 mL) was added and allowed to stir for 5 min. The reaction mixture was extracted with Et_2O (3 x 30 mL). The organic layers were combined and dried over anhydrous $MgSO_4$, filtered, and concentrated under reduced pressure.

Hydrazone cleavage

The resulting oil was hydrolysed by addition of Et_2O (5 mL), followed by 4 M HCl (0.5 mL) and allowed to stir vigorously, until all starting material had reacted (determined by TLC analysis (5 : 1, hexane : Et_2O)). Water (5 mL) was added and the mixture extracted with Et_2O (3 x 30 mL). The organic layers were combined and dried over anhydrous $MgSO_4$, filtered, and concentrated under reduced pressure. The crude product was purified using column chromatography on silica gel to give the pure product as a clear oil.

(*S*)-2-methyl-1-phenylpentan-3-one (*S*)-36

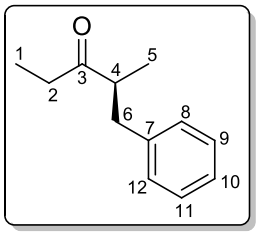

Spectroscopic characteristics were consistent with previously reported data.[192]

Enantioselectivity was determined by GC analysis: t_R = 7.1 (*R*-enantiomer) and 7.3 min (*S*-enantiomer) (120°C hold for 10 min, ramp 10°C/min to 140°C, hold for 5 min).

Solvent	Electrophile	Yield[a]	Ketone	*er R* : *S*	% *ee*
THF	BnBr	14%	**188**	50 : 50	Racemic
Et_2O	BnBr	33%	**(*S*)-188**	6 : 94	88%

[a]Isolated yield is over two steps.

Table 5.4.1 Solvent investigations for asymmetric alkylation using novel chiral auxiliary.

5.5 Synthesis *N,N*-Dimethylhydrazones for Asymmetric α-Alkylation via Intermolecular Chirality Transfer

General Procedure for the Synthesis of Hydrazones

The **ketone**, neat, was treated with non-symmetric *N,N*-dimethylhydrazine (1.5 equiv.) and acetic acid (few drops), and the reaction mixture was heated at reflux for 24 h. After cooling, water (10 mL) was added and the mixture extracted with Et_2O (3 x 30 mL). The organic layers were combined and dried over anhydrous $MgSO_4$, filtered, and concentrated under reduced pressure.

1,1-dimethyl-2-(pentan-3-ylidene)hydrazine 203

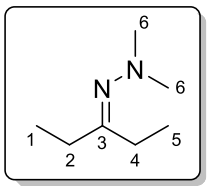

Prepared following the general procedure outlined above using 3-pentanone [256] and *N,N*-dimethylhydrazine. The crude product was purified using kugelrohr distillation to give the title compound **203** as a clear oil (5.01 g, 83%).

Spectroscopic characteristics were consistent with previously reported data.[257]

^{1}H NMR (300 MHz, $CDCl_3$): δ 1.08 (6H, t, *J* = 7.6 Hz, H-1, H-5), 2.24 (2H, q, *J* = 7.6 Hz, H-2), 2.42 (6H, s, H-6), 2.45 (2H, q, *J* = 7.6 Hz, H-4) ppm; ^{13}C NMR (75.5 MHz, $CDCl_3$): δ 11.1 (C-1), 11.6 (C-5), 22.5 (C-2), 28.7 (C-4), 47.6 (C-6), 174.5 (C-3) ppm; MS (ESI) *m/z*: 129 [M + H]$^+$.

(*E*)-1,1-dimethyl-2-(2-methylpentan-3-ylidene)hydrazine 207

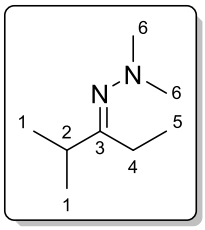

Prepared following the general procedure outlined above using 2-methyl-3-pentanone and *N,N*-dimethylhydrazine. The crude product was purified using kugelrohr distillation to give the title compound **207** as a clear oil (6.5 g, 92%).

Spectroscopic characteristics were consistent with previously reported data.[257]

Mixture of isomers: 3 : 1.

Major: ^{1}H NMR (300 MHz, $CDCl_3$): δ 1.08 (6H, d, *J* = 6.9 Hz, H-1), 1.09 (3H, t, *J* = 7.5 Hz, H-5), 2.37 (2H, q, *J* = 7.5 Hz, H-4), 2.38 (6H, s, H-6), 2.52 (1H, m, H-2) ppm; ^{13}C NMR (75.5 MHz, $CDCl_3$): δ 11.9 (C-5), 20.4 (C-1), 21.8 (C-4), 34.6 (C-2), 47.5 (C-6), 177.5 (C-3) ppm;

Minor: ^{1}H NMR (300 MHz, $CDCl_3$): δ 1.05 (6H, d, *J* = 6.9 Hz, H-1), 1.11 (3H, t, *J* = 7.5 Hz,

H-5), 2.17 (2H, q, *J* = 7.5 Hz, H-4), 2.39 (6H, s, H-6), 3.62 (1H, m, H-2) ppm; ^{13}C NMR (75.5 MHz, $CDCl_3$): δ 11.9 (C-5), 20.4 (C-1), 21.8 (C-4), 34.6 (C-2), 47.5 (C-6), 177.5 (C-3) ppm; MS (ESI) *m/z*: 143 $[M + H]^+$.

(*Z*)-2-(butan-2-ylidene)-1,1-dimethylhydrazine 208

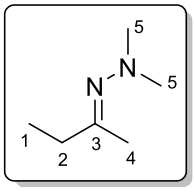

Prepared following the general procedure outlined above using 2-butanone and *N*,*N*-dimethylhydrazine. The crude product was purified using kugelrohr distillation to give the title compound **208** as a clear oil (6.93 g, 61%).

Spectroscopic characteristics were consistent with previously reported data.[258]

Mixture of isomers: 4 : 1.

Major: ^{1}H NMR (300 MHz, $CDCl_3$): δ 1.08 (3H, t, *J* = 7.5 Hz, H-1), 1.94 (3H, s, H-4), 2.21 (2H, q, *J* = 7.5 Hz, H-2), 2.43 (6H, s, H-5) ppm; ^{13}C NMR (75.5 MHz, $CDCl_3$): δ 11.5 (C-1), 15.9 (C-4), 32.2 (C-2), 47.0 (C-5), 168.8 (C-3) ppm; **Minor:** ^{1}H NMR (300 MHz, $CDCl_3$): δ 1.09 (3H, t, *J* = 7.6 Hz, H-1), 1.92 (3H, s, H-4), 2.41 (6H, s, H-5), 2.46 (2H, q, *J* = 7.6 Hz, H-2) ppm; ^{13}C NMR (75.5 MHz, $CDCl_3$): δ 10.9 (C-1), 22.1 (C-4), 24.5 (C-2), 47.5 (C-5), 170.3 (C-3) ppm; MS (ESI) *m/z*: 115 $[M + H]^+$.

(*E*)-1,1-dimethyl-2-(1-phenylpropylidene)hydrazine 209

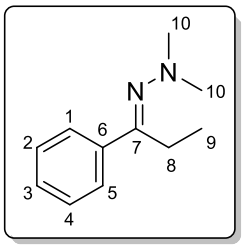

Prepared following the general procedure outlined above using propiophenone and *N*,*N*-dimethylhydrazine. The crude product was purified using kugelrohr distillation to give the title compound **209** as a clear oil (4.73 g, 90%).

Spectroscopic characteristics were consistent with previously reported data.[259]

Mixture of isomers: 4 : 1.

Major: ^{1}H NMR (300 MHz, $CDCl_3$): δ 1.07 (3H, t, *J* = 7.7 Hz, H-9), 2.56 (6H, s, H-10), 2.90 (2H, q, *J* = 7.7 Hz, H-8), 7.32-7.39 (3H, m, Ar-H), 7.61-7.69 (2H, m, Ar-H) ppm; ^{13}C NMR (75.5 MHz, $CDCl_3$): δ 11.9 (C-9), 21.8 (C-8), 47.9 (C-10), 127.0 (2 x Ar-CH), 128.3 (2 x Ar-CH), 129.2 (Ar-CH), 137.8 (C-6), 169.5 (C-7) ppm; **Minor:** ^{1}H NMR (300 MHz, $CDCl_3$): δ 1.02 (3H, t, *J* = 7.5 Hz, H-9), 2.36 (6H, s, H-10), 2.52 (2H, q, *J* = 7.5 Hz, H-8), 7.32-7.69 (5H, m, Ar-H) ppm; ^{13}C NMR (75.5 MHz, $CDCl_3$): δ 11.7 (C-9), 32.5 (C-8), 47.2 (C-10), 127.0 (Ar-CH), 127.8 (Ar-CH), 127.9 (Ar-CH), 128.3 (Ar-CH), 128.5 (Ar-CH), 132.9 (C-6), 165.2 (C-7) ppm; MS (ESI) *m/z*: 177 $[M + H]^+$.

(*E*)-2-(1-(4-methoxyphenyl)propylidene)-1,1-dimethylhydrazine 210

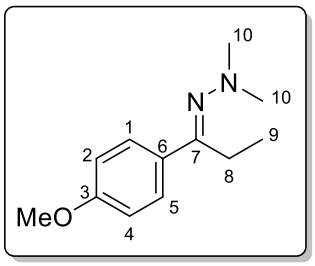

Prepared following the general procedure outlined above using 4-methoxypropiophenone and *N*,*N*-dimethylhydrazine. The crude product was purified using kugelrohr distillation to give the title compound **210** as a clear oil (2.75 g, 89%).

Mixture of isomers: 10 : 1.

IR (NaCl) $\bar{\nu}_{max}$: 2952 (C-H stretch, s), 1606 (C=N stretch, s), 1512 (Aromatic C=C stretch, s), 1464 (C-H bending, s) cm^{-1}; **Major:** ^{1}H NMR (300 MHz, $CDCl_3$): δ 1.08 (3H, t, *J* = 7.6 Hz, H-9), 2.54 (6H, s, H-10), 2.88 (2H, q, *J* = 7.6 Hz, H-8), 3.82 (3H, s, OMe), 6.85-6.93 (2H, m, Ar-H), 7.66-7.69 (2H, m, Ar-H) ppm; ^{13}C NMR (75.5 MHz, $CDCl_3$): δ 12.1 (C-9), 21.5 (C-8), 47.9 (C-10), 55.3 (OMe), 116.7 (2 x Ar-CH), 128.4 (2 x Ar-CH), 130.2 (Ar-C), 160.6 (Ar-C), 169.1 (C-7) ppm; **Minor:** ^{1}H NMR (300 MHz, $CDCl_3$): δ 1.01 (3H, t, *J* = 7.5 Hz, H-9), 2.36 (6H, s, H-10), 2.51 (2H, q, *J* = 7.5 Hz, H-8), 3.86 (3H, s, OMe), 7.32-7.39 (2H, m, Ar-H), 7.91-7.99 (2H, m, Ar-H) ppm; ^{13}C NMR (75.5 MHz, $CDCl_3$): δ 11.9 (C-9), 31.4 (C-8), 47.0 (C-10), 55.4 (OMe), 113.5 (2 x Ar-CH), 128.7 (2 x Ar-CH), 130.2 (Ar-C), 160.6 (Ar-C), 166.7 (C-7) ppm; HRMS (ESI) *m/z* calcd for $C_{12}H_{19}N_2O$ $[M + H]^+$: 207.1497, found 207.1492.

(*E*)-1,1-dimethyl-2-(5-methylhexan-3-ylidene)hydrazine 211

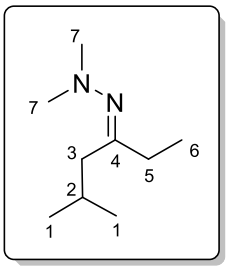

To diisopropylamine (27.5 mmol, 3.88 mL) in anhydrous THF, under N_2 atmosphere, was added *n*-BuLi (1.5 M, 30 mmol, 25 mL) at 0°C. The mixture was allowed to stir at 0°C for 30 min. The reaction mixture was cooled to -78°C, (*Z*)-2-(butan-2-ylidene)-1,1-dimethylhydrazine **208** was added dropwise, it was allowed warm to room temperature and allowed to stir for 6 h. The 2-iodopropane (5.1 g, 30 mmol) was added dropwise and the reaction was allowed warm to room temperature overnight. The reaction was quenched with saturated NH_4Cl (1.5 mL), Et_2O (10 mL) and NH_4Cl (10 mL) were added and the mixture was extracted with Et_2O (3 x 30 mL). The organic layers were combined and dried over anhydrous $MgSO_4$, filtered, and concentrated under reduced pressure. The crude product was purified using column chromatography (10 : 1, hexane : Et_2O, 4% Et_3N) on silica gel to give the title compound **211** as a clear oil (1.42 g, 37%).

The crude NMR showed a mixture of isomers: 8 : 1. However the compound rapidly interconverts over time and a mixture of isomers: 1 : 1 was observed upon purification.

R_f = 0.32 (4 : 1, hexane : Et_2O). IR (NaCl) $\bar{\nu}_{max}$: 2957 (C-H stretch, s), 1633 (C=N stretch, s), 1464 (C-H bending, s) cm^{-1}; **Major:** ^1H NMR (300 MHz, $CDCl_3$): δ 0.92 (6H, d, *J* = 6.6 Hz, H-1), 1.07 (3H, t, *J* = 7.6 Hz, H-6), 1.85-2.05 (1H, m, H-2), 2.22 (2H, q, *J* = 7.6 Hz, H-5), 2.34-2.39 (2H, d, *J* = 7.6 Hz, H-3), 2.37 (6H, s, H-7) ppm; ^{13}C NMR (75.5 MHz, $CDCl_3$): δ 11.9 (C-6), 22.6 (C-1), 25.8 (C-2), 29.3 (C-5), 37.9 (C-3), 47.3 (C-7), 173.2 (C-4) ppm; **Minor:** ^1H NMR (300 MHz, $CDCl_3$): δ 0.91 (6H, d, *J* = 6.5 Hz, H-1), 1.07 (3H, t, *J* = 7.6 Hz, H-6), 1.85-2.05 (1H, m, H-2), 2.10 (2H, d, *J* = 7.6 Hz, H-3), 2.38-2.48 (2H, m, H-5), 2.41 (6H, s, H-7) ppm; ^{13}C NMR (75.5 MHz, $CDCl_3$): δ 11.2 (C-6), 22.4 (C-1), 23.1 (C-5), 26.2 (C-2), 44.4 (C-3), 47.6 (C-7), 172.9 (C-4) ppm (Note: Exact structural assignment confirmed using COSY and HSQC); HRMS (ESI) *m/z* calcd for $C_9H_{21}N_2$ $[M + H]^+$: 157.1705, found 157.1698.

5.6 Asymmetric α-Alkylation via Intermolecular Chirality Transfer

5.6.1 Temperature, Solvent and Base Variations

General Procedure for the Asymmetric Alkylation using Intermolecular Chirality Transfer Methodology

To a schlenk tube, under a N_2 atmosphere, were added anhydrous **solvent** (1 mL/mmol of hydrazone) and (-)-sparteine **(-)-sp 100** or (+)-sparteine **(+)-sp 100** (1.2 equiv.) at room temperature. *sec*-BuLi (1.4 M, 1.1 equiv.) was added at -78°C and allowed to stir for 30 min. Hydrazone **203** (1 equiv.) was added dropwise at -78°C, allowed warm to room temperature and allowed to stir for 6 h at **deprotonation temperature**. The reaction was cooled to **alkylation temperature** and **electrophile** (1.2 equiv.) was added dropwise. The mixture was allowed to stir at **alkylation temperature** for 22 h.

At **alkylation temperature**, saturated NH_4Cl (0.5 mL) was added and the mixture allowed warm to room temperature. Et_2O (30 mL) was added and the mixture was washed with NH_4Cl (3 x 10 mL). The organic layer was dried over anhydrous $MgSO_4$, filtered, and concentrated under reduced pressure to afford the crude hydrazone. The crude hydrazone was used in the next step without further purification.

Hydrazone cleavage

The resulting oil was hydrolysed by addition of Et_2O (5 mL), followed by 4 M HCl (0.5 mL) and allowed to stir vigorously, until all starting material had reacted (determined by TLC analysis (5 : 1, hexane : Et_2O)). Water (5 mL) was added and the mixture extracted with Et_2O (3 x 30 mL). The organic layers were combined and dried over anhydrous $MgSO_4$, filtered, and concentrated under reduced pressure. The crude product was purified using column chromatography on silica gel to give the pure ketone.

Ligand	Electrophile	Deprot. Temp.	Alkyl. Temp.	Solvent	Yield[a]	Ketone	*er R* : *S*	% *ee*
(-)-sp 100	BnBr	RT	-78°C to RT	Toluene	53%	**(*S*)-36**	20 : 80	60%
(-)-sp 100	BnBr	RT	-70°C	Toluene	no reaction occurred			
(-)-sp 100	BnBr	RT	-55°C	Toluene	50%	**(*S*)-36**	28 : 72	44%
(-)-sp 100	BnBr	RT	-30°C	Toluene	57%	**(*S*)-36**	24 : 76	52%
(-)-sp 100	BnBr	RT	0°C	Toluene	50%	**(*S*)-36**	27 : 73	46%
(-)-sp 100	BnBr	RT	RT	Toluene	55%	**(*S*)-36**	29 : 71	42%
(-)-sp 100	BnBr	RT	70°C	Toluene	53%	**(*S*)-36**	30 : 70	40%
(-)-sp 100	BnBr	32°C	-30°C	Toluene	45%	**(*S*)-36**	23 : 77	54%
(+)-sp 100	BnBr	40°C	-30°C	Toluene	32%	**(*R*)-36**	70 : 30	40%
(-)-sp 100	BnBr	40°C	40°C	Toluene	52%	**(*S*)-36**	33 : 67	34%
(-)-sp 100	BnBr	70°C	70°C	Toluene	54%	**(*S*)-36**	36 : 64	28%

[a]Isolated yield is over two steps.

Table 5.6.1 Temperature variations.

Ligand	Electrophile	Deprot. Temp.	Alkyl. Temp.	Solvent	Yield[a]	Ketone	*er R* : *S*	% *ee*
(-)-sp 100	*n*-PeI	RT	-30°C	Toluene	46%	**(*S*)-188**	17 : 83	66%
(+)-sp 100	*n*-PeI	RT	-30°C	Et_2O	43%	**(*R*)-188**	78 : 22	56%
(-)-sp 100	*n*-PeI	RT	-30°C	MTBE	32%	**(*S*)-188**	33 : 67	34%
(-)-sp 100	BnBr	RT	-30°C	Toluene	57%	**(*S*)-36**	24 : 76	52%
(-)-sp 100	BnBr	RT	-30°C	Cumene	62%	**(*S*)-36**	25 : 75	50%
(-)-sp 100	BnBr	RT	-30°C	Benzene	45%	**(*S*)-36**	31 : 69	38%
(-)-sp 100	BnBr	RT	-30°C	Cyclohexane	23%	**(*S*)-36**	31 : 69	38%
(-)-sp 100	BnBr	RT	-30°C	THF	40%	**(*S*)-36**	Racemic	

[a]Isolated yield is over two steps.

Table 5.6.2 Solvent Investigations.

Ligand	Electrophile	Deprot. Temp.	Alkyl. Temp.	Alkyl Lithium Reagent	Yield[a]	Ketone	*er R* : *S*	% *ee*
(-)-sp 100	BnBr	RT	-30°C	PhLi	16%	**(*S*)-36**	20 : 80	60%
(-)-sp 100	BnBr	RT	-30°C	*n*-BuLi	44%	**(*S*)-36**	28 : 72	44%
(-)-sp 100	BnBr	RT	-30°C	*sec*-BuLi	57%	**(*S*)-36**	24 : 76	52%
(-)-sp 100	BnBr	RT	-30°C	*t*-BuLi	35%	**(*S*)-36**	24 : 76	52%

[a]Isolated yield is over two steps.

Table 5.6.3 Alkyl lithium reagent.

5.6.2 Substrate Investigations

General Procedure for the Asymmetric Alkylation using Intermolecular Chirality Transfer Methodology

To a schlenk tube, under a N_2 atmosphere, were added anhydrous toluene (1 mL/mmol of hydrazone) and (-)-sparteine **(-)-sp 100** or (+)-sparteine **(+)-sp 100** (1.2 equiv.) at room temperature. *sec*-BuLi (1.4 M, 1.1 equiv.) was added at -78°C and allowed to stir for 30 min. **Hydrazone** (1 equiv.) was added dropwise at -78°C, allowed warm to room temperature and allowed to stir at room temperature for 6 h. The reaction was cooled to -30°C and **electrophile** (1.2 equiv.) was added dropwise. The mixture was allowed to stir at -30°C for 22 h.

At -30°C, saturated NH_4Cl (0.5 mL) was added and the mixture allowed warm to room temperature. Et_2O (30 mL) was added and the mixture was washed with NH_4Cl (3 x 10 mL). The organic layer was dried over anhydrous $MgSO_4$, filtered, and concentrated under reduced pressure to afford the crude hydrazone. The crude hydrazone was used in the next step without further purification.

Hydrazone cleavage

The resulting oil was hydrolysed by addition of Et_2O (5 mL), followed by 4 M HCl (0.5 mL) and allowed to stir vigorously, until all starting material had reacted (determined by TLC analysis (5 : 1, hexane : Et_2O)). Water (5 mL) was added and the mixture extracted with Et_2O (3 x 30 mL). The organic layers were combined and dried over anhydrous $MgSO_4$, filtered, and concentrated under reduced pressure. The crude product was purified using column chromatography on silica gel to give the pure ketone.

(*S*)-2-methyl-1-phenylpentan-3-one (*S*)-36

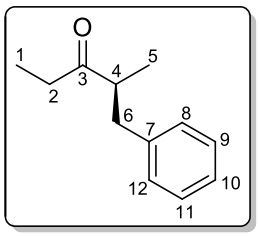

Prepared following the general procedure outlined above using hydrazone **203** and benzyl bromide. The crude product was purified using column chromatography (10 : 1, hexane : Et_2O) on silica gel to give the title compound **(*S*)-36** as a clear oil (0.098 g, 57% over two steps, 52% *ee*).

$[\alpha]_D^{23}$ + 31.7 (c 1.1, $CHCl_3$) (lit.[192] $[\alpha]_D^{23}$ + 70.9 (c 1.1, $CHCl_3$, for 99% *ee*, *S*-enantiomer)).

Spectroscopic characteristics were consistent with that of **36** shown earlier and with previously reported data.[192]

Enantioselectivity was determined by GC analysis: 24 : 76 *er*, t_R = 7.4 (*R*-enantiomer) and 7.8 min (*S*-enantiomer) (120°C hold for 10 min, ramp 10°C/min to 140°C, hold for 5 min).

(*R*)-2-methyl-1-(4-(trifluoromethyl)phenyl)pentan-3-one (*R*)-183

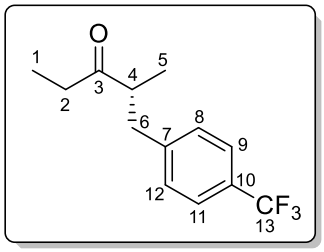

Prepared following the general procedure outlined above using hydrazone **203** and 4-trifluoromethylbenzyl bromide. The crude product was purified using column chromatography (15 : 1, hexane : Et_2O) on silica gel to give the title compound **(*R*)-183** as a clear oil (0.112 g, 46% over two steps, 32% *ee*).

$[\alpha]_D^{20}$ – 17.4 (c 1.11, Et_2O).

*Note: opposite stereochemistry due to the use of (+)-sparteine **(+)-sp 100** used as chiral ligand. Spectroscopic characteristics were consistent with that of **183** shown earlier and with previously reported data.[253]

Enantioselectivity was determined by GC analysis: 66 : 34 *er*, t_R = 10.4 (*R*-enantiomer) and 12.1 min (*S*-enantiomer) (120°C hold for 10 min, ramp 5°C/min to 140°C, hold for 5 min).

(*S*)-(*E*)-4-methyl-7-phenylhept-6-en-3-one (*S*)-184

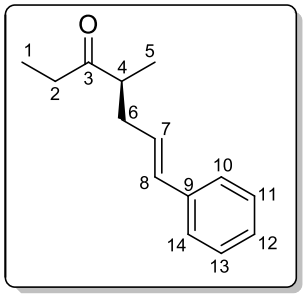

Prepared following the general procedure outlined above using hydrazone **203** and 3-bromo-1-phenyl-1-propene. The crude product was purified using column chromatography (15 : 1, hexane : Et_2O) on silica gel to give the title compound **(*S*)-184** as a clear oil (0.061 g, 30% over two steps, 58% *ee*).

$[\alpha]_D^{20}$ + 9.7 (c 0.36, Et_2O).

Spectroscopic characteristics were consistent with that of **184** shown earlier and with previously reported data.[254]

Enantioselectivity was determined by GC analysis: 21 : 79 *er*, t_R = 25.2 (*R*-enantiomer) and 26.5 min (*S*-enantiomer) (130°C hold for 30 min, ramp 10°C/min to 140°C, hold for 5 min).

(*S*)-(*E*)-4-methyloct-6-en-3-one (*S*)-185

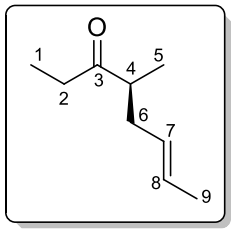

Prepared following the general procedure outlined above using hydrazone **203** and crotyl bromide. The crude product was purified using column chromatography (50 : 1, hexane : Et_2O) on silica gel to give the title compound **(*S*)-185** as a clear oil (0.275 g, 20% over two steps, 30% *ee*).

$[\alpha]_D^{20}$ + 3.6 (c 0.7, $CHCl_3$) (lit.[197] $[\alpha]_D^{20}$ + 23.9 (c 1.07, $CHCl_3$, for 98% *ee*, *S*-enantiomer)).

Spectroscopic characteristics were consistent with that of **185** shown earlier and with previously reported data.[197]

Enantioselectivity was determined by GC analysis: 35 : 65 *er*, t_R = 4.0 (*R*-enantiomer) and 4.4 min (*S*-enantiomer) (90°C hold for 5 min, ramp 10°C/min to 140°C, hold for 5 min).

(*S*)-1-(4-bromophenyl)-2-methylpentan-3-one (*S*)-186

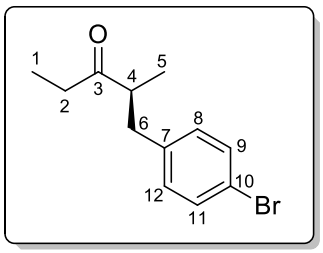

Prepared following the general procedure outlined above using hydrazone **203** and 4-bromobenzyl bromide. The crude product was purified using column chromatography (10 : 1, hexane : Et_2O) on silica gel to give the title compound **(*S*)-186** as a clear oil (0.070 g, 28% over two steps, 40% *ee*).

$[\alpha]_D^{20}$ + 1.2 (c 0.33, Et_2O).

Spectroscopic characteristics were consistent with that of **186** shown earlier and with previously reported data.[35]

Enantioselectivity was determined by GC analysis: 30 : 70 *er*, t_R = 15.7 (*R*-enantiomer) and 16.7 min (*S*-enantiomer) (140°C hold for 20 min).

(*S*)-2-methyl-1-*p*-tolylpentan-3-one (*S*)-187

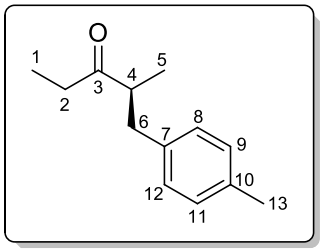

Prepared following the general procedure outlined above using hydrazone **203** and 4-methylbenzyl bromide. The crude product was purified using column chromatography (20 : 1, hexane : Et_2O) on silica gel to give the title compound **(*S*)-187** as a clear oil (0.094 g, 50% over two steps, 46% *ee*).

$[\alpha]_D^{20}$ + 28.7 (c 0.204, Et_2O).

Spectroscopic characteristics were consistent with that of **187** shown earlier.

Enantioselectivity was determined by GC analysis: 27 : 73 *er*, t_R = 12.2 (*R*-enantiomer) and 12.8 min (*S*-enantiomer) (120°C hold for 5 min, ramp 10°C/min to 140°C, hold for 5 min).

(*S*)-4-methylnonan-3-one (*S*)-188

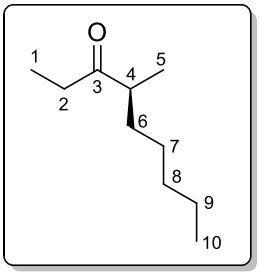

Prepared following the general procedure outlined above using hydrazone **203** and 1-iodopentane. The crude product was purified using column chromatography (10 : 1, hexane : Et_2O) on silica gel to give the title compound **(*S*)-188** as a clear oil (0.07 g, 46% over two steps, 66% *ee*).

$[\alpha]_D^{20}$ + 4.9 (c 0.528, Et_2O).

Spectroscopic characteristics were consistent with that of **188** shown earlier.

Enantioselectivity was determined by GC analysis: 17 : 83 *er*, t_R = 3.6 (*R*-enantiomer) and 3.8 min (*S*-enantiomer) (105°C hold for 10 min, ramp 10°C/min to 140°C, hold for 5 min).

(*S*)-1-(4-fluorophenyl)-2-methylpentan-3-one (*S*)-213

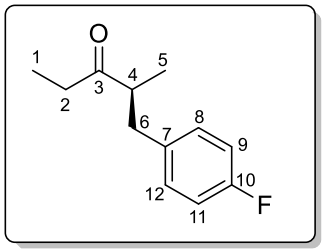

Prepared following the general procedure outlined above using hydrazone **203** and 4-fluorobenzyl bromide. The crude product was purified using column chromatography (10 : 1, hexane : Et_2O) on silica gel to give the title compound **(*S*)-213** as a clear oil (0.049 g, 26% over two steps, 40% *ee*).

Spectroscopic characteristics were consistent with previously reported data.[253]

R_f = 0.42 (5 : 1, hexane : Et_2O). $[\alpha]_D^{20}$ + 7.27 (c 0.22, Et_2O). ^{1}H NMR (300 MHz, $CDCl_3$): δ 0.96 (3H, t, *J* = 7.3 Hz, H-1), 1.07 (3H, d, *J* = 6.9 Hz, H-5), 2.24 (1H, dq, *J* = 17.9, 7.2 Hz, H-2), 2.44 (1H, dq, *J* = 17.9, 7.2 Hz, H-2), 2.54 (1H, dd, *J* = 7.0, 13.3 Hz, H-6), 2.73-2.87 (1H, m, H-4), 2.94 (1H, dd, *J* = 7.4, 13.3 Hz, H-6), 6.89-7.01 (2H, m, Ar-H), 7.03-7.14 (2H, m, Ar-H) ppm; ^{13}C NMR (75.5 MHz, $CDCl_3$): δ 7.6 (C-1), 16.7 (C-5), 35.2 (C-2), 38.4 (C-6), 48.0 (C-4), 115.1 (d, $^2J_{C\text{-}F}$ = 21.2 Hz, C-9, C-11), 130.3 (d, $^3J_{C\text{-}F}$ = 7.8 Hz, C-8, C-12), 135.5 (d, $^4J_{C\text{-}F}$ = 3.3 Hz, C-7), 161.5 (d, $J_{C\text{-}F}$ = 244.1 Hz, C-10), 214.6 (C-3) ppm; MS (ESI) *m/z*: 194 $[M + H]^+$.

Enantioselectivity was determined by GC analysis: 30 : 70 *er*, t_R = 8.8 (*R*-enantiomer) and 9.8 min (*S*-enantiomer) (120°C hold for 10 min, ramp 10°C/min to 140°C, hold for 5 min).

(*R*)-2-methyl-1-(*o*-tolyl)pentan-3-one (*S*)-216

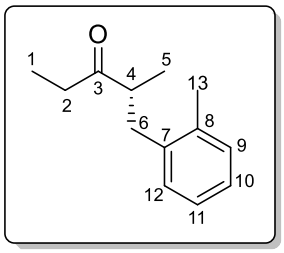

Prepared following the general procedure outlined above using hydrazone **203** and 2-methylbenzyl bromide, on 5 mmol scale. The crude product was purified using column chromatography (10 : 1, hexane : Et_2O) on silica gel to give the title compound **(*S*)-216** as a clear oil (0.52 g, 55% over two steps, 52% *ee*). *Note: opposite stereochemistry due to the use of (+)-sparteine **(+)-sp 100** used as chiral ligand.

Spectroscopic characteristics were consistent with previously reported data.[253]

R_f = 0.55 (5 : 1, hexane : Et_2O). $[\alpha]_D^{20}$ – 45.9 (c 1, Et_2O). ^{1}H NMR (300 MHz, $CDCl_3$): δ 0.97 (3H, t, *J* = 7.3 Hz, H-1), 1.09 (3H, d, *J* = 6.9 Hz, H-5), 2.23 (1H, dq, *J* = 17.9, 7.3 Hz, H-2), 2.31 (3H, s, H-13), 2.42 (1H, dq, *J* = 17.9, 7.3 Hz, H-2), 2.57 (1H, dd, *J* = 6.9, 13.4 Hz, H-6), 2.77-2.90 (1H, m, H-4), 2.97 (1H, dd, *J* = 6.9, 13.4 Hz, H-6), 6.97-7.19 (4H, m, Ar-H) ppm; ^{13}C NMR (75.5 MHz, $CDCl_3$): δ 7.6 (C-1), 16.6 (C-5), 19.4 (C-13), 35.2 (C-2), 36.5 (C-6), 46.4 (C-4), 125.9 (Ar-CH), 126.4 (Ar-CH), 129.7 (Ar-CH), 130.4 (Ar-CH), 136.0 (Ar-C), 138.0 (Ar-C), 214.8 (C-3) ppm (Note: Exact structural assignment confirmed using COSY and HSQC); MS (ESI) *m/z*: 191 $[M + H]^+$.

Enantioselectivity was determined by GC analysis: 76 : 24 *er*, t_R = 11.4 (*R*-enantiomer) and 11.9 min (*S*-enantiomer) (120°C hold for 20 min, ramp 10°C/min to 140°C, hold for 5 min).

(*S*)-1-(4-methoxyphenyl)-2-methylpentan-3-one (*S*)-215

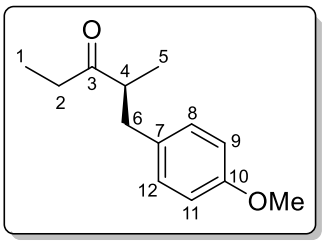

Prepared following the general procedure outlined above using hydrazone **203** and 4-methoxybenzyl bromide. The crude product was purified using column chromatography (10 : 1, hexane : Et_2O) on silica gel to give the title compound **(*S*)-215** as a clear oil (0.067 g, 33% over two steps, 34% *ee*).

Spectroscopic characteristics were consistent with previously reported data.[253]

R_f = 0.41 (4 : 1, hexane : Et_2O). $[\alpha]_D^{20}$ + 17.1 (c 0.88, CH_2Cl_2) (lit.[260] $[\alpha]_D^{20}$ + 61.1 (c 2, CH_2Cl_2, for 97.5% *ee*, configuration not specified)). ^{1}H NMR (300 MHz, $CDCl_3$): δ 0.96 (3H, t, *J* = 7.3 Hz, H-1), 1.07 (3H, d, *J* = 7.1 Hz, H-5), 2.25 (1H, dq, *J* = 17.9, 7.3 Hz, H-2), 2.42 (1H, dq, *J* = 17.9, 7.3 Hz, H-2), 2.51 (1H, dd, *J* = 6.9, 13.1 Hz, H-6), 2.71-2.86 (1H, m, H-4), 2.90 (1H, dd, *J* = 7.2, 13.1 Hz, H-6), 3.78 (3H, s, OMe), 6.74-6.85 (2H, m, Ar-H), 7.00-7.10 (2H, m, Ar-H) ppm; ^{13}C NMR (75.5 MHz, $CDCl_3$): δ 7.6 (C-1), 16.6 (C-5), 35.2 (C-2), 38.5 (C-6), 48.1 (C-4),

55.2 (OMe), 113.8 (2 x Ar-CH), 129.9 (2 x Ar-CH), 131.9 (Ar-C), 158.0 (Ar-C), 214.9 (C-3) ppm; MS (ESI) *m/z*: 207 $[M + H]^+$.

Enantioselectivity was determined by GC analysis: 33 : 67 *er*, t_R = 23.2 (*R*-enantiomer) and 23.6 min (*S*-enantiomer) (120°C hold for 25 min, ramp 10°C/min to 140°C, hold for 5 min).

(*R*)-1-(4-(*tert*-butyl)phenyl)-2-methylpentan-3-one (*S*)-214

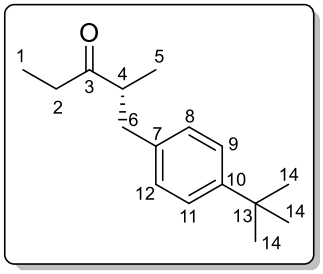

Prepared following the general procedure outlined above using hydrazone **203** and 4-*tert*-butylbenzyl bromide. The crude product was purified using column chromatography (10 : 1, hexane : Et_2O) on silica gel to give the title compound **(*S*)-214** as a clear oil (0.143 g, 62% over two steps, 42% *ee*).

*Note: opposite stereochemistry due to the use of (+)-sparteine **(+)-sp 100** used as chiral ligand. Spectroscopic characteristics were consistent with previously reported data.[253]

R_f = 0.45 (5 : 1, hexane : Et_2O). $[\alpha]_D^{20}$ – 25.1 (c 1, Et_2O). ^{1}H NMR (300 MHz, $CDCl_3$): δ 0.98 (3H, t, *J* = 7.3 Hz, H-1), 1.07 (3H, d, *J* = 6.9 Hz, H-5), 1.29 (9H, s, H-14), 2.28 (1H, dq, *J* = 17.9, 7.3 Hz, H-2), 2.43 (1H, dq, *J* = 17.9, 7.3 Hz, H-2), 2.52 (1H, dd, *J* = 6.9, 13.4 Hz, H-6), 2.74-2.89 (1H, m, H-4), 2.95 (1H, dd, *J* = 6.9, 13.4 Hz, H-6), 7.06 (2H, d, *J* = 8.2 Hz, Ar-H), 7.28 (2H, d, *J* = 8.2 Hz, Ar-H) ppm; ^{13}C NMR (75.5 MHz, $CDCl_3$): δ 7.6 (C-1), 16.6 (C-5), 31.4 (C-14), 34.4 (C-13), 34.9 (C-2) 38.7 (C-6), 47.9 (C-4), 125.3 (2 x Ar-CH), 128.6 (2 x Ar-CH), 136.7 (Ar-C), 149.0 (Ar-C), 214.8 (C-3) ppm (Note: Exact structural assignment confirmed using COSY and HSQC); MS (ESI) *m/z*: 233 $[M + H]^+$.

Enantioselectivity was determined by GC analysis: 71 : 29 *er*, t_R = 12.9 (*R*-enantiomer) and 13.2 min (*S*-enantiomer) (140°C hold for 20 min).

(*S*)-2-methyl-1-(4-nitrophenyl)pentan-3-one (*S*)-212

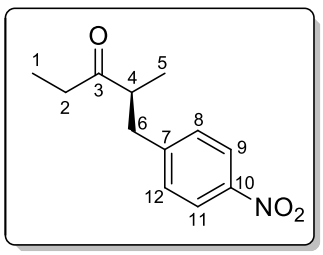

Prepared following the general procedure outlined above using hydrazone **203** and 4-nitrobenzyl bromide. The crude product was purified using column chromatography (10 : 1, hexane : Et_2O) on silica gel to give the title compound **(*S*)-212** as a clear oil (0.048 g, 22% over two steps, 20% *ee*).

R_f = 0.32 (4 : 1, hexane : Et_2O). $[\alpha]_D^{20}$ + 0.658 (c 0.38, Et_2O). IR (NaCl) $\bar{\nu}_{max}$: 2966-2930 (C-H stretch, s), 1712 (C=O stretch, s), 1518 (Aromatic C=C stretch, s), 1345 (N-O stretch, s) cm^{-1}; ^{1}H NMR (300 MHz, $CDCl_3$): δ 0.91 (3H, t, *J* = 7.2 Hz, H-1), 1.06 (3H, d, *J* = 7.0 Hz, H-5), 2.19

(1H, dq, *J* = 17.9, 7.2 Hz, H-2), 2.43 (1H, dq, *J* = 17.9, 7.2 Hz, H-2), 2.60 (1H, dd, *J* = 7.0, 13.4 Hz, H-6), 2.74-2.87 (1H, m, H-4), 3.03 (1H, dd, *J* = 7.0, 13.3 Hz, H-6), 7.02-7.28 (2H, m, Ar-H), 8.02-8.12 (2H, m, Ar-H) ppm; ^{13}C NMR (75.5 MHz, $CDCl_3$): δ 6.5 (C-1), 15.7 (C-5), 34.0 (C-2), 37.6 (C-6), 46.4 (C-4), 122.7 (2 x Ar-CH), 128.8 (2 x Ar-CH), 145.6 (Ar-C), 145.9 (Ar-C), 212.5 (C-3) ppm; HRMS (ESI) *m/z* calcd for $C_{12}H_{14}NO_3$ $[M - H]^-$: 220.0974, found 220.0972.

Enantioselectivity was determined by GC analysis: 40 : 60 *er*, t_R = 79.0 (*R*-enantiomer) and 93.1 min (*S*-enantiomer) (140°C hold for 100 min).

(*R*)-2,4-dimethyl-1-phenylpentan-3-one (*R*)-189

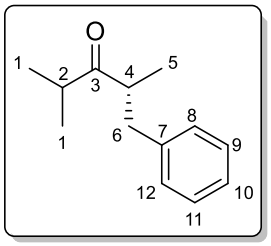

Prepared following the general procedure outlined above using hydrazone **207** and benzyl bromide. The crude product was purified using column chromatography (10 : 1, hexane : Et_2O) on silica gel to give the title compound **(*R*)-189** as a clear oil (0.089 g, 47% over two steps, 8% *ee*). *Note: opposite stereochemistry due to the use of (+)-sparteine **(+)-sp 100** used as chiral ligand.

$[\alpha]_D^{20}$ – 6.2 (c 0.86, $CHCl_3$) (lit.[255] $[\alpha]_D^{20}$ – 83.8 (c 1.07, $CHCl_3$ for > 99% *ee, R*-enantiomer)).

Spectroscopic characteristics were consistent with that of **189** shown earlier and with previously reported data.[255]

Enantioselectivity was determined by GC analysis: 54:46 *er*, t_R = 10.8 (*R*-enantiomer) and 11.1 min (*S*-enantiomer) (110°C hold for 20 min, ramp 10°C/min to 140°C, hold for 5 min).

2-methyl-1-phenylbutan-1-one 190

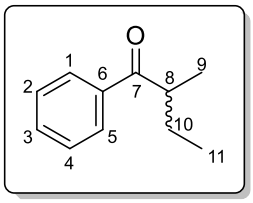

Prepared following the general procedure outlined above using hydrazone **209** and ethyl iodide. The crude product was purified using column chromatography (10 : 1, hexane : Et_2O) on silica gel to give the title compound **190** as a clear oil (0.090 g, 56% over two steps, racemic).

Spectroscopic characteristics were consistent with that of **190** shown earlier and with previously reported data.[256]

Enantioselectivity was determined by GC analysis: 50:50 *er*, t_R = 14.0 and 14.9 min (100°C hold for 20 min, ramp 5°C/min to 140°C, hold for 5 min).

2-methyl-1,3-diphenylpropan-1-one 191

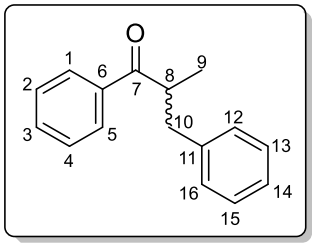

Prepared following the general procedure outlined above using hydrazone **209** and benzyl bromide. The crude product was purified using column chromatography (10 : 1, hexane : Et_2O) on silica gel to give the title compound **191** as a clear oil (0.139 g, 62% over two steps, racemic).

Spectroscopic characteristics were consistent with that of **191** shown earlier and with previously reported data.[256]

Enantioselectivity was determined by GC analysis: 50:50 *er*, t_R = 53.2 and 57.2 min (90°C hold for 5 min, ramp 10°C/min to 140°C, hold for 5 min).

1-(4-methoxyphenyl)-2-methyl-3-phenylpropan-1-one 218

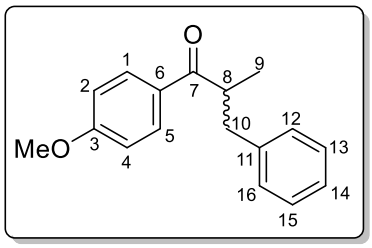

Prepared following the general procedure outlined above using hydrazone **210** and benzyl bromide. The crude product was purified using column chromatography (10 : 1, hexane : Et_2O) on silica gel to give the title compound **218** as a clear oil (0.129 g, 51% over two steps, racemic).

Spectroscopic characteristics were consistent with previously reported data.[256]

R_f = 0.41 (4 : 1, hexane : Et_2O). ^{1}H NMR (300 MHz, $CDCl_3$): δ 1.18 (3H, d, *J* = 6.8 Hz, H-9), 2.67 (1H, dd, *J* = 7.8, 13.7 Hz, H-10), 3.14 (1H, dd, *J* = 6.3, 13.7 Hz, H-10), 3.69 (1H, m, H-8), 3.86 (3H, s, OMe), 6.86-6.99 (2H, m, Ar-H), 7.09-7.34 (5H, m, Ar-H), 7.87-7.97 (2H, m, Ar-H) ppm; ^{13}C NMR (75.5 MHz, $CDCl_3$): δ 17.6 (C-9), 39.5 (C-10), 42.3 (C-8), 55.5 (OMe), 113.8 (2 x Ar-CH), 126.1 (Ar-CH), 128.3 (2 x Ar-CH), 129.1 (2 x Ar-CH), 129.5 (Ar-C), 130.6 (2 x Ar-CH), 140.1 (Ar-C), 163.4 (Ar-C), 202.3 (C-7) ppm; MS (ESI) *m/z*: 255 $[M + H]^+$.

Enantioselectivity was determined by GC analysis: 50:50 *er*, t_R = 200.3 and 202.6 min (140°C hold for 240 min).

(*R*)-2,5,8-trimethylnon-7-en-4-one (*R*)-219

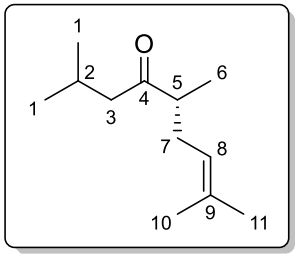

Prepared following the general procedure outlined above using hydrazone **211** and 3,3-dimethylallyl bromide. The crude product was purified using column chromatography (10 : 1, hexane : Et_2O) on silica gel to give the title compound **(*R*)-219** as a clear oil (0.050 g, 28% over two steps, 30% *ee*). *Note: opposite stereochemistry due to the use of (+)-sparteine **(+)-sp 100** used as chiral ligand.

Spectroscopic characteristics were consistent with previously reported data.[181]

R_f = 0.58 (5 : 1, hexane : Et_2O). $[\alpha]_D^{25}$ – 3.3 (c 1.3, $CHCl_3$) (lit.[181] $[\alpha]_D^{25}$ – 26.9 (c 1.3, $CHCl_3$, for 92% *ee*, *R*-enantiomer)). ^{1}H NMR (300 MHz, $CDCl_3$): δ 0.90 (6H, d, *J* = 6.6 Hz, H-1), 1.03 (3H, d, *J* = 6.9 Hz, H-6), 1.64 (3H, s, H-10), 1.68 (3H, s, H-11), 1.95-2.08 (1H, m, H-7), 2.09-2.22 (1H, m, H-2), 2.22-2.37 (3H, m, H-7, H-3), 2.43-2.58 (1H, m, H-5), 5.03 (1H, t, *J* = 7.4 Hz, H-8) ppm; ^{13}C NMR (75.5 MHz, $CDCl_3$): δ 15.9 (C-6), 17.8 (C-10), 22.5, 22.6 (C-1), 24.2 (C-2), 25.7 (C-11), 31.4 (C-7), 46.8 (C-5), 50.5 (C-3), 121.6 (C-8), 133.4 (C-9), 214.3 (C-4) ppm (Note: Exact structural assignment confirmed using COSY and HSQC); MS (ESI) *m/z*: 183 $[M + H]^+$.

GC analysis: 65:35 *er*, t_R = 27.1 (*R*-enantiomer) and 27.5 min (*S*-enantiomer) (75°C hold for 30 min, ramp 10°C/min to 140°C, hold for 5 min).

Ligand	Hydrazone	Electrophile	Yield[a]	Ketone	*er R* : *S*[b]	% *ee*
(-)-sp 100	**203**	benzyl bromide	57%	**(*S*)-36**	24 : 76	52%
(+)-sp 100	**203**	4-trifluoromethyl benzyl bromide	46%	**(*R*)-183**	66 : 34	32%
(-)-sp 100	**203**	3-bromo-1-phenyl-1-propene	30%	**(*S*)-184**	21 : 79	58%
(-)-sp 100	**203**	crotyl bromide	20%	**(*S*)-185**	35 : 65	30%
(-)-sp 100	**203**	4-bromobenzyl bromide	28%	**(*S*)-186**	30 : 70	40%
(-)-sp 100	**203**	4-methylbenzyl bromide	50%	**(*S*)-187**	27 : 73	46%
(-)-sp 100	**203**	1-iodopentane	46%	**(*S*)-188**	17 : 83	66%
(-)-sp 100	**203**	4-fluorobenzyl bromide	26%	**(*S*)-213**	30 : 70	40%
(+)-sp 100	**203**	2-methylbenzyl bromide	54%	**(*R*)-216**	76 : 24	52%
(-)-sp 100	**203**	4-methoxybenzyl bromide	33%	**(*S*)-215**	33 : 67	34%
(+)-sp 100	**203**	4-*tert*-butylbenzyl bromide	62%	**(*R*)-214**	71 : 29	42%
(-)-sp 100	**203**	4-nitrobenzyl bromide	22%	**(*S*)-212**	40 : 60	20%
(+)-sp 100	**207**	benzyl bromide	48%	**(*R*)-189**	54 : 46	8%
(-)-sp 100	**209**	ethyl iodide	56%	**190**	Racemic	
(-)-sp 100	**209**	benzyl bromide	62%	**191**	Racemic	
(-)-sp 100	**210**	benzyl bromide	51%	**218**	Racemic	
(+)-sp 100	**211**	3,3-dimethylallyl bromide	28%	**(*R*)-219**	65 : 35	30%

[a]Isolated yield is over two steps. [b]Absolute configuration assigned based on the optical rotation data of **(*S*)-36** and inferred for the others

Table 5.6.4 Summary of Substrate Scope.

5.6.3 Procedures for Work-up Investigations

(*R*)-1-(4-(*tert*-butyl)phenyl)-2-methylpentan-3-one (*R*)-214

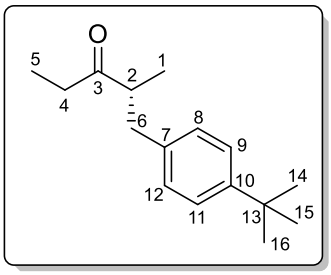

To a schlenk tube, under a N_2 atmosphere, were added anhydrous toluene (5 mL) and (+)-sparteine **(+)-sp 100** (0.28 g, 1.2 mmol) at room temperature. *sec*-BuLi (1.4 M, 1.1 mmol, 0.78 mL) was added at -78°C and allowed to stir for 30 min. Hydrazone **203** (0.128 g, 1 mmol) was added dropwise at -78°C, allowed warm to room temperature and allowed to stir at room temperature for 6 h. The reaction was cooled to -30°C and 4-*tert*-butylbenzyl bromide (0.27 g, 1.2 mmol) was added dropwise. The mixture was allowed to stir at -30°C for 22 h.

Work-up: The reaction was worked up using one of the methods detailed below.

Work-up A

At -30°C, saturated NH_4Cl (0.5 mL) was added and the mixture allowed warm to room temperature. Et_2O (30 mL) was added and the mixture was washed with NH_4Cl (3 x 10 mL). The organic layer was dried over anhydrous $MgSO_4$, filtered, and concentrated under reduced pressure. The crude hydrazone was subjected to the HCl hydrolysis method (see method A in section 5.6.4). The crude product was purified using column chromatography (10 : 1, hexane : Et_2O) on silica gel to give the title compound **(*R*)-214** as a clear oil (0.243 g, 62% over two steps, 42% *ee*).

Spectroscopic characteristics were consistent with that of **(*R*)-214** shown earlier and with previously reported data.[253]

Enantioselectivity was determined by GC analysis: 71 : 29 *er*, t_R = 12.9 (*R*-enantiomer) and 13.2 min (*S*-enantiomer) (140°C hold for 20 min).

Work-up B

At -30°C, MeOH (0.5 mL) was added and the mixture allowed warm to room temperature. The reaction mixture was concentrated under reduced pressure. Et_2O (10 mL) was added and the mixture extracted with Et_2O (3 x 10 mL). The organic layers were combined and dried over anhydrous $MgSO_4$, filtered, and concentrated under reduced pressure. The crude hydrazone purified using column chromatography (10 : 1, hexane : Et_2O, 4% Et_3N) on silica gel to give the pure hydrazone which was immediately subjected to the HCl hydrolysis method (see method A in section 5.6.4). The crude ketone was purified using column chromatography (10 :

1, hexane : Et_2O) on silica gel to give the title compound **(*R*)-214** as a clear oil (0.123 g, 53% over two steps, 42% *ee*).

Spectroscopic characteristics were consistent with that of **(*R*)-214** shown earlier and with previously reported data.[253]

Enantioselectivity was determined by GC analysis: 71 : 29 *er*, t_R = 12.9 (*R*-enantiomer) and 13.2 min (*S*-enantiomer) (140°C hold for 20 min).

Work-up C

At -30°C, pH 7 buffer solution (0.5 mL) was added and the mixture allowed warm to room temperature. Et_2O (10 mL) was added and the mixture extracted with Et_2O (3 x 20 mL). The organic layers were combined and dried over anhydrous $MgSO_4$, filtered, and concentrated under reduced pressure. The crude hydrazone was purified using column chromatography (10 : 1, hexane : Et_2O, 4% Et_3N) on silica gel to give the pure hydrazone which was immediately subjected to the HCl hydrolysis method (see method A in section 5.6.4). The crude ketone was purified using column chromatography (10 : 1, hexane : Et_2O) on silica gel to give the title compound **(*R*)-214** as a clear oil (0.120 g, 52% over two steps, 42% *ee*).

Spectroscopic characteristics were consistent with that of **(*R*)-214** shown earlier and with previously reported data.[253]

Enantioselectivity was determined by GC analysis: 71 : 29 *er*, t_R = 12.9 (*R*-enantiomer) and 13.2 min (*S*-enantiomer) (140°C hold for 20 min).

5.6.4 Hydrazone Cleavage Methods

(*R*)-2-methyl-1-(*o*-tolyl)pentan-3-one (*R*)-216

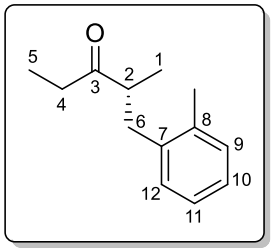

To a schlenk tube, under a N_2 atmosphere, were added anhydrous toluene (5 mL) and (+)-sparteine **(+)-sp 100** (1.686 g, 6 mmol) at room temperature. *sec*-BuLi (1.4 M, 5.5 mmol, 3.9 mL) was added at -78°C and allowed to stir for 30 min. Hydrazone **203** (0.64 g, 5 mmol) was added dropwise at -78°C, allowed warm to room temperature and allowed to stir at room temperature for 6 h. The reaction was cooled to -30°C and 2-methylbenzyl bromide (1.11 g, 6 mmol) was added dropwise. The mixture was allowed to stir at -30°C for 22 h.

At -30°C, saturated NH_4Cl (0.5 mL) was added and the mixture allowed warm to room temperature. Et_2O (30 mL) was added and the mixture was washed with NH_4Cl (3 x 10 mL). The organic layer was dried over anhydrous $MgSO_4$, filtered, and concentrated under reduced pressure.

The crude product was then subjected to one of the following hydrazone cleavage methods.

Hydrazone cleavage method A

The hydrazone (max. 5 mmol) was cleaved by addition of Et_2O (10 mL), followed by 4 M HCl (2.5 mL) and allowed to stir vigorously, until all starting material had reacted (determined by TLC analysis (5 : 1, hexane : Et_2O)). Water (10 mL) was added and the mixture extracted with Et_2O (3 x 30 mL). The organic layers were combined and dried over anhydrous $MgSO_4$, filtered, and concentrated under reduced pressure. The crude product was purified using column chromatography (10 : 1, hexane : Et_2O) on silica gel to give the title compound **(*R*)-216** as a clear oil (0.52 g, 55% over two steps, 52% *ee*).

Spectroscopic characteristics were consistent with that of **(*R*)-216** shown earlier and with previously reported data.[253]

Enantioselectivity was determined by GC analysis: 76 : 24 *er*, t_R = 11.4 (*R*-enantiomer) and 11.9 min (*S*-enantiomer) (120°C hold for 20 min, ramp 10°C/min to 140°C, hold for 5 min).

Hydrazone cleavage method B

The hydrazone (max. 2.5 mmol) was cleaved by adding SeO_2 (0.416 g, 3.75 mmol) and MeOH (37.5 mL) followed by pH 7 phosphate buffer (12.5 mL) and H_2O_2 (30%, 1.25 mL). After completion, saturated $NaHCO_3$ (20 mL) was added to the mixture and the aqueous layers were

extracted with Et_2O (3 x 50 mL). The organic layers were combined and dried over anhydrous $MgSO_4$, filtered, and concentrated under reduced pressure. The crude product was purified using column chromatography (10 : 1, hexane : Et_2O) on silica gel to give the title compound **(*R*)-216** as a clear oil (0.254 g, 54% over two steps, 52% *ee*).

Spectroscopic characteristics were consistent with that of **(*R*)-216** shown earlier and with previously reported data.[253]

Enantioselectivity was determined by GC analysis: 76 : 24 *er*, t_R = 11.4 (*R*-enantiomer) and 11.9 min (*S*-enantiomer) (120°C hold for 20 min, ramp 10°C/min to 140°C, hold for 5 min).

Hydrazone cleavage method C

The hydrazone (max. 2.5 mmol) was cleaved by adding acetone (25 mL) and water (2.5 mL), followed by Amberlyst® 15 hydrogen form beads (500 mg, 200 mg per mmol of hydrazone). The reaction mixture was heated at reflux, until all starting material had reacted (determined by TLC analysis (5 : 1, hexane : Et_2O)). The reaction mixture was cooled and the Amberlyst® beads were removed by filtration and washed with acetone (10 mL). The filtrate was concentrated under reduced pressure. To the resulting residue, water (10 mL) and Et_2O (10 mL) were added and the mixture was extracted with Et_2O (3 x 20 mL). The organic layers were combined and dried over anhydrous $MgSO_4$, filtered, and concentrated under reduced pressure. The crude product was purified using column chromatography (10 : 1, hexane : Et_2O) on silica gel to give the title compound **(*R*)-216** as a clear oil (0.219 g, 46% over two steps, 52% *ee*).

Spectroscopic characteristics were consistent with that of **(*R*)-216** shown earlier and with previously reported data.[253]

Enantioselectivity was determined by GC analysis: 76 : 24 *er*, t_R = 11.4 (*R*-enantiomer) and 11.9 min (*S*-enantiomer) (120°C hold for 20 min, ramp 10°C/min to 140°C, hold for 5 min).

5.6.5 Addition of Lithium Salts

(*R*)-1-(4-(*tert*-butyl)phenyl)-2-methylpentan-3-one (*R*)-214

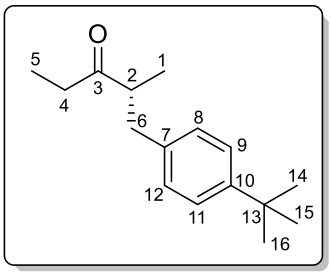

To a schlenk tube, under a N_2 atmosphere, were added **lithium salt** (1.1 mmol), anhydrous toluene (2 mL) and (+)-sparteine **(+)-sp 100** (0.28 g, 1.2 mmol) at room temperature. *sec*-BuLi (1.4 M, 1.1 mmol, 0.78 mL) was added at -78°C and allowed to stir for 30 min. Hydrazone **203** (0.128 g, 1 mmol) was added dropwise at -78°C, allowed warm to room temperature and allowed to stir at room temperature for 6 h. The reaction was cooled to -30°C and 4-*tert*-butylbenzyl bromide (0.27 g, 1.2 mmol) was added dropwise. The mixture was allowed to stir at -30°C for 22 h.

At -30°C, saturated NH_4Cl (0.5 mL) was added and the mixture allowed warm to room temperature. Et_2O (30 mL) was added and the mixture was washed with NH_4Cl (3 x 10 mL). The organic layer was dried over anhydrous $MgSO_4$, filtered, and concentrated under reduced pressure to afford the crude hydrazone.

Hydrazone cleavage

The resulting oil was hydrolysed by addition of Et_2O (5 mL), followed by 4 M HCl (0.5 mL) and allowed to stir vigorously, until all starting material had reacted (determined by TLC analysis (5 : 1, hexane : Et_2O)). Water (5 mL) was added and the mixture extracted with Et_2O (3 x 30 mL). The organic layers were combined and dried over anhydrous $MgSO_4$, filtered, and concentrated under reduced pressure. The crude product was purified using column chromatography (10 : 1, hexane : Et_2O) on silica gel to give the pure ketone **(*R*)-214**.

Spectroscopic characteristics were consistent with that of **(*R*)-214** shown earlier and with previously reported data.[253]

Enantioselectivity was determined by GC analysis: t_R = 12.9 (*R*-enantiomer) and 13.2 min (*S*-enantiomer) (140°C hold for 20 min).

Ligand	Hydrazone	Lithium Salt	Yield[a]	Ketone	*er R* : *S*	% *ee*
(+)-sp 100	**203**	Lithium chloride	35%	**(*R*)-214**	69 : 31	38%
(+)-sp 100	**203**	Lithium bromide	9%	**(*R*)-214**	59 : 41	18%
(+)-sp 100	**203**	Lithium iodide	7%	**(*R*)-214**	61 : 39	22%
(+)-sp 100	**203**	Lithium bromide	59%	**(*R*)-214**	71 : 29	42%[b]

[a]Yield determined using NMR and 1,3,5-trimethoxybenzene as internal standard. [b]2 equiv. lithium bromide were added after the deprotonation and allowed to stir for 45 min at room temperature, before cooling to -30°C for alkylation.

Table 5.6.5 Addition of Lithium Salts.

5.6.6 Procedures for Mechanistic Investigations

Using the general procedure as detailed in section 5.6.2 the following variations were also investigated and are summarised in Table 5.6.6, Table 5.6.7 and Table 5.6.8.

Ligand	Variation from standard conditions	Electrophile	Yield	Ketone	*er R* : *S*	% *ee*
(-)-sp 100	**(-)-sp 100** added @ RT after deprot.	benzyl bromide	25%[a]	**(*S*)-10**	23 : 77	54%[c]
(+)-sp 100	2 h alkylation	4-*tert*-butylbenzyl bromide	43%[b]	**(*R*)-214**	71 : 29	42%
(+)-sp 100	0.2 equiv. electrophile	2-methylbenzyl bromide	18%[b]	**(*R*)-216**	76 : 24	52%

[a]Isolated yield over two steps. [b]Yield determined using NMR and 1,3,5-trimethoxybenzene as internal standard. [c]Ligand was added after the deprotonation and allowed to stir for 45 min, before alkylation @ -30°C.

Table 5.6.6 Mechanistic Investigations.

Ligand	Variation from standard conditions	Electrophile	Yield	Ketone	*er R* : *S*	% *ee*
(+)-sp 100	0.4 equiv. **(+)-sp 100**	4-*tert*-butylbenzyl bromide	38%[a]	**(*R*)-214**	68 : 32	36%
(+)-sp 100	0.4 equiv. **(+)-sp 100** in ether	4-*tert*-butylbenzyl bromide	34%[a]	**(*R*)-214**	59 : 41	18%

[a]Yield determined using NMR and 1,3,5-trimethoxybenzene as internal standard. [b]Ligand was added after the deprotonation and allowed to stir for 45 min at room temperature, before cooling to -30°C for alkylation.

Table 5.6.7 Catalytic Use of Chiral Ligand.

Ligand	Variation from standard conditions	Electrophile	Yield[a]	Ketone	*er R* : *S*	% *ee*
(+)-sp 100	1.5 h alkylation (+)-sp/*sec*BuLi	4-*tert*-butylbenzyl bromide	20%	**(*R*)-214**	68 : 32	36%
No ligand	1.5 h alkylation Only *sec*BuLi	4-*tert*-butylbenzyl bromide	10%	**(*R*)-214**	n/a	n/a

[a]Yield determined using NMR and 1,3,5-trimethoxybenzene as internal standard.

Table 5.6.8 Sparteine/*sec*-BuLi versus *sec*-BuLi Rate Experiments.

5.7 Preparation of Chiral Ligands and their use in the Asymmetric Synthesis of α-Alkylated Ketones

5.7.1 Preparation of 2,2'-isopropylidenebis[(4*S*)-4-phenyl-4,5-dihydro-1,3-oxazole]

Synthetic route A

(*S*)-(+)-phenylglycinol (*S*)-232

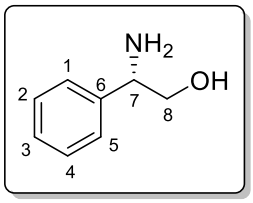

To sodium borohydride (4.5 g, 0.118 mol) under a N_2 atmosphere was added anhydrous THF (80 mL), followed by the dropwise addition of boron trifluoride diethyl etherate (0.237 mol, 29 mL). The suspension was allowed to stir for 15 min, followed by portion-wise addition of (*S*)-(+)-2-phenylglycine (8.9 g, 0.059 mol) over 10 min. The resulting suspension was allowed to stir at room temperature overnight, and heated at reflux for 12 h, allowed to cool to room temperature and allowed to stir overnight again. The reaction mixture was quenched with methanol until gas evolution ceased. The reaction mixture was concentrated under reduced pressure to yield a white solid. 20% aqueous sodium hydroxide solution (400 mL) was added and the basic solution was extracted with CH_2Cl_2 (3 x 200 mL). The organic layers were combined and dried over anhydrous $MgSO_4$, filtered, and concentrated under reduced pressure to afford **(*S*)-232** as a white solid (7.01 g, 97%). Mp 70-72°C (lit.[261] 72-74°C).

Spectroscopic characteristics were consistent with previously reported data.[261,262]

$[\alpha]_D^{22}$ + 27.4 (c 1.07, MeOH) (lit.[262] $[\alpha]_D^{22}$ – 28.5 (c 1, MeOH, for *R*-enantiomer)). ^{1}H NMR (300 MHz, $CDCl_3$): δ 2.01 (1H, bs, O-H), 3.55 (1H, dd, *J* = 8.5, 10.6 Hz, H-7), 3.74 (1H, dd, *J* = 4.2, 10.6 Hz, H-8), 4.05 (1H, dd, *J* = 4.2, 8.5 Hz, H-8), 7.21-7.41 (5H, m, Ar-H) ppm; ^{13}C NMR (75.5 MHz, $CDCl_3$): δ 57.3 (C-7), 68.1 (C-8), 126.4 (2 x Ar-CH), 127.6 (Ar-CH), 128.6 (2 x Ar-CH), 142.8 (C-6) ppm; MS (ESI) *m/z*: 138 $[M + H]^+$.

2,2-dimethyl malonyl dichloride 233

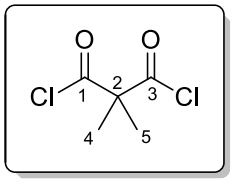

To thionyl chloride (54.0 g, 454 mmol) at 0°C was added malonic acid (12.0 g, 90.8 mmol). The reaction mixture was heated at reflux for 6 h. The excess thionyl chloride was removed under reduced pressure. The crude acid chloride was purified by kugelrohr distillation to give the pure acid chloride **233** as a yellow oil (8.48 g, 55%).

Spectroscopic characteristics were consistent with previously reported data.[213]

^{1}H NMR (300 MHz, $CDCl_3$): δ 1.68 (6H, s, H-4, H-5) ppm; ^{13}C NMR (75.5 MHz, $CDCl_3$): δ 23.0 (C-4, C-5), 69.1 (C-2), 172.0 (C-1, C-3) ppm; MS (ESI) *m/z*: 167 $[M + H]^+$.

N,N'-bis((*S*)-2-hydroxy-1-phenylethyl)-2,2-dimethylmalonamide (*S*,*S*)-234

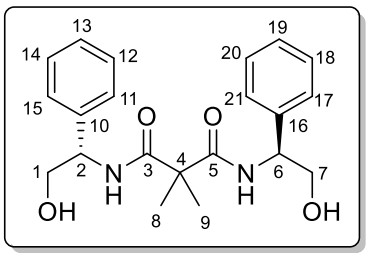

To a stirred solution of the amino alcohol **(*S*)-232** (13.6 g, 99.4 mmol) and Et_3N (248 mmol, 34.7 mL) in CH_2Cl_2 (150 mL) was added dropwise, a solution of the acid chloride **233** (8.4 g, 49.7 mmol) in CH_2Cl_2 (35 mL) at 0°C, and the mixture was allowed to stir overnight at room temperature. The formed solid was removed by filtration and was washed with CH_2Cl_2 (20 mL). For a second crop of product, the mother liquor was extracted with 10% HCl solution (250 mL), the aqueous layer was extracted with CH_2Cl_2 (50 mL). The combined organic extracts were washed with saturated aqueous $NaHCO_3$, water, and brine. The organic layer was dried over anhydrous $MgSO_4$, filtered, and concentrated under reduced pressure to afford the crude product, this was crystallised from 1 : 1, CH_2Cl_2 : hexane to give the pure bisamide **(*S*,*S*)-234** as a white solid (13.01 g, 71%). Mp 60-62°C.

$[\alpha]_D^{22}$ + 55.1 (c 1, MeOH). ^{1}H NMR (300 MHz, MeOD): δ 1.49 (6H, s, H-8, H-9), 3.72 (2H, dd, *J* = 7.8, 11.3 Hz, H-2, H-6), 3.79 (2H, dd, *J* = 5.0, 11.3 Hz, H-1, H-7), 5.04 (2H, dd, *J* = 5.0, 7.8 Hz, H-1, H-7), 7.15-7.36 (10H, m, Ar-H) ppm; ^{13}C NMR (75.5 MHz, MeOD): δ 24.3 (C-8, C-9), 51.5 (C-4), 57.3 (C-2, C-6), 66.0 (C-1, C-7), 127.8 (4 x Ar-CH), 128.4 (2 x Ar-CH), 129.5 (4 x Ar-CH), 140.9 (C-10, C-16), 175.8 (C-3, C-5) ppm; MS (ESI) *m/z*: 371 $[M + H]^+$.

Crystallographic data was also obtained for this compound (see Appendix).

2,2'-isopropylidenebis[(4*S*)-4-phenyl-4,5-dihydro-1,3-oxazole] (*S*,*S*)-227

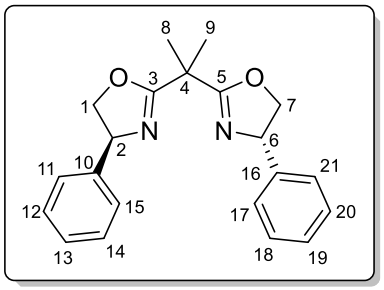

To a stirred solution of the bisamide **(*S*,*S*)-234** (8.0 g, 21.6 mmol), DMAP (0.26 g, 2.16 mmol) and Et_3N (94.9 mmol, 13.2 mL) in CH_2Cl_2 (100 mL) at 0°C was added a solution of *p*-toluenesulfonyl chloride (8.22 g, 43.14 mmol) in CH_2Cl_2 (20 mL) over a period of 10 min. The reaction mixture was allowed to stir at room temperature for 48 h. Saturated NH_4Cl (50 mL) was added to the reaction and the biphasic mixture was allowed to stir for 15 min. The layers were separated and the aqueous layer was extracted with CH_2Cl_2 (3 x 100 mL). The organic layers were combined and washed with saturated aqueous $NaHCO_3$ (100 mL). The aqueous

layer was extracted with CH_2Cl_2 (3 x 100 mL). The organic layers were combined and washed with brine (2 x 100 mL). The organic layer was dried over anhydrous $MgSO_4$, filtered, and concentrated under reduced pressure to afford the crude product. The crude product was purified using column chromatography (4 : 1, hexane : EtOAc, with 0.4% Et_3N) on silica gel to give the title compound **(*S*,*S*)-227** (0.74 g, 10%).

Spectroscopic characteristics were consistent with previously reported data.[216]

R_f = 0.55 (4 : 1, hexane : EtOAc, with 0.4% Et_3N). $[\alpha]_D^{20}$ – 141.3 (c 1, EtOH) (lit.[216] $[\alpha]_D^{20}$ + 153 (c 1, EtOH, for *S*,*S*-enantiomer)). ^{1}H NMR (300 MHz, $CDCl_3$): δ 1.69 (6H, s, H-8, H-9), 4.17 (2H, dd, *J* = 7.7, 8.3 Hz, H-1, H-7), 4.68 (2H, dd, *J* = 8.3, 10.1 Hz, H-2, H-6), 5.23 (2H, dd, *J* = 7.7, 10.1 Hz, H-1, H-7), 7.12-7.42 (10H, m, Ar-H) ppm; ^{13}C NMR (75.5 MHz, $CDCl_3$): δ 24.5 (C-8, C-9) 39.0 (C-4), 69.5 (C-2, C-6), 75.5 (C-1, C-7), 126.7 (4 x Ar-CH), 127.6 (2 x Ar-CH), 128.7 (4 x Ar-CH), 142.4 (C-10, C-16), 170.4 (C-3, C-5) ppm; MS (ESI) *m/z*: 335 $[M + H]^+$.

Synthetic route B[215,216]

2,2'-isopropylidenebis[(4*S*)-4-phenyl-4,5-dihydro-1,3-oxazole] (*S*,*S*)-227

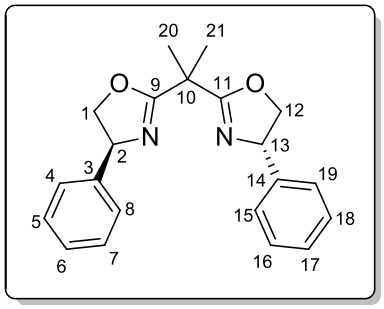

To a stirred solution of 2,2-dimethyl malononitrile (1.47 g, 15.6 mmol) and zinc triflate (5.73 g, 15.7 mmol) in anhydrous toluene (120 mL), was added a solution of the amino alcohol **(*S*,*S*)-232** (4.33 g, 31.4 mmol) in anhydrous toluene (60 mL). The solution was heated at reflux for 7 days. The reaction mixture was allowed to cool to room temperature. The reaction mixture was washed with brine (3 x 100 mL) and saturated aqueous $NaHCO_3$ (3 x 100 mL). The organic layer was dried over anhydrous $MgSO_4$, filtered, and concentrated under reduced pressure to afford the crude product. The crude product was purified using column chromatography (4 : 1, hexane : EtOAc, with 0.4% Et_3N) on silica gel to give the title compound **(*S*,*S*)-227** (2.15 g, 41%).

Spectroscopic characteristics were consistent with that of **(*S*,*S*)-227** shown earlier and with previously reported data.[216]

5.7.2 Preparation of (1*S*,2*S*)-N^1,N^1,N^2,N^2-tetramethyl-1,2-diphenylethane-1,2-diamine

(1*S*,2*S*)-N^1,N^1,N^2,N^2-tetramethyl-1,2-diphenylethane-1,2-diamine (*S*,*S*)-228

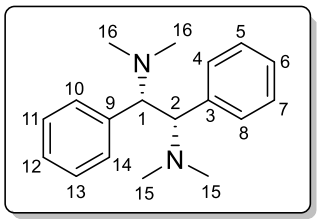

To a solution of (1*S*,2*S*)-1,2-diphenylethylenediamine (0.5 g, 2.34 mmol) in formic acid (90%, 56.3 mmol, 1.1 mL) was added formalin (37%, 37.2 mmol, 1.4 mL) dropwise. The reaction mixture was heated at reflux for 3 days. Formic acid (5.5 mL) and formalin (7 mL) were added and reflux was continued for 4 days. Again formic acid (5.5 mL) and formalin (7 mL) were added and reflux was continued for another 3 days. Once again formic acid (5.5 mL) and formalin (7 mL) were added and reflux was continued for another 7 days. The reaction mixture was allowed cool, and 10% HCl solution (40 mL) as added and the aqueous layer was washed with Et_2O (15 mL). After the addition of 50% NaOH solution (pH 11), the aqueous layer was extracted with EtOAc (50 mL) and the organic layer was washed with brine (15 mL). The organic layer was dried over anhydrous $MgSO_4$, filtered, and concentrated under reduced pressure to afford the crude product. The crude product was purified using column chromatography (4 : 1, hexane : EtOAc, with 0.4% Et_3N) on silica gel to give the title compound **(*S*,*S*)-228** (0.36 g, 45%). Mp 82-85°C (lit.[156] 88-90°C).

Spectroscopic characteristics were consistent with previously reported data.[156]

R_f = 0.33 (4 : 1, hexane : EtOAc, with 0.4% Et_3N). $[\alpha]_D^{20}$ + 53.8 (c 1.09, $CHCl_3$) (lit.[156] $[\alpha]_D^{20}$ + 57.2 (c 1, $CHCl_3$, for *S*,*S*-enantiomer)). ^{1}H NMR (300 MHz, $CHCl_3$): δ 2.25 (12H, s, H-15, H-16), 4.24 (2H, s, H-1, H-2), 6.95-7.18 (10H, m, Ar-H) ppm; ^{13}C NMR (75.5 MHz, $CHCl_3$): δ 40.8 (C-15, C-16), 67.9 (C-1, C-2), 126.6 (2 x Ar-CH), 127.2 (4 x Ar-CH), 129.9 (4 x Ar-CH), 133.8 (C-3, C-9) ppm; MS (ESI) *m/z*: 269 $[M + H]^+$.

5.7.3 Preparation of (1*R*,2*R*)-1,2-dimethoxy-1,2-diphenylethane

(1*R*,2*R*)-1,2-dimethoxy-1,2-diphenylethane (*R*,*R*)-229

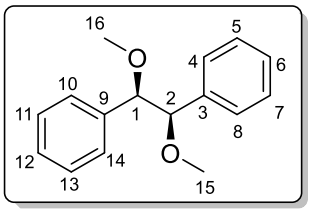

To a stirred suspension of NaH (1.2 g, 30.1 mmol, 60 % in oil, washed with anhydrous hexane (3 x 10 mL) in anhydrous THF (25 mL) was added a solution of (+)-hydrobenzoin (2.5 g, 11.7 mmol) in anhydrous THF (12 mL) at room temperature under a N_2 atmosphere. The reaction mixture was heated at reflux for 30 min. The reaction mixture was cooled to 0°C, dimethyl sulfate (3.1 g, 24.5 mmol, 2.33 mL) was added. The hard viscous mass was allowed to stir for 15 h at room temperature. NH_4Cl (5 mL) was added to quench the reaction. The mixture was extracted with Et_2O (2 x 25mL). The combined organic layers were washed with saturated $NaHCO_3$ (10 mL) and brine (10 mL). The organic layer was dried over anhydrous $MgSO_4$, filtered, and concentrated under reduced pressure to afford the crude product. The crude product was crystallized from hexane to give the title compound **(*R*,*R*)-229** as a colourless solid (1.93 g, 68%). Mp 94-96°C (lit.[156] 99-100°C).

Spectroscopic characteristics were consistent with previously reported data.[156]

$[\alpha]_D^{25}$ – 13.4 (c 1.22, $CHCl_3$) (lit.[156] $[\alpha]_D^{25}$ – 15.2 (c 1.22, $CHCl_3$, for *R*,*R*-enantiomer)). ^{1}H NMR (300 MHz, $CDCl_3$): δ 3.27 (6H, s, H-15, H-16), 4.31 (2H, s, H-1, H-2), 6.95-7.04 (4H, m, Ar-H), 7.12-7.20 (6H, m, Ar-H) ppm; ^{13}C NMR (75.5 MHz, $CDCl_3$): δ 57.2 (C-15, C-16), 87.7 (C-1, C-2), 127.6 (2 x Ar-CH), 127.8 (4 x Ar-CH), 127.9 (4 x Ar-CH), 138.2 (C-3, C-9) ppm; MS (ESI) *m/z*: 243 $[M + H]^+$.

5.7.4 Preparation of (*S*)-1-methyl-2-(pyrrolidin-1-ylmethyl)pyrrolidine

Synthetic route A

(*S*)-1-methyl-2-(pyrrolidin-1-ylmethyl)pyrrolidine (*S*)-230

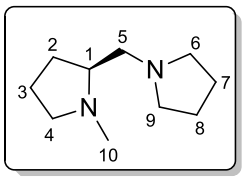

To a solution of (*S*)-(1-pyrrolidinylmethyl)-pyrrolidine **(*S*)-193** (1.5 g, 9.72 mmol) in water (10 mL) was added formic acid (90%, 215 mmol, 8.1 mL) and formalin (37%, 108 mmol, 8.1 mL) dropwise. The reaction mixture was heated at reflux for 24 h. The reaction mixture was allowed cool, 15% NaOH solution was added, until pH 11 was reached. The aqueous layer was extracted with EtOAc (3 x 20 mL). The organic layers were combined and dried over anhydrous $MgSO_4$, filtered, and concentrated under reduced pressure to afford the crude product. The product was further purified by kugelrohr distillation to give the title compound **(*S*)-230**, as a colourless oil (0.6 g, 38%).

Spectroscopic characteristics were consistent with previously reported data.[219,263] $[\alpha]_D^{21}$ – 83.5 (c 0.53, EtOH) (lit.[263] $[\alpha]_D^{21}$ – 84.5 (c 0.53, EtOH, for *S*-enantiomer)). ^{1}H NMR (300 MHz, $CDCl_3$): δ 1.45-1.79 (7H, m, H-2, H-3, H-7, H-8), 1.87-2.02 (1H, m, H-3), 2.03-2.29 (3H, m, H-4, H-5), 2.32 (3H, s, H-10), 2.38-2.51 (4H, m, H-6, H-9), 2.58 (1H, dd, *J* = 4.0, 11.5 Hz, H-5), 2.97 (1H, m, H-1) ppm; ^{13}C NMR (75.5 MHz, $CDCl_3$): δ 21.6 (C-2), 22.5 (C-7, C-8), 30.1 (C-3), 40.4 (C-10), 53.9 (C-6, C-9), 56.6 (C-4), 60.6 (C-5), 63.9 (C-1) ppm; MS (ESI) *m/z*: 169 $[M + H]^+$.

Synthetic route B[219]

(*S*)-(1-methylpyrrolidin-2-yl)(pyrrolidin-1-yl)methanone (*S*)-250

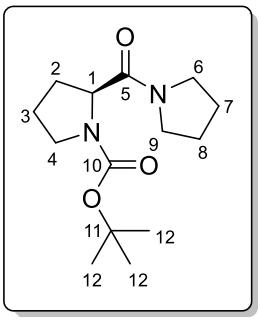

To a suspension of the (*S*)-boc-proline (21.5 g, 100 mmol) in CH_2Cl_2 (30 mL) was added a solution of DCC (20.6 g, 100 mmol) in CH_2Cl_2 (60 mL) at 0°C under a N_2 atmosphere. The reaction mixture was allowed to stir for 30 min at room temperature. To the reaction mixture was added a solution of pyrrolidine (100 mmol, 8.35 mL) in CH_2Cl_2 (60 mL) slowly at 0°C and the reaction temperature was increased to room temperature for 15 min. After 12 h, the reaction mixture was concentrated under reduced pressure. EtOAc (100 mL) was added to the residue. After insoluble materials were removed by filtration, the filtrate was washed with 1M HCl solution (20 mL), saturated $NaHCO_3$ (20 mL) and brine (2 x 100 mL). The organic layer was dried over anhydrous $MgSO_4$, filtered, and concentrated under reduced pressure to afford the crude product. The crude product was purified using column

chromatography (10 : 1, $CHCl_3$: EtOAc) on silica gel to give the title compound **(*S*)-250** (9.3 g, 35%). Mp 69-72°C (lit.[264] 85°C).

Spectroscopic characteristics were consistent with previously reported data.[265]

The *N*-amide moiety has energetically similar *cis* and *trans* isomers (rotamers). These rotamers have slightly different chemical shifts, both are reported here.

R_f = 0.15 (5 : 1, $CHCl_3$: EtOAc, with 0.4% Et_3N). $[\alpha]_D^{23}$ – 32.9 (c 1, MeOH) (lit.[265] $[\alpha]_D^{23}$ – 36.4 (c 1, MeOH, for *S*-enantiomer)). ^{1}H NMR (300 MHz, $CDCl_3$): δ 1.40 (9H, s, H-12), 1.46 (9H, s, H-12), 1.74-2.24 (16H, m, H-2, H-3, H-7, H-8), 3.32-3.80 (12H, m, H-4, H-6, H-9), 4.35 (1H, dd, *J* = 5.0, 7.9 Hz, H-1), 4.48 (1H, dd, *J* = 3.1, 7.7 Hz, H-1) ppm; ^{13}C NMR (75.5 MHz, $CDCl_3$): δ 23.8, 24.0, 24.1, 24.2, 26.2, 26.3, 29.5, 30.4, 45.9, 46.0, 46.1, 46.7, 46.8 (C-2, C-3, C-4, C-6, C-7, C-8, C-9), 28.4, 28.5 (C-12), 57.8, 58.0 (C-1), 79.3, 79.4 (C-11), 153.8, 154.5 (C-10), 171.0, 171.3 (C-5) ppm; MS (ESI) *m/z*: 269 $[M+H]^+$.

(*S*)-1-methyl-2-(pyrrolidin-1-ylmethyl)pyrrolidine (*S*)-230

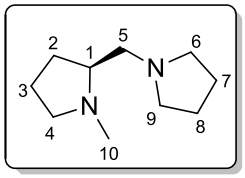

To $LiAlH_4$ (3.16 g, 83.4 mmol) in anhydrous THF (35 mL), under a N_2 atmosphere at 0°C, was added (*S*)-(1-methylpyrrolidin-2-yl)(pyrrolidin-1-yl)methanone **(*S*)-250** (9.0 g, 33.4 mmol) in anhydrous THF (35 mL). The reaction mixture was brought to room temperature and allowed to stir overnight. It was then heated at reflux for 4 h. The reaction mixture was allowed cool to room temperature and quenched by addition of water (4 mL), 15% NaOH solution (4 mL) and water (12 mL) and allowed to stir for 1 h, until a white precipitate had formed. The mixture was filtered through a pad of Celite® to remove the inorganic salts and washed with EtOAc (100 mL). The filtrate was dried over anhydrous $MgSO_4$, filtered, and concentrated under reduced pressure to give the crude product. The product was further purified by kugelrohr distillation to give the title compound **(*S*)-230**, as a colourless oil (2.85 g, 51%).

Spectroscopic characteristics were consistent with that of **(*S*)-230** shown earlier and with previously reported data.[219,263]

5.7.5 Preparation of (1*S*,2*S*)-N^1,N^2-bis(3,3-dimethylbutyl)-N^1,N^2-dimethylcyclohexane-1,2-diamine

(1*S*,2*S*)-(+)-1,2-diaminocyclohexane *D*-tartrate (*S*,*S*)-251

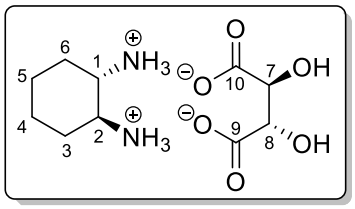

Trans-(±)-1,2-diaminocyclohexane (100 mmol, 20 mL) was added dropwise to a stirred solution of *D*-tartaric acid (12.5 g, 50 mmol) in water (45 mL), such that the internal temperature did not exceed 70°C (during this time a white precipitate forms, but this disappears by the point of complete addition). AcOH (5 mL) was added dropwise such that the internal temperature did not exceed 90°C. The resulting solution was allowed to cool in an ice bath and left in the refrigerator for 6 h. The solids were removed by filtration and the filter-cake was washed with cold water (20 mL) and MeOH (5 x 10 mL) (washings kept separate). The resulting white solid was dried to give the (1*S*,2*S*)-cyclohexane diamine *D*-tartaric acid salt **(*S*,*S*)-251** (13.1 g, 99%). Mp 265-268°C (lit.[97] 283-284°C).

Spectroscopic characteristics were consistent with previously reported data.[97]

$[\alpha]_D^{20}$ – 12.05 (c 4, H_2O) (lit.[266] $[\alpha]_D^{20}$ – 12.5 (c 4, H_2O, for *S*,*S*-enantiomer)). ^{1}H NMR (300 MHz, $CDCl_3$): δ 1.21-1.37 (2H, m, H-4, H-5), 1.37-1.56 (2H, m, H-4, H-5), 1.67-1.86 (2H, m, H-3, H-6), 2.01-2.17 (2H, m, H-3, H-6), 3.22-3.38 (2H, m, H-1, H-2), 4.26 (2H, s, H-7, H-8) ppm; ^{13}C NMR (75.5 MHz, $CDCl_3$): δ 22.8 (C-4, C-5) 29.4 (C-3, C-6), 52.2 (C-1, C-2), 73.8 (C-7, C-8), 178.5 (C-9, C-10) ppm; MS (ESI) *m/z*: 115 $[M + H]^+$ (1,2-diaminocyclohexane), 149 $[M - H]^-$ (*D*-tartaric acid).

(1*R*,2*R*)-(+)-1,2-diaminocyclohexane *L*-tartrate (*R*,*R*)-251

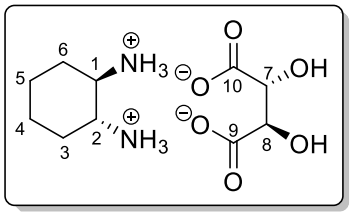

The aqueous filtrate was combined with the aqueous washings from the preparation of (1*S*,2*S*)-(+)-1,2-diaminocyclohexane D-tartrate **(*S*,*S*)-251** and cooled to 0°C. *L*-tartaric acid (12.5 g, 50 mmol) was added portion wise to the solution over 5 min. The resulting solution was allowed to stir at 0°C for 4 h. The solids were removed by filtration and the filter-cake was washed with cold water (20 mL) and MeOH (5 x 10 mL). The resulting white solid was dried to give the (1*R*,2*R*)-cyclohexane diamine *L*-tartaric acid salt **(*R*,*R*)-251** (10.1 g, 76%). Mp 260-262°C (lit.[97] 275-276°C).

Spectroscopic characteristics were consistent with that of **(*S*,*S*)-251** shown earlier and with previously reported data.[97]

$[\alpha]_D^{20}$ + 11.7 (c 4, H_2O) (lit.[266] $[\alpha]_D^{20}$ + 12.5 (c 4, H_2O, for *R*,*R*-enantiomer)).

dimethyl-(1*S*,2*S*)-cyclohexane-1,2-diyldicarbamate (*S*,*S*)-280

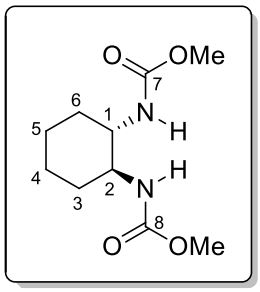

A solution of NaOH (12.2 g, 306 mmol) in water (20 mL) and methylchloroformate (6.20 mL, 80.3 mmol) were simultaneously added to a stirred suspension of (1*S*,2*S*)-cyclohexane diamine *D*-tartaric acid salt **(*S*,*S*)-251** (10.01 g, 37.9 mmol) in toluene (50 mL) at 0°C. This led to the formation of a gel-like precipitate. The resulting mixture was allowed to stir at room temperature for 48 h. $CHCl_3$ (50 mL) was added and the solids were removed by filtration and washed with $CHCl_3$ (2 x 25 mL). The filtrate was washed with water (25 mL). The aqueous layer was extracted with $CHCl_3$ (2 x 50 mL). The organic layers were combined and dried over anhydrous $MgSO_4$, filtered, and concentrated under reduced pressure to give the crude product as a white solid (7.27 g, 83%).

The crude product **(*S*,*S*)-280** was used in the next step without further purification.

Spectroscopic characteristics were consistent with previously reported data.[97]

^{1}H NMR (300 MHz, $CDCl_3$): δ 1.08-1.40 (4H, m, H-4, H-5), 1.65-1.83 (2H, m, H-3, H-6), 1.96-2.16 (2H, m, H-3, H-6), 3.14-3.44 (2H, m, H-1, H-2), 3.65 (6H, s, 2 x OMe), 4.95 (2H, bs, 2 x N-H) ppm; ^{13}C NMR (75.5 MHz, $CDCl_3$): δ 24.7 (C-4, C-5) 32.9 (C-3, C-6), 52.1 (2 x OMe), 55.5 (C-1, C-2), 157.5 (C-7, C-8) ppm; MS (ESI) *m/z*: 231 $[M + H]^+$.

(1*S*,2*S*)-N^1,N^2-dimethylcyclohexane-1,2-diamine (*S*,*S*)-252

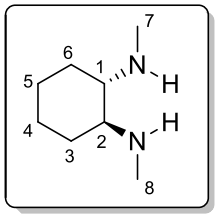

To a stirred suspension of $LiAlH_4$ (7.20 g, 189.6 mmol) in anhydrous THF (60 mL) at 0°C under a N_2 atmosphere, was added a solution of the crude carbamate **(*S*,*S*)-280** (max. 37.9 mmol) in anhydrous THF (60 mL), dropwise. The resulting solution was heated at reflux for 40 h. The solution was cooled to 0°C and Et_2O (50 mL) was added. The mixture was quenched by the slow addition of water (7 mL), 15% NaOH solution and water (21 mL) and allowed to stir for 1 h, a white precipitate formed. The mixture was filtered through a pad of Celite® to remove the inorganic salts and washed with 24 : 1, CH_2Cl_2 : MeOH (2 x 50 mL). The filtrate was dried over anhydrous $MgSO_4$, filtered, and concentrated under reduced pressure to give the crude product as a yellow oil (4.25 g, 79%).

The crude product **(*S*,*S*)-252** was used in the next step without further purification.

Spectroscopic characteristics were consistent with previously reported data.[97]

^{1}H NMR (300 MHz, $CDCl_3$): δ 0.85-1.07 (2H, m, H-4, H-5), 1.17-1.34 (2H, m, H-4, H-5), 1.69-1.82 (2H, m, H-3, H-6), 1.96-2.06 (2H, m, H-3, H-6), 2.06-2.15 (2H, m, H-1, H-2), 2.39 (6H,

s, H-7, H-8) ppm; ^{13}C NMR (75.5 MHz, $CDCl_3$): δ 25.0 (C-4, C-5) 30.7 (C-3, C-6), 33.5 (C-7, C-8), 55.5 (C-1, C-2) ppm; MS (ESI) *m/z*: 143 $[M + H]^+$.

(1*S*,2*S*)-N^1,N^2-(cyclohexane-1,2-diyl)bis(N,3,3-trimethylbutanamide) (*S*,*S*)-281

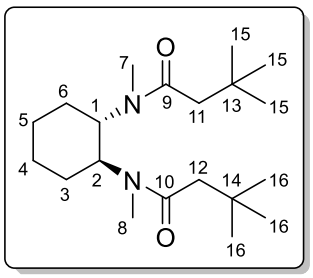

A solution of *tert*-butylacetylchloride (10.8 mL, 77.5 mmol) in CH_2Cl_2 (20 mL) was added dropwise to a stirred biphasic mixture of crude diamine **(*S*,*S*)-252** (max. 37.9 mmol) in CH_2Cl_2 (50 mL) and NaOH (7.06 g, 176 mmol) in water (25 mL) at 0°C. The resulting mixture was allowed to stir at room temperature for 40 h. The two layers were separated and the aqueous layer was extracted with CH_2Cl_2 (5 x 100 mL). The organic layers were combined and dried over anhydrous $MgSO_4$, filtered, and concentrated under reduced pressure to give the crude bis-amide as a white solid (10.2 g, 80%).

The crude product **(*S*,*S*)-281** was used in the next step without further purification.

Spectroscopic characteristics were consistent with previously reported data.[97]

^{1}H NMR (300 MHz, $CDCl_3$): δ 1.03 (18H, s, H-15, H-16), 1.25-1.85 (8H, m, H-3, H-4, H-5, H-6), 2.18 (2 x 2H, d, *J* = 14.0 Hz, H-11, H-12), 2.83 (6H, s, H-7, H-8), 4.66-4.79 (2H, m, H-1, H-2) ppm; ^{13}C NMR (75.5 MHz, $CDCl_3$): δ 25.1 (C-4, C-5) 29.5 (C-3, C-6), 29.9 (C-15, C-16), 30.9 (C-7, C-8), 31.5 (C-13, C-14), 45.4 (C-11, C-12), 51.6 (C-1, C-2), 171.9 (C-9, C-10) ppm; MS (ESI) *m/z*: 339 $[M + H]^+$.

(1*S*,2*S*)-N^1,N^2-dimethyl- N^1,N^2-bis(3,3-dimethylbutyl)cyclohexane-1,2-diamine (*S*,*S*)-113

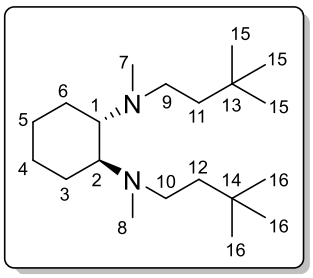

To a stirred suspension of $LiAlH_4$ (7.20 g, 189.6 mmol) in anhydrous THF (60 mL) at 0°C under a N_2 atmosphere, was added a solution of the bisamide **(*S*,*S*)-281** (max. 37.9 mmol) in anhydrous THF (60 mL), dropwise. The resulting solution was heated at reflux for 40 h. The solution was cooled to 0°C and Et_2O (50 mL) was added. The mixture was quenched by the slow addition of water (7 mL), 15% NaOH solution and water (21 mL) and allowed to stir for 1 h, a white precipitate formed. The mixture was filtered through a pad of Celite® to remove the inorganic salts and washed with 24 : 1, CH_2Cl_2 : MeOH (2 x 50 mL). The filtrate was dried over anhydrous $MgSO_4$, filtered, and concentrated under reduced pressure to give the crude product as a yellow oil. The product was further purified by kugelrohr distillation to give the title compound **(*S*,*S*)-113**, as a colourless oil (4.84 g, 41% over four steps).

Spectroscopic characteristics were consistent with previously reported data.[97] $[\alpha]_D^{20}$ + 27.1 (c 1, $CHCl_3$) (lit.[220] $[\alpha]_D^{20}$ – 31.1 (c 1.02, $CHCl_3$, for *R*,*R*-enantiomer)). ^{1}H NMR (300 MHz, $CDCl_3$): δ 0.89 (18H, s, H-15, H-16), 1.04-1.24 (4H, m, H-4, H-5), 1.32-1.44 (4H, t, *J* = 8.4 Hz, H-11, H-12), 1.62-1.84 (4H, m, H-3, H-6), 2.24 (6H, s, H-7, H-8), 2.37-2.59 (6H, m, H-1, H-2, H-9, H-10) ppm; ^{13}C NMR (75.5 MHz, $CDCl_3$): δ 25.1 (C-4, C-5), 25.9 (C-3, C-6), 29.6 (C-15, C-16), 29.8 (C-13, C-14), 37.0 (C-7, C-8), 42.2 (C-11, C-12), 50.1 (C-9, C-10), 62.6 (C-1, C-2) ppm; MS (ESI) *m/z*: 311 $[M + H]^+$.

5.7.6 Preparation of N^1,N^1,N^2,N^2-tetramethylcyclohexane-1,2-diamine

(1*S*,2*S*)-N^1,N^1,N^2,N^2-tetramethylcyclohexane-1,2-diamine (*S*,*S*)-231

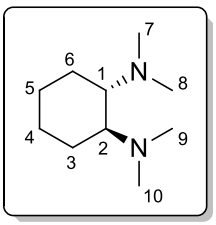

(1*S*,2*S*)-(+)-1,2-diaminocyclohexane *D*-tartrate **(*S*,*S*)-251** (4 g, 15.17 mmol) was dissolved in formic acid (90%, 159 mmol, 6 mL) and formalin (37%, 97.6 mmol, 8 mL) was added slowly at room temperature. The reaction mixture was heated at reflux for 2 h. The reaction mixture was allowed cool and made basic, until pH 14 was reached. The aqueous layer was extracted with Et_2O (3 x 20 mL). The organic layers were combined and dried over anhydrous $MgSO_4$, filtered, and concentrated under reduced pressure to afford the crude product. The product was further purified by kugelrohr distillation to give the title compound **(*S*,*S*)-231** as a colourless oil (1.82 g, 71%).

Spectroscopic characteristics were consistent with previously reported data.[220]

$[\alpha]_D^{20}$ + 58.3 (c 1.05, $CHCl_3$) (lit.[220] $[\alpha]_D^{20}$ – 62.9 (c 1.05, $CHCl_3$, for *R*,*R*-enantiomer)). ^{1}H NMR (300 MHz, $CDCl_3$): δ 1.00-1.23 (4H, m, H-4, H-5), 1.63-1.78 (2H, m, H-3, H-6), 1.78-1.91 (2H, m, H-3, H-6), 2.28 (12H, s, H-7, H-8, H-9, H-10), 2.35-2.42 (2H, m, H-1, H-2) ppm; ^{13}C NMR (75.5 MHz, $CDCl_3$): δ 22.9 (C-4, C-5), 25.6 (C-3, C-6), 40.1 (C-7, C-8, C-9, C-10), 63.9 (C-1, C-2) ppm; MS (ESI) *m/z*: 171 $[M + H]^+$.

(1*R*,2*R*)-N^1,N^1,N^2,N^2-tetramethylcyclohexane-1,2-diamine (*R*,*R*)-231

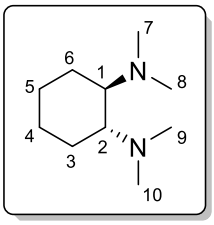

Prepared following the procedure outlined above for (1*S*,2*S*)-N1,N1,N2,N2-tetramethylcyclohexane-1,2-diamine **(*S*,*S*)-231**, using (1*R*,2*R*)-(+)-1,2-diaminocyclohexane *L*-tartrate **(*R*,*R*)-251** as starting material. The crude product was purified by kugelrohr distillation to give the title compound **(*R*,*R*)-231** as a colourless oil (1.4 g, 55%).

Spectroscopic characteristics were consistent with that of **(*S*,*S*)-231** shown earlier and with previously reported data.[220]

$[\alpha]_D^{20}$ – 59.9 (c 1.05, $CHCl_3$) (lit.[220] $[\alpha]_D^{20}$ – 62.9 (c 1.05, $CHCl_3$, for *R*-enantiomer)).

5.7.7 Chiral Ligand Screen in the Asymmetric Synthesis of α-Alkylated Ketones

General Procedure

To a schlenk tube, under a N_2 atmosphere, were added anhydrous toluene (1 mL) and **ligand** (1.2 mmol) at room temperature. *sec*-BuLi (1.4 M, 1.1 mmol, 0.78 mL) was added at -78°C and allowed to stir for 30 min. Hydrazone **203** (0.128 g, 1 mmol) was added dropwise at -78°C, allowed warm to room temperature and allowed to stir at room temperature for 6 h. The reaction was cooled to -30°C and **electrophile** (1.2 mmol) was added dropwise. The mixture was allowed to stir at -30°C for 22 h.

At -30°C, saturated NH_4Cl (0.5 mL) was added and the mixture allowed warm to room temperature. Et_2O (30 mL) was added and the mixture was washed with NH_4Cl (3 x 10 mL). The organic layer was dried over anhydrous $MgSO_4$, filtered, and concentrated under reduced pressure. The crude product was purified using column chromatography (10 : 1, hexane : Et_2O) on silica gel to give a clear oil.

Hydrazone cleavage

The resulting oil was hydrolysed by addition of Et_2O (5 mL), followed by 4 M HCl (0.5 mL) and allowed to stir vigorously, until all starting material had reacted (determined by TLC analysis (5 : 1, hexane : Et_2O)). Water (5 mL) was added and the mixture extracted with Et_2O (3 x 30 mL). The organic layers were combined and dried over anhydrous $MgSO_4$, filtered, and concentrated under reduced pressure. The crude product was purified using column chromatography (10 : 1, hexane : Et_2O) on silica gel to give the pure ketone.

Ligand	Electrophile	Deprot. Temp.	Alkyl. Temp.	Yield[a]	Product	*er R* : *S*	% *ee*
(-)-sp 100	*n*-PeI	RT	-30°C	34%	**(*S*)-188**	17 : 83	66%
(*S*,*S*)-227	*n*-PeI	RT	-30°C	No reaction occurred			
(*S*,*S*)-228	BnBr	RT	-30°C	31%	**(*S*)-36**	45 : 55	10%
(*R*,*R*)-229	BnBr	RT	-30°C	27%	**(*R*)-36**	57 : 43	14%
(*S*)-230	*n*-PeI	RT	-30°C	16%	**188**	50 : 50	Racemic
(*S*,*S*)-113	*n*-PeI	RT	-30°C	53%	**(*S*)-188**	29 : 71	42%
(*S*,*S*)-231	*n*-PeI	RT	-30°C	23%	**(*R*)-188**	58 : 42	16%

[a]Isolated yield over two steps

Table 5.7.1 Chiral ligand screen in the asymmetric synthesis of α-alkylated ketones.

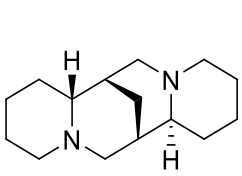

(-)-sp 100

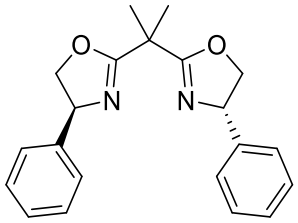

(*S*,*S*)-227

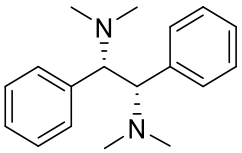

(*S*,*S*)-228

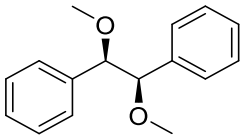

(*R*,*R*)-229

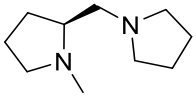

(*S*)-230

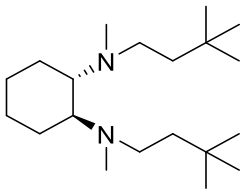

(*S*,*S*)-113

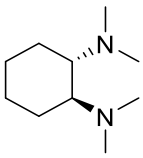

(*S*,*S*)-231

Figure 5.7.1

5.8 Aldol & Michael Reactions using (-)- and (+)-Sparteine

1-hydroxy-2-methyl-1-phenylpentan-3-one 254

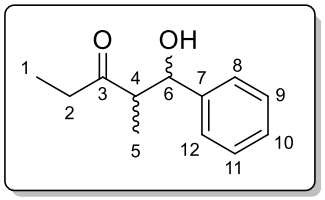

To a schlenk tube, under a N_2 atmosphere, were added anhydrous toluene (1 mL) and (-)-sparteine **(-)-sp 100** (0.281 g, 1.2 mmol) at room temperature. *sec*-BuLi (1.4 M, 1.1 mmol, 0.78 mL) was added at -78°C and allowed to stir for 30 min. Hydrazone **203** (0.128 g, 1 mmol) was added dropwise at -78°C, allowed warm to room temperature and allowed to stir at room temperature for 6 h. The reaction was cooled to -30°C and benzaldehyde (0.127 g, 1.2 mmol) was added dropwise. The mixture was allowed to stir at -30°C for 22 h.

At -30°C, saturated NH_4Cl (0.5 mL) was added and the mixture allowed warm to room temperature. Et_2O (30 mL) was added and the mixture was washed with NH_4Cl (3 x 10 mL). The organic layer was dried over anhydrous $MgSO_4$, filtered, and concentrated under reduced pressure to afford the crude hydrazone. The crude hydrazone was used in the next step without further purification.

Hydrazone Cleavage

The hydrazone was cleaved by adding acetone (10 mL) and water (1 mL), followed by Amberlyst® 15 hydrogen form beads (200 mg). The mixture was heated at reflux, until all starting material had reacted (determined by TLC analysis (1 : 1, hexane : Et_2O)). The reaction mixture was cooled and the Amberlyst® beads were removed by filtration and washed with acetone (10 mL). The filtrate was concentrated under reduced pressure. To the resulting residue, water (10 mL) and Et_2O (10 mL) were added and the mixture was extracted with Et_2O (3 x 20 mL). The organic layers were combined and dried over anhydrous $MgSO_4$, filtered, and concentrated under reduced pressure. The crude product was purified using column chromatography (5 : 1, hexane : Et_2O) on silica gel to give the title compound **254** as a clear oil, isolated as a mixture of diastereomers, 0.125 g, 65% over two steps, 60 : 40 *dr*, *syn* 52% *ee*, *anti* 30% *ee*.

Spectroscopic characteristics were consistent with previously reported data.[267]

R_f = 0.6 (1 : 1, hexane : Et_2O). **Syn diastereomer:** ^{1}H NMR (400 MHz, $CDCl_3$): δ 1.00 (3H, t, *J* = 7.3 Hz, H-1), 1.08 (3H, d, *J* = 7.2 Hz, H-5), 2.33 (1H, dq, *J* = 18.1, 7.3 Hz, H-2), 2.50 (1H, dq, *J* = 17.9, 7.3 Hz, H-2), 2.84 (1H, dq, *J* = 4.0, 7.2 Hz, H-4), 3.11 (1H, bs, O-H), 5.05 (1H, bd, *J* = 4.0 Hz, H-6), 7.20-7.39 (5H, m, Ar-H) ppm; ^{13}C NMR (75.5 MHz, $CDCl_3$): δ 7.5 (C-1), 10.5 (C-5), 35.4 (C-2), 52.2 (C-4), 73.3 (C-6), 125.9 (2 x Ar-CH), 127.4 (Ar-CH), 128.3 (2 x Ar-CH), 141.8 (C-7), 216.2 (C-3) ppm; **Anti diastereomer:** ^{1}H NMR (400 MHz, $CDCl_3$): δ

0.94 (3H, d, *J* = 7.2 Hz, H-5), 1.04 (3H, t, *J* = 7.3 Hz, H-1), 2.43 (1H, dq, *J* = 18.1, 7.3 Hz, H-2), 2.56 (1H, dq, *J* = 18.1, 7.3 Hz, H-2), 2.87-2.99 (1H, m, H-4), 4.69 (1H, bd, *J* = 5.0 Hz, O-H), 4.75 (1H, dd, *J* = 5.0, 8.2 Hz, H-6), 7.20-7.39 (5H, m, Ar-H) ppm; ^{13}C NMR (75.5 MHz, $CDCl_3$): δ 7.4 (C-1), 14.5 (C-5), 36.5 (C-2), 52.6 (C-4), 76.7 (C-6), 126.5 (2 x Ar-CH), 127.9 (Ar-CH), 128.5 (2 x Ar-CH), 142.2 (C-7), 216.0 (C-3) ppm; MS (ESI) *m/z*: 193 $[M + H]^+$.

Diastereoselectivity and enantioselectivity were determined by GC analysis: 60 : 40 *dr*, *syn* 23 : 77 *er*, *anti* 35 : 65 *er*, t_R = 17.3 (*syn*, major enantiomer), 19.5 min (*anti*, major enantiomer), 21.7 min (*anti*, minor enantiomer) and 22.6 min (*syn*, minor enantiomer) (130°C hold for 30 min).

4-methyl-6-nitro-5-phenylhexan-3-one 256

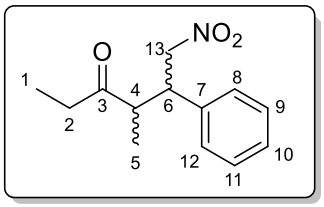

To a schlenk tube, under a N_2 atmosphere, were added anhydrous toluene (1 mL) and (+)-sparteine **(+)-sp 100** (0.281 g, 1.2 mmol) at room temperature. *sec*-BuLi (1.4 M, 1.1 mmol, 0.78 mL) was added at -78°C and allowed to stir for 30 min. Hydrazone **203** (0.128 g, 1 mmol) was added dropwise at -78°C, allowed warm to room temperature and allowed to stir at room temperature for 6 h. The reaction was cooled to -38°C and β-nitrostyrene (0.179 g, 1.2 mmol, in toluene (1 mL)) was added dropwise. The mixture was allowed to stir at -70°C for 22 h.

At -70°C, saturated NH_4Cl (0.5 mL) was added and the mixture allowed warm to room temperature. Et_2O (30 mL) was added and the mixture was washed with NH_4Cl (3 x 10 mL). The organic layer was dried over anhydrous $MgSO_4$, filtered, and concentrated under reduced pressure to afford the crude hydrazone. The crude hydrazone was used in the next step without further purification.

Hydrazone Cleavage

The resulting oil was hydrolysed by addition of Et_2O (5 mL), followed by 4 M HCl (0.5 mL) and allowed to stir vigorously, until all starting material had reacted (determined by TLC analysis (1 : 1, hexane : Et_2O)). Water (5 mL) was added and the mixture extracted with Et_2O (3 x 30 mL). The organic layers were combined and dried over anhydrous $MgSO_4$, filtered, and concentrated under reduced pressure. The crude product was purified using column chromatography (10 : 1, hexane : Et_2O) on silica gel to give the title compound **256** as a brown oil, 0.123 g, 53% over two steps, mixture of diastereomers, 88 : 12 *dr*, *syn* 2% *ee*, *anti* 2% *ee*.

Spectroscopic characteristics were consistent with previously reported data for both the *syn* and the *anti*.[268]

***Syn* diastereomer:** The *syn* diastereomer was isolated using column chromatography (10 : 1, hexane : Et_2O) on silica gel to give the title compound **256** as a brown oil, 0.105 g, 45% over two steps, *syn* 2% *ee*.

R_f = 0.52 (1 : 1, hexane : Et_2O). $[\alpha]_D^{23}$ – 0.278 (c 0.36, $CHCl_3$) (lit.[268] $[\alpha]_D^{23}$ – 185 (c 0.36, $CHCl_3$, for 96% *ee*, *S*,*R*-diastereomer)). ^{1}H NMR (300 MHz, $CDCl_3$): δ 0.97 (3H, d, *J* = 7.3 Hz, H-5), 1.07 (3H, t, *J* = 7.3 Hz, H-1), 2.41 (1H, dq, *J* = 18.0, 7.3 Hz, H-2), 2.61 (1H, dq, *J* = 18.0, 7.3 Hz, H-2), 2.99 (1H, dq, *J* = 9.6, 7.3 Hz, H-4), 3.62-3.76 (1H, m, H-6), 4.55-4.73 (2H, m, H-13), 7.13-7.20 (2H, m, Ar-H), 7.22-7.23 (3H, m, Ar-H) ppm; ^{13}C NMR (75.5 MHz, $CDCl_3$): δ 7.6 (C-1), 16.3 (C-5), 35.4 (C-2), 46.1 (C-4), 48.3 (C-6), 78.3 (C-13), 127.9 (2 x Ar-CH), 128.0 (Ar-CH), 129.0 (2 x Ar-CH), 137.6 (C-7), 213.5 (C-3) ppm; MS (ESI) *m/z*: 236 $[M + H]^+$.

***Anti* diastereomer:** The *anti* diastereomer was isolated using column chromatography (10 : 1, hexane : Et_2O) on silica gel to give the title compound **256** as a clear oil, (0.018 g, 8% over two steps, *anti* 2% *ee*).

R_f = 0.41 (1 : 1, hexane : Et_2O). $[\alpha]_D^{23}$ + 2.5 (c 0.26, $CHCl_3$) (lit.[268] $[\alpha]_D^{23}$ – 23 (c 0.26, $CHCl_3$, for 85% *ee*, *R*,*R*-diastereomer)). ^{1}H NMR (300 MHz, $CDCl_3$): δ 0.83 (3H, t, *J* = 7.3 Hz, H-1), 1.19 (3H, d, *J* = 6.9 Hz, H-5), 2.05 (1H, dq, *J* = 18.0, 7.3 Hz, H-2), 2.31 (1H, dq, *J* = 18.0, 7.3 Hz, H-2), 2.91-3.05 (1H, m, H-4), 3.72-3.84 (1H, m, H-6), 4.65-4.85 (2H, m, H-13), 7.11-7.47 (5H, m, Ar-H) ppm; ^{13}C NMR (75.5 MHz, $CDCl_3$): δ 7.3 (C-1), 14.5 (C-5), 35.8 (C-2), 45.9 (C-4), 49.1 (C-6), 77.6 (C-13), 127.7 (2 x Ar-CH), 127.8 (Ar-CH), 128.9 (2 x Ar-CH), 138.0 (C-7), 212.5 (C-3) ppm; MS (ESI) *m/z*: 236 $[M + H]^+$.

Diastereoselectivity and enantioselectivity were determined by GC analysis: 88 : 12 *dr*, *syn* 51 : 49 *er*, *anti* 51 : 49 *er*, t_R = 49.2 (*syn*, major enantiomer), 54.9 min (*anti*, major enantiomer), 56.5 min (*syn*, minor enantiomer) and 60.1 min (*anti*, minor enantiomer) (140°C hold for 80 min).

5.9 Procedures for NMR Investigations of Asymmetric Alkylation with (+)-Sparteine

Procedure for reaction to be analysed by NMR

(*R*)-1-(4-(*tert*-butyl)phenyl)-2-methylpentan-3-one (*R*)-214

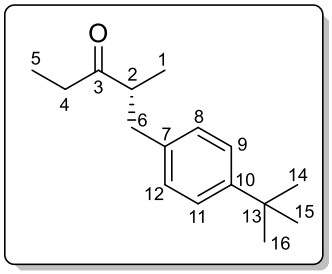

To a schlenk tube, under a N_2 atmosphere, were added anhydrous deuterated toluene (2 mL) and (+)-sparteine **(+)-sp 100** (0.28 g, 1.2 mmol) at room temperature. *sec*-BuLi (1.4 M, 1.1 mmol, 0.78 mL) was added at -78°C and allowed to stir for 30 min. Hydrazone **203** (0.128 g, 1 mmol) was added dropwise at -78°C, allowed warm to room temperature. After 30 min a sample was removed using a glass syringe (Figure 5.9.1), under a N_2 atmosphere, and transferred to the sealed NMR tube (Figure 5.9.2) and analysed via NMR. The reaction continued to stir at room temperature for a further 5.5 h. At room temperature, 4-*tert*-butylbenzyl bromide (0.27 g, 1.2 mmol) was added dropwise. After 30 min a sample was removed using a glass syringe (Figure 5.9.1), under a N_2 atmosphere, and transferred to the sealed NMR tube (Figure 5.9.2) and analysed via NMR. The mixture was allowed to stir at room temperature for 22 h.

Saturated NH_4Cl (0.5 mL) was added at room temperature. Et_2O (30 mL) was added and the mixture washed with NH_4Cl (3 x 10 mL). The organic layer was dried over anhydrous $MgSO_4$, filtered, and concentrated under reduced pressure to afford the crude hydrazone. Another sample was taken of the crude hydrazone after work-up and analysed via NMR.

Hydrazone cleavage

The resulting oil was hydrolysed by addition of Et_2O (5 mL), followed by 4 M HCl (0.5 mL) and allowed to stir vigorously, until all starting material had reacted (determined by TLC analysis (1 : 1, hexane : Et_2O)). Water (5 mL) was added and the mixture extracted with Et_2O (3 x 30 mL). The organic layers were combined and dried over anhydrous $MgSO_4$, filtered, and concentrated under reduced pressure. The crude product was purified using column chromatography (10 : 1, hexane : Et_2O) on silica gel to give the pure ketone (44%, yield determined using NMR and 1,3,5-trimethoxybenzene as internal standard, 28% *ee*).

Spectroscopic characteristics were consistent with that of **(*R*)-214** shown earlier and with previously reported data.[253]

Enantioselectivity was determined by GC analysis: 64 : 36 *er*, t_R = 12.9 (*R*-enantiomer) and 13.2 min (*S*-enantiomer) (140°C hold for 20 min).

Procedure for preparing NMR samples under inert atmosphere

An NMR tube, fitted with a rubber septum and wrapped in parafilm, was put under vacuum via a needle connected to a schlenk line (Figure 5.9.2). The tube was heated gently and filled with N_2, the NMR tube was allowed to cool under N_2 atmosphere. Using a glass syringe 0.6 mL of the reaction mixture was removed under inert atmosphere (Figure 5.9.1) and transferred to the NMR tube (Figure 5.9.2). The samples were analysed at 600 MHz on a Bruker AVANCE 600 instrument.

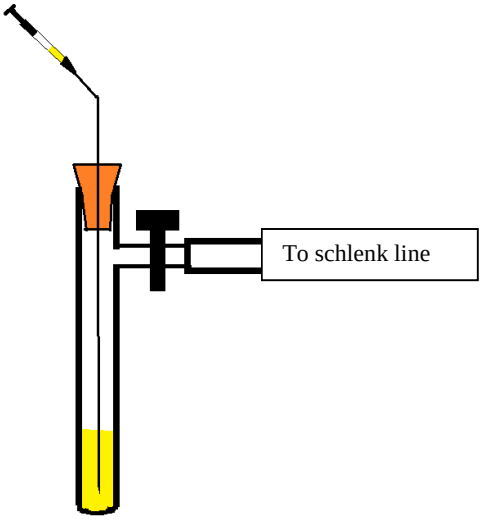

Figure 5.9.1

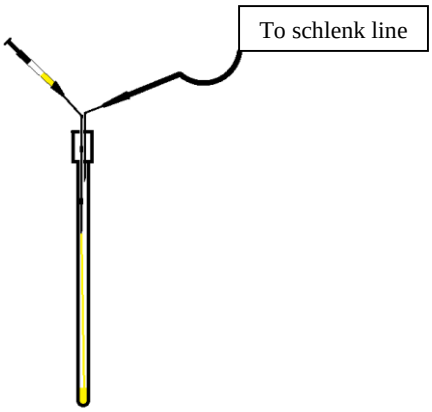

Figure 5.9.2

5.10 Asymmetric α-Alkylation and Synthesis of a 1,3-Amino Alcohol Precursors using Chiral Sulfinimines

5.10.1 Synthesis of *N*-*tert*-butanesulfinyl imines

General procedure for the synthesis of *N*-*tert*-butanesulfinyl imines

To a mixture of (*S*)-(-)-2-methyl-2-propanesulfinamide (1 equiv.) and the corresponding **ketone** (1 equiv.) in THF (4 mL per mmol of ketone), was added $Ti(OEt)_4$ (2 equiv.). The resulting mixture was heated at reflux overnight. The reaction mixture was allowed to cool to room temperature and brine (4 mL per mmol of ketone) and allowed to stir for 30 min before filtration through a pad of Celite®. The filtrate was dried over anhydrous $MgSO_4$, filtered, and concentrated under reduced pressure, to afford the crude *N*-*tert*-butanesulfinyl imine.

(*S*,*E*)-2-methyl-*N*-(1-phenylethylidene)propane-2-sulfinamide (*S*)-259

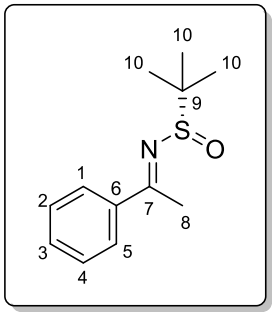

Prepared following the general procedure outlined above using acetophenone. The crude product was purified using column chromatography (10 : 1, hexane : EtOAc) on silica gel to give the title compound **(*S*)-259** as a yellow/green solid (0.802 g, 72%). Mp 36-40°C (lit.[269] Mp 36-40°C).

Spectroscopic characteristics were consistent with previously reported data.[269]

R_f = 0.2 (4 : 1, hexane : EtOAc). $[\alpha]_D^{20}$ + 14.0 (c 1.03, CH_2Cl_2) (lit.[269] $[\alpha]_D^{20}$ + 13.0 (c 1.03, CH_2Cl_2, for *S*-enantiomer)). ^{1}H NMR (300 MHz, $CDCl_3$): δ 1.22 (9H, s, H-10), 2.64 (3H, s, H-8), 7.23-7.42 (3H, m, Ar-H), 7.77 (2H, m, Ar-H) ppm; ^{13}C NMR (75.5 MHz, $CDCl_3$): δ 19.7 (C-8), 22.5 (C-10), 57.4 (C-9), 127.2 (2 x Ar-CH), 128.5 (2 x Ar-CH), 131.6 (Ar-CH), 138.6 (C-6), 176.4 (C-7) ppm; MS (ESI) *m/z*: 224 $[M + H]^+$.

(*S*,*E*)-2-methyl-*N*-(1-phenylpropylidene)propane-2-sulfinamide (*S*)-260

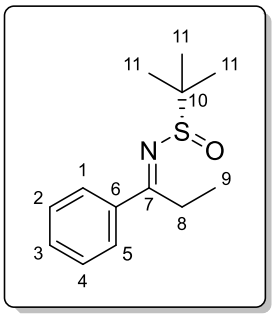

Prepared following the general procedure outlined above using propiophenone. The crude product was purified using column chromatography (10 : 1, hexane : EtOAc) on silica gel to give the title compound **(*S*)-260** as a yellow oil (0.691 g, 58%).

Spectroscopic characteristics were consistent with previously reported data.[269]

R_f = 0.35 (4 : 1, hexane : EtOAc). $[\alpha]_D^{20}$ + 7.9 (c 1.06, CH_2Cl_2) (lit.[269] $[\alpha]_D^{20}$ + 9 (c 1.06, CH_2Cl_2, for *S*-enantiomer)). ^{1}H NMR (300 MHz, $CDCl_3$): δ 1.28 (3H, t, *J* = 7.6 Hz, H-9), 1.33 (9H, s, H-11), 3.06-3.42 (2H, m, H-8), 7.34-7.6 (3H, m, Ar-H), 7.73-7.98 (2H, m, Ar-H) ppm; ^{13}C NMR (75.5 MHz, $CDCl_3$): δ 13.2 (C-9), 22.7 (C-11), 25.9 (C-8), 57.3 (C-10), 127.5 (Ar-CH), 128.6 (3 x Ar-CH), 131.5 (Ar-CH), 137.6 (C-6), 181.3 (C-7) ppm; MS (ESI) *m/z*: 238 $[M + H]^+$.

(*S*)-2-methyl-*N*-(pentan-3-ylidene)propane-2-sulfinamide (*S*)-261

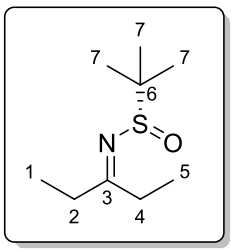

Prepared following the general procedure outlined above using 3-pentanone. The crude product was purified using column chromatography (10 : 1, hexane : EtOAc) on silica gel to give the title compound **(*S*)-261** as a yellow oil (1.194 g, 32%).

Spectroscopic characteristics were consistent with previously reported data.[270]

R_f = 0.3 (4 : 1, hexane : EtOAc). $[\alpha]_D^{20}$ + 156.8 (c 1, CH_2Cl_2). ^{1}H NMR (300 MHz, $CDCl_3$): δ 1.10 (3H, t, *J* = 7.2 Hz, H-1), 1.20 (3H, t, *J* = 7.6 Hz, H-5), 1.24 (9H, s, H-7), 2.37-2.54 (2H, m, H-2), 2.63-2.78 (2H, m, H-4) ppm; ^{13}C NMR (75.5 MHz, $CDCl_3$): δ 9.9 (C-1), 11.8 (C-5), 22.2 (C-7), 29.5 (C-2), 33.4 (C-4), 56.2 (C-6), 190.2 (C-3) ppm; MS (ESI) *m/z*: 190 $[M + H]^+$.

5.10.2 Asymmetric α-Alkylation using Chiral Sulfinimines

(*S*)-2-methyl-*N*-((*Z*)-2-methyl-1,3-diphenylpropylidene)propane-2-sulfinamide (*S*)-282

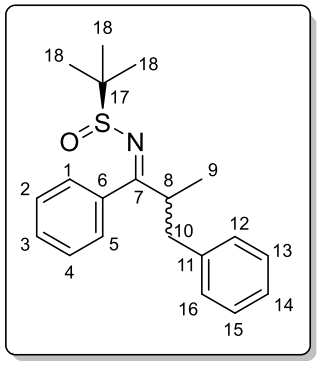

To a schlenk tube under N_2 atmosphere, containing diisopropylamine (1.2 mmol, 0.17 mL) in anhydrous THF (5 mL), was added *n*-BuLi (1.1 mmol, 1.6 M, 0.69 mL) at 0°C. The mixture was allowed to stir at 0°C for 30 min. The solution was cooled to -78°C and *tert*-butanesulfinyl imine **(*S*)-260** (0.237 g, 1 mmol, 0.22 mL) was added dropwise. After the reaction mixture was allowed to stir for 1 h at -78°C, benzyl bromide (0.222 g, 1.3 mmol) was added slowly. The reaction mixture was kept at -78°C for 3 h and was allowed warm to room temperature overnight. The reaction was quenched with saturated NH_4Cl (1.5 mL). NH_4Cl (10 mL) was added and the mixture was extracted with EtOAc (3 x 20 mL). The organic layers were combined and dried over anhydrous $MgSO_4$, filtered, and concentrated under reduced pressure.

^{1}H NMR analysis showed a complex mixture of products had formed.

This complex mixture of products were inseparable by column chromatography (10 : 1, hexane : EtOAc) on silica gel.

(*S*)-2-methyl-*N*-((*E*)-2-methyl-1-phenylpentan-3-ylidene)propane-2-sulfinamide (*S*)-283

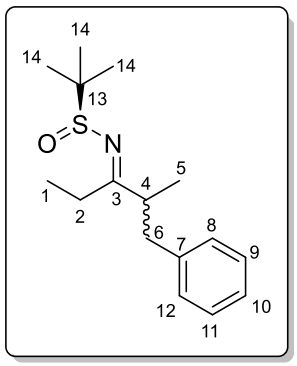

To a schlenk tube under N_2 atmosphere, containing diisopropylamine (1.2 mmol, 0.17 mL) in anhydrous THF (5 mL), was added *n*-BuLi (1.1 mmol, 1.6 M, 0.69 mL) at 0°C. The mixture was allowed to stir at 0°C for 30 min. The solution was cooled to -78°C and *tert*-butanesulfinyl imine **(*S*)-261** (0.189 g, 1 mmol, 0.22 mL) was added dropwise. After the reaction mixture was allowed to stir for 1 h at -78°C, benzyl bromide (0.222 g, 1.3 mmol) was added slowly. The reaction mixture was kept at -78°C for 3 h and was allowed warm to room temperature overnight. The reaction was quenched with saturated NH_4Cl (1.5 mL). NH_4Cl (10 mL) was added and the mixture was extracted with EtOAc (3 x 20 mL). The organic layers were combined and dried over anhydrous $MgSO_4$, filtered, and concentrated under reduced pressure.

^{1}H NMR analysis showed a complex mixture of products had formed.

5.10.3 Synthesis of 1,3-Amino Alcohol Precursors

(1*S*,3*S*)-1-(((*S*)-*tert*-butylsulfinyl)amino)-4,4-dimethyl-1-phenylpentan-3-yl pivalate (*S*,*S*,*S*)-270

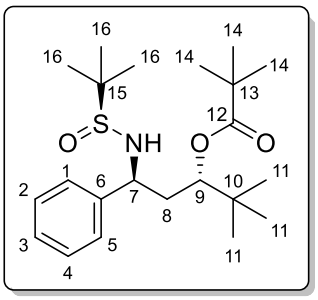

Method A

To a schlenk tube under N_2 atmosphere, containing diisopropylamine (1.2 mmol, 0.17 mL) in anhydrous THF (5 mL), was added *n*-BuLi (1.1 mmol, 1.5 M, 0.73 mL) at 0°C. The mixture was allowed to stir at 0°C for 30 min. The solution was cooled to -78°C and *tert*-butanesulfinyl imine **(*S*)-259** (0.223 g, 1 mmol) was added in one portion. After the reaction mixture was allowed to stir for 1 h at -78°C, pivaldehyde (0.189 g, 2.2 mmol) was added slowly. The reaction mixture was kept at -78°C for 3 h and was allowed warm to room temperature overnight. The reaction was quenched with saturated NH_4Cl (1.5 mL). NH_4Cl (10 mL) was added and the mixture was extracted with EtOAc (3 x 20 mL). The organic layers were combined and dried over anhydrous $MgSO_4$, filtered, and concentrated under reduced pressure. The crude product was purified using column chromatography (10 : 1, hexane : EtOAc) on silica gel to give the title compound **(*S*,*S*,*S*)-270** as a pale yellow solid (0.253 g, 64%, mixture of diastereomers, 90 : 10 *dr*).

Major diastereomer (S,S,S): The major diastereomer was isolated using column chromatography (10 : 1, hexane : EtOAc) on silica gel to give the title compound **(*S*,*S*,*S*)-270** as a pale yellow solid (0.232 g, 59%). Mp 162-168°C.

R_f = 0.15 (4 : 1, hexane : EtOAc). $[\alpha]_D^{23}$ + 37.9 (c 1, $CHCl_3$). IR (NaCl) $\bar{\nu}_{max}$: 3244 (N-H stretch, m), 2969 (C-H stretch, s), 1725 (C=O stretch, s), 1470 (C-H bending, s), 1163 (C-O stretch, s), 1039 (C-N stretch, s) cm^{-1}; ^1H NMR (300 MHz, $CDCl_3$): δ 0.95 (9H, s, H-11), 1.19 (9H, s, H-16), 1.23 (9H, s, H-14), 1.92 (1H, ddd, *J* = 3.0, 10.9, 14.1 Hz, H-8), 2.33 (1H, ddd, *J* = 1.5, 10.9, 14.1 Hz, H-8), 4.10 (1H, ddd, *J* = 3.0, 6.2, 10.9 Hz, H-7), 4.19 (1H, d, *J* = 6.2 Hz N-H), 5.07 (1H, dd, *J* = 1.5, 10.9 Hz, H-9), 7.22-7.41 (5H, m, Ar-H) ppm; ^{13}C NMR (75.5 MHz, $CDCl_3$): δ 22.6 (C-16), 26.1 (C-11), 27.4 (C-14), 34.9 (C-10), 37.2 (C-8), 39.1 (C-13), 56.2 (C-15), 57.3 (C-7), 77.3 (C-9), 127.4 (2 x Ar-CH), 127.6 (Ar-CH), 128.6 (2 x Ar-CH), 142.1 (C-

6), 178.6 (C-12) ppm (Note: Exact structural assignment confirmed using COSY, HSQC and HMBC); HRMS (ESI) *m/z* calcd for $C_{22}H_{38}NO_3S$ $[M + H]^+$: 396.2572, found 396.2559. Crystallographic data was also obtained for this compound (see Appendix).

Minor diastereomer: The absolute configuration was not determined.

The minor diastereomer was isolated using column chromatography (10 : 1, hexane : EtOAc) on silica gel to give the minor diastereomer of **270** as a yellow oil (0.021 g, 5%).

R_f = 0.22 (4 : 1, hexane : EtOAc). $[\alpha]_D^{23}$ + 57.5 (c 1, $CHCl_3$). IR (NaCl) $\bar{\nu}_{max}$: 3244 (N-H stretch, m), 2970 (C-H stretch, s), 1725 (C=O stretch, s), 1471 (C-H bending, s), 1164 (C-O stretch, s), 1039 (C-N stretch, s) cm^{-1}; ^1H NMR (300 MHz, $CDCl_3$): δ 0.89 (9H, s, H-11), 1.21 (9H, s, H-16), 1.27 (9H, s, H-14), 1.92 (1H, ddd, *J* = 3.0, 11.0, 14.4 Hz, H-8), 2.05 (1H, ddd, *J* = 3.0, 9.9, 14.4 Hz, H-8), 4.13-4.19 (1H, d, *J* = 2.7 Hz, N-H), 4.24 (1H, ddd, *J* = 2.7, 3.0, 9.9 Hz, H-7), 4.94 (1H, dd, *J* = 3.0, 11.0 Hz, H-9), 7.27-7.38 (5H, m, Ar-H) ppm; ^{13}C NMR (75.5 MHz, $CDCl_3$): δ 22.8 (C-16), 25.8 (C-11), 27.3 (C-14), 34.8 (C-10), 38.9 (C-8), 39.2 (C-13), 55.3 (C-7, C-15), 75.5 (C-9), 127.8 (Ar-CH), 127.9 (2 x Ar-CH), 128.5 (2 x Ar-CH), 141.7 (C-6), 178.6 (C-12) ppm (Note: Exact structural assignment confirmed using COSY, HSQC and HMBC); HRMS (ESI) *m/z* calcd for $C_{22}H_{38}NO_3S$ $[M + H]^+$: 396.2572, found 396.2559.

Isolated by-product from Aldol-Tishchenko Reaction

(*S*)-*N*-(3-hydroxy-4,4-dimethyl-1-phenylpentyl)-2-methylpropane-2-sulfinamide (*S*)-273

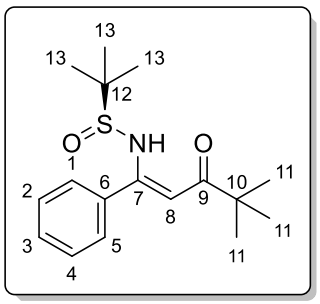

Yield: 0.078 g, 25%. Mp 82-85°C. R_f = 0.34 (4 : 1, hexane : EtOAc). $[\alpha]_D^{23}$ – 16.3 (c 0.43, $CHCl_3$). IR (NaCl) $\bar{\nu}_{max}$: 3583 (N-H stretch, m), 2962 (C-H stretch, s), 1558 (C=O stretch, s), 1081 (C-N stretch, s) cm^{-1}; ^1H NMR (300 MHz, $CDCl_3$): δ 1.19 (9H, s, H-11), 1.33 (9H, s, H-13), 5.69 (1H, s, H-8), 7.40-7.56 (5H, m, Ar-H), 12.07 (1H, bs, N-H) ppm; ^{13}C NMR (75.5 MHz, $CDCl_3$): δ 22.6 (C-13), 27.2 (C-11), 43.0 (C-10), 57.3 (C-12), 99.5 (C-8), 128.6 (2 x Ar-CH), 128.7 (2 x Ar-CH), 130.3 (Ar-CH), 135.0 (C-6), 160.9 (C-7), 207.7 (C-9) ppm; HRMS (ESI) *m/z* calcd for $C_{17}H_{26}NO_2S$ $[M + H]^+$: 308.1688, found 308.1684.

Crystallographic data was also obtained for this compound (see Appendix).

Method B

To a schlenk tube under N_2 atmosphere, containing diisopropylamine (1.2 mmol, 0.17 mL) in anhydrous THF (5 mL), was added *n*-BuLi (1.1 mmol, 1.5 M, 0.73 mL) at 0°C. The mixture was allowed to stir at 0°C for 30 min. The solution was cooled to -78°C and *tert*-butanesulfinyl imine **(*S*)-259** (0.223 g, 1 mmol) was added in one portion. After the reaction mixture was allowed to stir for 1 h at -78°C, $MgBr_2$ (0.368 g, 2 mmol) was added in one portion. The reaction mixture was allowed to stir for a further 45 min at -78°C. Pivaldehyde (0.189 g, 2.2 mmol) was added dropwise. The reaction mixture was kept at -78°C for 3 h and was allowed warm to room temperature overnight. The reaction was quenched with saturated NH_4Cl (1.5 mL), EtOAc (10 mL) and NH_4Cl (10 mL) were added and the mixture was extracted with EtOAc (3 x 20 mL). The organic layers were combined and dried over anhydrous $MgSO_4$, filtered, and concentrated under reduced pressure. The crude product was purified using column chromatography (10 : 1, hexane : EtOAc) on silica gel to give **270** as a clear oil (0.059 g, 15%, mixture of diastereomers, 79 : 21 *dr*).

Spectroscopic characteristics were consistent with that of **270** shown earlier.

(*S*)-*N*-((1*S*,3*S*)-3-hydroxy-4,4-dimethyl-1-phenylpentyl)-2-methylpropane-2-sulfinamide

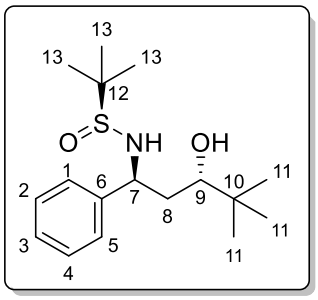

(*S*,*S*,*S*)-278

Method A

To potassium hydroxide (0.007 g, 0.126 mmol) in 1:1, EtOH : water, was added (1*S*,3*S*)-1-(((*S*)-*tert*-butylsulfinyl)amino)-4,4-dimethyl-1-phenylpentan-3-yl pivalate **(*S*,*S*,*S*)-270** (0.05 g, 0.126 mmol) at room temperature. This mixture was allowed to stir for 24 h. The reaction mixture was concentrated under reduced pressure to remove the EtOH. Water (1 mL) was added and the mixture was extracted with EtOAc (3 x 10 mL). The organic layers were combined and dried over anhydrous $MgSO_4$, filtered, and concentrated under reduced pressure to give a pale yellow solid.

^{1}H NMR analysis and TLC analysis showed the reaction was unsuccessful and that only starting material remained.

Method B

To (1*S*,3*S*)-1-(((*S*)-*tert*-butylsulfinyl)amino)-4,4-dimethyl-1-phenylpentan-3-yl pivalate **(*S*,*S*,*S*)-270** (0.091 g, 0.23 mmol) in MeOH (5 mL) was added potassium carbonate (0.079 g, 0.575 mmol) in one portion. The reaction mixture was heated at reflux overnight. The reaction mixture was cooled to room temperature. EtOAc (5 mL), water (2 mL), and a solution of saturated NH_4Cl (2 mL) were added. The resulting biphasic mixture was extracted with EtOAc (3 x 10 mL). The organic layers were combined and dried over anhydrous $MgSO_4$, filtered, and concentrated under reduced pressure to give a pale yellow solid.

^{1}H NMR analysis and TLC analysis showed the reaction was unsuccessful and that only starting material remained.

Method C

To a schlenk tube under N_2 atmosphere, containing DIBAL-H (0.315 mmol, 1 M, 0.315 mL) in anhydrous CH_2Cl_2 (2 mL), was added the (1*S*,3*S*)-1-(((*S*)-*tert*-butylsulfinyl)amino)-4,4-dimethyl-1-phenylpentan-3-yl pivalate **(*S*,*S*,*S*)-270** (0.05 g, 0.126 mmol, major diastereomer)

at -78°C. The mixture was allowed warm to room temperature and allowed to stir for 1 h at this temperature. The reaction was cooled to 0°C and MeOH (1 mL) was added slowly to quench the excess DIBAL-H. The reaction was allowed warm to room temperature. Aqueous 10% HCl was slowly added to hydrolyse the aluminium salts. The layers were separated and the organic layer was washed with aqueous $NaHCO_3$ and brine. The organic layer was dried over anhydrous $MgSO_4$, filtered, and concentrated under reduced pressure. The crude product was purified using column chromatography (4 : 1, hexane : EtOAc) on silica gel to give the title compound **(*S*,*S*,*S*)- 278** as a white solid (0.020 g, 51%, >98 : 2 *dr*). Mp 142-147°C.

R_f = 0.3 (1 : 1, hexane : EtOAc). $[\alpha]_D^{23}$ – 24.6 (c 1, $CHCl_3$) for *S*,*S*,*S* diastereomer. IR (NaCl) $\bar{\nu}_{max}$: 3263 (O-H stretch, s), 2957 (C-H stretch, s), 1479 (C-H bending, s), 1164 (C-O stretch, s), 1028 (C-N stretch, s) cm^{-1}, ^1H NMR (300 MHz, $CDCl_3$): δ 0.89 (9H, s, H-11), 1.16 (9H, s, H-13), 1.70-1.89 (2H, m, H-8), 2.77 (1H, bs, OH), 3.43 (1H, dd, *J* = 2.2, 10.1 Hz, H-9), 3.94 (1H, d, *J* = 7.2 Hz, N-H), 4.71 (1H, ddd, *J* = 3.9, 7.2, 11.1 Hz, H-7), 7.20-7.42 (5H, m, Ar-H) ppm; ^{13}C NMR (75.5 MHz, $CDCl_3$): δ 22.8 (C-13), 25.8 (C-11), 34.6 (C-10), 40.8 (C-8), 54.3 (C-7), 56.7 (C-12), 75.2 (C-9), 126.7 (2 x Ar-CH), 127.3 (Ar-CH), 128.7 (2 x Ar-CH), 143.5 (C-6) ppm (Note: Exact structural assignment confirmed using COSY, HSQC and HMBC); HRMS (ESI) *m/z* calcd for $C_{18}H_{30}NO_2$ $[M + H]^+$: 312.1997, found 312.2001.

(1*S*,3*S*)-1-amino-4,4-dimethyl-1-phenylpentan-3-yl pivalate.HCl (*S*,*S*,*S*)-279

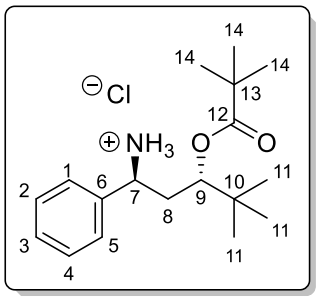

To *tert*-butylsulfinyl-amino-pivalate **(*S*,*S*,*S*)-270** (0.062 g, 0.16 mmol, major diastereomer) were added 1,4-dioxane (1.9 mL) and 4 M HCl (2.88 mL). The reaction mixture was heated at reflux overnight. The reaction mixture was cooled to room temperature and concentrated under reduced pressure. EtOAc (10 mL) was added at which point the product crashed out of solution. The solid was filtered and dried to afford the title compound **(*S*,*S*,*S*)-279** as a white solid (0.039g, 85%, >98 : 2 *dr*). Mp 218-220°C.

$[\alpha]_D^{23}$ + 7.7 (c 1, CH_2Cl_2). IR (NaCl) $\bar{\nu}_{max}$: 2959 (C-H stretch, s), 1716 (C=O stretch, s), 1458 (C-H bending, s), 1162 (C-O stretch, s), 1042 (C-N stretch, s) cm^{-1}; ^1H NMR (300 MHz, $CDCl_3$): δ 0.91 (9H, s, H-11), 1.11 (9H, s, H-14), 1.96 (1H, ddd, *J* = 4.8, 10.5, 15.0 Hz, H-8), 2.63 (1H, dd, *J* = 8.4, 15.0 Hz, H-8), 3.91-4.13 (1H, m, H-7), 4.79-5.03 (1H, m, H-9), 7.27-7.41 (3H, m, Ar-H), 7.41-7.55 (2H, m, Ar-H), 8.75 (3H, bs, N-H) ppm; ^{13}C NMR (75.5 MHz, $CDCl_3$): δ 25.9 (C-11), 27.2 (C-14), 34.9 (C-10), 35.9 (C-8), 39.1 (C-13), 54.5 (C-7), 77.6 (C-9), 127.6 (2 x Ar-CH), 129.0 (Ar-CH), 129.1 (2 x Ar-CH), 136.1 (C-6), 179.1 (C-12) ppm (Note: Exact structural assignment confirmed using COSY, HSQC and HMBC); HRMS (ESI) *m/z* calcd for $C_{18}H_{30}NO_2$ $[M + H]^+$: 292.2277, found 292.2276.

Chapter 6

Reference List

6.1 Reference List

1. Discrimination of Enantiomers by Biological Molecules: kshitij-iitjee.com. http://www.kshitij-iitjee.com/Discrimination-of-Enantiomers-by-Biological-Molecules (16-9-2014).

2. Nguyen, L. A.; He, H.; Pham-Huy, C. *Int. J. Biomed. Sci.* **2006,** *2*, 85-100.

3. Ojima, I. *Catalytic Asymmetric Synthesis;* 3rd ed.; John Wiley & Sons, Inc.: New York, 2010.

4. Chanan-Khan, A. A. A. In *Immunomodulating Drugs for the Treatment of Cancer*, 1st ed.; Lippincott Williams & Wilkins: Philadelphia, 2012.

5. Procter, G. *Asymmetric Synthesis;* 1st ed.; Oxford University Press: U.K., 1996.

6. Thomas, G. *Medicinal Chemistry: An Introduction;* 2nd ed.; John Wiley and Sons Ltd: West Sussex, U.K., 2007.

7. Dalko, P. I. *Angew. Chem. Int. Ed.* **2004,** *43*, 5138-5175.

8. Kohler, M. C.; Wengryniuk, S. E.; Coltart, D. M. In *Stereoselective synthesis of drugs and natural products*, 1st ed.; John Wiley & Sons. Inc.: New York, 2013.

9. Enders, D.; Wortmann, L.; Peters, R. *Acc. Chem. Res.* **2000,** *33*, 157-169.

10. Job, A.; Janeck, C. E.; Bettray, W.; Peters, R.; Enders, D. *Tetrahedron* **2002,** *58*, 2253-2329.

11. Paterson, I.; Norcross, R. D.; Ward, R. A.; Romea, P.; Lister, M. A. *J. Am. Chem. Soc.* **1994,** *116*, 11287-11314.

12. Stork, G.; Brizzolara, A.; Landesman, H.; Szmuszkovicz, J.; Terrell, R. *J. Am. Chem. Soc.* **1963,** *85*, 207-222.

13. House, H. O.; Liang, W. C.; Weeks, P. D. *J. Org. Chem.* **1974,** *39*, 3102-3107.

14. Ager, D. J.; Prakash, I.; Schaad, D. R. *Aldrichimica Acta* **1997,** *30*, 1-12.

15. Mea-Jacheet, D.; Horeau, A. *Bull. Soc. Chim. Fr.* **1968,** 4571-4575.

16. Yamada, S.; Hiroi, K.; Achiwa, K. *Tetrahedron Lett.* **1969,** *48*, 4233-4236.

17. Hashimoto, S. i.; Koga, K. *Tetrahedron Lett.* **1978,** *19*, 573-576.

18. Meyers, A. I.; Williams, D. R.; Druelinger, M. *J. Am. Chem. Soc.* **1976,** *98*, 3032-3033.

19. Meyers, A. I.; Williams, D. R. *J. Org. Chem.* **1978,** *43*, 3245-3247.

20. Enders, D.; Eichenauer, H. *Tetrahedron Lett.* **1977,** 191-194.

21. Enders, D. In *Asymmetric Synthesis*, 1st ed.; Morrison, J. D., Ed.; Academic Press: Orlando, Fl., 1984; Vol. 3.

22. Enders, D.; Fey, P.; Kipphard, H. *Org. Synth.* **1987,** *65*, 173-182.

23. Enders, D.; Eichenauer, H.; Pieter, R. *Chem. Ber.* **1979,** *112*, 3714.

24. Enders, D.; Kipphardt, H.; Gerdes, P.; Brena-Valle, L. J.; Bhushan, V. *Bull. Soc. Chim. Belg.* **1988,** *97*, 691-704.

25. Martens, J.; Lubben, S. *Liebigs Ann. Chem.* **1990,** *1990*, 949-952.

26. Wilken, J.; Thorey, C.; Groger, H.; Haase, D.; Saak, W.; Pohl, S.; Muzart, J.; Martens, J. *Liebigs Ann. Chem.* **1997,** *1997*, 2133-2146.

27. Enders, D.; Eichenauer, H. *Chem. Ber.* **1979,** *112*, 2933-2960.

28. Enders, D.; Eichenauer, H. *Tetrahedron* **1984,** *40*, 1345-1359.

29. Ahlbrecht, H.; Düber, E. O.; Dieter, E.; Eichenauer, H.; Weuster, P. *Tetrahedron Lett.* **1978,** *19*, 3691-3694.

30. Enders, D.; Bachstiidter, G.; Kremer, K. A. M.; Marsch, M.; Harms, K.; Boche, G. *Angew. Chem. Int. Ed. Engl.* **1988,** *27*, 1522-1524.

31. Andersen, M. W.; Hildebrandt, B.; Hoffmann, R. W. *Angew. Chem. Int. Ed. Engl.* **1991,** *103*, 90-92.

32. Enders, D.; Gatzweiler, W.; Jegelka, U. *Synthesis* **1991,** 1137-1141.

33. Nicolaou, K. C.; Ninkovic, S.; Sarabia, F.; Vourloumis, D.; He, Y.; Vallberg, H.; Finlay, M. R. V.; Yang, Z. *J. Am. Chem. Soc.* **1997,** *119*, 7974-7991.

34. Nicolaou, K. C.; Sarabia, F.; Ninkovic, S.; Finlay, M. R.; Boddy, C. N. C. *Angew. Chem. Int. Ed.* **1998,** *37*, 81-84.

35. Lim, D.; Coltart, D. M. *Angew. Chem. Int. Ed.* **2008,** *47*, 5207-5210.

36. Wengryniuk, S. E.; Lim, D.; Coltart, D. M. *J. Am. Chem. Soc.* **2011,** *133*, 8714-8720.

37. Krenske, E. H.; Houk, K. N.; Lim, D.; Wengryniuk, S. E.; Coltart, D. M. *J. Org. Chem.* **2010,** *75*, 8578-8584.

38. Garnsey, M. R.; Lim, D.; Yost, J. M.; Coltart, D. M. *Org. Lett.* **2010,** *12*, 5234-5237.

39. O'Brien, P. *J. Chem. Soc. Perkin Trans. 1* **1998,** 1439-1458.

40. Shirai, R.; Tanaka, M.; Koga, K. *J. Am. Chem. Soc.* **1986,** *108*, 543-545.

41. Simpkins, N. S. *J. Chem. Soc. Chem. Comm.* **1986,** 88-90.

42. Cain, C. M.; Cousins, R. P. C.; Coumbarides, G.; Simpkins, N. S. *Tetrahedron* **1990,** *46*, 523-544.

43. Cain, C. M.; Simpkins, N. S. *Tetrahedron Lett.* **1987,** *28*, 3723-3724.

44. Corey, E. J.; Gross, A. W. *Tetrahedron Lett.* **1984,** *25*, 495-498.

45. Kim, H.; Shirai, R.; Kawasaki, H.; Nakajima, M.; Koga, K. *Heterocycles* **1990,** *30*, 307-310.

46. Shirai, R.; Sato, D.; Aoki, K.; Tanaka, M.; Kawasaki, H.; Koga, K. *Tetrahedron* **1997,** *53*, 5963-5972.

47. Bunn, B. J.; Simpkins, N. S. *J. Org. Chem.* **1993,** *58*, 533-534.

48. Lipshutz, B. H.; Wood, M. R.; Lindsley, C. W. *Tetrahedron Lett.* **1995,** *36*, 4385-4388.

49. Majewski, M.; Lazny, R.; Nowak, P. *Tetrahedron Lett.* **1995,** *36*, 5465-5468.

50. Majewski, M.; Gleave, D. M.; Nowak, P. *Can. J. Chem.* **1995,** *73*, 1616-1626.

51. Sugasawa, K.; Shindo, M.; Noguchi, H.; Koga, K. *Tetrahedron Lett.* **1996,** *37*, 7377-7380.

52. Yamashita, T.; Sato, D.; Kiyoto, T.; Kumar, A.; Koga, K. *Tetrahedron Lett.* **1996,** *37*, 8195-8198.

53. Imai, M.; Hagihara, A.; Kawasaki, H.; Manabe, K.; Koga, K. *J. Am. Chem. Soc.* **1994,** *116*, 8829-8830.

54. Trost, B. M.; Lee, C.; In *Catalytic Asymmetric Catalysis;* Ojima, I. 2nd ed.; John Wiley & Sons, Inc.: New York, 2000.pp. 593-649.

55. Tsuji, J.; Takahashi, H.; Morikawa, M. *Tetrahedron Lett.* **1965,** *6*, 4387-4388.

56. Trost, B. M.; Fullerton, T. J. *J. Am. Chem. Soc.* **1973,** *95*, 292-294.

57. Trost, B. M.; Strege, P. E. *J. Am. Chem. Soc.* **1977,** *99*, 1649-1651.

58. Trost, B. M.; Schroeder, G. M. *J. Am. Chem. Soc.* **1999,** *121*, 6759-6760.

59. Behenna, D. C.; Stoltz, B. M. *J. Am. Chem. Soc.* **2004,** *126*, 15044-15045.

60. Trost, B. M.; Xu, J. *J. Am. Chem. Soc.* **2005,** *127*, 17180-17181.

61. Doyle, A. G.; Jacobsen, E. N. *J. Am. Chem. Soc.* **2004,** *127*, 62-63.

62. Dolling, U. H.; Davis, P.; Grabowski, E. J. J. *J. Am. Chem. Soc.* **1984,** *106*, 446-447.

63. Mastracchio, A.; Warkentin, A. A.; Walji, A. M.; MacMillan, D. W. C. *Proc. Natl. Acad. Sci. U. S. A* **2010,** *107*, 20648-20651.

64. Lazny, R.; Nodzewska, A. *Chem. Rev.* **2009,** *110*, 1386-1434.

65. Corey, E. J.; Enders, D. *Tetrahedron Lett.* **1976,** *17*, 3-6.

66. Corey, E. J.; Enders, D. *Chem. Ber.* **1978,** *111*, 1337-1361.

67. Bergbreiter, D. E.; Newcomb, M. *Tetrahedron Lett.* **1979,** *20*, 4145-4148.

68. Ludwig, J. W.; Newcomb, M.; Bergbreiter, D. E. *J. Org. Chem.* **1980,** *45*, 4666-4669.

69. Collum, D. B.; Kahne, D.; Gut, S. A.; DePue, R. T.; Mohamadi, F.; Wanat, R. A.; Clardy, J.; Van Duyne, G. *J. Am. Chem. Soc.* **1984,** *106*, 4865-4869.

70. Galiano-Roth, A. S.; Collum, D. B. *J. Am. Chem. Soc.* **1989,** *111*, 6772-6778.

71. Davenport, K. G.; Eichenauer, H.; Enders, D.; Newcomb, M.; Bergbreiter, D. E. *J. Am. Chem. Soc.* **1979,** *101*, 5654-5659.

72. Trost, B. M.; Fleming, I. In *Comprehensive Organic Synthesis*, Bergbreiter, D. E., Momongan, M., Eds.; Pergamon Press: Oxford, U.K., 1991; Vol. 2.

73. Corey, E. J.; Knapp, S. *Tetrahedron Lett.* **1976,** *17*, 3667-3668.

74. Corey, E. J.; Enders, D. *Tetrahedron Lett.* **1976,** *17*, 11-14.

75. Corey, E. J.; Enders, D.; Bock, M. G. *Tetrahedron Lett.* **1976,** *17*, 7-10.

76. Corey, E. J.; Knapp, S. *Tetrahedron Lett.* **1976,** *17*, 4687-4690.

77. Enders, D.; Weuster, P. *Tetrahedron Lett.* **1978,** *19*, 2853-2856.

78. Whitesell, J. K.; Whitesell, M. A. *Synthesis* **1983,** *1983*, 517-536.

79. Gawley, R. E.; Termine, E. J.; Aube, J. *Tetrahedron Lett.* **1980,** *21*, 3115-3118.

80. Enders, D.; Dyker, H.; Raabe, G.; Runsink, J. *Synlett* **1992,** *11*, 901-903.

81. The Nobel Prize in Chemistry 2001: Nobelprize.org. http://www.nobelprize.org/nobel_prizes/chemistry/laureates/2001/ (28-7-2014).

82. Knowles, W. S. *Acc. Chem. Res.* **1983,** *16*, 106-112.

83. Dang, T. P.; Kagan, H. B. *J. Chem. Soc. D* **1971,** 481.

84. Pfaltz, A.; Drury, W. J. *Proc. Natl. Acad. Sci. U. S. A* **2004,** *101*, 5723-5726.

85. Kizirian, J. C. *Chem. Rev.* **2008,** *108*, 140-205.

86. Stenhouse, J. *Annalen* **1851,** *78*, 1-30.

87. Orechoff, A.; Rabinowitch, M.; Kolowanowa, R. *Ber. Dtsch. Chem. Ges.* **1933,** *66*, 625.

88. Hoppe, D.; Hense, T. *Angew. Chem. Int. Ed. Engl.* **1997,** *36*, 2282-2316.

89. Marr, F.; Frohlich, R.; Hoppe, P. *Tetrahedron: Asymmetry* **2002,** *13*, 2587-2592.

90. Okamato, Y. *J. Polym. Sci. Part A: Polym. Chem.* **2004,** *42*, 4480–4491.

91. Tsuji, K.; Wagner, P.; Davis, M. E. *Microporous Mesoporous Mater.* **1991,** *28*, 461–469.

92. Denmark, S. E.; Nakajima, N.; Nicaise, O. J. C. *J. Am. Chem. Soc.* **1994,** *116*, 8797-8788.

93. McGrath, M. J.; Bilke, J. L.; O'Brien, P. *Chem. Commun.* **2006,** 2607–2609.

94. Mueller, J. A.; Jensen, D. R.; Sigman, M. S. *J. Am. Chem. Soc.* **2002,** *124*, 8202-8203.

95. Dearden, M. J.; Firkin, C. R.; Hermet, J. P.; O'Brien, P. *J. Am. Chem. Soc.* **2002,** *124*, 11870-11871.

96. Dearden, M. J.; McGrath, M. J.; O'Brien, P. *J. Org. Chem.* **2004,** *69*, 5789-5792.

97. Stead, D.; O'Brien, P.; Sanderson, A. *Org. Lett.* **2008,** *10*, 1409-1412.

98. Kizirian, J. C.; Cabello, N.; Pinchard, L.; Caille, J. C.; Alexakis, A. *Tetrahedron* **2005,** *61*, 8939-8946.

99. Kizirian, J. C.; Caille, J. C.; Alexakis, A. *Tetrahedron Lett.* **2003,** *44*, 8893-8895.

100. McGrath, M. J.; O'Brien, P. *J. Am. Chem. Soc.* **2005,** *127*, 16378-16379.

101. Zhou, P.; Chen, B. C.; Davis, F. A. *Tetrahedron* **2004,** *60*, 8003-8030.

102. Morton, D.; Stockman, R. A. *Tetrahedron* **2006,** *62*, 8869-8905.

103. Davis, F. A.; Friedman, A. J.; Kluger, E. W. *J. Am. Chem. Soc.* **1974,** *96*, 5000-5001.

104. Davis, F. A.; Zhou, P.; Chen, B. C. *Chem. Soc. Rev.* **1998,** *27*, 13-18.

105. Ellman, J. A.; Owens, T. D.; Tang, T. P. *Acc. Chem. Res.* **2002,** *35*, 984-995.

106. Cogan, D. A.; Ellman, J. A. *J. Am. Chem. Soc.* **1998,** *121*, 268-269.

107. Zhong, Y. W.; Dong, Y. Z.; Fang, K.; Izumi, K.; Xu, M. H.; Lin, G. Q. *J. Am. Chem. Soc.* **2005,** *127*, 11956-11957.

108. Evans, J. W.; Ellman, J. A. *J. Org. Chem.* **2003,** *68*, 9948-9957.

109. Barrow, J. C.; Ngo, P. L.; Pellicore, J. M.; Selnick, H. G.; Nantermet, P. G. *Tetrahedron Lett.* **2001,** *42*, 2051-2054.

110. Kochi, T.; Tang, T. P.; Ellman, J. A. *J. Am. Chem. Soc.* **2003,** *125*, 11276-11282.

111. Kochi, T.; Tang, T. P.; Ellman, J. A. *J. Am. Chem. Soc.* **2002,** *124*, 6518-6519.

112. Jacobsen, M. F.; Skrydstrup, T. *J. Org. Chem.* **2003,** *68*, 7112-7114.

113. Tang, T. P.; Ellman, J. A. *J. Org. Chem.* **2002,** *67*, 7819-7832.

114. Tang, T. P.; Ellman, J. A. *J. Org. Chem.* **1999,** *64*, 12-13.

115. Cogan, D. A.; Liu, G.; Ellman, J. *Tetrahedron* **1999,** *55*, 8883-8904.

116. Avenoza, A.; Busto, J. s. H.; Corzana, F.; Peregrina, J. s. M.; Sucunza, D.; Zurbano, M. a. M. *Synthesis* **2005,** *2005*, 575-578.

117. Naskar, D.; Roy, A.; Seibel, W. L.; Portlock, D. E. *Tetrahedron Lett.* **2003,** *44*, 8865-8868.

118. Shibahara, S.; Kondo, S.; Maeda, K.; Umezawa, H.; Ohno, M. *J. Am. Chem. Soc.* **1972,** *94*, 4353-4354.

119. Kozikowski, A. P.; Chen, Y. Y. *J. Org. Chem.* **1981,** *46*, 5248-5250.

120. Wang, Y. F.; Izawa, T.; Kobayashi, S.; Ohno, M. *J. Am. Chem. Soc.* **1982,** *104*, 6465-6466.

121. Hashiguchi, S.; Kawada, A.; Natsugari, H. *J. Chem. Soc. Perkin Trans. 1* **1991,** 2435-2444.

122. Knapp, S. *Chem. Rev.* **1995,** *95*, 1859-1876.

123. Sakai, R.; Kamiya, H.; Murata, M.; Shimamoto, K. *J. Am. Chem. Soc.* **1997,** *119*, 4112-4116.

124. Kempf, D. J.; Marsh, K. C.; Denissen, J. F.; McDonald, E.; Vasavanonda, S.; Flentge, C. A.; Green, B. E.; Fino, L.; Park, C. H.; Kong, X. P. *Proc. Natl. Acad. Sci. U. S. A* **1995,** *92*, 2484-2488.

125. Sham, H. L.; Zhao, C.; Li, L.; Betebenner, D. A.; Saldivar, A.; Vasavanonda, S.; Kempf, D. J.; Plattner, J. J.; Norbeck, D. W. *Bioorg. Med. Chem.* **2002,** *12*, 3101-3103.

126. Haight, A. R.; Stuk, T. L.; Allen, M. S.; Bhagavatula, L.; Fitzgerald, M.; Hannick, S. M.; Kerdesky, F. A. J.; Menzia, J. A.; Parekh, S. I.; Robbins, T. A.; Scarpetti, D.; Tien, J. H. *Org. Process Res. Dev.* **1999,** *3*, 94-100.

127. Shi, Z.; Harrison, B. A.; Verdine, G. L. *Org. Lett.* **2003,** *5*, 633-636.

128. Kondo, S.; Shibahara, S.; Takahashi, S.; Maeda, K.; Umezawa, H.; Ohno, M. *J. Am. Chem. Soc.* **1971,** *93*, 6305-6306.

129. Raju, B.; Mortell, K.; Anandan, S.; O'Dowd, H.; Gao, H.; Gomez, M.; Hackbarth, C.; Wu, C.; Wang, W.; Yuan, Z.; White, R.; Trias, J.; Patel, D. V. *Bioorg. Med. Chem. Lett.* **2003,** *13*, 2413-2418.

130. Naidu, S. V.; Kumar, P. *Tetrahedron Lett.* **2007,** *48*, 3793-3796.

131. Carlier, P. R.; Lo, M. M.; Lo, P. C.; Richelson, E.; Tatsumi, M.; Reynolds, I. J.; Sharma, T. A. *Bioorg. Med. Chem. Lett.* **1998,** *8*, 487-492.

132. Wang, X. B.; Kodama, K.; Hirose, T.; Yang, X. F.; Zhang, G. Y. *Tetrahedron: Asymmetry* **2010,** *21*, 75-80.

133. Geng, H.; Zhang, W.; Chen, J.; Hou, G.; Zhou, L.; Zou, Y.; Wu, W.; Zhang, X. *Angew. Chem. Int. Ed.* **2009,** *48*, 6052-6054.

134. Davis, F. A.; Gaspari, P. M.; Nolt, B. M.; Xu, P. *J. Org. Chem.* **2008,** *73*, 9619-9626.

135. Menche, D.; Arikan, F.; Li, J.; Rudolph, S. *Org. Lett.* **2007,** *9*, 267-270.

136. Keck, G. E.; Truong, A. P. *Org. Lett.* **2002,** *4*, 3131-3134.

137. Vilaplana, M. J.; Molina, P.; Arques, A.; Andrés, C.; Pedrosa, R. *Tetrahedron: Asymmetry* **2002,** *13*, 5-8.

138. Panev, S.; Linden, A.; Dimitrov, V. *Tetrahedron: Asymmetry* **2001,** *12*, 1313-1321.

139. Andrés, C.; Duque-Soladana, J. P.; Iglesias, J. M.; Pedrosa, R. *Tetrahedron Lett.* **1996,** *37*, 9085-9086.

140. Rice, G. T.; White, M. C. *J. Am. Chem. Soc.* **2009,** *131*, 11707-11711.

141. Lait, S. M.; Rankic, D. A.; Keay, B. A. *Chem. Rev.* **2007,** *107*, 767-796.

142. Yao, C. Z.; Xiao, Z. F.; Ning, X. S.; Liu, J.; Zhang, X. W.; Kang, Y. B. *Org. Lett.* **2014,** *16*, 5824-5826.

143. Sole, C.; Whiting, A.; Gulyas, H.; Fernandez, E. *Adv. Synth. Catal.* **2011,** *353*, 376-384.

144. Liu, G.; Cogan, D. A.; Ellman, J. A. *J. Am. Chem. Soc.* **1997,** *119*, 9913-9914.

145. Geissman, T. A. The Cannizzaro Reaction. In *Organic Reactions*, John Wiley & Sons, Inc.: New York, 2004.

146. Claisen, L. *Chem. Ber.* **1887,** *20*, 646-650.

147. Tishchenko, W. *J. Russ. Phys. Chem. Soc.* **1906,** *38*, 355.

148. Evans, D. A.; Hoveyda, A. H. *J. Am. Chem. Soc.* **1990,** *112*, 6447-6449.

149. Baramee, A.; Chaichit, N.; Intawee, P.; Thebtaranonth, C.; Thebtaranonth, Y. *J. Chem. Soc. , Chem. Commun.* **1991,** 1016-1017.

150. Caron, S.; Stoermer, D.; Mapp, A. K.; Heathcock, C. H. *J. Org. Chem.* **1996,** *61*, 9126-9134.

151. Mahrwald, R.; Costisella, B. *Synthesis* **1996,** 1087-1089.

152. Bodnar, P. M.; Shaw, J. T.; Woerpel, K. A. *J. Org. Chem.* **1997,** *62*, 5674-5675.

153. Rychnovsky, S. D.; Rogers, B.; Yang, G. *J. Org. Chem.* **1993,** *58*, 3511-3515.

154. Evans, D. A.; Rieger, D. L.; Gage, J. R. *Tetrahedron Lett.* **1990,** *31*, 7099-7100.

155. Heathcock, C. H.; Buse, C. T.; Kleschick, W. A.; Pirrung, M. C.; Sohn, J. E.; Lampe, J. *J. Org. Chem.* **1980,** *45*, 1066-1081.

156. Shindo, M.; Koga, K.; Tomioka, K. *J. Org. Chem.* **1998,** *63*, 9351-9357.

157. Mascarenhas, C. M.; Miller, S. P.; White, P. S.; Morken, J. P. *Angew. Chem. Int. Ed.* **2001,** *40*, 601-603.

158. Mlynarski, J.; Mitura, M. *Tetrahedron Lett.* **2004,** *45*, 7549-7552.

159. Gnanadesikan, V.; Horiuchi, Y.; Ohshima, T.; Shibasaki, M. *J. Am. Chem. Soc.* **2004,** *126*, 7782-7783.

160. Paterson, I.; Hulme, A. N. *J. Org. Chem.* **1995,** *60*, 3288-3300.

161. Molander, G. A.; Losada, C. D. *J. Org. Chem.* **1997,** *62*, 2935-2943.

162. Amedjkouh, M.; Ahlberg, P. *Tetrahedron: Asymmetry* **2002,** *13*, 2229-2234.

163. Lazny, R.; Nodzewska, A.; Zabicka, B. *J. Comb. Chem.* **2008,** *10*, 986-991.

164. Curtin, D. Y.; Kampmeier, J. A.; Farmer, M. L. *J. Am. Chem. Soc* **1965,** *87*, 874-882.

165. Clarke, S. L.; McSweeney, C. M.; McGlacken, G. P. *Tetrahedron: Asymmetry* **2014,** *25*, 356-361.

166. Richter, P. K.; Tomaszewski, M. J.; Miller, R. A.; Patron, A. P.; Nicolaou, K. C. *J. Chem. Soc. , Chem. Commun.* **1994,** 1151-1152.

167. Nicolaou, K. C.; Patron, A. P.; Ajito, K.; Richter, P. K.; Khatuya, H.; Bertinato, P.; Miller, R. A.; Tomaszewski, M. J. *Chem. Eur. J.* **1996,** *2*, 847-868.

168. Murakata, M.; Nakajima, M.; Koga, K. *J. Chem. Soc. , Chem. Commun.* **1990,** 1657-1658.

169. Imai, M.; Hagihara, A.; Kawasaki, H.; Manabe, K.; Koga, K. *Tetrahedron* **2000,** *56*, 179-185.

170. Stivala, C. E.; Zakarian, A. *J. Am. Chem. Soc.* **2011,** *133*, 11936-11939.

171. Trost, B. M.; Xu, J. *J. Am. Chem. Soc.* **2005,** *127*, 2846-2847.

172. Behenna, D. C.; Mohr, J. T.; Sherden, N. H.; Marinescu, S. C.; Harned, A. M.; Tani, K.; Seto, M.; Ma, S.; Novak, Z.; Krout, M. R.; McFadden, R. M.; Roizen, J. L.; Enquist, J. A.; White, D. E.; Levine, S. R.; Petrova, K. V.; Iwashita, A.; Virgil, S. C.; Stoltz, B. M. *Chem. Eur. J.* **2011,** *17*, 14199-14223.

173. Surendra, K.; Corey, E. J. *J. Am. Chem. Soc.* **2008,** *130*, 8865-8869.

174. Deiters, A.; Hoppe, D. *J. Org. Chem.* **2001,** *66*, 2842-2849.

175. Beak, P.; Du, H. *J. Am. Chem. Soc.* **1993,** *115*, 2516-2518.

176. Gross, K. M. B.; Jun, Y. M.; Beak, P. *J. Org. Chem.* **1997,** *62*, 7679-7689.

177. Wu, S.; Lee, S.; Beak, P. *J. Am. Chem. Soc.* **1996,** *118*, 715-721.

178. Hoppe, D.; Hintze, F.; Tebben, P. *Angew. Chem. Int. Ed. Engl.* **1990,** *29*, 1422-1424.

179. Stead, D.; Carbone, G.; O'Brien, P.; Campos, K. R.; Coldham, I.; Sanderson, A. *J. Am. Chem. Soc.* **2010,** *132*, 7260-7261.

180. Bilke, J. L.; Moore, S. P.; O'Brien, P.; Gilday, J. *Org. Lett.* **2009,** *11*, 1935-1938.

181. Enders, D.; Ridder, A. *Synthesis* **2000,** *13*, 1848-1851.

182. Shirini, F.; Zolfigol, M. A.; Khaleghi, M.; Mohammadpour-Baltork, I. *Synthetic Communications* **2003,** *33*, 1839-1844.

183. Arseniyadis, S.; Laurent, A.; Mison, P. *Bull. Soc. Chim. de France II* **1980,** 233-245.

184. Mitchell, T. N.; Costisella, B. *NMR - From Spectra to Structures;* 2 nd ed.; Springer Berlin Heidelberg: New York, 2007.

185. Carbone, G.; O'Brien, P.; Hilmersson, G. *J. Am. Chem. Soc.* **2010,** *132*, 15445-15450.

186. Gessner, V. H.; Daschlein, C.; Strohmann, C. *Chem. Eur. J.* **2009,** *15*, 3320-3334.

187. Reich, H. J. *Chem. Rev.* **2013,** *113*, 7130-7178.

188. Jones, A. C.; Sanders, A. W.; Bevan, M. J.; Reich, H. J. *J. Am. Chem. Soc.* **2007,** *129*, 3492-3493.

189. Anet, F. A. L.; Eves, C. R. *Can. J. Chem.* **1958,** *36*, 902-909.

190. Stierle, A. A.; Stierle, D. B.; Kelly, K. *J. Org. Chem.* **2006,** *71*, 5357-5360.

191. Fukui, H.; Yazaki, K.; Tabata, M. *Phytochemistry* **1984,** *23*, 2398-2399.

192. Lu, S. M.; Bolm, C. *Angew. Chem. Int. Ed.* **2008,** *47*, 8920-8923.

193. Bemis, G. W.; Murcko, M. A. *J. Med. Chem.* **1996,** *39*, 2887-2893.

194. Bafana, A. *OA Biotechnology* **2013,** *2*, 18.

195. Wang, J.; Sanchez-Rosello, M.; Acena, J. L.; del Pozo, C.; Sorochinsky, A. E.; Fustero, S.; Soloshonok, V. A.; Hong, L. *Chem. Rev.* **2014,** *114*, 2432-2506.

196. Munoz-Munz, O.; Juaristi, E. *Tetrahedron* **2003,** *59*, 4223-4229.

197. Enders, D.; Dhulut, S.; Steinbusch, D.; Herrbach, A. *Chem. Eur. J.* **2007,** *13*, 3942-3949.

198. Smith, A. B.; Liu, Z.; Simov, V. *Synlett* **2009,** *19*, 3131-3134.

199. Ballini, R.; Petrini, M. *J. Chem. Soc. , Perkin Trans. 1* **1988,** 2563-2565.

200. Reich, H. J. *J. Org. Chem.* **2012,** *77*, 5471-5491.

201. Beak, P.; Basu, A.; Gallagher, D. J.; Park, Y. S.; Thayumanavan, S. *Acc. Chem. Res.* **1996,** *29*, 552-560.

202. Thayumanavan, S.; Basu, A.; Beak, P. *J. Am. Chem. Soc.* **1997,** *119*, 8209-8216.

203. Hirsch, R.; Hoffmann, R. W. *Chem. Ber.* **1992,** *125*, 975-982.

204. Hoffmann, R. W.; Klute, W.; Dress, R. K.; Wenzel, A. *J. Chem. Soc. , Perkin Trans. 2* **1995,** 1721-1726.

205. Hoffmann, R. W.; Klute, W. *Chem. Eur. J.* **1996,** *2*, 694-700.

206. Hoffmann, R. W.; Ruhl, T.; Chemla, F.; Zahneisen, T. *Liebigs Ann. Chem.* **1992,** *1992*, 719-724.

207. DFT-B3CYP-6-31G calculations were carried out by Dr. Virginie Maggiotti in Floride State University. 2007.

208. Desimoni, G.; Faita, G.; Jorgensen, K. A. *Chem. Rev.* **2011,** *111*, 284-437.

209. Whitesell, J. K. *Chem. Rev.* **1989,** *89*, 1581-1590.

210. Rasappan, R.; Laventine, D.; Reiser, O. *Coord. Chem. Rev.* **2008,** *252*, 702-714.

211. Evans, D. A.; Miller, S. J.; Lectka, T.; von Matt, P. *J. Am. Chem. Soc.* **1999,** *121*, 7559-7573.

212. Thorhauge, J.; Roberson, M.; Hazell, R. G.; Jorgensen, K. A. *Chem. Eur. J.* **2002,** *8*, 1888-1898.

213. Evans, D. A.; Peterson, G. S.; Johnson, J. S.; Barnes, D. M.; Campos, K. R.; Woerpel, K. A. *J. Org. Chem.* **1998,** *63*, 4541-4544.

214. Tschantz, M. A.; Burgess, L. E.; Meyers, A. I. *Org. Synth.* **1996,** *73*, 221-225.

215. Cornejo, A.; Fraile, J. M.; Garcia, J. I.; Gil, M. J.; Martinez-Merino, V.; Mayoral, J. A.; Pires, E.; Villalba, I. *Synlett* **2005,** *2005*, 2321-2324.

216. Fraile, J. M.; Garcia, J. I.; Mayoral, J. A.; Roldan, M. *Org. Lett.* **2007,** *9*, 731-733.

217. Tomioka, K.; Shindo, M.; Koga, K. *J. Am. Chem. Soc.* **1989,** *111*, 8266-8268.

218. Oriyama, T.; Mukaiyama, T. *Chem. Lett.* **2015,** 2071-2074.

219. Hayashi, Y.; Tamura, T.; Shoji, M. *Adv. Synth. Catal.* **2004,** *346*, 1106-1110.

220. Kizirian, J. C.; Cabello, N.; Pinchard, L.; Caille, J. C.; Alexakis, A. *Tetrahedron* **2005,** *61*, 8939-8946.

221. Gille, S.; Cabello, N.; Kizirian, J. C.; Alexakis, A. *Tetrahedron: Asymmetry* **2006,** *17*, 1045-1047.

222. Mahrwald, R. *Chem. Rev.* **1999,** *99*, 1095-1120.

223. Nelson, S. G. *Tetrahedron: Asymmetry* **1998,** *9*, 357-389.

224. Csaky, A. G.; Plumet, J. *Chem. Soc. Rev.* **2001,** *30*, 313-320.

225. Mahrwald, R.; Evans, D. A. *Modern Aldol Reactions;* WILEY-VCH Verlag GmbH & Co. KGaA: Weinheim, 2004; Vol. 1 and 2.

226. Sibi, P.; Manyem, S. *Tetrahedron* **2000,** *56*, 8033-8061.

227. Takemoto, Y. *Org. Biomol. Chem.* **2005,** *3*, 4299-4306.

228. Li, H.; Wang, Y.; Tang, L.; Wu, F.; Liu, X.; Guo, C.; Foxman, B. M.; Deng, L. *Angew. Chem. Int. Ed.* **2005,** *44*, 105-108.

229. France, S.; Guerin, D. J.; Miller, S. J.; Lectka, T. *Chem. Rev.* **2003,** *103*, 2985-3012.

230. Evans, D. A.; Seidel, D. *J. Am. Chem. Soc.* **2005,** *127*, 9958-9959.

231. List, B. *Chem. Commun.* **2006,** 819-824.

232. Kochi, T.; Ellman, J. A. *J. Am. Chem. Soc.* **2004,** *126*, 15652-15653.

233. Kochi, T. *Asymmetric Syntheses of Amines Using N-Sulfinyl Metalloenamines*. Unpublished PhD Thesis, University of California, Berkeley, 2004.

234. Streitwieser, A.; Kim, Y. J.; Wang, D. Z. *Org. Lett.* **2001,** *3*, 2599-2601.

235. Davis, F. A.; Prasad, K. R.; Nolt, M. B.; Wu, Y. *Org. Lett.* **2003,** *5*, 925-927.

236. Kennedy, A.; Nelson, A.; Perry, A. *Synlett* **2004,** 967.

237. Huguenot, F.; Brigaud, T. *J. Org. Chem.* **2006,** *71*, 2159-2162.

238. Jha, V.; Kondekar, N. B.; Kumar, P. *Org. Lett.* **2010,** *12*, 2762-2765.

239. McCall, W. S.; Grillo, T. A.; Comins, D. L. *Org. Lett.* **2008,** *10*, 3255-3257.

240. McCall, W. S.; Grillo, T. A.; Comins, D. L. *J. Org. Chem.* **2008,** *73*, 9744-9751.

241. McCall, W. S.; Comins, D. L. *Org. Lett.* **2009,** *11*, 2940-2942.

242. Hunt, K. W.; Grieco, P. A. *Org. Lett.* **2002,** *4*, 245-248.

243. Ramachandran, P. V.; Prabhudas, B.; Chandra, J. S.; Reddy, M. V. R. *J. Org. Chem.* **2004,** *69*, 6294-6304.

244. Yadav, J. S.; Jayasudhan Reddy, Y.; Adi Narayana Reddy, P.; Subba Reddy, B. V. *Org. Lett.* **2013,** *15*, 546-549.

245. Foley, V. M.; McGlacken, G. P. *unpublished work* **2015**.

246. Vicinal Proton-Proton Coupling: Hans J.Reich, University of Wisconsin. http://www.chem.wisc.edu/areas/reich/nmr/05-hmr-05-3j.htm (18-8-2015).

247. Meerwein, H.; Schmidt, R. *Justus Liebigs Ann. Chem.* **1925,** *444*, 221-238.

248. Oppenauer, R. V. *Recl. Trav. Chim. Pays-Bas* **1937,** *56*, 137-144.

249. Mojtahedi, M. M.; Akbarzadeh, E.; Sharifi, R.; Abaee, M. S. *Org. Lett.* **2007,** *9*, 2791-2793.

250. Wuts, P. G. M.; Greene, T. W. Protection for the Hydroxyl Group, Including 1,2- and 1,3-Diols. In *Greene's Protective Groups in Organic Synthesis*, John Wiley & Sons, Inc.: New York, 2006; pp 16-366.

251. Huters, A. D.; Styduhar, E. D.; Garg, N. K. *Angew. Chem. Int. Ed.* **2012,** *51*, 3758-3765.

252. Fernandez, A. M.; Plaquevent, J. C.; Duhamel, L. *J. Org. Chem.* **1997,** *62*, 4007-4014.

253. Berthiol, F.; Doucet, H.; Santelli, M. *Tetrahedron* **2006,** *62*, 4372-4383.

254. Katritzky, A. R.; Huang, Z.; Fang, Y. *J. Org. Chem.* **1999,** *64*, 7625-7627.

255. Oppolzer, W.; Darcel, C.; Rochet, P.; Rosset, S.; De Brabander, J. *Helv. Chim. Acta.* **1997,** *80*, 1319-1337.

256. Cheon, C. H.; Kanno, O.; Toste, F. D. *J. Am. Chem. Soc.* **2011,** *133*, 13248-13251.

257. Stankovic, S.; Espenson, J. H. *J. Org. Chem.* **2000,** *65*, 2218-2221.

258. Sharma, S. D.; Pandhi, S. B. *J. Org. Chem.* **1990,** *55*, 2196-2200.

259. Crotti, P.; Di Bussolo, V.; Favero, L.; Macchia, F.; Pineschi, M.; Napolitano, E. *Tetrahedron* **1999,** *55*, 5853-5866.

260. Lu, W.-J.; Cheng, Y.-W.; Huang, X.-L. *Angew. Chem. Int. Ed.* **2008,** *47*, 10133-10136.

261. Tschantz, M. A.; Burgess, L. E.; Meyers, A. I. *Org. Synth.* **1998,** *9*, 457-461.

262. Wannaporn, D.; Ishikawa, T. *Mol Divers* **2005,** *9*, 321-331.

263. Kobayashi, S.; Uchiro, H.; Fujishita, Y.; Shiina, I.; Mukaiyama, T. *J. Am. Chem. Soc.* **1991,** *113*, 4247-4252.

264. Portevin, B.; Benoist, A.; Ramond, G.; Herve, Y.; Vincent, M.; Lepagnol, J.; De Nanteuil, G. *J. Med. Chem.* **1996,** *39*, 2379-2391.

265. Jarho, E. M.; Wallen, E. A.; Christiaans, J. A. M.; Forsberg, M. M.; Venäläinen, J. I.; Männistö, P. T.; Gynther, J.; Poso, A. *J. Med. Chem.* **2005,** *48*, 4772-4782.

266. Sigma Aldrich: http://www.sigmaaldrich.com/catalog/product/aldrich/416940?lang=en&region=IE. (5-8-2011).

267. Mahrwald, R.; Schetter, B. *Org. Lett.* **2006,** *8*, 281-284.

268. Xue, F.; Zhang, S.; Duan, W.; Wang, W. *Adv. Synth. Catal.* **2008,** *350*, 2194-2198.

269. Sirvent, J. A.; Foubelo, F.; Yus, M. *Chem. Commun.* **2012,** *48*, 2543-2545.

270. Carroll, W. A.; Meyer, M. D.; Wang, X.; Patel, M. V.; Dart, M. J.; Kolasa, T. Novel Compunds as Cannabinoid Receptor Ligand. USA Patent WO2008/63781 A2, May 29, 2008.

Appendix 1

Structure-function Analysis of the C-3 position in Analogues of Microbial Behavioural Modulator, HHQ

1.1 Introduction

1.1.1 Background

Currently, we are confronted with a worrying situation with respect to the lack of effective therapies against antibiotic-resistant bacterial infections. This predicament is attributed to the mode of action of marketed antibiotics, which is based on interference with bacterial growth. This therapeutic treatment inevitably results in the development of resistant strains.[1]

A promising strategy to overcome the growing and challenging resistance problem is to selectively target non-vital functions that are associated with the pathogenicity of a bacteria, such as the production of virulence factors.[2-5] The human opportunistic pathogen *Pseudomonas aeruginosa* is a Gram-negative bacterium and opportunistic pathogen that causes diseases in patients with impaired host defences and is often responsible for life-threatening nosocomial infections among immunocompromised individuals.[6,7] It is also the main morbidity- and mortality-causing agent in people suffering from cystic fibrosis. Aside from an extensive inflammatory response that is dominated by polymorphonuclear neutrophils,[8] virulence factors play a critical role in progressive lung deterioration during infection. Their production is controlled by a cell density-dependent extraordinary cell-to-cell communication system, which is known as quorum sensing.[9,10] Quorum sensing in *P. aeruginosa* is controlled by small organic molecules. With a focus on developing anti-infectives with novel modes of action, recent publications highlight quorum sensing inhibitors (QSIs) as potential powerful agents for anti-virulence therapy.[11-14]

P. aeruginosa uses quorum sensing to modulate gene expression in phenotypes such as swarming motility and the production of an arsenal of extracellular virulence factors that are capable of causing extensive tissue damage, bloodstream invasion, and consequently the promotion of systemic dissemination.[15] A key phenotype modulated by *P. aeruginosa* involves the formation of a protective biofilm which play a key role in its defence against antibiotics. Quorum sensing allows bacteria to regulate the gene expression of a large array of target genes in a cell population density-dependent manner via the exchange of small signalling molecules referred to as an autoinducers.[16,17]

There are two classes of quorum-sensing molecules produced by *P. aeruginosa*, the *N*-acylhomoserine lactone family including *N*-(3-oxo-dodecanoyl)-l-homoserine lactone **1** and *N*-butanoyl-homoserine lactone **2** (C_4-HSL) and the 2-alkylquinolones, including 2-heptyl-4-

quinolone **3** (HHQ) and the corresponding dihydroxylated derivative, 2-heptyl-3-hydroxy-4-quinolone or as it is better known *Pseudomonas* quinolone signal **4** (PQS) (Figure 1.1.1).[18-20]

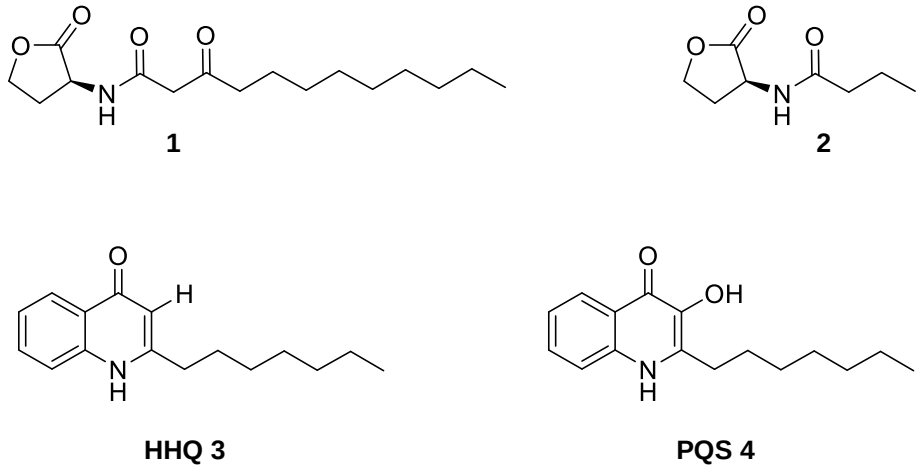

Figure 1.1.1

Acyl-homoserine lactone signalling can occur in vivo in the mouse lung, and acyl-homoserine lactone signals are produced by *P. aeruginosa* growing *ex vivo* within sputum samples from infected cystic fibrosis patients.[21] PQS-mediated cell-to-cell signalling occurs within the infected cystic fibrosis lung and therefore PQS has been recognised as a unique drug target for the development of new therapies for treating *P. aeruginosa* infections.[22]

1.1.2 The Biosynthesis of PQS

Studies on the biosynthesis of 4-quinolones have shown that they are derived from the condensation of anthranilic acid **5** and a β-keto-fatty acid **6**. Because PQS has a similar 4-quinolone base structure, it was predicted to have a similar metabolic route (Scheme 1.1.1). Calfee et al. confirmed that anthranilate was a precursor for PQS and also showed that an anthranilate analogue, methyl anthranilate, competes with anthranilate in this process, thereby decreasing the production of PQS.[23] Cells grown in the presence of methyl anthranilate were shown to have reduced elastase activity (a key feature of biofilm formation), suggesting that interfering with the PQS biosynthetic pathway may be a potential target to reduce the virulence of *P. aeruginosa*.[23] The primary metabolite anthranilate was shown to undergo a head-to-head condensation with β-keto-decanoic or β-keto-dodecanoic acid involving the release of the carboxylate of the fatty acid as CO_2 (Scheme 1.1.1) This study also verified this mechanism for the synthesis of PQS using labelling studies, since it showed that C-4 of PQS derives from anthranilic acid **5** and C-2 derives from the acetate **6**.[24]

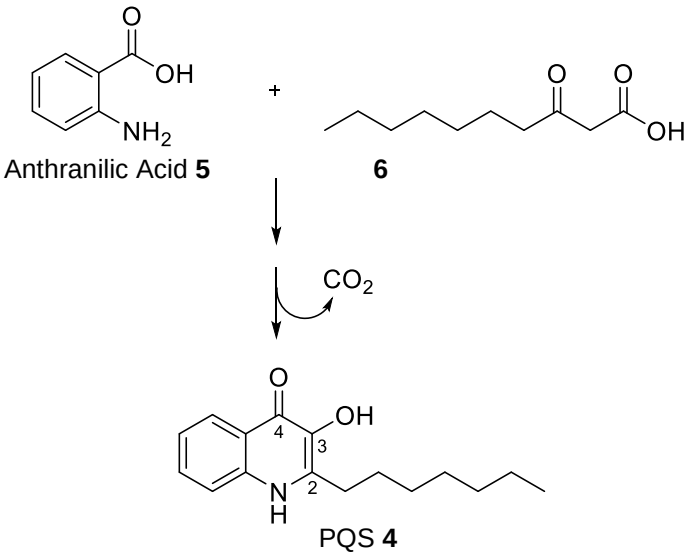

Scheme 1.1.1

In *P. aeruginosa*, anthranilate is synthesised by either the conversion of chorismate **7** via one of the two anthranilate synthases TrpEG and PhnAB, or by the breakdown of tryptophan **8** through the kynurenine pathway. The kynurenine pathway and the secondary anthranilate synthase PhnAB have been shown to provide anthranilate for the production of PQS (Scheme 1.1.2).[25]

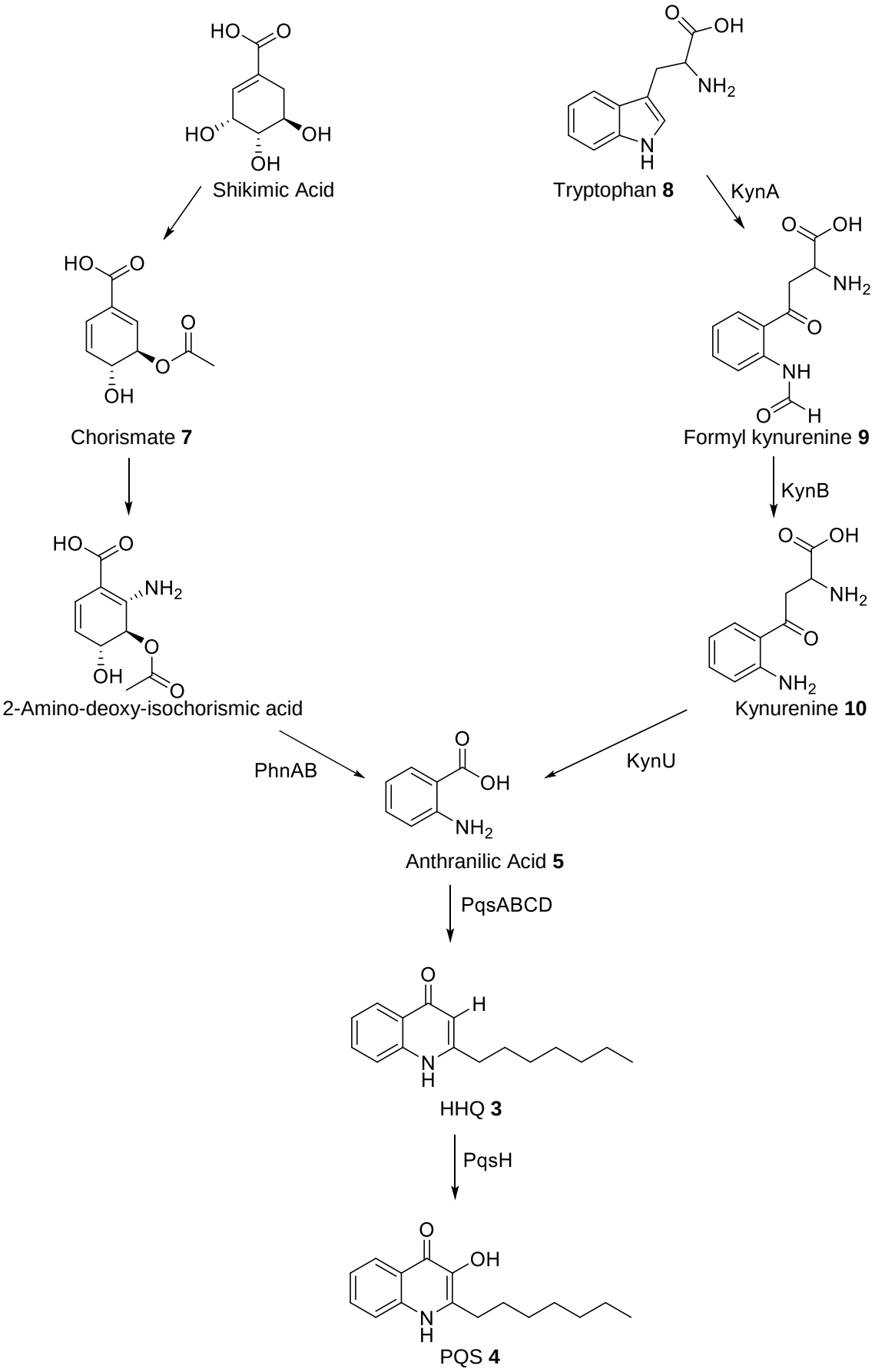
Shikimic Acid
Tryptophan **8**
KynA
Chorismate **7**
Formyl kynurenine **9**
KynB
2-Amino-deoxy-isochorismic acid
Kynurenine **10**
PhnAB
KynU
Anthranilic Acid **5**
PqsABCD
HHQ **3**
PqsH
PQS **4**

Scheme 1.1.2

In the kynurenine pathway, three genes (*kyn*A, *kyn*B and *kyn*U) of the anthranilate branch are responsible for converting tryptophan **8** to anthranilate, and these are present in *P. aeruginosa*.[26] This proposal was verified since a strain fed with radiolabelled tryptophan **8** produced radiolabelled PQS.[26] Experiments with mutant strains showed that *kyn*A and *kyn*U mutants did not produce PQS and a *kyn*B mutant did produce PQS but at a level which was much lower than wild-type.[26] Interestingly, none of the PQS detected from any of the mutant strains showed any radioactivity, indicating that a major source of the anthranilic acid **5** used in the synthesis of PQS via the kynurenine pathway.[26] The pathway is proposed to function via three enzymes: KynA, (a tryptophan 2,3-dioxygenase) converts tryptophan **8** to formyl kynurenine **9**, which is then converted to kynurenine **10** via KynB (kynurenine formidase), which is in turn converted to anthranilic acid **5** via a kynureninase, KynU.[26]

The fact that there are two separate pathways (Kyn and PhnAB) to anthranilate, which is a precursor to 4-quinolones, highlights the fact that this metabolite is important for the pathogenesis of *P. aeruginosa*.[26] Experiments to determine the relative importance of the two pathways show that in the *kyn* pathway mutants grown in minimal medium, PQS was still produced, however a *phn*A mutant did not produce PQS unless supplemented with anthranilate or *phn*AB genes.[26] In strains grown in rich medium it was determined that the *kyn* pathway was the main source of anthranilate.[26] It was therefore concluded that PhnAB is used to produce PQS when tryptophan **8** is unavailable, but when tryptophan **8** is present, the *kyn* pathway is the major route to anthranilic acid **5**.[26]

It is also interesting that sputum from the lungs of cystic fibrosis patients has been shown to contain a large proportion of amino acids.[27] It is suggested that these amino acids, and particularly aromatic amino acids provide the sole carbon source to support growth of *P. aeruginosa* in cystic fibrosis sputum and contribute to the induction of PQS.[27] In experiments, a *P. aeruginosa* strain grown in minimal medium produced three times more PQS when supplemented with tryptophan **8**.[27] Furthermore the strain produced five times more PQS when grown in cystic fibrosis sputum than when grown in a glucose medium.[27] This implies that the cystic fibrosis lung may provide an amino acid-rich environment which promotes the production of PQS.[26]

1.1.3 Cell-to-Cell Communication

P. aeruginosa's virulence depends on a large number of cell-associated and extracellular factors. Cell-to-cell signalling systems control the expression and allow a coordinated, cell-density-dependent production of many virulence factors.

Cell-to-cell signaling systems enable *P. aeruginosa* to overcome host defense mechanisms. Isolated production of extracellular virulence factors by a small number of bacteria lead to an efficient host response neutralizing these compounds. However, the coordinated expression of virulence genes by an entire bacterial population allow *P. aeruginosa* to secrete extracellular factors but only when they can be produced at high enough levels to overcome host defenses. These factors alter the precarious balance between host defenses and production of bacterial toxins, leading to invasion of blood vessels, dissemination, systemic inflammatory-response syndrome, and finally death. Even appropriate antibiotic therapies are often unable to stop this course; therefore, the process must be blocked early.[28]

The pathogenesis of *P. aeruginosa* is clearly multifactorial as underlined by the large number of virulence factors and the broad spectrum of diseases the bacterium causes. Many of the extracellular virulence factors required for tissue invasion and dissemination are controlled by cell-to-cell signaling systems involving homoserine lactone-based signal molecules and specific transcriptional activator proteins.[29-32] These regulatory systems enable *P. aeruginosa* to produce virulence factors in a coordinated, cell-density-dependent manner that could allow the bacteria to overwhelm the host defense mechanisms. Interference with cell-to-cell signaling dependent virulence factor production is a promising therapeutic approach for reducing illness and death associated with *P. aeruginosa* colonization and infection. The growing number of human pathogens found to contain cell-to-cell signaling systems highlights the importance of exploring interference with bacterial cell-to-cell signaling for new therapeutic interventions.[28]

1.1.4 Biological Functions and Applications

The quinolone PQS has a vast and varied array of biological functions, influencing iron homeostasis,[20,33] vesicle formation,[34] secondary metabolite production and biofilm formation.[35] *P. aeruginosa* PQS signalling is highly responsive to environmental and host-specific cues, including Mg^{2+} concentration and the cystic fibrosis therapeutic colistin.[36] Recent evidence has revealed that PQS is capable of modulating immune responses and human T-cell proliferation.[37,38] However, relatively little is known about their role within a host.[39]

P. aeruginosa infects the airways of almost 100% of cystic fibrosis patients. These patients have a defective immune system which is unable to clear the bacteria, leading to chronic lung infections which are notoriously difficult to treat, due to the development of resistance to antimicrobial therapy.[36] PQS production is altered in the lungs of the cystic fibrosis patient.[36] It has been demonstrated that PQS levels produced are 7 to 15 fold higher in cystic fibrosis patients aged 24-36 months than in a laboratory strain.[36] However in older patients there is a significant reduction in PQS production.[36] This suggests that PQS production varies during adaptation to the environment of the cystic fibrosis lung and therefore may be a target to exploit in attempts to alter early colonization.[36]

In the environment of the cystic fibrosis lung, *P. aeruginosa* forms a biofilm which protects the bacteria from attack from the host immune system and antibacterial agents, therefore rendering these infections very difficult to treat.[40] Bacterial biofilms are organised groups of cells existing in a polymer matrix which is generally self-produced and adhered to an inert or living surface. Extracellular DNA, polysaccharides and proteins can all function as components of the biofilm matrix. PQS has been indicated as being important in the formation of biofilms.[35] Growth of a *P. aeruginosa* biofilm on a stainless-steel coupon was increased on addition of PQS.[35] The molecular mechanism for this is not fully defined, however it was observed that lectin, which is under the control of PQS, may be involved, since *lec*A mutants formed poor biofilms[35] and further observations suggest that lectin plays a role in the maturation of biofilms.

The virulence of *P. aeruginosa* is also likely to be affected by the amount of PQS produced, since many virulence factors including elastase, rhamnolipids, the galactophilic lectin, LecA and pyocyanin are regulated by PQS. Gallagher et al. showed that *P. aeruginosa* strains which were unable to produce PQS had a reduced ability to kill nematodes, a group of cylindrically shaped worms.[41] Modern 4-quinolone antibiotics target DNA gyrase of bacteria, but this is often naturally mutated, especially in *P. aeruginosa*, to give resistant strains.[42] In spite of the growth

of these resistant strains, some 4-quinolones are shown to have an inhibitory effect, possibly because the quinolone reduces the synthesis of various virulence factors controlled by quorum sensing.

There is increasing evidence to suggest that environmental factors other than cell density play a role in signalling via quorum sensing systems.[39] Addition of exogenous PQS to *P. aeruginosa* depletes free iron from the growth medium, and probably functions as an iron trap, taking in iron from the growth medium and retaining it in association with the bacterial cell surface.[20] In this way PQS may promote trapping and storing of iron for future use, since iron is an essential nutrient for *P. aeruginosa*.[20,39] In addition, by using up available sources of iron, it may also starve competing bacterial species of free iron, promoting its chances of survival.[39]

1.2 Results and Discussion

1.2.1 Introduction

The anti-virulence therapy using QS inhibitors (QSIs) selectively intervening with pathogenicity, e.g. by repressing the production of virulence factors, without impairing bacterial viability has been proposed as an alternative approach to conventional anti-bacterial therapy. It is supposed that in this anti-virulence therapy the selection pressure is reduced. This treatment option is therefore regarded as a promising strategy to overcome the rising and challenging resistance problem. This approach is not bactericidal therefore resistance is not a problem.[23] PQS and HHQ have emerged as key regulators of bacterial cooperative behaviour in the antibiotic resistant human pathogen *P. aeruginosa* (as discussed in section 1.1) and would therefore become the targets of our investigations.

Our objective during this research project was twofold: Firstly, to synthesise 3-haloquinolin-4-ones as analogues of PQS. These substrates would facilitate mechanistic studies into PQS signalling in virulent *Pseudomonas* populations with important clinical applications. We would hope to interrupt PQS biosynthesis by inhibiting conversion of HHQ to PQS, and in turn disrupt the production of virulence factors of *P. aeruginosa* using C-3 analogues by functionalising the C-3 position. With these analogues hydrogen bonding would also not be possible, however an electron-withdrawing group would still be present, and the impact of this would be investigated.

Secondly, we wanted to explore if a new *N*-methyl version could be used in palladium cross-coupling reactions, thus providing access to an array of new biologically important quinolones. Importantly, the 2-heptyl chain is essential for certain biological functions such as the stimulation of outer vesicle formation in *P. aeruginosa* and thus synthetic procedures on compounds bearing this bulky and hydrophobic substituent are important. There are no reports of halogenation or subsequent cross-coupling of HHQ at the C-3 position. From a synthetic viewpoint, the presence of the long hydrophobic chain represents a challenge due to low solubility and the obvious steric hindrance.

The literature on the chemical synthesis of HHQ and PQS was scant at the onset of this project. The Somanathan et al. synthesis of HHQ involved condensation of the long chain acid chloride with the carbanion derived from ethyl acetoacetate **11** to give **12**, followed by deacetylation using sodium ethoxide to afford the corresponding β-keto-ester **13**. This β-keto-ester **13** was

condensed with aniline in the presence of *p*-toluene sulfonic acid and a Conrad–Limpach cyclisation gave HHQ **3** (Scheme 1.2.1).[43]

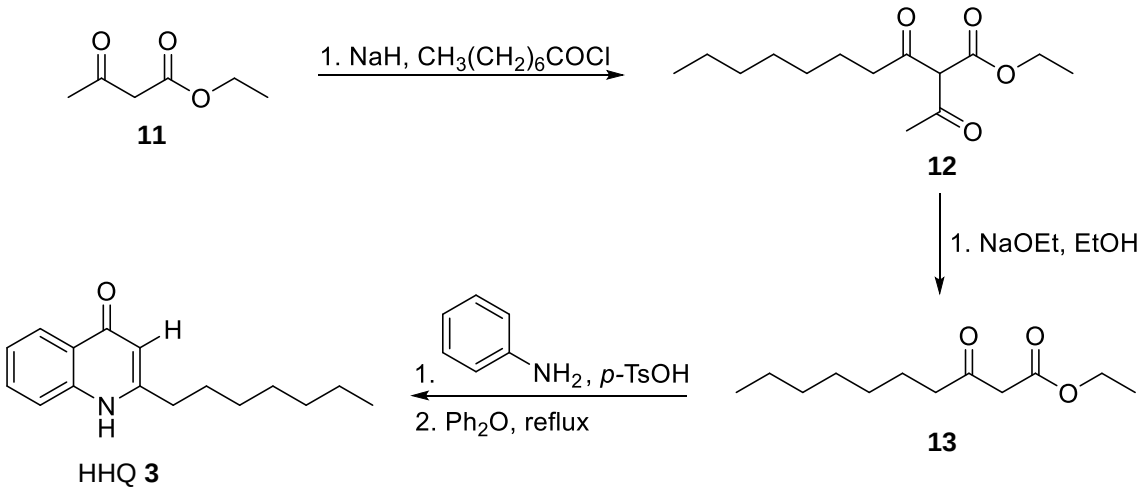

Scheme 1.2.1

In Woschek's synthesis of HHQ,[44] the β-keto-ester **13** was prepared using a procedure described by Epstein (Scheme 1.2.2).[45]

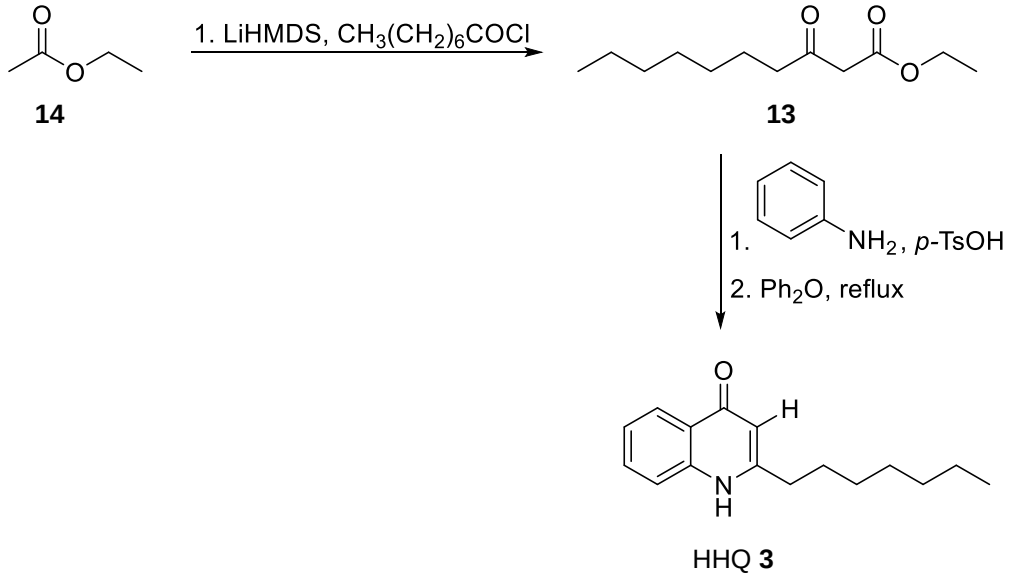

Scheme 1.2.2

Ethyl acetate **14** was deprotonated using lithium hexamethyldisilazide followed by reaction with octanoyl chloride. The β-keto-ester **13** was condensed with aniline and cyclised using diphenyl ether as described in Somanathan's synthesis above. An alternative method for the cyclisation step involves the use of sulphuric acid and acetic anhydride, also yielding HHQ.[46]

The conversion of HHQ to PQS via the formyl intermediate, which is oxidised with hydrogen peroxide in basic medium, has been described by Pesci et al.[42]

1.2.2 Synthesis of 2-heptylquinolin-4(1*H*)-one

For our synthesis of HHQ, we decided to employ a procedure from Oikawa et al. for the preparation of the β-keto-ester,[47] which takes advantage of the reactivity of Meldrum's acid **15**. Meldrum's acid **15** readily reacts with electrophiles, even in the absence of a strong base because of its high acidity (pK_a of 4.97).[47,47] Therefore, acylation of **15** is also expected to occur under similar conditions.[47]

Meldrum's acid **15** was reacted with octanoyl chloride in the presence of pyridine. The reaction was monitored by NMR analysis until all starting material had reacted. The mixture was then washed with 5% HCl solution several times and water. The organic layer was dried, filtered, and concentrated under reduced pressure, to afford the acylated Meldrum's acid **16** as a brown oil. This residue was used in the next step without further purification (Scheme 1.2.3). The spectroscopic data obtained for **16** was consistent with that previously reported.[48]

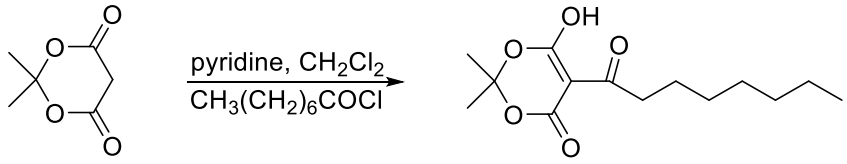

15 **16**

Scheme 1.2.3

Newly formed **16** was then subjected to methanolysis, instead of ethanolysis because of the excellent yields obtained by Oikawa, to afford the methyl β-keto-ester **17** in 66% yield over two steps (Scheme 1.2.4). The spectroscopic data corresponded to that previously reported in the literature.[48]

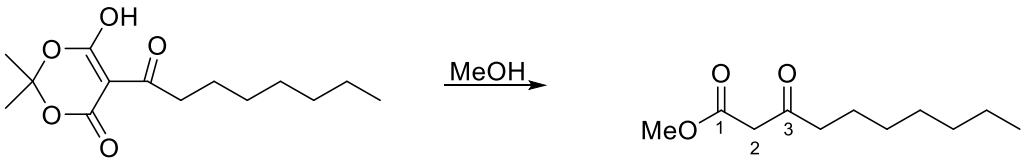

16 **17**, 66% over two steps

Scheme 1.2.4

For the remaining steps, we employed Somanathan's conditions.[43] β-keto-ester **17** was condensed with aniline in the presence of *p*-toluene sulfonic acid at reflux, using a Dean-Stark apparatus. The crude enamine **18** was used in the next step without further purification (Scheme 1.2.5). To the best of our knowledge there has been no previous report of compound **18** in the

literature. The ^{1}H NMR spectrum was distinctly different from that of the β-keto-ester **17**. A distinctive peak was observed at 4.73 ppm for the enamine hydrogen at C-2. A broad singlet was observed at 10.30 ppm for the NH signal, confirming incorporation of the aniline moiety into the target compound. A dramatic shift is also observed for C-2 in the ^{13}C NMR. The signal for the CH_2 at C-2 for the β-keto-ester **17** had been observed at 49.0 ppm, but was now present much further downfield at 84.5 ppm for the enamine. DEPT spectra confirmed this was a CH signal. A mass spectrum in the positive mode confirmed the presence of the protonated molecular ion at m/z = 276.

Enamine **18** was subjected to Conrad–Limpach cyclisation by refluxing in diphenyl ether. The formed MeOH was removed under reduced pressure. To the isolated residue, diethyl ether and 2 M hydrochloric acid solution were added. The mixture was allowed to stir vigorously for 5 min, then allowed stand at room temperature for 18 h. The crystalline solid which formed was filtered and washed with diethyl ether to afford a yellow solid. The crude product was crystallised from ethyl acetate and the pure **19** isolated as a cream solid in a 40% yield over two steps (Scheme 1.2.5).

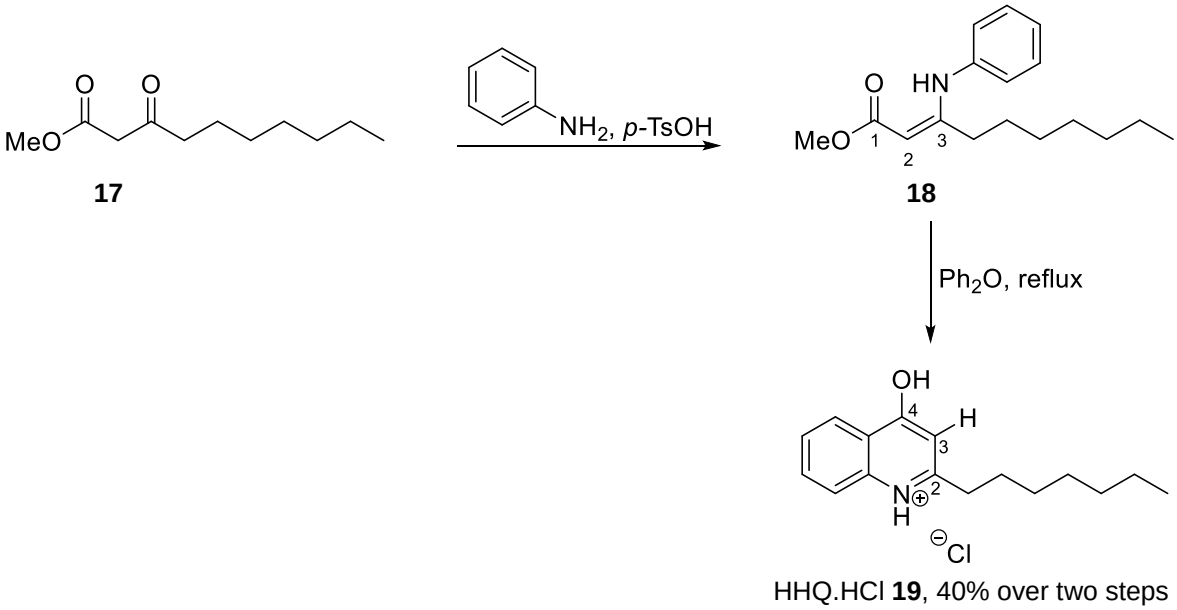

Scheme 1.2.5

Initially we were concerned that the ^{1}H NMR and ^{13}C NMR spectra did not correspond to previous data obtained for HHQ. The carbon at C-4 was observed much further upfield (169.7 ppm) then one would expect for a carbonyl in this system. We concluded this signal was more indicative of the C=**C**-OH and that HHQ must be present as the hydroxy-quinoline tautomer.

This was further supported by crystal structure analysis (Figure 1.2.1), which confirmed HHQ was isolated as the hydrochloride salt HHQ.HCl **19**.

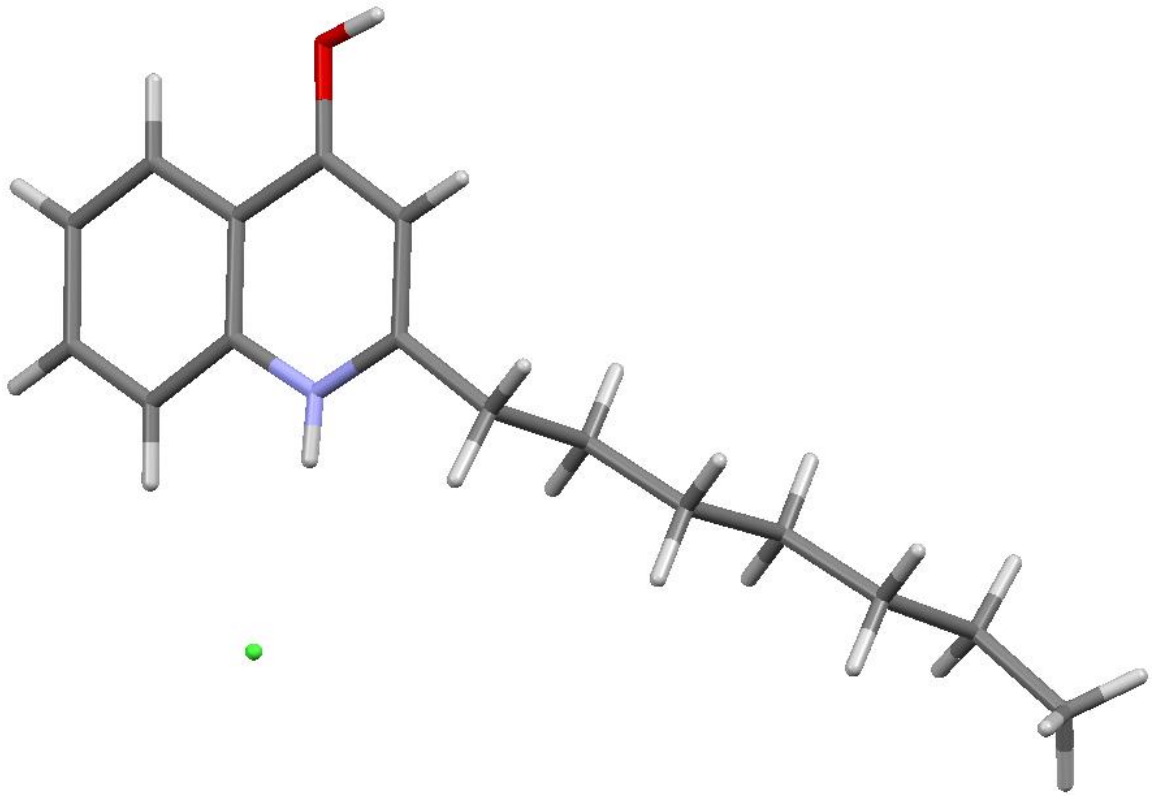

HHQ.HCl **19**

Figure 1.2.1

The free base, HHQ (Figure 1.2.2) was easily obtained by stirring the hydrochloride salt HHQ.HCl **19** in chloroform (due to poor solubility in other solvents) and adding 15% sodium hydroxide solution until the aqueous layer reached neutral pH. The mixture was separated and extracted with chloroform. The combined organic layers were dried, filtered and concentrated to afford HHQ **3** in a 95% yield.

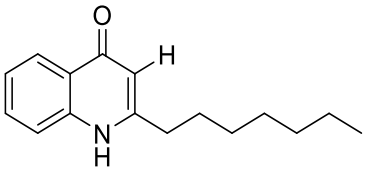

HHQ **3**

Figure 1.2.2

1.2.3 Synthesis of 3-halo-analogues of 2-heptylquinolin-4(1*H*)-one

At the onset of the project, structure–function analysis on HHQ and PQS had centred on the alkyl chain length[49,50] and substitution of the anthranilate ring.[49] The crucial C-3 position had not been investigated. Subsequent to our published investigations,[51,52] Hartmann and co-workers have reported 'blocking' the C-3 position of HHQ and repressing PQS biosynthesis using **20** (Figure 1.2.3).[14,53]

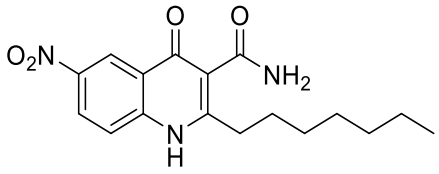

20

Figure 1.2.3

Therefore, the structure–function analysis in this project study was designed to provide key insights into the activity of the HHQ and PQS compounds both within *P. aeruginosa* and also towards non-pseudomonal bacterial and fungal species. To date there have been no reports of halogenation or cross-coupling of HHQ or its derivatives.

HHQ was subjected to chlorination using sodium dichloroisocyanurate **21** following a chlorination-procedure by Staskun.[54] Crystallisation from MeOH afforded the product **22** as colourless crystals in a 58% yield (Scheme 1.2.6). Successful chlorination was confirmed by the absence of the C-3 proton signal at 6.21 ppm in the ^{1}H NMR spectrum. A high resolution mass spectrum in the positive mode confirmed the presence of the protonated molecular ion at m/z = 278.1306.

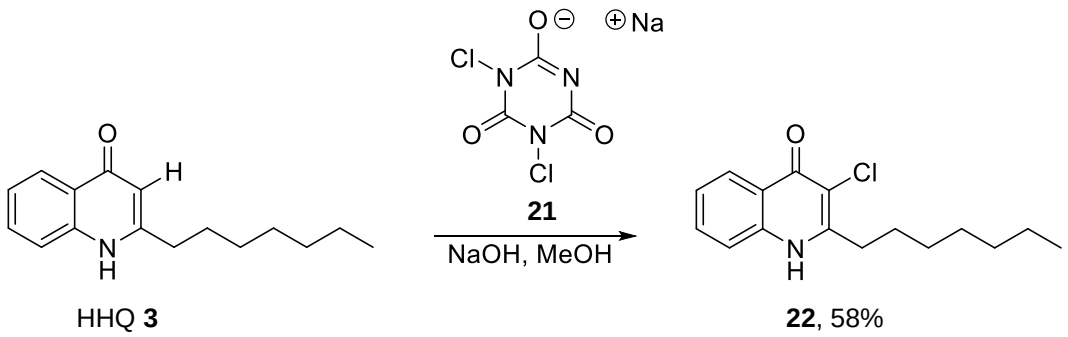

Scheme 1.2.6

Bromination of HHQ was achieved using pyridinium tribromide **23** and acetic acid. Aqueous sodium thiosulfate was added to quench the reaction and the formed precipitate was filtered and washed with ice-cold EtOH (15 ml). The crude solid was crystallised from EtOH to give **24** as pale yellow cystals in a 50% yield (Scheme 1.2.7). The successful incorporation of the bromine was evident in the ^{13}C NMR where a shift in the C-3 peak was observed from 108.5 ppm (for HHQ) to 105.1 ppm for **24**. Again the C-3 proton signal at 6.21 ppm, for HHQ was absent from the ^{1}H NMR spectrum. A high resolution mass spectrum in the positive mode confirmed the presence of the protonated molecular ion at m/z = 322.0812.

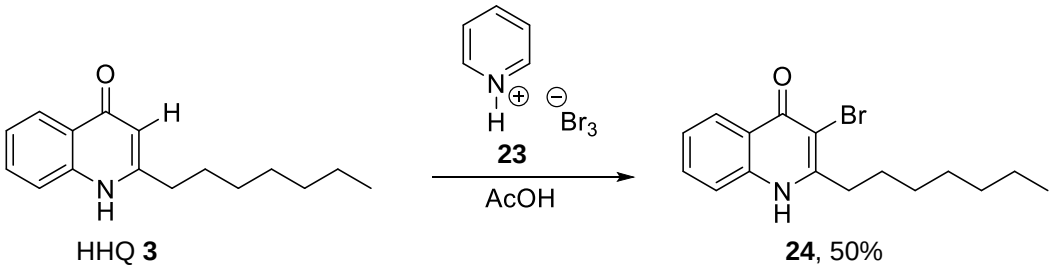

Scheme 1.2.7

Iodination was successful using iodine and sodium carbonate in THF. Sodium thiosulfate was used to quench the reaction and the precipitate which formed was collected by filtration and washed with ice cold water. The product **25** did not require further purification and was isolated in 48% yield (Scheme 1.2.8).

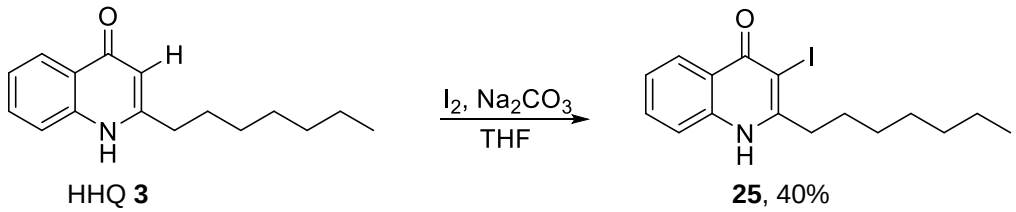

Scheme 1.2.8

Iodination was also evident in the ^{13}C NMR where a shift in the C-3 peak was observed from 108.5 ppm (for HHQ) to 85.7 ppm for **25**. Again the C-3 proton signal at 6.21 ppm, for HHQ was absent from the ^{1}H NMR spectrum. A high resolution mass spectrum in the positive mode confirmed the presence of the protonated molecular ion at m/z = 370.0656.

The anticipated low reactivity associated with the sterically demanding neighbouring alkyl chains never materialised in these reactions and moderate to good yields were achieved for all halogenations.

Furthermore, iodide **25** was easily methylated by deprotonation with sodium hydride, at 40°C for 5 h, followed by alkylation with methyl iodide, for 12 h at 40°C, affording **26** in 67% yield (Scheme 1.2.9).[55]

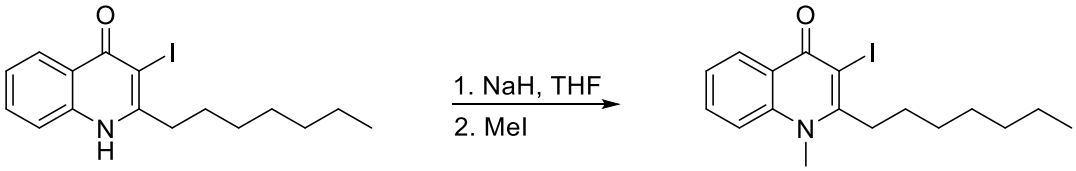

25 **26**, 67%

Scheme 1.2.9

We were aware that the structural isomer **27** (Figure 1.2.4) could also be formed from this reaction.

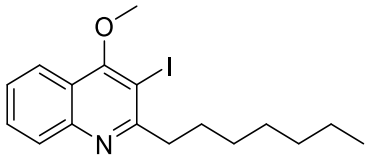

27

Figure 1.2.4

The spectroscopic data showed that one product had been formed. On comparison of the ^{13}C NMR spectra with the signals of similar compounds, **28**[56] and **29**,[53] in the literature (Figure 1.2.5), we elucidated, **26** had been prepared in preference to the structural isomer **27**.

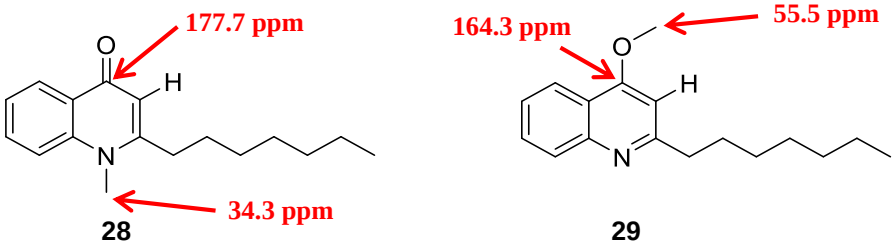

28 **29**

Figure 1.2.5

On analysis of the ^{13}C NMR spectra, the data clearly showed a distinct similarity to that of *N*-methylated **28**. In our ^{13}C NMR spectrum a signal at 173.8 ppm was observed which was indicative of a carbonyl moiety. Also a signal at 40.1 ppm supported our claims for the preferential formation of the *N*-methylated isomer, **26**.

Oxidative addition of HHQ to the palladium complex would be expected to be slow due to the large steric bulk of the seven carbon alkyl chain. However we were encouraged by reports previously in the literature, where a similar substrate successfully underwent Suzuki-Miyaura coupling at the C-3 position with the presence of a phenyl group at C-2.[55]

To our delight, we were able to successfully perform a Suzuki-Miyaura coupling reaction at C-3 using phenylboronic acid and palladium-tetrakis(triphenylphosphine) as precatalyst (Scheme 1.2.10).

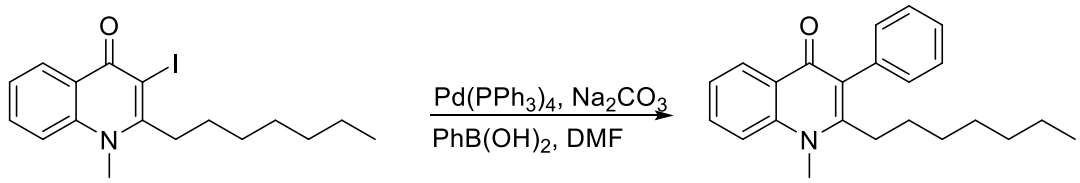

26 **30**, 50%

Scheme 1.2.10

After heating at 130°C for 30 min, palladium black was seen to precipitate and the reaction was stopped. The coupled product was purified using column chromatography (1:1, hexane:EtOAc) and **30** was isolated in 50% yield.

This reaction follows the general Suzuki-Miyaura coupling reaction mechanism[57,58] (Scheme 1.2.11).

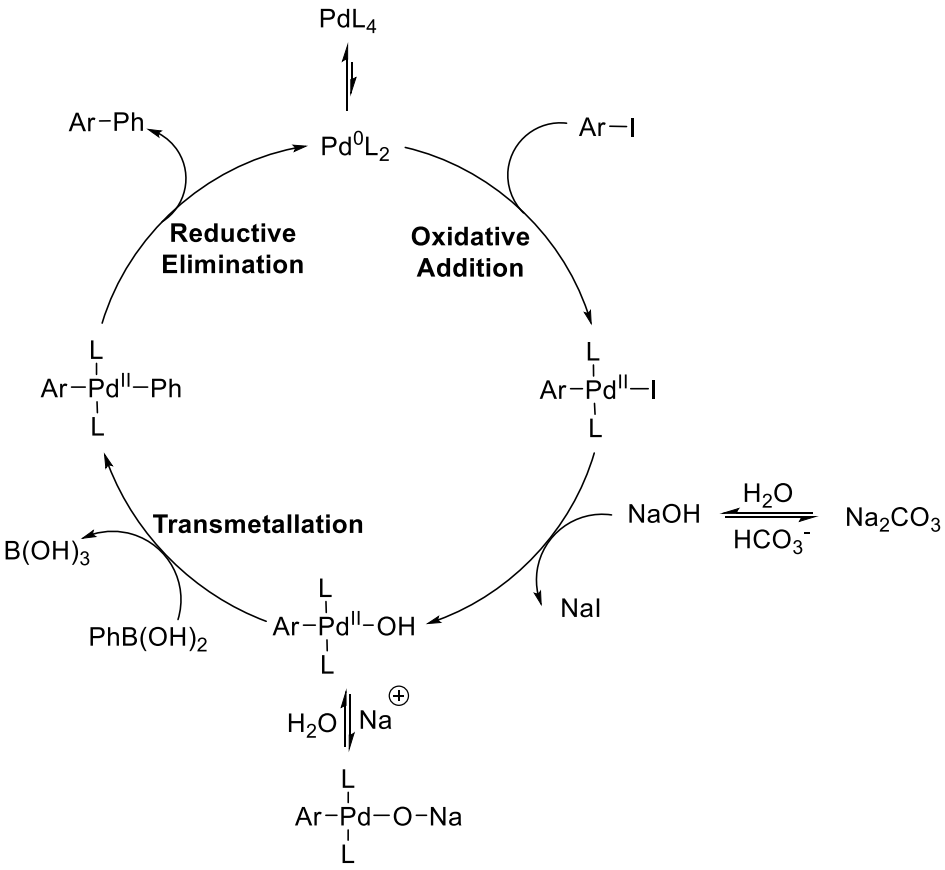

Scheme 1.2.11

1.2.4 Biological Results and Discussion

Biological studies were carried out by our collaborators Dr. Jerry Reen and Prof. Fergal O'Gara at the Microbiology Department, University College Cork.

The PQS signalling system, a key component of quorum sensing in *P. aeruginosa*, is known to control production of a range of virulence factors, including biofilm formation, elastase, rhamnolipid and the phenazine redox compound pyocyanin.[35,41] The synthesis of PQS itself was not completed as part of this PhD project but was prepared by another member of the group. It was hoped functionalisation at the C-3 position would identify either a potential antagonist in the biosynthesis of PQS or an antivirluence agent to interfere with the pathogency of *P. aeruginosa.*

Phenazine is important in *P. aeruginosa* for the production of pyocyanin. It is this compound which contributes to the ability of *P. aeruginosa* to colonise the lungs of cystic fibrosis patients. Phenazine natural products have been implicated in the virulence and competitive fitness of producing organisms. Phenazines can benefit *P. aeruginosa* by serving as signalling molecules, regulating persister cell formation, influencing colony morphology, and promoting iron acquisition and biofilm development.[59] By interfering with phenazine restoration we would be impeding a key virulence factor of *P. aeruginosa.*

Halo-analogues, **22**, **24** and **25** were first assessed for restoration of phenazine production in a *pqs*A mutant, in which the biosynthetic steps required for 2-alkylquinolone production have been disrupted.

While both HHQ **3** and PQS restored phenazine production in the *pqs*A mutant strain, the halo-analogues, **22**, **24** and **25**, were significantly less effective in triggering production of the phenazine (Figure 1.2.6), suggesting that the C-3 position is crucial for control of phenazine production in *P. aeruginosa* and identifying **22**, **24** and **25** as potential anti-virulence agents.

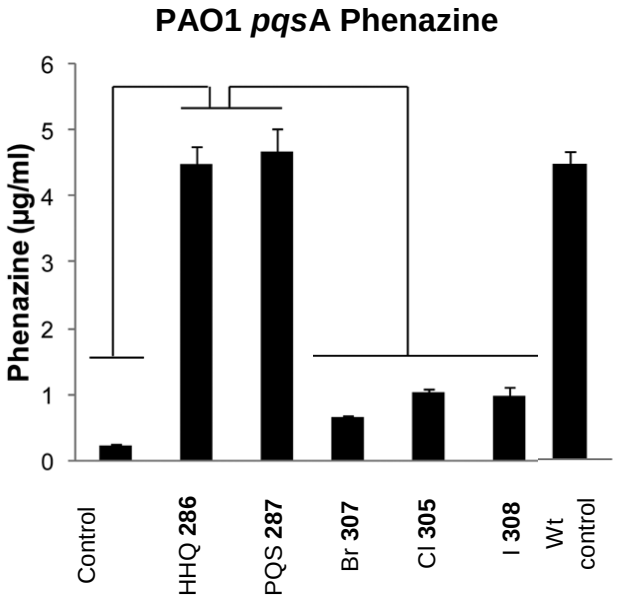

Figure 1.2.6

P. aeruginosa is notorious for its ability to cause chronic infections by its high level of drug resistance involving the formation of biofilms as previously mentioned. Biofilm formation[20,39] is a structured community of bacterial cells enclosed in a self-produced polymeric matrix adhering to an inert or living surface.[60] This mode of growth is particularly resistant to antibodies and antibiotics. In multi-drug resistant bacteria, biofilms play a key role in allowing the pathogen to overcome host defences and contribute to its virulence. PQS has been shown to mediate the formation of biofilm in *P. aeruginosa*.[35] *Bacillus substilis* is a Gram positive bacteria which co-inhabits the soil environment with *P. aeruginosa*.[61] *B. substilis* species are an excellent and well-utilised model system for Gram positive bacteria, and a cross-species influence with *P. aeruginosa* has been shown.[62] In light of this co-existance of *B. substilis* and *P. aeruginosa* in soil, it is perhaps unsurprising that communication mechanisms between both organisms would exist.

Given that both the quinolone (HHQ) and the HCl salt of its tautomer hydroxy-quinoline (HHQ.HCl **19**) were accessible, we felt it would be valuable to confirm that both exhibited identical activities for biofilm formation. Biofilm formation were similarly influenced in *B. subtilis* in the presence of HHQ **3** and HHQ.HCl **19** (Figure 1.2.7). This was determined using optical density measurments at 595 nm. Optical density, measured in a spectrophotometer, can be used to measure biofilm thickness. As visible light passes through a cell suspension the light is scattered. Greater scatter indicates thicker biofilm formation.

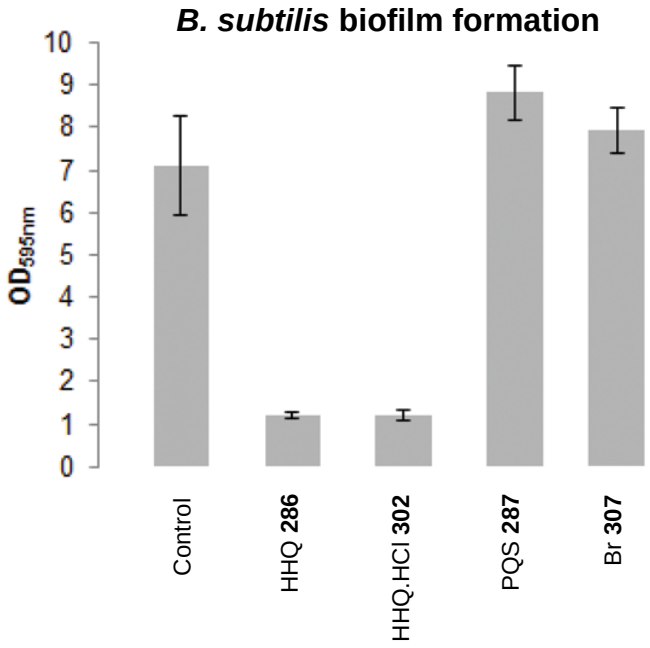

Figure 1.2.7

However, in contrast to HHQ and HHQ.HCl **19**, antibiofilm activity towards *B. subtilis* was abolished upon substitution at the C-3 position, i.e. halo-analogue **24** (Figure 1.2.7), highlighting the importance of the C-3 position in the biological role of these compounds.

Although PQS has been found in sputum of patients suffering from cystic fibrosis,[22] the impact and potential cytotoxic effects of these compounds on airway epithelial cells has not been investigated. Therefore, HHQ, PQS and compounds **22**, **24** and **25** were tested for cytotoxicity towards a human airway epithelial cell line (Figure 1.2.8).

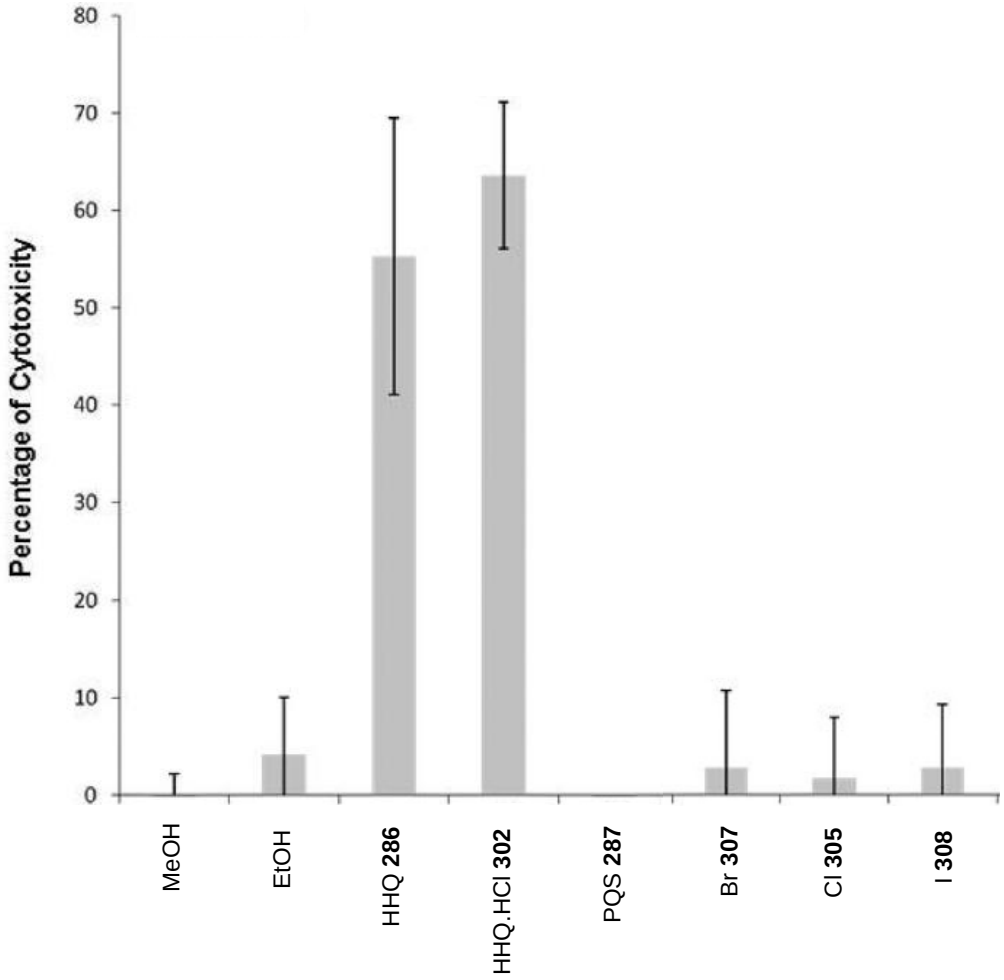

Figure 1.2.8

Interestingly, HHQ was found to be cytotoxic towards IB3-1 cells while PQS did not exhibit any cytotoxic activity. The cytotoxicity of both the quinolone (HHQ) and hydroxy-quinoline hydrochloride (HHQ.HCl **19)**, towards IB3-1 cells were comparable (~60%). The halo-analogues **22**, **24** and **25** did not exhibit cytotoxicity towards IB3-1 cells. This is further evidence to support the importance of the C-3 position in the biological functionality of the HHQ and PQS molecules.

1.3 Conclusions and Future Work

In conclusion the synthesis of multigram quantities of HHQ has been achieved.

For the first time, halo-analouges of HHQ have been prepared which showed potential as antivirulence agents in impeding the restoration of phenazine production. Disappointingly, halo-analogue **24** did not show any antibiofilm activity. However, these biological investigations highlight the strict structural requirements at the C-3 position for the biological activity of HHQ and PQS.

Also the first successful palladium-catalysed cross coupling reaction has been performed on *N*-methylated HHQ opening up the possibility of synthesising other novel alkylquinolones bearing aryl, heteroaryl and alkyl groups at the C-3 position. These would be useful for further structure function analysis of PQS analogues.

The future work of this project will expand the palladium-catalysed cross coupling to other reactions such as the Mizoroki-Heck reaction. Initial thoughts that oxidative addition would be problematic due to steric hindrance of the bulky alkyl chain at C-2 did not materialise.

Future structural studies will involve continued functionalisation of the 3-position (e.g. introduction of fluorine) with a view towards attaining a deeper understanding of the complex roles of these molecules in bacterial and fungal species.

Publications on this work to date are included in the Appendix.

1.4 Experimental

*Note: An arbitrary numbering system was employed to assist in the clear assignment of the spectroscopic data and does not correspond to the IUPAC number system for these compounds. Only carbon atoms were numbered in the experimental.

1.4.1 Synthesis of 2-heptylquinolin-4(1*H*)-one

5-(1-hydroxyoctylidiene)-2,2-dimethyl-1,3-dioxane-4,6-dione 16

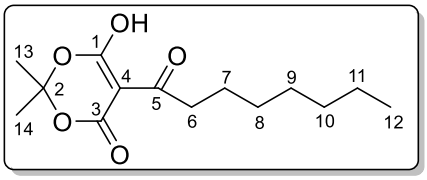

To a solution of 2,2-dimethyl-1,3-dioxane-4,6-dione **15** (Meldrum's Acid) (40 g, 0.278 mol), in distilled CH_2Cl_2 (400 mL) at 0°C under a N_2 atmosphere, was added pyridine (45 mL, 0.556 mol), followed by the dropwise addition of octanoyl chloride **31** (52.5 mL, 0.306 mol) over 5 min. After allowing the resulting orange liquid to stir at 0°C for 1 h, the reaction mixture was allowed warm to room temperature for 20 h. The reaction was monitored by NMR analysis until all starting material had reacted. The mixture was then washed with 5% HCl solution (6 x 200 mL) and water (200 mL). The organic layer was dried over anhydrous $MgSO_4$, filtered, and concentrated under reduced pressure, to afford the title compound **16** as a brown oil (73.9 g). This residue was used in the next step without further purification.

Spectroscopic characteristics were consistent with previously reported data.[48]

^{1}H NMR (300 MHz, $CDCl_3$): δ 0.88 (3H, t, *J* = 6.9 Hz, H-12), 1.20-1.45 (10H, m, H-11, H-10, H-9, H-8, H-7), 1.79 (6H, s, H-13, H-14), 3.04 (2H, t, *J* = 7.6 Hz, H-6), 15.30 (1H, br s, O-H) ppm; ^{13}C NMR (75.5 MHz, $CDCl_3$): δ 14.1 (C-12), 26.8 (2 x CH_3, C-13, C-14), 22.6, 26.2, 28.9, 29.0, 31.6, 35.8 (6 x CH_2, C-11, C-10, C-9, C-8, C-7, C-6), 91.7 (C-4), 104.8 (C-2), 160.2 (C-1), 170.6 (C-3), 198.4 (C-5) ppm; MS (ESI) *m/z*: 269 $[M - H]^-$.

methyl-3-oxo-decanoate 17

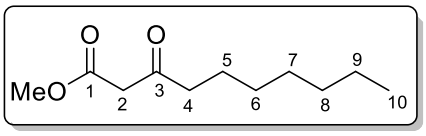

To MeOH (300 mL) was added 5-(1-hydroxyoctylidiene)-2,2-dimethyl-1,3-dioxane-4,6-dione **16** (max. 0.278 mol) from the previous step and the mixture was heated at reflux for 2.5 h. The reaction mixture was allowed to cool to room temperature and concentrated under reduced pressure, yielding an orange liquid. This crude product was purified by fractional distillation to afford the β- keto ester **17** as a clear oil (36.5 g, 66% over two steps).

Spectroscopic characteristics were consistent with previously reported data.[48]

^{1}H NMR (300 MHz, $CDCl_3$): δ 0.88 (3H, t, *J* = 6.7 Hz, H-10), 1.20-1.40 (8H, m, H-9, H-8, H-7, H-6), 1.52-1.66 (2H, m, H-5), 2.52 (2H, t, *J* = 7.4 Hz, H-4), 3.45 (2H, s, H-2), 3.74 (3H, s, OMe) ppm; ^{13}C NMR (75.5 MHz, $CDCl_3$): δ 14.1 (C-10), 22.6, 23.4, 28.9, 29.0, 31.6, 43.1 (6 x CH_2, C-9, C-8, C-7, C-6, C-5, C-4), 49.0 (C-2), 52.3 (OMe), 167.7 (C-1), 202.9 (C-3) ppm; MS (ESI) *m/z*: 201 $[M + H]^+$.

(*Z*)-methyl 3-(phenylamino)dec-2-enoate 18

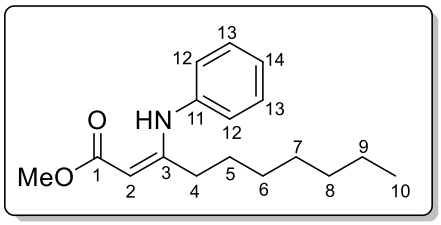

To methyl-3-oxo-decanoate **17** (36.5 g, 0.184 mol) was added aniline (17.6 g, 0.189 mol), hexane (300 mL) and *p*-toluene sulfonic acid (0.519 g, 0.003 mol) were added, at which point cloudiness was observed. The mixture was heated at reflux under a N_2 atmosphere for 5 h using a Dean-Stark apparatus and allowed to stir overnight at room temperature. The crude reaction mixture was dried over anhydrous $MgSO_4$, filtered, and concentrated under reduced pressure yielding **18** as a dark orange oil (51.4 g). This crude product was used in the next step without further purification.

^{1}H NMR (300 MHz, $CDCl_3$): δ 0.84 (3H, t, *J* = 6.8 Hz, H-10), 1.10-1.35 (8H, m, H-9, H-8, H-7, H-6), 1.35-1.47 (2H, m, H-5), 2.28 (2H, t, *J* = 7.8 Hz, H-4), 3.69 (3H, s, OMe), 4.73 (1H, s, H-2), 7.09 (2H, d, *J* = 7.5 Hz, H-12), 7.17 (1H, t, *J* = 7.3 Hz, H-14), 7.33 (2H, t, *J* = 7.5 Hz, H-13), 10.30 (1H, br s, N-H) ppm; ^{13}C NMR (75.5 MHz, $CDCl_3$): δ 14.2 (C-10), 22.6, 27.9, 28.8, 28.9, 31.6, 32.2 (6 x CH_2, C-9, C-8, C-7, C-6, C-5, C-4), 50.3 (OMe), 84.5 (C-2), 125.1 (2 x Ar-CH), 125.3 (Ar-CH), 129.1 (2 x Ar-CH), 139.2 (C-11), 163.8 (C-3), 171.0 (C-1) ppm; MS (ESI) *m/z*: 276 $[M + H]^+$.

2-heptylquinolin-4(1*H*)-one.HCl 19

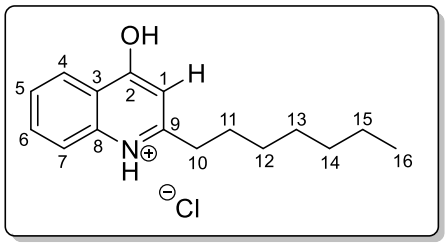

To diphenyl ether (45 mL, 0.264 mol) heated at reflux was added **18** (max. 0.184 mol), dropwise over 1.5 h, ensuring vigorous reflux was maintained. Heating was continued for 1 h. The reaction mixture was then cooled to room temperature. The formed MeOH was removed under reduced pressure. To the isolated residue, Et_2O (120 mL) and 2 M HCl solution (160 mL) were added. This mixture was allowed to stir vigorously for 5 min, then allowed stand at room temperature for 18 h. The crystalline solid which formed, was filtered and washed with Et_2O

to afford a yellow solid. The crude product was crystallised from EtOAc and the pure **19** isolated as a cream solid (19.9 g, 40% over two steps). Mp 111-114°C.

IR (KBr) $\bar{\nu}_{max}$: 3103 (O-H stretch, m), 2930-2728 (C-H stretch, s), 2442 (N-H stretch, s) 1639 (C=N stretch, s), 1594 (aromatic C=C, s), 1488 (C-H bending, m) cm^{-1}; ^{1}H NMR (300 MHz, $CDCl_3$): δ 0.77 (3H, t, *J* = 6.7 Hz, H-16), 1.05-1.30 (6H, m, H-15, H-14, H-13), 1.30-1.41 (2H, m, H-12), 1.75-1.91 (2H, m, H-11), 3.12 (2H, t, *J* = 7.8 Hz, H-10), 7.63 (1H, m, H-5), 7.63 (1H, s, H-1), 7.84 (1H, ddd, *J* = 1.2, 7.0, 8.4 Hz, H-6), 8.34 (1H, dd, *J* = 1.2, 8.4 Hz, H-4), 8.53 (1H, d, *J* = 8.4 Hz, H-7), 14.95 (1H, br s, O-H) ppm; ^{13}C NMR (75.5 MHz, $CDCl_3$): δ 14.0 (C-16), 22.5, 28.9, 29.3, 29.8, 31.6 (5 x CH_2, C-15, C-14, C-13, C-12, C-11), 34.3 (C-10), 105.4 (C-1), 119.5 (C-3), 119.9 (C-7), 123.8 (C-4), 127.2 (C-5), 133.9 (C-6), 139.7 (C-8), 160.9 (C-9), 169.7 (C-2) ppm (Note: Structural assignment confirmed using COSY, HSQC and HMBC); HRMS (ESI) *m/z* calcd for $C_{16}H_{22}NO$ $[M + H]^+$: 244.1701, found 244.1696 (HHQ). Anal. Calcd for $C_{16}H_{22}ClNO$: C, 68.68; H, 7.93; N, 5.01. Found: C, 68.99; H, 7.91; N, 5.02.

Crystallographic data was also obtained for this compound (see Appendix).

2-heptylquinolin-4(1*H*)-one 3

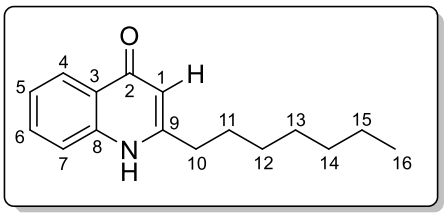

To a solution of 2-heptylquinolin-4(1*H*)-one.HCl **19** (0.050 g, 0.179 mmol) in $CHCl_3$ (2 mL) was added 15% NaOH solution, until neutral pH was achieved. The mixture was extracted with $CHCl_3$ (3 x 20 mL). The combined organic fractions were dried over anhydrous $MgSO_4$, filtered, and concentrated under reduced pressure, to afford **3** as a cream solid (0.041 g, 95% yield). Mp 143-146°C (Lit.[44] Mp 146-147°C).

Spectroscopic characteristics were consistent with previously reported data.[44]

^{1}H NMR (400 MHz, $CDCl_3$): δ 0.86 (3H, t, *J* = 7.0 Hz, H-16), 1.15-1.36 (8H, m, H-15, H-14, H-13, H-12), 1.68-1.76 (2H, m, H-11), 2.65 (2H, t, *J* = 7.7 Hz, H-10), 6.21 (1H, s, H-1), 7.32 (1H, ddd, *J* = 1.8, 6.4, 8.1 Hz, H-5), 7.51-7.61 (2H, m, H-6, H-7), 8.35 (1H, dd, *J* = 1.4, 8.1 Hz H-4), 10.37 (1H, br s, N-H) ppm; ^{13}C NMR (75.5 MHz, $CDCl_3$): δ 14.0 (C-16), 22.5, 28.7, 28.9, 29.1, 31.6 (5 x CH_2, C-15, C-14, C-13, C-12, C-11), 34.3 (C-10), 108.5 (C-1), 117.8 (C-7), 123.5 (C-5), 125.1 (C-3), 125.7 (C-4), 131.8 (C-6), 140.2 (C-8), 154.1 (C-9), 178.9 (C-2) ppm (Note: Structural assignment confirmed using COSY, HSQC and HMBC); MS (ESI) *m/z*: 244 $[M + H]^+$.

1.4.2 Synthesis of 3-halo-analogues of 2-heptylquinolin-4(1*H*)-one

3-chloro-2-heptylquinolin-4-ol 22

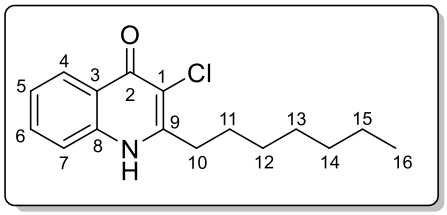

To a stirred solution of 2-heptylquinolin-4(1*H*)-one **3** (0.106 g, 0.435 mmol) in a mixture of MeOH (5 mL), 2 M NaOH (1.4 mL), and water (1.4 mL) at room temperature was added sodium dichloroisocyanurate (0.146 g, 0.79 mmol). After 40 min, the reaction mixture was filtered, and the combined filtrate and MeOH washings were acidified to pH 4 (2 M HCl) and cooled to 4°C in the refrigerator. The solid product **22** was collected by filtration and crystallised from MeOH to afford colourless crystals (0.070 g, 58%). Mp 269-272°C.

IR (KBr) $\bar{\nu}_{max}$: 3348 (N-H stretch, m), 2924 (C-H stretch, s), 1633 (C=O stretch, m), 1562 (aromatic C=C, s), 1031 (C-N, stretch, s) cm^{-1}; ^{1}H NMR (400 MHz, CD_3SOCD_3): δ 0.85 (3H, t, *J* = 6.9 Hz, H-16), 1.32 (8H, m, H-15, H-14, H-13, H-12), 1.69 (2H, m, H-11), 2.83 (2H, t, *J* = 7.8 Hz, H-10), 7.34 (1H, ddd, *J* = 1.3, 7.0, 8.0 Hz, Ar-H), 7.57 (1H, d, *J* = 8.4 Hz, Ar-H), 7.67 (1H, ddd, *J* = 1.3, 7.0, 8.4 Hz, Ar-H), 8.09 (1H, dd, *J* = 1.3, 8.0 Hz, Ar-H), 12.07 (1H, br s, N-H) ppm; ^{13}C NMR (125.8 MHz, CD_3SOCD_3): δ 13.9 (C-16), 21.9, 27.5, 28.3, 28.6, 31.1, 32.1 (6 x CH_2, C-15, C-14, C-13, C-12, C-11, C-10), 113.3 (C-1), 118.0 (Ar-CH), 123.4 (C-3), 123.5 (Ar-CH), 125.1 (Ar-CH), 131.8 (Ar-CH), 138.5 (C-8), 150.6 (C-9), 170.8 (C-2) ppm; HRMS (ESI) *m/z* calcd for $C_{16}H_{21}{}^{35}ClNO$ $[M + H]^+$: 278.1312, found 278.1306.

3-bromo-2-heptylquinolin-4-ol 24

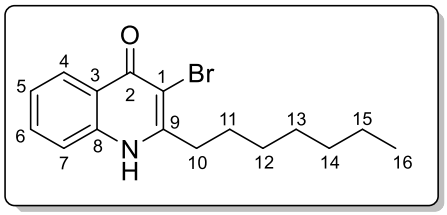

To a solution of 2-heptylquinolin-4(1*H*)-one **3** (0.038 g, 0.156 mmol) in acetic acid (0.78 mL, 5 mL per mmol of HHQ) was added pyridinium tribromide (0.100 g, 0.313 mmol). The reaction mixture was allowed to stir at room temperature for 3 h. Aqueous $Na_2S_2O_3$ was added to quench the reaction and the formed precipitate was filtered and washed with ice-cold EtOH (15 ml). The crude solid was crystallised from EtOH to give pale yellow crystals **24** (0.025 g, 50%). Mp 245-248°C.

IR (KBr) $\bar{\nu}_{max}$: 3432 (N-H stretch, m), 2926 (C-H stretch, s), 1631 (C=O stretch, m), 1581 (aromatic C=C, s), 1141 (C-N stretch, s) cm^{-1}; ^{1}H NMR (400 MHz, CD_3SOCD_3): δ 0.85 (3H, t, *J* = 6.8 Hz, H-16), 1.30 (8H, m, H-15, H-14, H-13, H-12), 1.70 (2H, m, H-11), 2.86 (2H, t, *J* = 7.8 Hz, H-10), 7.35 (1H, ddd, *J* = 1.4, 6.8, 8.1 Hz, Ar-H), 7.58 (1H, d, *J* = 8.3 Hz, Ar-H), 7.68 (1H, ddd, *J* = 1.4, 6.8, 8.3 Hz, Ar-H), 8.09 (1H, dd, *J* = 1.4, 8.1 Hz, Ar-H), 12.07 (1H, br s, N-

H) ppm; ^{13}C NMR (125.8 MHz, CD_3SOCD_3): δ 13.9 (C-16), 21.9, 27.6, 28.3, 28.6, 31.1, 34.5 (6 x CH_2, C-15, C-14, C-13, C-12, C-11, C-10), 105.5 (C-1), 117.9 (Ar-CH), 122.7 (C-3), 123.6 (Ar-CH), 125.2 (Ar-CH), 131.8 (Ar-CH), 138.7 (C-8), 152.1 (C-9), 171.2 (C-2) ppm; HRMS (ESI) *m/z* calcd for $C_{16}H_{21}{}^{79}BrNO$ $[M + H]^+$: 322.0807, found 322.0812.

3-heptyl-2-iodoquinolin-4(1*H*)-ol 25

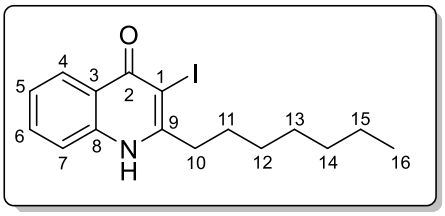

A mixture of 2-heptylquinolin-4(1*H*)-one **3** (0.2 g, 0.823 mmol), iodine (0.418 g, 1.65 mmol) and Na_2CO_3 (0.131 g, 1.235 mmol) in THF (4 mL) was allowed to stir at room temperature for 18 h. The mixture was quenched with $Na_2S_2O_3$ (0.613 g, 3.88 mmol) and the precipitate was collected by filtration before washing with ice cold water (50 mL). The product **25** did not require further purification (0.146 g, 48%). Mp 221-225°C.

IR (KBr) $\bar{\nu}_{max}$: 3419 (N-H stretch, s), 2920 (C-H stretch, m), 1627 (C=O stretch, m), 1556 (aromatic C=C, s), 1134 (C-N stretch, s) cm^{-1}; ^{1}H NMR (500 MHz, CD_3SOCD_3): δ 0.86 (3H, t, *J* = 7.0 Hz, H-16), 1.27-1.42 (8H, m, H-15, H-14, H-13, H-12), 1.68 (2H, m, H-11), 2.91 (2H, t, *J* = 7.9 Hz, H-10), 7.35 (1H, ddd, *J* = 1.2, 7.0, 8.3, Hz, Ar-H), 7.58 (1H, d, *J* = 8.3 Hz, Ar-H), 7.68 (1H, ddd, *J* = 1.2, 7.0, 8.3 Hz, Ar-H), 8.07 (1H, dd, *J* = 1.2, 8.3 Hz, Ar-H), 12.08 (1H, br s, O-H) ppm; ^{13}C NMR (125.8 MHz, CD_3SOCD_3): δ 13.9 (C-16), 21.9, 27.9, 28.3, 28.6, 31.1, 38.7 (6 x CH_2, C-15, C-14, C-13, C-12, C-11, C-10), 85.7 (C-1), 117.7 (Ar-CH), 120.6 (C-3), 123.8 (Ar-CH), 125.5 (Ar-CH), 131.9 (Ar-CH), 139.0 (C-8), 154.5 (C-9), 173.2 (C-2) ppm; HRMS (ESI) *m/z* calcd for $C_{16}H_{21}INO$ $[M + H]^+$: 370.0668, found 370.0656.

1.4.3 *N*-methylation and the Suzuki-Miyaura reaction

2-heptyl-3-iodo-1-methylquinolin-4(1*H*)-one 26

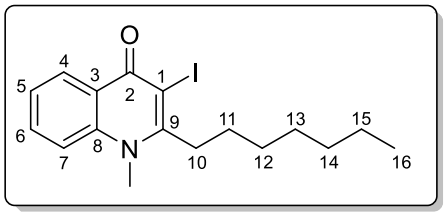

To stirred suspension of NaH (0.016 g, 0.669 mmol, 50% in oil, washed with anhydrous hexane (3 x 10 mL)) in dry THF (3 mL) was added 3-heptyl-2-iodoquinolin-4(1*H*)-one **25** (0.165 g, 0.446 mmol) at room temperature under a N_2 atmosphere. The reaction mixture was allowed to stir at 40°C for 5 h. The reaction mixture was treated with iodomethane (0.095 g, 0.669 mmol) and allowed to stir for 12 h at 40°C. Water (1 mL) was added to quench the reaction. The mixture was extracted with $CHCl_3$ (2 x 20 mL). The combined organic fractions were then washed with brine (10 mL). The organic layer was dried over anhydrous $MgSO_4$, filtered, and concentrated under reduced pressure. The product was purified using column chromatography (1:1, hexane : EtOAc) to afford **26** as a crystalline solid (0.082 g, 48%). Mp 66-69°C.

IR (KBr) $\bar{\nu}_{max}$: 2926-2854 (C-H stretch, s), 1617 (C=O stretch, s), 1592 (C=C stretch, s), 1519 (aromatic C=C, s) cm^{-1}; ^{1}H NMR (400 MHz, $CDCl_3$): δ 0.91 (3H, t, *J* = 6.8 Hz, H-16), 1.34-1.53 (8H, m, H-15, H-14, H-13, H-12), 1.55-1.70 (2H, m, H-11), 3.22 (2H, t, *J* = 8.3, H-10), 3.89 (3H, s, N-CH_3), 7.36 (1H, ddd, *J* = 1.3, 7.0, 8.1 Hz, Ar-H), 7.52 (1H, d, *J* = 8.6 Hz, Ar-H), 7.65 (1H, ddd, *J* = 1.3, 7.0, 8.6 Hz, Ar-H), 8.43 (1H, dd, *J* = 1.3, 8.1 Hz, Ar-H) ppm; ^{13}C NMR (100.6 MHz, $CDCl_3$): δ 14.1 (C-16), 22.6, 27.5, 28.8, 29.5, 31.7, 36.6 (6 x CH_2, C-15, C-14, C-13, C-12, C-11, C-10), 40.1 (N-CH_3), 90.4 (C-1), 115.3 (Ar-CH), 122.5 (C-3), 124.2 (Ar-CH), 127.8 (Ar-CH), 132.3 (Ar-CH), 140.8 (C-8), 155.1 (C-9), 173.8 (C-2) ppm; HRMS (ESI) *m/z* calcd for $C_{17}H_{23}INO$ $[M + H]^+$: 384.0824, found 384.0806.

2-heptyl-1-methyl-3-phenylquinolin-4(1*H*)-one 30

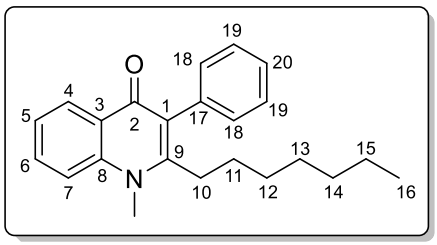

A mixture of 2-heptyl-3-iodo-1-methylquinolin-4(1*H*)-one **26** (0.055 g, 0.143 mmol), phenylboronic acid (0.035 g, 0.286 mmol) and $Pd(PPh_3)_4$ (0.008 g, 5 mol%) in DMF (1.5 mL) and aqueous 2 M Na_2CO_3 (1.5 mL) was heated at reflux for 2 h and then cooled to room temperature. The mixture was poured into ice-cold water and the precipitate was taken-up into $CHCl_3$ (10 mL), washed with brine (10 mL). The organic layer was dried over anhydrous $MgSO_4$, filtered, and concentrated under reduced pressure. The product was purified using column chromatography (1:1, hexane : EtOAc) affording the pure product **30** as a solid (0.024 g, 50%). Mp 213-215°C.

IR (KBr) $\bar{\nu}_{max}$: 2926-2854 (C-H stretch, s), 1618 (C=O stretch, s), 1592 (C=C stretch, s), 1538 (aromatic C=C, s) cm^{-1}; ^{1}H NMR (400 MHz, $CDCl_3$): δ 0.84 (3H, t, *J* = 7.1 Hz, H-16), 1.08-1.36 (8H, m, H-15, H-14, H-13, H-12), 1.49-1.62 (2H, m, H-11), 2.63 (2H, t, *J* = 8.2 Hz, H-10), 3.83 (3H, s, N-CH_3), 7.21-7.25 (2H, m, Ar-H), 7.35 (4H, m, Ar-H), 7.56 (1H, d, *J* = 8.6 Hz, Ar-H), 7.67 (1H, ddd, *J* = 1.6, 7.1, 8.6 Hz, Ar-H), 8.45 (1H, dd, *J* = 1.6, 8.0 Hz, Ar-H) ppm; ^{13}C NMR (100.6 MHz, $CDCl_3$): δ 14.0 (C-16), 22.5, 28.5, 28.9, 29.3, 31.5, 31.8 (6 x CH_2, C-15, C-14, C-13, C-12, C-11, C-10), 35.0 (N-CH_3), 115.2 (Ar-CH), 123.2 (Ar-CH), 124.3 (C-3), 126.2 (C-1), 127.0 (Ar-CH), 127.3 (Ar-CH), 128.4 (2 x Ar-CH), 130.6 (2 x Ar-CH), 131.9 (Ar-CH), 137.1 (C-17), 141.5 (C-8), 152.3 (C-9), 176.3 (C-2) ppm; HRMS (ESI) *m/z* calcd for $C_{23}H_{27}NO$ $[M + H]^+$: 334.2171, found 334.2164.

1.5 Reference List

1. Arias, C. A.; Murray, B. E. *N. Engl. J. Med.* **2009,** *360*, 439-443.
2. Cegelski, L.; Marshall, G. R.; Eldridge, G. R.; Hultgren, S. J. *Nat. Rev. Microbiol.* **2008,** *6*, 17-27.
3. Galloway, W. R. J. D.; Hodgkinson, J. T.; Bowden, S.; Welch, M.; Spring, D. R. *Trends in Microbiology* **2012,** *20*, 449-458.
4. Rasko, D. A.; Sperandio, V. *Nat. Rev. Drug Discovery* **2010,** *9*, 117-128.
5. O'Connell, K. M. G.; Hodgkinson, J. T.; Sore, H. F.; Welch, M.; Salmond, G. P. C.; Spring, D. R. *Angew. Chem. Int. Ed.* **2013,** *52*, 10706-10733.
6. Rello, J.; Diaz, E. *Crit. Care. Med.* **2003,** *31*, 2544-2551.
7. Chastre, J.; Fagon, J. Y. *Am. J. Respir. Crit. Care. Med.* **2002,** *165*, 867-903.
8. Downey, D. G.; Bell, S. C.; Elborn, J. S. *Thorax* **2009,** *64*, 81-88.
9. Swift, S. D. *Adv. Microb. Physiol.* **2001,** *45*, 199-270.
10. Rutherford, S. T.; Bassler, B. L. *Cold Spring Harbor Perspect. Med.* **2012,** *2*, a012427.
11. Frei, R.; Breitbach, A. S.; Blackwell, H. E. *Angew. Chem. Int. Ed.* **2012,** *51*, 5226-5229.
12. Brackman, G.; Celen, S.; Baruah, K.; Bossier, P.; Van Calenbergh, S.; Nelis, H. J.; Coenye, T. *Microbiology* **2009,** *155*, 4114-4122.
13. Storz, M. P.; Maurer, C. K.; Zimmer, C.; Wagner, N.; Brengel, C.; de Jong, J. C.; Lucas, S.; Musken, M.; Haussler, S.; Steinbach, A.; Hartmann, R. W. *J. Am. Chem. Soc.* **2012,** *134*, 16143-16146.
14. Lu, C.; Maurer, C. K.; Kirsch, B.; Steinbach, A.; Hartmann, R. W. *Angew. Chem. Int. Ed.* **2014,** *53*, 1109-1112.

15. Bjarnsholt, T.; Givskov, M. *Anal. Bioanal. Chem.* **2007,** *387*, 409-414.

16. Rumbaugh, K. P.; Griswold JA, F. A. U.; Hamood, A. N. *Microbes. Infect.* **2000,** *2*, 1721-1731.

17. Smith, R. S.; Iglewski, B. H. *Curr. Opin. Microbiol.* **2003,** *6*, 56-60.

18. Gambello, M. J.; Iglewski, B. H. *J. Bacteriol.* **1991,** *173*, 3000-3009.

19. Passador, L.; Cook, J. M.; Gambello, M. J.; Rust, L.; Iglewski, B. H. *Science* **1993,** *260*, 1127-1130.

20. Diggle, S. P.; Matthijs, S.; Wright, V. J.; Fletcher, M. P.; Chhabra, S. R.; Lamont, I. L.; Kong, X.; Hider, R. C.; Cornelis, P.; Camara, M.; Williams, P. *Chem Biol.* **2007,** *14*, 87-96.

21. Singh, P. K.; Schaefer, A. L.; Parsek, M. R.; Moninger, T. O.; Welsh, M. J.; Greenberg, E. P. *Nature* **2000,** *407*, 762-764.

22. Collier, D. N.; Anderson, L.; McKnight, S. L.; Noah, T. L.; Knowles, M.; Boucher, R.; Schwab, U.; Gilligan, P.; Pesci, E. C. *FEMS Microbiology Lett.* **2002,** *215*, 41-46.

23. Calfee, M. W.; Coleman, J. P.; Pesci, E. C. *Proc. Natl. Acad. Sci. U. S. A.* **2001,** *98*, 11633-11637.

24. Bredenbruch, F.; Nimtz, M.; Wray, V.; Morr, M.; Muller, R.; Haussler, S. *J. Bacteriol.* **2005,** *187*, 3630-3635.

25. D'Argenio, D. A.; Calfee, M. W.; Rainey, P. B.; Pesci, E. C. *J. Bacteriol.* **2002,** *184*, 6481-6489.

26. Farrow, J. M.; Pesci, E. C. *J. Bacteriol.* **2007,** *189*, 3425-3433.

27. Palmer, K. L.; Mashburn, L. M.; Singh, P. K.; Whiteley, M. *J. Bacteriol.* **2005,** *187*, 5267-5277.

28. Christian, V. D.; Barbara, H., I *Emerg. Infect. Dis.* **1998,** *4*, 551-560.

29. Pearson, J. P.; Passador, L. F.; Iglewski BH, F. A. U.; Greenberg, E. P. *Proc. Natl. Acad. Sci. U. S. A* **1995,** *92*, 1490-1494.

30. Ochsner, U. A.; Koch, A. K.; Fiechter, A.; Reiser, J. *J. Bacteriol.* **1994,** *176*, 2044-2054.

31. Latifi, A.; Winson MK, F. A. U.; Foglino, M. F.; Bycroft BW, F. A. U.; Stewart GS, F. A. U.; Lazdunski, A. F.; Williams, P. *Mol. Microbiol.* **1995,** *17*, 333-343.

32. Ochsner, U. A.; Reiser, J. *Proc. Natl. Acad. Sci. U. S. A.* **1995,** *92*, 6424-6428.

33. Bredenbruch, F. *Environ. Microbiol.* **2006,** *8*, 1318-1329.

34. Mashburn, L. M.; Whiteley, M. *Nature* **2005,** *437*, 422-425.

35. Diggle, S. P.; Winzer, K.; Chhabra, S. R.; Worrall, K. E.; Camara, M.; Williams, P. *Mol. Microbiol.* **2003,** *50*, 29-43.

36. Guina, T.; Purvine, S. O.; Yi, E. C.; Eng, J.; Goodlett, D. R.; Aebersold, R.; Miller, S. I. *Proc. Natl. Acad. Sci. U. S. A.* **2003,** *100*, 2771-2776.

37. Kim, K.; Kim, Y. U.; Koh, B. H.; Hwang, S. S.; Kim, S. H.; Lepine, F.; Cho, Y. H.; Lee, G. R. *Immunology* **2010,** *129*, 578-588.

38. Hooi, D. S. W.; Bycroft, B. W.; Chhabra, S. R.; Williams, P.; Pritchard, D. I. *Infect. Immun.* **2004,** *72*, 6463-6470.

39. Dubern, J. F.; Diggle, S. P. *Mol. BioSyst.* **2008,** *4*, 882-888.

40. Diggle, S. P.; Cornelis, P.; Williams, P.; Camara, M. *Int. J. Med. Microbiol.* **2006,** *296*, 83-91.

41. Gallagher, L. A.; McKnight, S. L.; Kuznetsova, M. S.; Pesci, E. C.; Manoil, C. *J. Bacteriol.* **2002,** *184*, 6472-6480.

42. Pesci, E. C.; Milbank, J. B. J.; Pearson, J. P.; McKnight, S.; Kende, A. S.; Grennberg, E. P.; Iglewski, B. H. *Proc. Natl. Acad. Sci. U. S. A.* **1999,** *96*, 11229-11234.

43. Somanathan, R.; Smith, K. M. *J. Het. Chem.* **1981,** *18*, 1077-1079.

44. Woscheka, A.; Mahouta, M.; Mereiterb, K.; Hammerschmidt, F. *Synthesis* **2007,** *10*, 1517–1522.

45. Epstein, J.; Cannon, P.; Swidler, R.; Baraze, A. *J. Org. Chem.* **1977,** *42*, 759-762.

46. Lepine, F.; Deziel, E.; Milot, S.; Rahme, L. G. *Biochim. Biophys. Acta* **2003,** *1622*, 36-41.

47. Oikawa, Y.; Sugano, K.; Yonemitsu, O. *J. Org. Chem.* **1978,** *43*, 2087-2088.

48. Lokot, I. P.; Pashkovsky, F. S.; Lakhvich, F. A. *Tetrahedron* **1999,** *55*, 4783-4792.

49. Hodgkinson, J.; Bowden, S. D.; Galloway, W. R. J. D.; Spring, D. R.; Welch, M. *J. Bacteriol.* **2010,** *192*, 3833-3837.

50. Fletcher, M. P.; Diggle, S. P.; Crusz, S. A.; Chhabra, S. R.; Camara, M.; Williams, P. *Environ. Microbiol.* **2007,** *9*, 2683-2693.

51. Reen, F. J.; Legendre, C.; O'Gara, F.; Clarke, S. L.; McSweeney, C. M.; Eccles, K. S.; Lawrence, S. E.; McGlacken, G. P. *Organic and Biomolecular Chemistry* **2012,** *10*, 8903-8910.

52. Reen, F. J.; Mooij, M. J.; Holcombe, L. J.; McSweeney, C. M.; McGlacken, G. P.; Morrissey, J. P.; O'Gara, F. *FEMS Microbiol. Ecol.* **2011,** *77*, 413-428.

53. Lu, C.; Kirsch, B.; Maurer, C. K.; de Jong, J. C.; Braunshausen, A.; Steinbach, A.; Hartmann, R. W. *Eur. J. Med. Chem.* **2014,** *79*, 173-183.

54. Staskun, B. *J. Org. Chem.* **1988,** *53*, 5287-5291.

55. Mphahele, M. J.; Nwamadi, M. S.; Mabeta, P. *J. Het. Chem.* **2006,** *43*, 255-260.

56. Liu, Z. L.; Chu, S. S.; Jiang, G. H. *J. Agric. Food Chem.* **2009,** *57*, 10130-10133.

57. Miyaura, N.; Suzuki, A. *Chem. Rev.* **1995,** *95*, 2457-2483.

58. Lennox, A. J. J.; Lloyd-Jones, G. C. *Angew. Chem. Int. Ed.* **2013,** *52*, 7362-7370.

59. Glasser, N. R.; Kern, S. E.; Newman, D. K. *Mol. Microbiol.* **2014,** *92*, 399-412.

60. Wei, Q.; Ma, L. Z. *Int. J. Mol. Sci.* **2013,** *14*, 20983-21005.

61. Burke, S. A.; Wright, J. D.; Robinson, M. K.; Bronk, B. V.; Warren, R. L. *Appl. Environ. Microbiol.* **2004,** *70*, 2786-2790.

62. Tashiro, Y.; Uchiyama, H.; Nomura, N. *Microbes. Environ.* **2012,** *25*, 120-125.

Appendix 2

II. Single Crystal Analysis Reports

*****Note: All single crystal analysis was carried out by members of the Dr. Simon Lawrence research group in University College Cork.

Crystallographic data for N,N'-bis((*S*)-2-hydroxy-1-phenylethyl)-2,2-dimethylmalonamide **(*S*,*S*)-240**

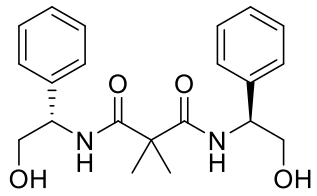

checkCIF/PLATON report

You have not supplied any structure factors. As a result the full set of tests cannot be run.

No syntax errors found. CIF dictionary Interpreting this report

Datablock: I

```
Bond precision:  C-C = 0.0045 A          Wavelength=0.71073

Cell:            a=8.423(3)    b=11.261(3)          c=11.347(4)
                 alpha=90      beta=91.054(12)      gamma=90
Temperature:     300 K
```

	Calculated	Reported
Volume	1076.1(6)	1076.1(7)
Space group	P 21	P 1 21 1
Hall group	P 2yb	P 2yb
Moiety formula	C21 H26 N2 O4, 2(H2 O)	C21 H26 N2 O4, 2(H2 O)
Sum formula	C21 H30 N2 O6	C21 H30 N2 O6
Mr	406.47	406.47
Dx,g cm-3	1.255	1.254
Z	2	2
Mu (mm-1)	0.092	0.092
F000	436.0	436.0
F000’	436.22	
h,k,lmax	9,13,13	9,13,13
Nref	1981[3754]	3505
Tmin,Tmax	0.985,0.995	0.960,1.000
Tmin’	0.965	

```
Correction method= MULTI-SCAN

Data completeness= 1.77/0.93      Theta(max)= 24.920

R(reflections)= 0.0411( 2599)     wR2(reflections)= 0.0944( 3505)

S = 1.016                 Npar= 290
```

The following ALERTS were generated. Each ALERT has the format
test-name_ALERT_alert-type_alert-level.
Click on the hyperlinks for more details of the test.

Alert level C

```
STRVA01_ALERT_4_C          Flack parameter is too small
          From the CIF: _refine_ls_abs_structure_Flack   -0.800
          From the CIF: _refine_ls_abs_structure_Flack_su    1.300
PLAT033_ALERT_4_C Flack x Parameter Value Deviates from Zero .....     -0.800
```

```
PLAT340_ALERT_3_C Low Bond Precision on  C-C Bonds ..............     0.0045 Ang
PLAT420_ALERT_2_C D-H Without Acceptor       N10    -   H10    ...          ?
```

Alert level G

```
REFLT03_ALERT_4_G  ALERT: MoKa measured Friedel data cannot be used to
                   determine absolute structure in a light-atom
                   study EXCEPT under VERY special conditions.
                   It is preferred that Friedel data is merged in such cases.
           From the CIF: _diffrn_reflns_theta_max           24.92
           From the CIF: _reflns_number_total               3505
           Count of symmetry unique reflns         1981
           Completeness (_total/calc)            176.93%
           TEST3: Check Friedels for noncentro structure
           Estimate of Friedel pairs measured      1524
           Fraction of Friedel pairs measured     0.769
           Are heavy atom types Z>Si present         no
PLAT002_ALERT_2_G Number of Distance or Angle Restraints on AtSite          6
PLAT005_ALERT_5_G No _iucr_refine_instructions_details in CIF ....          ?
PLAT032_ALERT_4_G Std. Uncertainty on Flack Parameter Value High .      1.300
PLAT791_ALERT_4_G Note: The Model has Chirality at C7     (Verify)          S
PLAT791_ALERT_4_G Note: The Model has Chirality at C19    (Verify)          S
PLAT860_ALERT_3_G Note: Number of Least-Squares Restraints .......          5
```

---

   0 **ALERT level A** = Most likely a serious problem - resolve or explain
   0 **ALERT level B** = A potentially serious problem, consider carefully
   4 **ALERT level C** = Check. Ensure it is not caused by an omission or oversight
   7 **ALERT level G** = General information/check it is not something unexpected

   0 ALERT type 1 CIF construction/syntax error, inconsistent or missing data
   2 ALERT type 2 Indicator that the structure model may be wrong or deficient
   2 ALERT type 3 Indicator that the structure quality may be low
   6 ALERT type 4 Improvement, methodology, query or suggestion
   1 ALERT type 5 Informative message, check

It is advisable to attempt to resolve as many as possible of the alerts in all categories. Often the minor alerts point to easily fixed oversights, errors and omissions in your CIF or refinement strategy, so attention to these fine details can be worthwhile. In order to resolve some of the more serious problems it may be necessary to carry out additional measurements or structure refinements. However, the purpose of your study may justify the reported deviations and the more serious of these should normally be commented upon in the discussion or experimental section of a paper or in the "special_details" fields of the CIF. checkCIF was carefully designed to identify outliers and unusual parameters, but every test has its limitations and alerts that are not important in a particular case may appear. Conversely, the absence of alerts does not guarantee there are no aspects of the results needing attention. It is up to the individual to critically assess their own results and, if necessary, seek expert advice.

Publication of your CIF in IUCr journals

A basic structural check has been run on your CIF. These basic checks will be run on all CIFs submitted for publication in IUCr journals (*Acta Crystallographica, Journal of Applied Crystallography, Journal of Synchrotron Radiation*); however, if you intend to submit to *Acta Crystallographica Section C* or *E*, you should make sure that full publication checks are run on the final version of your CIF prior to submission.

Publication of your CIF in other journals

Please refer to the *Notes for Authors* of the relevant journal for any special instructions relating to CIF submission.

PLATON version of 18/07/2011; check.def file version of 04/07/2011

Datablock I - ellipsoid plot

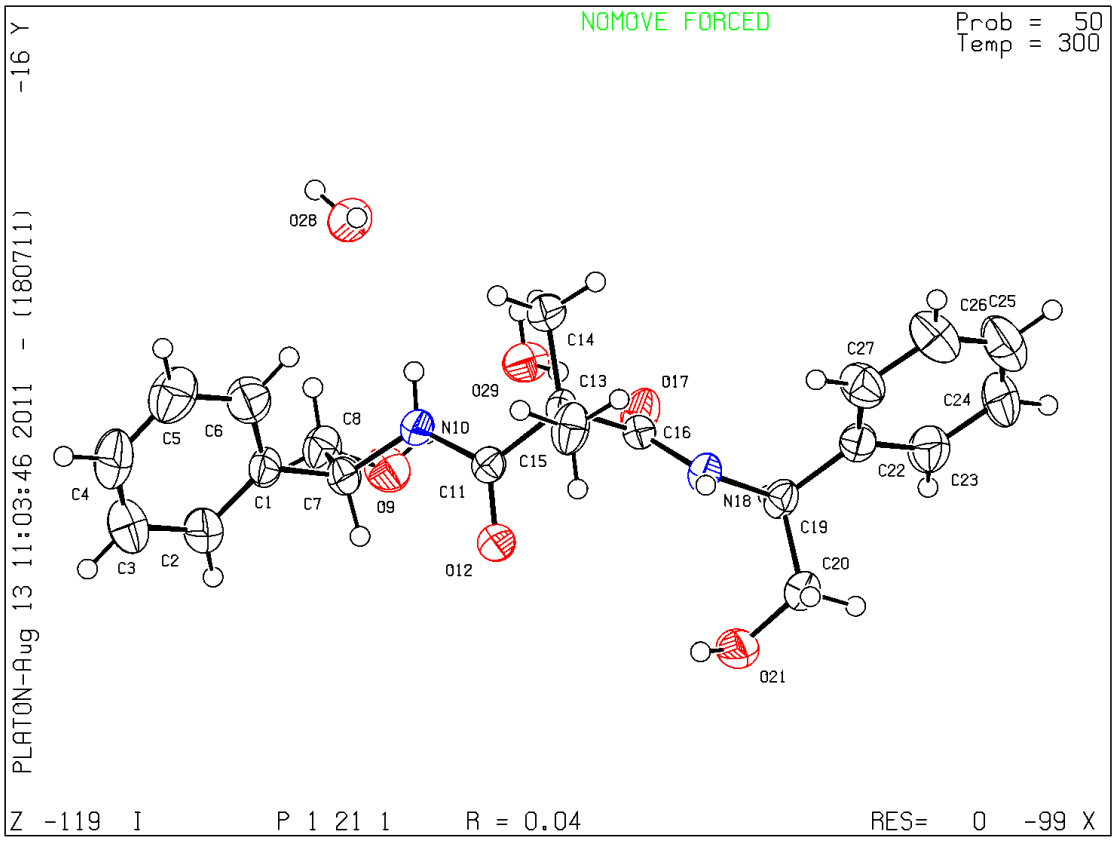

Crystallographic data for (1*S*,3*S*)-1-(((*S*)-*tert*-butylsulfinyl)amino)-4,4-dimethyl-1-phenylpentan-3-yl pivalate **(*S*,*S*,*S*)-275**

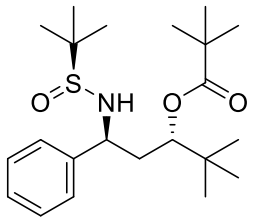

checkCIF/PLATON report

You have not supplied any structure factors. As a result the full set of tests cannot be run.

THIS REPORT IS FOR GUIDANCE ONLY. IF USED AS PART OF A REVIEW PROCEDURE FOR PUBLICATION, IT SHOULD NOT REPLACE THE EXPERTISE OF AN EXPERIENCED CRYSTALLOGRAPHIC REFEREE.

No syntax errors found. CIF dictionary Interpreting this report

Datablock: I

Bond precision: C-C = 0.0048 A Wavelength=0.71073

Cell: a=9.6296(11) b=10.9154(19) c=23.692(4)
alpha=90 beta=90 gamma=90
Temperature: 296 K

	Calculated	Reported
Volume	2490.3(7)	2490.3(6)
Space group	P 21 21 21	P 21 21 21
Hall group	P 2ac 2ab	P 2ac 2ab
Moiety formula	C22 H37 N O3 S	?
Sum formula	C22 H37 N O3 S	C22 H37 N O3 S
Mr	395.60	395.59
Dx,g cm-3	1.055	1.055
Z	4	4
Mu (mm-1)	0.149	0.149
F000	864.0	864.0
F000'	864.83	
h,k,lmax	12,13,29	12,13,29
Nref	5133[2918]	5094
Tmin,Tmax	0.968,0.987	0.870,0.990
Tmin'	0.927	

Correction method= MULTI-SCAN

Data completeness= 1.75/0.99 Theta(max)= 26.470

R(reflections)= 0.0494(3286) wR2(reflections)= 0.1164(5094)

S = 1.007 Npar= Npar = 257

The following ALERTS were generated. Each ALERT has the format
test-name_ALERT_alert-type_alert-level.
Click on the hyperlinks for more details of the test.

Alert level B

PLAT035_ALERT_1_B No _chemical_absolute_configuration info given . Please Do !
PLAT242_ALERT_2_B Low Ueq as Compared to Neighbors for ..... C25 Check

---

Alert level C

PLAT213_ALERT_2_C Atom C26 has ADP max/min Ratio ..... 3.2 prolat
PLAT220_ALERT_2_C Large Non-Solvent C Ueq(max)/Ueq(min) Range 4.6 Ratio
PLAT222_ALERT_3_C Large Non-Solvent H Uiso(max)/Uiso(min) .. 5.8 Ratio
PLAT230_ALERT_2_C Hirshfeld Test Diff for C25 -- C27 .. 5.8 su
PLAT241_ALERT_2_C High Ueq as Compared to Neighbors for ..... C3 Check
PLAT242_ALERT_2_C Low Ueq as Compared to Neighbors for ..... C1 Check
PLAT242_ALERT_2_C Low Ueq as Compared to Neighbors for ..... C10 Check
PLAT242_ALERT_2_C Low Ueq as Compared to Neighbors for ..... C18 Check
PLAT242_ALERT_2_C Low Ueq as Compared to Neighbors for ..... C23 Check
PLAT340_ALERT_3_C Low Bond Precision on C-C Bonds ..... 0.0048 Ang.

Alert level G

PLAT005_ALERT_5_G No _iucr_refine_instructions_details in the CIF Please Do !
PLAT791_ALERT_4_G The Model has Chirality at C7 ..... S Verify
PLAT791_ALERT_4_G The Model has Chirality at C9 ..... S Verify

---

0 **ALERT level A** = Most likely a serious problem - resolve or explain
2 **ALERT level B** = A potentially serious problem, consider carefully
10 **ALERT level C** = Check. Ensure it is not caused by an omission or oversight
3 **ALERT level G** = General information/check it is not something unexpected

1 ALERT type 1 CIF construction/syntax error, inconsistent or missing data
9 ALERT type 2 Indicator that the structure model may be wrong or deficient
2 ALERT type 3 Indicator that the structure quality may be low
2 ALERT type 4 Improvement, methodology, query or suggestion
1 ALERT type 5 Informative message, check

It is advisable to attempt to resolve as many as possible of the alerts in all categories. Often the minor alerts point to easily fixed oversights, errors and omissions in your CIF or refinement strategy, so attention to these fine details can be worthwhile. In order to resolve some of the more serious problems it may be necessary to carry out additional measurements or structure refinements. However, the purpose of your study may justify the reported deviations and the more serious of these should normally be commented upon in the discussion or experimental section of a paper or in the "special_details" fields of the CIF. checkCIF was carefully designed to identify outliers and unusual parameters, but every test has its limitations and alerts that are not important in a particular case may appear. Conversely, the absence of alerts does not guarantee there are no aspects of the results needing attention. It is up to the individual to critically assess their own results and, if necessary, seek expert advice.

Publication of your CIF in IUCr journals

A basic structural check has been run on your CIF. These basic checks will be run on all CIFs submitted for publication in IUCr journals (*Acta Crystallographica, Journal of Applied Crystallography, Journal of Synchrotron Radiation*); however, if you intend to submit to *Acta Crystallographica Section C* or *E*, you should make sure that full publication checks are run on the final version of your CIF prior to submission.

Publication of your CIF in other journals

Please refer to the *Notes for Authors* of the relevant journal for any special instructions relating to CIF submission.

PLATON version of 05/02/2014; check.def file version of 05/02/2014

Datablock I - ellipsoid plot

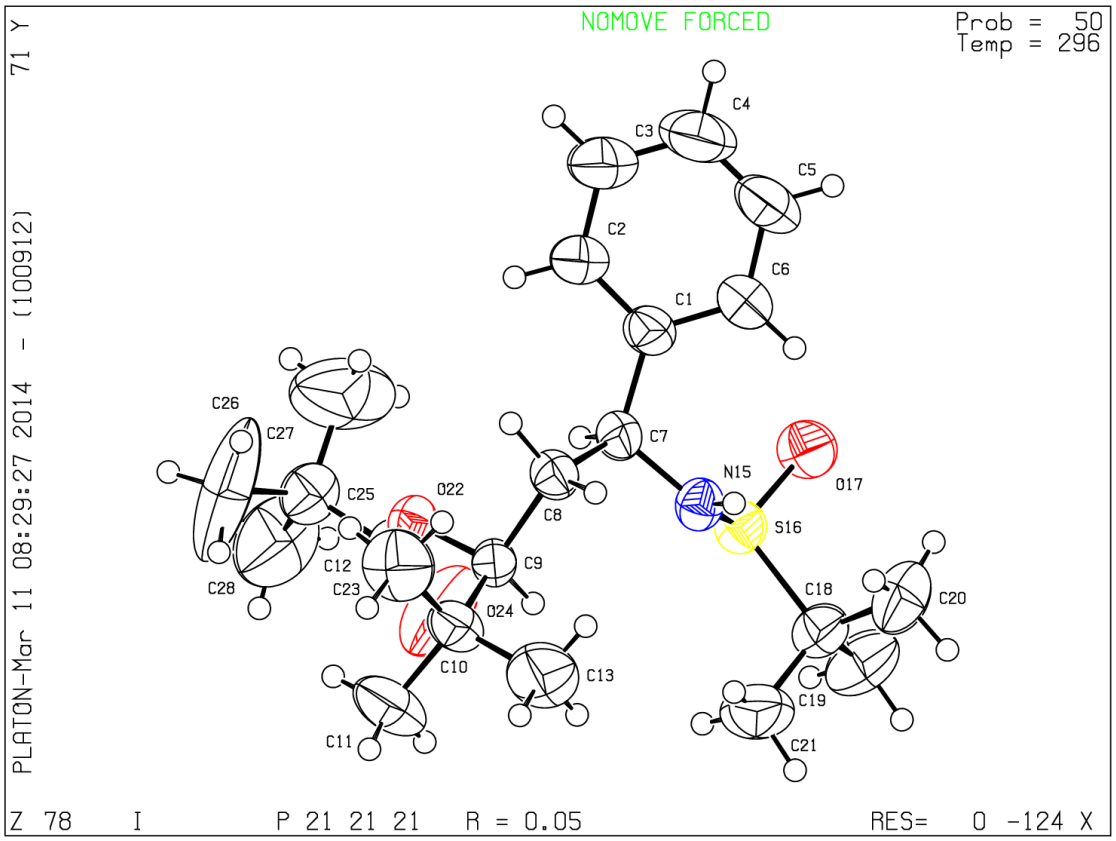

Crystallographic data for (*S*)-N-(3-hydroxy-4,4-dimethyl-1-phenylpentyl)-2-methylpropane-2-sulfinamide **(*S*)-278**

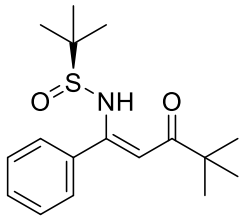

checkCIF/PLATON report

You have not supplied any structure factors. As a result the full set of tests cannot be run.

THIS REPORT IS FOR GUIDANCE ONLY. IF USED AS PART OF A REVIEW PROCEDURE FOR PUBLICATION, IT SHOULD NOT REPLACE THE EXPERTISE OF AN EXPERIENCED CRYSTALLOGRAPHIC REFEREE.

No syntax errors found. CIF dictionary Interpreting this report

Datablock: I

```
Bond precision:  C-C = 0.0095 A          Wavelength=0.71073

Cell:            a=10.200(9)    b=9.406(8)           c=10.462(9)
                 alpha=90       beta=116.167(13)     gamma=90
Temperature:     296 K

                 Calculated                Reported
Volume           900.9(14)                 900.9(13)
Space group      P 21                      P 1 21 1
Hall group       P 2yb                     P 2yb
Moiety formula   C17 H25 N O2 S            C17 H25 N O2 S
Sum formula      C17 H25 N O2 S            C17 H25 N O2 S
Mr               307.44                    307.44
Dx,g cm-3        1.133                     1.133
Z                2                         2
Mu (mm-1)        0.184                     0.184
F000             332.0                     332.0
F000'            332.37
h,k,lmax         12,11,13                  12,11,13
Nref             3892[ 2067]               3707
Tmin,Tmax        0.970,0.978               0.910,0.980
Tmin'            0.950

Correction method= MULTI-SCAN

Data completeness= 1.79/0.95      Theta(max)= 26.920

R(reflections)= 0.0632( 1776)     wR2(reflections)= 0.2204( 3707)

S = 1.058                 Npar= 195
```

The following ALERTS were generated. Each ALERT has the format
test-name_ALERT_alert-type_alert-level.
Click on the hyperlinks for more details of the test.

Alert level B

Crystal system given = monoclinic

PLAT201_ALERT_2_B Isotropic non-H Atoms in Main Residue(s) .... 3 Report

---

Alert level C

PLAT026_ALERT_3_C Ratio Observed / Unique Reflections too Low .... 48 %
PLAT029_ALERT_3_C _diffrn_measured_fraction_theta_full Low ..... 0.979 Note
PLAT230_ALERT_2_C Hirshfeld Test Diff for C17 -- C18 .. 5.2 su
PLAT242_ALERT_2_C Low Ueq as Compared to Neighbors for ..... C10 Check
PLAT242_ALERT_2_C Low Ueq as Compared to Neighbors for ..... C17 Check
PLAT340_ALERT_3_C Low Bond Precision on C-C Bonds ..... 0.0095 Ang.

Alert level G

PLAT002_ALERT_2_G Number of Distance or Angle Restraints on AtSite 10 Note
PLAT003_ALERT_2_G Number of Uiso or Uij Restrained non-H Atoms ... 1 Report
PLAT072_ALERT_2_G SHELXL First Parameter in WGHT Unusually Large. 0.11 Report
PLAT172_ALERT_4_G The CIF-Embedded .res File Contains DFIX Records 2 Report
PLAT301_ALERT_3_G Main Residue Disorder ..... Percentage = 14 Note
PLAT860_ALERT_3_G Number of Least-Squares Restraints ..... 35 Note

---

0 **ALERT level A** = Most likely a serious problem - resolve or explain
1 **ALERT level B** = A potentially serious problem, consider carefully
6 **ALERT level C** = Check. Ensure it is not caused by an omission or oversight
6 **ALERT level G** = General information/check it is not something unexpected

0 ALERT type 1 CIF construction/syntax error, inconsistent or missing data
7 ALERT type 2 Indicator that the structure model may be wrong or deficient
5 ALERT type 3 Indicator that the structure quality may be low
1 ALERT type 4 Improvement, methodology, query or suggestion
0 ALERT type 5 Informative message, check

It is advisable to attempt to resolve as many as possible of the alerts in all categories. Often the minor alerts point to easily fixed oversights, errors and omissions in your CIF or refinement strategy, so attention to these fine details can be worthwhile. In order to resolve some of the more serious problems it may be necessary to carry out additional measurements or structure refinements. However, the purpose of your study may justify the reported deviations and the more serious of these should normally be commented upon in the discussion or experimental section of a paper or in the "special_details" fields of the CIF. checkCIF was carefully designed to identify outliers and unusual parameters, but every test has its limitations and alerts that are not important in a particular case may appear. Conversely, the absence of alerts does not guarantee there are no aspects of the results needing attention. It is up to the individual to critically assess their own results and, if necessary, seek expert advice.

Publication of your CIF in IUCr journals

A basic structural check has been run on your CIF. These basic checks will be run on all CIFs submitted for publication in IUCr journals (*Acta Crystallographica, Journal of Applied Crystallography, Journal of Synchrotron Radiation*); however, if you intend to submit to *Acta Crystallographica Section C* or *E*, you should make sure that full publication checks are run on the final version of your CIF prior to submission.

Publication of your CIF in other journals

Please refer to the *Notes for Authors* of the relevant journal for any special instructions relating to CIF submission.

PLATON version of 20/08/2014; check.def file version of 18/08/2014

Datablock I - ellipsoid plot

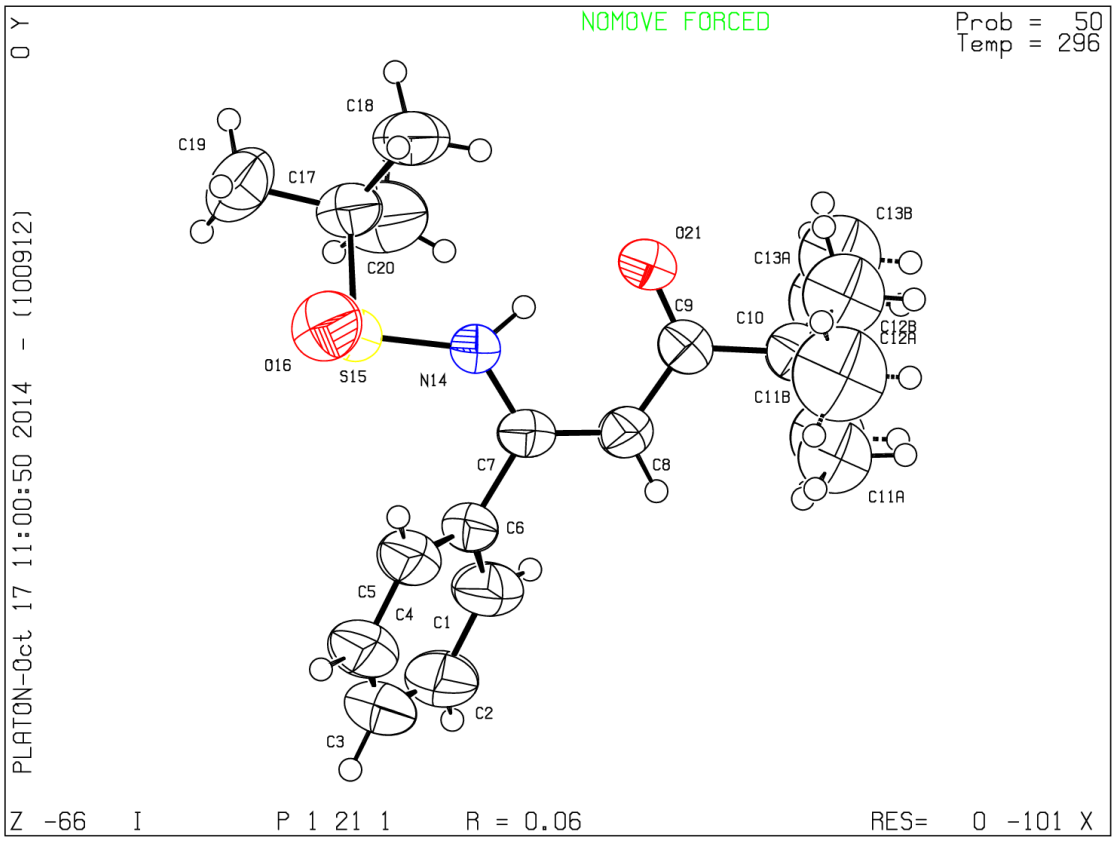

Crystallographic data for 2-heptylquinolin-4(1*H*)-one.HCl **307**

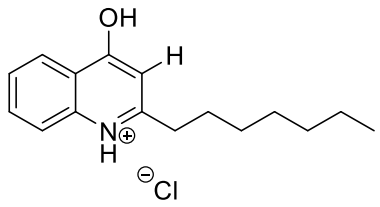

checkCIF/PLATON report

You have not supplied any structure factors. As a result the full set of tests cannot be run.

THIS REPORT IS FOR GUIDANCE ONLY. IF USED AS PART OF A REVIEW PROCEDURE FOR PUBLICATION, IT SHOULD NOT REPLACE THE EXPERTISE OF AN EXPERIENCED CRYSTALLOGRAPHIC REFEREE.

No syntax errors found. CIF dictionary Interpreting this report

Datablock: I

```
Bond precision:  C-C = 0.0049 A          Wavelength=0.71073

Cell:            a=10.221(7)    b=13.132(8)          c=12.143(8)
                 alpha=90       beta=106.090(18)     gamma=90
Temperature:     296 K
```

	Calculated	Reported
Volume	1566.0(18)	1566.0(17)
Space group	P 21/n	P 1 21/n 1
Hall group	-P 2yn	-P 2yn
Moiety formula	C16 H22 N O, Cl	C16 H22 N O, Cl
Sum formula	C16 H22 Cl N O	C16 H22 Cl N O
Mr	279.80	279.80
Dx,g cm-3	1.187	1.187
Z	4	4
Mu (mm-1)	0.237	0.237
F000	600.0	600.0
F000’	600.79	
h,k,lmax	12,16,15	12,16,15
Nref	3245	3226
Tmin,Tmax	0.961,0.974	0.637,0.745
Tmin’	0.951	

```
Correction method= MULTI-SCAN

Data completeness= 0.994          Theta(max)= 26.510

R(reflections)= 0.0559( 1682)     wR2(reflections)= 0.1690( 3226)

S = 1.087                 Npar= 177
```

The following ALERTS were generated. Each ALERT has the format
test-name_ALERT_alert-type_alert-level.
Click on the hyperlinks for more details of the test.

Alert level C

```
PLAT230_ALERT_2_C Hirshfeld Test Diff for    C5     --  C6      ..        6.0 su
PLAT340_ALERT_3_C Low Bond Precision on  C-C Bonds ..............     0.0049 Ang.
```

Alert level G

```
PLAT003_ALERT_2_G Number of Uiso or Uij Restrained non-H Atoms ...          1 Report
PLAT007_ALERT_5_G Number of Unrefined Donor-H Atoms ..............          1 Report
PLAT860_ALERT_3_G Number of Least-Squares Restraints .............          6 Note
```

```
   0 ALERT level A = Most likely a serious problem - resolve or explain
   0 ALERT level B = A potentially serious problem, consider carefully
   2 ALERT level C = Check. Ensure it is not caused by an omission or oversight
   3 ALERT level G = General information/check it is not something unexpected

   0 ALERT type 1 CIF construction/syntax error, inconsistent or missing data
   2 ALERT type 2 Indicator that the structure model may be wrong or deficient
   2 ALERT type 3 Indicator that the structure quality may be low
   0 ALERT type 4 Improvement, methodology, query or suggestion
   1 ALERT type 5 Informative message, check
```

It is advisable to attempt to resolve as many as possible of the alerts in all categories. Often the minor alerts point to easily fixed oversights, errors and omissions in your CIF or refinement strategy, so attention to these fine details can be worthwhile. In order to resolve some of the more serious problems it may be necessary to carry out additional measurements or structure refinements. However, the purpose of your study may justify the reported deviations and the more serious of these should normally be commented upon in the discussion or experimental section of a paper or in the "special_details" fields of the CIF. checkCIF was carefully designed to identify outliers and unusual parameters, but every test has its limitations and alerts that are not important in a particular case may appear. Conversely, the absence of alerts does not guarantee there are no aspects of the results needing attention. It is up to the individual to critically assess their own results and, if necessary, seek expert advice.

Publication of your CIF in IUCr journals

A basic structural check has been run on your CIF. These basic checks will be run on all CIFs submitted for publication in IUCr journals (*Acta Crystallographica*, *Journal of Applied Crystallography*, *Journal of Synchrotron Radiation*); however, if you intend to submit to *Acta Crystallographica Section C* or *E*, you should make sure that full publication checks are run on the final version of your CIF prior to submission.

Publication of your CIF in other journals

Please refer to the *Notes for Authors* of the relevant journal for any special instructions relating to CIF submission.

PLATON version of 20/08/2014; check.def file version of 18/08/2014

Datablock I - ellipsoid plot

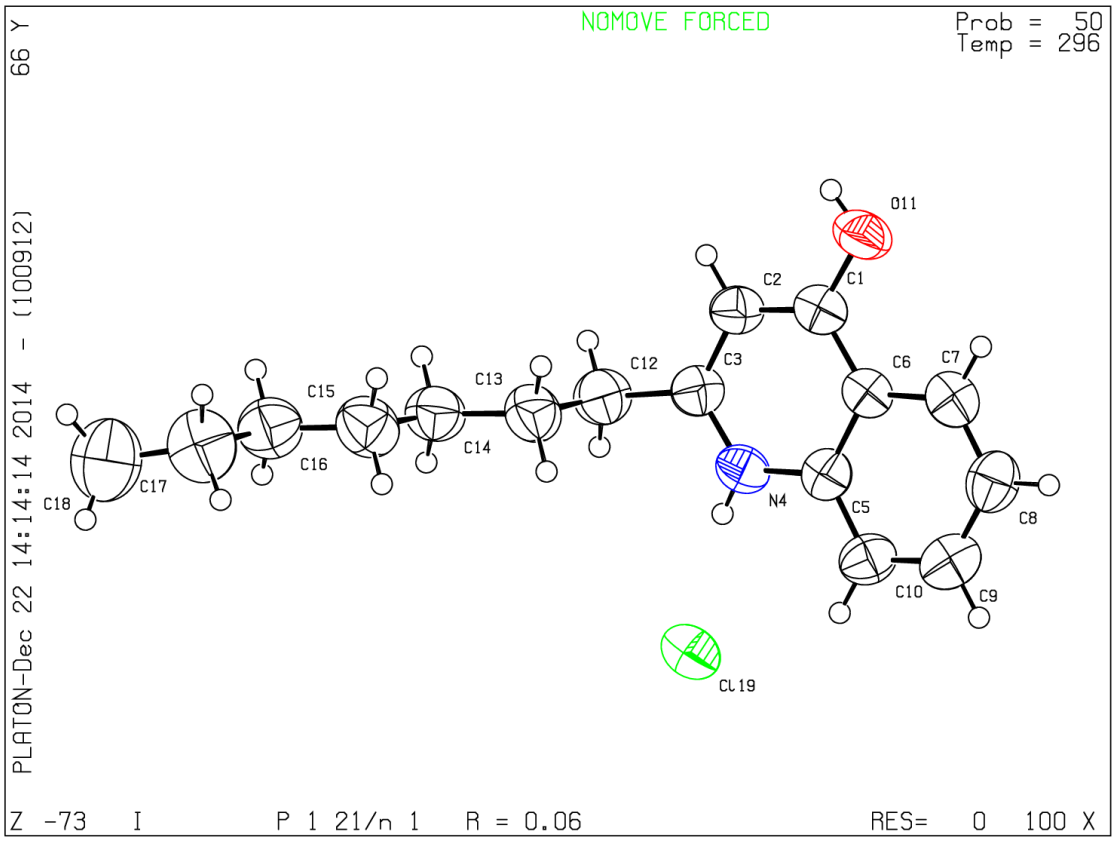

II. Publications

ChemComm

COMMUNICATION

View Article Online
View Journal | View Issue

Cite this: *Chem. Commun.*, 2014, **50**, 14817

Received 1st September 2014,
Accepted 30th September 2014

DOI: 10.1039/c4cc06895e

www.rsc.org/chemcomm

The asymmetric alkylation of dimethylhydrazones; intermolecular chirality transfer using sparteine as chiral ligand†

Christina M. McSweeney, Vera M. Foley and Gerard P. McGlacken*

The asymmetric alkylation of ketones represents a fundamental transformation in organic chemistry. Chiral auxiliaries have been used almost exclusively for this transformation. Herein we describe a strategy for the generation of enantiomerically enriched α-alkylated ketones up to an er of 83 : 17, using a chiral ligand protocol.

A large number of optically active drugs and natural products contain α-functionalized ketones, or simple derivatives there-of. Furthermore, chiral α-alkylated ketones are very useful synthons and have found widespread use in total synthesis.[1] Thus, the asymmetric alkylation of ketones represents a very useful transformation in organic chemistry. Surprisingly however, only one effective methodology is available for acyclic systems, and this involves the use of chiral auxiliaries.

The well-known, proline derived, SAMP/RAMP auxiliaries (Scheme 1(i)) have found numerous applications in asymmetric alkylation.[1c] For example, Nicolaou *et al.* applied the SAMP auxiliary of 3-pentanone in an asymmetric alkylation en route to swinholide A.[2] More recently Coltart has introduced *N*-amino cyclic carbamate (ACC) chiral auxiliaries (Scheme 1(ii)).[3] These auxiliaries do not require the extremely low alkylation temperatures used with SAMP/RAMP hydrazones. The ACC methodology has already been utilized in the synthesis of several biologically important compounds.[4]

Moreover, it is worth noting that despite the advances in the use of homo chiral lithium amide bases,[5] transition metal catalysis[6] and organocatalysis,[7] none of these areas of research have managed to achieve the asymmetric α-alkylation of acyclic ketones.

Our approach to chiral α-alkylated ketones involves the use of simple non-chiral dimethylhydrazones and effecting their asymmetric alkylation using a chiral diamine ligand (Scheme 1(iii)).

The use of lithium bases to furnish small aliphatic α-alkylated ketones, often proceeds in poor yield.[8] In light of this, we chose the dimethylhydrazone methodology.[9] Additionally, we postulated that deprotonation using an alkyl lithium–chiral diamine system would furnish a highly structured azaenolate benefiting from added chelation of the dimethylamino group (Scheme 2). Subsequent alkylation with high facial selectivity could provide chiral, alkylated dimethylhydrazones.

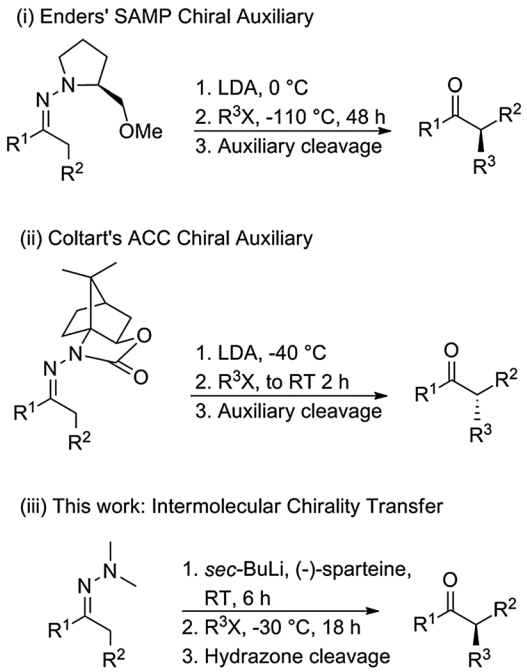

Scheme 1 Comparison of previously used methodology and our work.

Of the numerous chiral diamines available,[10] (−)-sparteine ((−)-sp) was chosen due to its efficiency and breadth of application.[11] For example, (−)-sp/lithium systems have proven useful in a number transformations involving asymmetric deprotonations and substitutions.[12] O'Brien and co-workers have used (−)-sp in the catalytic asymmetric deprotonation of *N*-Boc pyrrolidine.[13]

Firstly, 3-pentanone dimethylhydrazone **1**, 4-heptanone dimethylhydrazone **2** and cycloheptanone dimethylhydrazone

Analytical and Biological Chemistry Research Facility and Department of Chemistry, University College Cork, Cork, Ireland. E-mail: g.mcglacken@ucc.ie

† Electronic supplementary information (ESI) available. See DOI: 10.1039/c4cc06895e

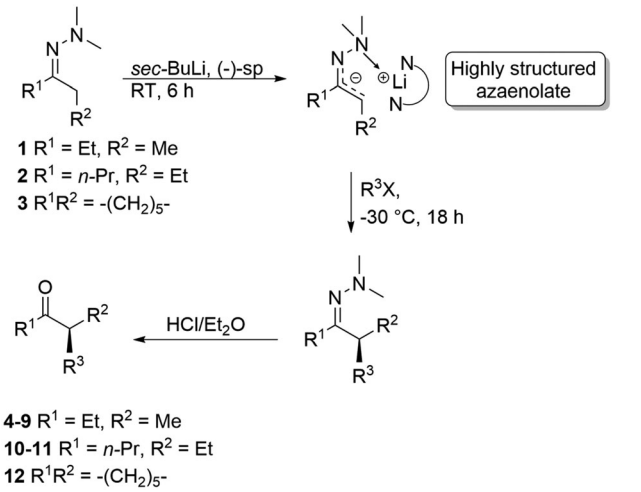

Scheme 2 General scheme for asymmetric alkylations *via* intermolecular chirality transfer.

Table 1 Solvent optimization studies on the dimethylhydrazones of 3-pentanone

Entry	Ligand	R^3X	Solvent	Yield[a] (%)	Ketone	er[c] *R*:*S*
1	(−)-sp	BnBr	THF	40	**4**	Racemic
2	(−)-sp	BnBr	Toluene	57	**4**	24:76
3	(−)-sp	BnBr	Cumene	62[b]	**4**	25:75
4	(−)-sp	BnBr	Benzene	45	**4**	31:69
5	(−)-sp	BnBr	Cyclohexane	23	**4**	31:69
6	(−)-sp	*n*-PeI	Toluene	34	**5**	17:83
7	(−)-sp	*n*-PeI	MTBE	32	**5**	33:67
8	(+)-sp	*n*-PeI	Et_2O	43	**5**	78:22

[a] Isolated yields over 2 steps after purification by column chromatography. [b] Yield determined using NMR and 1,3,5-trimethoxybenzene as internal standard. [c] er determined by chiral GC and absolute configuration assigned based on the optical rotation data of **4** and inferred for the others.

3 were prepared in near quantitative yields using dimethylhydrazine in the presence of a catalytic amount of AcOH. We focused our initial studies on establishing an optimum solvent for these reactions. Hydrazone **1** was subjected to (−)-sp/*sec*-BuLi deprotonation (room temperature for 6 h) and alkylated with either benzyl bromide or 1-iodopentane (−30 °C for 18 h), in a range of solvents (Table 1). The resultant alkylated hydrazones were hydrolysed using a biphasic 4 M HCl–diethyl ether system and the enantiomeric excess of the ketones **4** and **5** determined.[14] The enantioselectivity showed a high solvent dependence. The use of THF as solvent, afforded ketone **4** with no enantioenrichment (entry 1), probably due to competing coordination with (−)-sp to lithium.[15] Cumene as solvent gave good conversion to alkylated ketone (62% NMR yield over 2 steps) (entry 3).[16] The use of benzene, cyclohexane and MTBE gave poor enantioselectivity (entries 4, 5 and 7, Table 1). Diethyl ether afforded ketone **5** in good enantioselectivity (78:22 er) and moderate yield (43%) over 2 steps (entry 8). In this case, to demonstrate the accessibility of both enantiomers of the chiral ketone, (+)-sp was utilised.

Toluene was found to be the prime solvent for these reactions giving the best enantioenrichment of both **4** and **5**, 24:76 er (entry 2) and 17:83 er (entry 6), respectively. While conversion to product in toluene was high, yields remained moderate, most likely due to the high volatility of the resulting ketones.[17]

Table 2 Substrate scope in asymmetric alkylations using sparteine as chiral ligand

Entry[a]	Ligand	Hydrazone	R^3X	Yield[b] (%)	Ketone	er[c] *R*:*S*
1	(−)-sp	**1**	*n*-PeI	34	**5**	17:83
2	(+)-sp	**1**	*n*-PeI	31	**5**	81:19
3	(−)-sp	**1**	BnBr	57	**4**	24:76
4	(−)-sp	**1**	$C_6H_5CH{=}CHCH_2Br$	30	**6**	21:79
5	(+)-sp	**1**	$2\text{-}CH_3C_6H_4CH_2Br$	54	**7**	76:24
6	(+)-sp	**1**	$C_6(CH_3)_5CH_2Br$	60	**8**	81:19
7	(+)-sp	**1**	$4\text{-}t\text{-}BuC_6H_4CH_2Br$	62	**9**	71:29
8	(−)-sp	**2**	*n*-PeI	39	**10**	18:82
9	(+)-sp	**2**	*n*-HexI	53	**11**	80:20
10	(+)-sp	**3**	AllylBr	19	**12**	68:32[d]

[a] All reactions were performed in anhydrous toluene using optimized conditions as shown in Scheme 2. [b] Isolated yields over 2 steps after purification by column chromatography. [c] er determined by chiral GC. [d] Absolute configuration not determined.

Next we probed the scope of the reaction with a range of simple alkyl halides (Table 2). A clear trend is apparent, with the long chain alkyl halides proving less reactive (entries 1, 2, 8 and 9) compared with benzyl bromides (entries 3 and 5–7). Introduction of *n*-pentyl and *n*-hexyl moieties require an iodide leaving group. However, these slower reacting electrophiles did result in products (**5**, **10**, **11**) displaying the highest enantioenrichment.

The introduction of a methyl group at the 2-position of benzyl bromide (entry 5) had no effect on enantioselectivity in comparison to the unsubstituted benzyl bromide (entry 3), but the use of pentamethyl benzyl bromide showed a distinct increase in enantioselectivity (entry 6) in the final ketone. Also increased yields were observed for electrophiles resulting in less volatile ketone products (entries 6 and 7). Finally, cycloheptanone dimethylhydrazone was subjected to the standard conditions. The resulting allylated ketone **12** was isolated in 19% yield with an er of 68:32.

Interestingly, deprotonation of hydrazone **2** with LDA, followed by subsequent addition of (−)-sp, *n*-iodopentane and hydrolysis gave **10** in an er of 21:79 (Scheme 3). Significantly, only a slight drop in enantiomeric excess and yield is noticed in comparison to reaction when (−)-sp is added prior to deprotonation (entry 8, Table 2). In light of this we postulate that

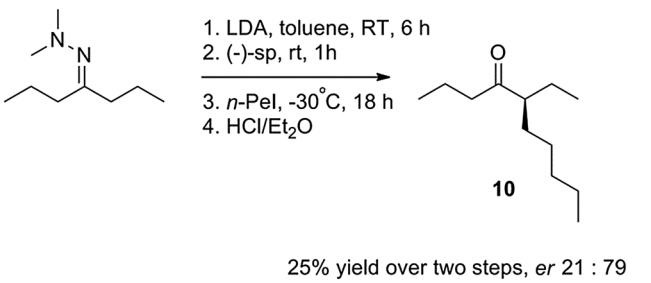

Scheme 3 Deprotonation prior to (−)-sp addition.

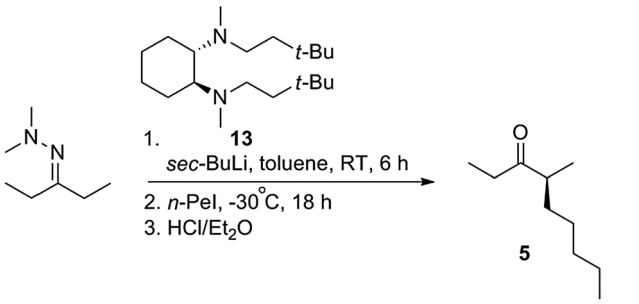

Scheme 4 Use of an easily-prepared chiral diamine.

asymmetric alkylation rather than (or at least in addition to) asymmetric deprotonation is operative.[18] Interestingly, the low nucleophilicity of LDA indicates that this methodology could be extended to the α-substitution of hydrazones derived from aldehydes, and esters.

Preliminary investigations show that easily-prepared chiral diamines such as **13**[19] can mediate these transformations also (Scheme 4). In contrast to sparteine, these ligands can be easily modified. Optimisation of ligands such as **13** and application to asymmetric alkylation reactions are currently underway.

In summary, to the best of our knowledge this report details the first example of asymmetric alkylation to a non-chiral acyclic aza(enolate). Optimisation studies involving the use of other chiral diamines are ongoing and will be reported in due course.

We thank Science Foundation Ireland (09/RFP/CHS2353) and the Irish Research Council for funding.

Notes and references

1 (*a*) M. C. Kohler, S. E. Wengryniuk and D. M. Coltart, Asymmetric α-alkylation of aldehydes, ketones, and carboxylic acids, in *Stereoselective Synthesis of Drugs and Natural Products*, John Wiley & Sons. Inc., Hoboken, NJ, 1st edn, 2013, pp. 183–213; (*b*) D. Enders, L. Wortmann and R. Peters, *Acc. Chem. Res.*, 2000, **33**, 157–169; (*c*) A. Job, C. E. Janeck, W. Bettray, R. Peters and D. Enders, *Tetrahedron*, 2002, **58**, 2253–2329.

2 (*a*) K. C. Nicolaou, K. Ajito, A. P. Patron, H. Khatuya, P. K. Richter and P. Bertinato, *J. Am. Chem. Soc.*, 1996, **118**, 3059–3060; (*b*) K. C. Nicolaou, A. P. Patron, K. Ajito, P. K. Richter, H. Khatuya, P. Bertinato, R. A. Miller and M. J. Tomaszewski, *Chem. – Eur. J.*, 1996, **2**, 847–868.

3 (*a*) D. Lim and D. M. Coltart, *Angew. Chem., Int. Ed.*, 2008, **47**, 5207–5210; (*b*) S. E. Wengryniuk, D. Lim and D. M. Coltart, *J. Am. Chem. Soc.*, 2011, **133**, 8714–8720. Coltart's methodology also elegantly allows for α,α′-bisalkylation.

4 For an example see: M. R. Garnsey, D. Lim, J. M. Yost and D. M. Coltart, *Org. Lett.*, 2010, **12**, 5234–5237.

5 (*a*) M. Murakata, M. Nakajima and K. Koga, *J. Chem. Soc., Chem. Commun.*, 1990, 1657–1658; (*b*) M. Imai, A. Hagihara, H. Kawasaki, K. Manabe and K. Koga, *J. Am. Chem. Soc.*, 1994, **116**, 8829–8830; (*c*) M. Imai, A. Hagihara, H. Kawasaki, K. Manabe and K. Koga, *Tetrahedron*, 2000, **56**, 179–185; (*d*) C. E. Stivala and A. Zakarian, *J. Am. Chem. Soc.*, 2011, **133**, 11936–11939.

6 Trost and Stoltz have both described Pd-catalyzed allylic alkylation of ketones through allyl enol carbonates and silyl enol ethers for the introduction of an allyl group in some substrates. For example see: (*a*) B. M. Trost and J. Xu, *J. Am. Chem. Soc.*, 2005, **127**, 2846–2847; (*b*) B. M. Trost and J. Xu, *J. Am. Chem. Soc.*, 2005, **127**, 17180–17181; (*c*) B. M. Stoltz, *et al.*, *Chem. – Eur. J.*, 2011, **17**, 14199–14223.

7 A general method for the organocatalytic alkylation of ketones is unknown. However MacMillan have achieved the alkylation of aldehydes *via* transient chiral enamine derivatives. For example see: (*a*) D. A. Nicewicz and D. W. C. MacMillan, *Science*, 2008, **322**, 77–80; (*b*) T. D. Beeson, A. Mastracchio, J.-B. Hong, K. Ashton and D. W. C. MacMillan, *Science*, 2007, **316**, 582–585. Aldehyde alkylations have also been reported by List and Enders. For examples see: (*c*) N. Vignola and B. List, *J. Am. Chem. Soc.*, 2004, **126**, 450–451; (*d*) D. Enders, C. Wang and J. W. Bats, *Angew. Chem., Int. Ed.*, 2008, **47**, 7539–7542.

8 A large variation in yields is observed in the literature. The direct alkylation of ketones occurred in consistently low yields in our hands. For a literature example of the allylation of 3-pentanone (<30% yield) see: G. A. Molander and C. D. Losada, *J. Org. Chem.*, 1997, **62**, 2935–2943.

9 For an example of the use of dimethylhydrazones see: K. Surendra and E. J. Corey, *J. Am. Chem. Soc.*, 2008, **130**, 8865–8869.

10 For a review of chiral diamines see: J. C. Kizirian, *Chem. Rev.*, 2008, **108**, 140–205.

11 For a review see: D. Hoppe and T. Hense, *Angew. Chem., Int. Ed. Engl.*, 1997, **36**, 2282–2316.

12 (*a*) A. Deiters and D. Hoppe, *J. Org. Chem.*, 2001, **66**, 2842–2849; (*b*) P. Beak and H. Du, *J. Am. Chem. Soc.*, 1993, **115**, 2516–2518; (*c*) K. M. B. Gross, Y. M. Jun and P. Beak, *J. Org. Chem.*, 1997, **62**, 7679–7689; (*d*) S. Wu, S. Lee and P. Beak, *J. Am. Chem. Soc.*, 1996, **118**, 715–721; (*e*) P. Tebben, F. Hintze and D. Hoppe, *Angew. Chem., Int. Ed. Engl.*, 1990, **29**, 1422–1433; (*f*) D. Stead, P. O'Brien and A. Sanderson, *Org. Lett.*, 2008, **10**, 1409–1412; (*g*) D. Stead, G. Carbone, P. O'Brien, K. R. Campos and A. Sanderson, *J. Am. Chem. Soc.*, 2010, **132**, 7260–7261.

13 (*a*) M. J. McGrath and P. O'Brien, *J. Am. Chem. Soc.*, 2005, **127**, 16378–16379; (*b*) J. L. Bilke, S. P. Moore, P. O'Brien and J. Gilday, *Org. Lett.*, 2009, **11**, 1935–1938.

14 A range of different cleavage methods (Amberlyst® 15 hydrogen form beads in acetone–water, copper chloride in THF and ozone in DCM) were investigated. All gave similar enantioselectivity.

15 G. Carbone, P. O'Brien and G. Hilmersson, *J. Am. Chem. Soc.*, 2010, **132**, 15445–15450.

16 Removal of this high boiling point solvent in the presence of volatile ketones proved difficult. Ketone product was lost as a result.

17 A notable decrease in mass was observed upon lengthy rotary evaporation.

18 For a thorough discussion of the origins of enantioselectivity in related systems see: P. Beak, A. Basu, D. J. Gallagher, Y. S. Park and S. Thayumanavan, *Acc. Chem. Res.*, 1996, **29**, 552–560.

19 See ref. 12*f* for an example of the use of diamine **13** in asymmetric deprotonation reactions.

Tetrahedron: *Asymmetry* 25 (2014) 356–361

Contents lists available at ScienceDirect

Tetrahedron: *Asymmetry*

journal homepage: www.elsevier.com/locate/tetasy

Investigation of a novel diamine based chiral auxiliary in the asymmetric alkylation of ketones

Sarah L. Clarke, Christina M. McSweeney, Gerard P. McGlacken *

Analytical and Biological Chemistry Research Facility and Department of Chemistry, University College Cork, Cork, Ireland

ARTICLE INFO

Article history:
Received 5 December 2013
Accepted 6 January 2014

ABSTRACT

A novel chiral auxiliary containing a pyrrolidine ring has been utilised in the preparation of various chiral ketones with good to excellent enantioselectivities (up to 92%). It has been successfully employed in aldol and Michael reactions giving moderate to high selectivity.

1. Introduction

The α-alkylation of ketones is a fundamental reaction in organic synthesis. However there exists a very limited number of methods to carry out this transformation in an asymmetric manner. The use of SAMP/RAMP methodology almost exclusively accounts for these types of transformations.[1] SAMP/RAMP hydrazones have been widely employed as key steps in the synthesis of numerous natural products, for example, indanomycine,[2] (+)-eremophilenolide[3] and stigmatellin A.[4] Previous alteration of the basic SAMP/RAMP framework has included the use of more sterically hindered groups on the arm to give chiral auxiliaries such as SADP, SAEP, SAPP[5] and RAMBO.[6] Replacement of the terminal methoxy group with a trimethylsiloxy group showed comparable enantioselectivities to SAMP in asymmetric α-alkylation reactions and very good selectivities with aldol reactions.[7] More recently, Coltart has successfully used chiral *N*-amino cyclic carbamate hydrazones as an alternative to SAMP-type hydrazones, allowing the preparation of both α-alkylated and α,α-bisalkylated ketones in a convenient and scalable manner.[8]

With such a limited number of routes available to chiral α-alkylated ketones, there remains significant scope for the exploration of new, easily prepared chiral auxiliaries for use in their synthesis. We set out to investigate if a nitrogen (as part of a pyrrolidine system) could ligate to lithium as effectively as in the SAMP/RAMP system (where a –OMe group is utilised). We herein report the chromatography-free synthesis of a novel chiral auxiliary incorporating a pyrrolidine ring. The chiral hydrazine is available in four steps from N-protected proline **1** or only two steps from commercially available (*S*)-(+)-1-(2-pyrrolidinylmethyl)pyrrolidine **3**. Subsequent reaction with symmetrical and unsymmetrical ketones followed by deprotonation, alkylation (using both alkyl and the rarely reported benzyl electrophiles) and hydrolysis gave valuable chiral ketones in very good ee and moderate yields. The chiral auxiliary can be applied to both aldol and Michael reactions.

2. Results and discussion

Chiral auxiliary **5** was formed in a five step sequence from commercially available (*S*)-*N*-(benzyloxycarbonyl)proline **1** via DCC coupling to provide amide **2** in 81% yield. Two reduction steps afforded chiral diamine **3** in good yield. Nitrosation gave **4** and a final $LiAlH_4$ reduction furnished hydrazine **5**. Chiral auxiliary **5** was reacted with 3-pentanone to give chiral hydrazone **6** in 80% yield (46% yield after purification by distillation) (Scheme 1). In a similar manner, **5** was combined with propiophenone, *p*-methoxypropiophenone and *p*-fluoropropiophenone to afford hydrazones **7a**, **7b** and **7c** in 52%, 54% and 48% yields, respectively (Scheme 2).

Chiral hydrazone **6** was then subjected to LDA (5 h, room temperature) deprotonation and alkylated with benzyl bromide (addition at −110 °C, temperature held for 1 h at −110 °C then for 5 h at −70 °C) in either diethyl ether, toluene or tetrahydrofuran. The resultant alkylated hydrazone **8** was hydrolysed using a biphasic 4 M HCl/diethyl ether system and ketone **9** was analysed for enantioselectivity using chiral gas chromatography (Scheme 3). The use of diethyl ether as the solvent for the alkylation step afforded **9** with very good enantioselectivity (89% ee) in comparison to toluene and tetrahydrofuran (66% and 61% ee, respectively) albeit in moderate yields (20–30%).[9]

Improved yields were obtained on extension of the deprotonation time to 16 h and by decreasing the temperature to 0 °C. In these cases complete conversion to the alkylated hydrazone was observed. Yields remained moderate, most likely due to the high volatility of the resulting ketones.[10]

Various methods for the cleavage of α-substituted hydrazones to the corresponding ketones have been utilised.[11] Oxalic acid is reported as a convenient, high yielding, racemisation-free method for the hydrolytic cleavage of SAMP hydrazones.[12] However, when

* Corresponding author. Tel.: +353 21 4902866; fax: +353 21 4274097.
E-mail address: g.mcglacken@ucc.ie (G.P. McGlacken).

0957-4166/$ - see front matter © 2014 Elsevier Ltd. All rights reserved.
http://dx.doi.org/10.1016/j.tetasy.2014.01.006

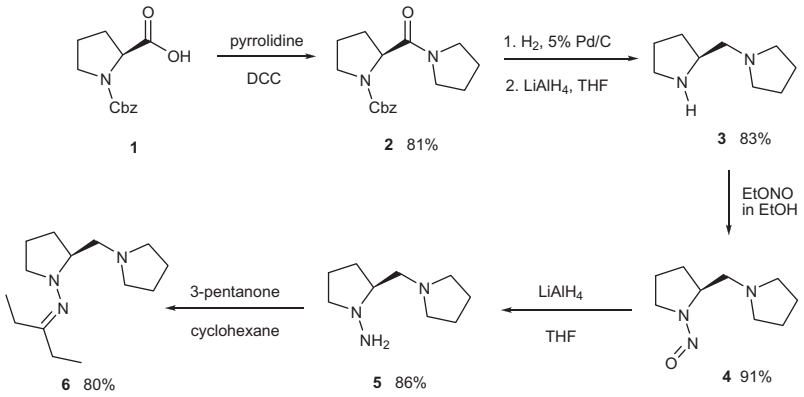

Scheme 1. Synthesis of the chiral auxiliary and the corresponding 3-pentanone hydrazone.

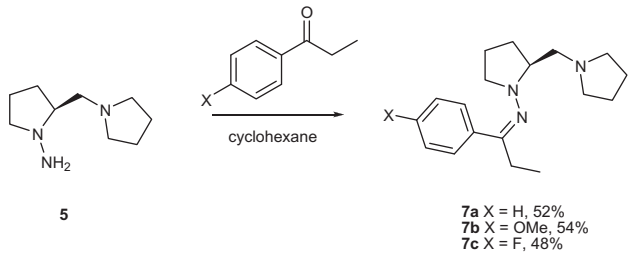

Scheme 2. Synthesis of propiophenone-based hydrazones.

we employed oxalic acid as a hydrazone cleavage method only moderate enantioselectivity was observed in the chiral ketones.[13] We suspected that racemisation was occurring, possibly due to some protonation of the pyrrolidine and increased solubility and exposure to the aqueous acidic layer. In order to investigate this possibility, both chiral hydrazone **7a** and the corresponding SAMP variant **11** were prepared and subjected to LDA and benzylbromide (Scheme 4). Both hydrazones were hydrolysed using oxalic acid and HCl/diethyl ether. Using the SAMP hydrazine, benzylated propiophenone **10** was obtained in 92% and 88% ee using oxalic acid and HCl/diethyl ether cleavage methods, respectively. A larger variation in the enantioselectivity was observed between the two cleavage methods when chiral auxiliary **7a** was employed in the reaction (51% and 78% ee). This clearly indicates that racemisation does occur when oxalic acid is used in combination with our chiral auxiliary and underlines the need for a thorough investigation of cleavage methods in such cases. To the best of our knowledge, the enzymatic cleavage of chiral hydrazones has not been reported. Porcine pancreatic lipase (PPL) was chosen as an appropriate enzyme because of its use in the cleavage of dimethylhydrazones.[14] Its use furnished ketone **9** in low (ca. 10%) yield (over two steps) albeit in 83% ee (Table 1, entry 8). Finally, a biphasic hydrolysis method (HCl/diethylether) was attempted. Clean conversion from alkylated hydrazones to ketones was observed with little or no racemisation occurring.

With usable hydrolysis conditions in hand, a variety of electrophiles were reacted with the azaenolate derived from **6**. The reaction of 3-pentanone hydrazone **6** with LDA and pentyliodide gave ketone **12** with 92% ee, albeit in moderate yield (Table 1, entry 1). When *t*-BuLi was employed as the base instead of LDA, the selectivity dropped to 82% ee (entry 2). Various other aliphatic electrophiles were employed to afford ketones **13**–**16** (entries 3–6) with very good enantioselectivities. We next turned our

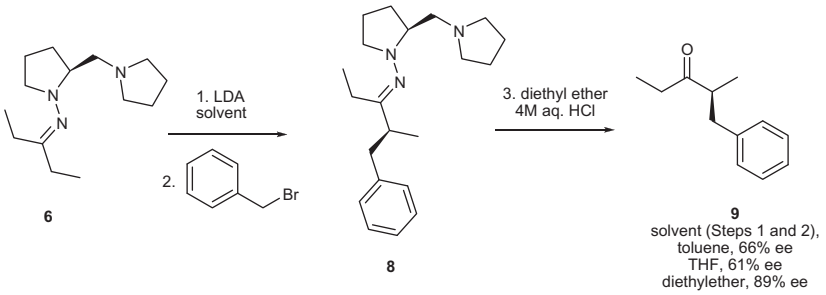

Scheme 3. Solvent screen for the alkylation step of a chiral hydrazone.

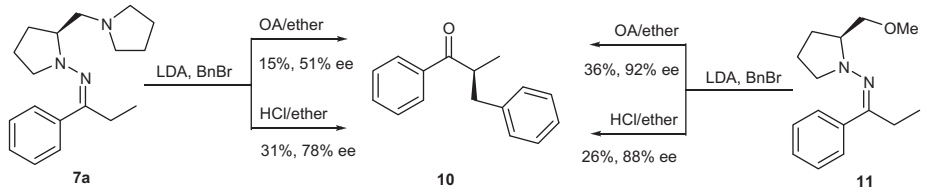

Scheme 4. Racemisation studies of chiral hydrazone **7a** and the SAMP variant **11** using oxalic acid (OA) or a biphasic 4 M HCl mediated cleavage. Isolated yields quoted over two steps.

Table 1
Results of alkylation reactions of hydrazones

Entry	Hydrazone	Electrophile	Product ketone	% Yield (over two steps)	% ee[e]
1	**6**	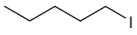	**12**	13	**92**[a]
2	**6**		**12**	29	82[a,b]
3	**6**		**13**	**63**	55[c]
4	**6**		**14**	23	90[a]
5	**6**	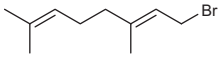	**15**	15	86[a]
6	**6**	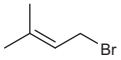	**16**	19	89[a]
7	**6**	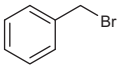	**9**	7	89[a]
8	**6**		**9**	10	83[d]
9	**6**	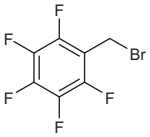	**17**	34	48[a]
10	**6**	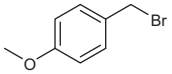	**18**	24	84[a]
11	**6**	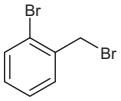	**19**	21	86[a]
12	**6**	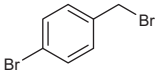	**20**	19	62[c]
13	**6**	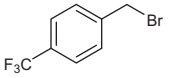	**21**	14	73[c]
14	**6**	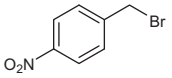	**22**	6	58[a]
15	**6**	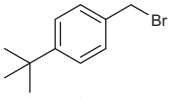	**23**	28	87[a]
16	**7a**	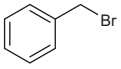	**10**	15	78[a]
17	**7a**		**24**	25	89[a]
18	**7b**		**25**	29	79[a]
19	**7c**		**26**	33	90[a]

Yield is calculated over two steps; alkylation of the parent hydrazone and hydrolysis of the alkylated hydrazone to the product ketone. Alkylated hydrazone is not isolated.
[a] HCl/diethyl ether hydrolysis.
[b] *t*-BuLi used as the base.
[c] Satd aq oxalic acid/diethyl ether hydrolysis.
[d] PPL hydrolysis. The ketone products have been assigned as (*S*) by comparison of the specific rotation value of **24** with that reported in the literature and others by analogy.[15]
[e] All ee values were determined using chiral GC analysis and confirmed by comparison with independently prepared racemic ketones.

attention to the use of benzyl bromides as electrophiles. Their use in hydrazone chiral auxiliary methodology has been very limited. In fact, no thorough investigation of benzyl based electrophiles has been reported using chiral hydrazone methodology. A plethora of electrophiles were used affording ketones **9**, and **17**–**23**, all with good enantioselectivity. Substituted benzyl groups allowed us to probe the effect of electron withdrawing and donating groups present on the electrophiles. The presence of electron withdrawing groups on the benzyl moiety caused a decrease in the enantioselectivity of the resultant ketone when compared to the unsubstituted benzyl bromide (entry 7, 89%), which is most apparent with the use of perfluorobenzyl bromide (entry 9, 48%). The presence of an electron donating group, for example the use of *p*-methoxybenzyl bromide (entry 10, 84%), had little effect on the enantioselectivity observed.

Further to these studies it was decided to investigate the effect of the electronic substituents on the hydrazone moiety. Propiophenone, *p*-methyoxypropiophenone and *p*-fluoropropiophenone hydrazones **7a**–**c** were chosen as substrates and subjected to the standard conditions using allyl bromide as the electrophile. The resultant ketones **24**–**26** demonstrate that the presence of an electron donating substituent on the ring (entry 18, 79% ee) results in a decrease in the enantioselectivity when compared to the unsubstituted ketone (entry 17, 89% ee). The presence of an electron withdrawing substituent (entry 19, 90% ee), had little effect on the enantioselectivity.

We then applied our methodology to an aldol reaction (Scheme 5). Hydrazone **6** was deprotonated using LDA, reacted with benzaldehyde and hydrolysed using Amberlyst® to afford **27** in 39% yield over two steps. Enantiomeric excesses of 63% and

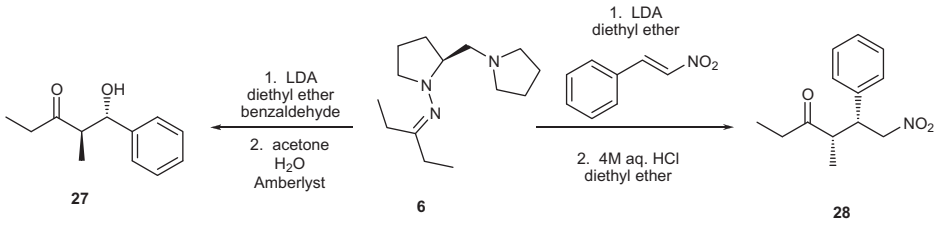

Scheme 5. Aldol and Michael reactions. Absolute stereochemistry unknown.

15% were obtained for *anti*- and *syn*-**27**, respectively. A diastereomeric ratio of 86:14 *anti*/*syn*, determined by GC, was identical to that observed by ^{1}H NMR.[16] The relative stereochemistry observed (*anti*) was opposite to that usually seen in aldol reactions using SAMP (*syn*).

Our novel chiral auxiliary was then applied to a Michael reaction (Scheme 5). Hydrazone **6** was treated with LDA and *trans*-β-nitrostyrene followed by subsequent hydrolysis to afford crude **28**, which was subjected to GC analysis. Enantiomeric excesses of 84% and 47% were determined for *syn*- and *anti*-**28**, respectively, with an excellent diastereomeric ratio of 94:6 *syn*/*anti* as determined by GC and NMR analysis. Again the relative orientation was opposite to that usually formed when using a SAMP chiral auxiliary in Michael reactions.[1c,17] Purification using column chromatography allowed isolation of *syn*-**28** in 84% ee and 13% yield over two steps.

3. Conclusion

A novel hydrazone-based chiral auxiliary has been established involving a pyrrolidine arm. The chiral auxiliary has been formed in good yields in five steps from commercially available (*S*)-*N*-(benzyloxycarbonyl)proline **1** (or only two steps from commercially available (*S*)-(+)-1-(2-pyrrolidinylmethyl)pyrrolidine **3**) without the need for silica column chromatography purification. Enantiomeric excesses of up to 92% were achieved in the α-alkylated aliphatic ketones formed and up to 89% in the less studied aromatic ketones. While the overall yields were moderate (in many cases due to product volatility), comparison studies with the SAMP chiral auxiliary showed comparable yields (Scheme 4). However, given the remarkably few methods available to access these compounds and the excellent enantioselectivities observed, we are pleased to report our novel chiral auxiliary as a viable route to these chiral synthons. Initial unoptimised studies into the use of our chiral auxiliary in Michael reactions have proven to be successful.

4. Experimental

4.1. Procedure for synthesis of the chiral auxiliary:

4.1.1. (*S*)-1-[*N*-(benzyloxycarbonyl)proly]-pyrrolidine 2[18]

To a CH_2Cl_2 solution (120 mL) of (*S*)-*N*-(benzyloxycarbonyl)proline (74.57 g, 0.3 mol) was added dropwise a CH_2Cl_2 solution (120 mL) of DCC (61.69 g, 0.3 mol) at 0 °C under a nitrogen atmosphere. After stirring for 30 min, a CH_2Cl_2 solution (120 mL) of pyrrolidine (24.7 mL, 0.3 mol) was slowly added dropwise to the reaction mixture at 0 °C via an addition funnel. The reaction mixture was allowed to warm to room temperature overnight. The precipitate was removed by filtration through a pad of Celite® and washed with CH_2Cl_2. The filtrate was washed with 0.5 M HCl (2 × 150 mL), satd aq $NaHCO_3$ solution (150 mL), H_2O (150 mL) and brine (150 mL). The organic layer was dried over $MgSO_4$, concentrated in vacuo and the crude product recrystallised from ethyl acetate to yield product **2** as a white, crystalline solid (73.52 g, 81% yield). $[\alpha]_D^{22} = -13.3$ (*c* 1.60, MeOH) {lit.[19] $[\alpha]_D^{22} = -14.1$ (*c* 1.61, MeOH)}. Mp 123–125 °C [lit.[19] 130–130 °C]. δ_H ($CDCl_3$, 300 MHz) (mixture of rotamers) 1.56–2.20 (8H, m, 4× CH_2), 3.25–3.75 (6H, m, 3× CH_2), 4.39–4.54 (1H, m, CH), 4.97–5.22 (2H, m, CH_2), 7.28–7.37 (5H, m, ArH). δ_C ($CDCl_3$, 75.5 MHz) (mixture of rotamers) 23.8, 23.9 (CH_2), 24.1, 24.4 (CH_2), 26.0, 26.3 (CH_2), 29.5, 30.5 (CH_2), 46.0, 46.0 (CH_2), 46.1, 46.3 (CH_2), 46.7, 47.3 (CH_2), 57.7, 58.2 (CH_2), 66.9, 67.1 (CH), 127.8, 127.9 (2× ArCH), 128.0, 128.1 (ArCH), 128.4, 128.4 (2× ArCH), 136.7, 136.8 (quaternary C), 154.2, 154.9 (C=O), 170.7, 171.0 (C=O). *m*/*z* (ES+) 303 [$(M+H)^+$, 100%].

4.1.2. (*S*)-2-(1-Pyrrolidinylmethyl)-pyrrolidine 3[20]

To a methanol (350 mL) solution of **2** (75.40 g, 250 mmol) was added Pd/C (5%, 4.78 g). The reaction mixture was then stirred under hydrogen at atmospheric pressure for 22 h while monitoring the reaction progress by TLC analysis. The crude reaction mixture was filtered through a pad of Celite® and washed with methanol to elute the product. The filtrate was concentrated in vacuo to yield the crude amide as a yellow oil (39.84 g, 95% yield). $[\alpha]_D^{26} = -89.6$ (*c* 1.7, EtOH) {lit.[21] $[\alpha]_D^{26} = -112.2$ (*c* 1.7, EtOH)}. δ_H ($CDCl_3$, 300 MHz) 1.60–2.02 (7H, m, 7× CH_2), 2.05–2.14 (1H, m, CH_2), 2.77–2.85 (1H, m, CH_2), 2.93 (1H, br s, NH), 3.15–3.22 (1H, m, CH_2), 3.36–3.57 (4H, m, 2× CH_2), 3.73–3.77 (1H, dd, *J* = 6.5, 8.6 Hz, CH). δ_C ($CDCl_3$, 75.5 MHz) 24.0, 26.0, 26.5, 30.4, 45.9, 46.0, 47.7 (7× CH_2), 59.5 (CH), 172.7 (C=O). *m*/*z* (ES+) 169 [$(M+H)^+$, 100%]. A solution of amide (19.02 g, 113 mmol) in dry THF (80 mL) was added dropwise over 3 h to $LiAlH_4$ (15.00 g, 396 mmol) in dry THF (140 mL) under a nitrogen atmosphere at 0 °C. The reaction mixture was allowed to stir at room temperature overnight, heated at reflux for 4 h, then allowed to stir at room temperature overnight. The reaction mixture was quenched by the dropwise addition of satd aq Na_2SO_4 solution (20 mL). The crude reaction mixture was filtered through a pad of Celite® and washed with ethyl acetate. The mother liquor was concentrated in vacuo to give the crude product as a yellow oil (14.54 g, 83% yield). Additional purification was achieved by Kugelrohr distillation yielding **3** as a colourless oil (11.22 g, 64% yield). $[\alpha]_D^{20} = +5.2$ (*c* 2.4, EtOH) [lit.[21] $[\alpha]_D^{20} = +8.9$ (*c* 2.4, EtOH)]. δ_H ($CDCl_3$, 300 MHz) 1.22–1.43 (1H, m, CH_2), 1.68–1.81 (6H, m, 3× CH_2), 1.82–1.95 (1H, m, CH_2), 2.31–2.37 (1H, dd, *J* = 5.2, 11.9 Hz, CH_2), 2.45–2.61 (6H, m, 3× CH_2, NH), 2.81–2.89 (1H, m, CH_2), 2.94–3.02 (1H, m, CH_2), 3.17–3.26 (1H, m, CH). δ_C ($CDCl_3$, 75.5 MHz) 23.4 (2× CH_2), 25.0, 30.1, 46.1 (3× CH_2), 54.6 (2× CH_2), 57.4 (CH), 62.1 (CH_2). *m*/*z* (ES+) 155 [$(M+H)^+$, 100%].

4.1.3. (*S*)-1-Nitroso-2-(pyrrolidin-1-ylmethyl)pyrrolidine 4

At first, 10–20% ethyl nitrite in ethanol (taken to be 15%) (5.45 mL, 8.63 mmol) was added to **3** (1.065 g, 6.90 mmol). The reaction vessel was covered in aluminium foil and allowed to stir at room temperature with progress monitored by ^{1}H NMR spectroscopy. After 45 h, ethanol was removed in vacuo to yield **4** as a yellow oil (1.15 g, 91% yield). δ_H ($CDCl_3$, 300 MHz) 1.76–

1.81 (4H, m, 2× CH_2), 1.91–2.25 (4H, m, 2× CH_2), 2.54–2.67 (4H, m, 2× CH_2), 2.80 (1H, dd, J = 8.8, 12.2 Hz, CH_2), 3.00 (1H, dd, J = 5.1, 12.2 Hz, CH_2), 3.52–3.75 (2H, m, CH_2), 4.59–4.67 (1H, m, CH). δ_C ($CDCl_3$, 75.5 MHz) 20.7 (CH_2), 23.5 (2× CH_2), 28.7, 45.6 (2× CH_2), 54.7 (2× CH_2), 59.5 (CH_2), 60.3 (CH). Since nitrosamines are potentially carcinogenic, no further data was obtained and the crude reaction mixture was used without purification in the next step.

4.1.4. (*S*)-2-(Pyrrolidin-1-ylmethyl)pyrrolidin-1-amine 5

To a solution of $LiAlH_4$ (2.61 g, 69 mmol) in dry THF (120 mL) was added dropwise a solution of **4** (6.30 g, 34 mmol) in dry THF (60 mL) under a nitrogen atmosphere at 0 °C. The reaction mixture was allowed to stir at 0 °C for 1 h, then at room temperature for 1 h before being heated at reflux for 4.5 h and stirred at room temperature overnight. The reaction progress was monitored by ^1H NMR spectroscopy. On completion, the reaction vessel was transferred to an ice bath and quenched by the dropwise addition of H_2O (2.6 mL), 3 M aq NaOH (2.6 mL) and H_2O (7.2 mL). The reaction mixture was filtered through a pad of Celite® using ether to elute the product. The mother liquor was concentrated in vacuo to yield **5** as a yellow oil (4.98 g, 86%). $[\alpha]_D^{20} = -11.4$ (c 1, EtOH). ν_{max}/cm^{-1} (KBr): 3306 (N–H stretch, m), 1591 (N–H bending, m), 1137 (C–N stretch, m). δ_H ($CDCl_3$, 300 MHz) 1.41–1.54 (1H, m, CH_2), 1.68–1.85 (6H, m, 3× CH_2), 1.93–2.07 (1H, m, CH_2), 2.26–2.41 (3H, m, 2× CH_2), 2.45–2.53 (2H, m, CH_2), 2.54–2.62 (2H, m, CH_2), 2.69–2.72 (3H, m/br s, CH_2/NH_2), 2.85–2.91 (1H, m, CH_2), 3.22–3.29 (1H, m, CH). δ_C ($CDCl_3$, 75.5 MHz) 20.6 (CH_2), 23.5 (2× CH_2), 28.7 (CH_2), 54.8 (2× CH_2), 59.6 (CH_2), 61.5 (CH_2), 67.8 (CH). Exact mass calcd for $C_8H_{11}IO_2$ [(M+H)$^+$], 170.1657. Found 170.1674.

4.1.5. (*S*)-*N*-(Pentan-3-ylidine)-2-(pyrrolidin-1-ylmethyl)pyrrolidin-1-amine 6

3-Pentanone (9.34 mL, 88 mmol) was added dropwise to a stirred solution of **5** (4.98 g, 29 mmol) in cyclohexane (8 mL) under an atmosphere of nitrogen. The reaction mixture was then allowed to stir at room temperature overnight and reaction progress monitored by ^1H NMR spectroscopy. On completion, the reaction mixture was poured into 6:1 DCM/H_2O and the organic layer extracted. The organic layer was dried over $MgSO_4$ and concentrated in vacuo to give the crude product as a yellow oil (5.61 g, 80% yield). Purification was achieved by Kugelrohr distillation to yield the product as a colourless oil (4.52 g, 65% yield). $[\alpha]_D^{20} = +114$ (c 1, EtOH). ν_{max}/cm^{-1} (NaCl): 1637 (C=N stretch, s), 1342, 1138 (C–N stretch, m). δ_H ($CDCl_3$, 300 MHz) 1.07 (6H, q, 2× CH_3), 1.53–1.66 (1H, m, CH_2), 1.69–1.91 (6H, m, 3× CH_2), 2.02–2.14 (1H, m, CH_2), 2.17–2.29 (2H, m, CH_2), 2.30–2.55 (9H, m, 4× CH_2, CH), 2.97–3.10 (2H, m, CH_2). δ_C ($CDCl_3$, 75.5 MHz) 10.9 (2× CH_3), 11.8, 21.8, 23.5, 23.5, 28.6, 28.7, 54.8, 55.0, 61.4 (10× CH_2), 66.1 (CH), 173.3 (CN). Exact mass calcd for $C_{14}H_{27}N_3$ [(M+H)$^+$], 238.2277. Found 238.2283.

4.2. General procedure for synthesis of racemic ketones

To THF (5 mL) was added commercially available LDA (1.1 equiv) at −78 °C. The reaction was stirred for 5 min and 3-pentanone was added dropwise. The reaction was stirred at −78 °C for 30 min and the electrophile (1.1 equiv) was added (in 3 mL THF if solid). The reaction was allowed to warm to room temperature overnight. Next, at. aq NH_4Cl solution (10 mL) was added and the crude product extracted with ethyl acetate or ether (3× 15 mL), dried over $MgSO_4$ and concentrated in vacuo to yield the crude product, which was purified by silica column chromatography.

4.3. General procedure for HCl/diethyl ether hydrolysis

At first, 4 M HCl (0.5 mL) and water (0.5 mL) were added to a vigorously stirred solution of alkylated hydrazone in diethyl ether (5 mL). The reaction progress was monitored by TLC analysis every 10 min. On completion, water (10 mL) was added, followed by extraction with diethyl ether (3× 25 mL). The organic layers were combined and washed with water (2× 10 mL), dried over $MgSO_4$ and concentrated in vacuo to yield the ketone, which was purified by silica column chromatography.

4.4. Procedure for PPL hydrolysis

To a solution of PPL (100 mg) in water (10 mL) was added a solution of alkylated hydrazone (1.05 mmol) in acetone (6 mL). The reaction was allowed to stir at room temperature for 23 h, diluted with diethyl ether (20 mL), washed with brine (3× 15 mL), dried over $MgSO_4$ and concentrated in vacuo. Purification was achieved using silica column chromatography to yield **9** as a yellow oil (19.3 mg, 10% yield over two steps).

4.5. General procedure for oxalic acid hydrolysis

At first, satd aq oxalic acid (1.5 vol with respect to mmol hydrazone) was added to a vigorously stirred solution of alkylated hydrazone in diethyl ether (4 vol with respect to mmol hydrazone). The reaction progress was monitored by TLC analysis and on completion were added water (5 mL) and diethyl ether (3× 20 mL). Organic extracts were combined, dried over $MgSO_4$ and concentrated in vacuo to yield the ketone which was purified by silica column chromatography.

4.6. Example procedure for the alkylation of chiral hydrazone

To a stirred solution of dry diisopropylamine (0.16 mL, 1.16 mmol) in dry diethyl ether (4 mL) in an N_2 filled Schlenk tube at −78 °C was added 1.6 M *n*-BuLi (0.86 mL, 1.21 mmol). The solution was allowed to stir at 0 °C for 30 min to generate a solution of LDA. Hydrazone **6** (250 mg, 1.05 mmol) was added slowly dropwise at −78 °C and allowed to stir at 0 °C for 16 h. A solution of *n*-pentyl iodide (250 mg, 1.26 mmol) in dry diethyl ether (2 mL) in a separate Schlenk, which was previously evacuated and filled with N_2 three times, was added dropwise to a solution of deprotonated hydrazone at −110 °C. The temperature of the reaction was kept at −110 °C for 1 h, then at −70 °C for 5 h before being allowed to warm gradually to room temperature overnight. Next, satd aq NH_4Cl solution (10 mL) was added to quench the reaction followed by extraction with diethyl ether (3 × 20 mL). The organic layers were combined, dried over $MgSO_4$ and concentrated in vacuo to yield the crude alkylated hydrazone as a yellow oil, which was hydrolysed using HCl/diethyl ether to yield the crude product as a yellow oil. Purification was carried out using silica column chromatography eluting with 95:5 hexane/diethyl ether to afford **12** as a pale yellow oil (22 mg, 13% and 92% ee). $[\alpha]_D^{20} = +5.5$ (c 0.2, Et_2O). ν_{max}/cm^{-1} (film) 2961, 2932 (alkane CH stretches), 1714 (C=O). δ_H ($CDCl_3$, 300 MHz) 0.88 (3H, t, J = 6.8 Hz, CH_3), 1.04 (3H, t, J = 7.3 Hz, CH_3) 1.06 (3H, d, J = 6.9 Hz, CH_3), 1.17–1.35 (8H, m, 4× CH_2), 2.46 (2H, dq, J = 1.5, 7.3 Hz, CH_2), 2.48–2.58 (1H, m, CH). δ_C ($CDCl_3$, 125 MHz) 7.8, 14.1, 16.5 (3× CH_3), 22.5, 27.0, 31.9, 33.1, 34.2 (5× CH_2), 46.1 (CH), 215.7 (C=O). Exact mass calcd for $C_{10}H_{21}O$ [(M+H)$^+$], 157.1592. Found 157.1584. Sample for GC made up at 1 mg/mL in dry dichloromethane and run on Agilent Technologies 7820A GC System using G4513A Injector and Astec Chiraldex G-TA fused silica capillary column purchased from Sigma Aldrich Supelco using conditions 105 °C hold 10 min, ramp 10 °C/min to 140 °C hold 5 min, flow 1 mL/min, inj. vol. 0.2 μL, split ratio 10:1, front inlet 150 °C, detector 155 °C. Retention time: 3.63 min (minor), 3.87 min (major).

4.7. Example of the procedure for the Michael reaction

To a stirred solution of dry diisopropylamine (0.2 mL, 1.39 mmol) in dry diethyl ether (4 mL) in an N_2 filled Schlenk tube at −78 °C was added 1.6 M *n*-BuLi (0.91 mL, 1.45 mmol). The solution was then allowed to stir at 0 °C for 30 min to generate a

solution of LDA. Hydrazone **6** (299 mg, 1.26 mmol) was slowly added dropwise at −78 °C and allowed to stir at 0 °C for 16 h. Next, *trans*-β-nitrostyrene (245 mg, 1.64 mmol) was dissolved in dry diethyl ether (3 mL), cooled to −78 °C and then slowly added dropwise to a solution of deprotonated hydrazone at −110 °C via a cannula. The temperature of the reaction was kept at −110 °C for 1 h, then at −70 °C for 5 h before being allowed to warm gradually to room temperature overnight. Next, satd aq NH_4Cl solution (10 mL) was added to quench the reaction followed by extraction with diethyl ether (3× 20 mL). The organic layers were combined, dried over $MgSO_4$ and concentrated in vacuo to yield a product as a dark yellow solid, which was hydrolysed using HCl/diethyl ether to yield the crude product as a pale brown oil (GC analysis of crude obtained), which was purified using silica column chromatography eluting with 90:10 hexane/diethyl ether to afford *syn*-**28** as a yellow oil (37 mg, 13% and 84% ee). $[\alpha]_D^{22} = +3.5$ (*c* 0.2, $CHCl_3$). {lit.[22] $[\alpha]_D^{22} = +8.9$ (*c* 0.2, $CHCl_3$)}. δ_H ($CDCl_3$, 300 MHz) 0.97 (3H, d, *J* = 7.1 Hz, CH_3), 1.07 (3H, t, *J* = 7.3 Hz, CH_3), 2.41 (1H, dq, *J* = 7.3, 18.0 Hz, CH_3CH_2), 2.61 (1H, dq, *J* = 7.3, 18.0 Hz, CH_3CH_2), 2.94–3.05 (1H, m, CH_3CH), 3.66–3.73 (1H, m, *CH*Ar), 4.57–4.71 (2H, m, CH_2NO_2), 7.14–7.17 (2H, m, ArH), 7.29–7.33 (3H, m, ArH). δ_C ($CDCl_3$, 75.5 MHz) 7.6, 16.3 (2× CH_3), 35.4 (CH_2), 46.1, 48.3 (2× CH), 78.3 (CH_2), 127.9, 129.0 (5× ArC), 137.6 (quaternary C), 213.6 (C=O). *m*/*z* (ES+) 235 [$(M+H)^+$, 78%]. Samples for GC made up at 1 mg/mL in dry dichloromethane and ran on Agilent Technologies 7820A GC System using G4513A Injector and Astec Chiraldex G-TA fused silica capillary column purchased from Sigma Aldrich Supelco using conditions 140 °C hold 70 min, flow 1 mL/min, inj. vol. 0.2 μL, split ratio 10:1, front inlet 150 °C, detector 155 °C. *anti*-**28** could not be isolated. Retention times: 44.95 min (*syn*), 51.05 min (*anti*), 52.40 min (*syn*), 55.53 min (*anti*).

Acknowledgements

The authors wish to thank the Irish Research Council for Science, Engineering and Technology (IRCSET) and Pfizer Process Development Centre, Cork for funding under the Enterprise partnership scheme (S.L.C. and G.P.M.) and Science Foundation Ireland (C.M.S. and G.P.M. grant number 09/RFP/CH52353).

References

1. (a) Enders, D. *Asymmetric Synthesis*; Academic Press: New York, 1984; (b) Enders, D.; Eichenauer, H.; Baus, U.; Schubert, H.; Kremer, K. A. M. *Tetrahedron* **1984**, *40*, 1345–1359; (c) Job, A.; Janeck, C. F.; Bettray, W.; Peters, R.; Enders, D. *Tetrahedron* **2002**, *58*, 2253–2329.
2. (a) Nicolaou, K. C.; Papahatjis, D. P.; Claremon, D. A.; Dolle, R. E. *J. Am. Chem. Soc.* **1981**, *103*, 6967–6969; (b) Nicolaou, K. C.; Claremon, D. A.; Papahatjis, D. P.; Magolda, R. L. *J. Am. Chem. Soc.* **1981**, *103*, 6969–6971.
3. Pennanen, S. I. *Acta Chem. Scand. B* **1981**, *35*, 555–557.
4. Enders, D.; Geibel, G.; Osborne, S. *Chem. Eur. J.* **2000**, *6*, 1302–1309.
5. Enders, D.; Kipphardt, H.; Gerdes, P.; Breña-Valle, L. J.; Bhushan, V. *Bull. Soc. Chim. Belg.* **1988**, *97*, 691–704.
6. Martens, J.; Lübben, S. *Liebigs Ann. Chem.* **1990**, 949–952.
7. McGlacken, G. P.; Breeden, S. W. *Tetrahedron: Asymmetry* **2005**, *16*, 3615–3618.
8. (a) Lim, D.; Coltart, D. M. *Angew. Chem., Int. Ed.* **2008**, *47*, 5207–5210; (b) Wengryniuk, S. E.; Lim, D.; Coltart, D. M. *J. Am. Chem. Soc.* **2011**, *133*, 8714–8720.
9. Other similar chiral auxiliaries were prepared, for example, **29** but gave poorer enantioselectivies.

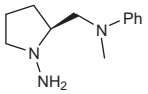

29

10. A notable decrease in mass was observed upon lengthy rotary evaporation.
11. Enders, D.; Wortmann, L.; Peters, R. *Acc. Chem. Res.* **2000**, *33*, 157–169.
12. Enders, D.; Hundertmark, T.; Lazny, R. *Synlett* **1998**, 721–722.
13. Although oxalic acid caused some racemisation during the hydrolysis process, the chiral auxiliary could be recycled in our hands using the method outlined in the literature.[12]
14. Mino, T.; Matsuda, T.; Hiramatsu, D.; Yamashita, M. *Tetrahedron Lett.* **2000**, *41*, 1461–1463.
15. Trost, B. M.; Xu, J. *J. Am. Chem. Soc.* **2005**, *127*, 17180–17181.
16. Purification using silica column chromatography was attempted however an inseparable mixture of diastereomers was obtained.
17. Further studies are underway to evaluate if our chiral auxiliary and SAMP give consistently opposite relative stereochemistry, despite possessing the same orientation.
18. Chowdhury, R.; Ghosh, S. K. *Org. Lett.* **2009**, *11*, 3270–3273.
19. Otani, G.; Yamada, S. *Chem. Pharm. Bull.* **1973**, *21*, 2112–2118.
20. Amedjkouh, M.; Ahlberg, P. *Tetrahedron: Asymmetry* **2002**, *13*, 2229–2234.
21. Nagasawa, K.; Takahashi, H.; Hiori, K.; Yamadam, S.-I. *Yakugaku Zasshi* **1975**, *95*, 33–45.
22. McCooey, S. H.; Connon, S. J. *Org. Lett.* **2007**, *9*, 599.

RESEARCH ARTICLE

The *Pseudomonas* quinolone signal (PQS), and its precursor HHQ, modulate interspecies and interkingdom behaviour

F. Jerry Reen[1], Marlies J. Mooij[1], Lucy J. Holcombe[1], Christina M. McSweeney[2], Gerard P. McGlacken[2], John P. Morrissey[3] & Fergal O'Gara[1]

[1]BIOMERIT Research Centre, Department of Microbiology, University College Cork, Ireland; [2]Department of Chemistry and Analytical and Biological Research Facility, University College Cork, Ireland; and [3]Department of Microbiology, University College Cork, Ireland

Correspondence: Fergal O'Gara, BIOMERIT Research Centre, Department of Microbiology, University College Cork, Ireland. Tel.: +353 21 490 2646; fax: +353 21 427 5934; e-mail: f.ogara@ucc.ie

Received 11 December 2010; revised 22 March 2011; accepted 22 April 2011.
Final version published online 26 May 2011.

DOI:10.1111/j.1574-6941.2011.01121.x

Editor: Julian Marchesi

Keywords
interspecies/interkingdom; *Pseudomonas* quinolone signal; PQS; HHQ; biofilm; motility.

Abstract

The *Pseudomonas* quinolone signal (PQS), and its precursor 2-heptyl-4-quinolone (HHQ), play a key role in coordinating virulence in the important cystic fibrosis pathogen *Pseudomonas aeruginosa*. The discovery of HHQ analogues in *Burkholderia* and other microorganisms led us to investigate the possiblity that these compounds can influence interspecies behaviour. We found that surface-associated phenotypes were repressed in Gram-positive and Gram-negative bacteria as well as in pathogenic yeast in response to PQS and HHQ. Motility was repressed in a broad range of bacteria, while biofilm formation in *Bacillus subtilis* and *Candida albicans* was repressed in the presence of HHQ, though initial adhesion was unaffected. Furthermore, HHQ exhibited potent bacteriostatic activity against several Gram-negative bacteria, including pathogenic *Vibrio vulnificus*. Structure–function analysis using synthetic analogues provided an insght into the molecular properties that underpin the ability of these compounds to influence microbial behaviour, revealing the alkyl chain to be fundamental. Defining the influence of these molecules on microbial–eukaryotic-host interactions will facilitate future therapeutic strategies which seek to combat microorganisms that are recalcitrant to conventional antimicrobial agents.

Introduction

Cooperative behaviour has changed our perception of how bacteria interact and cohabit within diverse ecological and clinical environments. The mobilization of diffusible signal molecules among populations of bacteria facilitates coordination of cellular activities towards the benefit of the population as a whole rather than the individual cell. While these signalling molecules are often species-specific, the ability to 'listen in' and decipher a competitor's messages is a valuable asset in mixed microbial communites, such as those that exist during infection of the cystic fibrosis (CF) lung. This phenomenon, often referred as interspecies or interkingdom signalling, is emerging as a key influence on the outcome of infectious diseases, although currently a dearth of knowledge exists regarding the signals involved in many of these interactions.

Pseudomonas aeruginosa is a highly adaptable organism, capable of colonizing a wide variety of niches including burn wounds and immunocompromised patients and it is the main pathogen associated with morbidity and mortality in CF patients (Govan & Deretic, 1996). *Pseudomonas aeruginosa* produces $>$ 50 alkylquinolones that differ structurally on the basis of substitution at the C3 position, *N*-oxide substitution of the quinolone nitrogen and modification of the alkyl side chain (Pesci *et al.*, 1999; Lepine *et al.*, 2004). Many of these alkylquinolones have been characterized with respect to their antibiotic activities (Wratten *et al.*, 1977; Leisinger and Margraff, 1979; Lepine *et al.*, 2004), while a role as signal molecules in cell–cell communication has been revealed for 2-heptyl-3-hydroxy-4-quinolone [*Pseudomonas* quinolone signal (PQS)] and its immediate precursor 2-heptyl-4-quinolone (HHQ) (Pesci *et al.*, 1999; McKnight *et al.*, 2000; Diggle *et al.*, 2003; Deziel *et al.*, 2004).

PQS signalling is pleiotropic, regulating biofilm formation, secondary metabolite production, pigment and virulence factor production, motility and membrane vesicle formation (Diggle *et al.*, 2003, 2007b; Dubern & Diggle,

2008; Mashburn-Warren *et al.*, 2009). Many of these phenotypes are mediated through the LysR-type transcriptional regulator PqsR, for which both HHQ and PQS act as coinducers (Wade *et al.*, 2005; Xiao *et al.*, 2006). Several important phenotypes such as iron chelation and pro-oxidant activities have since been attributed to PQS (Diggle *et al.*, 2003; Bredenbruch *et al.*, 2006; Haussler and Becker, 2008). While PQS has poor solubility in aqueous solution and is packaged into self-promoted vesicles to facilitate trafficking (Mashburn-Warren *et al.*, 2009), HHQ is known to passively diffuse out of the cell into the extracellular milieu (Deziel *et al.*, 2004).

Recent studies have identified HHQ biosynthetic systems in non-*Pseudomonas* species (Diggle *et al.*, 2006; Vial *et al.*, 2008). While the function of HHQ analogues in these species remains to be elucidated, strong structural similarities with *P. aeruginosa* HHQ suggest the existence of a conserved interspecies signalling system. However, although the spectrum of influence of alkylquinolones has been extensively reviewed in recent years (most recently by Heeb *et al.*, 2010 and Huse & Whiteley, 2010), the question remains as to whether HHQ and PQS signal molecules have an interspecies/interkingdom communication role.

In this study we reveal a role for both PQS and HHQ as modulators of key phenotypes in Gram-positive and Gram-negative bacteria, as well as towards the eukaryotic yeast *Candida albicans*. In addition, we provide evidence for the structural requirements that define the interkingdom role of these molecules.

Materials and methods

Strains and growth conditions

Strains, media composition and growth conditions are described in Table 1. One of the *Bacillus subtilis* strains used in this study, NCTC 10073, has been renamed *Bacillus atrophaeus*, with both species being indistinguishable using standard characterization methods (Fritze & Pukall 2001). However, as this strain is still listed as *B. subtilis* in the NCTC collection, we have used that designation throughout the paper. Trypticase soy agar (TSA) (Merck, Germany) was routinely used to culture *Bacillus*, *Escherichia* and *Staphylococcus* species. *Listeria monocytogenes* was cultured on brain–heart infusion (BHI) agar. *Vibrio cholerae*, *Vibrio vulnificus* and *Vibrio parahaemolyticus* were cultured on Luria–Bertani (LB) [tryptone 1% (w/v), yeast extract 0.5% (w/v), agar 1.5% (w/v)] supplemented with 0.5%, 2% and 3% (w/v) NaCl, respectively. *Vibrio fischeri* was cultured on LBS [Tryptone 1% (w/v), yeast extract 0.5% (w/v), NaCl 2% (w/v), agar 1.5% (w/v) and 20 mM Tris-HCl (pH 7.5)]. Marine agar was used to culture sea-sponge isolates and was constituted as 10 g of soluble starch, 4 g of yeast extract, 2 g of peptone, 15 g of Bacto agar, 33.3 g of InstantOcean (Aquarium Systems, Mentor, OH) and 1 L of distilled water. *Candida albicans* was grown in non-filament-inducing media; YPD [2% (w/v) Bacto peptone, 1% (w/v) yeast extract and 2% (w/v) glucose] or YNB [1 × YNB salts with ammonium sulphate (Difco 291940), 0.2% (w/v) glucose and 0.1% (w/v) maltose] and filament-inducing media; YNBNP [YNB supplemented with 25 mM phosphate buffer (pH 7) and 2.5 mM *N*-acetylglucosamine (Sigma A-8625)], or Spider media (10 g of nutrient broth, 10 g of mannitol and 2 g of K_2HPO_4 in 1 L distilled water pH 7.2) as described previously (Liu *et al.*, 1994; McAlester *et al.*, 2008).

Chemical synthesis of alkylquinolone derivatives

HHQ was prepared using a procedure we have recently reported (McGlacken *et al.*, 2010) starting with Meldrum's acid in a four-step procedure. Conversion to the aldehyde proceeded using a Duff formylation reaction using a modified method to that described by Pesci *et al.* (1999). Transformation to PQS occurred as described previously (Pesci *et al.*, 1999). Synthesis of the methyl derivative of PQS was achieved through reaction of the appropriate anthranilic acid with chloroacetone under basic conditions followed by cyclization of the corresponding anthranilate in refluxing *N*-methylpyrrolidone. This procedure described by Hradil *et al.* (1999) gave the quinolone in good yield (> 50% over two steps). Synthesis of the methyl derivative of HHQ was achieved by reaction of ethyl acetoacetate and aniline followed by cyclization in refluxing diphenylether. All alkylquinolone compounds (Supporting Information, Table S1) were solubilized in methanol and stored at $-20\,^{\circ}C$.

Antibacterial activity assays

Antibacterial activity of all alkylquinolone derivatives was initially investigated using agar plate assays. Bacteria were streaked onto growth agar (Table 1) and incubated overnight at an appropriate temperature (Table 1). Where growth was altered on plates, kinetics were measured in liquid culture in microtitre plates using a BioScreen C analyser (Oy Growth Curves Ab Ltd, Helsinki). To initiate time kill-curve assays, overnight cultures were standardized to $OD_{600\,nm}$ 0.2, to which HHQ was added at 1, 10 or 50 μM. Equal volumes of methanol were added to control cultures. Samples were taken at 1 h intervals and viable cell counts were enumerated on LBS (*V. fischeri*) or LB (*Escherichia coli* and *V. cholerae*) agar.

Semi-solid motility assays

Motility of *B. subtilis* and *Bacillus cereus* was analysed on LB and TSA 0.3% (w/v) agar, *Staphylococcus aureus* colony spreading was assessed on LB and TSA 0.24% (w/v) agar,

Table 1. List of strains and routine growth conditions used in this study

Strain	Description	Temperature (°C)	Media	Source/reference
Gram negative				
Pseudomonas aeruginosa PA14		37	LB	Liberati *et al*. (2006)
P. aeruginosa PA14 *pqsH*$^-$	*pqsH*::Tn*M*	37	LB	Liberati *et al*. (2006)
Escherichia coli NCIMB11943		37	LB	NCIMB
Vibrio fischeri ES114	*E. scolopes*, Hawai'i	25	LBS	E. Ruby lab, UW
V. fischeri MJ11	*M. japonica*, Japan	25	LBS	E. Ruby lab, UW
V. cholerae 0395	O1 Classical, India	30	LB	UCC Collection
V. vulnificus YJ016	Biotype 1, Taiwan	30	LB 2% NaCl	UCC Collection
V. parahaemolyticus RIMD2210633	03:K6, Japan	30	LB 3% NaCl	UCC Collection
Salmonella Typhimurium LT2		37	LB	UCC Collection
Serratia marcescens	Clinical isolate 58272	30	LB	J. Clair, Mercy Hospital
Serratia sp. 39006		30	LB	Poulter *et al*. (2010)
Proteus vulgaris NCIMB12426		37	LB	NCIMB
Gram positive				
Bacillus subtilis NCTC10073	Renamed *Bacillus atrophaeus* (Fritze & Rüdiger 2001)	30	TSB	NCTC
B. subtilis NCDO1789		30	TSB	NCDO
B. cereus NCIMB9373		30	TSB	NCIMB
Staphylococcus aureus NCDO949		37	TSB	NCDO
S. epidermidis DMSZ3095		37	TSB	DMSZ
S. gallinarum DMSZ4616		37	TSB	DMSZ
Micrococcus luteus NCIMB9278		37	TSB	NCIMB
Listeria monocytogenes LO28	Serotype 1/2c	37	BHI	C. Hill lab, UCC
Marine sponge isolates*				
Vibrio sp.	*P. boletiformis* isolate	23	MA	UCC Collection
Algoriphagus sp.	*P. boletiformis* isolate	23	MA	UCC Collection
Bacillus sp.	*P. boletiformis* isolate	23	MA	UCC Collection
Pseudoalteromonas sp.	*P. boletiformis* isolate	23	MA	UCC Collection
Spongibacter sp.	*P. boletiformis* isolate	23	MA	UCC Collection
Shewanella sp.	*P. boletiformis* isolate	23	MA	UCC Collection
Micrococcus sp.	*P. boletiformis* isolate	23	MA	UCC Collection
Pseudovibrio sp.	*A. dissimilis* isolate	23	MA	UCC Collection
Yeast				
Candida albicans SC5314		37	YPD	Gillum *et al*. (1984)
C. albicans BCa2-10	*tup1/tup1*	37	YPD	Braun & Johnson (1997)
C. glabrata ATCC2001		37	YPD	ATCC
Kluyveromyces marxianus CBS608		37	YPD	CBS
Saccharomyces cerevisiae BY4741		37	YPD	Brachmann *et al*. (1998)

*Marine sponges were collected at the Lough Hyne Marine Nature Reserve, Co. Cork. Ireland.

and *L. monocytogenes* motility was analysed on BHI 0.3% (w/v) agar. Swarming motility in Gram-negative bacteria was analysed on Eiken Agar [0.6% (w/v) supplemented with 0.5% (w/v) glucose], while swimming motility was assessed on LB and TSA 0.3% (w/v) agar. *Vibrio fischeri* motility was assayed on TB-SW 0.25% (w/v) agar, while *P. aeruginosa* twitching motility was assessed on LB agar [1% (w/v)]. Alkylquinolone derivatives were added to the molten medium at a final concentration of 10 μM immediately before pouring plates. $FeCl_3$ was added to molten agar medium at a final concentration of 100 μM. Aliquots of overnight cultures (3 μL) were spotted into the centre of the plate and the zone of motility was measured against control plates containing methanol. Alternatively, toothpicks were used to inoculate colonies from plates, incubated overnight, onto the centre of Eiken agar plates. All experiments were performed in triplicate and data presented is the result of at least three independent biological replicates.

Attachment and pellicle formation analysis

Bacterial cultures were incubated overnight and transferred into fresh TSB to an $OD_{600\,nm}$ of 0.05. Aliquots (1 mL) were transferred into 24-well plates and alkylquinolone derivates or controls added at a final concentration of 10 μM. Plates were incubated overnight and attachment/biofilm was evaluated by crystal violet staining after washing to quantify attached cells. For analysis of migration from the air–liquid surface interface, plates were prepared as described above and incubated at a 45° angle overnight. Liquid was removed

preserving the attached pellicle, and plates were visualized microscopically. To analyse the impact of HHQ on the specific stages of *B. subtilis* pellicle formation, six-well plates were prepared as above and incubated at 30 °C. Aliquots (2 μL) were removed from the bottom of the wells at 4 h intervals, stained with crystal violet on glass slides, and visualized under a microscope.

Cultivation of biofilms using flow-cell technology

Biofilms were grown at room-temperature in flow chambers with individual channel dimensions of $1 \times 4 \times 40$ mm. The flow system was assembled and prepared as described previously by Moller *et al.* (1998). Before inoculation, cells were pre-exposed to 10 μM HHQ or methanol control for 12 h, with a starting $OD_{600\,nm}$ of 0.05, shaking at 30 °C in TSB. Subsequently, the flow channels were inoculated with 250 μL of these cells diluted to an $OD_{600\,nm}$ of 0.05 in TSB media. After inoculation, the flow chambers were inverted without flow for 1 h, after which the flow was started using a Watson Marlow 205S peristaltic pump at a mean flow velocity of 0.2 mm s^{-1}, and the flow chambers were reverted again. The chambers were either supplied with TSB containing either 10 μM HHQ, 10 μM PQS or an equal volume of methanol. Biofilms were visualized 9 h postinoculation following addition of 250 μL of 5 μM SYTO9 (Invitrogen) into the flow cells. The flow was stopped for the incubation period of the dye (15 min), after which the flow was reinstated and the biofilm was visualized. Three independent experiments were performed.

Microscopy and image acquisition

Microscopic observations and image acquisition of the biofilms were performed with a Zeiss LSM 5 Exciter (Carl Zeiss, Jena, Germany) equipped with an argon laser and detector and filter sets for monitoring green fluorescence from SYTO9 (excitation, 488 nm; emission 505–550 nm). Images and Z-stacks were obtained using a $\times$40/0.75 NA objective and images were generated using the IMARIS Software package (Bitplane AG, Zürich, Switzerland). Images of *C. albicans* were captured using a Leica DM1000 microscope ($\times$40/0.65 objective lens) attached to a Leica DFC290 HD camera (Solms, Germany).

Candida albicans biofilm assay

Biofilm formation in *C. albicans* was measured in 96-well polystyrene plates (Sarstedt) as described previously (Ramage *et al.*, 2001). Briefly, *C. albicans* cells were grown as yeast cultures at 30 °C in YNB medium overnight. Yeast cells were diluted in YNBNP filament inducing medium to $OD_{600\,nm}$ 0.05, treated with HHQ, PQS or cHHQ (10, 50 or 100 μM) and 100 μL cultures were placed in the wells of the plate for an initial incubation period of 1 h at 37 °C. The media and nonadherent cells were removed and the wells were washed twice with 100 μL of fresh growth medium to remove nonadhered cells. Fresh growth medium (100 μL) supplemented with HHQ, PQS or cHHQ, was added to the wells, and the plates were reincubated statically for 24 h. Biofilm formation was measured using a semi-quantitative XTT (Sigma) reduction assay (Hawser, 1996; Tunney *et al.*, 2004). Cultures with no added supernatant and cultures containing an equivalent volume of methanol were used as controls. Experiments were repeated in triplicate with six technical replicates. Means were compared using pairwise *t*-tests ($P \leq 0.05$).

Phenazine quantification assay

Overnight cultures of PA14 wild-type and the *pqsH*$^{-}$ mutant obtained from the nonredundant PA14 *Tn*M mutant library were inoculated 1 : 100 into fresh LB containing 10 μM HHQ, PQS, cHHQ, HHQ-C_1, PQS-C_1 or methanol and incubated overnight at 37 °C, 200 r.p.m. Pyocyanin was extracted as previously described and quantified spectrophotometrically at $A_{520\,nm}$ (Essar *et al.*, 1990).

Thin layer chromatography (TLC) analysis

TLC analysis of HHQ, PQS and derivative molecules was performed using the protocol described by Fletcher *et al.* (2007). The stationary phase silica plate (Merck) was soaked for 30 min in KH_2PO_4 and activated at 100 °C for 1 h before use, while the mobile phase used was dichloromethane : methanol 95 : 5. As controls, extracts were obtained from PA14 wild-type, PA14 *Tn*M *pqsH*$^{-}$ and PA14 *Tn*M *pqsA*$^{-}$.

Results

HHQ exhibits species-specific antibacterial activity

The consequences of interspecies and interkingdom communication vary from coercive growth inhibition to more subtle signal related modulation of microbial behaviour. Initially, it was necessary to determine if physiological concentrations of HHQ and PQS [10 μM (Calfee *et al.*, 2005)] exhibited antimicrobial activity against a range of Gram-negative and Gram-positive microorganisms, which were chosen to reflect the diverse ecological niches occupied by *P. aeruginosa* isolates. HHQ and PQS were also tested for antimicrobial activity against several yeast species including the pathogens *C. albicans* and *Candida glabrata* (results are summarized in Table 2). Growth inhibition ranged from complete inhibition, to partial inhibition, and finally to no alteration in growth. The growth of *V. fischeri*, *V. vulnificus*

Table 2. Summary of HHQ and PQS influences on microbial behaviour

	Phenotype																	
	Growth						Motility						Biofilm					
Species	M	P	cH	H	mP	mH	M	P	cH	H	mP	mH	M	P	cH	H	mP	mH
Gram negative																		
P. aeruginosal PA14	+	+	+	+	+	+	+	--[†]	nt[†]	+	+	+	+	+	+	+	+	+
E. coli NCIMB11943	+	+	+	+	+	+	+	---[†]	nt[†]	+	+	+	+	+	+	+	+	+
Serratia sp. 39006	+	+	+	+	+	+	+	--[†]	nt[†]	+	+	+	+	+	+	+	+	+
Serratia marcescens	+	+	+	+	+	+	+	--[†]	nt[†]	+	+	+	+	+	+	+	+	+
S. Typhimurium LT2	+	+	+	+	+	+	nm	nm	nm	nm	nm	nm	+	+	+	+	+	+
P. vulgaris NCIMB12426	+	+	+	+	+	+	nm	nm	nm	nm	nm	nm	+	+	+	+	+	+
V. cholerae O395	+	+	+	-	+	+	+	+	+	-[*]	+	+	+	+	+	+	+	+
V. fischeri ES114	+	+	+	---	+	+	+	+	+	---[*]	+	+	+	+	+	+	+	+
V. fischeri MJ11	+	+	+	---	+	+	+	+	+	---[*]	+	+	+	+	+	+	+	+
V. vulnificus YJ016	+	+	+	---	+	+	+	+	+	+	+	+	+	+	+	+	+	+
V. parahaemolyticus RIMD2210633	+	+	+	+	+	+	nt	nt	nt	nt	nt	nt	nt	nt	nt	nt	nt	nt
Shewanella sp.	+	+	+	-	+	+	nt	nt	nt	nt	nt	nt	nt	nt	nt	nt	nt	nt
Vibrio sp.	+	+	+	-	+	+	nt	nt	nt	nt	nt	nt	nt	nt	nt	nt	nt	nt
Pseudovibrio sp.	+	+	+	+	+	+	nt	nt	nt	nt	nt	nt	nt	nt	nt	nt	nt	nt
Algoriphagus sp.	+	+	+	---	+	+	nt	nt	nt	nt	nt	nt	nt	nt	nt	nt	nt	nt
Pseudoalteromonas sp.	+	+	+	-	+	+	nt	nt	nt	nt	nt	nt	nt	nt	nt	nt	nt	nt
Spongibacter sp.	+	+	+	+	+	+	nt	nt	nt	nt	nt	nt	nt	nt	nt	nt	nt	nt
Gram positive																		
B. subtilis NCTC10073	+	+	+	+	+	+	+	---	--	-	+	+	+	+	--	---	+	+
B. subtilis NCDO1789	+	+	+	+	+	+	+	---	--	-	+	+	+	+	--	---	+	+
B. cereus NCIMB9373	+	+	+	+	+	+	+	---	--	-	+	+	+	+	+	+	+	+
Bacillus sp.	+	+	+	+	+	+	nt	nt	nt	nt	nt	nt	nt	nt	nt	nt	nt	nt
S. aureus NCDO949	+	+	+	+	+	+	+	---	---	---	+	+	+	+	+	+	+	+
S. epidermidis DMSZ3095	+	+	+	+	+	+	+	---	--	--	+	+	+	+	+	+	+	+
S. gallinarum DMSZ4616	+	+	+	+	+	+	+	---	+	+	+	+	+	+	+	+	+	+
L. monocytogenes LO28	+	+	+	+	+	+	+	---	-	-	+	+	+	+	+	+	+	+
M. luteus NCIMB9278	+	+	+	+	+	+	nm	nm	nm	nm	nm	nm	+	+	+	+	+	+
Micrococcus sp.	+	+	+	+	+	+	nt	nt	nt	nt	nt	nt	nt	nt	nt	nt	nt	nt
Yeast																		
C. albicans SC5314	+	+	+	+	+	+	+	+	+	+	+	+	+	+	--	---	+	+
C. glabrata ATCC2001	+	+	+	+	+	+	nt	nt	nt	nt	nt	nt	nt	nt	nt	nt	nt	nt
S. cerevisiae BY4741	+	+	+	+	+	+	nt	nt	nt	nt	nt	nt	nt	nt	nt	nt	nt	nt
K. marxianus CBS608	+	+	+	+	+	+	nt	nt	nt	nt	nt	nt	nt	nt	nt	nt	nt	nt

[*]Growth inhibiting.

[†]Denotes swarming motility. Swimming motility was unaffected in these organisms.

+, Normal phenotype; ---, 80–100% reduction; --, 50–79% reduction; -, 20–49% reduction; nt, not tested; nm, nonmotile; M, MeOH; P, PQS; cH, cHHQ; H, HHQ; mP, PQS-C_1; mH, HHQ-C_1.

and a marine sponge isolate *Algoriphagus* sp. was completely inhibited on agar plates supplemented with 10 μM HHQ (Fig. 1a and Table 2). Growth of the human pathogen *V. cholerae* and several marine sponge isolates was also altered, though not completely inhibited, in the presence of HHQ (Table 2). Addition of 10 μM HHQ to both agar and broth had no effect on the growth of the other Gram-negative and Gram-positive bacteria tested, including the pathogens *S. aureus* and *V. parahaemolyticus*, or on any of the yeast species (Fig. 1a and Table 2). Subsequently, the kinetics of HHQ-induced growth inhibition were investigated using a BioScreen C multiwell system and confirmed the spectrum of HHQ-sensitive species (Fig. S1 and data not shown). Growth of *V. cholerae* and *V. fischeri* was inhibited in the presence of 10 μM HHQ, with the latter being almost completely repressed (Fig. S1) and time kill-curve analysis revealed the activity to be bacteriostatic (Fig. 1b).

PQS and HHQ repress microbial motility

Bacterial motility and chemotaxis have been associated with virulence in several bacterial species (Josenhans and Suerbaum, 2002; Krukonis and DiRita, 2003). To investigate the impact of HHQ and PQS on microbial motility, both

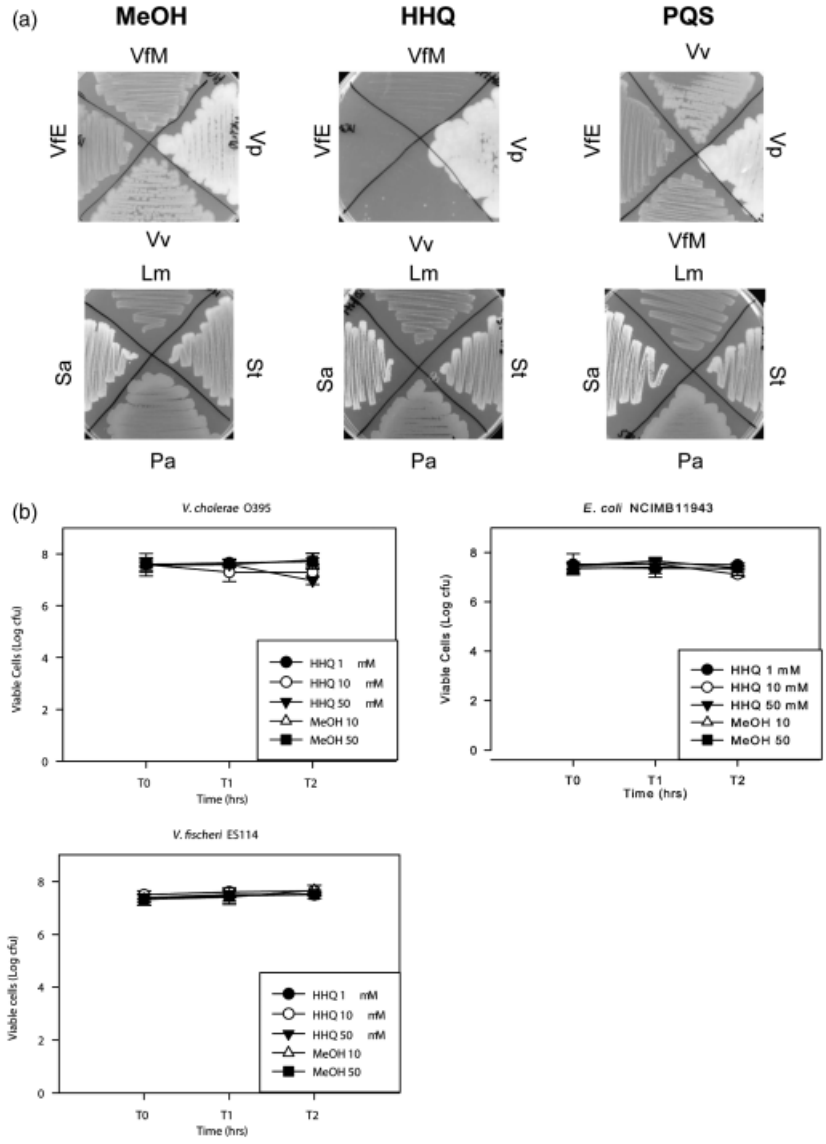

Fig. 1. HHQ but not PQS exhibits potent species-specific bacteriostatic activity. (a) Growth of *Vibrio fischeri* ES114 (VfE), *V. fischeri* MJ11 (VfM), *Vibrio vulnificus* YJ016 (Vv), *Vibrio parahaemolyticus* RIMD2210663 (Vp), *Listeria monocytogenes* LO28 (Lm), *Staphylococcus aureus* NCDO949 (Sa), *Pseudomonas aeruginosa* PA14 (Pa) and *S. enterica* serovar Typhimurium LT2 (St) in the presence of either HHQ or PQS (10 μM). (b) Time kill-curve analysis of HHQ towards *Escherichia coli*, *Vibrio cholerae* and *V. fischeri*.

compounds were added to semi-solid motility agar. Motility of all Gram-positive bacteria tested was significantly repressed in the presence of PQS, independent of any growth defect (Fig. 2 and Fig. S2; Table 2). With the exception of *S. aureus*, HHQ exhibited a less potent repression of motility than PQS (Fig. 2a and Fig. S2). Repression of *S. aureus* spreading motility by HHQ was not due to small colony variation and correlated with increased production of an orange pigment, likely to be staphyloxanthin, which became more pronounced after storage at 4 °C (Fig. S3). As PQS has previously been shown to act as an iron-trap (Bredenbruch *et al.*, 2006; Diggle *et al.*, 2007b), and several studies report that bacterial motility is reduced under iron-limiting conditions (Matilla *et al.*, 2007; Tang and Grossart, 2007; Glick *et al.*, 2010), we investigated the possibility that motility could be repressed in Gram-positive bacteria as a consequence of iron limitation. However, addition of 100 μM $FeCl_3$ to semi-solid agar plates did not restore motility, and repression in the presence of both $FeCl_3$ and PQS was comparable to that observed in the presence of PQS alone (Fig. 2c and Fig. S2). Swarming motility of Gram-negative bacteria was also reduced in the presence of PQS (Fig. 2a), while swimming motility and *P. aeruginosa* twitching motility was not influenced by the presence of PQS, HHQ or any of their derivatives (Fig. S2, data not shown and Table 2).

HHQ interferes with pellicle and biofilm formation in *B. subtilis*

The ability to form biofilms is another key cooperative trait that enables bacteria to persist in extreme and hostile environments, and is closely associated with motility in

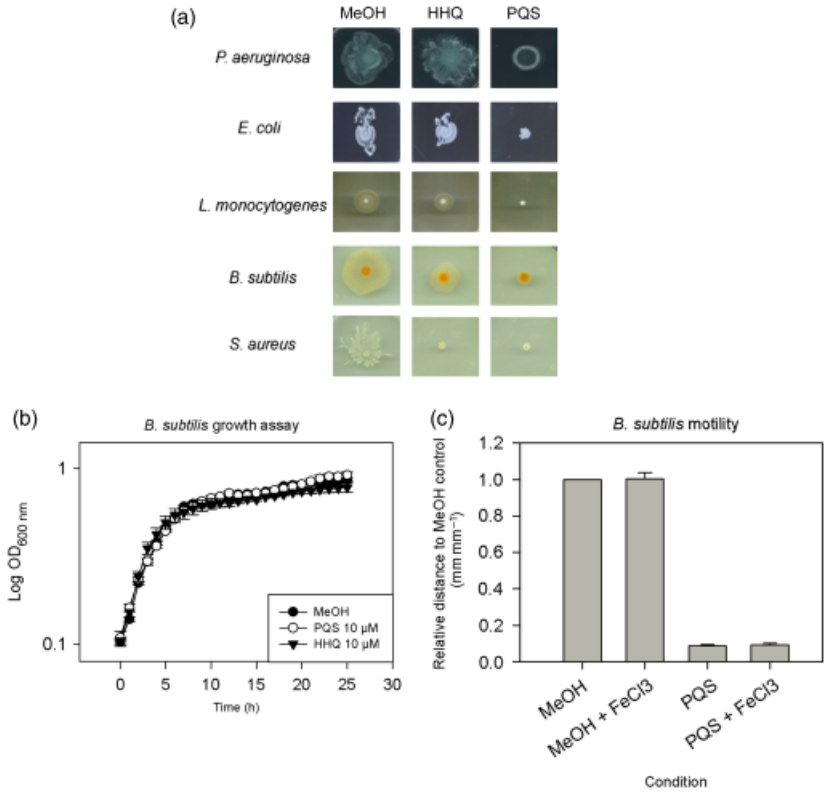

Fig. 2. HHQ and PQS influence microbial motility. (a) Motility of Gram-positive and Gram-negative bacteria on semi-solid TSA and Eiken agar plates supplemented with 10 μM HHQ or PQS. (b) Growth kinetics analysis of *Bacillus subtilis* in the presence of 10 μM HHQ or PQS on a BioScreen C analyser. (c) Motility of *B. subtilis* on semi-solid TSA plates supplemented with 10 μM PQS ± 100 μM $FeCl_3$.

several organisms. We therefore assessed the impact of the alkylquinolone signal molecules on biofilm formation in a range of Gram-negative and Gram-positive bacteria. A significant reduction in biofilm attachment/formation was observed upon addition of HHQ to *B. subtilis* cultures, while this phenotype was unaffected in several other Gram-positive and Gram-negative organisms, including *S. aureus* and *B. cereus* (Fig. S4 and Table 2). Microscopic visualization of 24-well assay plates incubated overnight at a 45° angle confirmed the impact of HHQ on formation of the *B. subtilis* pellicle (Fig. 3a). As pellicle formation in *B. subtilis* is known to progress through distinct genetic steps, involving defined groups of transcriptional regulators (Kobayashi, 2007), the biofilm assay was repeated in six-well plates and cells were visualized microscopically at 4 h intervals. This revealed that the early stages of biofilm development, including head-to-tail chain formation of *B. subtilis* cells and aggregation into clusters, were unaffected in the presence of HHQ (Fig. 3b). Biofilm formation was also dramatically reduced in flow chambers through which HHQ-treated cultures were passed (Fig. 3c). The biofilm structures were less frequent and ordered during HHQ treatment and this correlated with the reduced attachment observed after 1 h in HHQ-treated cultures (Fig. 3c). Interestingly, HHQ was unable to cause dispersal of preformed *B. subtilis* biofilms (data not shown) indicating that this compound exclusively targets formation of the mature biofilm. Consistent with microtitre assays, addition of PQS to flow cell cultures did not reduce pellicle formation, attachment or formation of mature biofilms (Fig. 3 and data not shown). The biofilm modulating activity of HHQ revealed in this analysis adds another layer of complexity to the capacity of this compound to influence microbial behaviour.

HHQ interferes with biofilm formation in *C. albicans*

Having established an interspecies influence for HHQ and PQS, we subsequently sought to address the possibilty that these compounds may also influence behaviour of eukaryotic pathogens. Bidirectional signalling between prokaryotes and eukaryotes is emerging as a key trait of the clinically important *Pseudomonas–Candida* interaction (Cugini *et al.*, 2007; Cugini *et al.*, 2010) and several molecules produced by *P. aeruginosa* have been shown to impact on *C. albicans* (Hogan and Kolter, 2002; Hogan *et al.*, 2004; Davies and Marques, 2009; Holcombe *et al.*, 2010). There was a significant reduction in the ability of *C. albicans* to form biofilms in the presence of HHQ, revealing an interkingdom dimension to HHQ function. Biofilm reduction could be observed at 10 μM HHQ but the phenomenon was greatly enhanced at concentrations of 50 or 100 μM HHQ (Fig. 4a and Fig. S5a). To further analyse the biofilm-specific effects of HHQ, and in particular whether the yeast-hyphal switch is implicated in biofilm inhibition, we used a constitutively filamenting *tup1/tup1* mutant. This strain

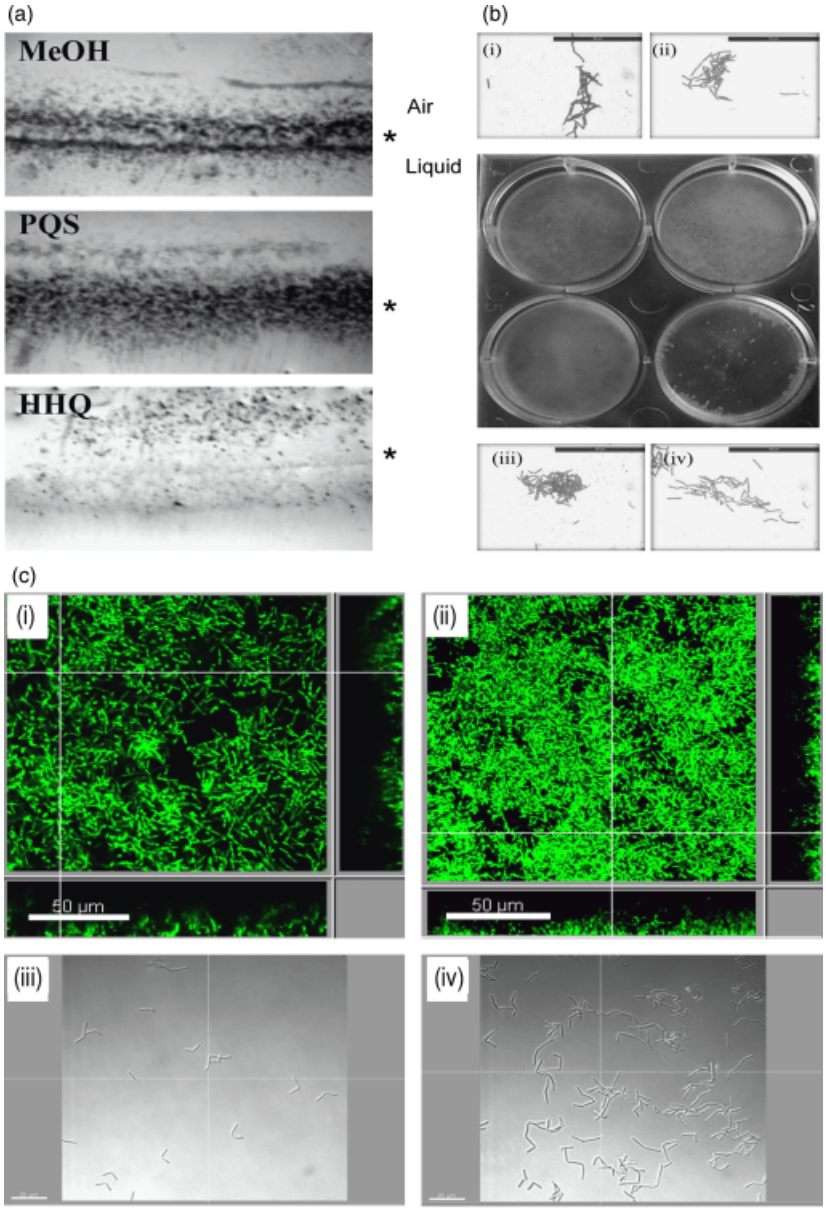

Fig. 3. Pellicle formation in *Bacillus subtilis* is disrupted by HHQ. (a) Pellicle formation assay of static *B. subtilis* cultures incubated at a 45° angle in 24-well plates supplemented with 10 μM HHQ or PQS. The migration and attachment of cells from the liquid–air interface was visualized after removal of unattached cells. (b) Cells sampled at 8 h to assess cell-morphological changes associated with pellicle formation in *B. subtilis*: (i) methanol, (ii) PQS, (iii) untreated, and (iv) HHQ. This figure is representative of six biological replicates. (c) Visualization of SYTO9-stained *B. subtilis* biofilms grown in TSB media for 9 h (i) in the presence of HHQ or (ii) in the presence an equal volume of methanol. Attachment was evaluated in cells treated with HHQ (iii) or methanol (iv) for 1 h. *Air–liquid interface.

lacks the hyphal repressor *TUP1* and as a result is 'locked' in the hyphal form. In contrast to the wild-type strain, no reduction in biofilm formation was observed in this strain after treatment with 100 μM HHQ (Fig. 4a). Biofilm reduction by HHQ in microtitre wells was not due to a decrease in the total cellular growth, supported by measurements of growth on solid media and in liquid shaking culture (Fig 4b and data not shown). When HHQ was present only during adhesion there was no effect on biofilms (Fig. S5b), however, when HHQ was added only during development there was a reduction in biofilm formation similar to that observed when HHQ was present throughout the assay (Fig. S5b), suggesting that initial adhesion is not a target of HHQ. Filamentation is crucial for the virulence of *C. albicans*, and the *P. aeruginosa* *N*-acylhomoserine lactone (AHL) molecule 3-oxo-C12 has been shown to target this morphological switch from yeast to hyphal growth (Hogan *et al.*, 2004). Using filamentation-inducing media, HHQ or PQS did not influence *C. albicans* morphology or the morphological switch during planktonic growth. Hyphae were produced normally on solid spider media and in liquid culture (Fig. 4c) and there was no difference in hyphal biomass production in response to HHQ (data not shown). Thus, in addition to the interspecies role revealed for HHQ and PQS, our analysis reveals an interkingdom role for HHQ, influencing biofilm formation in the major pathogenic yeast *C. albicans*.

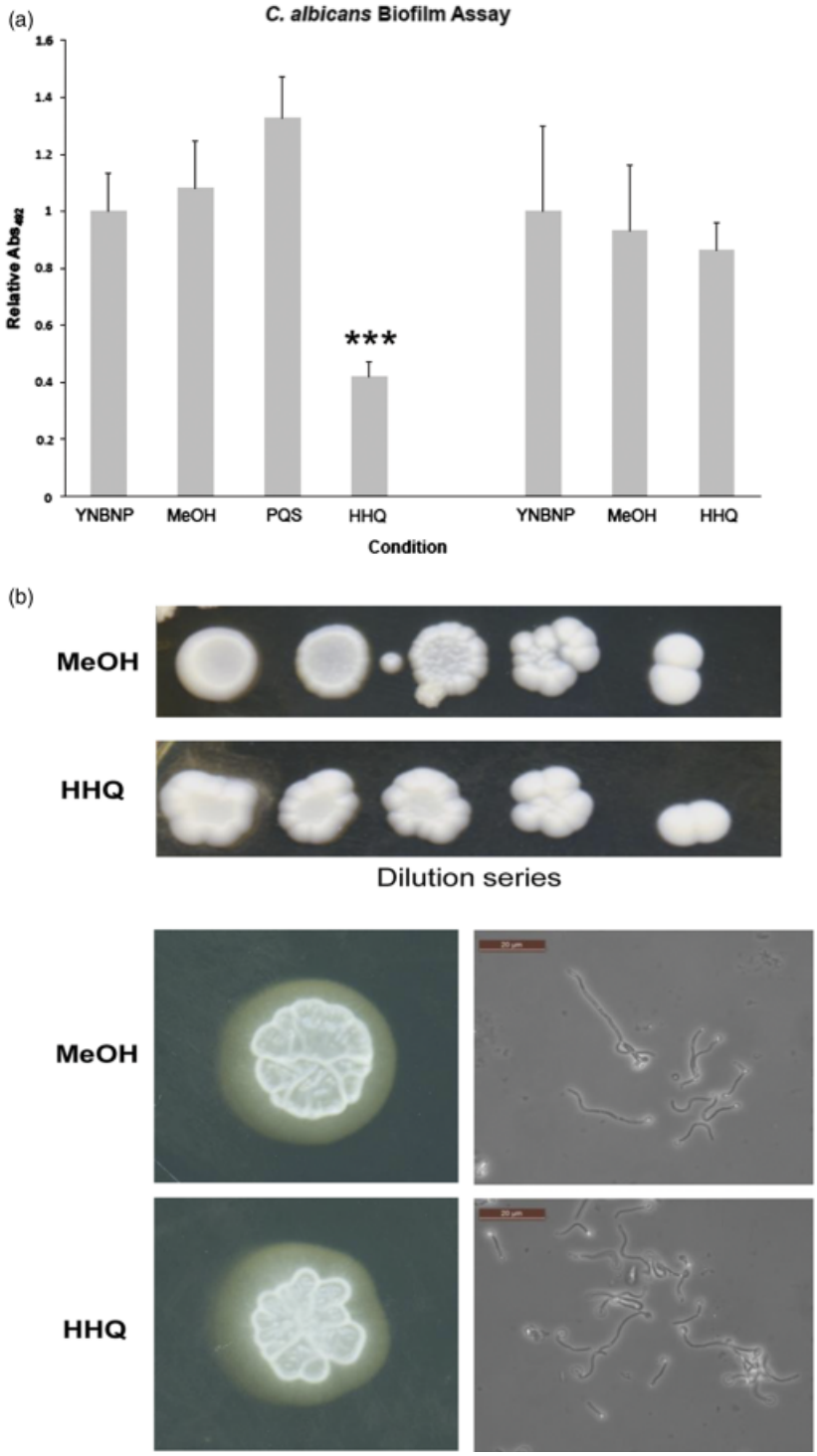

Fig. 4. HHQ interferes with biofilm formation in the eukaryotic yeast pathogen *C. albicans*. (a) *Candida albicans* SC5314 (wild type) and *tup1/tup1* mutant (constitutively hyphal) biofilm formation in filament-inducing medium with 100 μM PQS, HHQ or methanol in polystyrene microtitre wells. The *y*-axis represents $A_{492\,nm}$ values for each condition normalized to untreated YNBNP. Statistical differences are shown compared with methanol control (***$P \leq 0.001$ *t*-test). Error bars represent ± SD (three biological replicates). (b) Serial dilutions of wild-type *C. albicans* plated on YPD media containing 100 μM HHQ or an equivalent volume of methanol. (c) Microscopic visualization of the morphological transition from yeast to hyphae in planktonic cells. Filamentation on solid spider media in the presence of 100 μM HHQ (left panel). Filament-inducing media containing 100 μM HHQ or equivalent methanol (right panel). Images were captured after 4 h incubation with aeration at 37 °C.

Structure–function analysis of HHQ and PQS analogues provides insight into their influence on interkingdom behaviour

To gain an insight into the molecular characteristics that delineate the interspecies and interkingdom influence of HHQ and PQS uncovered in this study, we prepared analogues of HHQ and PQS for phenotypic analysis. These consisted of a C3 formyl substituted HHQ (cHHQ) and derivatives of HHQ and PQS where the C_7 alkyl side chain was replaced with a C_1 methyl group (Table S1). In contrast to the bacteriostatic activity of HHQ, addition of cHHQ,

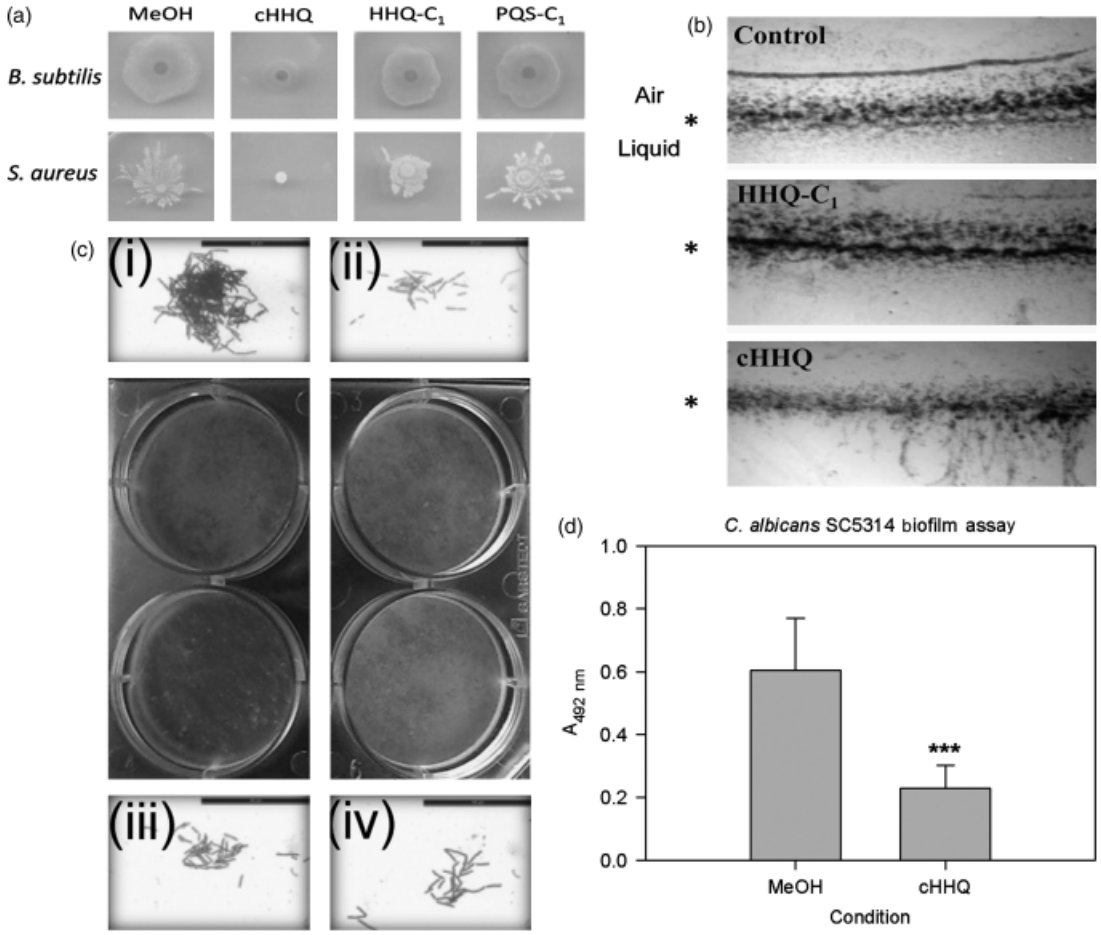

Fig. 5. Influence of HHQ structural analogues on microbial behaviour. (a) Motility of Gram-positive bacteria on semi-solid agar supplemented with cHHQ, HHQ-C_1 and PQS-C_1. (b) Pellicle formation and migration from the air–liquid surface interface in *Bacillus subtilis*, in the presence of cHHQ, HHQ-C_1 and PQS-C_1. (c) Pellicle formation in *B. subtilis* in the presence of cHHQ (i), HHQ (ii), methanol (iii) and HHQ-C_1 (iv). (d) Biofilm formation in *Candida albicans* in the presence of cHHQ and a methanol control (***$P \leq 0.001$ *t*-test). *Air–liquid interface.

HHQ-C_1, and PQS-C_1 to solid media did not influence the growth of any of the organisms tested (Table 2). Addition of 10 μM cHHQ to semi-solid agar did, however, reduce motility in Gram-positive bacteria to an extent that was intermediate between that observed in the presence of HHQ and PQS (Fig. 5a). The cHHQ molecule was also capable of interfering with biofilm formation/attachment in *B. subtilis* and *C. albicans*, albeit to a lesser degree than HHQ (Fig. 5b–d and Fig. S6; Table 2). TLC analysis revealed that the C_1 derivatives exhibited a markedly lower R_f-value than their parent compounds in a mobile phase of dichloromethane:-methanol (95 : 5) (Fig. 6a). Interestingly, although the Rf value of cHHQ was comparable to PQS, reflecting simliar polarities in this solvent, the dark colour of the cHHQ compound was comparable to that of HHQ possibly reflecting similar chemical properties (Fig. 6b). Structure analysis suggests that while both PQS and cHHQ possess moieties capable of an inductive electron-withdrawing effect, the potential aromaticity of the system would introduce resonance effects. In such cases the ring system of PQS would be expected to possess increased electron density compared with the aldehyde, with the ring of HHQ possessing intermediate electron density (Fig. 6c). Furthermore, while the C-3 hydroxyl group of PQS has the capacity to act as a H-bond donor, the C-3 aldehyde group of cHHQ does not have this function. However, the oxygen group at C-3 in both PQS and the aldehyde form could potentially act as a H-bond acceptor in biological systems. Interestingly, when supplied to a *P. aeruginosa* PA14 *pqsH*$^-$ mutant, which is capable of synthesizing HHQ but not PQS, the biological activity of cHHQ and the methyl analogues was consistent with their influence on microbial behaviour (Fig. 6d). While PQS was capable of restoring phenazine production in this mutant, HHQ and the two C_1 derivatives were deficient in this regard. In contrast, the cHHQ molecule restored phenazine production almost to wild-type levels (Fig. 6d).

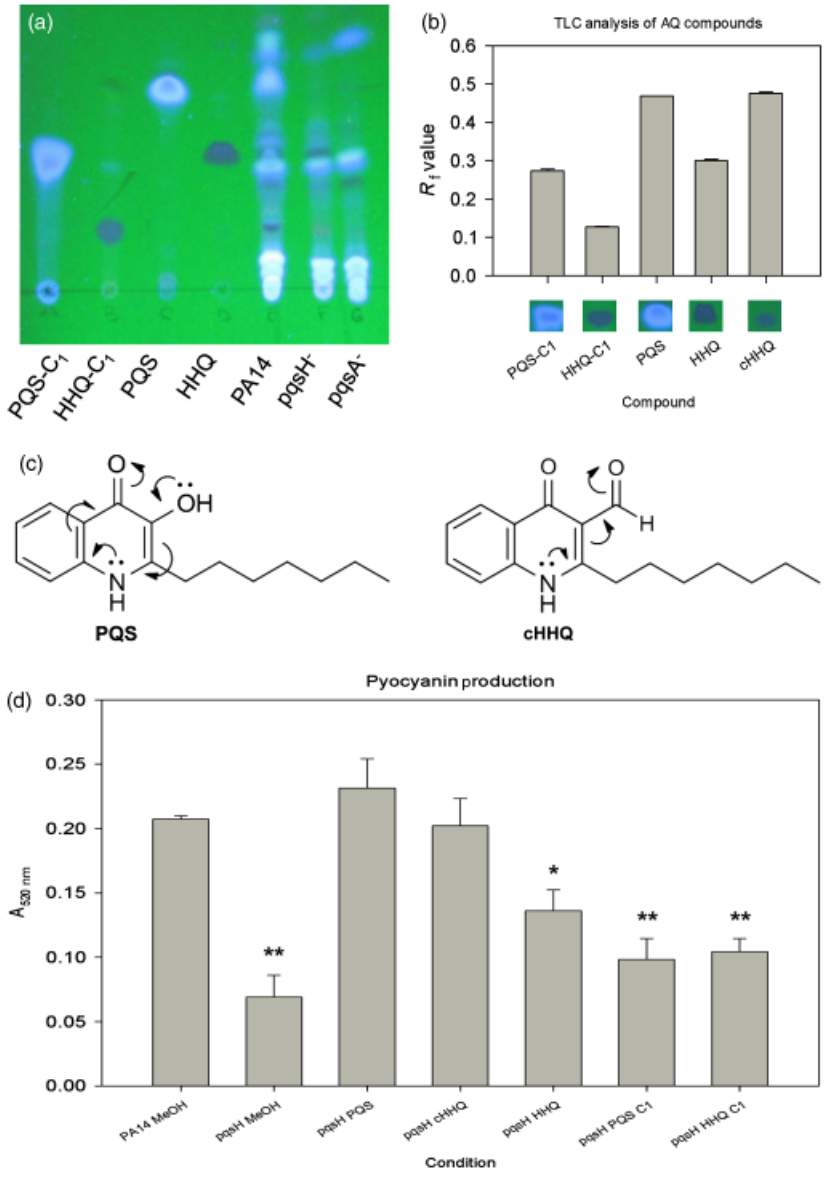

Fig. 6. Structure–function analysis of alkylquinolone compounds used in this study. (a) TLC analysis of the alkylquinolone compounds compared with PA14, PA14 *pqsA* and PA14 *pqsH* supernatant extracts. (b) Bar graph representation of TLC analysis revealing that both PQS and cHHQ have similar R_f values in the dichloromethane : methanol (95 : 5) mobile phase. (c) Resonance structure analysis of PQS and cHHQ molecules. In PQS, electron density would be released into the ring system. In contrast, an aldehyde group is more likely to act as a resonance electronic withdrawing group. HHQ would be close to 'neutral' in this respect. (d) Quantification of phenazine production in a *Pseudomonas aeruginosa* PA14 *pqsH*$^-$ mutant supplemented with the HHQ, PQS and their derivatives. Data presented is the SD of three independent experiments ($^*P \leq 0.05$, $^{**}P \leq 0.005$).

Therefore, the alkyl side chain and the H-bond accepting ability of the hydroxyl group are potentially defining features of the interkingdom modulating capacity of these signal compounds, while the hydrophobicity of both compounds must also be considered.

Discussion

Our analysis has revealed a novel interkingdom role for the PQS and its precursor HHQ, two *P. aeruginosa* signal molecules that have been shown to coordinate molecular circuitry and cellular function in this important opportunistic human pathogen. *Pseudomonas aeruginosa* inhabits a diverse array of niches, including soil and water, as well as being the principal nosocomial pathogen associated with mortality in CF patients (Janda and Bottone, 1981; Govan and Deretic, 1996). Many other important human pathogens are also found in both environmental and host niches where interaction with *P. aeruginosa* signal molecules is a strong possibility. Both *Listeria* and *Bacillus* species are soil- and water-borne human pathogens, with *Bacillus* in particular being an important colonizer of the plant rhizosphere (Berg *et al.*, 2005; Bottone, 2010). *Staphylococci* have also been isolated from the plant rhizosphere, which is emerging as a possible reservoir for opportunistic human pathogens (Berg *et al.*, 2005). A role for PQS and HHQ in moderating the polymicrobial communities that inhabit these environmentally and biotechnologically important niches must now be considered.

Pseudomonas aeruginosa is the predominant organism in chronic lung infection of CF patients, with up to 80% of the

adult CF population being chronically infected (Hansen *et al.*, 2008). *Staphylococcus aureus*, *Burkholderia cepacia* and *C. albicans* are also strongly associated with CF-infections and successfully colonize the CF-lung, often forming mixed biofilms with *P. aeruginosa* (FitzSimmons, 1993; Govan & Deretic, 1996; Hoiby, 1998; Bakare *et al.*, 2003). PQS has been detected at 2 μM in CF samples from sputum, bronchoalveolar lavage fluid and mucopurulent fluid from distal airways of end-stage lungs removed at transplant, and this is considered to be an underestimate due to limitations of the extraction technique (Collier *et al.*, 2002). Subsequently, isolates obtained from infant CF-patients under 3 years of age were found to overproduce PQS, suggesting that it may be instrumental in adaptation of *P. aeruginosa* to the airways of young CF-patients (Guina *et al.*, 2003a). Transcriptomic and functional genomic studies have provided further evidence for the importance of PQS and HHQ during adaptation to the CF-lung (Palmer *et al.*, 2005; Lindsey *et al.*, 2008) and have also revealed several environmental and host-related stimuli that influence production of alkylquinolones in *P. aeruginosa* (Guina *et al.*, 2003b; Jensen *et al.*, 2006; Cummins *et al.*, 2009; Schertzer *et al.*, 2010). More recently, PQS has been implicated in *P. aeruginosa* pathogenesis in animal models of infection (Zaborin *et al.*, 2009), while Kim *et al.* (2010a, b) reported immunomodulation and inhibition of macrophage activation by HHQ and PQS. These findings, and the scope of the modulation of microbial behaviour described in this study, suggest that both HHQ and PQS may be more influential during infection than previously thought.

The complexity of bacterial–fungal biofilms during infection has a major influence on the host response, in particular during the chronic stage of infection (Cugini *et al.*, 2007; McAlester *et al.*, 2008; Allard *et al.*, 2009; Gibson *et al.*, 2009). We have recently shown that supernatants from *P. aeruginosa* could inhibit *C. albicans* biofilms in an HSL-independent manner, an effect that was also observed in a constitutively hyphal *tup1*/*tup1* mutant (Holcombe *et al.*, 2010). The finding that HHQ inhibits biofilm formation in *C. albicans* wild type, but not in a *tup1*/*tup1* mutant, implies that yet another mechanism is involved. Tup1 regulates many different sets of genes involved in hyphal and biofilm development, and one possibility is that HHQ may potentially modulate the interactions of Tup1 with some of its binding partners leading to the observed biofilm-specific effects. Previous studies have shown that production of PQS and HHQ is influenced by farnesol, a *C. albicans* derived signalling molecule involved in interspecies and intraspecies interactions, highlighting the intricacy of the interactions surrounding these organisms (Cugini *et al.*, 2007; Cugini *et al.*, 2010).

The role of HHQ and PQS uncovered in this study mirrors the expanding influence of *P. aeruginosa* AHL signal molecules on microbial and eukaryotic systems. 3-oxo-C12-HSL has been shown to be involved in bacterial cross-talk (Riedel *et al.*, 2001; Qazi *et al.*, 2006) and also interferes with the yeast-hyphal transition in *C. albicans* (Hogan *et al.*, 2004). AHLs share structural homology with many eukaryotic hormones, and influence gene expression in a number of cell types (Telford *et al.*, 1998; Lawrence *et al.*, 1999; Tateda *et al.*, 2003; Li *et al.*, 2004) modulating the host inflammatory and immune response in mammals (Hooi *et al.*, 2004; Kim *et al.*, 2010a, b). While recent studies have implicated peroxisome proliferator-activated receptors as binding receptors for 3-oxo-C12-HSL (Jahoor *et al.*, 2008; Cooley *et al.*, 2010), the targets of HHQ and PQS remain to be elucidated. Along with AHLs, the alkylquinolone signal molecules are typically internalized (Williams, 2007), suggesting that receptors for these compounds may, at least in some species, be intracellular. Recently, PQS has been shown to mediate membrane vesicle formation in *E. coli* and *B. subtilis*, indicating that the Gram-negative membrane structure may not be a limiting determinant for interaction with PQS (Tashiro *et al.*, 2010). An exciting new finding reports that microorganisms may communicate both intra- and interspecies through nanotubes (Dubey & Ben-Yehuda, 2011), although *P. aeruginosa* remains to be characterized in this regard.

Several studies have discussed the requirements for true signal molecules (Winzer *et al.*, 2002; Diggle *et al.*, 2007a; Atkinson and Williams, 2009). Basic conditions are that the molecule must (1) diffuse from the cell, (2) be taken up by a neighbouring cell, (3) trigger an evolved response from that cell beyond that required to simply metabolize the molecule, and (4) benefit both the producer and the receiver (Diggle *et al.*, 2007a). While PQS and HHQ conform to these rules in *P. aeruginosa*, future studies will seek to determine the response networks that exist in other species. While the influence described in this study would suggest an antagonistic action towards other microorganisms, the species-specific response observed to the presence of HHQ and PQS suggests that their interspecies communication role cannot simply be explained by metabolism of the signal.

So, how might other species perceive and respond to the presence of HHQ and PQS in their extracellular milieu? Although the mechanisms through which both HHQ and PQS mediate their interkingdom modulation remains unknown, the fact that Gram-negative swimming motility was not affected by either compound suggests that flagellar activity is not targeted directly. Furthermore, the species-specific influence of HHQ on biofilm formation raises the possibility that other human pathogens such as *S. aureus*, which responds to HHQ by increasing pigment production and repressing spreading motility, may have adapted to its presence. Some further insight into how microorganisms perceive and respond to these compounds may be gleaned

from the formyl derivative molecule cHHQ, which influenced Gram-positive behaviour to an extent that was intermediate relative to HHQ and PQS. Structure function analysis suggests that hydrophobicity and H-bond accepting potential may be important in delineating PQS and HHQ effects, while the evidence for polarity and resonance effects is not supported by the phenotypic data. An indication of the diverse functionality of these alkylquinolone compounds has arisen from recent structure–function analysis performed on HHQ and PQS analogues in *P. aeruginosa*, where the anthranilate ring was altered by substitution (Hodgkinson *et al*., 2010). The authors reported a different structure–activity profile for each phenotype investigated, further evidence that the signalling mechanism of HHQ and PQS may be multifactorial.

The ability of HHQ and PQS to influence cross-kingdom behaviour suggests that alkylquinolone-signalling may play a fundamental role in the interspecies interactions that are the hallmark of polymicrobial communities. Furthermore, the diversity of clinically and biotechnologically relevant niches inhabited by the species investigated in this study highlights the potential for developing novel therapeutic and commercial strategies based on these compounds. Defining the interkingdom influence of HHQ and PQS will require a systems based approach that encompasses the physiology and complexity of both the producing and responding organisms. Furthermore, the insights gained through structure–function and multispecies analysis will facilitate mechanistic studies that seek to identify the molecular pathways responsible for transducing the PQS and HHQ influence and lead to a better understanding of how the alkylquinolone signal molecules influence gene expression in microbial pathogens.

Acknowledgements

We thank Pat Higgins for excellent technical assistance during the course of this work. We also thank Eimear Plower for performing flow-cell biofilm experiments and David Woods for performing time kill-curve assays. We thank Dr T. Barbosa for insightful discussion on *B. subtilis*-related phenotypes. *Candida albicans BCa2-10* was a kind gift from A. Johnson, and *L. monocytogenes* LO28, *Staphylococcus gallinarum* DMSZ4616 and *Staphylococcus epidermidis* DMSZ3095 were received from C. Hill. This research was supported in part by grants awarded by the European Commission (MTKD-CT-2006-042062; O36314), Science Foundation Ireland (SFI 04/BR/B0597; 07/IN.1/B948; 08/RFP/GEN1295; 08/RFP/GEN1319; 09/RFP/BMT2350), the Department of Agriculture and Food (DAF RSF 06 321; DAF RSF 06 377; FIRM 08/RDC/629), the Irish Research Council for Science, Engineering and Technology (05/EDIV/FP107), the Health Research Board (RP/2006/271; RP/2007/290; HRA/2009/146), the Environmental Protection Agency (EPA2006-PhD-S-21; EPA2008-PhD-S-2), the Marine Institute (Beaufort award C2CRA 2007/082) and the Higher Education Authority of Ireland (PRTLI3). G.M.G. would like to thank Science Foundation Ireland for a Research Frontiers Programme grant (No. 09/RFP/CHS2353).

References

Allard JB, Rinaldi L, Wargo MJ, Allen G, Akira S, Uematsu S, Poynter ME, Hogan DA, Rincon M & Whittaker LA (2009) Th2 allergic immune response to inhaled fungal antigens is modulated by TLR-4-independent bacterial products. *Eur J Immunol* **39**: 776–788.

Atkinson S & Williams P (2009) Quorum sensing and social networking in the microbial world. *J R Soc Interface* **6**: 959–978.

Bakare N, Rickerts V, Bargon J & Just-Nubling G (2003) Prevalence of *Aspergillus fumigatus* and other fungal species in the sputum of adult patients with cystic fibrosis. *Mycoses* **46**: 19–23.

Berg G, Ebrl L & Hartmann A (2005) The rhizosphere as a reservoir for opportunistic human pathogenic bacteria. *Environ Microbiol* **7**: 1673–1685.

Bottone EJ (2010) *Bacillus cereus*, a volatile human pathogen. *Clin Microbiol Rev* **23**: 382–398.

Brachmann CB, Davies A, Cost GJ, Caputo E, Li JC, Hieter P & Boeke JD (1998) Designer deletion strains derived from *Saccharomyces cerevisiae* S288C: a useful set of strains and plasmids for PCR-mediated gene disruption and other applications. *Yeast* **14**: 115–132.

Braun BR & Johnson AD (1997) Control of filament formation in *Candida albicans* by the transcriptional repressor TUP1. *Science* **277**: 105–109.

Bredenbruch F, Geffers R, Nimtz M, Buer J & Haussler S (2006) The *Pseudomonas aeruginosa* quinolone signal (PQS) has an iron-chelating activity. *Environ Microbiol* **8**: 1318–1329.

Calfee MW, Shelton JG, McCubrey JA & Pesci EC (2005) Solubility and bioactivity of the *Pseudomonas* quinolone signal are increased by a *Pseudomonas aeruginosa*-produced surfactant. *Infect Immun* **73**: 878–882.

Collier DN, Anderson L, McKnight SL, Noah TL, Knowles M, Boucher R, Schwab U, Gilligan P & Pesci EC (2002) A bacterial cell to cell signal in the lungs of cystic fibrosis patients. *FEMS Microbiol Lett* **215**: 41–46.

Cooley MA, Whittall C & Rolph MS (2010) Pseudomonas signal molecule 3-oxo-C12-homoserine lactone interferes with binding of rosiglitazone to human PPARgamma. *Microbes Infect* **12**: 231–237.

Cugini C, Calfee MW, Farrow JM, Morales DK, Pesci EC & Hogan DA (2007) Farnesol, a common sesquiterpene, inhibits PQS production in *Pseudomonas aeruginosa*. *Mol Microbiol* **65**: 896–906.

Cugini C, Morales DK & Hogan DA (2010) *Candida albicans*-produced farnesol stimulates PQS production in LasR-

defective *Pseudomonas aeruginosa* strains. *Microbiology* **156**: 3096–3107.

Cummins J, Reen FJ, Baysse C, Mooij MJ & O'Gara F (2009) Subinhibitory concentrations of the cationic antimicrobial peptide colistin induce the *Pseudomonas* quinolone signal in *Pseudomonas aeruginosa*. *Microbiology* **155**: 2826–2837.

Davies DG & Marques CN (2009) A fatty acid messenger is responsible for inducing dispersion in microbial biofilms. *J Bacteriol* **191**: 1393–1403.

Deziel E, Lepine F, Milot S, He J, Mindrinos MN, Tompkins RG & Rahme LG (2004) Analysis of *Pseudomonas aeruginosa* 4-hydroxy-2-alkylquinolines (HAQs) reveals a role for 4-hydroxy-2-heptylquinoline in cell-to-cell communication. *P Natl Acad Sci USA* **101**: 1339–1344.

Diggle SP, Winzer K, Chhabra SR, Worrall KE, Camara M & Williams P (2003) The *Pseudomonas aeruginosa* quinolone signal molecule overcomes the cell density-dependency of the quorum sensing hierarchy, regulates *rhl*-dependent genes at the onset of stationary phase and can be produced in the absence of LasR. *Mol Microbiol* **50**: 29–43.

Diggle SP, Lumjiaktase P, Dipilato F, Winzer K, Kunakorn M, Barret DA, Chhabra SR, Camara M & Williams P (2006) Functional genetic analysis reveals a 2-alkyl-4-quinolone signaling system in the human pathogen *Burkholderia pseudomallei* and related bacteria. *Chem Biol* **13**: 701–710.

Diggle SP, Gardner A, West SA & Griffin AS (2007a) Evolutionary theory of bacterial quorum sensing: when is a signal not a signal? *Philos T Roy Soc B* **362**: 1241–1249.

Diggle SP, Matthijs S, Wright VJ *et al.* (2007b) The *Pseudomonas aeruginosa* 4-quinolone signal molecules HHQ and PQS play multifunctional roles in quorum sensing and iron entrapment. *Chem Biol* **14**: 87–96.

Dubern JF & Diggle SP (2008) Quorum sensing by 2-alkyl-4-quinolones in *Pseudomonas aeruginosa* and other bacterial species. *Mol Biosyst* **4**: 882–888.

Dubey GP & Ben-Yehuda S (2011) Intercellular nanotubes mediate bacterial communication. *Cell* **144**: 590–600.

Essar DW, Eberly L, Han CY & Crawford IP (1990) DNA-sequences and characterization of 4 early genes of the tryptophan pathway in *Pseudomonas aeruginosa*. *J Bacteriol* **172**: 853–866.

FitzSimmons SC (1993) The changing epidemiology of cystic fibrosis. *J Pediatr* **122**: 1–9.

Fletcher MP, Diggle SP, Camara M & Williams P (2007) Biosensor-based assays for PQS, HHQ and related 2-alkyl-4-quinolone quorum sensing signal molecules. *Nat Protoc* **2**: 1254–1262.

Fritze D & Pukall R (2001) Reclassification of bioindicator strains *Bacillus subtilis* DSM 675 and *Bacillus subtilis* DSM 2277 as *Bacillus atrophaeus*. *Int J Syst Evol Micr* **51**: 35–37.

Gibson J, Sood A & Hogan DA (2009) *Pseudomonas aeruginosa–Candida albicans*. Interactions: localization and fungal toxicity of a phenazine derivative. *Appl Environ Microb* **75**: 504–513.

Gillum AM, Tsay EYH & Kirsch DR (1984) Isolation of the *Candida albicans* gene for orotidine-5′-phosphate decarboxylase by complementation of *S. cerevisiae* URA3 and *Escherichia coli* PyrF mutations. *Mol Gen Genet* **198**: 179–182.

Glick R, Gilmour C, Tremblay J, Satanower S, Avidan O, Deziel E, Greenberg EP, Poole K & Banin E (2010) Increase in rhamnolipid synthesis under iron-limiting conditions influences surface motility and biofilm formation in *Pseudomonas aeruginosa*. *J Bacteriol* **192**: 2973–2980.

Govan JR & Deretic V (1996) Microbial pathogenesis in cystic fibrosis: mucoid *Pseudomonas aeruginosa* and *Burkholderia cepacia*. *Microbiol Rev* **60**: 539–574.

Guina T, Purvine SO, Yi EC, Eng J, Goodlett DR, Aebersold R & Miller SI (2003a) Quantitative proteomic analysis indicates increased synthesis of a quinolone by *Pseudomonas aeruginosa* isolates from cystic fibrosis airways. *P Natl Acad Sci USA* **100**: 2771–2776.

Guina T, Wu MH, Miller SI, Purvine SO, Yi EC, Eng J, Goodlett DR, Aebersold R, Ernst RK & Lee KA (2003b) Proteomic analysis of *Pseudomonas aeruginosa* grown under magnesium limitation. *J Am Soc Mass Spectr* **14**: 742–751.

Hansen CR, Pressler T & Hoiby N (2008) Early aggressive eradication therapy for intermittent *Pseudomonas aeruginosa* airway colonization in cystic fibrosis patients: 15 years experience. *J Cyst Fibros* **7**: 523–530.

Haussler S & Becker T (2008) The *Pseudomonas* quinolone signal (PQS) balances life and death in *Pseudomonas aeruginosa* populations. *PLoS Pathog* **4**: e1000166.

Hawser S (1996) Comparisons of the susceptibilities of planktonic and adherent *Candida albicans* to antifungal agents: a modified XTT tetrazolium assay using synchronised *C.albicans* cells. *J Med Vet Mycol* **34**: 149–152.

Heeb S, Fletcher MP, Chhabra SR, Diggle SP, Williams P & Camara M (2010) Quinolones: from antibiotics to autoinducers. *FEMS Microbiol Rev.* **35**: 247–274.

Hodgkinson J, Bowden SD, Galloway WR, Spring DR & Welch M (2010) Structure–activity analysis of the *Pseudomonas* quinolone signal molecule. *J Bacteriol* **192**: 3833–3837.

Hogan DA & Kolter R (2002) *Pseudomonas–Candida* interactions: an ecological role for virulence factors. *Science* **296**: 2229–2232.

Hogan DA, Vik A & Kolter R (2004) A *Pseudomonas aeruginosa* quorum-sensing molecule influences *Candida albicans* morphology. *Mol Microbiol* **54**: 1212–1223.

Hoiby N (1998) *Pseudomonas in Cystic Fibrosis: Past, Present, and Future*. Cystic Fibrosis Trust, London.

Holcombe LJ, McAlester G, Munro CA, Enjalbert B, Brown AJP, Gow NAR, Ding C, Butler G, O'Gara F & Morrissey JP (2010) *Pseudomonas aeruginosa* secreted factors impair biofilm development in *Candida albicans*. *Microbiology* **156**: 1476–1486.

Hooi DSW, Bycroft BW, Chhabra SR, Williams P & Pritchard DI (2004) Differential immune modulatory activity of *Pseudomonas aeruginosa* quorum-sensing signal molecules. *Infect Immun* **72**: 6463–6470.

Hradil P, Hlavac J & Lemr K (1999) Preparation of 1,2-disubstituted-3-hydroxy-4(1H)-quinolinones and the influence of substitution on the course of cyclization. *J Heterocyclic Chem* **36**: 141–144.

Huse H & Whiteley M (2010) 4-Quinolones smart phones of the microbial world. *Chem Rev* **111**: 152–159.

Jahoor A, Patel R, Bryan A, Do C, Krier J, Watters C, Wahli W, Li G, Williams SC & Rumbaugh KP (2008) Peroxisome proliferator-activated receptors mediate host cell proinflammatory responses to *Pseudomonas aeruginosa* autoinducer. *J Bacteriol* **190**: 4408–4415.

Janda JM & Bottone EJ (1981) *Pseudomonas aeruginosa* enzyme profiling: predictor of potential invasiveness and use as an epidemiological tool. *J Clin Microbiol* **14**: 55–60.

Jensen V, Lons D, Zaoui C, Bredenbruch F, Meissner A, Dieterich G, Munch R & Haussler S (2006) RhlR expression in *Pseudomonas aeruginosa* is modulated by the *Pseudomonas* quinolone signal via PhoB-dependent and -independent pathways. *J Bacteriol* **188**: 8601–8606.

Josenhans C & Suerbaum S (2002) The role of motility as a virulence factor in bacteria. *Int J Med Microbiol* **291**: 605–614.

Kim K, Kim SH, Lepine F, Cho YH & Lee GR (2010a) Global gene expression analysis on the target genes of PQS and HHQ in J774A.1 monocyte/macrophage cells. *Microb Pathogenesis* **49**: 174–180.

Kim K, Kim YU, Koh BH, Hwang SS, Kim SH, Lepine F, Cho YH & Lee GR (2010b) HHQ and PQS, two *Pseudomonas aeruginosa* quorum-sensing molecules, down-regulate the innate immune responses through the nuclear factor-kappa B pathway. *Immunology* **129**: 578–588.

Kobayashi K (2007) *Bacillus subtilis* pellicle formation proceeds through genetically defined morphological changes. *J Bacteriol* **189**: 4920–4931.

Krukonis ES & DiRita VJ (2003) From motility to virulence: sensing and responding to environmental signals in *Vibrio cholerae*. *Curr Opin Microbiol* **6**: 186–190.

Lawrence RN, Dunn WR, Bycroft B, Camara M, Chhabra SR, Williams P & Wilson VG (1999) The *Pseudomonas aeruginosa* quorum-sensing signal molecule, *N*-(3-oxododecanoyl)-L-homoserine lactone, inhibits porcine arterial smooth muscle contraction. *Brit J Pharmacol* **128**: 845–848.

Leisinger T & Margraff R (1979) Secondary metabolites of the fluorescent Pseudomonads. *Microbiol Rev* **43**: 422–442.

Lepine F, Milot S, Deziel E, He JX & Rahme LG (2004) Electrospray/mass spectrometric identification and analysis of 4-hydroxy-2-alkylquinolines (HAQs) produced by *Pseudomonas aeruginosa*. *J Am Soc Mass Spectr* **15**: 862–869.

Li L, Hooi D, Chhabra SR, Pritchard D & Shaw PE (2004) Bacterial *N*-acylhomoserine lactone-induced apoptosis in breast carcinoma cells correlated with down-modulation of STAT3. *Oncogene* **23**: 4894–4902.

Liberati NT, Urbach JM, Miyata S, Lee DG, Drenkard E, Wu G, Villanueva J, Wei T & Ausubel FM (2006) An ordered, nonredundant library of *Pseudomonas aeruginosa* strain PA14 transposon insertion mutants (vol 103, pg 2833, 2006). *P Natl Acad Sci USA* **103**: 19931–19931.

Lindsey TL, Hagins JM, Sokol PA & Silo-Suh LA (2008) Virulence determinants from a cystic fibrosis isolate of *Pseudomonas aeruginosa* include isocitrate lyase. *Microbiology* **154**: 1616–1627.

Liu H, Kohler J & Fink GR (1994) Suppression of hyphal formation in *Candida albicans* by mutation of a STE12 homolog. *Science* **266**: 1723–1726.

Mashburn-Warren L, Howe J, Brandenburg K & Whiteley M (2009) Structural requirements of the *Pseudomonas* Quinolone signal for membrane vesicle stimulation. *J Bacteriol* **191**: 3411–3414.

Matilla MA, Ramos JL, Duque E, de Dios Alche J, Espinosa-Urgel M & Ramos-Gonzalez MI (2007) Temperature and pyoverdine-mediated iron acquisition control surface motility of *Pseudomonas putida*. *Environ Microbiol* **9**: 1842–1850.

McAlester G, O'Gara F & Morrissey JP (2008) Signal-mediated interactions between *Pseudomonas aeruginosa* and *Candida albicans*. *J Med Microbiol* **57**: 563–569.

McGlacken GP, McSweeney CM, O'Brien T, Lawrence SE, Elcoate CJ, Reen FJ & O'Gara F (2010) Synthesis of 3-halo-analogues of HHQ, subsequent cross-coupling and first crystal structure of *Pseudomonas* quinolone signal (PQS). *Tetrahedron Lett* **51**: 5919–5921.

McKnight SL, Iglewski BH & Pesci EC (2000) The *Pseudomonas* quinolone signal regulates *rhl* quorum sensing in *Pseudomonas aeruginosa*. *J Bacteriol* **182**: 2702–2708.

Moller S, Sternberg C, Andersen JB, Christensen BB, Ramos JL, Givskov M & Molin S (1998) *In situ* gene expression in mixed-culture biofilms: Evidence of metabolic interactions between community members. *Appl Environ Microb* **64**: 721–732.

Palmer KL, Mashburn LM, Singh PK & Whiteley M (2005) Cystic fibrosis sputum supports growth and cues key aspects of *Pseudomonas aeruginosa* physiology. *J Bacteriol* **187**: 5267–5277.

Pesci EC, Milbank JBJ, Pearson JP, McKnight S, Kende AS, Greenberg EP & Iglewski BH (1999) Quinolone signaling in the cell-to-cell communication system of *Pseudomonas aeruginosa*. *P Natl Acad Sci USA* **96**: 11229–11234.

Poulter S, Carlton TM, Su XB, Spring DR & Salmond GPC (2010) Engineering of new prodigiosin-based biosensors of *Serratia* for facile detection of short-chain *N*-acyl homoserine lactone quorum-sensing molecules. *Environ Microbiol Rep* **2**: 322–328.

Qazi S, Middleton B, Muharram SH, Cockayne A, Hill P, O'Shea P, Chhabra SR, Camara M & Williams P (2006) *N*-acylhomoserine lactones antagonize virulence gene expression and quorum sensing in *Staphylococcus aureus*. *Infect Immun* **74**: 910–919.

Ramage G, Vande Walle K, Wickes BL & Lopez-Ribot JL (2001) Standardized method for *in vitro* antifungal susceptibility testing of *Candida albicans* biofilms. *Antimicrob Agents Ch* **45**: 2475–2479.

Riedel K, Hentzer M, Geisenberger O, Huber B, Steidle A, Wu H, Hoiby N, Givskov M, Molin S & Ebrl L (2001)

N-acylhomoserine-lactone-mediated communication between *Pseudomonas aeruginosa* and *Burkholderia cepacia* in mixed biofilms. *Microbiology* **147**: 3249–3262.

Schertzer JW, Brown SA & Whiteley M (2010) Oxygen levels rapidly modulate *Pseudomonas aeruginosa* social behaviours via substrate limitation of PqsH. *Mol Microbiol* **77**: 1527–1538.

Tang KW & Grossart HP (2007) Iron effects on colonization behavior, motility, and enzymatic activity of marine bacteria. *Can J Microbiol* **53**: 968–974.

Tashiro Y, Ichikawa S, Nakajima-Kambe T, Uchiyama H & Nomura N (2010) *Pseudomonas* quinolone signal affects membrane vesicle production in not only gram-negative but also gram-positive bacteria. *Microb Environ* **25**: 120–125.

Tateda K, Ishii Y, Horikawa M, Matsumoto T, Miyairi S, Pechere JC, Standiford TJ, Ishiguro M & Yamaguchi K (2003) The *Pseudomonas aeruginosa* autoinducer *N*-3-oxododecanoyl homoserine lactone accelerates apoptosis in macrophages and neutrophils. *Infect Immun* **71**: 5785–5793.

Telford G, Wheeler D, Williams P, Tomkins PT, Appleby P, Sewell H, Stewart GS, Bycroft BW & Pritchard DI (1998) The *Pseudomonas aeruginosa* quorum-sensing signal molecule *N*-(3-oxododecanoyl)-L-homoserine lactone has immunomodulatory activity. *Infect Immun* **66**: 36–42.

Tunney MM, Ramage G, Field TR, Moriarty TF & Storey DG (2004) Rapid colorimetric assay for antimicrobial susceptibility testing of *Pseudomonas aeruginosa*. *Antimicrob Agents Ch* **48**: 1879–1881.

Vial L, Lepine F, Milot S, Groleau MC, Dekimpe V, Woods DE & Deziel E (2008) *Burkholderia pseudomallei*, *B. thailandensis*, and *B. ambifaria* produce 4-hydroxy-2-alkylquinoline analogues with a methyl group at the 3 position that is required for quorum-sensing regulation. *J Bacteriol* **190**: 5339–5352.

Wade DS, Calfee MW, Rocha ER, Ling EA, Engstrom E, Coleman JP & Pesci EC (2005) Regulation of *Pseudomonas* quinolone signal synthesis in *Pseudomonas aeruginosa*. *J Bacteriol* **187**: 4372–4380.

Williams P (2007) Quorum sensing, communication and cross-kingdom signalling in the bacterial world. *Microbiology* **153**: 3923–3938.

Winzer K, Hardie KR & Williams P (2002) Bacterial cell-to-cell communication: sorry, can't talk now – gone to lunch! *Curr Opin Microbiol* **5**: 216–222.

Wratten SJ, Wolfe MS, Andersen RJ & Faulkner DJ (1977) Antibiotic metabolites from a marine Pseudomonad. *Antimicrob Agents Ch* **11**: 411–414.

Xiao GP, Deziel E, He JX, Lepine F, Lesic B, Castonguay MH, Milot S, Tampakaki AP, Stachel SE & Rahme IG (2006) MvfR, a key *Pseudomonas aeruginosa* pathogenicity LTTR-class regulatory protein, has dual ligands. *Mol Microbiol* **62**: 1689–1699.

Zaborin A, Romanowski K, Gerdes S *et al.* (2009) Red death in *Caenorhabditis elegans* caused by *Pseudomonas aeruginosa* PAO1. *P Natl Acad Sci USA* **106**: 6327–6332.

Supporting Information

Additional Supporting Information may be found in the online version of this article:

Fig. S1. HHQ exhibits species-specific antibacterial activity.
Fig. S2. PQS and HHQ repress microbial motility.
Fig. S3. Several stress response and quorum sensing regulated phenotypes are unaffected by HHQ and PQS.
Fig. S4. Alkyl quinolones interfere with attachment/biofilm formation in *Bacillus subtilis*.
Fig. S5. HHQ exhibits a dose dependent effect on *Candida albicans* biofilm formation but does not influence initial adhesion.
Fig. S6. Influence of alkylquinolone structural analgoues on microbial biofilm formation.
Table S1. HHQ, PQS and derivative compounds.

Please note: Wiley-Blackwell is not responsible for the content or functionality of any supporting materials supplied by the authors. Any queries (other than missing material) should be directed to the corresponding author for the article.

Tetrahedron Letters 51 (2010) 5919–5921

Contents lists available at ScienceDirect

Tetrahedron Letters

journal homepage: www.elsevier.com/locate/tetlet

Synthesis of 3-halo-analogues of HHQ, subsequent cross-coupling and first crystal structure of *Pseudomonas* quinolone signal (PQS)

Gerard P. McGlacken [a,*], Christina M. McSweeney [a], Timothy O'Brien [b], Simon E. Lawrence [a], Curtis J. Elcoate [a], F. Jerry Reen [c], Fergal O'Gara [c]

[a] Department of Chemistry and Analytical and Biological Research Facility, University College Cork, Ireland
[b] School of Pharmacy, University College Cork, Ireland
[c] BIOMERIT Research Centre, Department of Microbiology, University College Cork, Ireland

ARTICLE INFO

Article history:
Received 15 July 2010
Revised 16 August 2010
Accepted 3 September 2010
Available online 15 September 2010

Keywords:
PQS
HHQ
Quorum signaling
Quinolone
Pd-catalysis

ABSTRACT

2-Aryl- and 2-alkyl-quinolin-4-ones and their N-substituted derivatives have several important biological functions such as the *Pseudomonas* quinolone signal (PQS) molecule participation in quorum sensing. Herein, we report the synthesis of its biological precursor, 2-heptyl-4-hydroxy-quinoline (HHQ) and possible isosteres of PQS; the C-3 Cl, Br and I analogues. N-Methylation of the iodide was also feasible and the usefulness of this compound showcased in Pd-catalysed cross-coupling reactions, thus allowing access to a diverse set of biologically important molecules. The first crystal structure of PQS is also included.

Quinolones are best known as broad-spectrum antibacterial agents,[1] for example, fluoroquinolone sales accounted for 18% of the antibacterial market in 2006.[2] An attractive feature of these molecules is their ability to kill bacteria very rapidly; an ability not widely attributable to other antibacterial agents. The related 2-aryl and 2-alkylquinolin-4-ones have recently received considerable attention due to their more wide ranging pharmacological applications. For example, 2-arylquinolin-4-one derivatives also exhibit anti-bacterial[3] and anti-tumour properties.[4] N-Substituted 2-arylquinoline derivatives can act as anti-malarial agents, immunostimulants and non-nucleoside HIV-1 inhibitors.[5] 2-Heptyl-4-hydroxyquinoline N-oxide (HHQNO) is effective against *Staphylococcus aureus*.[6] 2-Heptyl-3-hydroxy-4-quinolone,[7] otherwise known as the *Pseudomonas* quinolone signal (PQS, Fig. 1), has emerged as a key regulator of bacterial cooperative behaviour known as quorum sensing in the antibiotic resistant human pathogen *Pseudomonas aeruginosa*.[8] Derived from its biological precursor, 2-heptyl-4-quinolone (HHQ), PQS has a vast and varied array of biological functions[9] influencing iron homeostasis,[10] vesicle formation,[11] secondary metabolite production and biofilm formation.[12] *P. aeruginosa* PQS signaling is highly responsive to environmental and host-specific cues, including Mg^{2+} and the CF therapeutic colistin.[13] Recent evidence has revealed that PQS is capable of modulating immune responses and human T-cell proliferation.[14]

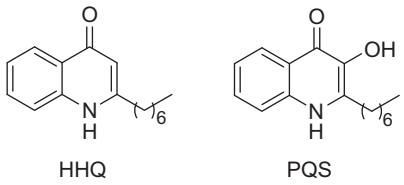

Figure 1. HHQ and PQS structures.

Our interest is twofold; firstly, in the synthesis of 3-haloquinolin-4-ones as analogues of PQS. These substrates will facilitate mechanistic studies into PQS signaling in virulent *Pseudomonas* populations with important clinical applications. Secondly, to explore if a new *N*-methyl version can be used in palladium cross-coupling reactions, thus providing access to an array of new biologically important quinolones. Importantly, the 2-heptyl chain is essential for certain biological functions such as the stimulation of outer vesicle formation in *P. aeruginosa*[11] and thus synthetic procedures on compounds bearing this bulky and hydrophobic substituent are important. There are no reports of halogenation or subsequent cross-coupling of HHQ. From a synthetic viewpoint, the presence of the long hydrophobic chain represents a challenge due to low solubility and the obvious steric hindrance.

* Corresponding author. Fax: +353 021 427 4097.
E-mail address: g.mcglacken@ucc.ie (G.P. McGlacken).

0040-4039/$ - see front matter © 2010 Elsevier Ltd. All rights reserved.
doi:10.1016/j.tetlet.2010.09.013

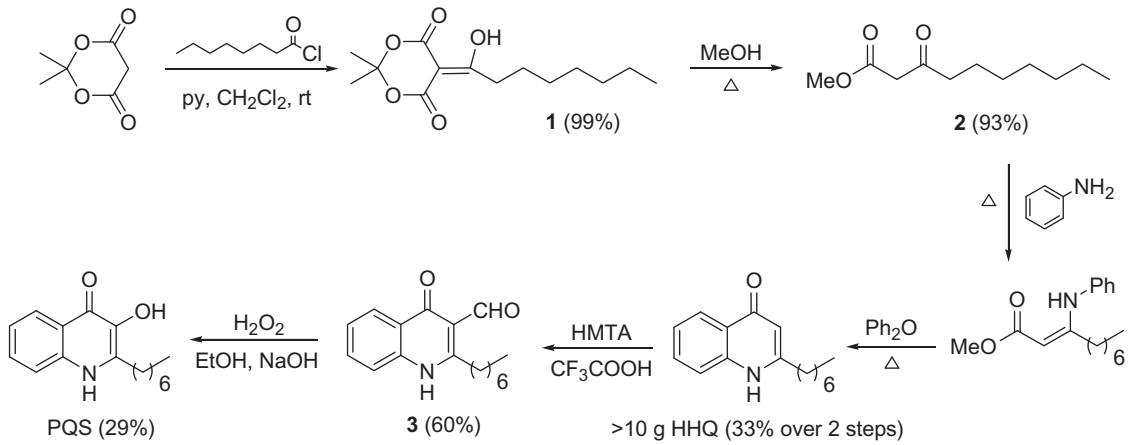

Scheme 1. Synthesis of HHQ and PQS.

Our initial goal was the synthesis of multi-gram quantities of the useful precursor HHQ and to investigate if HHQ could be halogenated at the 3-position. A modified route was designed. Initially Meldrum's acid (0.14 mol) was reacted with octanoyl chloride giving compound **1** followed by boiling in MeOH affording β-ketoester **2** in excellent yield (Scheme 1).[15] Formation of the enamine by reaction with aniline using Dean–Stark apparatus occurred with >98% conversion (^{1}H NMR) over 16 h.[16] Conrad–Limpach cyclisation occurred best using a method described by Bangdiwala and Desai.[17] An alternative cyclisation method reported by Woschek et al. failed to give any product in our hands.[18] As quantities of PQS were also required for biological testing, we carried out our synthesis based on conditions described by Pesci et al.[7]

The Duff formylation reaction proved problematic. In fact no isolable aldehyde could be obtained using the experimental conditions reported. We found using two equivalents of hexamine (HMTA) crucial to obtain a decent yield of aldehyde **3**. Oxidation of precursor **3** proceeded with moderate yield to give PQS as described.[7] For the first time X-ray crystallographic data were obtained for PQS (Fig. 2).[19] Interesting dimeric H-bonding indicates the potential for similar interactions in biological systems.

Chlorination of HHQ occurred smoothly using sodium dichloroisocyanurate.[20] Bromination also proceeded in reasonable yield with either pyridinium tribromide (PTB) or Br_2. Iodination with I_2 in basic THF afforded **6**.[21] The anticipated low reactivity associated with the sterically demanding neighbouring alkyl chain never materialised in these reactions. Furthermore, iodide **6** could be easily methylated under standard conditions affording **7** in 67% yield (Scheme 2).[22] To our delight, Pd-cross-coupling reactions could be carried out on **7**. Using $Pd(PPh_3)_4$ as catalyst a phenyl group could be introduced at the 3-position.[23]

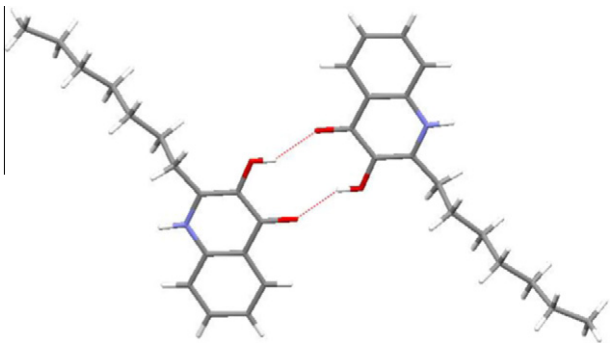

Figure 2. X-ray crystal structure of PQS depicting dimeric H-bonding.[19]

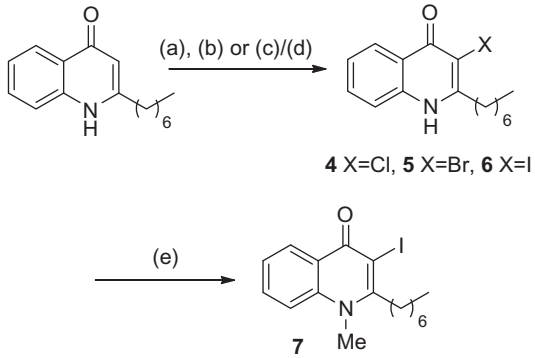

Scheme 2. Reagents and conditions: (a) $C_3Cl_2N_3NaO_3$, 2 M NaOH, MeOH, H_2O, 59% (b) PTB, AcOH, 68% (c) Br_2, 1 I_2 crystal, AcOH, 44% (d) I_2, Na_2CO_3, THF, 48% (e) NaH, DMF, MeI.

After heating at 130 °C for 30 min, palladium black was seen to precipitate and the reaction was stopped. The coupled product **8** was isolated in 50% yield.[24] An alkenyl group was also introduced using the Mizoroki–Heck reaction, iodide **7** and styrene giving alkene **9**. Two catalytic systems were tried over 16 h at 100 °C using $Pd_2(dba)_3$.dba and $Pd(PPh_3)_4$ with NMR analysis indicating conversions of ca. 15% and 30%, respectively. Using $Pd(PPh_3)_4$ at 120 °C only improved the conversion to 60% with an isolated yield of 52% (Scheme 3). No further optimisation was carried out.

In conclusion, we have described the synthesis of >10 g quantities of HHQ, its halogenation at the 3-position, subsequent

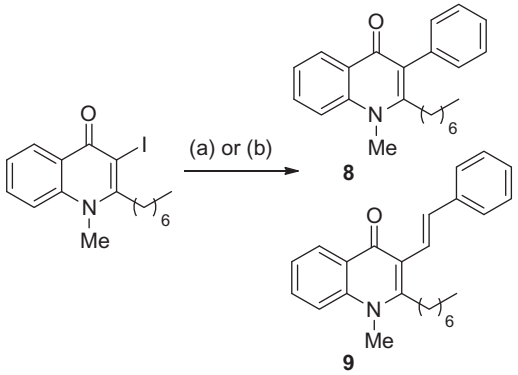

Scheme 3. Reagents and conditions: (a) $PhB(OH)_2$, $Pd(PPh_3)_4$, DMF, 2 M Na_2CO_3, 50% (b) styrene, $Pd(PPh_3)_4$, NMP, Et_3N, 52%.

N-methylation and finally Pd-cross coupling of 3-iodo-HHQ. The crystal structure of the prominent biological agent PQS is also described. These compounds and analogues are currently undergoing full biological evaluation, which will be reported in due course.

Acknowledgements

The authors thank Science Foundation Ireland (G.P.M., C.M.S. Grant No. 09/RFP/CHS2353, S.E.L., C.J.E. Grant No. 07/SRC/B1158 and 05/PICA/B802/EC07) for funding, Mary Ellen Buckley for earlier work on the synthesis of HHQ, J. B. Milbank for helpful discussion and Johnson-Matthey for the gift of transition metal catalysts. F.OG. thanks the European Commission (MTKD-CT-2006-042062; O36314), SFI (SFI 04/BR/B0597; 07/IN.1/B948; 08/RFP/GEN1295; 09/RFP/BMT2350), the Department of Agriculture and Food (DAF RSF 06 321; DAF RSF 06 377; FIRM 08/RDC/629), Irish Research Council for Science, Engineering and Technology (05/EDIV/FP107), the Health Research Board (RP/2006/271; RP/2007/290; HRA/2009/146), the Environmental Protection Agency (EPA2006-PhD-S-21; EPA2008-PhD-S-2), the Marine Institute (Beaufort award) and the Higher Education Authority of Ireland (PRTLI3).

References and notes

1. Drlica, K.; Malik, M.; Kerns, R. B.; Zhao, X. *Antimicrob. Agents Chemother.* **2008**, *52*, 385.
2. Kresse, H.; Belsey, M.; Rovini, H. *Nat. Rev. Drug Disc.* **2007**, *6*, 19.
3. (a) Wang, M.; Liu, Y.; Huang, Z. *Tetrahedron Lett.* **2001**, *42*, 2553; (b) Hadjeri, M.; Mariotte, A.; Boumendjel, A. *Chem. Pharm. Bull.* **2001**, *49*, 1352.
4. Xia, Y.; Yang, Z.; Xia, P.; Hackl, T.; Hamel, E.; Mauger, A.; Wu, J.; Lee, K. J. *J. Med. Chem.* **2001**, *44*, 3932.
5. (a) Moyer, M. P.; Weber, F. H.; Gross, J. L. *J. Med. Chem.* **1992**, *35*, 4595; (b) Palacios, F.; de Retana, A. M. O.; Oyarzabal, J. *Tetrahedron* **1999**, *55*, 5947.
6. Hoffman, L. R.; Déziel, E.; D'Argenio, D. A.; Lépine, F.; Emerson, J.; McNamara, S.; Gibson, R. L.; Ramsey, B. W.; Miller, S. I. *Proc. Natl. Acad. Sci. U.S.A.* **2006**, *26*, 19890.
7. Pesci, E. C.; Milbank, J. B.; Pearson, J. P.; McKnight, S.; Kende, A. S.; Greenberg, E. P.; Iglewski, B. H. *Proc. Natl. Acad. Sci. U.S.A* **1999**, *96*, 11229.
8. (a) Parsek, M. R.; Greenburg, E. P. *Trends Microbiol.* **2005**, *13*, 27; (b) Swift, S.; Downie, J. A.; Whitehead, N. A.; Barnard, A. M. L.; Salmond, G. P. C.; Williams, P. *Adv. Microb. Physiol.* **2001**, *45*, 199; (c) Williams, P.; Winzer, K.; Chan, W.; Camara, M. *Philos. Trans. R. Soc. London, Ser. B* **2007**, *362*, 1119.
9. Dubern, J.-F.; Diggle, S. P. *Mol. Biosyst.* **2008**, *4*, 882.
10. (a) Diggle, S. P.; Matthijs, S.; Wright, V. J.; Fletcher, M. F.; Chhabra, S. R.; Lamont, L. I.; Kong, X.; Hider, R. C.; Cornelis, P.; Cámara, M.; Williams, P. *Chem. Biol.* **2007**, *14*, 87; (b) Bredenenbruch, F.; Geffers, R.; Nimtz, M.; Buer, J.; Häussler, S. *Environ. Microbiol.* **2006**, *8*, 1318.
11. Mashburn-Warren, L.; Howe, J.; Brandenberg, K.; Whitely, M. *J. Bacteriol.* **2009**, *191*, 3411.
12. Diggle, S. P.; Winzer, K.; Chhabra, S. R.; Worrall, K. E.; Cámara, M.; Williams, P. *Mol. Microbiol.* **2003**, *50*, 29.
13. (a) Cummins, J.; Reen, F. J.; Baysse, C.; Mooij, M. J.; O'Gara, F. *Microbiology* **2009**, *155*, 2826; (b) Guina, T.; Purvine, S. O.; Yi, E. C.; Eng, J.; Goodlett, D. R.; Aebersold, R.; Miller, S. I. *Proc. Natl. Acad. Sci. U.S.A.* **2003**, *100*, 2771.
14. (a) Kim, K.; Kim, Y. U.; Koh, B. H.; Hwang, S. S.; Kim, S.-H.; Lépine, F.; Cho, Y.-H.; Lee, G. R. *Immunology* **2010**, *129*, 578; (b) Hooi, D. S. W.; Bycroft, B. W.; Chhabra, S. R.; Williams, P.; Pritchard, D. I. *Infect. Immun.* **2004**, *72*, 6463.
15. Kocieński, P. J.; Pelotier, B.; Pons, J.-M.; Prideaux, H. *J. Chem. Soc.* **1998**, 1373.
16. Lokot, I. P.; Pashkovsky, F. S.; Lakhvich, F. A. *Tetrahedron* **1999**, *55*, 4783.
17. Bangdiwala, B. P.; Desai, C. M. *J. Indian Chem. Soc.* **1953**, *30*, 655.
18. Woschek, A.; Mahout, M.; Mereiter, K.; Hammerschmidt, F. *Synthesis* **2007**, 1517.
19. Notable features include a dimeric structure with two moderate strength hydroxy-carbonyl intermolecular H-bonds with a discrete amino carbonyl H-bond capping the dimer. A second crystallographically different dimer was also observed (omitted in diagram for clarity). The data has been deposited at the CCDC 780780.
20. Staskun, B. *J. Org. Chem.* **1988**, *53*, 5287.
21. Example of halogenation: 3-Iodo-2-heptylquinolin-4(1*H*)-one: A mixture of HHQ (0.2 g, 0.823 mmol), iodine (0.418 g, 1.646 mmol) and Na_2CO_3 (0.131 g, 1.235 mmol) in THF (4 mL) was stirred at rt for 18 h. The mixture was quenched with $Na_2S_2O_3$ (0.613 g, 3 equiv) and the precipitate was collected by filtration before washing with ice-cold H_2O (50 mL). Recrystallisation was carried out (EtOH) affording **6** (146 mg) in 48% yield. Mp: 241–243 °C. IR ν_{max} (KBr): 3210, 3060, 2923, 2851, 2360 1628, 1578, 1555, 1497, 1473, 1435 cm^{-1}; ^1H NMR (400 MHz CD_3SOCD_3) δ: 0.86 (3H, t, *J* 8.5), 1.27–1.42 (8H, m), 1.68 (2H, m), 2.91 (2H, t, *J* 9.9), 7.33–7.38 (1H, m), 7.58 (1H, d, *J* 10.1), 7.65–7.7 (1H, m), 8.07 (1H, d, *J* 8.7), 12.08 (1H, br s); ^{13}C NMR (400 MHz CD_3SOCD_3) δ: 13.9, 22.0, 27.9, 28.3, 28.6, 31.1, 38.7, 85.7, 117.8, 120.6, 123.8, 125.5, 131.9, 139.0, 154.6, 173.2. Exact mass calcd for $C_{16}H_{21}INO$ $(M+H)^+$, 370.0668. Found 370.0656.
22. N-Methylation: 2-Heptyl-3-iodo-1-methylquinolin-4(1*H*)-one: A stirred suspension of **6** (120 mg, 0.446 mmol) in dry DMF (3 mL) was treated with NaH (60% dispersion, 1.5 equiv) at room temperature under a nitrogen atmosphere then stirred at 40 °C for 5 h. The mixture was treated with iodomethane (1.5 equiv, 69 mg) and stirred for 12 h at 40 °C. The mixture was quenched with cold H_2O. The product was extracted with $CHCl_3$, washed with brine and dried ($MgSO_4$). The solvent was evaporated and the product was purified using column chromatography (1:1 hexane/EtOAc) affording **7** (82 mg) in 66% yield. Mp: 67–69 °C. IR ν_{max} (KBr): 3374, 2926, 2854, 2361, 1617, 1592.8, 1519, 1462 cm^{-1}; ^1H NMR (400 MHz $CDCl_3$) δ: 0.91 (3H, t, *J* 6.9), 1.34 (6H, m), 1.53 (2H, m), 1.68 (2H, m), 3.22 (2H, t, *J* 7.9), 3.89 (3H, s), 7.36 (1H, t, *J* 7.1), 7.52 (1H, d, *J* 8.6), 7.62–7.65 (1H, m), 8.44 (1H, d, *J* 6.6); ^{13}C NMR (400 MHz $CDCl_3$) δ: 14.1, 22.6, 27.6, 28.9, 29.6, 31.7, 36.7, 40.1, 90.4, 115.3, 122.6, 124.2, 127.9, 132.4, 140.9, 155.0, 173.8. Exact mass calcd for $C_{17}H_{23}INO$ $(M+H)^+$, 384.0824. Found 384.0806.
23. For a similar reaction, see: Mphahele, M. J.; Nwamadi, M. S.; Mabeta, P. *J. Heterocycl. Chem.* **2006**, *43*, 255.
24. Example of Pd-coupling: 2-heptyl-1-methyl-3-phenylquinolin-4-one: A stirred mixture of **7** (55 mg, 0.143 mmol), phenylboronic acid (2 equiv, 35 mg) and $Pd(PPh_3)_4$ (5 mol %) in DMF (2.5 ml) and aqueous 2 M Na_2CO_3 (1.5 mL) was heated at 130 °C for 2 h and then cooled to room temperature. The mixture was poured into ice-cold H_2O and the precipitate was taken-up into $CHCl_3$, washed with brine and dried. The solvent was evaporated and the product was purified using column chromatography (1:1 hexane/EtOAc) affording **8** (24 mg) in 50% yield. Mp: 211–215 °C. IR ν_{max} (KBr): 2926, 2854, 1618, 1592, 1538, 1498 cm^{-1}; ^1H NMR (400 MHz $CDCl_3$) δ: 0.85 (3H, t, *J* 7.2), 1.19 (8H, m), 1.55 (2H, m), 2.63 (2H, t, *J* 8.2), 3.83 (3H, s), 7.20–7.45 (6H, m), 7.55 (1H, d, *J* 8.6), 7.65–7.75 (1H, m), 8.5 (1H, dd, *J* 1.4, 8); ^{13}C NMR (400 MHz $CDCl_3$) δ: 14.0, 22.6, 28.5, 28.9, 29.4, 31.5, 31.8, 35.0, 115.2, 123.3, 124.3, 126.2, 127.0, 127.3, 128.4, 130.7, 132.0, 137.2, 141.6, 152.4, 176.4. Exact mass calcd for $C_{23}H_{28}NO$ $(M+H)^+$, 334.2171. Found 334.2164.

Organic & Biomolecular Chemistry

Cite this: *Org. Biomol. Chem.*, 2012, **10**, 8903

www.rsc.org/obc

PAPER

Structure–function analysis of the C-3 position in analogues of microbial behavioural modulators HHQ and PQS†

F. Jerry Reen,[a] Sarah L. Clarke,[b] Claire Legendre,[a] Christina M. McSweeney,[b] Kevin S. Eccles,[b] Simon E. Lawrence,[b] Fergal O'Gara*[a] and Gerard P. McGlacken*[b]

Received 12th June 2012, Accepted 26th September 2012
DOI: 10.1039/c2ob26823j

2-Heptyl-3-hydroxy-4-quinolone (PQS) and its precursor 2-heptyl-4-quinolone (HHQ) are key signalling molecules of the important nosocomial pathogen *Pseudomonas aeruginosa*. We have recently reported an interkingdom dimension to these molecules, influencing key virulence traits in a broad spectrum of microbial species and in the human pathogenic yeast *Candida albicans*. For the first time, targeted chemical derivatisation of the C-3 position was undertaken to investigate the structural and molecular properties underpinning the biological activity of these compounds in *P. aeruginosa*, and using *Bacillus subtilis* as a suitable model system for investigating modulation of interspecies behaviour.

Microbial populations coordinate cellular behaviour through the mobilisation of diffusible signal molecules, which activate gene expression upon accumulation above a threshold or quorum.[1] This phenomenon (quorum sensing), is an essential communication system utilised by a broad spectrum of Gram-negative and Gram-positive bacteria, and is a central control mechanism for virulence and pathogenesis.[2] 2-Heptyl-3-hydroxy-4-quinolone, the Pseudomonas Quinolone Signal (PQS) is a key regulator of quorum sensing in *Pseudomonas aeruginosa*.[1,3,4] *P. aeruginosa* is best known as an antibiotic resistant human pathogen associated with hospital-acquired infections and is the primary cause of morbidity and mortality in people with cystic fibrosis (CF).[5] Controlling *P. aeruginosa* infection is thus of great clinical importance.[6–9] Research into PQS activity has revealed a vast and varied array of biological functions.[10–16] In addition to controlling expression of key components of the QS regulon, PQS also modulates biofilm formation, secondary metabolite production, pigment and virulence factor production, motility and membrane vesicle formation.[11–13,15] 2-Heptyl-4-quinolone (HHQ), the biological precursor of PQS, also possesses a plethora of roles including quorum sensing responsibilities.[13] PQS has been detected at 2 μM in CF samples from sputum, bronchoalveolar lavage fluid and mucopurulent fluid from distal airways of end-stage lungs removed at transplant.[17] Isolates obtained from infant CF-patients under 3 years of age overproduce PQS, suggesting that it may be instrumental in adaptation of *P. aeruginosa* to the airways of young CF-patients.[18] Transcriptomic and functional genomics studies have provided further evidence for the importance of PQS and its precursor HHQ during adaptation to the CF-lung[19,20] while Kim *et al.*[21,22] reported immunomodulation and inhibition of macrophage activation by HHQ and PQS. Diggle *et al.* reported that pathogenic bacteria other than *P. aeruginosa* synthesise 2-alkyl-4-quinolones (AQs). *Burkholderia pseudomallei*, for example, produces AQs and employs a structurally similar molecule to HHQ but does not produce PQS.[13,23] Intriguingly, it has recently been shown that both PQS and HHQ can also control the behaviour of other bacterial and fungal species.[24,25] We found that surface-associated phenotypes were repressed in a number of Gram-positive and Gram-negative bacteria as well as in pathogenic yeast in response to PQS and HHQ.[24] Motility was repressed in a broad range of bacteria, while biofilm formation in *Bacillus subtilis* and *Candida albicans* was repressed in the presence of HHQ, though initial adhesion was unaffected. Furthermore, HHQ exhibited potent bacteriostatic activity against several marine species of Gram-negative bacteria, including pathogenic *Vibrio vulnificus*.

To take advantage of signalling pathways in a clinical setting we take two routes: (1) the early detection of biomarkers such as HHQ and PQS[26–28] and (2) interference with bacterial signals by the synthesis of molecular analogues capable of interrupting key virulence traits such as biofilm formation and motility. To date, the limited structure–function analysis performed on HHQ and PQS has centred on the alkyl chain length[7,29] and substitution of the anthranilate ring.[7] The crucial C-3 position has not been investigated, notwithstanding the divergent biological activities

[a]*BIOMERIT Research Centre, Department of Microbiology, University College Cork, Ireland. E-mail: f.ogara@ucc.ie; Fax: +353 21 4903101; Tel: +353 21 4903101*
[b]*Department of Chemistry and Analytical & Biological Chemistry Research Facility (ABCRF), University College Cork, Ireland. E-mail: g.mcglacken@ucc.ie; Fax: +353 21 4274097; Tel: +353 21 4274097*

†Electronic supplementary information (ESI) available: Full experimental procedures, biological data, ^{1}H spectra of novel compounds and additional crystallographical data are included. CCDC 885400. For ESI and crystallographic data in CIF or other electronic format see DOI: 10.1039/c2ob26823j

identified for HHQ and PQS towards other bacterial and fungal pathogens. Therefore, the structure–function analysis detailed in this study was designed to provide key insights into the activity of the HHQ and PQS compounds both within *P. aeruginosa* and also towards non-pseudomonal bacterial and fungal species. These included several key cystic fibrosis pathogens such as *Staphylococcus aureus* and *C. albicans*, for which *B. subtilis* proved to be a suitable model for single species analysis of swarming motility and biofilm formation. Assigning the structural modules of the quinolone compounds to biological functions would provide significant insight into their underlying mechanism of action. This would form the basis for development of innovative therapies, for example where disruption of biofilm formation would expose microbial pathogens to normal antibacterial action. In this report we present our findings on the biological activity of eight molecules of interest, 2-heptyl-4-quinolone (**3**, **HHQ**), aldehyde **4**, 2-heptyl-3-hydroxyquinolin-4(1*H*)-one (**5**, **PQS**), 3-methyl analogue **8**, halogenated versions **9**, **10** and **11** and finally **12** which possesses a potential hydrogen donor/acceptor at the 3-position.

Chemical synthesis

HHQ was prepared starting with Meldrum's acid (0.14 mol) which was reacted with octanoyl chloride followed by boiling in methanol (MeOH), reaction with aniline[30] and a Conrad–Umpach cyclisation (Scheme 1).†[31] An alternative cyclisation method reported by Woschek *et al.* failed to give any product in our hands.[32] As quantities of **4** and PQS were also required, their synthesis from HHQ was achieved using conditions described by *Pesci et al.*[33] although an excellent method for the direct synthesis of PQS has recently been reported.[34] The Duff formylation of HHQ proved problematic and 2 equivalents of hexamine (HMTA) was found to be crucial to obtaining decent yields.[35] Reaction of aldehyde **4** with MCPBA gave PQS in 29% yield.

The 3-methyl analogue **8** was synthesised in a similar fashion over five steps (Scheme 2).† Again Meldrum's acid was reacted with octanoyl chloride followed by β-ketoester formation. Methylation was carried out using K_2CO_3 and MeI giving **6**. Reaction with aniline gave enamine **7** and a final Conrad–Limpach cyclisation in diphenyl ether afforded analogue **8**.[31,35]

Bromo-analogue **9** was prepared using *N*-bromosuccinimide in 37% yield (after recrystallisation) or using Br_2 in 47% yield (Scheme 3). The 3-chloro-quinolone **10** was synthesised in one step using sodium dichloroisocyanurate (DCIC).[36] Recrystallisation afforded **10** in 46% yield. Iodo-analogue **11** was formed in the presence of *N*-iodosuccinimide in 48% yield (halogenation yields not optimised).

Novel 2-heptylquinazolin-4-one **12** was synthesised *via* a convenient one-step synthesis by reaction of anthranilamide with octanal, and following recrystallisation from ethanol, afforded the product in 76% yield (Scheme 4).

Given that both the quinolone and quinoline tautomeric structures (both structures have been arbitrarily depicted in the literature[37]) of HHQ were accessible, the latter as its hydrochloride salt (Fig. 1), we felt it would be valuable to confirm that both

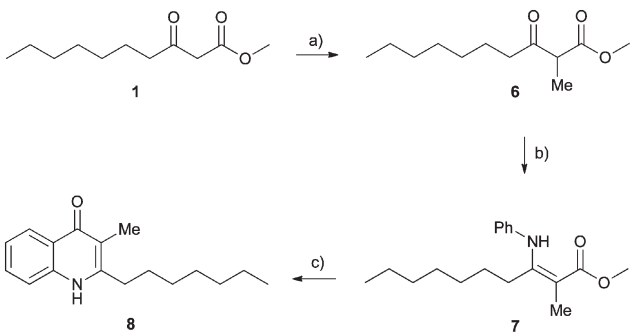

Scheme 2 Synthesis of 3-Me analogue **8**. Conditions: (a) K_2CO_3, MeI, reflux, 40%. (b) $PhNH_2$, reflux, 79% (c) Ph_2O, reflux, 10%.

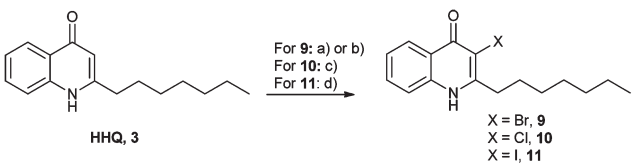

Scheme 3 Halogenation of HHQ. Conditions: (a) NBS, MeOH, 37% (b) Br_2, AcOH, 47% (c) DCIC, H_2O, 46% (d) NIS, AcOH, 48%.

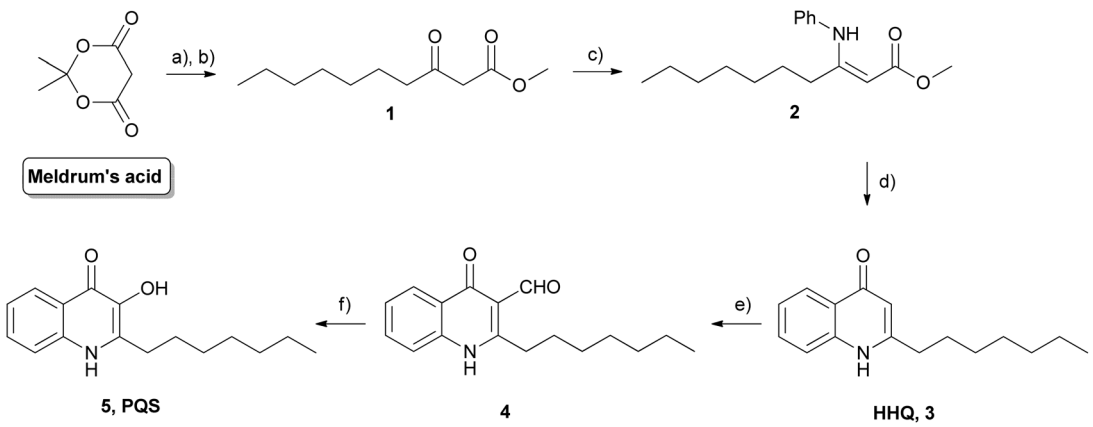

Scheme 1 Synthesis of HHQ and PQS. Conditions: (a) octanoyl chloride, pyridine, DCM (b) MeOH, reflux, 34% over 2 steps (c) $PhNH_2$, reflux, 79% (d) Ph_2O, reflux, 33% (e) HMTA, TFA, reflux, 56% (f) H_2O_2, NaOH, 29%.

the free quinolone and quinoline hydrochloride exhibited identical biological activities. Both compounds **3** (HHQ) and **3·HCl** (HHQ·HCl) were found to be interchangeable when used in biological systems and exerted a common influence on inter-kingdom behaviour. Both motility and biofilm formation were similarly influenced in *B. subtilis* in the presence of **3** and **3·HCl** when tested under physiological pH (Fig. 3 and 4).

Biological studies

In order to assess the importance of the C-3 position to the biological activity of HHQ and PQS, the capacity for analogues functionalised at this position to replace the native compounds in *P. aeruginosa* was investigated. The PQS signalling system, a key component of QS in *P. aeruginosa*, is known to control production of a range of virulence factors, including elastase, rhamnolipid and the phenazine redox compound pyocyanin.[11,38] Therefore, the analogues were first assessed for restoration of phenazine production in a *pqsA* mutant, in which the biosynthetic steps required for AQ production have been disrupted. While both HHQ and PQS restored phenazine production in the *pqsA* mutant strain, the analogues were significantly less effective in triggering production of the pigment, with **12** being the least effective (Fig. 2A), suggesting that the C-3 position is crucial for control of phenazine production in *P. aeruginosa*. Interestingly, addition of equimolar concentrations of the analogues to the wild-type PAO1 and PA14 strains, which produce both HHQ and PQS, did not interfere with phenazine production (Fig. 2B). In *P. aeruginosa*, PQS also plays a fundamental role in the structural formation of biofilms and PQS-deficient mutants have been shown to produce thin flat biofilms, which are markedly different to the mushroom shaped structures produced by the wild-type strain.[39] However, neither mutation of *pqsA* nor addition of analogues markedly influenced the initial stages of biofilm formation in *P. aeruginosa* as seen in crystal violet multi-well assays (ESI†).

Aside from their key role as signalling compounds in *P. aeruginosa*, both HHQ and PQS exert distinct influences on the behaviour of a range of microbial pathogens.[24] Differing only at the 3-position, yet displaying diverse biological functionalities suggests a key role for the C-3 position in modulating interspecies microbial behaviour. Microbial swarming motility and biofilm formation require cooperative multicellular behaviour and provide a mechanism for bacterial cells to establish and persist during infection. While motility was shown to be altered in *S. aureus* in the presence of HHQ and PQS, *C. albicans* biofilm formation was repressed in the presence of HHQ. As we have previously shown both phenotypes to be affected in *B. subtilis* in the presence of HHQ, this species was chosen as a model organism upon which to test the interspecies influence of the alkylquinolone compounds.

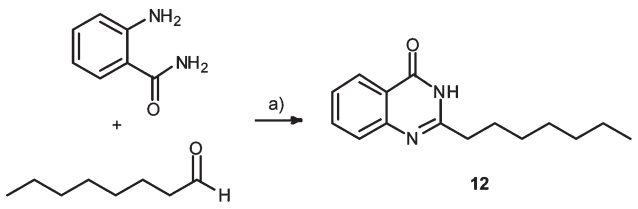

Scheme 4 Synthesis of PQS analogue. Conditions: (a) $NaSO_3H$, DMA, reflux, 76%.

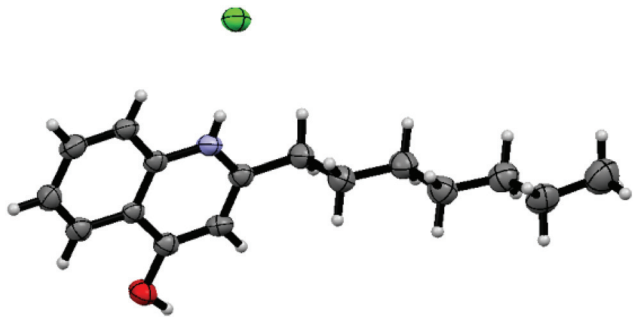

Fig. 1 Crystal structure of **3·HCl** (HHQ·HCl).†

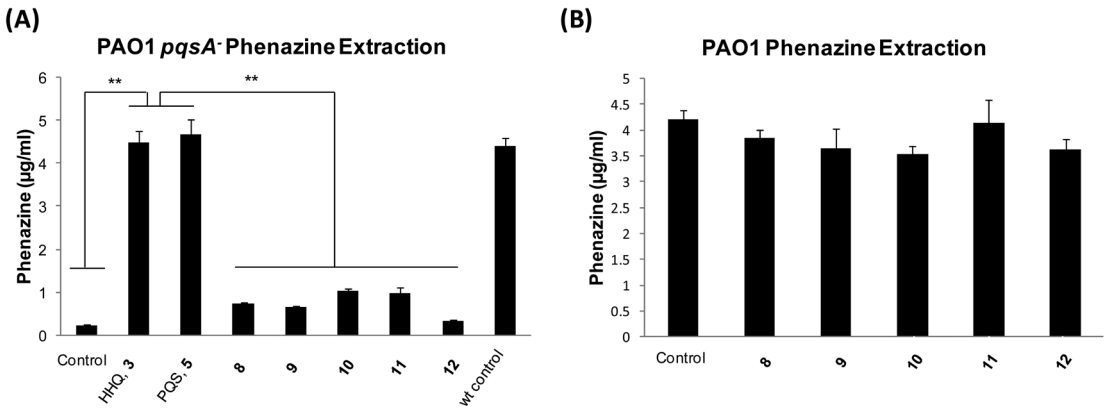

Fig. 2 Influence of functionalised derivatives on PQS-dependent phenotypes in *P. aeruginosa*. (**A**) The ability of HHQ and PQS (10 µM) to restore phenazine production in a *pqsA* mutant was lost to the derivative compounds indicating that the C-3 position is crucial in this regard. (**B**) Addition of 10 µM concentrations of derivative compounds did not interfere with phenazine production in the wild-type PAO1 strain. Data presented is representative of three independent experiments (Students *t*-test, ***p*-value ≤ 0.005).

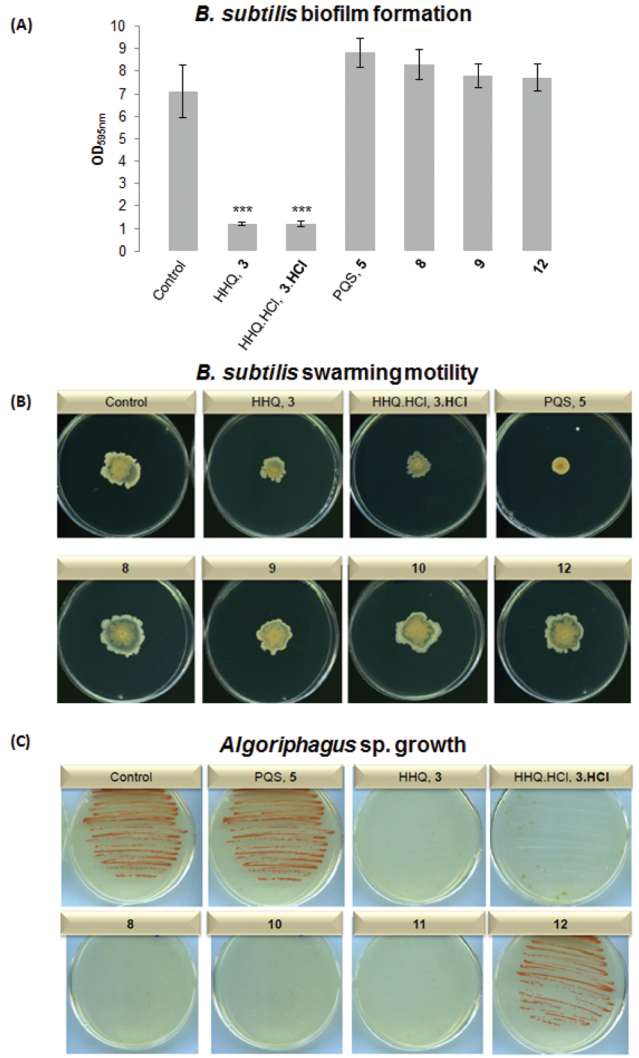

Fig. 3 Structural variation of the C-3 position interferes with the biological activity of *P. aeruginosa* AQ molecules. (**A**) Crystal violet staining of 18 h cultures grown static in multi-well plates revealed that HHQ interferes with *B. subtilis* biofilm formation irrespective of its tautomeric form (HHQone and HHQine). Furthermore, the anti-biofilm activity of the HHQ chloride salt was comparable to HHQ. However, this anti-biofilm activity was abolished upon substitution at the C-3 position, irrespective of the nature of that substitution (**8–12**). All compounds were added at a final concentration of 10 μM and statistical significance was provided by paired Student's *t*-test (***, *p*-value ≤ 0.001). (**B**) *B. subtilis* swarming motility was assessed after 16 h on 0.3% (w/v) TSA plates. Notably, substitution with methyl and halogen groups (**8–11**) which would be sterically consistent with PQS, was enough to abolish the anti-swarming activity of the parent compounds, again highlighting the structural specificity underpinning the biological activity of these compounds. All images are provided to scale. (**C**) The ability of HHQ to repress the growth of a marine isolate on SYP agar was maintained in both tautomeric forms, and upon substitution with methyl and halogen groups (**8–11**). However, **12** did not exhibit antibacterial activity towards the marine bacteria, similar to PQS. Data presented is representative of at least three independent biological replicates.

Unlike **3** and **3·HCl**, analogues **6–12** did not exhibit anti-biofilm activity towards *B. subtilis* (Fig. 3A), highlighting the importance of the C-3 position in underpinning the biological role of these compounds. Furthermore, the inability of **10** to affect biofilm formation in *C. albicans*, a human pathogenic yeast and an important CF pathogen (data not shown), underlines the importance of the C-3 position for biological functionality of the AQ compounds. The influence of **6–12** on microbial swarming motility was negligible compared to HHQ and PQS (Fig. 3B). Interestingly, the methyl and halogen substituted compounds **8–11** retained antimicrobial activity towards an *Algoriphagus* marine isolate, which was previously shown to be susceptible to HHQ, while PQS and quinazolinone **12** did not suppress growth of this species (Fig. 3C).

HHQ and PQS have previously been shown to influence transcription in a mouse monocyte/macrophage cell line.[40] However, although PQS has been found in CF sputum,[17] the impact and potential cytotoxic effects of these compounds on airway epithelial cells has not been investigated. Therefore, HHQ, PQS and compounds **8–12** were tested for cytotoxicity towards a human airway epithelial cell line (IB3-1 cells) for 16 h at concentrations ranging from 10 to 100 μM by quantification of the lactate dehydrogenase (LDH) release, in comparison with treatment by 0.1% Triton X-100, used as a positive control for cytotoxicity. Interestingly, HHQ was found to be cytotoxic towards IB3-1 cells while PQS did not exhibit any cytotoxic activity (Fig. 4). The cytotoxicity of HHQ decreased with decreasing concentrations and was less than 10% at 10 μM (data not shown). As above, the cytotoxicity of both the quinolone and quinoline compounds towards IB3-1 cells was comparable (~60%). With the exception of quinazolinone **12** which exhibited a significant level of cytotoxicity, the C-3 substituted analogues (**8–11**) did not exhibit cytotoxicity towards IB3-1 cells, reinforcing the importance of the C-3 position in the functionality of the HHQ and PQS molecules. Notably, IB3-1 cellular morphological analysis revealed massive cellular damage caused by HHQ at a concentration of 100 μM (Fig. 4) and significant cellular change for **12**. While PQS (Fig. 4) and to a lesser extent **8–11** (data not shown) caused moderate changes in cellular morphology, the plasma membrane remained intact, consistent with the lack of LDH release, compared to 0.1% Triton X-100.

Conclusions

The *P. aeruginosa* AQ signalling molecules are emerging as key components of the highly dynamic and bidirectional molecular dialogue that exists between pathogen and host and within the mixed microbial populations that are characteristic of infection. This is the first report highlighting the strict structural requirements at the C-3 position underpinning the biological activity of HHQ and PQS. The control of phenazine production in *P. aeruginosa* involves a complex interplay between PqsR, AQs and the last component of the PQS biosynthetic operon, PqsE.[38,41,42] The inability of any of the AQ analogues described in this study to restore phenazine production in a *P. aeruginosa pqsA* mutant suggests that the C-3 position is crucial for HHQ and PQS activity in this important nosocomial pathogen. Interestingly, addition of the analogues to wild-type cultures did not interfere with phenazine production, suggesting that they may not be effective inhibitors in *P. aeruginosa*. Multi-well biofilm assays suggest that the analogues do not interfere with the initial stages

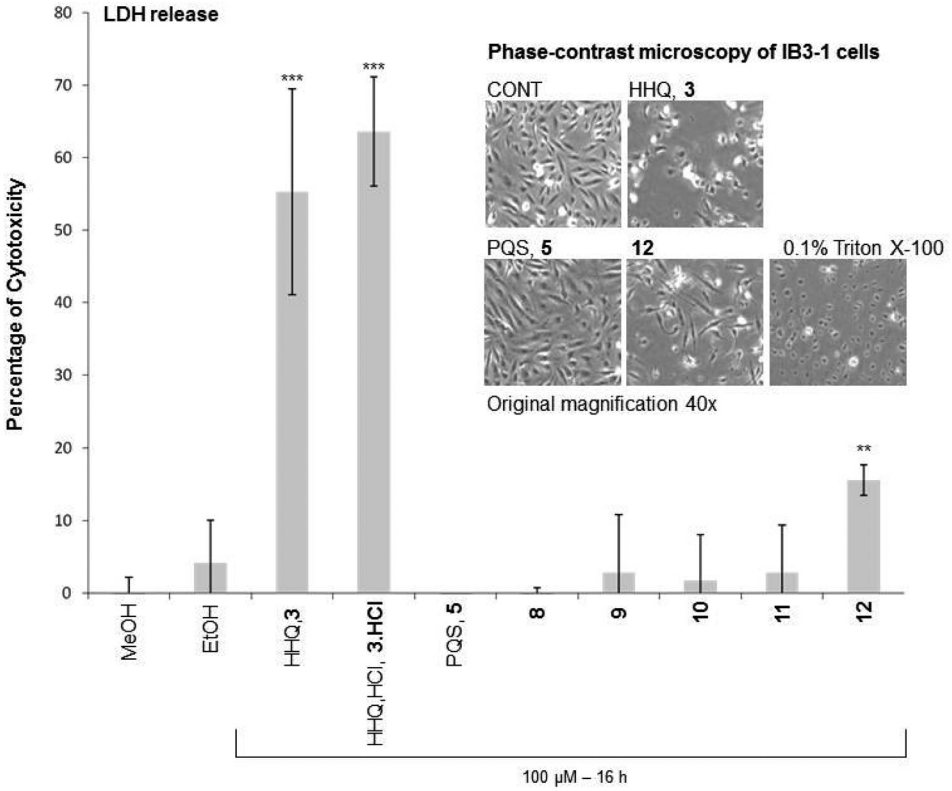

Fig. 4 C-3 substitution abrogates cytotoxic activity of HHQ. Cytotoxicity is expressed as a percentage of the total amount of LDH released from cells treated with 0.1% Triton X-100 (given the percentage of 100). The release of LDH was measured in cell culture medium of IB3-1 cells treated with methanol or ethanol, or with 100 μM of HHQ, the HHQ chloride salt, PQS, methylated HHQ analogue **8**, halogenated HHQ analogues **9–11** or analogue **12**. Data (means ± SD) are representative of three independent biological experiments. Two-tailed unpaired student's *t*-test was performed by comparison of IB3-1 cells treated with HHQ analogue molecules with IB3-1 cells treated with methanol or ethanol (**, *p*-value ≤ 0.01; ***, *p*-value ≤ 0.001). Phase-contrast microscopy of IB3-1 cells untreated (CONT) or treated with HHQ, PQS, or **12** at a concentration of 100 μM for 16 h. Triton X-100 (0.1%) was used as a control in these studies. Original magnification 40×.

of biofilm formation in *P. aeruginosa*, which is perhaps unsurprising as attachment and microcolony formation in *pqsA* mutants have previously been shown to be largely comparable to wild-type.[43,44] Flow-cell technology and confocal laser microscopy will be required to assess the full impact of these analogues on *P. aeruginosa* biofilm architecture and maturation. Notwithstanding this, the correlation between loss of function both within *P. aeruginosa* and towards other microbial species upon functionalisation of the C-3 position is striking. While the molecular mechanism underpinning the response to HHQ and PQS in other microbial species remains to be defined, it is interesting to speculate that some structural conservation may exist.

If a simple electron withdrawing group was required at C-3 then halogenation at this point (**9–11**) would be expected to produce molecules with similar biological activity. Alternatively introduction of an NH-group as in **12** (another tautomer can exist here also) could mimic the –OH group in PQS. However in both cases the capacity to modulate either *P. aeruginosa* or interkingdom behaviour was lost in these compounds. Therefore it is clear that the 3-H and 3-OH groups in HHQ and PQS respectively, play a more complex role in these biological systems. Methylation of the C-3 position (**8**) led to the generation of a known signal molecule produced by several *Burkholderia* species, which do not have the capacity to produce PQS. Interestingly, **8** appeared to have lost its ability to restore phenazine production or influence interspecies multicellular behaviour, although it did retain antibacterial activity against *Algoriphagus sp*. Therefore, although both compounds are structurally similar, and produced by important pathogens of the CF-lung, their interspecies activity profiles are distinct. Again introduction of a nitrogen at C-3 (**12**) led to complete loss of biological activity relative to HHQ, while we have previously shown that an aldehyde substituted analogue (**4**) had intermediate activity relative to both compounds.[24] Although from a chemical perspective, bacterial conversion of HHQ to PQS would go some way to explaining this observation, the evolutionary rationale underpinning this has yet to be established. Future structural studies will involve further manipulation of the 3-site with a view towards attaining a deeper understanding of the complex roles of these molecules in bacterial and fungal species.

Experimental (see ESI† for full details)

Preparation of 6

To 3-oxo-methyl-decanoate[45] (2.74 g, 13.7 mmol) was added dry acetone (35 mL). This solution was added to a flask containing dry potassium carbonate (1.76 g, 12.7 mmol) over a N_2

atmosphere. The reaction mixture was allowed stir for 20 min before the addition of methyliodide (1.02 mL, 16.4 mmol). Stirring was continued at room temperature overnight before being heated at reflux for 6 h. The mixture was allowed to cool and the solvent was removed *in vacuo* to yield the crude product as a yellow oil. Purification was carried out using silica column chromatography to yield **6** as a pale yellow oil (1.17 g, 40%). (Found: C, 67.15; H, 10.2. $C_{12}H_{22}O_3$ requires C, 67.3; H, 10.35%.) ν_{max} (film)/cm^{-1} 2930 (CH stretch), 2857 (CH stretch), 1749 (C═O ketone), 1717 (C═O ester), 1456 (CH scissor, bending), 1204 (C–O ester). δ_H ($CDCl_3$, 300 MHz) 0.88 (3H, t, J = 6.7 Hz, CH_3), 1.23–1.27 (8H, m, 4 × CH_2), 1.33 (3H, d, J = 7.2 Hz, CO–CH(C*H*$_3$)–CO), 1.53–1.66 (2H, m, C*H*$_2$CH$_2$CO), 2.52 (2H, qt, J = 7.4, 17.2, 27.4, 44.6 Hz, C*H*$_2$CO), 3.53 (1H, q, J = 7.1 Hz, CO–C*H*(CH$_3$)–CO), 3.73 (3H, s, OCH_3). δ_C ($CDCl_3$, 75.5 MHz) 12.8, 14.0 (2 × CH_3), 22.6, 23.5, 28.98, 29.00, 31.6, 41.4 (6 × CH_2), 52.3 (CO–*C*H–CO), 52.7 (OCH_3), 171.1 (C═O ester), 205.9 (C═O ketone). Exact mass calculated for $C_{12}H_{23}O_3$ [(M + H)$^+$], 215.1647. Found 215.1642, m/z (ES$^+$) 215 [(M + H)$^+$, 30%].

Preparation of 7

To a solution of 2-methyl-3-oxo-methyl-decanoate (1.27 g, 5.94 mmol) in dry hexane (30 mL) was added aniline (0.57 mL, 6.24 mmol) and *p*-toluene sulfonic acid (0.023 g, 0.12 mmol). The reaction mixture was heated at reflux under a N_2 atmosphere for 16 h. The reaction was allowed to cool and the solvent was removed *in vacuo* yielding **7** as an orange oil (1.35 g, 79%). (Found: C, 74.3; H, 9.2; N, 5.2. $C_{18}H_{27}NO_2$ requires C, 74.7; H, 9.4; N, 4.8%.) ν_{max} (film)/cm^{-1} 3216 (NH stretch), 2952 (CH stretch), 2928 (CH stretch), 2856 (CH stretch), 1744 (C═O), 1657 (C═C), 1612, 1594 (NH bend), 1252 (C–O), 1229 (C–O), 1164 (C–O). δ_H ($CDCl_3$, 400 MHz) 0.84 (3H, t, J = 7.0 Hz, CH_3), 1.17–1.29 (8H, m, 4 × CH_2), 1.37–1.46 (2H, m, CH_2), 1.59 (1H, s, CH_3), 1.86 (1H, s, CH_3), 2.26–2.30 (1H, m, CH_2), 2.34–2.38 (1H, m, CH_2), 3.52–3.75 (4H, m, CH_3), 7.03–7.10 (2H, m, 2 × ArH), 7.13–7.19 (1H, m, ArH), 7.26–7.35 (2H, m, 2 × ArH), 10.81 (1H, bs, OH). δ_C ($CDCl_3$, 75.5 MHz) 12.5, 14.0 (2 × CH_3), 22.6, 27.7, 28.7, 28.8, 29.4, 31.6 (6 × CH_2), 50.7 (CH_3), 124.8 (quaternary C), 125.1, 125.6, 128.9, 129.1, 129.3 (5 × ArC), 160.8 (ArC–N), 163.8 (C–N), 171.7 (C═O). Exact mass calculated for $C_{18}H_{28}NO_2$ [(M + H)$^+$], 290.2120. Found 290.2116, m/z (ES$^+$) 290 [(M + H)$^+$, 56%].

Preparation of 8

Diphenyl ether (45 mL) was heated at reflux (270 °C) and the enamine (1.35 g, 4.68 mmol) was added dropwise over 90 min ensuring reflux was maintained and the mixture was heated for an additional 1 h. The mixture was then allowed cool to room temperature and the formed methanol was removed *in vacuo*. 4 M HCl (6 mL) was then added and the organic layer extracted with ethyl acetate (2 × 8 mL) dried over anhydrous $MgSO_4$, filtered and the solvent removed *in vacuo* to yield crude product as a brown oil. Purification was achieved using silica column chromatography to yield product as a dark brown solid followed by two recrystallisations from methanol to yield **8** as a white crystalline solid (10.6 mg, 10%). δ_H (CD_3OD, 400 MHz) 0.88 (3H, t, J = 6.8 Hz, CH_3), 1.30–1.46 (8H, m, 4 × CH_2), 1.68–1.75 (2H, m, CH_2), 2.15 (3H, s, CH_3), 2.81 (2H, t, J = 7.9 Hz, CH_2), 7.33 (1H, t, J = 8.1 Hz, ArH), 7.53–7.55 (1H, m, ArH), 7.60–7.64 (1H, m, ArH), 8.22 (1H, d, J = 7.5 Hz, ArH). δ_C (CD_3OD, 75.5 MHz) 10.8, 14.4 (2 × CH_3), 23.7, 30.0, 30.2, 30.5, 32.9, 33.5 (6 × CH_2), 116.2 (quaternary C), 118.7 (ArC), 124.4 (quaternary C), 124.5, 126.2, 132.7 (3 × ArC), 140.6, 153.4 (2 × quaternary C), 179.5 (C═O), m/z (ES$^+$) 258 [(M + H)$^+$, 100%].

Preparation of 3-bromo-2-heptylquinolin-4(1*H*)-one, 9

Method A. To a stirred solution of **3** (0.5 g, 2.05 mmol) in dichloromethane (10 mL) and methanol (2.5 mL) was added portionwise *N*-bromosuccinimide (0.73 g, 4.1 mmol) and the reaction was stirred at room temperature for 24 h. The solvent was removed *in vacuo* and the crude product was purified by recrystallisation in ethanol yielding **9** as a white solid (0.245 g, 37%).

Method B. To a stirred solution of **3** (0.389 g, 1.6 mmol) in acetic acid (4 mL) was added dropwise over 30 min, a solution of bromine (0.1 mL, 1.8 mmol) in acetic acid (1 mL). Reaction progress was monitored by TLC analysis. After 1 h, the reaction mixture was poured into 1% aqueous sodium sulfite (100 mL). The precipitate was filtered and washed with water yielding the product **9** as a white solid (0.245 g, 47%). Mp 245–248 °C (EtOH). ν_{max} (KBr)/cm^{-1} 3432 (OH stretch), 2926 (CH stretch), 2855 (CH stretch), 1631 (C═N), 1607 (aromatic), 1559 (C═N conjugated), 1475 (C═C stretch aromatic), 572 (C–Br). δ_H ([CD_3]$_2$SO, 300 MHz) 0.85 (3H, s, CH_3), 1.26–1.34 (8H, m, 4 × CH_2), 1.70 (2H, m, CH_2), 2.84–2.89 (2H, m, CH_2), 7.33–7.38 (1H, m, ArH), 7.57–7.70 (2H, m, 2 × ArH), 8.09 (1H, d, J = 7.9 Hz, ArH), 12.03 (1H, bs, OH). δ_C ([CD_3]$_2$SO, 75 MHz) 13.9 (CH_3), 22.0, 27.6, 28.3, 28.6, 31.1, 34.5 (6 × CH_2), 105.5 (C–Br), 117.8 (ArC), 122.7 (quaternary C), 123.6, 125.2 131.9 (3 × ArC), 138.7 (quaternary C), 152.0 (C═N), 171.24 (C–OH). Exact mass calculated for $C_{16}H_{21}NOBr$ [(M + H)$^+$], 322.0807. Found 322.0792, m/z ES$^+$ 322.3 [(M + H)$^+$, 100%].

Preparation of 3-chloro-2-heptylquinolin-4(1*H*)-one, 10

HHQ·HCl (**3·HCl**)† (0.839 g, 3.0 mmol) was dissolved in methanol (50 mL) before addition of 2 M NaOH until neutral followed by water (10 mL). Sodium dichloroisocyanurate (0.363 g, 1.65 mmol) was then added to the reaction mixture. The reaction was allowed stir at room temperature overnight. The precipitate was filtered and washed with methanol. The filtrate was then acidified to pH 4 and placed in the fridge overnight. The precipitate was filtered to give an off-white solid. Purification by recrystallisation in ethanol yielded **10** as a white crystalline solid (0.167 g, 46%). Mp 269–272 °C (EtOH). (Found: C, 68.7; H, 7.1; N, 5.1; Cl, 12.5. $C_{16}H_{20}ONCl$ requires C, 69.2; H, 7.3; N, 5.0; Cl, 12.8%.) ν_{max} (KBr)/cm^{-1} 3454 (OH stretch), 2927 (CH stretch), 2857 (CH stretch), 1634 (C═C stretch, conjugated), 1563 (C═N conjugated), 1504 (C–C stretch, in ring, aromatic), 1477 (C═C stretch, aromatic), 1356 (CN stretch), 584 (C–Cl). δ_H ([CD_3]$_2$SO, 300 MHz) 0.88 (3H, t, J = 6.7 Hz,

CH_3), 1.26–1.34 (8H, m, 4 × CH_2), 1.65–1.75 (2H, m, CH_2), 2.84 (2H, t, J = 7.8 Hz, CH_2), 7.32–7.37 (1H, m, ArH), 7.57–7.70 (2H, m, 2 × ArH), 8.1 (1H, d, J = 8.1 Hz, ArH), 12.03 (1H, bs, OH). δ_C ([CD_3]$_2$SO, 150 MHz) 13.9 (CH_3), 22.0, 27.5, 28.4, 28.6, 31.1, 32.1 (6 × CH_2), 113.3 (C–Cl), 118.0 (Ar–CH), 123.4 (quaternary C), 123.5, 125.1, 131.8 (3 × Ar–CH), 138.6 (quaternary C), 150.7 (ArC), 170.9 (C═O). Exact mass calculated for $C_{16}H_{21}NOCl$ [$(M + H)^+$], 278.1312. Found 278.1317, m/z (ES^+) 278 [$(M + H)^+$, 100%].

Preparation of 3-iodo-2-heptylquinolin-4(1*H*)-one, 11

To a stirred solution of **3** (0.333 g, 1.37 mmol) in glacial acetic acid (10 mL) was added portionwise *N*-iodosuccinimide (0.315 g, 1.40 mmol). Reaction progress was monitored by TLC analysis and after 2 h, the precipitate was filtered, washed with acetic acid and acetonitrile. Purification was achieved by silica column chromatography (80/20 ethyl acetate/hexane, ramping to 100% ethyl acetate) to yield **11** as a white crystalline solid (0.22 g, 48%). Mp 221–225 °C (EtOAc). (Found: C, 52.4; H, 5.4; N, 3.9. $C_{16}H_{20}INO$ requires C, 52.0; H, 5.5; N, 3.8%.) ν_{max} (film)/cm^{-1} 3419 (OH stretch), 2921 (CH stretch), 1627 (C═N), 1557 (C═N conjugated), 1474 (C═C stretch aromatic), 1134 (C–O alcohol), 571 (C–I). δ_H ([CD_3]$_2$SO, 300 MHz) 0.84–0.88 (3H, m, CH_3). 1.27–1.37 (8H, m, 4 × CH_2), 1.63–1.71 (2H, m, CH_2), 2.88–2.93 (2H, m, CH_2), 7.30–7.35 (1H, m, ArH), 7.57–7.68 (2H, m, 2 × ArH), 8.05–8.08 (1H, d, J = 8.1 Hz, ArH). δ_C ([CD_3]$_2$SO, 75 MHz) 13.9 (CH_3), 22.0, 27.9, 28.3, 28.7, 31.1, 38.7 (6 × CH_2), 85.8 (C–I), 117.8 (ArC), 120.6 (quaternary C), 123.8, 125.4, 131.9 (3 × ArC), 139.0 (quaternary C), 154.5 (C═N), 173.1 (C–OH). Exact mass calculated for $C_{16}H_{21}NOI$ [$(M + H)^+$], 370.0668. Found 370.0664, m/z ES^+ 370.3 [$(M + H)^+$, 100%]. (Assigned as the quinoline tautomer.)

Preparation of 12

A mixture of anthranilamide (20.5 mmol, 2.791 g), *n*-octanal (20.5 mmol, 3.2 mL) and sodium bisulfite (30.75 mmol, 3.2 g) in dimethylacetamide (30 mL) was stirred at 150 °C for 2 h. Reaction progress was monitored by TLC analysis. The reaction mixture was poured into water (500 mL) and the precipitate filtered. The precipitate was recrystallised from ethanol to give product **12** as an off-white crystalline solid (3.82 g, 76%). Mp 124–127 °C (EtOH). (Found: C, 73.4; H, 8.2; N, 11.4. $C_{15}H_{20}N_2O$ requires C, 73.7; H, 8.25; N, 11.5%.) ν_{max} (KBr)/cm^{-1} 3448 (OH stretch), 3034 (C–H stretch aromatic), 2919 (CH stretch), 2855 (CH stretch) 1674 (C═C), 1616 (C═N), 1470 (CH_2 bend), 1341 (C–N stretch), 1149 (C–O alcohol). δ_H ($CDCl_3$, 300 MHz) 0.88 (3H, t, J = 6.8 Hz, CH_3), 1.25–1.51 (8H, m, 4 × CH_2), 1.82–1.92 (2H, m, CH_2), 2.74–2.79 (2H, m, CH_2), 7.44–7.49 (1H, m, ArH), 7.68–7.80 (2H, m, 2 × ArH), 8.29 (1H, dd, J = 1.1, 8.0 Hz, ArH), 11.10 (1H, bs, OH). δ_C ($CDCl_3$, 75 MHz) 14.1 (CH_3), 22.6, 27.6, 29.0, 29.2, 31.7, 36.1 (6 × CH_2), 120.5 (quaternary C), 126.3, 126.4, 127.2, 134.8 (4 × ArC), 149.4 (quaternary C), 156.8 (C═N), 164.0 (C–OH). Exact mass calculated for $C_{15}H_{20}N_2O$ [$(M + H)^+$], 245.1654. Found 245.1654, m/z ES^+ 245 [$(M + H)^+$, 80%].

Acknowledgements

This research was supported in part by grants awarded to FOG by the European Commission (FP7-KBBE-2012-6, CP-TP-312184; FP7-KBBE-2012-6, CP-TP-311975; OCEAN.2011-2, 287589; MTKD-CT-2006-042062, O36314), Science Foundation Ireland (07/IN.1/B948; 08/RFP/GEN1295; 08/RFP/GEN1319; 09/RFP/BMT2350), the Department of Agriculture and Food (DAF RSF 06 321; DAF RSF 06 377; FIRM 08/RDC/629), the Irish Research Council for Science, Engineering and Technology (RS/2010/2413; 05/EDIV/FP107), the Health Research Board (RP/2006/271; RP/2007/290; HRA/2009/146), the Environmental Protection Agency (EPA2006-PhD-S-21; EPA2008-PhD-S-2), the Marine Institute (Beaufort award C2CRA 2007/082) and the Higher Education Authority of Ireland (PRTLI3; PRTLI4). GMG also thanks Science Foundation Ireland (09/RFP/CHS2353).

References

1 S. Swift, J. A. Downie, N. A. Whitehead, A. M. L. Barnard, G. P. C. Salmond and P. Williams, *Adv. Microb. Physiol.*, 2001, **45**, 199–270.
2 T. R. de Kievit and B. H. Iglewski, *Infect. Immun.*, 2000, **68**, 4839–4849.
3 M. R. Parsek and E. P. Greenburg, *Trends Microbiol*, 2005, **13**, 27–33.
4 P. Williams, K. Winzer, W. C. Chan and M. Cámara, *Phil. Trans. R. Soc. London B Biol. Sci.*, 2007, **362**, 1119–1134.
5 P. K. Singh, A. L. Schaefer, M. R. Parsek, T. O. Moninger, M. J. Welsh and E. P. Greenberg, *Nature*, 2000, **407**, 762–764.
6 Q. Seet and L.-H. Zhang, *Mol. Microbiol.*, 2011, **80**, 951–965.
7 J. T. Hodgkinson, S. D. Bowden, W. R. J. D. Galloway, D. R. Spring and M. Welch, *J. Bacteriol.*, 2010, **192**, 3833–3837.
8 J.-H. Lee, M. Hwan Cho and J. Lee, *Environ. Microbiol.*, 2011, **13**, 62–73.
9 G. Singh, B. Wu, M. S. Baek, A. Camargo, A. Nguyen, N. A. Slusher, R. Srinivasan, J.-P. Wiener-Kronish and S. V. Lynch, *Microb. Pathog.*, 2010, **49**, 196–203.
10 J. Cummins, F. J. Reen, C. Baysse, M. J. Mooij and F. O'Gara, *Microbiology*, 2009, **155**, 2826–2837.
11 S. P. Diggle, K. Winzer, S. R. Chhabra, K. E. Worrall, M. Cámara and P. Williams, *Mol. Microbiol.*, 2003, **50**, 29–43.
12 J.-F. Dubern and S. P. Diggle, *Mol. BioSyst.*, 2008, **4**, 882–888.
13 S. P. Diggle, S. Matthijs, V. J. Wright, M. P. Fletcher, S. R. Chhabra, I. L. Lamont, X. Kong, R. C. Hider, P. Cornelis, M. Cámara and P. Williams, *Chem. Biol.*, 2007, **14**, 87–96.
14 F. Bredenenbruch, R. Geffers, M. Nimtz, J. Buer and S. Häussler, *Environ. Microbiol.*, 2006, **8**, 1318–1329.
15 L. Mashburn-Warren, J. Howe, K. Brandenberg and M. Whitely, *J. Bacteriol.*, 2009, **191**, 3411–3414.
16 T. Guina, S. O. Purvine, E. C. Yi, J. Eng, D. R. Goodlett, R. Aebersold and S. I. Miller, *Proc. Natl. Acad. Sci. U. S. A.*, 2003, **100**, 2771–2776.
17 D. N. Collier, L. Anderson, S. L. McKnight, T. L. Noah, M. Knowles, R. Boucher, U. Schwab, P. Gilligan and E. C. Pesci, *FEMS Microbiol. Lett.*, 2002, **215**, 41–46.
18 J. R. Guina, S. O. Purvine, E. C. Yi, J. Eng, D. R. Goodlett, R. Aebersold and S. I. Miller, *Proc. Natl. Acad. Sci. U. S. A.*, 2003, **100**, 2771–2776.
19 K. L. Palmer, L. M. Mashburn, P. K. Singh and M. Whiteley, *J. Bacteriol.*, 2005, **187**, 5267–5277.
20 N. T. Lindsey, J. M. Hagins, P. A. Sokol and L. A. Silo-Suh, *Microbiology*, 2008, **154**, 1616–1627.
21 K. Kim, S. H. Kim, F. Lepine, Y. H. Cho and G. R. Lee, *Microb. Pathog.*, 2010, **49**, 174–180.
22 K. Kim, Y. U. Kim, B. H. Koh, S. S. Hwang, S. H. Kim, F. Lepine, Y. H. Cho and G. R. Lee, *Immunology*, 2010, **129**, 578–588.
23 S. P. Diggle, P. Lumjiaktase, F. Dipilato, K. Winzer, M. Kunakorn, D. A. Barrett, S. R. Chhabra and P. Williams, *Chem. Biol.*, 2006, **13**, 701–710.

24 F. J. Reen, M. J. Mooij, L. J. Holcombe, C. M. McSweeney, G. P. McGlacken, J. P. Morrissey and F. G. O'Gara, *FEMS Microbiol. Ecol.*, 2011, **77**, 413–428.
25 R. Fernández-Piñar, M. Cámara, J.-F. Dubern, J. L. Ramos and M. Espinosa-Urgel, *Res. Microbiol.*, 2011, **162**, 773–781.
26 L. Zhou, J. A. Glennon, J. H. T. Luong, F. J. Reen, F. O'Gara, C. M. McSweeney and G. P. McGlacken, *Chem. Commun.*, 2011, **47**, 10347–10349.
27 M. F. Fletcher, S. P. Diggle, M. Cámara and P. Williams, *Nat. Protocols*, 2007, **2**, 1254–1262.
28 Z. Zhou, F. J. Reen, F. O'Gara, C. M. McSweeney, S. L. Clarke, J. D. Glennon, J. H. T. Luong and G. P. McGlacken, *J. Chromatogr., A*, 2012, **1251**, 169–175.
29 M. P. Fletcher, S. P. Diggle, S. A. Crusz, S. R. Chhabra, M. Cámara and P. Williams, *Environ. Microbiol.*, 2007, **9**, 2683–2693.
30 I. P. Lokot, F. S. Pashkovsky and F. A. Lakhvich, *Tetrahedron*, 1999, **55**, 4783–4792.
31 B. P. Bangdiwala and C. M. Desai, *J. Indian Chem. Soc.*, 1953, **30**, 655–656.
32 A. Woschek, M. Mahout, K. Mereiter and F. Hammerschmidt, *Synthesis*, 2007, 1517–1522.
33 E. C. Pesci, J. B. Milbank, J. P. Pearson, S. McKnight, A. S. Kende, E. P. Greenberg and B. H. Iglewski, *Proc. Natl. Acad. Sci. U. S. A.*, 1999, **96**, 11229–11234.
34 J. T. Hodgkinson, W. R. J. D. Galloway, M. Welch and D. R. Spring, *Nat. Protocols*, 2012, **7**, 1184–1192.
35 G. P. McGlacken, C. M. McSweeney, T. O'Brien, S. E. Lawrence, C. J. Elcoate, F. J. Reen and F. O'Gara, *Tetrahedron Lett.*, 2010, **51**, 5919–5921.
36 B. Staskun, *J. Org. Chem.*, 1988, **53**, 5287–5291.
37 S. Heeb, M. P. Fletcher, S. R. Chhabra, S. P. Diggle, P. Williams and M. Cámara, *FEMS Microbiol. Rev.*, 2011, **35**, 247–274.
38 L. A. Gallagher, S. L. McKnight, M. S. Kuznetsova, E. C. Pesci and C. Manoil, *J. Bacteriol.*, 2002, **172**, 884–900.
39 M. Allesen-Holm, K. B. Barken, L. Yang, M. Klausen, J. S. Webb, S. Kjelleberg, S. Molin, M. Givskov and T. Tolker-Nielsen, *Mol. Microbiol.*, 2006, **59**, 1114–1128.
40 K. Kim, Y. U. Kim, B. H. Koh, S. S. Hwang, S.-H. Kim, F. Lépine, Y.-H. Cho and G. R. Lee, *Immunology*, 2010, **129**, 578–588.
41 G. Rampioni, C. Pustelny, M. P. Fletcher, V. J. Wright, M. Bruce, K. P. Rumbaugh, S. Heeb, M. Cámara and P. Williams, *Environ. Microbiol.*, 2010, **12**, 1659–1673.
42 D. G. Ha, J. H. Merritt, T. H. Hampton, J. T. Hodgkinson, M. Janecek, D. R. Spring, M. Welch and G. A. O'Toole, *J. Bacteriol.*, 2011, **193**, 6770–6780.
43 M. Bacalso, T. Xu, K. Yeung and D. Zheng, *J. Exp. Micro. Immunol.*, 2011, **15**, 84–89.
44 C. L. Haley, J. A. Colmer-Hamood and A. N. Hamood, *BMC Microbiol.*, 2012, **12**, 181.
45 M. Nakahata, M. Imaida, H. Ozaki, T. Harada and A. Tai, *Bull. Chem. Soc. Jpn.*, 1982, **55**, 2186–2189.

